Instituto de Investigación, Desarrollo e Innovación en Biotecnología Sanitaria de Elche

Universidad Miguel Hernández de Elche

Tesis Doctoral 2019

Polifenoles de plantas comestibles como reprogramadores metabólicos en condiciones de glucolipotoxicidad

---

Polyphenols from edible plants as metabolic reprogrammers under glucolipotoxic conditions

Mariló Olivares Vicente

Director: Dr. Vicente Micol Molina

Codirectora: Dra. María Herranz López

Programa de Doctorado en Biología Molecular y Celular

La presente Tesis Doctoral se presenta como un compendio de trabajos previamente publicados, o aceptados para revisión, que se citan a continuación:

- María Herranz-López[1], Isabel Borrás-Linares[1], **Mariló Olivares-Vicente**, Julio Gálvez, Antonio Segura-Carretero, Vicente Micol. *Correlation between the cellular metabolism of quercetin and its glucuronide metabolite and oxidative stress in hypertrophied 3T3-L1 adipocytes*. Phytomedicine 25 (2017) 25-28. doi: 10.1016/j.phymed.2016.12.008. [1]Estos autores contribuyeron igualmente en este trabajo.

- Cecilia Jiménez-Sánchez, **Mariló Olivares-Vicente**, Celia Rodríguez-Pérez, María Herranz-López, Jesús Lozano-Sánchez, Antonio Segura-Carretero, Alberto Fernández-Gutiérrez, José Antonio Encinar, Vicente Micol. *AMPK modulatory activity of olive-tree leaves phenolic compounds: Bioassay-guided isolation on adipocyte model and in silico approach.* PLOS One. 2017. 12(3):e0173074. doi: 10.1371/journal.pone.0173074.

- **Mariló Olivares-Vicente**, Enrique Barrajón-Catalán, María Herranz-López, Antonio Segura-Carretero, Jorge Joven, José Antonio Encinar, Vicente Micol. *Plant-derived polyphenols in human health: Biological activity, metabolites and putative molecular targets.* Current Drug Metabolism 19 (2018) 351-369. doi:10.2174/ 1389200219666180220095236.

- María Herranz-López[1], **Mariló Olivares-Vicente**[1], Marina Boix-Castejón, Nuria Caturla, Enrique Roche, Vicente Micol. *Differential effects of a combination of Hibiscus sabdariffa and Lippia citriodora polyphenols in overweight/obese subjects: A randomized controlled trial*. Scientific Reports, 2019, 28;9(1):2999. doi: 10.1038/s41598-019-39159-5. [1]Estos autores contribuyeron igualmente en este trabajo.

El **Dr. Vicente Micol Molina**, catedrático en el Área de Bioquímica y Biología Molecular de la Universidad Miguel Hernández, y la **Dra. María Herranz López**, profesora asociada del Departamento de Bioquímica y Biología Molecular de la Universidad Miguel Hernández e Investigadora del Instituto de Investigación, Desarrollo e Innovación en Biotecnología Sanitaria de Elche (IDiBE),

CERTIFICAN que el trabajo de investigación que conduce a la obtención del grado de Doctora, titulado "**Polifenoles de plantas comestibles como reprogramadores metabólicos en condiciones de glucolipotoxicidad**", del que es autora Dña. María Dolores Olivares Vicente, ha sido realizado bajo su dirección en el Instituto de Investigación, Desarrollo e Innovación en Biotecnología Sanitaria de Elche (IDiBE) de la Universidad Miguel Hernández,

Y **DAN SU CONFORMIDAD** para la presentación de dicha Tesis Doctoral bajo la modalidad de **Compendio de Publicaciones**.

Para que conste a los efectos oportunos, firman el presente certificado en Elche a ……. de …… de 2019.

Dr. Vicente Micol Molina	Dra. María Herranz López
Director/Tutor de la Tesis Doctoral	Codirectora de la Tesis Doctoral

El **Dr. Ricardo Mallavia Marín**, catedrático en el Área de Química Inorgánica y coordinador del Programa de Doctorado en Biología Molecular y Celular del Instituto de Investigación, Desarrollo e Innovación en Biotecnología Sanitaria de Elche (IDiBE),

DA SU CONFORMIDAD a la lectura de la Tesis Doctoral, titulada "**Polifenoles de plantas comestibles como reprogramadores metabólicos en condiciones de glucolipotoxicidad**", realizada por Dña. María Dolores Olivares Vicente en el Instituto de Investigación, Desarrollo e Innovación en Biotecnología Sanitaria de Elche (IDiBE) de la Universidad Miguel Hernández para optar al grado de **Doctora con Mención Internacional**.

Para que conste a los efectos oportunos, firma el presente certificado en Elche a ……. de …… de 2019.

Dr. Ricardo Mallavia Marín

Coordinador del Programa de Doctorado

en Biología Molecular y Celular

Dña. María Dolores Olivares Vicente ha realizado la presente Tesis Doctoral gracias a la concesión de una beca predoctoral con número de expediente ACIF/2016/230 correspondiente al Programa de Subvenciones para la contratación de personal investigador de carácter predoctoral concedidas por la Generalitat Valenciana y cofinanciadas por el Fondo Social Europeo. Asimismo, la doctoranda ha realizado una estancia de nueve meses en el *Laboratoire de Pharm-Ecologie Cardiovasculaire* (EA 4278 LaPEC) de la Universidad de Aviñón (Francia) gracias a la concesión de tres ayudas del Programa de Subvenciones para estancias de contratados predoctorales en centros de investigación fuera de la Comunitat Valenciana, con números de expediente BEFPI/2017/030, BEFPI/2018/047 y BEFPI/2019/047.

AGRADECIMIENTOS

Me gustaría expresar mi gratitud a todas aquellas personas que, desde la parte más técnica a la parte más emocional, han hecho que esta Tesis sea posible.

En primer lugar, quiero agradecer a mis directores de Tesis: el Dr. Vicente Micol y la Dra. María Herranz, por su dirección, dedicación, motivación y contribución en mi formación académica y profesional. Gracias, Vicente, por abrirme las puertas de tu laboratorio, por tu valioso asesoramiento, por la transmisión de conocimientos y por ofrecerme los medios necesarios para llevar a cabo este proyecto. Gracias, María, por haber sido mi directora y compañera, por tu disponibilidad, por toda tu ayuda y por las innombrables veces que me has empujado a seguir cuando perdía la motivación. Sin tu espíritu alentador y optimista, esto habría sido muy difícil.

Al Dr. Enrique Barrajón, por su ayuda incondicional y sus valiosos consejos en materia de ciencia.

Al Dr. José Antonio Encinar, por sus aportaciones en los estudios computacionales y su contribución en la elaboración de los artículos.

Agradezco especialmente al Dr. Enrique Roche. Gracias, Enrique, por abrirme horizontes, por motivarme y por el apoyo y la ayuda que siempre estás dispuesto a ofrecer. Eres un referente en lo profesional y en lo personal.

Merci à Dr. Agnes Vinet pour m'avoir ouvert les portes de son laboratoire, et à toute l'équipe du LaPEC, qui m'a gentillement accueilli comme un membre du groupe. En particulier, merci à Dr. Catherine Riva pour sa supervision, sa disponibilité et sa contribution à ma formation scientifique. Mon expérience au LaPEC m'a permis d'apprendre nouvelles techniques et acquérir de nouvelles compétences scientifiques. Merci à Alex, pour son aide inconditionnelle dans le labo et dehors, et à Charly, pour me transmettre son énergie et sa positivité.

Al grupo de investigación del Centro Tecnológico de Investigación y Desarrollo del Alimento Funcional (CIDAF), dirigido por el Dr. Antonio Segura, y al grupo de Recerca Biomédica, dirigido por el Dr. Jorge Joven, por sus contribuciones experimentales.

A mis compañeras del lab: Vero, Almu, Luz, María L. y Noelia. Gracias, chicas, por todo lo que me habéis ayudado y por compartir conmigo tantos momentos de alegría y desahogo. También a Javi, Marina, Jesica y todos aquellos que habéis formado parte del grupo. Mucho ánimo y suerte en vuestros caminos.

Al grupo técnico del IDiBE, especialmente Maite, por su ayuda y disposición y por poner siempre orden cuando nos reina el caos.

A todos los miembros del IDiBE que, de alguna manera u otra, han contribuido en la gestión, administración y asesoramiento de esta Tesis. En particular, al director del Instituto, el Dr. Antonio Ferrer, por brindarme la oportunidad de realizar mi Tesis Doctoral en este centro, y al director del Programa de Doctorado, el Dr. Ricardo Mallavia, por su disponibilidad y su imprescindible labor en nuestra formación como doctores. También quiero agradecer al personal de administración, tanto los que estaban cuando comencé, como Javier, May y Bea, como los que están ahora que termino, Maite, Pepi, Vicente y Eva.

A mi querida amiga Sara, por todo lo que hemos compartido dentro y fuera del laboratorio. Y por las veces que has cuidado de mis celulitas. Te deseo un futuro lleno de éxitos y felicidad, porque no mereces otra cosa.

A mi querida amiga Tere, la que llegó siendo mi alumna y la que ha terminado enseñándome a mí. Eres una luchadora nata y sé que vas a llegar muy lejos.

A mis queridos Ceci y Aitor, porque sin vosotros me habría hundido muchas veces. Gracias por todo el apoyo que me dais y por estar siempre tan cerca, aun cuando estáis tan lejos.

A mi familia, el pilar clave que me ha sustentado todos estos años. A mis abuelos, que siempre me deseáis felicidad en aquello que hago. A mis tíos Martín y Toñi, por preocuparos por mí y desearme siempre lo mejor. A mis tíos David y José, por aportarme momentos de paz y desconexión. A mis María Puñetas: Mar y Noelia, por estar siempre y antes que nadie, porque sois mis primas, pero también mis mejores amigas.

A mi Tete, por enseñarme a afrontar los problemas desde el sentido del humor. Y a Jenny, por motivarme y saber escucharme en mis momentos de frustración.

Y, por supuesto, a mis padres. Porque os lo debo todo y absolutamente todo. Porque sois los pilares de todo lo que construyo, aguantando y soportando todas las adversidades. Vosotros me enseñáis que la vida es lucha, perseverancia y sacrificio y que, solamente así, se consiguen los verdaderos éxitos. Y esto es un gran éxito.

Gracias de todo corazón.

"La felicidad del cuerpo se funda en la salud;

la del entendimiento, en el saber."

Tales de Mileto

RESUMEN

Las plantas representan una enorme fuente de compuestos con importantes propiedades terapéuticas. Concretamente, los polifenoles han sido ampliamente estudiados no sólo por su inherente capacidad antioxidante, sino además porque su gran diversidad estructural les hace partícipes en multitud de procesos biológicos. Debido a este carácter pleiotrópico, los polifenoles son idóneos candidatos como compuestos bioactivos en el tratamiento de enfermedades multifactoriales como la obesidad y sus patologías asociadas. No obstante, muchos estudios que han empleado modelos celulares se centran en los efectos biológicos de estos compuestos sin considerar la biotransformación que sufren cuando son ingeridos. Considerando aspectos sobre la bioactividad y la biodisponibilidad, el objetivo fundamental de la presente Tesis ha sido profundizar en los mecanismos moleculares de los metabolitos derivados de polifenoles de *Hibiscus sabdariffa* (HS), *Lippia citriodora* (LC) y *Olea europaea*, demostrando su implicación en la mejora de las alteraciones asociadas con la obesidad.

Los resultados de la presente Tesis, obtenidos mediante el empleo de un modelo celular de adipocitos hipertróficos inducidos por alta glucosa, indican que los polifenoles y sus metabolitos pueden alcanzar dianas intracelulares revirtiendo las alteraciones metabólicas que ocurren en el tejido adiposo obeso, como el estrés oxidativo, la excesiva acumulación de triglicéridos, la disfunción mitocondrial y la inflamación. Asimismo, se ha visto que los polifenoles pueden mediar sus efectos modulando la expresión génica de proteínas implicadas en el metabolismo lipídico, como la sintasa de ácidos grasos (FASN) o el receptor activado por proliferadores de peroxisomas alfa (PPARα), y la actividad de proteínas como la quinasa activada por AMP (AMPK), un regulador clave del metabolismo energético que representa una diana terapéutica potencial en patologías metabólicas. Además, los estudios computacionales sugieren que algunos polifenoles pueden desempeñar su papel de manera específica modulando directamente la actividad de sus dianas.

A pesar de su baja biodisponibilidad, los estudios de intervención en humanos confirman la eficacia de estos polifenoles cuando son consumidos de forma regular en periodos relativamente cortos. En un estudio llevado a cabo con voluntarias obesas y con sobrepeso, se ha demostrado que la ingesta de una combinación de HS y LC puede mejorar parámetros antropométricos y el perfil lipídico, y reducir la tensión arterial sistólica y el pulso cardíaco. Se postula que estos cambios pueden ser mediados por la modulación de AMPK a nivel del tejido adiposo o actuando directamente sobre el sistema cardiovascular. Los resultados de esta Tesis ofrecen un conocimiento global sobre los potenciales metabolitos responsables de la bioactividad de plantas, así como sus posibles dianas moleculares.

ABSTRACT

Plants represent an enormous source of compounds with important therapeutic properties. Specifically, polyphenols have been widely studied not only because of their inherent antioxidant capacity, but also because their high structural diversity makes them participants in a multitude of biological processes. Due to this pleiotropic nature, polyphenols become suitable candidates as bioactive compounds in the treatment of multifactorial diseases such as obesity and its related diseases. However, many studies using cellular models focus on the biological effects of these compounds without considering the biotransformation they suffer when ingested. Based on bioactivity and bioavailability data, the main objective of this Thesis has been to deepen the molecular mechanisms of polyphenol-derived metabolites from *Hibiscus sabdariffa* (HS), *Lippia citriodora* (LC) and *Olea europaea*, demonstrating their implication on the amelioration of obesity-associated alterations.

Using a hypertrophic adipocyte cell model induced by high glucose, the results of this Thesis indicate that polyphenols and their metabolites can reach intracellular targets reversing the metabolic alterations occurred in obese adipose tissue, such as oxidative stress, excessive triglyceride accumulation, mitochondrial dysfunction and inflammation. Likewise, it has been observed that polyphenols can mediate their effects through modulation of gene expression of proteins involved in lipid metabolism, such as fatty acid synthase (FASN) or peroxisome proliferator-activated receptor alpha (PPARα), and the activity of AMP-activated protein kinase (AMPK), a key regulator of energy metabolism that represents a potential therapeutic target in metabolic pathologies. In addition, computational studies suggest that some polyphenols may play their role through a direct modulation of the activity of their targets.

Despite the low bioavailability, human intervention studies confirm the efficacy of these polyphenols when consumed regularly in relatively short periods. In a study carried out with obese and overweight volunteers, it has been shown that the intake of a combination of HS and LC can improve anthropometric parameters and lipid profile and reduce systolic blood pressure and heart rate. It is postulated that these changes can be mediated by the modulation of AMPK in adipose tissue or through a direct action on the cardiovascular system. The results of this Thesis offer an extensive knowledge about the potential metabolites responsible for the bioactivity of plants, as well as their possible molecular targets.

ABREVIATURAS

AC, circunferencia abdominal

ACC, acetil-CoA carboxilasa

ADaM, *allosteric drug and metabolite-binding site*

ADMET, absorción, distribución, metabolismo, excreción y toxicidad

ADP, adenosín difosfato

AICAR, 5-aminoimidazol-4-carboxamida-1-β-4-ribofuranósido

AID, dominio autoinhibitorio (*autoinhibitory domain*)

AMP, adenosín monofosfato

AMPc, adenosín monofosfato cíclico

AMPK, proteína quinasa activada por AMP

ATGL, lipasa adiposa de triglicéridos

ATP, adenosín trifosfato

BSA, albúmina sérica bovina

BF, grasa corporal

CaMKKβ, quinasa β dependiente de Ca^{2+} y calmodulina

CBM, módulo de unión a carbohidratos (*carbohydrate-binding module*)

CBS, motivos *cystathionine-β-synthase*

C/EBPs, proteínas potenciadoras de unión a elementos CCAAT

DAD, detector de diodo

DBP, presión arterial diastólica

ΔG, variación de energía libre de Gibbs

DMEM, *Dulbecco's Modified Eagle's Medium*

DMSO, dimetilsulfóxido

ERO, especies reactivas de oxígeno

ESI, ionización por electrospray

FA, ácido graso

FASN, sintasa de ácidos grasos

FBS, suero bovino fetal

FICI, índice fraccional de concentración inhibitoria

GLP-1, péptido similar al glucagón tipo 1

H_2O_2, peróxido de hidrógeno

HPLC, cromatografía líquida de alto rendimiento

HS, *Hibiscus sabdariffa*

HSL, lipasa sensible a hormonas

IBMX, 3-isobutil-1-metilxantina

IMC, Índice de Masa Corporal

IL, interleucina

IT, trampa de iones

KD, dominio quinasa convencional de serinas y treoninas (*kinase domain*)

LC, *Lippia citriodora*

LKB1, quinasa hepática B1

LPL, lipoproteína lipasa

MCP-1, proteína quimioatrayente de monocitos 1

MS, espectrometría de masas

NCD-RisC, *NCD Risk Factor Collaboration*

Nrf2, factor nuclear eritroide 2 (*nuclear factor erythroid 2-related factor 2*)

NF-κB, factor nuclear kappa B

OL, hoja de *Olea europaea* (*olive leaf*)

OMS, Organización Mundial de la Salud

pAMPK, AMPK fosforilada

PEHS, extracto polifenólico de HS

pGLM-ENH, plásmido con la región potenciadora del gen de MCP-1 humano

PPARα, receptor activado por el proliferador de peroxisomas alfa

PPARγ, receptor activado por el proliferador de peroxisomas gamma

Pref-1, factor de preadipocito

Q, quercetina

Q3GA, quercetina-3-glucurónido

ROS, *reactive oxygen species*

RP, fase inversa

RPMI-1640, *Roswell Park Memorial Institute medium*

SBP, presión arterial sistólica

ST-loop, lazo flexible rico en Ser y Thr

TAB, tejido adiposo blanco

TAM, tejido adiposo marrón

TG, triglicérido

TOF, tiempo de vuelo

TNF-α, factor de necrosis tumoral alfa

UCP1, proteína desacoplante

UGT, uridinadifosfato glucuroniltransferasa (*UDP-glucuronosyltransferase*)

ZMP, AICAR monofosfato

ÍNDICE

ÍNDICE

INTRODUCCIÓN GENERAL

1 OBESIDAD

1.1 OBESIDAD. LA PANDEMIA DEL SIGLO XXI

Según la Organización Mundial de la Salud (OMS), "el sobrepeso y la obesidad se definen como una acumulación anormal o excesiva de grasa" que puede agravar seriamente la salud. El método más generalizado para estimar el estado nutricional de una persona es el Índice de Masa Corporal (IMC), que se calcula dividiendo el peso de una persona en kilogramos por el cuadrado de su altura en metros. Según la clasificación publicada por la OMS, una persona presenta obesidad cuando su IMC es igual o superior a 30 kg/m^2, y sobrepeso cuando su IMC es igual o superior a 25 kg/m^2 (**Fig. 1**) [1]. No obstante, el IMC es un parámetro orientativo que debe interpretarse con cautela, dado que no considera variables importantes como el género o la edad, así como tampoco el porcentaje de grasa corporal o su localización en las distintas partes del cuerpo [2].

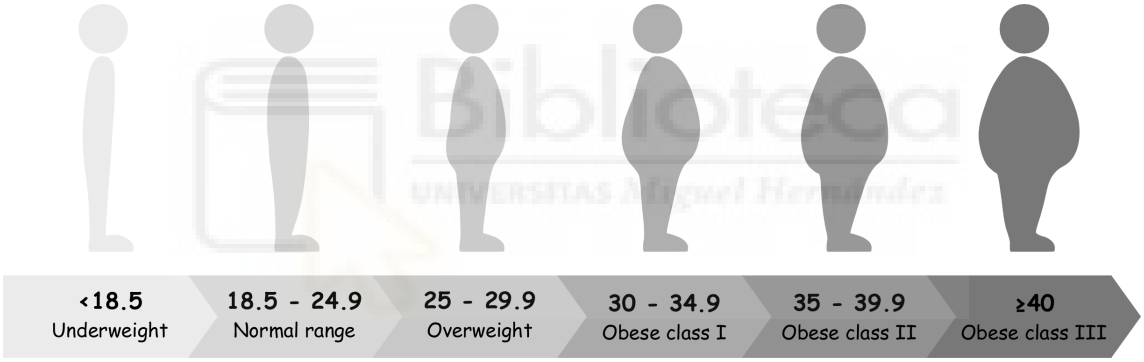

Figura 1. Clasificación según la OMS del estado nutricional de acuerdo con el IMC. Datos obtenidos a partir del informe "*Obesity: preventing and managing the global epidemic*" publicado en el año 2000 por la OMS [3].

Desde 1975 a 2016, la prevalencia mundial de obesidad ha aumentado progresivamente. Aunque siempre se ha considerado un problema limitado a países de altos ingresos, esta enfermedad prevalece cada vez más en aquellos de medianos y bajos ingresos. La *NCD Risk Factor Collaboration* (NCD-RisC), una red mundial de profesionales del ámbito de la salud que proporciona datos rigurosos sobre los factores de riesgo de enfermedades no transmisibles, manifiesta que el número de mujeres con obesidad a nivel mundial ha aumentado de 69 millones en 1975 a 390 millones en 2016 y el de hombres, de 31 millones en 1975 a 281 millones en 2016 (**Fig. 2**) [4]. Se trata, por tanto, de una situación alarmante para la salud pública a nivel global, dado que la obesidad es un importante factor de riesgo para el desarrollo de enfermedades cardiovasculares, diabetes e incluso algunos tipos de cáncer.

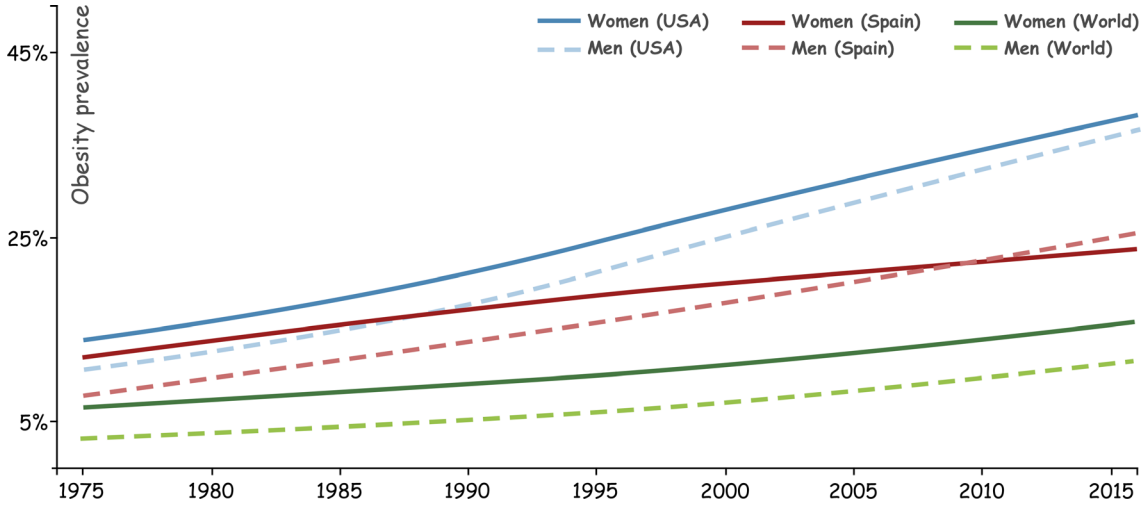

Figura 2. Comparativa de la tendencia de la prevalencia de obesidad desde 1975 hasta 2016 entre Estados Unidos, España y a nivel mundial. En 2016, el porcentaje de mujeres obesas alcanzó el 38.2 % en EE. UU., el 23.8 % en España y el 15.7 % a nivel mundial, mientras que el de hombres obesos representó el 36.5 % en EE. UU., el 25.5 % en España y el 11.6 % a nivel mundial. Adaptación de los datos poblaciones publicados por la NCD-RisC a partir de una población de participantes mayores de 19 años desde 1975 hasta 2016 [5].

2 TEJIDO ADIPOSO Y SUS ALTERACIONES EN LA OBESIDAD

2.1 TEJIDO ADIPOSO. MÁS QUE UN SIMPLE RESERVORIO DE ENERGÍA

LIPOGÉNESIS Y LIPÓLISIS

El tejido adiposo se ha considerado como un mero órgano especializado en acumular energía en forma de grasa. No obstante, dicha función es vital para mantener la homeostasis energética de todo el organismo, ya que los adipocitos proveen nutrientes a otros tejidos ante una escasez de ingesta calórica mientras que, en condiciones de abundancia, los almacenan en forma de triglicéridos [6]. Estos dos procesos antagónicos son llevados a cabo por proteínas altamente reguladas, como la lipoproteína lipasa (LPL), la lipasa adiposa de triglicéridos (ATGL) o la lipasa sensible a hormonas (HSL). La LPL hidroliza los triglicéridos de los quilomicrones y las proteínas de muy baja densidad (VLDL) circulantes, liberando ácidos grasos que son esterificados de nuevo por los adipocitos para su almacenaje [7]. Por otro lado, la ATGL y la HSL son dos enzimas implicadas en las primeras etapas de la lipólisis, proceso mediante el cual los triglicéridos almacenados son hidrolizados a ácidos grasos y glicerol [8]. Estos ácidos grasos son entonces transportados y empleados para producir energía en forma de ATP a través de la β-oxidación mitocondrial (**Fig. 3**).

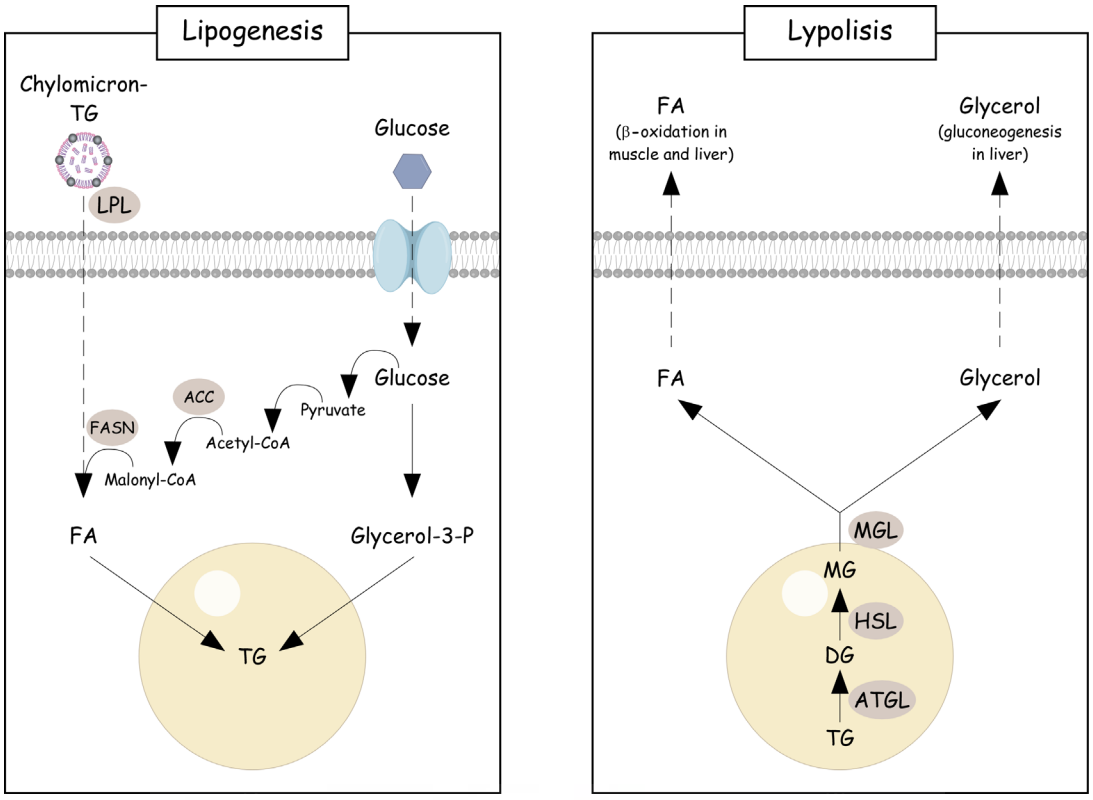

Figura 3. Lipogénesis y lipólisis en un adipocito. TG, triglicéridos; LPL, lipoproteína lipasa; FA, ácidos grasos; ACC, acetil-CoA carboxilasa; FASN, sintasa de ácidos grasos; DG, diglicéridos; MG, monoglicéridos; ATGL, lipasa adiposa de triglicéridos; HSL, lipasa sensible a hormonas; MGL, monoacilglicerol lipasa. Adaptación de la revisión publicada por Vázquez-Vela *et al.* [9].

TIPOS DE TEJIDO ADIPOSO EN HUMANOS

En humanos, se han descrito dos tipos fundamentales de tejido adiposo: el tejido adiposo blanco (TAB) y el tejido adiposo marrón (TAM) [10]. La función descrita anteriormente es propia del TAB, mientras que el TAM disipa la energía en forma de calor a través de la termogénesis, proceso llevado a cabo por la proteína desacoplante 1 (UCP1) [11, 12]. El TAB se encuentra distribuido a lo largo de todo el organismo, distinguiéndose dos depósitos principales: el subcutáneo y el visceral. Cabe destacar que la obesidad abdominal derivada de la excesiva acumulación de grasa en el TAB visceral es la que se asocia con un mayor riesgo de sufrir complicaciones metabólicas [13], como la resistencia a la insulina, la diabetes tipo 2 y los problemas cardiovasculares. Por otro lado, el TAM queda limitado a neonatos, pero recientemente se han descrito depósitos de TAM funcional en adultos, especialmente en la región cervical y supraclavicular [14, 15]. Por ello, la manipulación farmacológica del TAM ha emergido recientemente como una estrategia terapéutica potencial frente a las complicaciones de la obesidad.

Actualmente, se ha identificado un nuevo tipo de adipocito que subyace dentro del TAB. Se conocen como adipocitos beige porque presentan características genotípicas y fenotípicas propias de un adipocito marrón (gran cantidad de mitocondrias, presencia de vacuolas lipídicas multiloculares y expresión de UCP1) en respuesta a ciertos estímulos como el frío, el ejercicio o el tratamiento con agonistas de PPARγ [16] (**Fig. 4**). A pesar de estas similitudes, los adipocitos marrones y los beige provienen de linajes celulares distintos. Los adipocitos marrones clásicos proceden de precursores que expresan el factor miogénico 5, al igual que las células del músculo esquelético. Por otro lado, el origen de los adipocitos beige se desconoce, pero se postula que comparten un ancestro común con los adipocitos blancos y pueden originarse a partir de células precursoras beige o blancas o a partir de la transdiferenciación de adipocitos blancos maduros [17]. Estudios en animales evidencian que ciertas moléculas, como los polifenoles procedentes de plantas, pueden estimular la actividad beige del TAB previniendo la obesidad, la resistencia a la insulina y la esteatosis hepática [18-20].

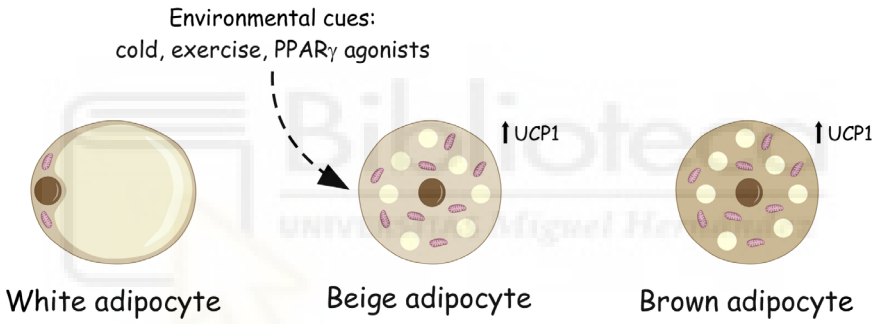

Figura 4. Tipos de adipocitos. Los adipocitos blancos se caracterizan por presentar una gran vacuola lipídica en su citoplasma y pocas mitocondrias. El adipocito marrón presenta vacuolas lipídicas multiloculares, una gran cantidad de mitocondrias y una alta expresión de UCP1. El adipocito beige exhibe las características propias de un adipocito marrón bajo la inducción de diversos factores como el frío, el ejercicio o el tratamiento con agonistas de PPARγ. Adaptación del trabajo publicado por Brestoff y Artis [21].

PAPEL ENDOCRINO DEL TEJIDO ADIPOSO

Más allá de representar el principal reservorio energético del organismo, el tejido adiposo blanco desempeña también un importante papel endocrino. Los adipocitos secretan polipéptidos señalizadores llamados adipoquinas que regulan el peso corporal y procesos como la sensibilidad a la insulina o la inflamación (**Fig. 5**) [9, 22]. Por ejemplo, la leptina, una de las primeras adipoquinas descritas, regula el apetito y el gasto energético actuando directamente sobre el hipotálamo. La adiponectina es una hormona que aumenta la sensibilidad a la insulina a nivel sistémico, promueve el metabolismo de los lípidos y la glucosa en hígado y músculo, y desempeña un papel antiinflamatorio en el tejido adiposo.

Por otro lado, los adipocitos también pueden regular la respuesta inflamatoria a través de la secreción de citoquinas como el factor de necrosis tumoral alfa (TNF-α) o interleucinas (IL-1β, IL-6, IL-8, IL-10, IL-15, entre otras).

No obstante, cabe considerar que los adipocitos representan un tercio del tejido adiposo, coexistiendo con otros tipos celulares como fibroblastos, preadipocitos, macrófagos, células T, linfocitos, neutrófilos y células endoteliales (**Fig. 8**). Estas células participan activamente en la función secretora del tejido adiposo garantizando el mantenimiento de la homeostasis energética. Sin embargo, el desequilibrio entre los diferentes tipos celulares, así como entre la producción de adipoquinas y otras hormonas en el tejido adiposo, está estrechamente relacionado con el desarrollo de las alteraciones metabólicas asociadas a la obesidad [23].

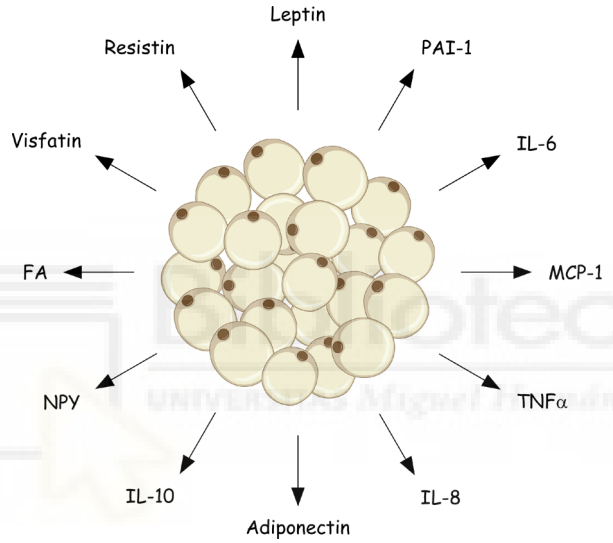

Figura 5. Adipoquinas secretadas por los adipocitos. Mediante la secreción de estas moléculas, los adipocitos regulan procesos como el metabolismo lipídico, la homeostasis de la glucosa, la sensibilidad a la insulina, la inflamación o la angiogénesis, entre otros. PAI-1, inhibidor del activador de plasminógeno 1; IL, interleucina; MCP-1, proteína quimioatrayente de monocitos 1; TNFα, factor de necrosis tumoral alfa; NPY, neuropéptido Y; FA, ácidos grasos. Adaptación de los trabajos publicados por Trayhurn *et al.* [24] y Vázquez-Vela *et al.* [9].

2.2 EXPANSIÓN DEL TEJIDO ADIPOSO Y SUS ALTERACIONES METABÓLICAS EN LA OBESIDAD

El tejido adiposo puede expandirse de dos formas: por un aumento en el tamaño de los adipocitos (hipertrofia) o por la formación de nuevos adipocitos (hiperplasia) [25]. Si bien la hiperplasia (fenómeno más común en la infancia y adolescencia) podría considerarse un medio para tratar las alteraciones metabólicas de la obesidad, ya que se ha descrito en adultos obesos metabólicamente sanos [26]; la hipertrofia de los adipocitos es la que se

considera perjudicial para la función del tejido adiposo y la que deriva, por tanto, en una resistencia a la insulina y otras alteraciones descritas en la obesidad [27]. Cuando el aporte calórico supera el gasto energético de forma prolongada, los adipocitos acumulan el exceso de nutrientes aumentando considerablemente su tamaño. Como se detalla a continuación, la hipertrofia del adipocito provoca una serie de alteraciones que comprometen la función del tejido adiposo, con importantes consecuencias a nivel sistémico.

ESTRÉS OXIDATIVO

Una de las alteraciones asociadas a la hipertrofia es el desequilibrio en el estado oxidativo, como consecuencia de una alta producción de especies reactivas de oxígeno (ERO). Las ERO son moléculas reactivas inestables que pueden oxidar componentes celulares como lípidos, DNA o proteínas. Entre ellas, se encuentran el anión superóxido ($O_2^{\cdot-}$), el peróxido de hidrógeno (H_2O_2) y el radical hidroxilo ($OH^{\cdot}$). La mitocondria, a través de las reacciones redox que tienen lugar en la cadena de trasporte de electrones, es la principal fuente endógena de ERO [28]. Asimismo, las ERO también pueden formarse a través de reacciones enzimáticas llevadas a cabo por enzimas como la NADPH oxidasa, entre otras [29].

Las ERO desempeñan un importante papel en el mantenimiento de la homeostasis celular ya que, cuando existe un equilibrio prooxidante-antioxidante, estas moléculas participan en la regulación de vías de señalización a través de la oxidación reversible de ciertas proteínas. Por ejemplo, las ERO derivadas de la cadena respiratoria mitocondrial en células madre mesenquimales inducen la expresión del receptor activado por el proliferador de peroxisomas gamma (PPARγ), un factor transcripcional clave en el proceso de adipogénesis [30]. También se ha demostrado que el tratamiento transitorio de adipocitos 3T3-L1 con H_2O_2 aumenta la captación de glucosa a través de la activación de la vía de señalización de la insulina [31].

No obstante, una exposición prolongada a altos niveles de glucosa y lípidos aumenta la actividad β-oxidativa de las mitocondrias y, con ello, los niveles de ERO en los adipocitos. Este desequilibrio oxidativo, acompañado por la incapacidad de las enzimas antioxidantes de eliminar el exceso de ERO, puede provocar la oxidación irreversible de ciertas biomoléculas, afectando a su actividad o resultando tóxicas para el adipocito. Además, la alta producción de ERO contribuye a su vez al estado hipertrófico del tejido adiposo, ya que favorece la acumulación de lípidos al inhibir la formación de nuevos adipocitos y bloquear la cadena respiratoria en los adipocitos maduros (**Fig. 6**) [32].

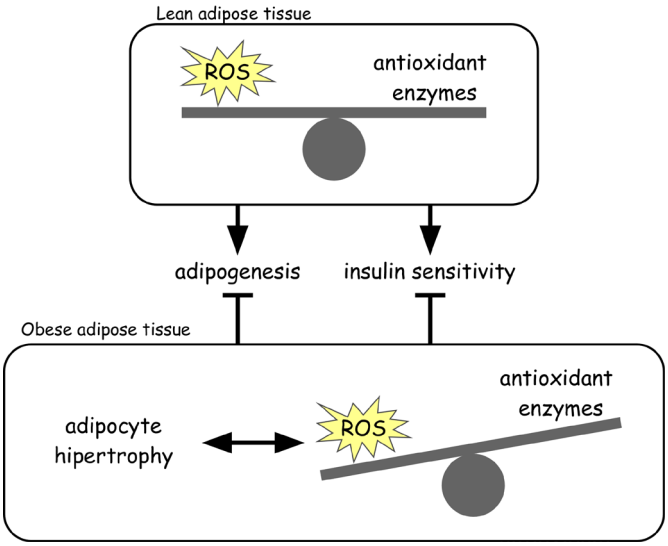

Figura 6. Papel de las ERO en el tejido adiposo. En situaciones de normopeso, el tejido adiposo se encuentra en un equilibrio entre la producción de ERO y la expresión de enzimas antioxidantes, favoreciéndose la formación de nuevos adipocitos y la sensibilidad a la insulina. En la obesidad, la hipertrofia de los adipocitos produce un desequilibrio entre la alta producción de ERO y la expresión disminuida de enzimas antioxidantes, inhibiéndose los procesos de adipogénesis y las vías de señalización de la insulina y promoviendo el estado hipertrófico de los adipocitos. ROS, *reactive oxygen species*. Adaptación de los trabajos publicados por Tormos [30], Ma [31] y Castro [32].

DISFUNCIÓN MITOCONDRIAL

Otro de los trastornos producidos en el adipocito hipertrófico debido a la expansión patológica del tejido adiposo en la obesidad es una disfunción a nivel mitocondrial, como consecuencia principalmente de la alta producción de ERO. Esta disfuncionalidad se ve acompañada por alteraciones en la morfología y en los procesos de fisión y fusión de las mitocondrias, una reducción en la biogénesis mitocondrial, una mayor producción de ERO y una pérdida del potencial de membrana mitocondrial (**Fig. 7**) [33]. La mitocondria ha sido ampliamente estudiada en el músculo esquelético, los adipocitos marrones, el corazón y el hígado [34], pero su papel en los adipocitos blancos siempre había quedado relegado por su baja abundancia. No obstante, cada vez se conoce más la importancia de este orgánulo en el mantenimiento de la homeostasis metabólica del tejido adiposo blanco y se defiende que la disfunción mitocondrial debida a mutaciones en el DNA o a la oxidación de las proteínas mitocondriales es causa de la resistencia a la insulina en este tejido [35], por lo que la mitocondria constituye una diana terapéutica *per se* en el tratamiento de las enfermedades asociadas a la obesidad.

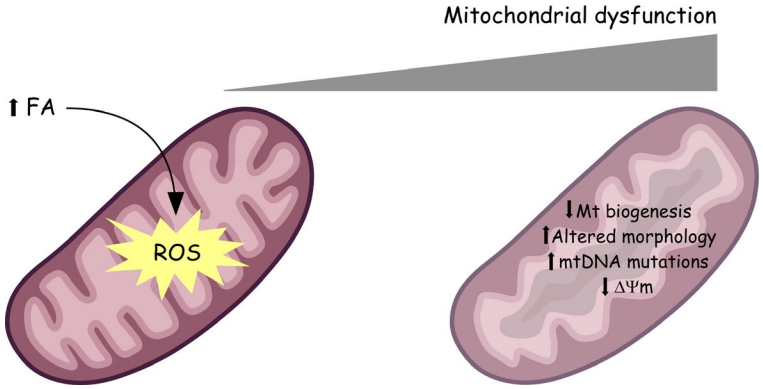

Figura 7. Evolución de la mitocondria en la obesidad. El exceso de ácidos grasos (FA) aumenta la actividad oxidativa de la mitocondria dando como resultado una alta producción de ERO que, a su vez, afectan a la función de la mitocondria alterando su morfología, provocando mutaciones en el DNA mitocondrial y la oxidación de proteínas de la cadena respiratoria, disminuyendo la biogénesis mitocondrial y ocasionando una pérdida del potencial de membrana mitocondrial (ΔΨm). Adaptación del trabajo publicado por Gao *et al.* [33].

INFLAMACIÓN

La hipertrofia del adipocito, el aumento en la producción de ERO y la disfunción mitocondrial impulsan el establecimiento de un estado inflamatorio crónico de bajo grado en el tejido adiposo (**Fig. 8**). Además de disminuir la secreción de adipoquinas antiinflamatorias como la adiponectina, los adipocitos hipertróficos liberan una mayor cantidad de citoquinas proinflamatorias como TNF-α, IL-6 e IL-8, moléculas de adhesión endotelial como VCAM-1 y factores quimioatrayentes como la proteína quimioatrayente de monocitos 1 (MCP-1). Esto promueve la infiltración de los monocitos circulantes al endotelio, su migración al tejido adiposo y la polarización de los macrófagos al fenotipo clásicamente activado o tipo M1 [36], amplificando la respuesta inflamatoria en el tejido adiposo.

RESISTENCIA A LA INSULINA

En última instancia, estas alteraciones metabólicas e inflamatorias conducen a una resistencia a la insulina en el tejido adiposo (**Fig. 8**). Por ejemplo, la adiponectina es una adipoquina estrechamente relacionada con la regulación de la sensibilidad a la insulina y se encuentra disminuida en el plasma de individuos obesos con resistencia a la insulina [37]. Asimismo, los individuos diabéticos presentan altos niveles plasmáticos de IL-6 y TNF-α, pero estos niveles son incluso mayores en aquellos que además presentan obesidad asociada [38]. Estas citoquinas, junto con las ERO, pueden disminuir la sensibilidad a la insulina a través de la expresión y translocación del factor nuclear kappa B (NF-κB), el cual

inhibe la vía de señalización de insulina y además aumenta la expresión de citoquinas proinflamatorias [39, 40].

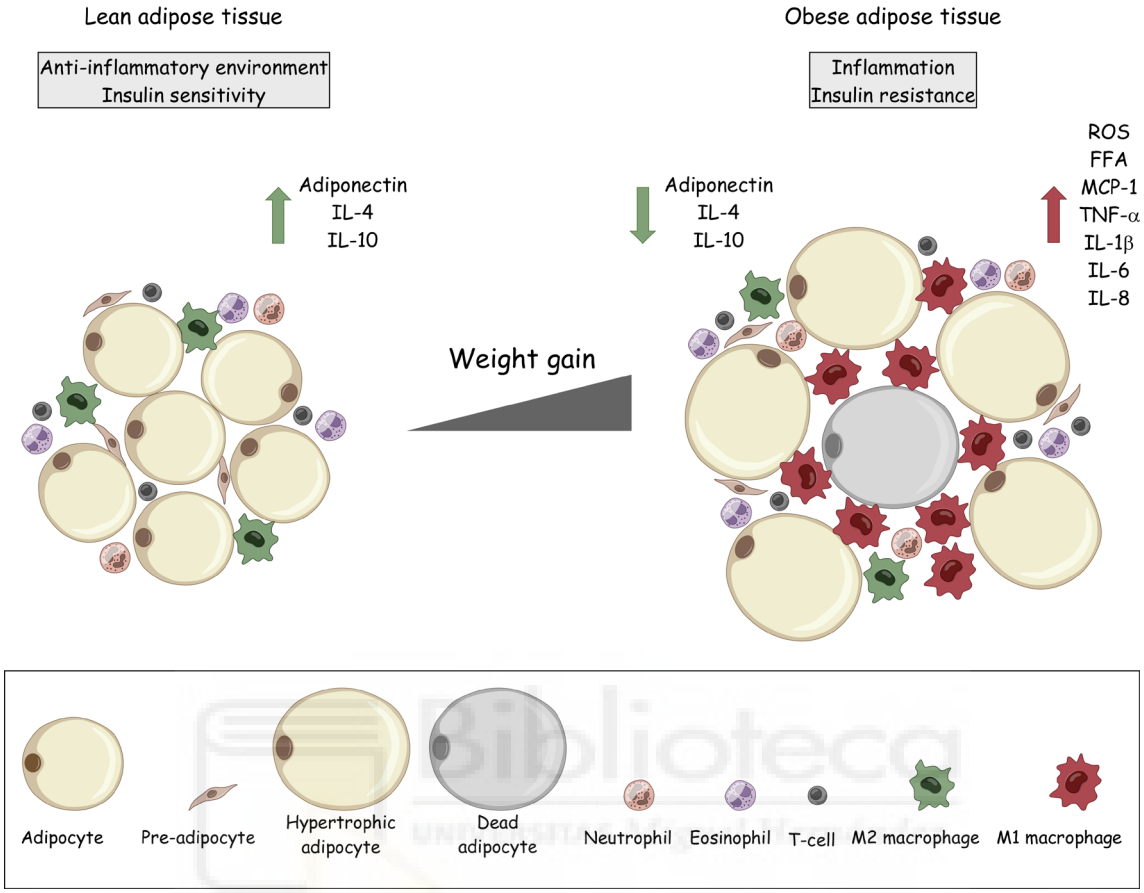

Figura 8. Evolución del tejido adiposo en la obesidad. El tejido adiposo está formado por adipocitos, preadipocitos, células inmunes y células vasculares que coexisten en equilibrio favoreciendo un ambiente antiinflamatorio y la sensibilidad a la insulina. En la obesidad, la hipertrofia de los adipocitos está acompañada por un aumento de ERO, disfunción mitocondrial, hipoxia, muerte de adipocitos, liberación de ácidos grasos (FFA), disminución en la secreción de adiponectina, reclutamiento de células inmunes, polarización de los macrófagos al fenotipo M1 y aumento en la producción de citoquinas proinflamatorias. Todas estas alteraciones promueven un estado de inflamación crónico de bajo grado y resistencia a la insulina en el tejido adiposo. Adaptación del trabajo publicado por Trim *et al.* [41].

CONSECUENCIAS DE LA OBESIDAD A NIVEL SISTÉMICO

La incapacidad del tejido adiposo por acumular los lípidos excedentes, así como la inflamación del tejido, llevan consigo importantes consecuencias a nivel sistémico. La aparición de resistencia a la insulina, la hiperglicemia, la hipertensión y la dislipidemia son una serie de sintomatologías asociadas a la obesidad que se recogen dentro de un cuadro clínico conocido como síndrome metabólico [42]. Dichos signos suponen los principales factores de riesgo al desarrollo de otras enfermedades.

La diabetes tipo 2 asociada a la obesidad se origina cuando los lípidos circulantes que no son capturados por los adipocitos permanecen en el torrente sanguíneo hasta acabar depositándose en otros órganos y tejidos como el hígado, el páncreas y el músculo esquelético. Esta deposición ectópica de grasa, así como la cantidad de señales inflamatorias que se liberan desde el tejido adiposo, provocan también la pérdida de sensibilidad a la insulina en el hígado y en el músculo esquelético y la disfunción de las células β pancreáticas [43]. A nivel hepático, la disfunción de este órgano puede desembocar en el desarrollo de una esteatosis hepática o también conocida como la enfermedad del hígado graso no asociada al alcohol. Por otro lado, la inflamación y el estrés oxidativo también provocan la disfunción del endotelio vascular produciendo una arteriosclerosis y, por tanto, el riesgo a desarrollar toda una serie de trastornos cardiovasculares (**Fig.9**).

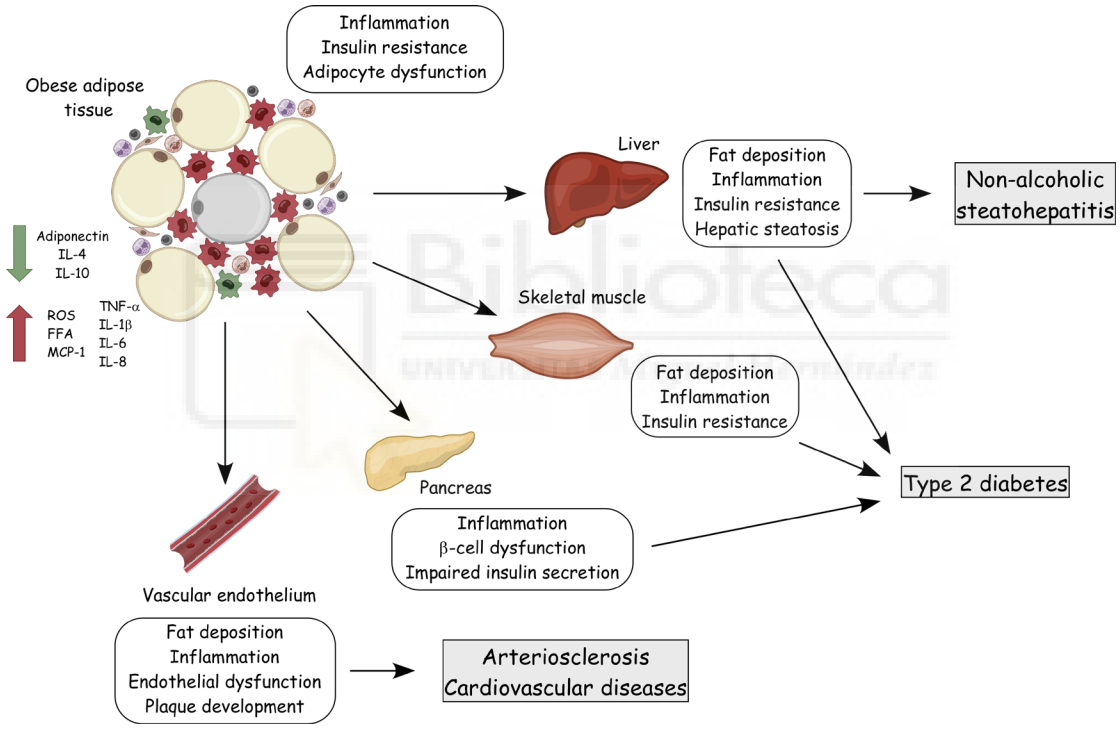

Figura 9. Alteraciones sistémicas en obesidad. En la obesidad, la liberación de citoquinas proinflamatorias por el tejido adiposo y la deposición ectópica de grasa en órganos como el hígado, el músculo esquelético, el páncreas o el endotelio promueven la disfunción de estos órganos dando lugar a la aparición de esteatosis hepática, diabetes tipo 2, arteriosclerosis y enfermedades cardiovasculares. Adaptación del trabajo publicado por Gauthier *et al.* [44].

3 ADIPOGÉNESIS Y MODELOS CELULARES DE ESTUDIO

3.1 PROCESO DE ADIPOGÉNESIS

La adipogénesis es el proceso por el cual una célula precursora denominada preadipocito se diferencia a adipocito. Aunque la formación de nuevos adipocitos en humanos es un fenómeno que ocurre durante la etapa de la gestación fetal, la capacidad de expansión del tejido adiposo está presente durante toda la vida y se estimula en función de las demandas de almacenamiento energético del organismo. No obstante, este proceso se da especialmente tras el nacimiento volviendo a desencadenarse en la adolescencia, y decae en la edad adulta [6]. La comprensión del proceso de diferenciación de los adipocitos es clave para conocer el entramado de eventos que provocan el incremento del tejido adiposo y los mecanismos que pueden revertir las alteraciones metabólicas asociadas a la obesidad.

La conversión de un preadipocito a un adipocito maduro ocurre por la activación en cascada de factores de transcripción que inducen la expresión secuencial de genes destinados a establecer el fenotipo del adipocito. Uno de los factores transcripcionales esenciales en el proceso de la adipogénesis es el receptor activado por el proliferador de peroxisomas gamma (PPARγ). Esta proteína pertenece a una familia de receptores nucleares hormonales activados por ligandos que regulan procesos como el metabolismo energético, la proliferación celular y la inflamación [45, 46]. A su vez, las proteínas potenciadoras de unión a elementos CCAAT (C/EBPα, C/EBPβ y C/EBPδ) constituyen una familia de factores transcripcionales que intervienen, junto con PPARγ, en la diferenciación del adipocito [47]. Tras la activación hormonal de la adipogénesis, la cascada transcripcional que se desencadena comienza con la expresión de las C/EBPβ y C/EBPδ. Seguidamente, estas dos proteínas inician la expresión de C/EBPα y PPARγ, las cuales se activan mutuamente manteniéndose así durante toda la etapa de la diferenciación [48, 49] (**Fig.10**).

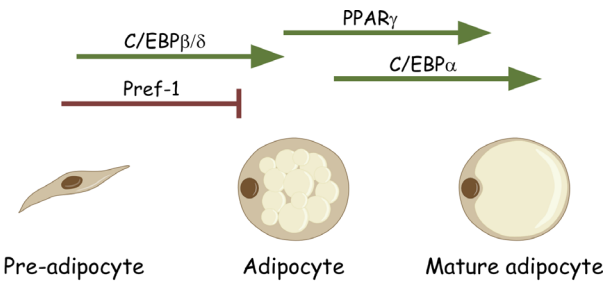

Figura 10. Diferenciación de un adipocito. Los preadipocitos se mantienen en un estado no diferenciado por la acción del factor de preadipocito Pref-1. Ante la estimulación hormonal, se induce el proceso de adipogénesis iniciado por la activación de C/EBPβ y C/EBPδ, seguido de PPARγ y C/EBPα, culminando en la expresión de genes que establecen el fenotipo de adipocito maduro. Adaptación del capítulo publicado por de Villiers *et al.* [50].

3.2 MODELO DE ADIPOGÉNESIS *IN VITRO*

El modelo celular más empleado para el estudio de la adipogénesis *in vitro* es la línea celular de fibroblastos 3T3-L1, aislada a partir de embriones de ratón albino suizo [51]. Los fibroblastos 3T3-L1 son inducidos en cultivo con un cóctel que contiene insulina, dexametasona (un glucocorticoide sintético) y 3-isobutil-1-metilxantina (IBMX, un inhibidor de fosfodiesterasas que aumenta la concentración intracelular de AMPc). Estos tres agentes estimulan vías que culminan en la activación de las C/EBPβ y C/EBPδ, poniendo en marcha todo el mecanismo transcripcional de la adipogénesis (**Fig. 11**) [52, 53].

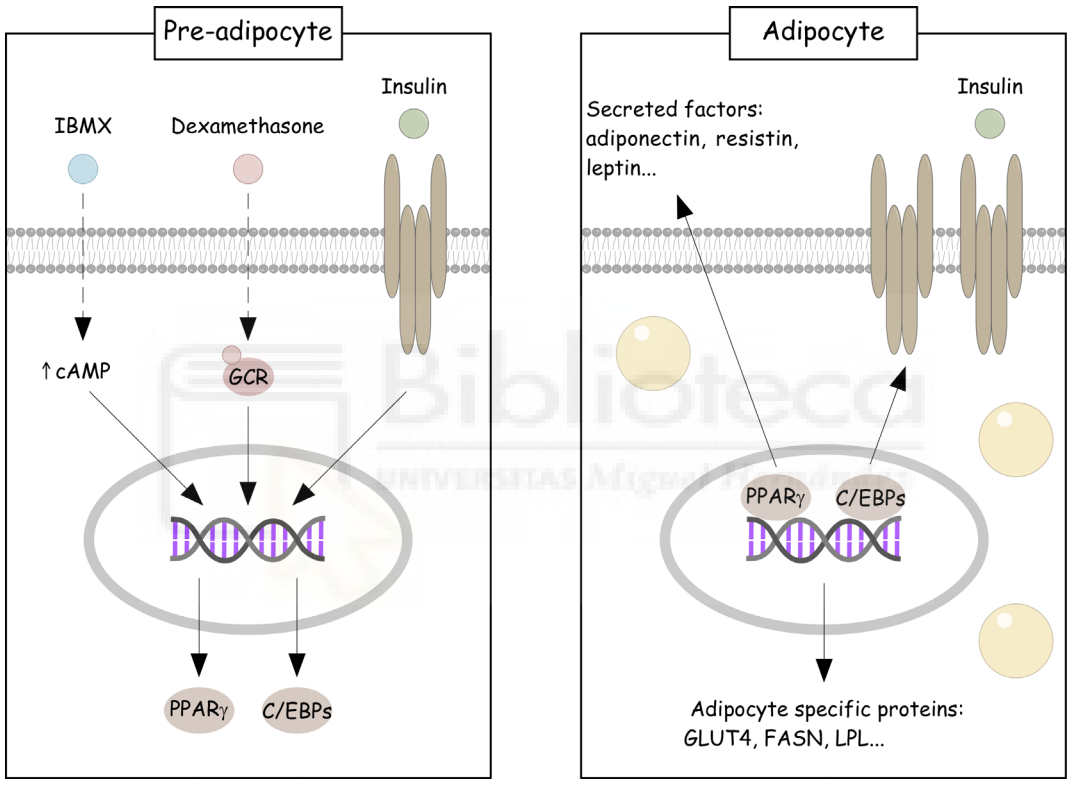

Figura 11. Proceso de adipogénesis *in vitro*. El IBMX aumenta los niveles intracelulares de AMP cíclico (cAMP), la dexametasona se une al receptor de glucocorticoides (GCR) y la insulina se une al receptor de insulina. Las tres vías culminan en la activación de genes de la familia de las C/EBPs y PPARγ. Estos factores activan genes específicos del adipocito que codifican factores de secreción, el receptor de insulina y proteínas implicadas en la síntesis y la unión de ácidos grasos. GLUT4, transportador de glucosa 4. Adaptación de la ficha técnica de Merck [54].

Según el modelo de adipogénesis exhibido por los fibroblastos 3T3-L1, el proceso de diferenciación se desarrolla en cuatro etapas a través de las cuales se producen cambios cronológicos en la expresión de genes [48]. Inicialmente, los preadipocitos se encuentran en un estado no diferenciado bajo la acción del factor de preadipocito Pref-1, exhibiendo la morfología propia de un fibroblasto. Durante esta etapa, los preadipocitos crecen y

proliferan hasta alcanzar la confluencia, momento en el que el contacto célula-célula inhibe la proliferación. En la siguiente etapa se produce la expansión clonal mitótica, en la que se producen sucesivas rondas de replicación de DNA y duplicación celular. A continuación, tiene lugar la etapa temprana de la diferenciación, donde se desencadena la activación de las C/EBPs y PPARγ, seguida de una etapa terminal en la que aumenta la expresión de genes específicos de adipocito. De esta manera, los preadipocitos pierden su morfología fibroblástica adquiriendo una forma esférica con la presencia de gotas lipídicas en el citoplasma.

3.3 MODELO DE ADIPOCITOS HIPERTRÓFICOS 3T3-L1

La línea de preadipocitos 3T3-L1 es también un modelo válido para el estudio de las alteraciones que ocurren como consecuencia de la hipertrofia de los adipocitos en la obesidad. Esta hipertrofia se puede inducir incubando adipocitos 3T3-L1 maduros con altas concentraciones de glucosa durante un tiempo prolongado. De esta manera, los adipocitos convierten el exceso de glucosa en triglicéridos aumentando considerablemente el tamaño de las vacuolas lipídicas (**Fig. 12**). Una vez alcanzado el estado de hipertrofia, los adipocitos presentan estrés oxidativo, disfunción mitocondrial, inflamación y resistencia a la insulina. Por ello, el establecimiento del estado de hipertrofia en la línea celular 3T3-L1 convierte a esta línea en un modelo óptimo para estudiar las alteraciones metabólicas que tienen lugar en el tejido adiposo de un individuo obeso [55].

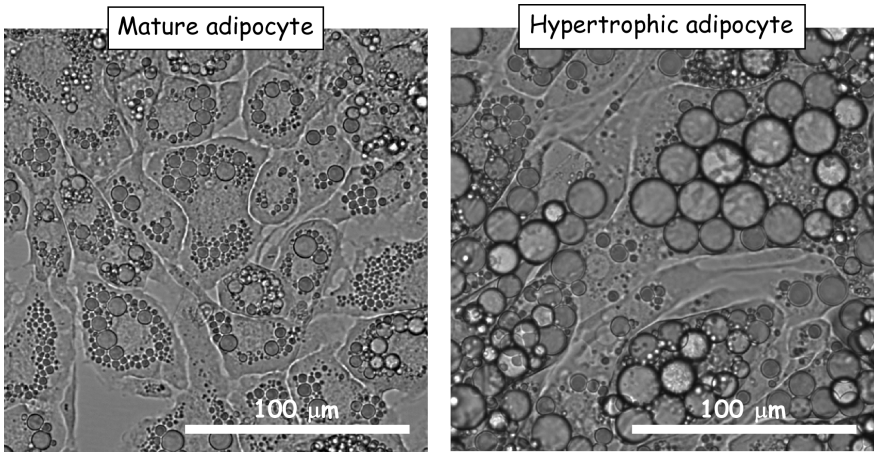

Figura 12. Adipocitos maduros e hipertróficos obtenidos a partir de la diferenciación de fibroblastos 3T3-L1. La incubación de adipocitos maduros (10 días de diferenciación) con altas concentraciones de glucosa durante, al menos, una semana permite la obtención de adipocitos hipertróficos, que exhiben un gran tamaño celular y grandes gotas lipídicas en el citoplasma. Microfotografías en campo claro obtenidas por microscopía digital.

4 AMPK COMO DIANA TERAPÉUTICA EN LA OBESIDAD

4.1 AMPK. ESTRUCTURA Y ACTIVACIÓN

La proteína quinasa activada por AMP (AMPK) es el sensor energético por excelencia de las células eucariotas. Se trata de una serina/treonina quinasa que activa e inhibe otras quinasas en respuesta a las demandas energéticas de la célula, con la finalidad de garantizar la homeostasis energética celular y la del organismo entero. Estructuralmente, es un complejo heterotrimérico compuesto por tres subunidades: una subunidad catalítica α y dos subunidades reguladoras β y γ. En mamíferos, existen dos isoformas de la subunidad α (α1 y α2) y de la subunidad β (β1 y β2) y tres de la subunidad γ (γ1, γ2 y γ3) codificadas por distintos genes, dando lugar a 12 posibles combinaciones heterotriméricas de AMPK. No obstante, la expresión de las diferentes combinaciones parece ser específica del tejido y de la localización subcelular, mostrando incluso propiedades regulatorias y funcionales distintas [56].

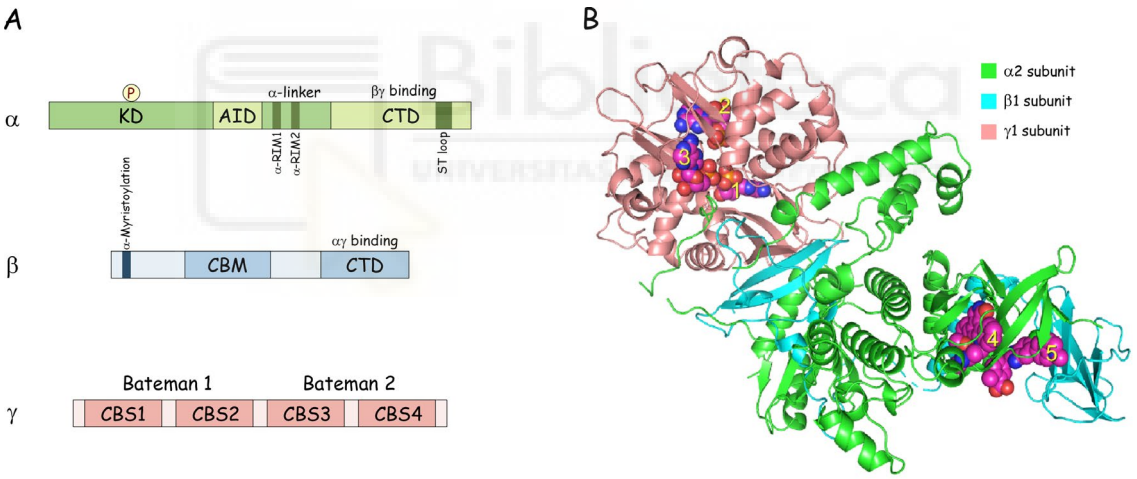

Figura 13. Estructura de AMPK. (A) AMPK se compone de una subunidad catalítica (α) y dos subunidades reguladoras (β y γ). KD, dominio quinasa; AID, dominio autoinhibitorio; α-RIM (dominio α de interacción con las subunidades reguladoras); CTD (dominio C-terminal), ST-loop (lazo rico en Ser y Thr); CBM (módulo de unión a carbohidratos); CBS (motivos *cystathionine-β-synthase*). Adaptación del trabajo publicado por García *et al.* [59]. (B) Se muestra la estructura secundaria de la proteína. Los números 1, 2 y 3 indican los 3 sitios CBS funcionales de la subunidad γ, el número 4 corresponde al sitio de unión a ATP en el KD de la subunidad α y el número 5 representa la zona de interacción entre las subunidades α y β. En esferas se muestran posibles ligandos en sitios reguladores de AMPK. Estructura 5iso adaptada usando el programa PyMol 2.0 (Capítulo 2).

La subunidad α contiene el dominio quinasa convencional de serinas y treoninas (KD, *kinase domain*) que alberga el residuo treonina 172 (Thr172) en el lazo de activación. La fosforilación de este residuo es necesaria para la activación de la proteína. Además, presenta

un dominio autoinhibitorio (AID, *autoinhibitory domain*) y un lazo flexible rico en Ser y Thr (ST-loop) [57]. La subunidad β contiene un módulo de unión a carbohidratos (CBM) que permite la unión a glucógeno [58]. La subunidad γ presenta el dominio de unión a nucleótidos de adenina, que se compone de dos dominios Bateman, cada uno compuesto por dos repeticiones en tándem de motivos CBS (*cystathionine-β-synthase*). En mamíferos, sólo tres de estas cuatro repeticiones CBS unen nucleótidos de adenina (CBS1, CBS3 y CBS4). Los sitios 1 y 3 unen competitivamente AMP, ADP y ATP, mientras que el sitio 4 une sólo AMP o ATP, siendo mayor la afinidad por AMP [59] (**Fig. 13**).

La activación de AMPK se produce por un mecanismo triple: 1) por la acción de quinasas que fosforilan la Thr172 del lazo de activación, 2) por la protección del lazo de activación frente a la acción de las fosfatasas y 3) por la activación alostérica inducida por la unión de AMP. Este último mecanismo a su vez es antagonizado por ATP, mientras que la unión de ADP protege frente a la defosforilación del lazo de activación, pero sin inducir la activación alostérica [60].

Las principales quinasas descritas que activan AMPK a través de la fosforilación de Thr172 son la quinasa hepática B1 (LKB1) y la quinasa β dependiente de Ca^{2+} y calmodulina (CaMKKβ). La fosforilación de AMPK por la CaMKKβ es un mecanismo dependiente de los niveles intracelulares de Ca^{2+} [61], mientras que la LKB1 requiere del cambio conformacional inducido por la unión alostérica de AMP en la subunidad γ de AMPK [62]. Por otro lado, la activación de AMPK también puede ser modulada por la fosforilación de otros residuos de la proteína. Por ejemplo, se ha demostrado que la fosforilación mediada por Akt del residuo Ser487 del ST-loop bloquea el acceso a las quinasas para fosforilar la Thr172 [63].

La regulación alostérica de AMPK por AMP ocurre por la unión de este nucleótido a los tres sitios CBS funcionales de la subunidad γ. Se postula que la región enlazadora (*α-linker*) de la subunidad α interactúa con el sitio CBS2 y con el AMP que se une al sitio CBS3, actuando como sensor que transduce la señal de activación al KD [57]. Asimismo, la unión de más moléculas de AMP a los sitios CBS1 y CBS4 estabiliza la unión de AMP al sitio CBS3. Por el contrario, la unión del nucleótido ATP impide la unión de AMP y, a su vez, reduce la interacción con la subunidad α [64]. La unión de AMP al sitio CBS3 también desestabiliza la interacción entre el KD y el AID favoreciendo de esta manera la conformación activa de AMPK. A su vez, se ha descrito que tanto AMP como ADP inducen un cambio conformacional que dificulta la accesibilidad de las fosfatasas al lazo de activación e impide la desfosforilación de la Thr172 [57].

4.2 PAPEL METABÓLICO DE AMPK

Cuando la relación citosólica de AMP/ATP aumenta por estímulos como la contracción muscular, los bajos niveles de glucosa, la deprivación de nutrientes, la hipoxia o la isquemia, AMPK se activa y fosforila todo un arsenal de sustratos con el fin de inhibir rutas biosintéticas que consumen ATP y activar vías que regeneran el ATP a través de la oxidación de biomoléculas (**Fig. 14**). Por ejemplo, AMPK controla el metabolismo de los lípidos a través de la inhibición por fosforilación de la ACC, que reduce consecuentemente los niveles intracelulares de malonil-CoA. Esto estimula la activación de la carnitina palmitoiltransferasa 1 (CPT1), una proteína que transloca los ácidos grasos desde el citosol a la matriz mitocondrial aumentando la β-oxidación. Además, el malonil-CoA es un sustrato de la sintasa de ácidos grasos (FASN), por lo que la reducción de este precursor disminuye también la síntesis de ácidos grasos [65]. De esta manera, AMPK es capaz de modular la actividad y la expresión de proteínas implicadas en el metabolismo de la glucosa, lípidos y esteroles, y otros procesos como la síntesis de proteínas, la biogénesis mitocondrial o la autofagia [59].

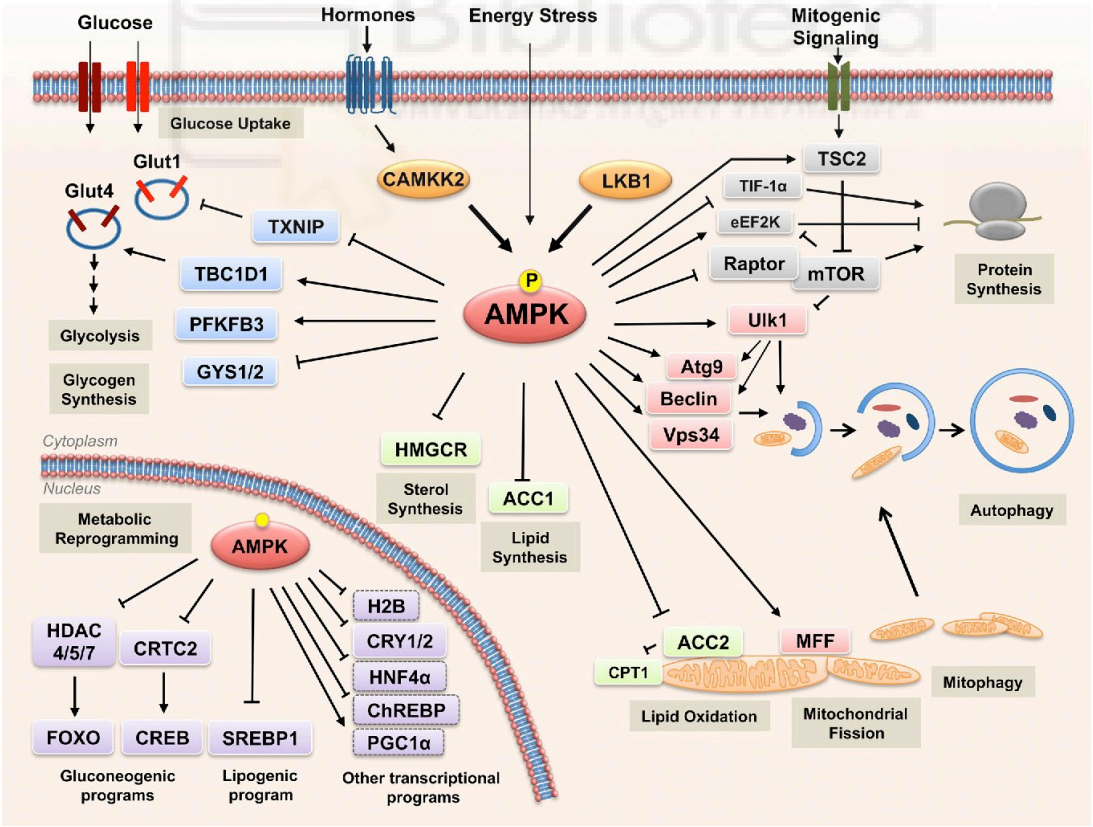

Figura 14. Vías de señalización reguladas por AMPK. En condiciones de estrés energético, AMPK es activada por fosforilación a través de la acción de proteínas como LKB1 y CaMKKβ. Tras la activación, AMPK fosforila sustratos metabólicos que llevan a la activación e inhibición de rutas que producen y consumen ATP, respectivamente. Esquema extraído del trabajo publicado por García *et al.* [59].

4.3 AMPK COMO DIANA FARMACOLÓGICA

Dado el papel de AMPK como regulador del balance energético en el organismo, existe un interés creciente en la búsqueda de moléculas que modulen esta proteína para su uso terapéutico en enfermedades metabólicas como la obesidad, la diabetes o enfermedades cardiovasculares. Actualmente, se han elucidado algunos de los mecanismos de acción de los fármacos prescritos en clínica. La mayoría promueven la activación de AMPK de forma indirecta a través del aumento de la relación AMP/ATP en las células [66]. Este es el caso de la metformina, un derivado sintético de la guanidina que se emplea actualmente para tratar la diabetes tipo 2 por reducir la producción de glucosa hepática y aumentar la sensibilidad a la insulina. Se ha propuesto que la metformina ejerce parte de sus efectos antidiabéticos activando AMPK a través de la inhibición del complejo I de la cadena respiratoria mitocondrial, lo que conlleva a una reducción de los niveles celulares de ATP [67]. No obstante, es posible que ciertas moléculas puedan inducir la activación indirecta de AMPK a través de diversas vías simultáneas, como ocurre con las tiazolidinedionas (TZDs), como la rosiglitazona y la pioglitazona. Estos fármacos antidiabéticos comparten el mecanismo de acción de la metformina, pero también pueden activar AMPK a través del aumento de adiponectina inducido por la activación de PPARγ [68]. Otras moléculas con capacidad de activar AMPK son los polifenoles. Entre ellos, se ha descrito que el resveratrol de la uva, la epigalocatequina galato del té verde o la quercetina presente en varias frutas y verduras modulan diversas vías de señalización que conducen a un aumento en los niveles celulares de AMP, lo que promueve la activación de AMPK [66].

No obstante, el mecanismo indirecto por el que algunos de estos compuestos activan AMPK puede dar lugar a la aparición de ciertos efectos secundarios e, incluso, algunos de ellos han sido retirados en fases clínicas [69]. En este sentido, es importante la búsqueda de moduladores directos de AMPK que actúen de forma específica sobre la proteína. El principal modulador directo descrito de AMPK es el 5-aminoimidazol-4-carboxamida-1-β-4-ribofuranósido (AICAR) [59]. Se trata de un análogo de adenosina que, tras ser absorbido por las células, es fosforilado dando lugar a AICAR monofosfato (ZMP). ZMP mimetiza el mecanismo de acción del AMP uniéndose a los sitios CBS de la subunidad γ. Sin embargo, como análogo de AMP, AICAR puede activar otras rutas metabólicas en las que este nucleótido participa [66].

Asimismo, AMPK también puede ser modulada a través de la interacción con otros sitios de unión distintos a los de AMP y ATP. El activador A-769662 (Abbott Laboratories), el compuesto 991 (Merck Sharp and Dohme Corporation and Metabasis Therapeutics) y el

salicilato (el metabolito activo de la aspirina) se han propuesto como activadores directos de AMPK, pero sus mecanismos de acción difieren del de AICAR. Estas moléculas pueden activar alostéricamente AMPK interactuando con la interfaz comprendida entre el KD de la subunidad α y el CBM de la subunidad β, denominada el sitio ADaM (*allosteric drug and metabolite-binding site*). Además, la modulación de AMPK a través del sitio ADaM protege también de la defosforilación de la Thr172 [59]. Otro activador directo de AMPK es el compuesto 2 (C2, *5-(5-hydroxyl-isoxazol-3-yl)-furan-2-phosphonic acid*). Este compuesto es incluso más potente que A-769662 y mimetiza la acción de AMP, aunque se postula que la interacción es a través de sitios de unión de la subunidad γ distintos a los de AMP [70].

5 TRATAMIENTOS FRENTE A LA OBESIDAD

5.1 LA FARMACOTERAPIA EN LA OBESIDAD

La adopción de un estilo de vida saludable mediante una dieta equilibrada y una actividad física óptima es la principal forma de prevenir y de tratar la obesidad. Sin embargo, la estrategia mundial enfocada a promover un estilo de vida saludable en la sociedad obesogénica actual no ha tenido el impacto esperado, dadas las cifras ascendentes en la prevalencia de esta patología. Las modificaciones en el estilo de vida de la población obesa es una tarea difícil de mantener en el tiempo y, en la mayoría de los casos, fallan en su intento de prevenir el desarrollo de patologías asociadas. Por ello, se hace necesaria la implementación de farmacoterapias que ayuden no sólo a la reducción de peso, sino también a mejorar otros trastornos relacionados con la obesidad como la hipertensión, la resistencia a la insulina, la hiperglicemia o la dislipidemia.

Durante las últimas décadas, la mayoría de los fármacos empleados para bajar de peso han sido retirados por su dudosa seguridad, debido a que se ven acompañados de complicaciones cardiovasculares y psiquiátricas. La mayoría de los fármacos retirados, aprobados o en fases clínicas median sus efectos a nivel periférico o central, reduciendo la absorción de grasas a nivel intestinal o suprimiendo el apetito y aumentando el gasto energético a nivel del sistema nervioso. Entre los fármacos aprobados hasta la fecha, se encuentran Orlistat, un inhibidor de lipasas pancreáticas; Liraglutide (Saxenda®), un agonista del receptor del péptido similar al glucagón tipo 1 (GLP-1); Naltrexone/Bupropion (Mysimba®), una combinación entre un antagonista opiáceo y un inhibidor del transportador de dopamina y noradrenalina; Lorcaserin (Belviq®), un agonista de serotonina; y Phentermine/Topiramate (Qsymia®), una combinación entre un inhibidor

del transportador de noradrenalina y un agonista del ácido γ-aminobutírico (GABA). No obstante, estos fármacos que presentan menos efectos adversos también ofrecen una eficacia limitada [71, 72].

En definitiva, parece que la cura farmacológica de la obesidad está lejos de ser una realidad y se hace necesaria la búsqueda de nuevas moléculas efectoras y dianas farmacológicas que modulen vías metabólicas más específicas sin causar efectos adversos graves. En este sentido, las plantas que tradicionalmente han sido empleadas para tratar diversas dolencias con base en un conocimiento puramente empírico, hoy día se sabe que son una potente fuente de moléculas bioactivas capaces de intervenir en multitud de mecanismos metabólicos. Este carácter pleiotrópico convierte a los fitoquímicos en candidatos potenciales más seguros para tratar enfermedades multifactoriales como la obesidad.

5.2 BENEFICIOS DE LOS POLIFENOLES DE PLANTAS

Los polifenoles son metabolitos secundarios sintetizados por las plantas que desempeñan un importante papel en diversas funciones como el crecimiento, la lignificación, la estructura, la pigmentación, la polinización o la defensa frente a patógenos, predadores y radiación ultravioleta [73]. Se caracterizan por la presencia de uno o más grupos fenoles en sus estructuras y pueden asociarse a otras moléculas como carbohidratos, ácidos orgánicos e incluso otros polifenoles, lo que les confiere una enorme diversidad estructural y, por tanto, un amplio espectro de acción. En función del número de grupos fenoles y el esqueleto de carbono de los polifenoles, estos pueden agruparse en distintas clases: ácidos fenólicos (ácidos hidroxibenzoicos y ácidos cinámicos), flavonoides (flavonoles, flavonas, isoflavonas, flavanonas, flavanoles, y antocianos), estilbenos y lignanos (**Fig. 15**).

Numerosos estudios demuestran el papel beneficioso de los polifenoles sobre la salud y su implicación en enfermedades multifactoriales como el cáncer o las asociadas con la obesidad. Estos compuestos presentan propiedades antioxidantes, antitumorales, antimicrobianas, antivirales, antiinflamatorias, antiaterogénicas, antihipertensivas y antilipogénicas. Durante décadas, los efectos biológicos de los polifenoles han sido atribuidos principalmente a su importante papel como agentes antioxidantes [74]. Este fundamento se basa en el hecho de que las enfermedades metabólicas e inflamatorias están estrechamente asociadas con el estrés oxidativo, el cual puede verse mermado por la capacidad de los polifenoles de secuestrar los radicales libres. Recientemente, se ha propuesto que el papel de los polifenoles no es exclusivo de su capacidad antioxidante, sino

que la diversidad estructural de estas moléculas las hace partícipes en multitud de vías de señalización, actuando como moduladores de la actividad y la expresión de un gran número de proteínas.

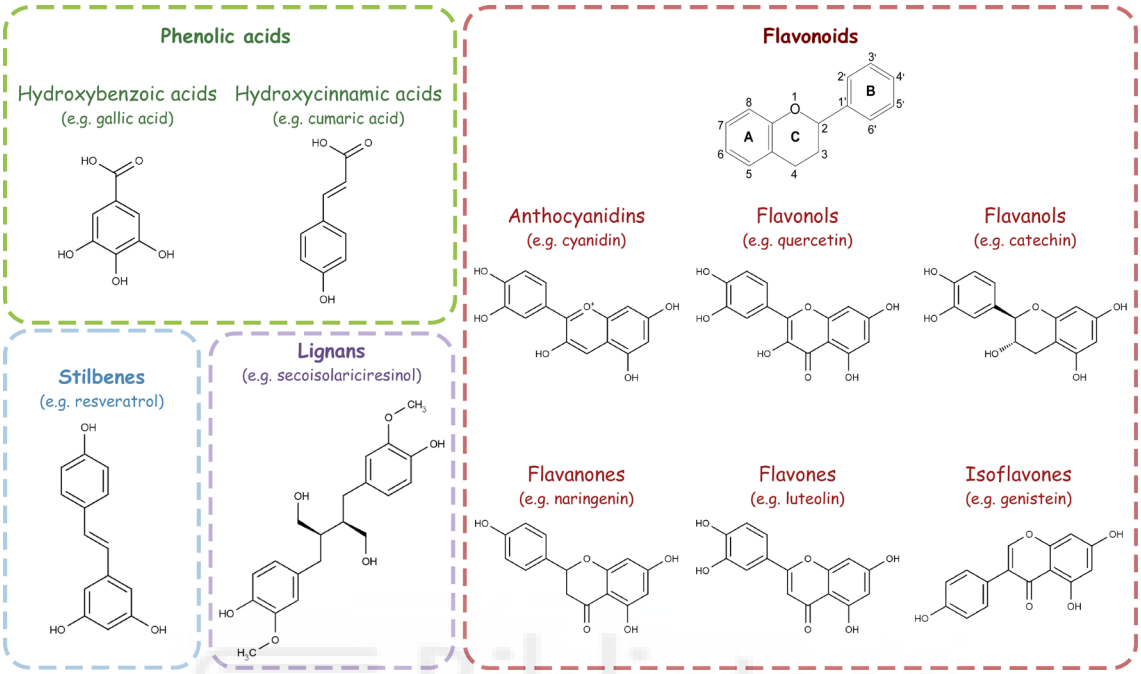

Figura 15. Clasificación de los polifenoles.

Numerosas plantas medicinales han sido evaluadas en estudios *in vitro* e *in vivo* demostrando sus efectos "antiobesidad" [75]. Durante la última década, se han recopilado suficientes evidencias que nos llevan a postular que los polifenoles derivados de plantas comestibles como *Hibiscus sabdariffa* (HS), *Lippia citriodora* (LC) y *Olea europaea* (**Fig. 16**) pueden contribuir a la prevención y al tratamiento de la obesidad. De acuerdo con los efectos moleculares observados de estas plantas en ensayos *in vitro* e *in vivo*, los polifenoles pueden mediar sus funciones a través de una gran variedad de mecanismos, como se describe a continuación.

REGULADORES DE LA HOMEOSTASIS REDOX INTRACELULAR

La obesidad se ha correlacionado con una alta producción de ERO en el tejido adiposo, una alta expresión y actividad de la NADPH oxidasa y una reducción en la expresión de enzimas antioxidantes como la superóxido dismutasa, la catalasa, la glutatión peroxidasa y la glutatión reductasa [76]. Como consecuencia, el daño inducido por estrés oxidativo ocurre no sólo por la alta producción de ERO, sino también por la incapacidad del sistema de

defensa de la célula de eliminar eficientemente estos agentes oxidantes. Ciertos polifenoles, como el ácido clorogénico o las quercetinas de HS, el verbascósido de LC y la oleuropeína o el hidroxitirosol de la hoja de olivo (OL), pueden proteger frente al daño oxidativo a través del secuestro directo de radicales libres y/o de la inducción de la actividad y expresión de enzimas antioxidantes modulando factores transcripcionales, como el factor nuclear eritroide 2 (Nrf2) [77-82].

INHIBIDORES DE LA PRODUCCIÓN DE CITOQUINAS PROINFLAMATORIAS

La respuesta inflamatoria, altamente asociada al estrés oxidativo, puede verse reducida como consecuencia del efecto antioxidante de los polifenoles, pero también por la modulación directa de las vías metabólicas y/o inflamatorias de las citoquinas [83]. Por ejemplo, se postula que los polifenoles de HS pueden reducir la producción de citoquinas como IL-6, IL-8, TNF-α y MCP-1 a través de la inhibición de las vías de las MAPK y NF-κB [55, 84, 85]. Asimismo, los polifenoles también pueden mediar la respuesta inflamatoria a través de la modulación de PPARγ, la producción de adiponectina y la activación de AMPK [86].

MODULADORES DE LAS VÍAS DE SEÑALIZACIÓN QUE REGULAN EL METABOLISMO Y LA GESTIÓN DE LA ENERGÍA

Los polifenoles de HS y de LC han demostrado reducir la acumulación de triglicéridos en adipocitos hipertróficos 3T3-L1 y en modelos animales de obesidad a través de la modulación de la actividad y la expresión génica de proteínas implicadas en el metabolismo de los lípidos, como AMPK, FASN y PPARα [86, 87]. Además de inducir cambios en la expresión génica de proteínas metabólicas, los experimentos computacionales de acoplamiento molecular sostienen la idea de que los polifenoles pueden mediar sus efectos también a través de la interacción directa con los sitios reguladores o catalíticos de las proteínas diana.

MODULADORES DEL EPIGENOMA

Se sabe que ciertas alteraciones metabólicas están ligadas a la desregulación de las modificaciones epigenéticas. La epigenética comprende todos aquellos cambios reversibles en el DNA que modulan la expresión de los genes, como son las metilaciones del DNA, las

acetilaciones/desacetilaciones de las histonas y la expresión de microRNAs. Ciertos estudios indican que algunos polifenoles, como el resveratrol, las quercetinas o la oleaceína, pueden corregir las alteraciones asociadas a ciertas patologías crónicas modulando los mecanismos epigenéticos [87-89]. Concretamente, se ha evidenciado que los polifenoles pueden regular la expresión de genes metabólicos alterando los patrones de metilación del DNA, modulando las acetiltransferasas y deacetilasas de histonas y alterando la expresión de microRNAs.

A B C

Figura 16. *Hibiscus sabdariffa* (A), *Lippia citriodora* (B) y *Olea europaea* (C). Imágenes obtenidas de Internet [90-92].

5.3 LOS EFECTORES DE LOS POLIFENOLES. BIODISPONIBILIDAD Y METABOLISMO

A pesar de la amplia evidencia científica sobre los mecanismos de acción de los polifenoles y sus implicaciones en la mejora de ciertas enfermedades metabólicas, poco se sabe acerca de los cambios metabólicos que pueden sufrir estos compuestos *in vivo*. Por ello, conocer la farmacocinética de los polifenoles es clave para el entendimiento de su bioactividad, dado que la biodisponibilidad y el metabolismo de estas moléculas en el organismo determinan su modo de acción.

Los polifenoles existen en numerosas y diversas formas químicas en las plantas, lo que determina su absorción una vez ingeridos. Son pocos los polifenoles que pueden atravesar la barrera intestinal por difusión pasiva y alcanzar el torrente sanguíneo de forma intacta. Otros van a requerir de una previa metabolización en el tracto gastrointestinal para poder ser absorbidos, por lo que los metabolitos que consiguen llegar a la circulación plasmática pueden diferir estructuralmente de sus formas nativas.

Ciertas clases de polifenoles, como los flavonoides o ácidos fenólicos, aparecen frecuentemente glicosilados en las plantas. Las glicosilaciones, a su vez, suelen ser muy diversas pudiendo darse la unión de una o más moléculas de azúcar (glucosa, ramnosa y

galactosa, entre otras) en distintas posiciones de la estructura polifenólica. Sin embargo, la absorción de estas moléculas en la barrera intestinal requiere de la deglicosilación enzimática previa del polifenol. Las células humanas expresan algunas β-glucosidasas, por lo que ciertos polifenoles ligados a glucosas pueden ser susceptibles de ser deglicosilados, pero no así otras formas glicosiladas como los ramnósidos. De igual modo, la absorción de los polifenoles también puede verse dificultada por la esterificación de algunos ácidos fenólicos con otras moléculas como ácidos orgánicos y lípidos, así como por el gran peso molecular que tienen algunos polifenoles como los polímeros de antocianos. Ante estas limitaciones, la flora intestinal puede desempeñar un papel importante catabolizando estos compuestos y favoreciendo su absorción en el intestino grueso [93, 94].

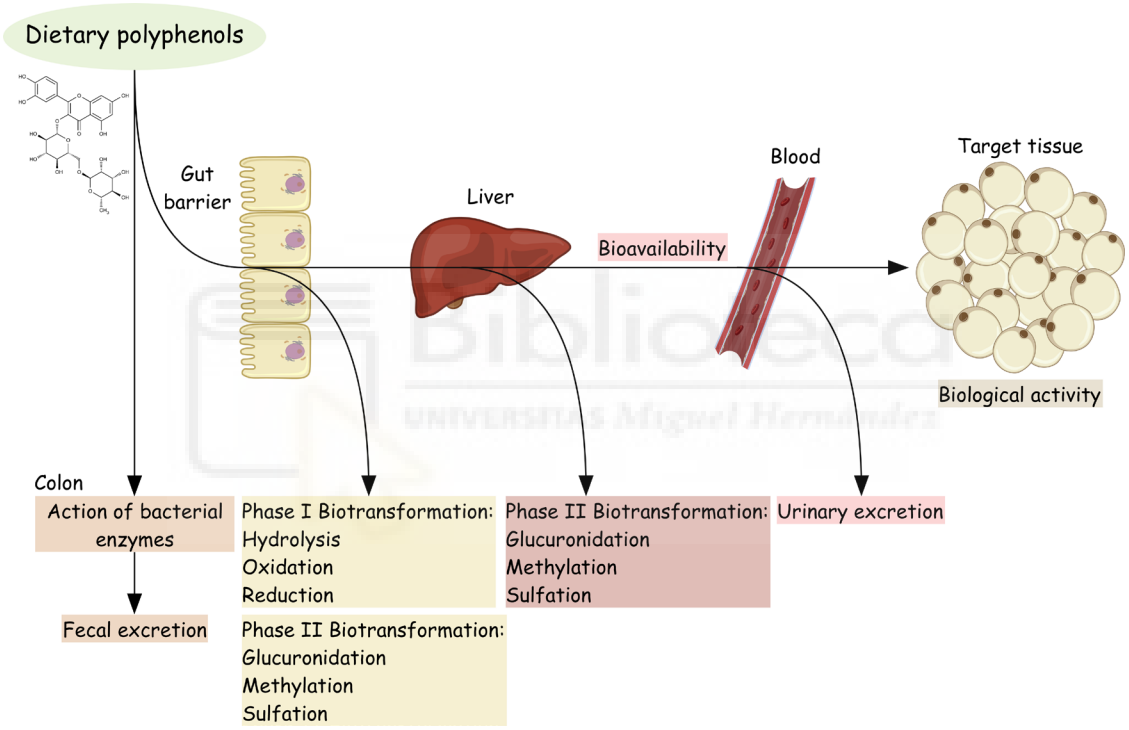

Figura 17. Biodisponibilidad y metabolismo de los polifenoles tras una ingestión oral. Tras la ingestión, los polifenoles pueden ser metabolizados por reacciones de fase I y II en el tracto gastrointestinal y en el hígado. Los metabolitos que alcanzan el torrente sanguíneo pueden ser transportados a los tejidos diana y ejercer su actividad biológica. Adaptación del trabajo publicado por Duynhoven *et al.* [96].

Además del tracto gastrointestinal, los polifenoles pueden sufrir también importantes reacciones de fase I y fase II en el hígado, fundamentalmente metilaciones, sulfataciones y glucuronidaciones. Aunque estas modificaciones ocurren con la finalidad de favorecer la excreción de estos compuestos a través de la bilis o la orina, los productos de estas metabolizaciones podrían ser los auténticos efectores de los polifenoles. De esta manera, cuando los polifenoles o sus metabolitos llegan al torrente sanguíneo, estos pueden ser

captados por las células de los tejidos diana donde efectúan su mecanismo de acción. A su vez, una vez en el tejido diana, estos compuestos pueden ser acumulados o sufrir nuevas biotransformaciones (**Fig. 17**) [95].

6 TÉCNICAS DE CRIBADO VIRTUAL

6.1 ACOPLAMIENTO MOLECULAR COMO HERRAMIENTA EN LA BÚSQUEDA DE MOLÉCULAS BIOACTIVAS FRENTE A DIANAS TERAPÉUTICAS

El descubrimiento de moléculas bioactivas que muestren un efecto farmacológico frente a una determinada enfermedad es un proceso largo que precisa, en primer lugar, de la identificación de una diana biológica implicada en el desarrollo de la patología y la selección de una o varias moléculas que puedan modular dicha diana. Tras esta primera etapa, se evalúa la eficacia y seguridad de los candidatos mediante estudios *in vitro* e *in vivo* y ensayos clínicos. No obstante, las fuentes de búsqueda de estas moléculas son numerosas. La naturaleza y, especialmente las plantas, ofrecen todo un arsenal de moléculas terapéuticas que, además, pueden ser modificadas por síntesis química ampliando aún más el abanico de posibilidades. En la práctica, la evaluación de todos estos compuestos con potencial terapéutico se hace inviable sin la adopción de herramientas computacionales que permitan reducir las librerías de millones de compuestos en un número de moléculas experimentalmente abordables, reduciendo así los tiempos de búsqueda y minimizando los costes.

El proceso de cribado virtual comienza con la adquisición de las estructuras cristalográficas de alta resolución de la proteína diana y de las estructuras químicas de las moléculas (ligandos) en formato electrónico. Para la selección de los ligandos, existe una amplia variedad de librerías químicas en las que se pueden encontrar las estructuras moleculares de polifenoles, como Phenol-Explorer, o de metabolitos, como Human Metabolome Database (HMDB), Madison Metabolomics Consortium Database (MMCD) o Metlin. Cabe destacar que el éxito biológico de un modulador candidato depende además de factores farmacocinéticos como la absorción, distribución, metabolismo, excreción y toxicidad (ADMET) de las moléculas una vez administradas, por lo que únicamente aquellos compuestos que muestren un perfil ADMET óptimo deben ser evaluados *in silico*. Existen aplicaciones de Internet que permiten predecir el perfil ADMET de una molécula, por lo que puede emplearse como una previa selección de los candidatos reduciendo la librería a aquellos que muestren un perfil farmacocinético positivo.

El cribado *in silico* de la batería de moléculas candidatas frente a la diana a estudio se lleva a cabo mediante programas que permiten realizar experimentos de acoplamiento molecular, como AutoDock/Vina. Estos programas enfrentan las estructuras moleculares de los ligandos frente a los sitios catalíticos y reguladores de la proteína diana y predicen todas las posibles conformaciones ligando-receptor calculando las energías de afinidad de las pequeñas moléculas en los sitios de unión de la proteína. De esta manera, aquellas moléculas que presenten las mejores energías de afinidad pueden ser propuestas como candidatas para su evaluación posterior en los experimentos *in vitro*. Por ello, los experimentos de acoplamiento molecular pueden ser empleados como técnicas de cribado que permitan la búsqueda y predicción de polifenoles que puedan modular dianas metabólicas como AMPK.

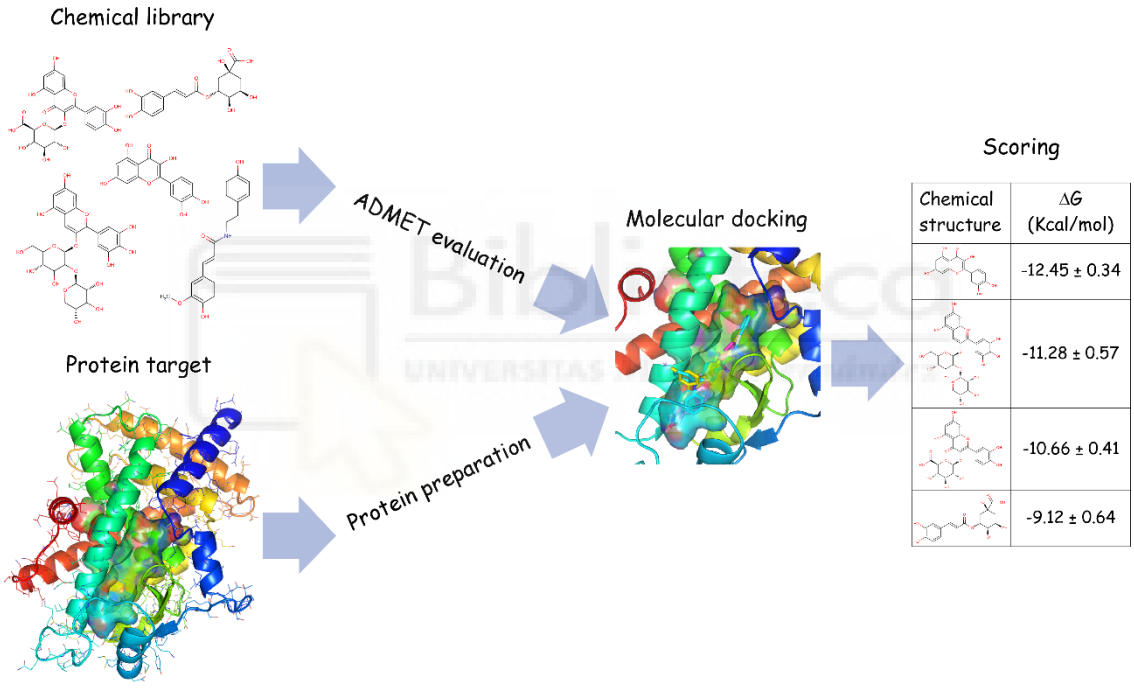

Figura 20. Esquema del proceso de cribado virtual de una librería de compuestos polifenólicos frente a una proteína diana mediante técnicas de acoplamiento molecular. Las estructuras químicas son evaluadas previamente por criterios ADMET y la estructura de alta resolución de la proteína diana es preparada para los experimentos de acoplamiento. A continuación, las estructuras químicas seleccionadas son enfrentadas computacionalmente a los sitios de unión de la proteína diana calculando puntuaciones basadas en los valores de energía de afinidad (ΔG). Aquellas moléculas con mejores ΔG son seleccionadas para su evaluación *in vitro* e *in vivo*. Esquema adaptado del trabajo publicado por Olivares-Vicente *et al.* [95].

OBJETIVOS

OBJETIVOS

Dadas las evidencias científicas presentadas en esta memoria sobre el potencial de los compuestos polifenólicos para paliar las complicaciones metabólicas asociadas a la obesidad, el **objetivo general** que se plantea es identificar los polifenoles (así como sus metabolitos) procedentes fundamentalmente de OL, LC e HS potencialmente responsables de regular el metabolismo energético a través de la modulación de AMPK y del mantenimiento del equilibrio redox y la homeostasis lipídica en adipocitos hipertróficos, así como también estudiar los efectos del consumo de una combinación de polifenoles de HS y LC en sujetos obesos y con sobrepeso. Para alcanzar este objetivo general, se han propuesto los siguientes objetivos específicos:

OBJETIVOS DEL CAPÍTULO 1

La OL presenta un alto contenido en polifenoles [97], lo que suscita un gran interés por su uso como nutracéutico con fines terapéuticos. Por ello, el objetivo de este capítulo es **determinar la implicación de un extracto de OL en la obesidad estudiando su efecto sobre la acumulación de triglicéridos en adipocitos 3T3-L1 hipertróficos y su capacidad de activar AMPK** mediante una técnica optimizada de inmunofluorescencia. Asimismo, se plantea realizar un fraccionamiento del extracto guiado por bioensayo y un análisis de acoplamiento molecular para identificar los compuestos responsables de la activación de AMPK.

OBJETIVOS DEL CAPÍTULO 2

Previamente, estudios del grupo han demostrado la capacidad de un extracto de LC de mejorar las alteraciones metabólicas que ocurren en la obesidad en adipocitos hipertróficos y ratones hiperlipidémicos [86]. El objetivo de este capítulo es **evaluar la capacidad de este extracto y de sus compuestos aislados de activar AMPK en adipocitos** mediante la técnica de inmunofluorescencia. Además, se pretende determinar las posibles interacciones sinérgicas entre los compuestos más activos a través de un estudio de sinergia y predecir la energía de afinidad de estos compuestos frente a AMPK mediante un análisis *in silico*.

OBJETIVOS DEL CAPÍTULO 3

A pesar de las evidencias científicas que demuestran el papel beneficioso de HS en la obesidad, se desconocen los compuestos responsables de sus efectos. Estudios previos sugieren que la quercetina y sus derivados glucuronidados, como la quercetina-3-glucurónido, son los principales metabolitos en plasma y pueden ejercer sus efectos en el hígado [87, 98, 99]. No obstante, se desconoce si pueden alcanzar el tejido adiposo y las dianas intracelulares de los adipocitos. Por ello, los objetivos del capítulo 3 son:

1. **Estudiar el metabolismo de la quercetina y la quercetina-3-glucurónido en adipocitos hipertróficos y correlacionar la reversión del estrés oxidativo asociado a la hipertrofia** con la presencia de metabolitos intracelulares.

2. **Determinar el papel de los principales metabolitos plasmáticos identificados de un extracto polifenólico de HS sobre el estrés metabólico inducido por glucolipotoxicidad en adipocitos hipertróficos**, evaluando sus efectos sobre el estrés oxidativo, la inflamación, los defectos en la mitocondria y la modulación sobre la actividad y expresión de ciertas dianas metabólicas.

OBJETIVOS DEL CAPÍTULO 4

Considerando la eficacia de LC y HS sobre el metabolismo lipídico y de la glucosa en animales hiperlipidémicos [55, 86], se plantea que los polifenoles de estos extractos alcanzan dianas similares y complementarias [100]. El objetivo de este capítulo es **comparar la eficacia de una formulación de LC e HS entre dos grupos de sujetos obesos y con sobrepeso para estudiar los efectos diferenciales** sobre parámetros antropométricos, metabólicos y hematológicos asociados con el síndrome metabólico, así como la presión arterial y el ritmo cardíaco. Finalmente, se propone evaluar la actividad de la mezcla polifenólica sobre AMPK y la acumulación de lípidos en adipocitos hipertróficos.

OBJETIVOS DEL CAPÍTULO 5

El último objetivo de este trabajo es **ofrecer un resumen de los datos acumulados en la bibliografía sobre la actividad farmacológica y el comportamiento farmacocinético de los polifenoles más representativos presentes en las tres plantas estudiadas en esta Tesis** y otras comúnmente consumidas y beneficiosas en el tratamiento de patologías metabólicas, proponiendo los posibles metabolitos activos responsables de tales efectos.

MATERIALES Y MÉTODOS

1 MATERIALES

1.1 CULTIVO CELULAR

La línea de fibroblastos 3T3-L1 de embrión de ratón albino suizo se obtuvo de *American Type Culture Collection* (ATCC® CL-173™, Manassas, VA, EE. UU.). *Dulbecco's Modified Eagle's Medium* (DMEM), *Roswell Park Memorial Institute medium* (RPMI-1640), la mezcla de antibióticos penicilina-estreptomicina, HEPES y D-glucosa se compraron a Gibco (Grand Island, NY, EE. UU.). Suero de ternera y suero bovino fetal (FBS) de HyClone™ se obtuvieron de ThermoFisher Scientific (Cramlington, Northumberland, Reino Unido). Dexametasona, IBMX, insulina, piruvato de sodio, ácido palmítico, β-mercaptoetanol, dimetilsulfóxido (DMSO), paraformaldehído y Triton X-100 se adquirieron de Sigma-Aldrich (Madrid, España). Albúmina sérica bovina (BSA) se obtuvo de EMD Millipore (Billerica, EE. UU.).

1.2 ESTÁNDARES Y EXTRACTOS

Quercetina y verbascósido se obtuvieron de Extrasynthese (Genay, Francia). Quercetina-3-glucurónido, ácido clorogénico y ácido L-ascórbico se compraron a Sigma-Aldrich (Steinheim, Alemania). Ácido logánico, luteolina-7-diglucurónido e isoverbascósido se adquirieron de PhytoLab (Vestenbergsgreuth, Alemania). Los extractos de HS, LC y la combinación de ambos (MetabolAid®) para los ensayos celulares y el estudio clínico fueron amablemente suministrados por Monteloeder, SL (Elche, Alicante, España).

2 MÉTODOS

2.1 FRACCIONAMIENTO DE LOS EXTRACTOS DE OL Y LC POR CROMATOGRAFÍA SEMI-PREPARATIVA

Se llevó a cabo un fraccionamiento semi-preparativo de los extractos de OL (capítulo 1) y LC (capítulo 2) empleando el sistema HPLC preparativo de Gilson (Gilson, Middleton, WI, EE. UU.), equipado con una solución de manejo de líquidos automatizado (modelo GX-271), una bomba binaria (modelo 331/332) y un detector de UV-Vis (modelo UV-Vis 156). Las columnas cromatográficas, las condiciones de separación, las fases móviles y la detección por DAD se detallan en la sección Materiales y Métodos de cada estudio.

2.2 CARACTERIZACIÓN Y CUANTIFICACIÓN DE MUESTRAS CITOPLASMÁTICAS Y EXTRACTOS POR HPLC

La caracterización de los extractos y fracciones de OL y LC (capítulo 1 y 2, respectivamente) y la identificación y cuantificación de metabolitos intracelulares de quercetina en adipocitos (capítulo 3) se llevó a cabo por cromatografía líquida de alto rendimiento acoplada a espectrometría de masas con tiempo de vuelo equipado con fuente de ionización por electrospray (HPLC-DAD-ESI-TOF/MS). Se empleó el sistema Agilent 1200 RRLC (Agilent Technologies, Palo Alto, CA, EE. UU.) de Series Rapid Resolution acoplado a un analizador de masas microTOF (Bruker Daltonik, Bremen, Alemania) con interfaz ESI (modelo G1607A, Agilent Technologies) operando en modo negativo. La composición de la combinación de LC-HS (capítulo 4) fue analizada por HPLC (Agilent LC 214 1100 series; Agilent Technologies, Inc., Palo Alto, CA, EE. UU.), acoplada a un espectrómetro de masas Esquire 3000+ (Bruker Daltonics, GmbH, Bremen, Alemania), equipado con ESI y trampa de iones. Las columnas cromatográficas, las condiciones de separación, las fases móviles, la detección por DAD y los datos de calibración se detallan en la sección Materiales y Métodos de cada estudio.

2.3 PROPAGACIÓN DE LA LÍNEA CELULAR 3T3-L1 Y DIFERENCIACIÓN A ADIPOCITOS MADUROS E HIPERTRÓFICOS

La línea de fibroblastos 3T3-L1 se propagó en DMEM completo bajo en glucosa (5 mM de glucosa, 10 % de suero de ternera, 100 µg/mL de estreptomicina y 100 U/mL de penicilina) bajo condiciones óptimas (37°C, 95 % de humedad y 5 % de CO_2). El proceso de diferenciación a adipocito se realizó usando fibroblastos confluentes mediante un protocolo establecido [55]. Brevemente, la diferenciación se indujo incubando con DMEM alto en glucosa (20 mM) suplementado con un 10 % de FBS y los agentes inductores de la adipogénesis (10 µg/mL de insulina, 1 µM de dexametasona y 0.5 mM de IBMX) durante 48 h. Seguidamente, las células se mantuvieron con DMEM alto en glucosa suplementado con insulina, remplazándose cada 2-3 días, hasta obtener adipocitos maduros entre el octavo y décimo día de la diferenciación. La inducción de la hipertrofia del adipocito se consiguió entre el decimoséptimo y el decimonoveno día de la diferenciación con el mismo medio.

2.4 INDUCCIÓN DE GLUCOLIPOTOXICIDAD EN ADIPOCITOS Y CÉLULAS Β-PANCREÁTICAS

Los preadipocitos 3T3-L1 se cultivaron y diferenciaron como se describió anteriormente. La línea de células β-pancreáticas INS 832/13 (proporcionada amablemente por el laboratorio del Dr. Enrique Roche Collado) se cultivó en RPMI-1640 completo (11 mM glucosa, 10 mM HEPES, 10 % FBS, 2 mM L-glutamina, 1 mM de piruvato de sodio y 50 µM de β-mercaptoetanol) [101]. Una de las formas de inducir estrés metabólico en adipocitos es mediante la incubación prolongada con altas concentraciones de glucosa. La glucotoxicidad promueve la hipertrofia del adipocito [102]. De igual modo, la glucolipotoxicidad puede ser inducida *in vitro* por la incubación con altas concentraciones de glucosa unida con la adición de ácidos grasos saturados, como el ácido palmítico [103-105]. Para ello, células β-pancreáticas INS 832/13 y adipocitos maduros 3T3-L1 fueron incubados con 20 mM de glucosa y 0.5 mM de palmitato unido a 0.5 % de BSA durante 24 h y 7 días, respectivamente, renovando el medio de cultivo diariamente.

2.5 TRATAMIENTO DE ADIPOCITOS 3T3-L1

Previa a la determinación biológica, los adipocitos maduros o hipertróficos fueron tratados con compuestos puros o extractos a distintos tiempos de incubación y concentraciones, según se especifica en cada estudio. Para garantizar la esterilidad del cultivo celular, los compuestos o extractos se disolvieron en el medio de cultivo y se filtraron empleando filtros de acetato de celulosa de 0.2 µM de tamaño de poro (Advantec, Japón). En algunos casos, los compuestos/extractos fueron disueltos previamente en DMSO sin exceder una concentración tóxica del 0.5 % en el cultivo celular.

2.6 DETERMINACIONES CELULARES: ERO, LÍPIDOS, MASA MITOCONDRIAL Y CITOQUINAS PROINFLAMATORIAS

Los niveles de ERO intracelulares se cuantificaron empleando la sonda 2',7'-diclorodihidrofluoresceína diacetato (H_2DCFDA, Sigma-Aldrich, Madrid, España). La acumulación de lípidos intracelulares se determinó utilizando el reactivo AdipoRed™ (Lonza, Walkersville, MD, EE. UU.). El contenido mitocondrial se analizó mediante marcaje con la sonda MitoTracker™ Green (Molecular Probes, Invitrogen, Carlsbad, CA, EE. UU.). Los

niveles de adipoquinas secretadas se cuantificaron mediante un kit de ELISA de ratón (Signosis, Inc., Sunnyvale, CA, EE. UU.), que determina 8 citoquinas relacionadas con la obesidad (leptina, TNF-α, IGF-1, IL-6, VEGF, IL-1α, IL-1β y MCP-1). Para todas las determinaciones, se siguieron las instrucciones de los fabricantes.

2.7 Cuantificación de AMPK y AMPK fosforilada (pAMPK) por inmunofluorescencia en adipocitos

Los adipocitos se fijaron con formaldehído al 4 %, permeabilizaron con Triton X-100 al 0.25 % y bloquearon con suero de cabra al 4 %. Los anticuerpos primarios empleados fueron: anti-AMPK de ratón (ab80039, Abcam, Cambrigde, UK) y anti-pAMPK (Thr172) de conejo (2535, Cell Signaling Tech., Danvers, MA, EE. UU.). Los anticuerpos secundarios fueron: anti-ratón IgG-FITC (F0257) y anti-conejo IgG-CF594 (SAB4600107), ambos de Sigma-Aldrich. La fluorescencia correspondiente a los niveles de proteína de AMPK total y pAMPK se detectó y cuantificó empleando el lector de placas multimodal y de captura de imágenes celulares Cytation 3 (Biotek Instruments, Winooski, VT, EE. UU.). La activación de AMPK se expresa como la relación entre los niveles de pAMPK y AMPK total.

2.8 Cuantificación de AMPK, pAMPK, PPARα y FASN en adipocitos mediante la técnica Western blot

Para la extracción de proteína, los adipocitos se lisaron mediante ciclos de congelación y descongelación empleando un tampón de lisis (20 mM Tris-HCl, 150 mM NaCl, 1 mM EDTA, 1 % CHAPS, 1 mM Pefabloc y 1 % inhibidor de fosfatasas no. 2, Sigma-Aldrich Inc., Steinheim, Alemania). Se cuantificó proteína usando el espectrofotómetro NanoDrop (NanoDrop Technologies, Wilmington, DE). La electroforesis se llevó a cabo empleando geles de poliacrilamida en gradiente Bis-Tris 4-12 % o Tris-Gly 4-20 % (Invitrogen, Barcelona, España). Las proteínas se transfirieron a membranas de nitrocelulosa empleando el sistema de transferencia iBlot (Invitrogen). Los anticuerpos empleados fueron: anti-AMPK de conejo (2532, Cell Signaling Tech., Danvers, MA, EE. UU.), anti-pAMPK (Thr172) de conejo (2531, Cell Signaling Tech.), anti-FASN de conejo (3180, Cell Signaling Tech.), anti-PPARα de conejo (H-98, St. Cruz Biotech., Heidelberg, Alemania) y anti-β-actina de conejo (H-300, St. Cruz Biotech.). Los anticuerpos secundarios empleados fueron: anti-conejo-HRP de cabra (Dako, Glostrup, Dinamarca) y anti-cabra-HRP (Dako, Glostrup, Dinamarca). La detección

quimioluminiscente se realizó usando el kit de detección ECL Advance Western Blotting (Amersham, GE Healthcare, Barcelona, España) y las membranas se analizaron con el sistema ChemiDoc (Bio-Rad, España). Los niveles de proteína se cuantificaron por densitometría de banda normalizada a la señal de β-actina utilizando el programa Image Lab (Version 3.0 build 11, Bio-Rad, Madrid, España).

2.9 ANÁLISIS DEL POTENCIADOR DEL GEN DE MCP-1 HUMANO POR TRANSFECCIÓN DE ADIPOCITOS

La evaluación de la expresión de MCP-1 a nivel transcripcional se realizó transfectando adipocitos 3T3-L1 con 5 días de diferenciación con un plásmido que contiene la región potenciadora del gen de MCP-1 humano (pGLM-ENH) acoplada al gen de la luciferasa (Osaka University, Japón). El plásmido se introdujo en el interior de los adipocitos usando el sistema de transfección Neon® de Invitrogen, siguiendo las instrucciones del fabricante. La expresión de MCP-1 se midió a partir de la luz producida por la actividad luciferasa usando el sistema de ensayo luciferasa de Promega y el luminómetro POLARstar (Omega, BMG LABTECH).

2.10 ESTUDIO DE SINERGIA ENTRE COMPUESTOS ACTIVADORES DE AMPK EN ADIPOCITOS

Se obtuvieron adipocitos maduros en placas de 96 pocillos y se incubaron los compuestos por parejas siguiendo la técnica del tablero de ajedrez (*checkerboard*). La actividad de AMPK se analizó por inmunofluorescencia. Las interacciones sinérgicas se determinaron calculando el "índice fraccional de concentración inhibitoria" (FICI), cuya fórmula fue adaptada en valores de activación. Se consideró sinergia cuando FICI ≤ 0.5; efecto aditivo cuando 0.5 < FICI ≤ 1; efecto indiferente cuando 1 < FICI < 2; y antagonismo cuando FICI ≥ 2, de acuerdo con la interpretación de EUCAST [106, 107].

2.11 EXPERIMENTOS DE ACOPLAMIENTO MOLECULAR *IN SILICO*

Las estructuras moleculares de los ligandos (polifenoles) se obtuvieron a partir de la base de datos Pubchem del *National Center for Biotechnology Information* (NCBI). Las estructuras de las proteínas (PPARα, FASN y AMPK) se obtuvieron de la base de datos *Research*

Collaboratory for Structural Bioinformatics (RCSB) *Protein Data Bank* (PDB). Las estructuras de las proteínas se visualizaron usando el programa PyMol 2.0 (PyMOL Molecular Graphics System, Version 2.0 Schrödinger, LLC). Los experimentos de acoplamiento molecular se llevaron a cabo usando el programa YASARA v18.12.27 [108], que calculó las variaciones de energía libre de Gibbs (ΔG, kcal/mol) como indicador de la energía de afinidad de los ligandos por los sitios de unión de las proteínas.

2.12 ESTUDIO DE INTERVENCIÓN EN MUJERES OBESAS Y CON SOBREPESO

Se llevó a cabo un ensayo controlado por placebo, doble ciego y aleatorizado de 8 semanas de duración en mujeres con sobrepeso y obesidad. Un total de 46 voluntarias entre 36-69 años con un IMC entre 24 a 34 Kg/m^2 completaron el estudio. Durante los dos meses de estudio, el grupo control recibió dos cápsulas de placebo y el grupo tratamiento recibió dos cápsulas de 250 mg cada una de una formulación preparada a partir de una mezcla de LC e HS. Ambos grupos acompañaron el tratamiento con una dieta isocalórica y la recomendación de 30 minutos al día de realización de ejercicio físico. Las medidas se tomaron al inicio y a los 30 y 60 días de estudio. El principal objetivo fue medir el efecto de la mezcla LC-HS sobre parámetros antropométricos y circulatorios. Los parámetros antropométricos incluyeron el peso corporal y la altura, el grosor del pliegue cutáneo del tríceps y la circunferencia abdominal (AC) medida en dos sitios diferentes: entre la apófisis xifoides y el ombligo (AC1) y a nivel del ombligo (AC2). Para medir el peso corporal y la altura se empleó una báscula con barra de altura y, a partir de estos datos, se calculó el IMC. El grosor del pliegue del tríceps se midió usando un plicómetro y AC1 y AC2 se midieron usando una cinta métrica. El porcentaje de grasa corporal (% BF) se calculó a partir del peso corporal, la altura y la AC empleando la ecuación de Weltman para mujeres obesas [109]. Se extrajeron muestras de plasma en ayunas para determinar la glucosa total, la hemoglobina glicosilada y el perfil lipídico (triglicéridos, colesterol total, lipoproteína de alta densidad y lipoproteína de baja densidad). Como segundo objetivo, se evaluó la presión arterial midiendo la presión sistólica (SBP) y diastólica (DBP) y el pulso cardíaco al principio y a los 30 y 60 días de la intervención usando el monitor de presión arterial oscilométrico Omron HEM-7320-LA (Omron Healthcare Co. Ltd, Kyoto, Japón).

RESULTADOS

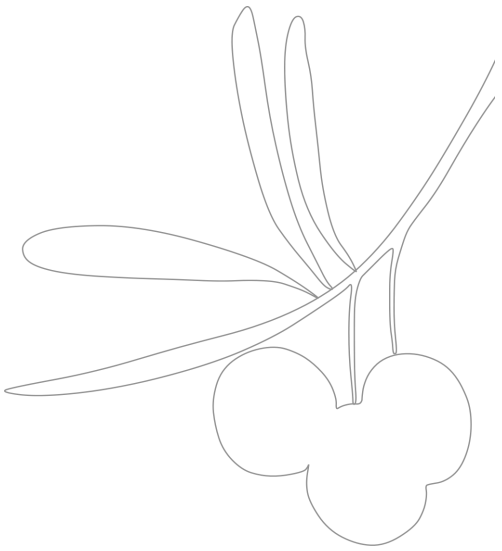

CAPÍTULO 1

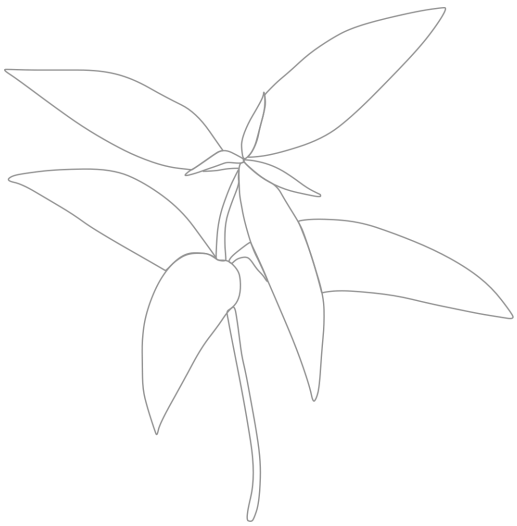

PLOS One, 2017, 12(3):e0173074

AMPK modulatory activity of olive-tree leaves phenolic compounds: Bioassay-guided isolation on adipocyte model and *in silico* approach

Cecilia Jiménez-Sánchez, Mariló Olivares-Vicente, Celia Rodríguez-Pérez, María Herranz-López, Jesús Lozano-Sánchez, Antonio Segura-Carretero, Alberto Fernández-Gutiérrez, José Antonio Encinar, Vicente Micol.

DOI: 10.1371/journal.pone.0173074

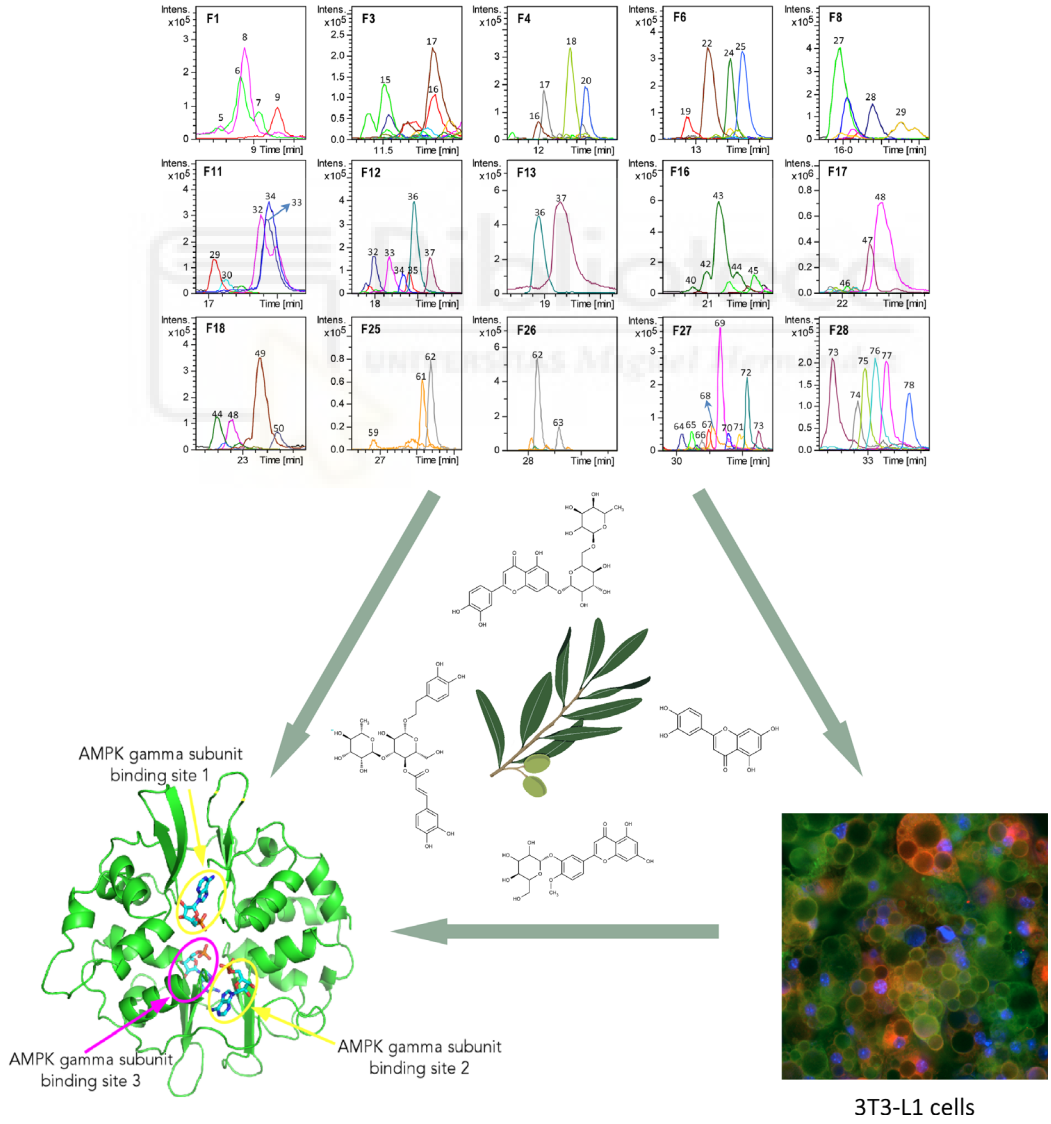

RESUMEN DE LOS RESULTADOS

En este trabajo, se estudió la capacidad de un extracto de OL de modular la acumulación de triglicéridos y la activación de AMPK en adipocitos 3T3-L1 hipertróficos. Previamente, el extracto de OL fue caracterizado por RP-HPLC-ESI-TOF/MS, identificándose un total de 78 compuestos. La mayoría pertenecían a la clase de compuestos fenólicos, especialmente iridoides (secoiridoides), ácidos cinámicos, derivados de feniletanoides, fenilpropanoides, cumarinas, flavonoides y lignanos. El extracto de OL disminuyó significativamente la acumulación de lípidos intracelulares en los adipocitos tras 48 h de incubación a 800 μg/mL, alcanzando una reducción del 16 % respecto al control. Asimismo, dicha disminución lipídica se correlacionó con un aumento significativo de la activación de AMPK por fosforilación en Thr172.

Con el fin de determinar los compuestos bioactivos responsables de activar AMPK, se llevó a cabo un fraccionamiento del extracto mediante HPLC-ESI-TOF/MS semi-preparativa. De esta manera, se obtuvieron un total de 28 fracciones que se analizaron en el modelo de adipocitos hipertróficos. Las fracciones que activaron AMPK estaban compuestas fundamentalmente por secoiridoides (isómeros de oleósido / secologanósido, ácido elenólico glucósido / metiloleósido, dimetiloleuropeína, hidroxioleuropeína / hidroxioleurósido, oleuropeína glucósido / *neonuezhenide*, isómeros de oleuropeína / oleurósido, dimetil hidroxi octenoiloxi secologanósido, ligstrósido, oleuropeína metil éter), ácidos cinámicos, feniletanoides y fenilpropanoides (ácido *p*-cumárico glucósido, verbascósido e isómeros de calcelariósido), flavonoides (isómeros de glucosil ramnosilquercetina-rutina-, luteolina rutinósido, luteolina glucósido, diosmetina glucósido, luteolina, quercetina, resinósido) y lignanos (olivil).

A continuación, se llevó a cabo un análisis de acoplamiento molecular de los compuestos presentes en las fracciones de OL que activaron AMPK en adipocitos frente a los sitios de unión de las tres subunidades de la proteína. Los resultados indicaron que algunos de los compuestos presentes en dichas fracciones podrían actuar como ligandos potenciales de la subunidad γ de AMPK. No obstante, los valores de ΔG de estos compuestos cuando se acoplaron a las subunidades α y β fueron más altos que los exhibidos por sus respectivos ligandos cristalográficos, lo que indica que la modulación de la proteína a través de estas dos subunidades es menos probable.

PLOS ONE

RESEARCH ARTICLE

AMPK modulatory activity of olive–tree leaves phenolic compounds: Bioassay-guided isolation on adipocyte model and in silico approach

Cecilia Jiménez-Sánchez[1,2], Mariló Olivares-Vicente[3], Celia Rodríguez-Pérez[1,2], María Herranz-López[3], Jesús Lozano-Sánchez[1,2], Antonio Segura-Carretero[1,2], Alberto Fernández-Gutiérrez[1,2], José Antonio Encinar[3‡], Vicente Micol[3,4‡*]

1 Department of Analytical Chemistry, University of Granada. Granada, Spain, **2** Research and Development of Functional Food Centre (CIDAF), PTS, Granada, Spain, **3** Instituto de Biología Molecular y Celular (IBMC), Miguel Hernández University (UMH), Elche, Alicante, Spain, **4** CIBER: CB12/03/30038, Fisiopatología de la Obesidad y la Nutrición, CIBERobn, Instituto de Salud Carlos III (ISCIII), Palma de Mallorca, Spain

‡ These authors are joint senior authors on this work.
* vmicol@umh.es

Citation: Jiménez-Sánchez C, Olivares-Vicente M, Rodríguez-Pérez C, Herranz-López M, Lozano-Sánchez J, Segura-Carretero A, et al. (2017) AMPK modulatory activity of olive–tree leaves phenolic compounds: Bioassay-guided isolation on adipocyte model and in silico approach. PLoS ONE 12(3): e0173074. doi:10.1371/journal.pone.0173074

Editor: Turgay Unver, Dokuz Eylul Universitesi, TURKEY

Received: November 7, 2016

Accepted: February 14, 2017

Published: March 9, 2017

Data Availability Statement: All relevant data are within the paper and its Supporting Information files.

Funding: This work was supported by the projects BFU2014-52433-C3-2-R, AGL2011-29857-C03-02 (Spanish Ministry of Science and Innovation); projects AGL2015-67995-C3-1-R, AGL2015-67995-C3-2-R, Torres Quevedo grants PTQ-13-06429 and PTQ-14-07243 and scholarship FPU

Abstract

Scope

Olive-tree polyphenols have demonstrated potential for the management of obesity-related pathologies. We aimed to explore the capacity of Olive-tree leaves extract to modulate triglyceride accumulation and AMP-activated protein kinase activity (AMPK) on a hypertrophic adipocyte model.

Methods

Intracellular triglycerides and AMPK activity were measured on the hypertrophic 3T3-L1 adipocyte model by AdipoRed and immunofluorescence microscopy, respectively. Reverse phase high performance liquid chromatography coupled to time-of-flight mass detection with electrospray ionization (RP-HPLC-ESI-TOF/MS) was used for the fractionation of the extract and the identification of the compounds. In-silico molecular docking of the AMPK alpha-2, beta and gamma subunits with the identified compounds was performed.

Results

Olive-tree leaves extract decreased the intracellular lipid accumulation through AMPK-dependent mechanisms in hypertrophic adipocytes. Secoiridoids, cinnamic acids, phenylethanoids and phenylpropanoids, flavonoids and lignans were the candidates predicted to account for this effect. Molecular docking revealed that some compounds may be AMPK-gamma modulators. The modulatory effects of compounds over the alpha and beta AMPK subunits appear to be less probable.

AP2010-2793 from the Spanish Ministry of Economy and Competitiveness (MINECO); P09-CTS-4564, P10-FQM-6563 and P11-CTS-7625 grants from Andalusian Regional Government Council of Innovation and Science; PROMETEO/2016/006, and ACIF/2016/230 from Generalitat Valenciana; CIBER (CB12/03/30038, Fisiopatologia de la Obesidad y la Nutricion, CIBERobn, Instituto de Salud Carlos III).

Competing interests: The authors have declared that no competing interests exist.

Abbreviations: ADP, adenosine diphosphate; AICAR, 5-Aminoimidazole-4-carboxamide ribonucleotide; AMP, adenosine monophosphate; AMPK, AMP-activated protein kinase; BCS, bovine calf serum; BPC, Base peak chromatogram; CaMKKβ, Calcium/calmodulin-dependent protein kinase 2; DEX, Dexamethasone; DMEM, Dulbecco's modified Eagle's medium; FA, fatty acid; FBS, fetal bovine serum; HPC, high-precision calibration; IBMX, 3-isobutyl-1-methylxanthine; LKB1, liver kinase 1; mTOR, mammalian target of rapamycin; pAMPK, phospho AMP-activated protein kinase; PVD, polyvinyldifluoride; RP-HPLC-ESI-TOF/MS, Reversed-phase High-Performance Liquid Chromatography coupled to Electrospray Time-of-Flight Mass Spectrometry; Thr172, Threonine172; WHO, World Health Organization.

Conclusions

Olive-tree leaves polyphenols modulate AMPK activity, which may become a therapeutic aid in the management of obesity-associated disturbances. The natural occurrence of these compounds may have important nutritional implications for the design of functional ingredients.

Introduction

Obesity is a multifactorial complex disease of global significance. This disease is defined by excess adipose mass and adipose tissue expansion, which occurs through adipocyte hypertrophy and hyperplasia [1]. Importantly, adipocyte size is a major determinant of obesity in adults [2]. Adipose tissue is a key energy storage organ, and adipose endocrine function is critical to the overall energy balance and homeostasis with adipocyte-derived pro- and anti-inflammatory adipokines playing key roles [3]. When the production and secretion of proinflammatory adipokines prevails, systemic inflammation, insulin resistance and obesity-related metabolic disorders arise [4].

Recently, AMP-activated protein kinase (AMPK) has been revealed to be an important regulator of cellular energy homeostasis. AMPK is a sensor of the cellular energy status that directs metabolic adaptation to support cellular growth and survival, restoring energy homeostasis. AMPK is involved in the regulation of carbohydrate and lipid metabolism, resulting in the inhibition of ATP-consuming anabolic pathways, including FA (fatty acid) synthesis, cholesterol and isoprenoid synthesis, hepatic gluconeogenesis and mTOR (mammalian target of rapamycin)-mediated protein translation. In parallel, AMPK activation stimulates ATP production by increasing FA oxidation, muscle glucose transport, mitochondrial biogenesis and caloric intake [5,6]. It also plays a major role in hormonal signaling and is a central node of such signaling pathways. It can regulate the endocrine system, and at the same time, its activity is regulated by a number of hormones and cytokines (adipokines) such as leptin, interleukin-6, resistin, ghrelin, and adiponectin. In addition, it controls the appetite through a neuroendocrine system that makes it a key regulator of energy metabolism at the whole body level [7].

AMPK is activated by phosphorylation at Thr172, which is modulated by the binding of AMP. Although allosteric activation is only caused by AMP, it has recently been found that similar effects on phosphorylation and dephosphorylation can also be produced by ADP [8]. Specifically, AMPK is phosphorylated by upstream kinases. The primary upstream AMPK kinase is the liver kinase B1 (LKB1), a product of a tumor suppressor gene, which provides anti-tumor functions through the direct phosphorylation of AMPK Thr172 *in vitro* and *in vivo* [9,10]. Secondly, Calcium/calmodulin-dependent protein kinase 2 (CaMKKβ), triggers the activation of AMPK in response to increases in cell Ca^{2+} [11]. Increases in the Ca^{2+} influx usually accompany such processes as the activation of motor proteins and messages of increased energy consumption. Thus, this activation mechanism anticipates ATP deficiency before it has occurred [12]. The classical pathways through which AMPK is activated by upstream kinases or Ca^{2+} are now becoming well understood, although the understanding of how phosphatases dephosphorylate the protein in Thr172 remains incomplete [13]. Although changes in the AMP, ATP, or Ca^{2+} levels are triggered by metabolic stresses, recent work suggests that AMPK can also be switched on by numerous plant-derived phenolic compounds [14–17]. To date, sufficient evidence has been accumulated to support that phenolic compounds of *Olea europaea* might be able to activate AMPK pathways in cancer cell lines through the AMPK/mTOR

axis [18,19]. These findings led us to postulate that these compounds could also have important implications in metabolic stress-related disorders such as obesity through AMPK-dependent mechanisms.

In this context, we have studied the capacity of an Olive-tree leaves extract to modulate triglyceride accumulation and AMPK activation using the well-established 3T3-L1 adipocyte model. The characterization of the phenolic extract was achieved using RP-HPLC-ESI-TOF/MS, and semi-preparative fractionation was performed to identify putative candidates for the attributed biological activity. A molecular docking approach was utilized to obtain the free energy variation of the molecular structures of the identified compounds on the AMPK alpha-2, beta and gamma subunits to search for direct AMPK interaction. Finally, a correlation between the most active Olive-tree leaves compounds in the cellular model and those bearing lower free energy values is proposed for the rational understanding of AMPK modulation by the extract.

Materials and methods

Materials

For the semi-preparative fractionation of the Olive-tree leaves extract, all chemicals were of analytical reagent grade and were used as received. Methanol used for the extraction was purchased from Panreac (Barcelona, Spain). Acetic acid and acetonitrile for semi-preparative HPLC were purchased from Fluka and Sigma-Aldrich (Steinheim, Germany), respectively. Water was purified by a Milli-Q system from Millipore (Bedford, MA, USA). 3T3-L1 mouse embryo fibroblasts were purchased from the American Type Culture Collection (Manassas, VA, USA). Dexamethasone (DEX), 3-isobutyl-1-methylxanthine (IBMX), insulin, penicillin—streptomycin, calf serum, fetal bovine serum (FBS) (both being HyClone), paraformaldehyde solution, and Triton X-100 were obtained from Sigma-Aldrich (Madrid, Spain). Dulbecco's modified Eagle's medium (DMEM) was purchased from Gibco (ThermoFisher Scientific, Waltham, MA, USA). Polyvinyldifluoride (PVD) filters, 0.22 μm, were obtained from Millipore (Bedford, MA, USA), and Dulbecco's phosphate buffered saline (PBS) was obtained from Sigma-Aldrich (St. Louis, MO, USA). The staining AdipoRed Assay Reagent was obtained from Lonza (Walkersville, MD USA).

Preparation of the Olive-tree leaves extract

Olive-tree leaves (*Olea europaea*) from the 'Arbequina' cultivar were used in this study. They were air-dried in the laboratory, and sample extraction was performed as described elsewhere [20]. Briefly, dry leaves (5 g) were crushed and extracted via Ultra—Turrax T18 basic reagent (IKA, Staufen, Germany) using 300 mL of MeOH/H_2O (80/20). After solvent evaporation, the extracts were reconstituted with MeOH/H_2O (50/50) to achieve a concentration of 50 mg/mL. Three extraction replicates were processed.

Analytical characterization of the Olive-tree leaves extract and isolated fractions

The Olive-tree leaves extract was analytically characterized by RP-HPLC-ESI-TOF/MS, performed in an Agilent 1200-HPLC system (Agilent Technologies, Waldbronn, Germany) of the Series Rapid Resolution equipped with a vacuum degasser, autosampler, a binary pump, and a UV-vis detector. The chromatographic separation was carried out as reported elsewhere [21]. The extract and the fractions were injected at a concentration of 1 mg/mL.

The compounds separated were monitored with a mass-spectrometry detector. MS was performed using a microTOF (Bruker Daltonik, Bremen, Germany), which was equipped with an ESI interface (model G1607A from Agilent Technologies, Palo Alto, CA, USA) operating in the negative-ion mode. The optimum values of the source and transfer parameters were described elsewhere [22]. The accurate mass data for the molecular ions were processed using the software Data Analysis 3.4 (Bruker Daltonik).

Semi-preparative fractionation of the Olive-tree leaves extract

Semi-preparative fractionation of the Olive-tree leaves extract was achieved using a Gilson preparative HPLC system (Gilson, Middleton, WI, USA) equipped with a binary pump (model 331/332), an automated liquid-handling solution (model GX-271), and a UV-Vis detector (model UV-Vis 156). The extract was fractionated at room temperature. A 250 mm x 10 mm i.d., 5 μm Phenomenex RP-C18 column was used to separate the compounds. The mobile phases consisted of acetic acid 0.5% (A) and acetonitrile (B). The following multi-step linear gradient was applied: 0 min, 5% B; 5 min, 15% B; 53 min, 27% B; 54 min, 28% B; 60 min, 100% B; 65 min, 100% B; 70 min, 5% B; 75 min, 5% B. The injection volume was 500 μL and the flow rate used was set at 10 mL/min. The compounds separated were monitored with UV-Vis (240 and 280 nm) and MS, using the time-of-flight mass spectrometer detector microTOF (Bruker Daltonik, Bremen, Germany), as reported in the previous section.

Cell culture and treatment and intracellular lipid quantitation

The 3T3-L1 preadipocyte cell line was cultured and differentiated as described elsewhere [23]. Hypertrophied adipocytes were obtained using high glucose medium containing insulin (4.5 mg/mL) after differentiation [24]. Under these conditions, cells become hypertrophic adipocytes, a cell model characterized by a high level of cytoplasmic lipid accumulation, insulin-resistance, and exacerbated oxidative stress, a situation reasonably similar to that of obese adipose tissue [16,24]. On day 18, cells were treated with the respective extract or fractions, which were dissolved in 10% FBS/high glucose (4.5 mg/mL) DMEM medium with 1 μM insulin and maintained for 48 h. For cell treatments, extract or fractions were reconstituted in cell culture medium plus DMSO at a maximum final concentration of 0.3% v/v after solvent evaporation. The crystal violet assay was performed as reported to dismiss the possible cytotoxic effects of the extract/fractions at the working concentrations [24,25]. Quantification of intracellular lipid droplets in hypertrophic adipocytes was performed as reported [24] using the staining AdipoRed Assay Reagent and the Cytation 3 cell imaging multi-mode microplate reader (Biotek Instruments, Winooski, VT, USA).

Quantification of the AMPK and pAMPK levels

For AMPK and phospho-AMPK (pAMPK) detection, an immunofluorescence assay was carried out. Cells were washed with PBS, fixed for 15 min in 4% paraformaldehyde, permeabilized in 0.25% Triton X-100 for 5 min, and washed with PBS. After blocking in 4% goat serum at room temperature for 1 h, the cells were washed and incubated overnight at 4˚C with mouse monoclonal to AMPK alpha 1 + AMPK alpha 2 antibodies (Abcam, Cambridge, UK) or rabbit monoclonal phospho-AMPKα (Thr172) antibodies (Cell Signaling Technology, Danvers, MA, USA). Cells were washed 3 times with PBS and incubated at ambient temperatures for 6 hours with Hoechst staining (2.5 μg/mL) together with each corresponding polyclonal secondary antibody, goat anti-rabbit IgG CF 594, or goat anti-mouse polyvalent immunoglobulins (G,A, M)-FITC, all from Sigma-Aldrich (St. Louis, MO, USA). Cells were washed 3 times with PBS and read with a Cytation 3 cell imaging multi-mode microplate reader (Biotek Instruments,

Winooski, VT, USA). AMPK was detected by measuring the fluorescence with excitation at 490 nm and emission at 520 nm for AMPK and with excitation at 590 nm and emission at 620 nm for pAMPK. To ensure that the extracts/fractions were not cytotoxic, the cell count was performed by taking microphotographs of the Hoechst-stained cells at 4x, using the DAPI imaging filter cube.

Molecular docking procedures

To date, several crystal structures of the three AMPKs have been solved and deposited into the Protein Data Bank, many of them with their inhibitors that delimitate their binding site. For AMPK catalytic subunit alpha-2 (UniProt P54646), the following structures have been used as a receptor in the molecular docking experiments for AMPK beta subunit (UniProt Q9Y478): 4CFE, 4CFF, 4ZHX, 5EZV. Finally, for the AMPK gamma subunit (UniProt P54619), several crystal structures were chosen: 2UV4, 2UV5, 2UV6, 2UV7, 4CFE, 4CFF, 4RER, 4REW, and 4ZHX. Prior to initiating the docking procedure, the protein (receptor) and ligand structures should be prepared [26]. A grid with the dimensions of 22 x 22 x 22 points was centered to ensure coverage of the binding site of the structure. AutoDock/Vina was set up on a Microsoft Windows 10 system using configuration files, including the usage of two CPUs and an effectiveness of 20.

Statistical analysis

Values are represented as the mean ± standard deviation (S.D.) of the mean. The values were subjected to statistical analysis (one-way ANOVA, and Dunett's test for multiple comparisons/non-parametric approaches). The differences were considered to be statistically significant at $p < 0.05$. All analyses were performed using Graph Pad Prism 6 (GraphPad Software, Inc. La Jolla, CA, USA). $^{*}p < 0.05$, $^{**}p < 0.01$ and $^{***}p < 0.001$ on the bars indicate statistically significant differences compared to the control, unless otherwise stated. All cellular measurements were derived from three independent experiments. Each experiment was performed in sextuplicate, unless otherwise specified.

Results

Characterization of the Olive-tree leaves extract by RP-HPLC-ESI-TOF

The Olive-tree leaves extract obtained as described in the materials and methods section was characterized using the RP-HPLC-ESI-TOF/MS methodology. The identification was performed by comparing the retention times from the MS data provided by the TOF analyzer and those from the literature (Fig 1).

The chromatographic profile obtained by RP-HPLC-ESI-TOF/MS showed several peaks, of which a total of 78 were tentatively identified. Compound numbers were assigned according to their elution order.

As shown in Table 1, most of the compounds belonged to the phenolic compound classes, specifically to the iridoid (most of them being secoiridoids), phenylethanol derivative, cinnamic acid, phenylpropanoid, coumarin, flavonoid, and lignan subclasses. The chemical structures of the identified compounds are included in S1 Fig.

The effects of *Olea euroapea* leaf extract on triglyceride accumulation and AMPK activity modulation in 3T3-L1 hypertrophic adipocytes

Hypertrophic and insulin resistant adipocytes were treated for 48 hours with different concentrations of the crude extract. After 48 h, the quantification of intracellular lipids was measured

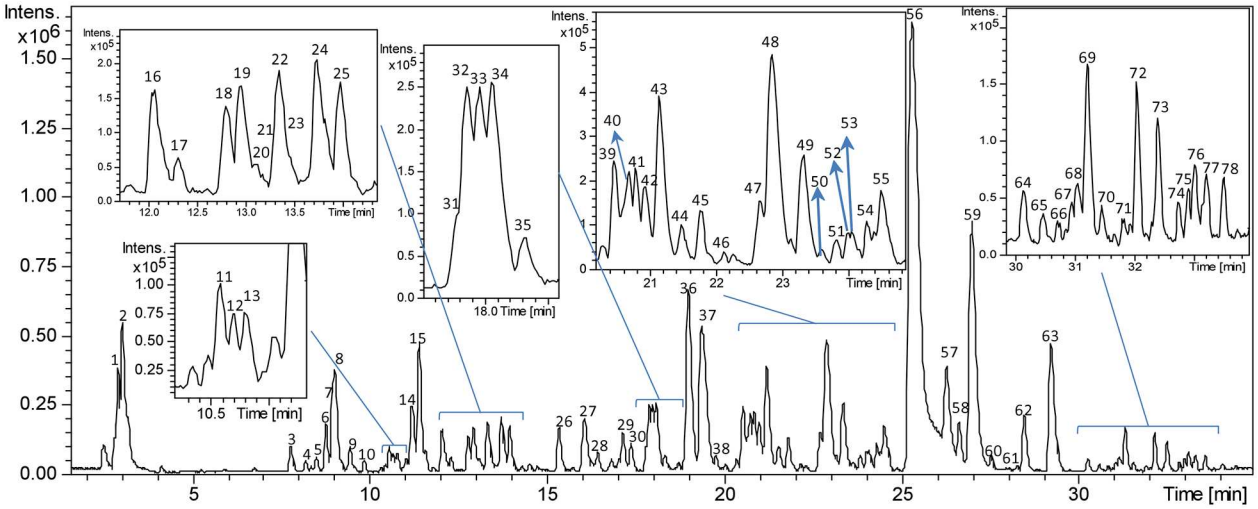

Fig 1. HPLC-MS characterization of Olive-tree leaves extract. Base peak chromatogram (BPC) of the Olive-tree leaves extract in the negative ion mode obtained by RP-HPLC-ESI-TOF/MS, in which the peaks are identified by numbers 1–78 according to the elution order.

doi:10.1371/journal.pone.0173074.g001

with the probe AdipoRed. Cells treated with 400, 600, and 800 μg/mL of the extract decreased triglyceride accumulation by 93, 92, and 86%, respectively (Fig 2), but statistically significant differences compared with the non-treated cells maintained in high glucose medium were found only at 800 μg/mL of the extract ($p<0.01$). Microscopic observation of cells treated with 800 μg/mL of the extract revealed a significant reduction in the intracellular triglyceride accumulation.

With the aim of unveiling the possible molecular mechanisms of the reduction of intracellular lipid accumulation, we studied the effects of the Olive-tree leaves crude extract on the activation of AMPK through the phosphorylation of Thr172. After 48 hours of treatment with increasing concentrations of the extract, the levels of AMPK and pAMPK at Thr 172 (pAMPK) were quantified by immunofluorescence (Fig 3). No significant changes in the total AMPK protein levels were detected (Fig 3A), while the phosphorylation of the protein showed a dose-response behavior upon the increase of the Olive-tree leaves extract concentration, exhibiting significant differences at 800 μg/mL compared to the high glucose-treated control cells ($p<0.05$). At this concentration, the Olive-tree leaves extract promoted an important AMPK activation, considering that one observed with the AMPK activator AICAR, an AMP synthetic analog (Fig 3B). Microscopic observation of the treated cells also revealed a significant increase in the fluorescence intensity corresponding to pAMPK levels in cells treated with the complete extract at 800 μg/mL (Fig 3G) compared to the control (Fig 3D).

Bio-assay guided isolation of AMPK modulators derived from the Olive-tree leaves extract by semipreparative liquid chromatography

To delimit the bioactive compounds responsible for the observed AMPK activation of the Olive-tree leaves extract, we developed a semi-preparative HPLC-ESI-TOF/MS methodology to fractionate the extract according to the UV and MS information. Twenty-eight fractions were obtained to be analyzed for AMPK activation (S2 Fig).

To study which individual compounds were responsible for the mentioned AMPK activation/inhibition, fractions were incubated for 48 hours at a concentration of 400 μg/mL. The levels of AMPK and pAMPK were quantified by immunofluorescence as described in the Methods (Fig 4). Some fractions, such as F1, F8 and F11, exhibited increased levels of total

Table 1. Relevant mass data of the proposed compounds detected in the Olive-tree leaves extract analyzed by RP-HPLC-ESI-TOF/MS. From left to right: peak number, retention time, calculated *m/z*, calculated *m/z*, molecular formula, error (ppm), millisigma value, proposed compound; and reference and matrix in which the proposed compound has been previously described.

Pk	RT (min)	*m/z* exp.	*m/z* calc.	Mol. formula	Error (ppm)	mSigma	Proposed compound	Reference	Matrix
1	2.86	341.1086	341.1089	$C_{12}H_{22}O_{11}$	0.9	89.4	Sucrose	[49]	Olive-tree leaves
2	3.096	191.057	191.0561	$C_7H_{12}O_6$	4.8	14.8	Quinic acid	[21]	Olive-tree leaves
3	7.811	375.1296	375.1297	$C_{16}H_{24}O_{10}$	0.3	9.2	(Epi)loganic acid isomer1	[50]	Olive pomace
4	8.229	389.1073	389.1089	$C_{16}H_{22}O_{11}$	4.1	9.9	Oleoside/ Secologanoside isomer 1	[21,51]	Olive-tree leaves
5	8.631	389.1074	389.1089	$C_{16}H_{22}O_{11}$	4	12.3	Oleoside/ Secologanoside isomer 2	[21,51]	Olive-tree leaves
6	8.797	315.1086	315.1085	$C_{14}H_{20}O_8$	0.1	16.5	Hydroxytyrosol-glucoside isomer 1	[51–53]	Olive-tree leaves
7	8.849	315.1101	315.1085	$C_{14}H_{19}O_8$	5	33.3	Hydroxytyrosol-glucoside isomer 2	[51–53]	Olive-tree leaves
8	9.048	389.1112	389.1089	$C_{16}H_{22}O_{11}$	5.7	13.7	Oleoside/ Secologanoside isomer 3	[21,51]	Olive-tree leaves
9	9.466	375.1299	375.1297	$C_{16}H_{24}O_{10}$	0.5	20.3	(Epi)loganic acid isomer 2	[50,53]	Olive pomace
10	9.868	153.0543	153.0557	$C_8H_{10}O_3$	9.3	16	Hydroxytyrosol	[21,52,53]	Olive-tree leaves
11	10.353	299.1136	299.1121	$C_{14}H_{20}O_7$	5	23.8	Tyrosol glucoside	[54]	Olive-tree leaves
12	10.486	341.0875	341.0878	$C_{15}H_{18}O_9$	1	5	Caffeoylglucoside	[55]	Olive mill wastewater
13	10.687	339.0702	339.0722	$C_{15}H_{16}O_9$	5.8	12.2	Esculin	[53]	Olive-tree leaves
14	11.189	403.1246	403.1246	$C_{17}H_{24}O_{11}$	0.2	19.8	Elenolic acid glucoside/methyloleoside isomer 1	[21,51]	Olive-tree leaves
15	11.423	389.1106	389.1089	$C_{16}H_{22}O_{11}$	4.2	14.6	Oleoside/ Secologanoside isomer 4	[21,51]	Olive-tree leaves
16	12.125	403.1241	403.1246	$C_{17}H_{24}O_{11}$	1.3	11.8	Elenolic acid glucoside/methyloleoside isomer 2	[21,51]	Olive-tree leaves
17	12.309	325.0918	325.0918	$C_{15}H_{18}O_8$	3.5	5.7	*p*-oumaric acid glucoside	[56]	*Ligustrum purpurascens* leaves (Oleaceae)
18	12.794	519.1727	519.1872	$C_{22}H_{32}O_{14}$	2.7	50.6	Unknown	–	–
19	12.878	401.1476	401.1453	$C_{18}H_{26}O_{10}$	3.7	21.6	Unknown	[51]	Olive-tree leaves
20	12.944	593.1524	593.1512	$C_{27}H_{30}O_{15}$	2	9.2	Unknown	–	–
21	13.246	387.2001	387.2024	$C_{19}H_{32}O_8$	6	15.2	Unknown	–	–
22	13.329	403.1258	403.1246	$C_{17}H_{24}O_{11}$	2.9	20.5	Elenolic acid glucoside/methyloleoside isomer 3	[21,51]	Olive-tree leaves
23	13.43	537.2002	537.1978	$C_{26}H_{34}O_{12}$	-4.5	3.3	Olivil glucoside	[53]	Olive stem
24	13.684	377.1461	377.1453	$C_{19}H_{22}O_8$	2.2	10.9	Oleuropein aglycone	[49,52]	Olive-tree leaves
25	14.099	609.1486	609.1461	$C_{27}H_{30}O_{16}$	4.1	10.4	Glucosyl rhamnosylquercetin (rutin) isomer 1	[54]	Olive-tree leaves
26	15.352	403.1222	403.1246	$C_{17}H_{24}O_{11}$	5.8	13.9	Elenolic acid glucoside methyloleoside isomer 4	[21,51]	Olive-tree leaves
27	16.055	415.1628	415.161	$C_{19}H_{28}O_{10}$	4.4	21	Phenethyl primeveroside	[57]	Isolated from olive cells
28	16.391	403.1958	403.1974	$C_{19}H_{32}O_9$	3.8	24.9	Ethyl-glucopyranosyloxy-oxopropyl-cyclohexaneacetic acid	[58]	Olive-tree leaves
29	17.445	511.2374	511.2396	$C_{22}H_{40}O_{13}$	4.3	6.9	Unknown	–	–
30	17.476	525.1611	525.1614	$C_{24}H_{30}O_{13}$	0.4	7.6	Demethyloleuropein	[53]	Olive-tree leaves
31	17.794	701.2279	701.2298	$C_{31}H_{42}O_{18}$	2.7	8.1	Oleuropein glucoside/neonuezhenide isomer 1	[52]	Olive-tree leaves
32	17.843	555.1744	555.1719	$C_{25}H_{32}O_{14}$	4.4	19.9	Hydroxyoleuropein isomer 1	[21]	Olive-tree leaves
33	17.877	609.1476	609.1461	$C_{27}H_{30}O_{16}$	2.5	20.9	Glucosyl rhamnosylquercetin (rutin) isomer 2	[54]	Olive-tree leaves
34	17.795	593.154	593.1512	$C_{27}H_{30}O_{15}$	4.7	29.2	Luteolin rutinoside/luteolin neohesperidoside/apigenin diglucoside	[21,53]	Olive-tree leaves
35	18.799	375.1426	375.1449	$C_{20}H_{24}O_7$	6.2	14.8	Olivil	[53]	Olive-tree leaves
36	18.982	623.2004	623.1981	$C_{29}H_{36}O_{15}$	6.2	8.4	Verbascoside	[21,49]	Olive-tree leaves
37	19.601	447.0964	447.0933	$C_{21}H_{20}O_{11}$	6.9	61.7	Luteolin glucoside isomer 1	[21,51,52]	Olive-tree leaves
38	19.735	477.1393	477.1402	$C_{23}H_{26}O_{11}$	2	26.7	Unknown	–	–
39	20.486	555.1722	555.1719	$C_{25}H_{32}O_{14}$	0.5	23.9	Hydroxyoleuropein isomer 2	[21]	Olive-tree leaves

(*Continued*)

Table 1. (*Continued*)

Pk	RT (min)	*m/z* exp.	*m/z* calc.	Mol. formula	Error (ppm)	mSigma	Proposed compound	Reference	Matrix
40	20.703	701.2329	701.2298	$C_{31}H_{42}O_{18}$	-4.4	16.5	Oleuropein glucoside/neonuezhenide isomer 2	[52]	Olive-tree leaves
41	20.806	577.1582	577.1563	$C_{27}H_{30}O_{14}$	-3.3	33.7	Apigenin rutinoside/apigenin neohesperidoside	[21,53]	Olive-tree leaves
42	20.937	701.2318	701.2298	$C_{31}H_{42}O_{18}$	-2.8	15.9	Oleuropein glucoside/neonuezhenide isomer 3	[52]	Olive-tree leaves
43	20.772	701.2329	701.2298	$C_{31}H_{42}O_{18}$	-4.4	16.5	Oleuropein glucoside/neonuezhenide isomer 4	[52]	Olive-tree leaves
44	21.489	701.2374	701.2298	$C_{31}H_{42}O_{18}$	-10.7	28.2	Oleuropein glucoside/neonuezhenide isomer 5	[52]	Olive-tree leaves
45	21.756	607.166	607.1668	$C_{28}H_{32}O_{15}$	1.4	17.3	Diosmetin rhamnoside glucoside (diosmin) isomer 1	[53]	Olive-tree leaves
46	22.275	607.1668	607.1668	$C_{28}H_{32}O_{15}$	0	26.8	Diosmetin rhamnoside glucoside (diosmin) isomer 2	[53]	Olive-tree leaves
47	22.642	431.0977	431.0984	$C_{21}H_{20}O_{10}$	1.5	22.8	Apigenin glucoside	[21,49]	Olive-tree leaves
48	22.826	447.0982	447.0933	$C_{21}H_{20}O_{11}$	-11.1	38.6	Luteolin glucoside isomer 2	[21,51,52]	Olive-tree leaves
49	23.311	461.1112	461.1089	$C_{22}H_{22}O_{11}$	-4.9	18.6	Diosmetin glucoside	[54]	Olive-tree leaves
50	23.463	491.155	491.1559	$C_{24}H_{28}O_{11}$	1.8	5.6	Calceolarioside isomer 1	[53]	Olive-tree leaves
51	23.779	541.1925	541.1927	$C_{25}H_{34}O_{13}$	0.2	16.5	Hydro-oleuropein	[59]	Olives and olive oil-derived matrices
52	24.049	491.1535	491.1559	$C_{24}H_{28}O_{11}$	4.9	12.1	Calceolarioside isomer 2	[53]	Olive-tree leaves
53	23.948	539.1778	539.177	$C_{25}H_{32}O_{13}$	-1.4	492.2	Oleuropein/oleuroside isomer 1	[21,49,52]	Olive-tree leaves
54	24.247	569.1906	569.1876	$C_{26}H_{34}O_{14}$	-5.4	7.6	Methoxyoleuropein	[51]	Olive-tree leaves
55	24.532	447.0951	447.0933	$C_{21}H_{20}O_{11}$	-4	4.4	Luteolin glucoside isomer 3	[21,51,53]	Olive-tree leaves
56	25.152	539.1808	539.177	$C_{25}H_{32}O_{13}$	-7	25.3	Oleuropein/oleuroside isomer 2	[21,49,52]	Olive-tree leaves
57	26.221	539.1804	539.177	$C_{25}H_{32}O_{13}$	-6.3	35	Oleuropein/oleuroside isomer 3	[21,49,52]	Olive-tree leaves
58	26.756	537.1571	537.1614	$C_{25}H_{30}O_{13}$	8	223	Unknown	–	–
59	26.923	539.1793	539.177	$C_{25}H_{32}O_{13}$	-4.3	7.1	Oleuropein/oleuroside isomer 4	[21,49,52]	Olive-tree leaves
60	27.441	557.2363	557.224	$C_{26}H_{38}O_{13}$	-4.3	8.9	[Dimetyl hydroxy octenoyloxi] secologanoside isomer 1	[21]	Olive-tree leaves
61	28.16	793.2821	793.2866	$C_{45}H_{46}O_{13}$	-1.9	59.1	Unknown	–	-
62	28.378	601.2156	601.2138	$C_{27}H_{38}O_{15}$	-3.1	6	Piperchabaoside/(epi)frameroside)/ ligustalisode dimethylacetal	[60]	*Ligustrum ovalifolium*
63	29.13	523.1802	523.1821	$C_{25}H_{32}O_{12}$	3.7	6.1	Ligstroside isomer 1	[21,49,51,52]	Olive-tree leaves
64	30.15	593.1285	593.1301	$C_{30}H_{26}O_{13}$	2.7	12.9	Unknown	-	-
65	30.485	557.2276	557.224	$C_{26}H_{38}O_{13}$	6.6	18.7	Ddimethyl hydroxy octenoyloxi secologanoside isomer 2	[21]	Olive-tree leaves
66	30.719	523.18	523.1821	$C_{25}H_{32}O_{12}$	3.9	31.6	Ligstroside isomer 2	[21,49,51,52]	Olive-tree leaves
67	30.936	553.1948	553.1927	$C_{26}H_{34}O_{13}$	-3.9	19	Oleuropein methyl ether	[61]	Olive wood
68	31.02	539.178	539.177	$C_{25}H_{32}O_{13}$	1.7	4.4	Oleuropein/oleuroside isomer 5	[21,49]	Olive-tree leaves
69	31.204	285.0412	285.0405	$C_{15}H_{10}O_6$	-2.7	19.2	Luteolin	[21,51,53]	Olive-tree leaves
70	31.454	301.036	301.0354	$C_{15}H_{10}O_7$	-2.1	5.9	Quercetin	[51,53]	Olive-tree leaves
71	31.789	613.195	613.1927	$C_{31}H_{34}O_{13}$	-3.9	13.3	Resinoside	[62]	Eucalyptus leaves
72	32.259	615.2125	615.2083	$C_{31}H_{36}O_{13}$	-6.8	6.5	Unknown	–	–
73	32.726	327.2178	327.2177	$C_{18}H_{32}O_5$	-0.3	14	Unknown	–	–
74	32.876	331.2502	331.249	$C_{18}H_{36}O_5$	3.6	16.5	Trihydroxystearic acid	[63]	Olive-tree leaves
75	32.96	269.0479	269.0455	$C_{15}H_{10}O_5$	-8.7	9.5	Apigenin	[52]	Olive-tree leaves
76	33.196	329.2339	329.2333	$C_{18}H_{34}O_5$	-1.8	28.9	Trihydroxy-octadecenoic acid	[64]	*Artemisia vulgaris* leaf
77	33.38	285.0417	285.0405	$C_{15}H_{10}O_6$	-4.5	8	Unknown	–	–
78	33.715	287.2206	287.2228	$C_{16}H_{32}O_4$	7.6	4.6	Dihydroxyhexadecanoic acid	[63]	Olive-tree leaves

doi:10.1371/journal.pone.0173074.t001

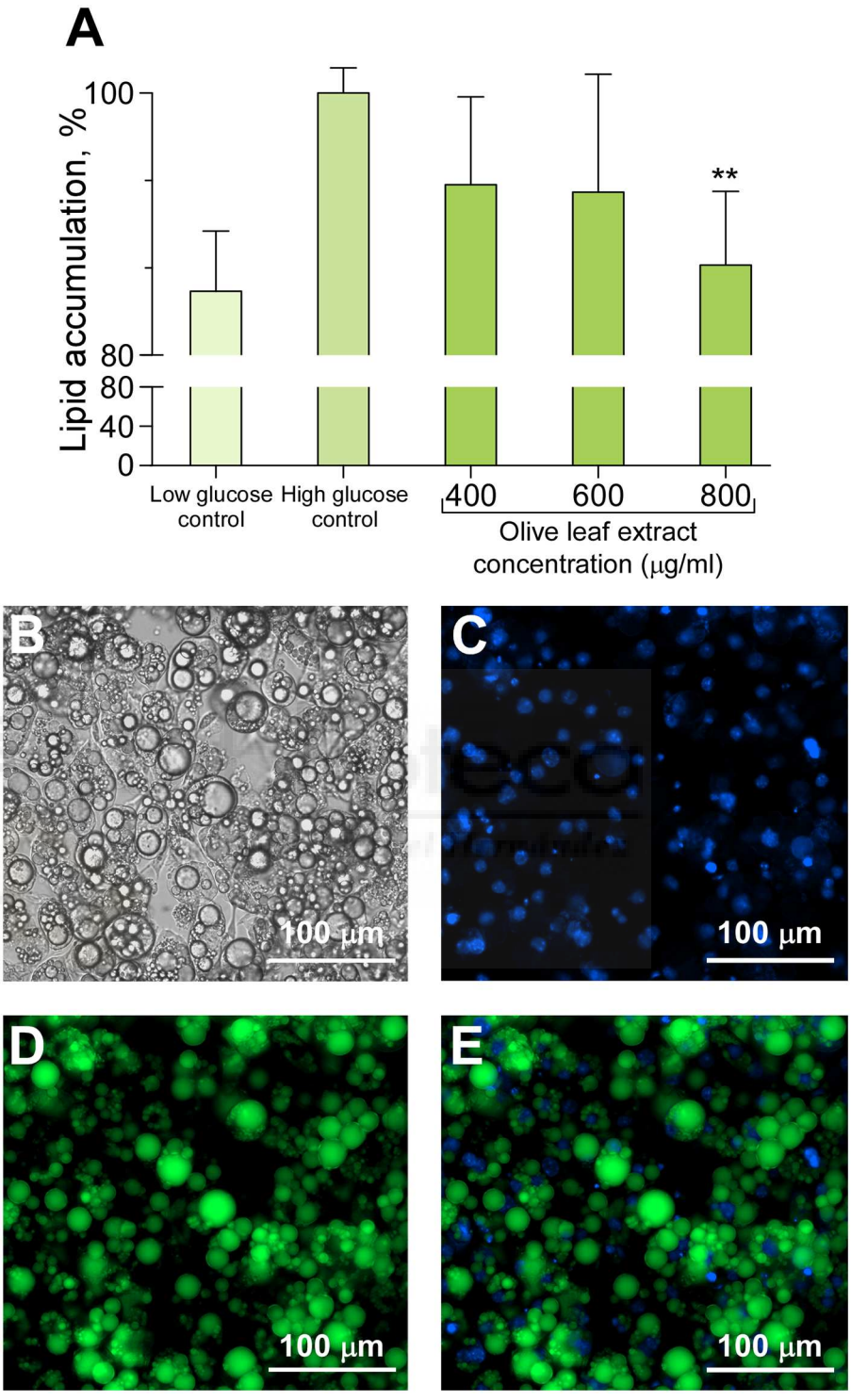

Fig 2. Intracellular triglyceride accumulation inhibitory effect of the complete Olive-tree leaves extract in 3T3-L1 hypertrophic adipocytes. (A) Quantitative assessment of lipid vesicles in hypertrophic adipocytes incubated with 400, 600, or 800 μg/mL of Olive-tree leaves extract and compared to the control in a high glucose medium. Values have been normalized with respect to the control incubated in a high glucose medium. ** $p<0.01$ indicates significant differences compared to the control. Representative microphotographs for the qualitative assessment of 3T3-L1 lipid droplets: hypertrophic adipocytes differentiated for 22 days, phase contrast (panel B), same cells stained for triglycerides in lipid droplets (green, panel D) and nuclei stained with DAPI to show the localization of nuclear DNA (blue, panel C). Superimposed lipid droplets and cellular nucleus (panel E).

doi:10.1371/journal.pone.0173074.g002

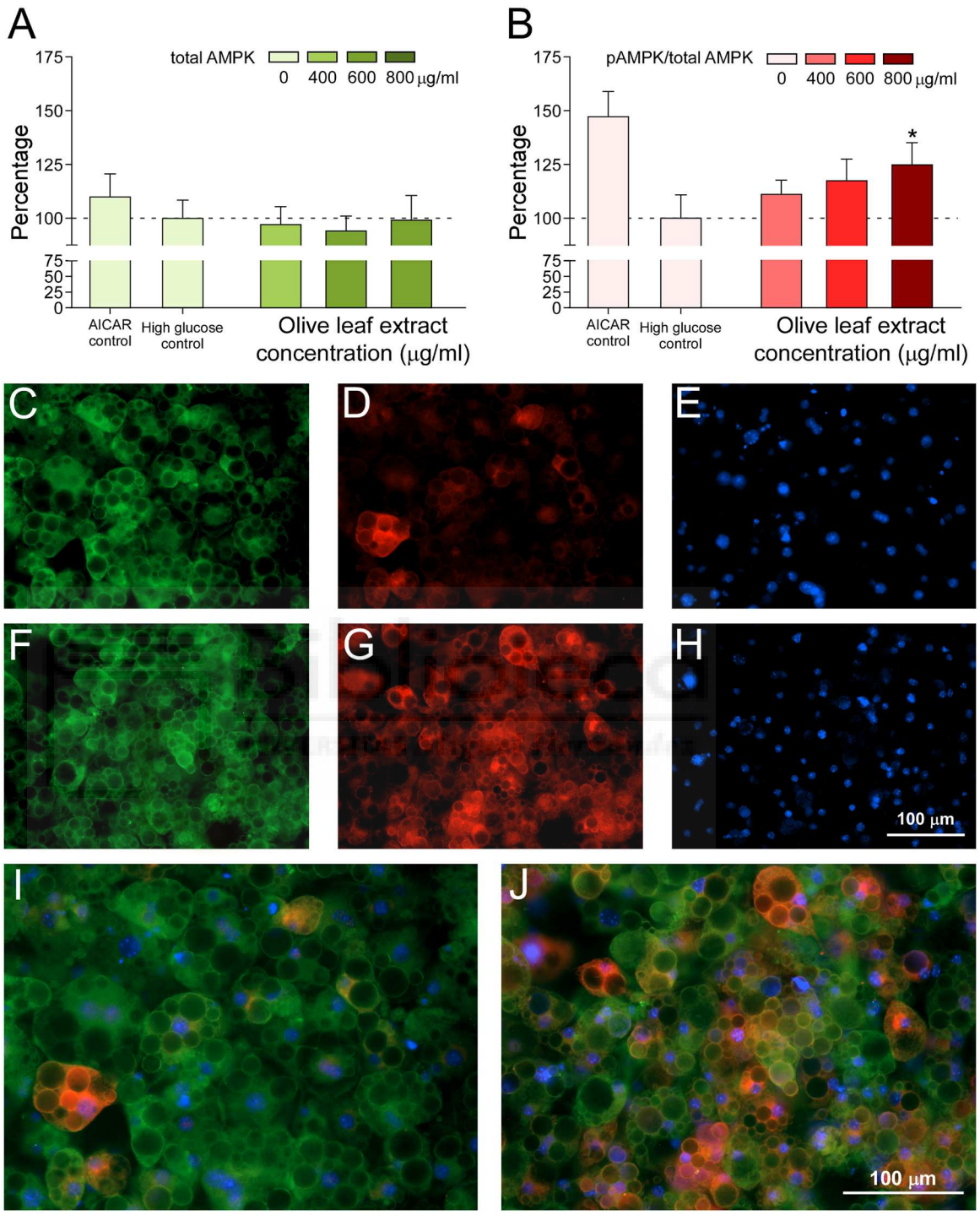

Fig 3. Olive-tree leaves extract activates AMPK in hypertrophic adipocytes. Measurement of the total AMPK expression levels (A) and the activation/inhibition rate (%), measured as the ratio pAMPK/AMPK, (B) Immunofluorescence microscopy of hypertrophic adipocytes treated with 400, 600, and 800 μg/mL of the olive-tree leaves extract and incubated in high glucose medium. Values were normalized with respect to the high glucose control. With comparative aims, the positive control 5-Aminoimidazole-4-carboxamide ribonucleotide (AICAR) has also been included. *p<0.05 indicates significant differences compared to the control incubated in high glucose medium. Representative microphotographs taken with a fluorescence microscope at 20x: control cells incubated in high glucose medium (total AMPK, green fluorescence, C; pAMPK, red fluorescence, D; nuclei, blue fluorescence, E; superimposed image, I) *vs.* cells incubated with 800 μg/mL of olive-tree leaves extract (total AMPK, F; pAMPK, G; nuclei, H; superimposed image, J).

doi:10.1371/journal.pone.0173074.g003

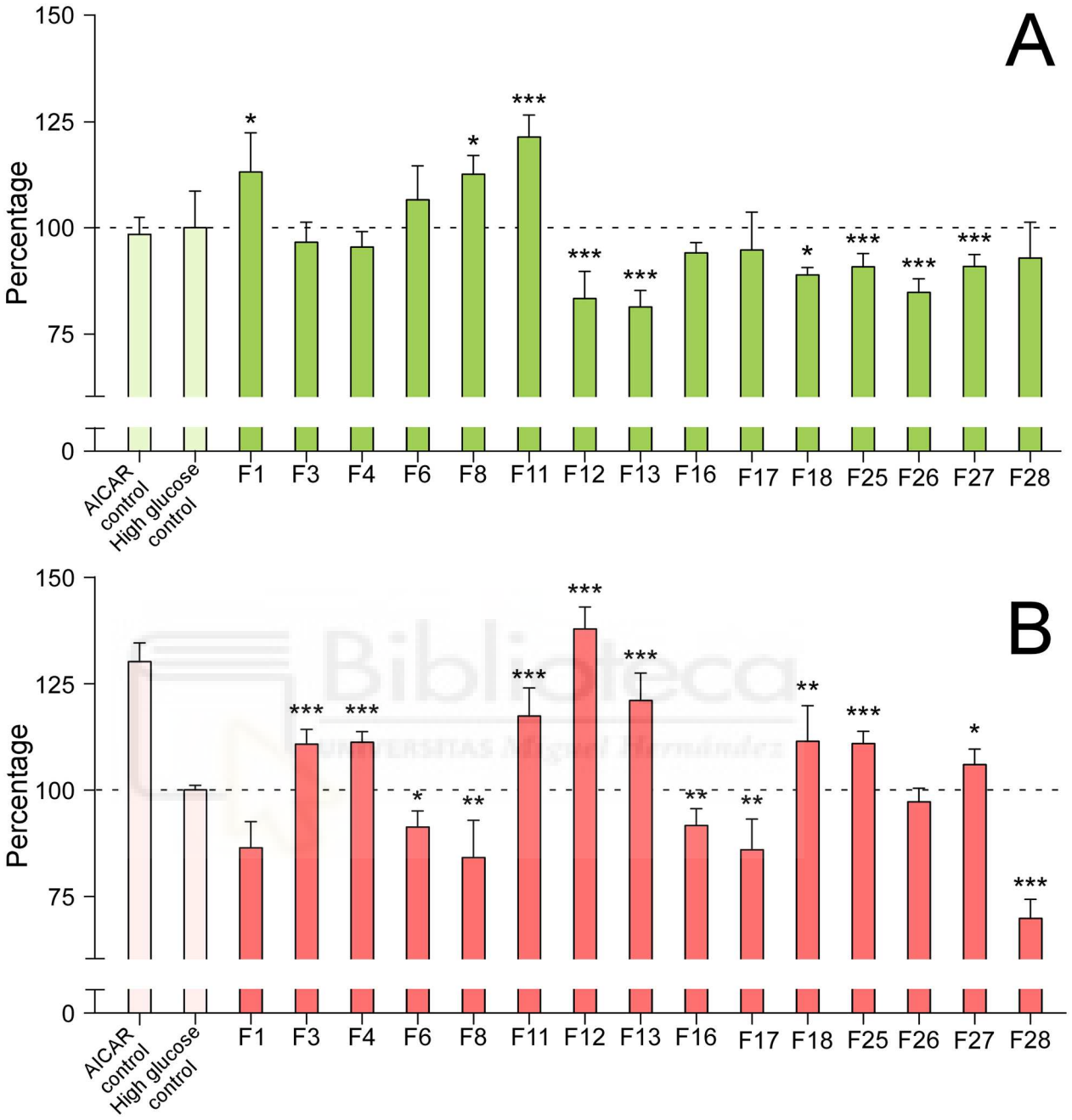

Fig 4. Modulation of AMPK expression and/or activity by Olive-tree leaves fractions. Measurement of the total AMPK expression levels (A) and the activation/inhibition rate (%), measured as the ratio pAMPK/AMPK (B) of the selected olive-tree leaves extract fractions in 3T3-L1 hypertrophic adipocytes. The modulatory effects on the AMPK expression levels and the effects on the pAMPK/AMPK ratio were quantified by immunofluorescence microscopy at a concentration of 400 μg/mL in cells incubated in high glucose medium. Values are normalized with respect to the high glucose control. With comparative aims, the positive control 5-Aminoimidazole-4-carboxamide ribonucleotide (AICAR) was also included. *, **, and *** indicate significant differences with respect to the control incubated in high glucose medium ($p<0.05$, $p<0.01$, and $p<0.001$, respectively).

doi:10.1371/journal.pone.0173074.g004

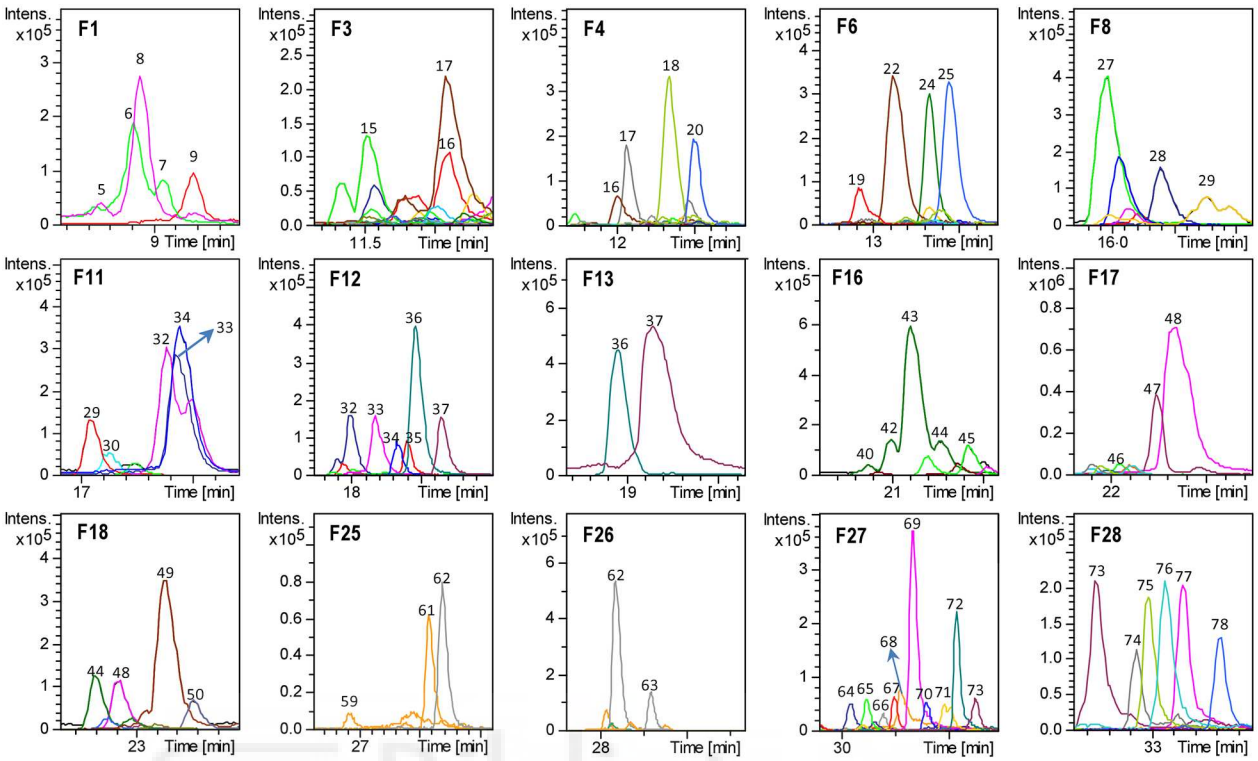

Fig 5. HPLC-MS characterization of the Olive-tree leaves fractions. Base peak chromatogram (BPC) of the selected fractions (F1-F28) in negative ion mode obtained by RP-HPLC-ESI-TOF/MS. The resulting peaks are identified with numbers 1–78, according to the order of elution.

doi:10.1371/journal.pone.0173074.g005

AMPK expression, while some others showed a weak but significant decrease in the AMPK expression levels compared to the controls, i.e., F12, F13, F18, F25, F26 and F27, (Fig 4A). In addition, some fractions showed a significant AMPK activation (F3, F4, F11, F12, F13, F18, F25 and F27), whereas others exhibited an AMPK inhibition (F6, F8, F16, F17 and F28) (Fig 4B).

Those fractions showing activation/inhibition capacity or expression level modulation of AMPK compared to the control were analyzed and fully characterized at the analytical scale by RP-HPLC-ESI-TOF/MS, as described in the Methods, to identify the responsible compounds for such an effect (Fig 5). The rest of the isolated fractions were not subjected to subsequent RP-HPLC-TOF/MS analysis.

Among the fractions showing AMPK activation (Fig 5), fraction 3 contained compounds 15 (oleoside/secologanoside isomer 4), 16 (elenolic acid glucoside/methyloleoside isomer 2), and 17 (*p*-coumaric acid glucoside), the latter being the most abundant compound. Fraction 4 contained compounds 16, 17, 18, and 20 (unknown); fraction 11 was composed of small quantities of compounds 29 (unknown), 30 (demethyloleuropein), and larger quantities of 32 (hydroxyoleuropein/hydroxyoleuroside isomer 1), 33 (glucosyl rhamnosylquercetin isomer 2), and 34 (luteolin rutinoside isomer 2). Fraction 12 contained compounds 32, 33, 34, 35 (olivil), 36 (verbascoside) as major compounds, along with 37 (luteolin glucoside isomer 1). Fraction 13 contained compounds 36, and 37; fraction 18 contained compounds 44 (oleuropein glucoside/neonuezhenide isomer 5), 48 (luteolin glucoside isomer 2), and 49 (diosmetin glucoside) as the major compounds, along with compound 50 (calceolarioside isomer 1). Fraction 25 contained compounds 59 (oleuropein/oleuroside isomer 4), 60 (unknown), and 61 (unknown).

Finally, fraction 27 mostly contained compounds 69 (luteolin) and 72 (unknown) and minor amounts of compounds 64 (unknown), 65 (dimethyl hydroxy octenoyloxi secologanoside isomer 2), 66 (ligstroside isomer 2), 67 (oleuropein methyl ether), 68 (oleuropein/oleuroside isomer 5), 70 (quercetin), 71 (resinoside) and 73 (unknown).

In contrast, some other fractions showed a significant inhibition of AMPK activity (Fig 5) Fraction F6 contained compounds 22 (elenolic acid glucoside/methyloleoside isomer 3), 24 (oleuropein aglycone), and 25 (glucosyl rhamnosyl quercetin -–rutin—isomer), along with minor quantities of compound 19 (unknown). F8 contained mostly compound 27 (phenethyl primeveroside) and also significant amounts of compounds 28 (ethyl-glucopyranosyloxy-oxo-propyl-cyclohexaneacetic acid) and 29 (unknown). F16 mostly contained compound 43 (oleuropein glucoside isomer 4) and minor quantities of compounds 40, 42, 44 (oleuropein glucoside/nuezhenide isomers 2, 3, and 5, respectively), and 45 (diosmetin rhamnoside glucoside—diosmin—isomer 1). F17 contained compounds 47 (apigenin glucoside) and 48 (luteolin glucoside isomer 2) and minor quantities of compound 46 (diosmetin rhamnoside glucoside —diosmin—isomer 2). Finally, F28, which drastically decreased the level of AMPK activation through phosphorylation by 30% ($p<0.001$), contained compounds 73 (unknown), 74 (trihydroxystearic acid), 75 (apigenin), 76 (trihydroxy-octadecenoic acid), 77 (unknown), and 78 (dihydroxyhexadecanoic acid).

Among those fractions showing a potent AMPK activation capacity through phosphorylation, a distinct behavior was observed for the total AMPK expression levels. The total AMPK levels were not significantly altered by fractions 3, and 4, were significantly increased ($p<0.001$) by fraction 11, and were significantly reduced ($p<0.001$) by fractions 12, 13, 18, 25 and 27. Most fractions with inhibitory AMPK activity showed no change in the total AMPK expression levels, i.e., fractions 6, 16, 17 and 28. However, fraction 8 exhibited decreased AMPK expression levels compared to the control.

Molecular docking of the identified compounds against AMPK binding sites

The aim of molecular docking is to predict the structure of the ligand-receptor complex using computational methods. In the current study, all known x-ray structures of AMPK alpha, beta and gamma have been docked with the identified compounds of each fraction (see S3 Fig). The Gibbs free energy variation (ΔG) is represented in Fig 6. All solved structures for the different subunits of AMPK have different co-crystallized ligands, which allows us to define the binding sites on which to perform the molecular docking (see S3 Fig). Additionally, we have performed molecular docking with the x-ray crystallographic ligands over its binding sites as a control of the best ΔG in each binding site. All three x-ray ligands of the AMPK gamma subunit present a $\Delta G \approx -6.5 \pm 0.5$ Kcal/mol when docked over its respective binding sites (PDB: 2UV4, 2UV5, 2UV6, 2UV7, 4CFE, 4CFF, 4RER, 4REW, and 4ZHX). As we can see in Fig 6, when the compounds contained in the Olive-tree leaves fractions bearing biological activity over AMPK (Fig 5) were docked to these three sites of the gamma subunit, the ΔG was less than or equal to the corresponding value for the crystallographic ligands. These results may indicate that these Olive-tree leaves compounds might act as potential ligands for the AMPK gamma subunit.

In contrast, when the same compounds were docked against the AMPK alpha subunit binding site or the AMPK beta subunit regulatory binding site, the ΔG for the Olive-tree leaves compounds exhibited higher values than those shown by the respective x-ray ligands of these binding sites. Only a few compounds showed ΔG values that were relatively close to those observed for the x-ray ligands, i.e., lower than -8.0 ± 0.5 Kcal/mol. These included compounds

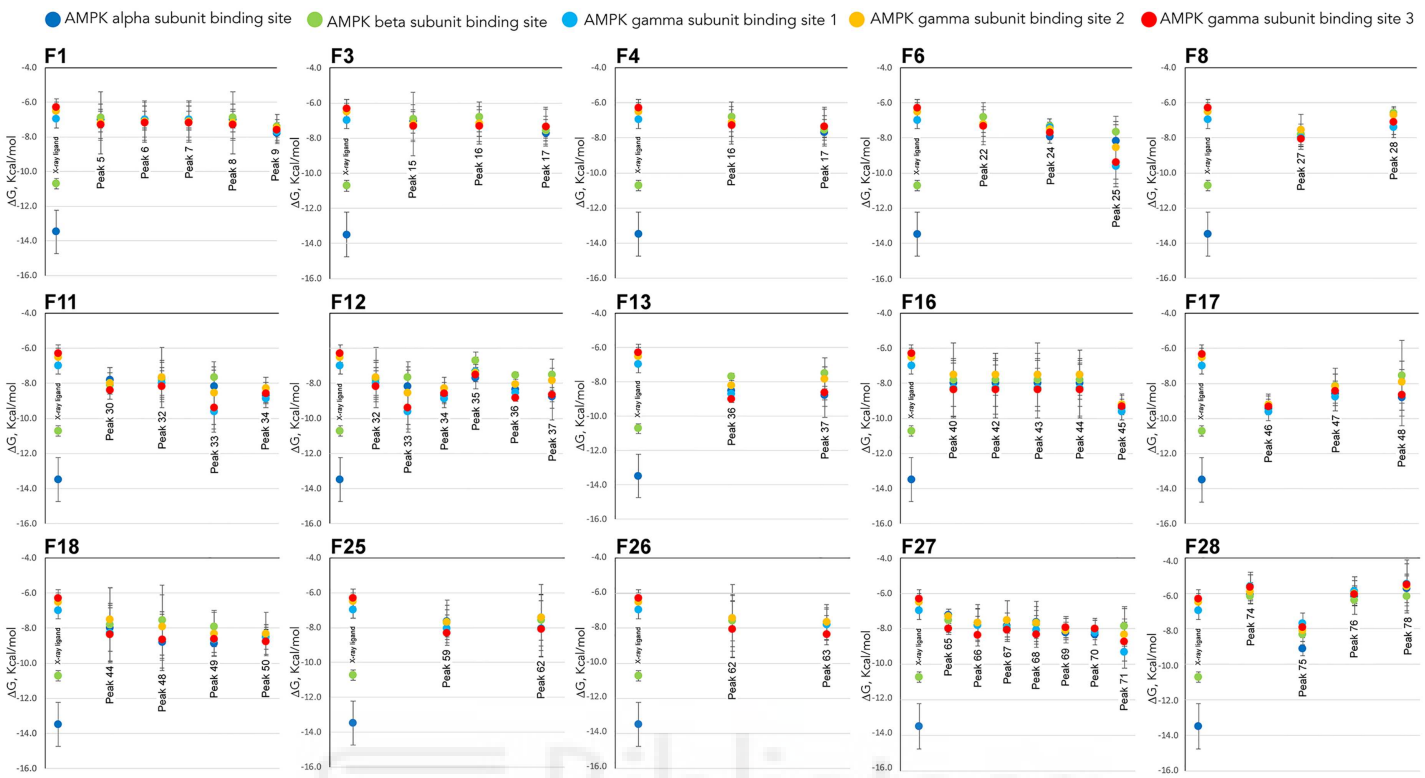

Fig 6. Comparison of the free energy variation (ΔG) of the Olive-tree leaves phenolic compounds and ligand against the binding sites of the three AMPK subunits obtained by molecular docking. Comparison of the free energy variation (ΔG) for all the identified compounds (Table 1 and S2 Fig) contained in those fractions showing activation/inhibition capacity of AMPK (Figs 4 and 5), based on molecular docking analysis against all known binding sites of AMPK (S3 Fig).

doi:10.1371/journal.pone.0173074.g006

34, 36, 37, 45, 46, 47, 48, 49, 69, 70, 71 and 75 for the AMPK alpha subunit and compounds 34, 45, 46, 47, 50, 69, 70 and 75 for the AMPK beta subunit regulatory binding site.

Discussion

Plant polyphenols are the most intensively studied natural products, as they are a recognized source of active compounds used to alleviate noncommunicable diseases such as obesity [16,27]. Plant derived polyphenols such as epigallocatechin gallate from green tea, resveratrol from grapes, curcumin from turmeric, quercetin from onion, phenylpropanoids from *Lippia citriodora*, or anthocyanins/flavonols from *Hibiscus sabdariffa* [4,16,17,24,28] have demonstrated either the inhibition of adipogenesis or the attenuation of intracellular lipid accumulation in 3T3-L1 adipocytes, a well characterized model of *in vitro* adipogenesis that becomes hypertrophic and insulin resistant when induced with high-glucose conditions [16,23,24]. Nevertheless, to date, there are no other reports on this ameliorative effect for Olive-tree leaves extracts. Our results suggest that Olive-tree leaves extracts have the potential to reduce lipid accumulation in hypertrophic and insulin resistant adipocytes. AMPK activation by phosphorylation at Thr-172 has also been correlated with a reduced lipid accumulation in the cytoplasm of 3T3-L1 adipocytes by several phenolic extracts [16,24,29], which is in agreement with our results of Olive-tree leaves extracts from using hypertrohic adipocytes.

In this regard, several lines of evidence have indicated a direct link between AMPK and lipid metabolism. It has been reported that AMPK exerts multiple effects that lead to the

normalization of lipid metabolism in adipose tissue. It directly phosphorylates acetylCoA carboxylase (ACC), which leads to the inhibition of fatty acid synthesis and the stimulation of fatty acid uptake into mitochondria through malonylCoA decrease [15,30]. It inhibits lipolysis through the phosphorylation of hormone sensitive lipase [31]. It inhibits the synthesis of triglycerides and phospholipids via the inactivation of glycerol phosphate acyl transferase (GPAT), and it downregulates the transcription of lipogenic genes, including those encoding ACC, fatty acid synthase (FAS), and GPAT [32,33]. Although the Olive-tree leaves extract is able to reduce the intracellular lipid accumulation in 3T3-L1 hypertrophic adipocytes through AMPK-dependent mechanisms, more studies will need to be performed to decipher which downstream targets are involved.

The fractionation of the Olive-tree leaves extract through semi-preparative RP-HPLC-ESI-TOF/MS allowed us to delimit the number of possible candidate compounds responsible for the observed activation of AMPK. Specifically, the components that might contribute to this effect in a higher extent belonged to the secoiridoids (isomers of oleoside/secologanoside, elenolic acid glucoside/methyloleoside, demethyloleuropein, hydroxyoleuropein/hydroxyoleuroside, oleuropein glucoside/neonuezhenide, oleuropein/oleuroside isomers, dimethyl hydroxy octenoyloxi secologanoside, ligstroside, oleuropein methyl ether), the cinnamic acids, phenylethanoids and phenylpropanoids (*p*-coumaric acid glucoside, verbascoside, and calcelarioside isomers), the flavonoids (isomers of glucosyl rhamnosylquercetin—rutin–, luteolin rutinoside, luteolin glucoside, diosmetin glucoside, luteolin, quercetin, resinoside), and the lignans (olivil) subclassess. The fact that fractions 12 and 13 share compounds 36 (verbascoside) and 37 (luteolin glucoside isomer 1) and that the adjacent fraction (14) contained almost exclusively compound 37 and did not exhibit AMPK activation suggests that verbascoside could be the main agent responsible for AMPK activation in these fractions. However, confirmation with the pure standard should be carried out to verify this hypothesis. Moreover, elenolic acid glucoside and -coumaric glucoside, which are both present in fractions 3 and 4, diosmetin glucoside in fraction 18, unknown compounds 61 and 62 in fraction 25 and luteolin and unknown compound 72 in fraction 27, might contribute to the observed AMPK activation in these particular fractions.

It should be highlighted that fractions F11, F12 and F13, which contained verbascoside (F12 and F13), and hydroxyoleuropein, rutin and luteolin rutinoside (F11 and F12) exhibited the maximum level of AMPK activation, and this activation was as potent as that obtained with the AMPK synthetic activator AICAR. In agreement with our results, lemon verbena polyphenolic extract and its major compound verbascoside have recently exhibited the capacity to activate AMPK concomitantly to the peroxisome proliferator-activated receptor gamma (PPAR-gamma)-dependent transcriptional upregulation of adiponectin, the upregulation of PPAR-alpha mRNA expression and the downregulation of the mRNA expression of fatty acid synthase [16].

The molecular mechanism by which these Olive-tree leaves polyphenols exert their activation needs to be elucidated. On the one hand, these compounds may reach upstream AMPK targets such as LKB1 or CaMKKβ kinases, adipokines or ROS-dependent calcium channel activation [10,11,14]. Furthermore, our *in silico* study also suggests the possibility that some Olive-tree leaves polyphenols may act as direct modulators of AMPK at different binding sites. The binding of AMP to the gamma subunit causes the allosteric activation of AMPK kinase. The binding of either AMP or ADP promotes and maintains the phosphorylation of threonine 172 within the activation loop of the kinase [8]. Increased AMPK activity leads to a concomitant increase in the phosphorylation of its downstream targets. In addition to regulation by adenine nucleotides, a number of small molecules have been identified that directly activate AMPK [34]. The kinase domain of the α-subunit and the carbohydrate-binding module of the

β-subunit are connected and define a new regulatory binding site (see S3 Fig, panels C and D). Molecular docking of the A-769662 compound, a small activator of AMPK kinase [35] for this regulatory site, presents a $\Delta G \approx -10.72 \pm 0.30$ Kcal/mol. Several compounds identified by RP-HPLC-TOF/MS show good enough ΔG values to be considered as putative AMPK ligands or regulators, i.e., $-10.1 \pm 0.8 < \Delta G < 8.0 \pm 0.2$ Kcal/mol. As an example, the compounds demethyloleuropein, 10-hydroxyoleuropein, (7"S)-hydroxyoleuropein, luteolin 7-rutinoside, diosmin, quercetin, etc., satisfy this condition and could, therefore, have a regulatory effect on this binding site, although obviously with less intensity than the activator A-769662. Staurosporine is an ATP-competitive kinase inhibitor that binds to many kinases with a high affinity, though with little selectivity. This compound is co-crystalized at the ATP-binding site of the AMPK alpha subunit (PDB: 4CFE, 4CFF, 4ZHX, and 5EZV), and its molecular coupling shows a $\Delta G \approx -13.5 \pm 1.3$ Kcal/mol. Free energy variation of all identified compounds from the Olive-tree leaves AMPK alpha subunit have significantly higher values than staurosporine; therefore, no inhibitory effect on the AMPK catalytic subunit should be expected for these compounds. However, some of these compounds could act as fine regulators of the AMPK alpha subunit and beta subunit.

It has been reported that polyphenols such as *p*-coumaric, luteolin, and quercetin, in their aglycone form, are able to increase the phosphorylation of AMPK in 3T3-L1 cells [16,31,36,37]. Unlike previous findings, our results also suggest that some of the phenolic compounds from Olive-tree leaves exhibit AMPK activation as glycosides when added to the extracellular media. In agreement with our results, some authors have demonstrated the antiadipogenic effect of luteolin glucoside on 3T3-L1 adipocytes, which might indicate that such phenolic glucosides could either be able to go through the plasmatic membrane [15] or could be metabolized to luteolin aglycone at the intracellular level. The fact that the treatment of adipocytes or hepatocytes with PPAR activators, such as plant polyphenols [26], enhanced glucuronidation activity and UDP-glucuronosyltransferase expression suggests that the glucuronide metabolites of polyphenols may also reach intracellular targets [38]. Surprisingly, other authors have found an adipogenic effect of quercetin (10 μM) on human mesenchymal stem cells [39]. This apparent discrepancy may be attributed to the different experimental model used or even to the different adipogenic induction timing. In any case, the inhibitory capacity of quercetin on adipogenesis is well documented in murine cell and animal model [28,40]. An explanation could be that differentiation into adipocytes may be independent of mitotic clonal expansion depending on the type of cell line.

However, we should express caution when extrapolating cell model data to in vivo conditions. Most glycosylated phenolic compounds are converted into their aglycones on the cell surface of the intestinal epithelial cells and bacteria. Upon absorption, the aglycone forms are subjected to enzymatic modification, and their different metabolites, (glucuronide, sulfated, or methylated metabolites) reach their target tissues and organs [24].

Most of the fractions showing inhibitory activity on AMPK (F6, F8, F16, F17 and F28) behaved as mild inhibitors. Nevertheless, the potent inhibitory effect of fraction 28 ($p<0.001$), which contains the flavone apigenin among other compounds, should be noted. Although apigenin has been shown to have an antiadipogenic effect through AMPK activation in the adipocyte model [41], the inhibitory effect of this fraction could be due to the inhibition of AMPK reported for some saturated fatty acids also present in this fraction [42]. In relation to the potential inhibitory mechanism, it is known that the phosphorylation of AMPK is reversed by phosphatases, although the exact mechanisms that modulate this action remain poorly understood [43].

Although beyond the scope of the present study, it has been found that the overactivation of AMPK has been observed in several neurodegenerative diseases, such as Alzheimer's

disease, progressive supranuclear palsy, corticobasal degeneration, Pick's disease, Parkinson's disease, and others [7]. Therefore, AMPK inhibitors could also be relevant as therapeutic therapies against these types of diseases.

Some secoiridoids from extra virgin olive oil, i.e., oleuropein aglycone and decarboxymethyl oleuropein aglycone, have been demonstrated to activate AMPK, which results in the inhibition of the mammalian target of rapamycin (mTOR) in breast cancer cells [18,27]. It has been postulated that chronic diseases associated with aging, such as cancer or obesity, are driven by the overactivation of the nutrient-sensing mTOR gerogene due to the loss of responsiveness to active AMPK, a suppressor of mTOR. In this manner, some secoiridoids from the Olive-tree may act as gerosuppressors, triggering AMPK activation and exerting a transcriptomic signature that reduces mTOR-driven aging. In agreement with this assumption, our findings support the hypothesis that some secoiridoids from *Olea europaea* (oleoside/secologanoside, elenolic acid glucoside, demethyloleuropein/demethyloleuroside, oleuropein/oleuroside, oleuropein glucoside and hydroxyoleuropein/ hydroxyoleuroside) may contribute to the activation of AMPK by Olive-tree leaves extract in 3T3-L1 adipocytes, although this should be confirmed using isolated pure compounds in the cell model.

Due to the diverse nature of the natural AMPK activators, one important question arises: how do they manage to activate AMPK despite the fact that their structures are so different? A previous study that used a cell line expressing an AMP- and ADP- insensitive AMPK mutant proposed that phenolic compounds such as quercetin activate AMPK indirectly by increasing cellular AMP and ADP levels, usually by inhibiting mitochondrial ATP synthesis [44]. It has also been reported that oleuropein aglycone indirectly actives AMPK through calcium concentration increases and the subsequent activation of CaMKKβ in SH-SY5Y neuroblastoma cells [19]. Nevertheless, the direct activation of kinases, such as AMPK, by phenolic compounds at the nucleotide binding site has also been proposed [45,46], which is consistent with our results. Whether phenolic compounds exert their AMPK modulation through direct or indirect mechanisms in our cell model should be further confirmed.

Our evidences support that Olive-tree may become a source for bioactive compounds with a potential use in chronic human diseases. Nevertheless, olive-tree leaves composition show a remarkable variability due to location, climate, cultivation practices and seasonal factors. Understanding the factors that control the genetic basis of fruit and leave composition may be necessary for the harvesting and production of suitable extracts to be applied in human health [47,48].

Conclusion

Olive-tree leaves extract decreases intracellular lipid accumulation through AMPK-dependent mechanisms in a hypertrophic and insulin resistant adipocyte model. The fractionation of the extract revealed that fractions containing compounds that belonged to the secoiridoids, cinnamic acids, phenylethanoids and phenylpropanoids, flavonoids and lignans subclasses were the best candidates to account for such effects. Our *in silico* results suggest the possibility that some of these compounds may be considered putative AMPK ligands or regulators at the three sites of the AMPK gamma subunit. However, the interaction of these compounds with the AMPK alpha subunit binding site or the AMPK beta subunit regulatory binding site is less probable, although a subtle regulation may occur. In conclusion, Olive-tree leaves compounds deserve further attention as a therapeutic aid in the management of obesity and/or its associated disturbances. Nevertheless, further research using pure isolated compounds in cell and animal models and including cell metabolic studies will be required to identify the compounds responsible for such effects.

Supporting information

S1 Fig. Proposed molecular structure of the identified compounds showed on Table 1 for selected fractions with biological activity over AMPK kinase.
(DOCX)

S2 Fig. Base Peak Chromatogram (BPC) made by HPLC-ESI-TOF. This BPC was obtained in negative ion mode of the olive leaf extract, with the optimized semi-preparative conditions, and the collected fractions highlighted in blue.
(DOCX)

S3 Fig. AMPK binding sites. Panels A, C and E show the secondary structure of alpha, beta and gamma subunits of AMPK kinase (4CFE.pdb), respectively. Panels B, D and F represent the electrostatic potential surface with a co-crystalized ligand indicating the position of each binding sites.
(DOCX)

Acknowledgments

This work was supported by the projects BFU2014-52433-C3-2-R, AGL2011-29857-C03-02 (Spanish Ministry of Science and Innovation); projects AGL2015-67995-C3-1-R, AGL2015-67995-C3-2-R, AGL2015-67995-C3-3-R, Torres Quevedo grants PTQ-13-06429 and PTQ-14-07243 and scholarship FPU AP2010-2793 from the Spanish Ministry of Economy and Competitiveness (MINECO); P09-CTS-4564, P10-FQM-6563 and P11-CTS-7625 grants from Andalusian Regional Government Council of Innovation and Science; PROMETEO/2016/006, and ACIF/2016/230 from Generalitat Valenciana; CIBER (CB12/03/30038, Fisiopatologia de la Obesidad y la Nutricion, CIBERobn, Instituto de Salud Carlos III).

Author Contributions

Conceptualization: CJS MOV MHL JLS ASC JAE VM.

Data curation: CJS MOV.

Formal analysis: MHL JAE VM.

Funding acquisition: MHL JLS ASC AFG JAE VM.

Investigation: CJS CRP JAE.

Methodology: CJS MOV MHL CRP.

Project administration: MHL ASC AFG JAE VM.

Resources: ASC AFG JAE VM.

Software: MHL JAE.

Supervision: MOV MHL JLS JAE VM.

Validation: ASC MHL JAE VM.

Visualization: CJS MHL MOV JAE.

Writing – original draft: CJS JAE VM.

Writing – review & editing: MHL JLS JAE VM.

References

1. Siriwardhana N, Kalupahana NS, Cekanova M, LeMieux M, Greer B, Moustahid—Moussa N. Modulation of adipose tissue inflammation by bioactive food compounds. J Nutr Biochem. 2013; 24: 613–623. doi: 10.1016/j.jnutbio.2012.12.013 PMID: 23498665
2. Ma S, Jing F, Xu C, Zhou L, Song Y, Yu C, et al. Thyrotropin and obesity: increased adipose triglyceride content through glycerol-3-phosphate acyltransferase 3. Sci Rep. 2015; 5: 7633. doi: 10.1038/srep07633 PMID: 25559747
3. Kalupahana NS, Moustaid-Moussa N, Claycombe KJ. Immunity as a link between obesity and insulin resistance. Mol Aspects Med. 2012; 33: 26–34. doi: 10.1016/j.mam.2011.10.011 PMID: 22040698
4. Wang S, Moustaid-Moussa N, Chen L, Mo H, Shastri A, Su R, et al. Novel insights of dietary polyphenols and obesity. J Nutr Biochem. 2014; 25: 1–18. doi: 10.1016/j.jnutbio.2013.09.001 PMID: 24314860
5. Bijland S, Mancini SJ, Salt IP. Role of AMP-activated protein kinase in adipose tissue metabolism and inflammation. Clin Sci (Lond). 2013; 124: 491–507.
6. Carling D, Thornton C, Woods A, Sanders MJ. AMP-activated protein kinase: new regulation, new roles? Biochem J. 2012; 445: 11–27. doi: 10.1042/BJ20120546 PMID: 22702974
7. Novikova DS, Garabadzhiu AV, Melino G, Barlev NA, Tribulovich VG. AMP-activated protein kinase: structure, function, and role in pathological processes. Biochemistry (Mosc). 2015; 80: 127–144.
8. Xiao B, Sanders MJ, Underwood E, Heath R, Mayer FV, Carmena D, et al. Structure of mammalian AMPK and its regulation by ADP. Nature. 2011; 472: 230–233. doi: 10.1038/nature09932 PMID: 21399626
9. Shaw RJ, Kosmatka M, Bardeesy N, Hurley RL, Witters LA, DePinho RA, et al. The tumor suppressor LKB1 kinase directly activates AMP-activated kinase and regulates apoptosis in response to energy stress. Proc Natl Acad Sci USA. 2004; 101: 3329–3335. doi: 10.1073/pnas.0308061100 PMID: 14985505
10. Shackelford DB, Shaw RJ. The LKB1-AMPK pathway: metabolism and growth control in tumour suppression. Nat Rev Cancer. 2009; 9: 563–575. doi: 10.1038/nrc2676 PMID: 19629071
11. Woods A, Dickerson K, Heath R, Hong SP, Momcilovic M, Johnstone SR, et al. Ca2+/calmodulin-dependent protein kinase kinase-beta acts upstream of AMP-activated protein kinase in mammalian cells. Cell Metab. 2005; 2: 21–33. doi: 10.1016/j.cmet.2005.06.005 PMID: 16054096
12. Sanders MJ, Grondin PO, Hegarty BD, Snowden MA, Carling D. Investigating the mechanism for AMP activation of the AMP-activated protein kinase cascade. Biochem J. 2007; 403: 139–148. doi: 10.1042/BJ20061520 PMID: 17147517
13. Hardie DG, Ross FA, Hawley SA. AMPK: a nutrient and energy sensor that maintains energy homeostasis. Nat Rev Mol Cell Biol. 2012; 13: 251–262. doi: 10.1038/nrm3311 PMID: 22436748
14. Ko HJ, Lo CY, Wang BJ, Chiou RYY, Lin SM. Theaflavin-3,3'-digallate, a black tea polyphenol, stimulates lipolysis associated with the induction of mitochondrial uncoupling proteins and AMPK-FoxO3A-MnSOD pathway in 3T3-L1 adipocytes. J Funct Foods. 2015; 17: 271–282.
15. Kim J, Lee I, Seo J, Jung M, Kim Y, Yim N, et al. Vitexin, orientin and other flavonoids from Spirodela polyrhiza inhibit adipogenesis in 3T3-L1 cells. Phytother Res. 2010; 24: 1543–1548. doi: 10.1002/ptr.3186 PMID: 20878708
16. Herranz-Lopez M, Barrajon-Catalan E, Segura-Carretero A, Menendez JA, Joven J, Micol V. Lemon verbena (*Lippia citriodora*) polyphenols alleviate obesity-related disturbances in hypertrophic adipocytes through AMPK-dependent mechanisms. Phytomedicine. 2015; 22: 605–614. doi: 10.1016/j.phymed.2015.03.015 PMID: 26055125
17. Joven J, Espinel E, Rull A, Aragones G, Rodriguez-Gallego E, Camps J, et al. Plant-derived polyphenols regulate expression of miRNA paralogs miR-103/107 and miR-122 and prevent diet-induced fatty liver disease in hyperlipidemic mice. Biochim Biophys Acta. 2012; 1820: 894–899. doi: 10.1016/j.bbagen.2012.03.020 PMID: 22503922
18. Menendez JA, Joven J, Aragones G, Barrajon-Catalan E, Beltran-Debon R, Borrás-Linares I, et al. Xenohormetic and anti-aging activity of secoiridoid polyphenols present in extra virgin olive oil: a new family of gerosuppressant agents. Cell Cycle. 2013; 12: 555–578. doi: 10.4161/cc.23756 PMID: 23370395
19. Rigacci S, Miceli C, Nediani C, Berti A, Cascella R, Pantano D, et al. Oleuropein aglycone induces autophagy via the AMPK/mTOR signalling pathway: a mechanistic insight. Oncotarget. 2015; 6: 35344–35357. doi: 10.18632/oncotarget.6119 PMID: 26474288
20. Talhaoui N, Gomez-Caravaca AM, Leon L, De la Rosa R, Segura-Carretero A, Fernández-Gutiérrez A. Determination of phenolic compounds of 'Sikitita' olive leaves by HPLC-DAD-TOF-MS. Comparison with its parents 'Arbequina' and 'Picual' olive leaves. LWT—Food Sci Technol. 2014; 58: 28–34.

21. Quirantes-Pine R, Lozano-Sanchez J, Herrero M, Ibanez E, Segura-Carretero A, Fernández-Gutiérrez A. HPLC-ESI-QTOF-MS as a Powerful Analytical Tool for Characterising Phenolic Compounds in Olive-leaf Extracts. Phytochem Anal. 2013; 24: 213–223. doi: 10.1002/pca.2401 PMID: 22987739

22. Lozano-Sanchez J, Segura-Carretero A, Menendez JA, Oliveras-Ferraros C, Cerretani L, Fernández-Gutiérrez A. Prediction of extra virgin olive oil varieties through their phenolic profile. Potential cytotoxic activity against human breast cancer cells. J Agric Food Chem. 2010; 58: 9942–9955. doi: 10.1021/jf101502q PMID: 20795736

23. Green H, Kehinde O. An established preadipose cell line and its differentiation in culture. II. Factors affecting the adipose conversion. Cell. 1975; 5: 19–27. PMID: 165899

24. Herranz-Lopez M, Fernandez-Arroyo S, Perez-Sanchez A, Barrajon-Catalan E, Beltran-Debon R, Menéndez JA, et al. Synergism of plant-derived polyphenols in adipogenesis: perspectives and implications. Phytomedicine. 2012; 19: 253–261. doi: 10.1016/j.phymed.2011.12.001 PMID: 22280831

25. Feoktistova M, Geserick P, Leverkus M. Crystal Violet Assay for Determining Viability of Cultured Cells. Cold Spring Harb Protoc. 2016;

26. Encinar JA, Fernandez-Ballester G, Galiano-Ibarra V, Micol V. In silico approach for the discovery of new PPARgamma modulators among plant-derived polyphenols. Drug Des Devel Ther. 2015; 9: 5877–5895. doi: 10.2147/DDDT.S93449 PMID: 26604687

27. Barrajon-Catalan E, Herranz-Lopez M, Joven J, Segura-Carretero A, Alonso-Villaverde C, Menéndez JA, et al. Molecular promiscuity of plant polyphenols in the management of age-related diseases: far beyond their antioxidant properties. Adv Exp Med Biol. 2014; 824: 141–159. doi: 10.1007/978-3-319-07320-0_11 PMID: 25038998

28. Moon J, Do HJ, Kim OY, Shin MJ. Antiobesity effects of quercetin-rich onion peel extract on the differentiation of 3T3-L1 preadipocytes and the adipogenesis in high fat-fed rats. Food and Chem Toxicol. 2013; 58: 347–354.

29. Sung J, Lee J. Capsicoside G, a furostanol saponin from pepper (*Capsicum annuum* L.) seeds, suppresses adipogenesis through activation of AMP-activated protein kinase in 3T3-L1 cells. J Funct Foods. 2016; 20: 148–158.

30. Gonzalez-Barroso MM, Anedda A, Gallardo-Vara E, Redondo-Horcajo M, Rodriguez-Sanchez L, Rial E. Fatty acids revert the inhibition of respiration caused by the antidiabetic drug metformin to facilitate their mitochondrial beta-oxidation. Biochim Biophys Acta. 2012; 1817: 1768–1775. doi: 10.1016/j.bbabio.2012.02.019 PMID: 22386881

31. Kang SI, Shin HS, Kim HM, Hong YS, Yoon SA, Kang SW, et al. Immature *Citrus sunki* peel extract exhibits antiobesity effects by beta-oxidation and lipolysis in high-fat diet-induced obese mice. Biol Pharm Bull. 2012; 35: 223–230. PMID: 22293353

32. Li Y, Xu S, Mihaylova MM, Zheng B, Hou X, Jiang B, et al. AMPK phosphorylates and inhibits SREBP activity to attenuate hepatic steatosis and atherosclerosis in diet-induced insulin-resistant mice. Cell Metab. 2011; 13: 376–388. doi: 10.1016/j.cmet.2011.03.009 PMID: 21459323

33. Yuan HD, Piao GC. An active part of Artemisia sacrorum Ledeb. inhibits adipogenesis via the AMPK signaling pathway in 3T3-L1 adipocytes. Int J Mol Med. 2011; 27: 531–536. doi: 10.3892/ijmm.2011.620 PMID: 21327327

34. Cool B, Zinker B, Chiou W, Kifle L, Cao N, Perham M, et al. Identification and characterization of a small molecule AMPK activator that treats key components of type 2 diabetes and the metabolic syndrome. Cell Metab. 2006; 3: 403–416. doi: 10.1016/j.cmet.2006.05.005 PMID: 16753576

35. Goransson O, McBride A, Hawley SA, Ross FA, Shpiro N, Foretz M, et al. Mechanism of action of A-769662, a valuable tool for activation of AMP-activated protein kinase. J Biol Chem. 2007; 282: 32549–32560. doi: 10.1074/jbc.M706536200 PMID: 17855357

36. Strobel P, Allard C, Perez-Acle T, Calderon R, Aldunate R, Leighton F. Myricetin, quercetin and catechin-gallate inhibit glucose uptake in isolated rat adipocytes. Biochem J. 2005; 386: 471–478. doi: 10.1042/BJ20040703 PMID: 15469417

37. Xiao N, Mei F, Sun Y, Pan G, Liu B, Liu K. Quercetin, luteolin, and epigallocatechin gallate promote glucose disposal in adipocytes with regulation of AMP-activated kinase and/or sirtuin 1 activity. Planta Med. 2014; 80: 993–1000. doi: 10.1055/s-0034-1382864 PMID: 25057854

38. Barbier O, Villeneuve L, Bocher V, Fontaine C, Torra IP, Duhem C, et al. The UDP-glucuronosyltransferase 1A9 enzyme is a peroxisome proliferator-activated receptor alpha and gamma target gene. J Biol Chem. 2003; 278: 13975–13983. doi: 10.1074/jbc.M300749200 PMID: 12582161

39. Casado-Diaz A, Anter J, Dorado G, Quesada-Gomez JM. Effects of quercetin, a natural phenolic compound, in the differentiation of human mesenchymal stem cells (MSC) into adipocytes and osteoblasts. J Nutr Biochem. 2016; 32: 151–162. doi: 10.1016/j.jnutbio.2016.03.005 PMID: 27142748

40. Seo MJ, Lee YJ, Hwang JH, Kim KJ, Lee BY. The inhibitory effects of quercetin on obesity and obesity-induced inflammation by regulation of MAPK signaling. J Nutr Biochem. 2015; 26: 1308–1316. doi: 10.1016/j.jnutbio.2015.06.005 PMID: 26277481

41. Ono M, Fujimori K. Antiadipogenic effect of dietary apigenin through activation of AMPK in 3T3-L1 cells. J Agric Food Chem. 2011; 59: 13346–13352. doi: 10.1021/jf203490a PMID: 22098587

42. Kwon B, Querfurth HW. Palmitate activates mTOR/p70S6K through AMPK inhibition and hypophosphorylation of raptor in skeletal muscle cells: Reversal by oleate is similar to metformin. Biochimie. 2015; 118: 141–150. doi: 10.1016/j.biochi.2015.09.006 PMID: 26344902

43. Russo GL, Russo M, Ungaro P. AMP-activated protein kinase: a target for old drugs against diabetes and cancer. Biochem Pharmacol. 2013; 86: 339–350. doi: 10.1016/j.bcp.2013.05.023 PMID: 23747347

44. Hawley SA, Ross FA, Chevtzoff C, Green KA, Evans A, Fogarty S, et al. Use of cells expressing gamma subunit variants to identify diverse mechanisms of AMPK activation. Cell Metab. 2010; 11: 554–565. doi: 10.1016/j.cmet.2010.04.001 PMID: 20519126

45. Corominas-Faja B, Santangelo E, Cuyas E, Micol V, Joven J, Ariza X, et al. Computer-aided discovery of biological activity spectra for anti-aging and anti-cancer olive oil oleuropeins. Aging (Albany NY). 2014; 6: 731–741.

46. Taha MO, Khanfar MA. Oleuropein potently inhibits mammalian target of rapamycin: possible involvement of tandem anomeric hyperconjugation-Michael reaction. Med Chem Res. 2015; 24: 616–623.

47. Dundar E, Suakar O, Unver T, Dagdelen A. Isolation and expression analysis of cDNAs that are associated with alternate bearing in Olea europaea L. cv. Ayvalik. BMC Genomics. 2013; 14: 219. doi: 10.1186/1471-2164-14-219 PMID: 23552171

48. Yanik H, Turktas M, Dundar E, Hernandez P, Dorado G, Unver T. Genome-wide identification of alternate bearing-associated microRNAs (miRNAs) in olive (*Olea* europaea L.). BMC Plant Biol 2013; 13: 10. doi: 10.1186/1471-2229-13-10 PMID: 23320600

49. Guinda A, Castellano JM, Santos-Lozano JM, Delgado-Hervas T, Gutierrez-Adanez P, Rada M. Determination of major bioactive compounds from olive leaf. LWT—Food Sci Technol. 2015; 64: 431–438.

50. Peralbo-Molina A, Priego-Capote F, Luque de Castro MD. Tentative identification of phenolic compounds in olive pomace extracts using liquid chromatography-tandem mass spectrometry with a quadrupole-quadrupole-time-of-flight mass detector. J Agric Food Chem. 2012; 60: 11542–11550. doi: 10.1021/jf302896m PMID: 23106267

51. Toth G, Alberti A, Solyomvary A, Barabas C, Boldizsar I, Noszal B. Phenolic profiling of various olive bark-types and leaves: HPLC-ESI/MS study. Ind Crops Prod. 2015; 67: 432–438.

52. Fu S, Arraez-Roman D, Segura-Carretero A, Menendez JA, Menendez-Gutierrez MP, MIcol V, et al. Qualitative screening of phenolic compounds in olive leaf extracts by hyphenated liquid chromatography and preliminary evaluation of cytotoxic activity against human breast cancer cells. Anal Bioanal Chem. 2010; 397: 643–654. doi: 10.1007/s00216-010-3604-0 PMID: 20238105

53. Michel T, Khlif I, Kanakis P, Termentzi A, Allouche N, Halabalaki M, et al. UHPLC-DAD-FLD and UHPLC-HRMS/MS based metabolic profiling and characterization of different Olea europaea organs of Koroneiki and Chetoui varieties. Phytochem Lett. 2015; 11: 424–439.

54. Talhaoui N, Gomez-Caravaca AM, Roldan C, Leon L, De la Rosa R, Fernández-Gutiérrez A, et al. Chemometric Analysis for the Evaluation of Phenolic Patterns in Olive Leaves from Six Cultivars at Different Growth Stages. J Agric Food Chem. 2015; 63: 1722–1729. doi: 10.1021/jf5058205 PMID: 25613562

55. Borja R, Martin A, Maestro R, Alba J, Fiestas JA. Enhancement of the anaerobic-digestion of olive mill waste-water by the removal of phenolic inhibitors. Process Biochem. 1992; 27: 231–237.

56. She GM, Wang D, Zeng SF, Yang CR, Zhang YJ. New phenylethanoid glycosides and sugar esters from ku-ding-cha, a herbal tea produced from *Ligustrum purpurascens*. J Food Sci. 2008; 73: C476–481. PMID: 19241537

57. Saimaru H, Orihara Y. Biosynthesis of acteoside in cultured cells of *Olea europaea*. J Nat Med. 2010; 64: 139–145. doi: 10.1007/s11418-009-0383-z PMID: 20037799

58. Taamalli A, Arraez-Roman D, Ibanez E, Zarrouk M, Segura-Carretero A, Fernández-Gutiérrez A. Optimization of microwave-assisted extraction for the characterization of olive leaf phenolic compounds by using HPLC-ESI-TOF-MS/IT-MS^2. J Agric Food Chem. 2012; 60: 791–798. doi: 10.1021/jf204233u PMID: 22206342

59. Klen TJ, Wondra AG, Vrhovsek U, Vodopivec BM. Phenolic Profiling of Olives and Olive Oil Process-Derived Matrices Using UPLC-DAD-ESI-QTOF-HRMS Analysis. J Agric Food Chem. 2015; 63: 3859–3872. doi: 10.1021/jf506345q PMID: 25782340

60. Hosny M, Ragab E, Mohammed A, Shaheen U. New secoiridoids from *Ligustrum ovalifolium* and their hypotensive activity. Pharmacognosy Res. 2009; 1: 91–97.

61. Perez-Bonilla M, Salido S, van Beek TA, de Waard P, Linares-Palomino PJ, Sánchez A, et al. Isolation of antioxidative secoiridoids from olive wood (*Olea europaea* L.) guided by on-line HPLC-DAD-radical scavenging detection. Food Chem. 2011; 124: 36–41.

62. Goodger JQ, Cao B, Jayadi I, Williams SJ, Woodrow IE. Non-volatile components of the essential oil secretory cavities of Eucalyptus leaves: discovery of two glucose monoterpene esters, cuniloside B and froggattiside A. Phytochemistry. 2009; 70: 1187–1194. doi: 10.1016/j.phytochem.2009.06.004 PMID: 19604527

63. Meakins GD, Swindells R. The structures of two acids from olive leaves. J Chem Soc. 1959: 1044–1047.

64. Melguizo-Melguizo D, Diaz-de-Cerio E, Quirantes-Pine R, Svarc-Gajic J, Segura-Carretero A The potential of *Artemisia vulgaris* leaves as a source of antioxidant phenolic compounds. J Funct Foods. 2014; 10: 192–200.

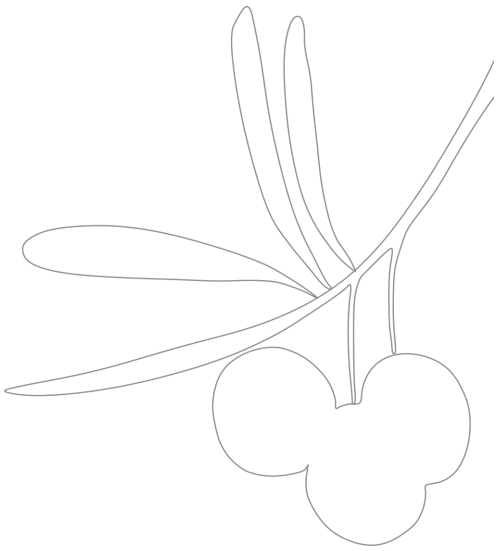

CAPÍTULO 2

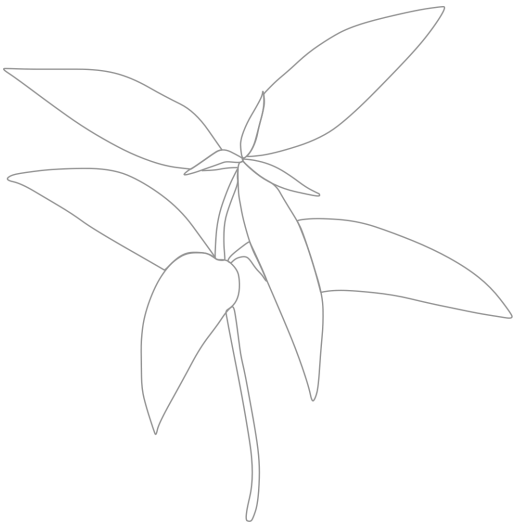

Nutrients (submitted)

The potential synergistic modulation of AMPK by *Lippia citriodora* polyphenols as a target in metabolic disorders

Mariló Olivares-Vicente, Noelia Sánchez-Marzo, José Antonio Encinar, María de la Luz Cádiz-Gurrea, Jesús Lozano-Sánchez, Antonio Segura-Carretero, David Arraez-Roman, Enrique Barrajón-Catalán, María Herranz-López, Vicente Micol.

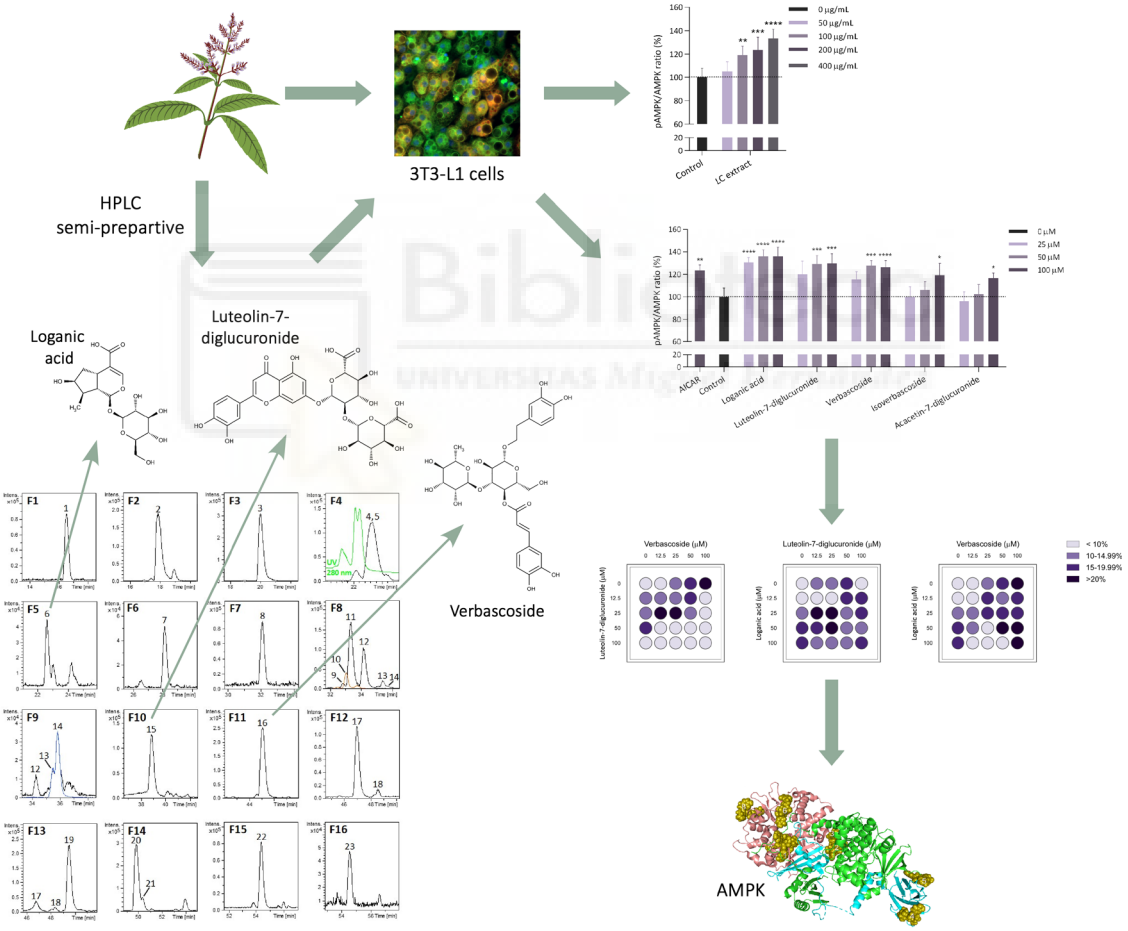

RESUMEN DE LOS RESULTADOS

El objetivo de este trabajo fue identificar los compuestos responsables de la capacidad de un extracto de LC de activar AMPK en adipocitos 3T3-L1. Para ello, se aislaron los compuestos previamente identificados en el extracto mediante RP-HPLC-ESI-TOF-MS semi-preparativa, obteniéndose un total de 16 fracciones constituidas por compuestos en una alta pureza o en combinación con otros minoritarios. Entre los compuestos identificados en las fracciones, se encuentran iridoides como *shanziside*, tevésido, gardósido, *shanziside* metil éster y ácido logánico; fenilpropanoides glicosilados como verbasósido, isómeros de cistanósido F, β-hidroxi-(iso)-verbascósido, martinósido, verbascósido, isoverbascósido, forsitósido A y leucosceptósido A; flavonoides como luteolina-7-diglucurónido, crisoeriol-7-diglucurónido, acacetina-7-diglucurónido y diooflavona; y monoterpenos como isómeros del ácido tuberónico glucósido y sacranósido A.

El extracto de LC enriquecido en verbascósido mostró capacidad de activar AMPK en adipocitos 3T3-L1 maduros tras 24 h de incubación a 100, 200 y 400 µg/mL, aumentando hasta un 19.3 %, 23.5 % y 33.2 % respecto al control, respectivamente. Asimismo, los compuestos de LC se evaluaron a 25, 50 y 100 µM. Entre ellos, los compuestos más activos fueron el ácido logánico, el verbascósido y la luteolina-7-diglucurónido (aumentando la actividad hasta 35.8 %, 26.2 % and 29.6 %, respectivamente), mientras que el isoverbascósido y la acacetina-7-diglucurónido activaron levemente AMPK a la última concentración evaluada. El extracto evaluado en adipocitos contenía aproximadamente un 27.41 % (p/p) de verbascósido, un 0.05 % de ácido logánico y un 0.53 % de luteolina-7-diglucurónido. Estos datos indican que el verbascósido es el principal responsable de la capacidad del extracto de activar AMPK.

Con el fin de estudiar las posibles interacciones sinérgicas entre los tres compuestos más activos, se llevó a cabo un estudio de sinergia. Los valores FICI calculados indicaron un efecto sinérgico para la combinación ácido logánico + luteolina-7-diglucurónido y un efecto aditivo para las combinaciones ácido logánico + verbascósido y verbascósido + luteolina-7-diglucurónido. El análisis de acoplamiento molecular de estos 3 compuestos frente a AMPK mostró valores de $\Delta G < -9$ Kcal/mol frente a algunas posiciones reguladoras de la proteína, como los tres sitios de unión a AMP de la subunidad γ y la zona de interacción entre la subunidad γ y β. De forma global, estos resultados sugieren que la combinación del ácido logánico, verbascósido y luteolina-7-diglucurónido en proporciones adecuadas podría potenciar sinérgicamente la capacidad del extracto de activar AMPK y que dicha activación podría darse a través de la interacción directa con sitios reguladores de la proteína.

The potential synergistic modulation of AMPK by *Lippia citriodora* polyphenols as a target in metabolic disorders

Mariló Olivares-Vicente[1], Noelia Sánchez-Marzo[2,3], José Antonio Encinar[1], María de la Luz Cádiz-Gurrea[2,3], Jesús Lozano-Sánchez[2,3], Antonio Segura-Carretero[2,3], David Arraez-Roman[2,3], Enrique Barrajón-Catalán[1], María Herranz-López[1]*†, Vicente Micol[1,4]†.

[1]Instituto de Investigación, Desarrollo e Innovación en Biotecnología Sanitaria de Elche (IDiBE), Instituto de Biología Molecular y Celular (IBMC), Miguel Hernández University (UMH). Elche, Spain.

[2]Department of Analytical Chemistry, University of Granada. Granada, Spain.

[3]Research and Development of Functional Food Centre (CIDAF), PTS. Granada, Spain.

[4]CIBER: CB12/03/30038, Fisiopatología de la Obesidad y la Nutrición, CIBERobn, Instituto de Salud Carlos III (ISCIII). Palma de Mallorca, Spain.

*Corresponding author. Address: mherranz@umh.es

† These authors shared author co-seniorship.

Abbreviations: AICAR (5-aminoimidazole-4-carboxamide-1-β-4-ribofuranoside), AMP (adenosine 5'-monophosphate), AMPK (AMP-activated protein kinase), CBM (carbohydrate-binding module), ΔG (Gibbs free energy variation), DMSO (dimethylsulfoxide), FASN (fatty acid synthase), KD (kinase domain), LC (*Lippia citriodora*), MAC (minimum activating concentration), pAMPK (phospho-AMPK), PPARα (peroxisome proliferator-activated receptor alpha), RP-HPLC-ESI-TOF-MS (reversed-phase high-performance liquid chromatography coupled to electrospray ionization time-of-flight mass spectrometry).

ABSTRACT

Lippia citriodora (LC) extract is a complex plant-derived mixture that has shown beneficial properties against obesity-related metabolic disorders through AMPK-mediated mechanism in cell and animal models. In this work, we aimed to elucidate the contribution of the different LC active compounds to the activity of the whole extract. For that purpose, we have used semi-preparative reversed-phase HPLC coupled to electrospray ionization time-of-flight mass spectrometry (RP-HPLC-ESI-TOF-MS) to achieve the identification and the bioassay-guided fractionation of the major compounds and an adipocyte cell model for the measurement of AMPK activity.

Among the 16 nearly pure fractions obtained, three compounds, i.e. verbascoside, luteolin-7-diglucuronide and loganic acid showed the highest capacity to activate AMPK in adipocytes. The synergy study using the checkerboard and FICI method exhibited synergistic behavior between loganic acid and luteolin-7-diglucuronide, while pairwise combination with verbascoside showed additive effects. The proportion of these three compounds in the extract (27.41 % (w/w) verbascoside, 0.05 % loganic acid and 0.53 % luteolin-7-diglucuronide) suggested that verbascoside is the main responsible for the AMPK activating capacity of LC, but the enrichment of the extract in these other minor compounds could enhance this activity. Further, molecular docking experiments revealed that these compounds could bind to the regulatory sites of AMPK gamma subunit and at the interface of the beta and gamma subunits, which postulate them as potential agonists of the enzyme, besides activating AMPK pathway at different levels. These findings may contribute to the development of optimized combinations of polyphenols as a new nutritional strategy against obesity-related metabolic disorders.

Keywords*: Lippia citriodora, polyphenol, adipocyte, AMPK, molecular docking, synergy.*

Introduction

According to the World Health Organization, the global prevalence of overweight and obesity has tripled in the last 4 decades. In 2016, about 39 % of the world's adult population were overweight and about 13 % were obese. Overweight and obesity are defined as abnormal or excessive accumulation of fat that is closely linked to the development of chronic disorders such as cardiovascular diseases [1], type 2 diabetes [2], musculoskeletal disorders [3] and some cancers [4]. Nevertheless, obesity can be prevented by taking measures at the individual level, restricting caloric intake and increasing regular physical activity, but also placing strong emphasis on health promoting a healthy lifestyle.

For a long time, numerous plants have been used as traditional remedies against diverse disorders, including those associated with obesity [5]. In recent years, there is a growing number of studies that demonstrate the mechanisms by which the compounds of these plants, especially polyphenols, confer such benefits [6-12]. Nevertheless, due to the complexity of plant extracts, the identification of the compounds responsible of their bioactivity becomes difficult to accomplish. Several approaches have been established in order to find the compounds responsible for the health effect, but this has been hindered due to the sample complexity and the low commercial availability of pure compounds or metabolites. Given this, the bioassay-guided fractionation of botanical extracts by semi-preparative high performance liquid chromatography (HPLC) and their characterization by reversed-phase HPLC coupled to electrospray ionization time-of-flight mass spectrometry (RP-HPLC-ESI-TOF-MS) become the appropriate approach to obtain isolated compounds and to properly characterize these complex mixtures.

In particular, polyphenols from *Lippia citriodora* (LC) have shown potential clinical applications in obesity through polypharmacological effects. Its main component, verbascoside, is a phenylpropanoid with demonstrated antioxidant capacity that has been proposed as the main responsible for the properties of LC extract [13-15]. Nevertheless, it has been also proposed that the presence of other minor compounds in the extract may provide synergistic effects [13]. Previous studies have shown that polyphenols from LC can ameliorate metabolic alterations that occur in obesity, by decreasing oxidative stress and mitochondrial dysfunction and modulating the expression or activity of some metabolic proteins such as peroxisome proliferator-activated receptor alpha (PPARα) and fatty acid synthase (FASN) [13]. Evidences from cellular and animal models of obesity and also from human trials suggest that the activation of AMP-activated protein kinase (AMPK) by LC

polyphenols might be one of the mechanisms involved in the modulation of fat metabolism [6, 16, 17].

AMPK is a crucial nutrient and energy sensor that regulates energy homeostasis [18]. This protein responds to energy demands activating or inhibiting pathways that produce or consume ATP, respectively. It consists of a heterotrimeric complex composed of one catalytic subunit (α1/α2) and two regulatory subunits (β1/β2 and γ1/γ2/γ3) [19]. The alpha subunit contains the Ser/Thr kinase domain (KD), which comprises Thr172 within the activation loop, followed by an autoinhibitory domain and a C-terminal domain (α-CTD), which interacts with beta subunit [20]. The beta subunit contains a carbohydrate-binding module (CBM) in their N-terminus and a C-terminal domain, which contains the αγ-subunit-binding sequence (αγ-SBS) domain, involved in binding to alpha and gamma subunits [21]. Finally, the gamma subunit contains four tandem repeats of a structural module called cystathione-β-synthase (CBS) motifs, three of which constitute the adenine nucleotide binding sites [20].

AMPK is allosterically activated by AMP followed by phosphorylation of Thr172 in the alpha subunit [22]. This protein can be activated by upstream kinases such as liver kinase B1 (LKB1) and Ca^{2+}/calmodulin-dependent kinase β (CaMKKβ) [23, 24]. In addition, several exogenous molecules have been also described as AMPK activators such as metformin, that has been used as an anti-diabetic drug [25], or AICAR (5-aminoimidazole-4-carboxamide-1-β-4-ribofuranoside), which is a direct agonist of AMPK demonstrated in *in vitro* experiments [26]. Some plant-derived polyphenols such as resveratrol, quercetin or verbascoside can also activate this protein, although the mechanism involved may vary considerably [13, 27, 28]. Due to their structural diversity [29], it is proposed that polyphenols can modulate signaling pathways that culminate in the activation of AMPK, or even directly interact with the binding sites of the protein facilitating its enzymatic activation via phosphorylation. In this point, computational techniques such as molecular docking and molecular dynamics are a useful tool to predict the molecular interactions between the target protein and polyphenolic ligands [30]. In addition, the multitargeted character of these molecules suggests that the combinations of certain polyphenols present in plant mixtures may exert synergistic interactions, producing an effect higher than that achieved by the simple addition of their individual components [29, 31]. This becomes an opportunity in the formulation of new dietary supplements focused to prevent and manage obesity-related pathologies.

Previous research demonstrates that LC extract and its main component, verbascoside, display a great ability to activate AMPK in hypertrophic adipocytes [13]. In addition, fractions containing several polyphenols and iridoids obtained by bioassay-guided fractionation of LC extract exhibited AMPK activating capacity [32]. In this work, we aimed to determine the contribution of several pure compounds present in the extract to the AMPK activation. In addition, we carried out a synergy study among the most active compounds to elucidate possible synergistic interactions, and an *in silico* analysis to predict the affinity energy of these compounds against the binding sites of AMPK. These results may contribute to design improved combinations of AMPK-activating polyphenols as a part of the strategy against obesity-related metabolic disorders.

Materials and methods

Materials

For the characterization and semi-preparative isolation of LC compounds, solvents were of HPLC-MS grade and were used as received. Acetic acid and methanol were obtained from Fluka (Sigma-Aldrich, Germany) and Lab-Scan (Gliwice, Poland), respectively. Water was purified by a Milli-Q system from Millipore (Bedford, MA, USA). The standard compounds loganic acid, luteolin-7-diglucuronide and isoverbascoside were purchased from PhytoLab (Vestenbergsgreuth, Germany). Verbascoside was acquired from Extrasynthese (Genay, France). The compounds of LC were isolated from a commercial extract of LC leaves (10 % verbascoside, w/w) provided by Monteloeder, S.L. (Elche, Spain). For the evaluation of AMPK activation in adipocytes and quantitation of compounds, an enriched LC extract (27 % verbascoside, w/w) from Monteloeder was used [13]. The purchased compounds were dissolved in dimethylsulfoxide (DMSO) (Sigma-Aldrich, St. Louis., MO, USA) and the isolated compounds were collected in water. Afterwards, the extract and compounds were prepared in culture medium and filtered before use in cell experiments.

For propagation and differentiation of 3T3-L1 preadipocytes (ATCC® CL-173™), Dulbecco's Modified Eagle Medium (DMEM) and the mix of antibiotics (penicillin/streptomycin) were acquired from Gibco (ThermoFisher Scientific, Waltham, MA, USA). Calf and fetal bovine serums were obtained from Fisher Scientific (Utah, USA). 3-isobutyl-1-methylxanthine (IBMX), dexamethasone and insulin were obtained from Sigma-Aldrich.

Isolation of LC compounds by semi-preparative method

For compound isolation, 50 mg of extract were dissolved in 1 mL of water and the result solution was vortexed for 1 min. The sample was filtered through a 0.25 mm filter before its introduction in the semi-preparative HPLC system. The isolation of LC compounds was carried out using a Gilson preparative HPLC system (Gilson Inc., Middleton, WI, USA) which equipped with automated liquid handling solution (model GX-271), a binary pump (model 331/332) and UV-Vis detector (model UV-Vis 156). A semi-preparative Ascentis C18 column (250 x 212 mm, 10 μm) was used to separate the compounds at room temperature. The mobile phases consisted of 0.5 % acetic acid in water (A) and acetonitrile (B). The multi-step linear gradient developed in the previous study was employed with some changes with the aim to optimize the compound purification: 0 min, 5 % B; 15 min, 20 % B; 21 min, 23 % B; 28 min, 25 % B; 32 min, 32 % B; 48 min, 40 % B, 65 min, 60 % B; 68 min, 65 % B; 70 min, 5 % B; 80 min, 5 % B [33]. The flow rate used was reduce to 10 mL/min and the injection volume was 500 μL. The UV-Vis detector was set at 240 and 280 nm while separated compounds were also monitored coupling this system to the time-of-flight (TOF) mass spectrometer mentioned below.

Afterwards, 16 fractions were collected, and their solvent was evaporated at 35˚C under vacuum in a Savant SpeedVac Concentrator SC250 EXP (Thermo Scientific, CA, USA). The residue of each fraction was dissolved in water at 800-1033.3 ppm depending of its weight and samples were filtered as mentioned above before analytical characterization.

Analytical characterization of the collected fractions by RP-HPLC-ESI-TOF-MS

Analyses of fractions were carried out in an Agilent 1200 series rapid-solution LC system (Agilent Technologies, Palo Alto, CA, USA) which includes an autosampler, a binary pump and a diode-array detector (DAD). Samples (10 μL) were injected onto a Zorbax Eclipse Plus C18 column (1.8 μm, 150 x 4.6 mm) for RP-HPLC at room temperature. The flow rate was set at 0.4 mL/min and the following multi-step linear gradient was applied: 0 min, 5 % B; 3 min, 10 % B; 15 min, 20 % B; 17 min, 23 % B; 24 min, 35 % B; 30 min, 40 % B, 40 min, 45 % B; 55 min, 60 % B; 60 min, 95 % B, 62 min, 5 % B; 70 min, 5 % B. The initial conditions were maintained for 10 min. Elution of compounds was monitored with UV-Vis in the spectrum range of 190-950 nm by the DAD detector.

Furthermore, the HPLC system was coupled to a TOF mass spectrometer (Bruker Daltonics, Bremen, Germany) for compound identification considering a m/z range of 50–1000. This detector was equipped with an electrospray ionization (ESI) interface (model G1607A, Agilent Technologies) working in negative ion mode. The optimum values for the source and transfer parameters were described in our previous work where external calibration was also explained [33]. The software DataAnalysis 4.0 (Bruker Daltonics) allowed the processing of the accurate mass data for the molecular ions.

Quantitation of compounds in the LC extract by RP-HPLC

Stocks solutions of loganic acid, luteolin-7-diglucuronide and verbascoside were prepared in methanol:water (50:50, v/v). The first two compounds were obtained with a stock concentration of 750 µg/mL, while verbascoside stock solution was prepared at 1500 µg/mL taking into consideration its higher expected amount. Standard solutions were obtained by dilution from stock solutions to final concentrations of 0.3125-500 µg/mL. For the quantification of these compounds, the enriched LC extract was dissolved in methanol:water (50:50, v/v) per duplicate each at 3 and 5 mg/mL in different days (interday), and resulting solutions were filtered using the filters mentioned above.

All samples were analyzed by RP-HPLC using the same mobile phase and multi-step linear gradient described in the characterization of the collected fractions. In this case, compounds were monitored by the DAD detector at 235, 320 and 350 nm wavelengths.

Propagation and differentiation of pre-adipocytes

The 3T3-L1 cells were propagated in DMEM containing 10 % bovine calf serum and antibiotics (100 U/mL penicillin and 100 µg/mL streptomycin) under optimal conditions (37°C, 95 % humidity, 5 % CO_2). To differentiate into adipocytes, cells were seeded in 96-well plates and maintained until confluence. Subsequently, preadipocytes were induced by incubating in DMEM containing 4.5 g/L glucose, 10 % fetal bovine serum and adipogenic agents (0.5 mM IBMX, 1 µM dexamethasone and 10 µg/mL insulin) for 48 h. Then, medium supplemented with insulin was replaced every 2-3 days until obtaining mature adipocytes. More than 90 % of the cells became mature adipocytes on the 8th day of differentiation and they were treated for 24 h with LC extract at 50, 100, 200 and 400 µg/mL or identified compounds from LC at 25, 50 and 100 µM. For the compounds dissolved in DMSO, the amount of solvent did not exceed 0.5 % in cells.

Determination of the AMPK and pAMPK levels by immunofluorescence assay

Levels of activated AMPK (phospho-AMPK, pAMPK) and total AMPK were determined in adipocytes by an immunofluorescence assay. In brief, treated cells were fixed in 4 % paraformaldehyde (Sigma-Aldrich), permeabilized in 0.3 % Triton X-100 (Sigma-Aldrich) and blocked in 4 % goat serum (Sigma-Aldrich). Then, cells were incubated with primary antibodies overnight, i.e. mouse anti-AMPK (ab80039, Abcam, Cambrigde, UK) and rabbit anti-pAMPK (Thr172) (#2535, Cell Signaling Tech., Danvers, MA, USA); followed by secondary antibodies for 6 h, i.e. anti-mouse IgG-FITC (F0257) or anti-rabbit IgG-CF594 (SAB4600107), both from Sigma-Aldrich. The fluorescence signal of each protein was measured by using a cell-imaging multi-mode microplate reader (Cytation 3, Biotek Instruments, Winooski, VT, USA). To dismiss any cytotoxic effect, the Hoechst 33342 dye (Molecular Probes, Invitrogen, Carlsbad, CA, USA) was co-incubated to stain and count nuclei by taking microphotographs with a DAPI imaging filter cube. Expression of AMPK was calculated as the ratio between total AMPK and nuclei, meanwhile activation of AMPK was expressed as the ratio between pAMPK and total AMPK. Representative pictures of fluorescent cells were taking with Bright Field, DAPI, Texas Red and GFP filter cubes at 20x.

Synergy study

The technique used to quantify the possible pairwise interactions between the AMPK activators was the checkerboard assay. Pre-adipocytes were seeded and differentiated into mature adipocytes in 96-well plates, as described above. Four concentrations of each compound were prepared within the activation range observed previously (25, 50, 100 and 200 μM). Compounds were added to the cells in pairs. For one compound, 50 μL of each preparation was added across the x-axis of the plate, while 50 μL of the other compound was added across the y-axis. Treated cells were incubated for 24 h and AMPK activation was determined by an immunofluorescence assay. Non-treated cells were used as a control of the AMPK basal activation and an increase of the activation equal to or greater than 15 % was considered statistically significant based on AMPK activation values previously achieved (Fig. 2). This minimum activating concentration (MAC) was used to calculate the synergic interactions by calculating the fractional inhibitory concentration index (FICI), whose formula in activation values would be: FICI = (MAC of compound X in combination / MAC of compound X alone) + (MAC of compound Y in combination / MAC of compound Y alone). Synergy was considered when FICI ≤ 0.5; an additive effect when 0.5 < FICI ≤ 1; an

indifferent effect when 1 < FICI < 2; and antagonism when FICI ≥ 2, according to the interpretation of EUCAST [31, 34].

Molecular docking

Human AMPK (2.63 Å resolution, pdb code **5ISO**) structure has been obtained from the Research Collaboratory for Structural Bioinformatics (RCSB) Protein Data Bank (PDB). The specific edition of the protein structure was made using PyMol 2.0 software (The PyMOL Molecular Graphics System, Version 2.0 Schrödinger, LLC, at http://www.pymol.org/) without further optimization. The molecular docking experiments have been performed using the YASARA v19.3.26 software [35] that has executed the AutoDock 4 algorithm [36], in which a 999 flexible docking runs were set and clustered (7 Å) around the putative binding sites. The AMBER99 force field have been used. The YASARA pH command was set to 7.4. The YASARA software calculates the Gibbs free energy variation (ΔG, kcal/mol), with more positive energy values indicating stronger binding. However, all the values included in the supplementary table's results were included with a negative sign as a best docked. Solely the ΔG value for the best compound docked in each cluster was shown. Dissociation constants were recalculated from the average binding energy of all compound of each cluster. The number of docked molecules (loganic acid or luteolin-7-diglucuronide or verbascoside) included in each cluster of compound has been indicated as "Members" in percentage in Supplementary Tables 1, 2 and 3. The theoretical dissociation constant of each ligand (loganic acid or luteolin-7-diglucuronide or verbascoside) at its putative binding site can be determined by calculating the binding energy of the ligand-receptor complex.

Statistical analysis

AMPK activation values are expressed as the mean ± standard deviation. Treatments were normalized to their respective controls incubated with the amount of DMSO or water used in each treatment. Data were subjected to one-way ANOVA analysis and Tukey's test for multiple/non-parametric approaches. Differences were considered statistically significant at $p < 0.05$. Statistical analyses were performed using GraphPad Prism version 6.00 (GraphPad Software, San Diego, CA, USA). *$p < 0.05$, **$p < 0.01$, ***$p < 0.001$ and ****$p < 0.0001$ on the bars indicate statistically significant differences compared to the control. All experiments were performed in quintupled.

Results

Isolation of LC compounds using semi-preparative HPLC and their characterization by RP-HPLC-ESI-TOF-MS

The purification strategy using semi-preparative HPLC was improved for isolating compounds that are not commercially available [33]. A total of 16 fractions (F1-F16) were collected (**Fig. 1**) and their composition was analyzed by the detailed RP-HPLC-ESI-TOF-MS method (**Table 1**). Relative percentage of each compound was estimated considering the relative area of the corresponding peak in the collected fraction.

The results showed that the main groups identified from the collected fractions were iridoid, glycosylated phenylpropanoid, flavonoid and monoterpenoid compounds. Regarding iridoids, shanziside (m/z 391) and theveside (m/z 389) were obtained completely pure in fractions F1 and F7, respectively. Fraction F2 contained mainly gardoside (m/z 373). Shanziside methyl ester (m/z 405) was obtained in fraction F6 as the major compound. Fraction F5 was the fraction where loganic acid (m/z 375) was found.

On the other hand, seven different fractions mainly contained glycosylated phenylpropanoids. Fraction F3 showed pure verbasoside (m/z 461), while cistanoside F isomers (m/z 487), β-hydroxy-(iso)-verbascoside (m/z 639), and martynoside (m/z 651) were contained as major compounds in F4, F9, and F16, respectively. Verbascoside (m/z 623) was isolated in fraction F11, while isoverbascoside (m/z 623) was obtained in F13. A different position isomer of verbascoside and isoverbascoside was obtained in fraction F14: forsythoside A (m/z 623). This compound has been identified in the characterization of a LC extract by other authors [37]. Leucosceptoside A (m/z 637) was also present in F10 as minor compound.

Moreover, three flavones in their glucuronide form were isolated: luteolin-7-diglucuronide (m/z 637) in F10, chrysoeriol-7-diglucuronide (m/z 651) in F12 and acacetin-7-diglucuronide (m/z 635) in F15. In this last fraction, diooflavone (m/z 621), a biflavonoid identified for the first time in LC in our previous work, was present as minor compound [33]. Fraction F8 contained not only tuberonic acid glucoside isomers (m/z 387) but also sacranoside A (m/z 445), both monoterpenoids, and β-hydroxy-(iso)-verbascoside (m/z 639).

Phenylpropanoid, iridoid and flavonoid compounds from LC modulate AMPK in adipocytes

Mature 3T3-L1 adipocytes were obtained to evaluate the capacity of the LC extract and its compounds to activate AMPK. After 24 h of incubation, LC extract significantly increased the activation of AMPK through phosphorylation of Thr172 at 100, 200 and 400 μg/mL in a dose-dependent manner (**Fig. 2A**). The phosphorylation of this kinase increased up to 19.3 % at 100 μg/mL, 23.5 % at 200 μg/mL and 33.2 % at 400 μg/mL of extract compared to basal activation levels observed in cells without extract. The LC extract was assessed at non-cytotoxic concentrations in 3T3-L1 adipocytes (**Supplementary Fig. 1A**).

For the evaluation of the isolated compounds, equivalent concentrations to the amount of verbascoside contained in 50, 100 and 200 μg/mL of LC extract (27 % w/w) were selected. Accordingly, the compounds were prepared at 25, 50 and 100 μM. Among all the compounds evaluated, five of them exhibited a significant AMPK activity (**Fig. 2B**). The strongest activators were loganic acid, verbascoside and luteolin-7-diglucuronide, which increased AMPK phosphorylation up to 35.8 %, 26.2 % and 29.6 %, respectively, respect to the non-treated control. Furthermore, these three compounds showed higher activation values than that one exerted by the agonist AICAR at 100 μM (123.2 %). In addition, the polyphenols isoverbascoside and acacetin-7-diglucuronide also activated AMPK, but this effect was very weak and only achieved at the highest concentration (119.1 % and 116.5 %, respectively). None of the activator compounds showed cytotoxic effect (**Supplementary Fig. 1B**).

Quantitation of the main AMPK activators compounds in the LC extract by RP-HPLC

In view of the results obtained above, loganic acid, luteolin-7-diglucuronide and verbascoside were selected as the three main AMPK activators and were quantified by RP-HPLC in the whole extract. As expected, verbascoside showed a percentage of 27.41 ± 0.52 % (w/w) in the extract, while luteolin-7-diglucuronide and loganic acid showed percentages of 0.53 ± 0.04 % and 0.05 ± 0.01 % (w/w), respectively (**Table 2**).

Verbascoside, luteolin-7-diglucuronide and loganic acid from LC might exhibit potential synergic and additive interactions on AMPK activation

To explore the possible synergic effects on AMPK modulation, we monitored a synergy study with the three most active compounds of LC (loganic acid, luteolin-7-diglucuronide and verbascoside). To address this, the compounds were added to the adipocytes in pairs at

different concentrations by the checkerboard method. After 24 h of incubation, AMPK activation was quantified by an immunofluorescence assay to calculate the FICI values of each combination (**Fig. 3**). The FICI values of the three combinations between loganic acid, verbascoside and luteolin-7-diglucuronide are represented in **Table 3**. The FICI analyses showed a synergistic effect for the combination loganic acid + luteolin-7-diglucuronide, with a FICI value = 0.5. The combinations loganic acid + verbascoside and verbascoside + luteolin-7-diglucuronide presented FICI values = 0.75, indicating an additive effect in both cases.

The potential direct interaction of verbascoside, luteolin-7-diglucuronide and loganic acid with AMPK through the regulatory binding sites

Molecular docking techniques aims to predict the structure of the ligand-receptor complex using computational methods and needs high-resolution structural information on the target structure. The docking software has a scoring function to make an approximate calculation of the binding free energy between the target (human AMPK) and the ligand (loganic acid or luteolin-7-diglucuronide or verbascoside) in each binding pose. To search for potential binding sites in each protein of interest, from the aforementioned compounds, a global molecular docking procedure was performed with AutoDock 4 [36] implemented in YASARA software [38].

The results obtained are shown in **Figure 4** and **Supplementary Tables 1 to 3**. A first observation of the results obtained shows that for the three all ligands, the clusters with lower ΔG for each compound are located in regulatory positions previously described in the literature. **Figure 4B** shows the 3 AMP binding sites in the gamma subunit, the ATP binding site in the catalytic subunit and the regulatory site at the interface of the alpha and beta subunits (see chain E, A, and B in **Fig. 4B**, respectively, ligands are represented as spheres). None of the three compounds tested is located at the ATP binding site while various occupancy of any of the three AMP binding sites can be observed in the gamma subunit. This would explain their behavior as AMPK agonists. A second interesting observation is that none of the three compounds localizes clusters of compounds with high affinity in the binding site that is established in the zone of interaction between AMPKα catalytic and AMPKβ-regulatory subunits. Finally, a third observation of interest is that different sites of high affinity have been found in the interaction zones between the gamma and beta subunits for the three compounds analyzed (**Fig. 4** and **Supplementary Tables 1 to 3**). The occupation of these sites could increase the catalytic activity of the alpha subunit.

Discussion

Previously, an extract from *Lippia citriodora* (LC) has been reported to ameliorate lipid metabolism in hypertrophic adipocytes and mice with diet-induced obesity. It is postulated that such effects can be partly mediated through AMPK activation [13]. In this work, we have identified the specific compounds responsible for the AMPK activating capacity of the extract in a cellular model. The potential synergistic effects of the combination containing the main activator compounds have been also observed in cultured adipocytes. Additionally, molecular docking data of the compounds with greater activation capacity on AMPK showed their high affinity binding to some known regulatory sites of the enzyme. This strongly suggests that they could directly exert their action on AMPK.

Given that the complex composition of plant extracts often hinders their clinical effectiveness, the identification of the active compounds in these mixtures seems an indispensable step to optimize the extraction process aimed to increase the efficiency in humans. In a previous work, we carried out a fractionation of LC extract by semi-preparative chromatography in order to obtain fractions composed of few compounds [32]. The evaluation of these fractions on hypertrophic 3T3-L1 adipocytes exhibited that most of the fractions exerted capacity to activate AMPK. In this work, our purpose was to isolate the components of LC fractions obtained in this previous study to identify the responsible candidates of the AMPK activity in adipocyte model. For this purpose, we have optimized the semi-preparative purification process to improve chromatographic separation and to obtain nearly pure compounds in each fraction [39].

A total of 22 compounds contained in 16 fractions were identified in the LC extract. Among them, five iridoids, ten glycosylated phenylpropanoids, four flavones and three monoterpenoids were detected in agreement with previous studies [32, 37]. In contrast to our previous work [32], most of the identified LC compounds were obtained in fractions with a high purity, such as shanziside in F1, gardoside in F2, verbasoside in F3, shanziside methyl ester in F6, theveside in F7, luteolin-7-diglucuronide in F10 and acacetin-7-diglucuronide in F15. Meanwhile, the isolation of verbascoside in F11 and martynoside in F16 was also achieved in this previous study. Additionally, other fractions were composed of major contributors (cistanoside F isomers in F4, loganic acid in F5, tuberonic acid glucoside isomer in F8, β-hydroxy-(iso)-verbascoside in F9, chysoeriol-7-diglucuronide in F12, isoverbascoside in F13 and forsythoside A in F14) together with a few minor compounds. Major compounds from fractions F5 (loganic acid), F10 (luteolin-7-

448 diglucuronide), F11 (verbascoside), and F13 (isoverbascoside) are phytochemicals which
449 are commercially available, so that pure commercial standard compounds were used for
450 bioactivity assays after consideration of the relative area in the mentioned fractions.
451
452 After isolation, we tested the LC compounds in mature 3T3-L1 adipocytes to evaluate the
453 AMPK activation. With a comparative purpose, the selected doses of compounds for the
454 cellular assay were equivalent to the concentration of verbascoside present at the
455 concentrations evaluated for the whole extract. Among the compounds, loganic acid,
456 luteolin-7-diglucuronide and verbascoside showed the strongest capacity to activate AMPK,
457 whereas isoverbascoside and acacetin-7-diglucuronide exhibited a weak effect on AMPK
458 activation at the highest concentration evaluated (100 μM). In agreement with our previous
459 work [32], the five activator compounds, evaluated here in a pure form, were present in LC
460 fractions that exhibited AMPK activating capacity in hypertrophic adipocytes. Our results
461 suggest that these compounds could be responsible for the activity of these fractions. In this
462 preceding study, other activator fractions contained compounds that did not exhibit AMPK
463 activity in our study. Nevertheless, a reliable comparison is difficult to establish as the
464 concentrations tested and incubation time were higher than those selected for our study.
465
466 In this work, the AMPK activation achieved by verbascoside was similar to that obtained by
467 the whole extract at equivalent doses. Considering that verbascoside is the major compound
468 of LC extract, our data suggest that this phenylpropanoid is likely one of the main
469 responsible for the AMPK activating capacity. In agreement with these findings, a bioassay-
470 guided fractionation of an olive leaf extract showed that the fractions that exhibited the
471 highest capacity to activate AMPK in adipocytes were mainly composed of verbascoside
472 [40]. In addition, the bioactivity of verbascoside in hypertrophic adipocytes has been
473 previously demonstrated [13], exhibiting a modulating capacity on other metabolic
474 proteins, such as PPARα and FASN. However, these effects were lower than the obtained by
475 the whole extract, suggesting the presence of other active compounds. Accordingly, we
476 carried out a synergy study with the most active compounds of LC (loganic acid, luteolin-7-
477 diglucuronide and verbascoside) in order to investigate if these compounds, in an
478 appropriate proportion, could enhance the activity against AMPK. We did not consider
479 isoverbascoside and acacetin-7-diglucuronide in this analysis as they showed weak AMPK
480 activation values in the cellular assay at concentrations difficult to achieve *in vivo*.
481
482 When we evaluated the three most active compounds in pairwise combinations, the
483 compounds showed additive effects on AMPK activation and even a synergistic interaction

484 between loganic acid and luteolin-7-diglucuronide. However, verbascoside represents
485 27.41 ± 0.52 % (w/w) on the extract, whereas loganic acid and luteolin-7-diglucuronide
486 constitute 0.05 ± 0.01 and 0.53 ± 0.04 % (w/w), respectively. The low relative proportion
487 of these two last compounds in the extract reinforces that the AMPK activity of LC is mainly
488 exhibited by verbascoside. Despite this, our data suggest that the presence of these minor
489 compounds in adequate proportions, together with verbascoside, could synergistically
490 enhance the bioactivity of LC extracts.
491
492 It should be considered that the *in vivo* activity of LC extract depends essentially on the
493 absorption and metabolism of its compounds in the gut, so that the effector metabolites in
494 the target tissue may differ considerably from the ingested compounds. In this regard, data
495 derived from cellular experiments do not contemplate these pharmacokinetic processes
496 and should be interpreted with caution. Previously, other authors reported the phenolic
497 metabolites of LC in plasma samples of rats after an oral administration of the extract and
498 correlated with an antioxidant protection in blood cells [10]. In this study, verbascoside was
499 found as the major metabolite, suggesting that this phenylpropanoid can be absorbed in its
500 native form. In addition, low levels of luteolin-7-diglucuronide were detected in plasma,
501 probably by a prior deglycosylation of the flavone in the gut barrier and subsequent
502 glucuronidation. With the aforementioned, it is reasonable to postulate that verbascoside
503 and luteolin-7-diglucuronide may reach molecular targets *in vivo*. Regarding loganic acid,
504 this iridoid has been proposed to exert anti-obesity effects in an ovariectomy-female mouse
505 model and reduce adipogenesis on 3T3-L1 pre-adipocytes through regulation of some
506 adipogenesis-related genes [41]. Nevertheless, whether this compound is absorbed in its
507 native form or undergoes phase II biotransformation reactions deserves further research.
508
509 Further, our computational docking data suggest that these compounds could act directly
510 as AMPK agonists. As derived from the molecular docking experiment, the three most active
511 compounds of LC showed poses with ΔG below -9 Kcal/mol for several regulatory positions
512 of AMPK. Some of these positions corresponded to any of the three AMP binding sites of the
513 gamma subunit, suggesting that the LC compounds may activate AMPK by mimicking the
514 allosteric mechanism of AMP. This mechanism has been previously described for other
515 agonists such as AICAR, which is phosphorylated inside the cell into AICA riboside
516 monophosphate (ZMP), an analogue of AMP [26]. In addition, different interaction zones in
517 the gamma subunit were found and it is not excluded that these LC compounds could
518 modulate the kinase by interacting with binding sites in the gamma subunit different from
519 adenine nucleotide sites, as reported with the activator 5-(5-hydroxyl-isoxazol-3-yl)-furan-

2-phosphonic acid [42]. Similarly, the occupation of LC compounds in different sites of the interaction zones between the gamma and beta subunits could also exert an increase in the catalytic activity of AMPK. Finally, none of the three LC compounds seemed to interact either with the ATP binding site of the alpha subunit or the interface established between the alpha subunit KD and the beta subunit CBM. This latter is called the allosteric drug and metabolite (ADaM) site, as it has been described as a binding site of activators such as A-769662, compound 911 and salicylate [42, 43]. Therefore, the additive and synergistic effects between the three LC compounds on AMPK activity could be explained through the co-interaction of these compounds in different binding sites of the protein. Although we show here that some LC compounds may be direct activators of AMPK, the possibility that these compounds could target other upstream kinases of AMPK should be considered in further studies.

Conclusion

Considering the role of AMPK in energy metabolism, this protein is considered a key pharmacological target in the treatment of metabolic diseases such as obesity. LC is a plant that can contribute to ameliorate this problem and its action seems to be mediated through the activation of AMPK mainly exerted by its major component, verbascoside. In addition, other minor compounds such as loganic acid and luteolin-7-diglucuronide show a strong capacity to activate this enzyme and the synergy study and molecular docking experiment reveal that the three bioactive compounds together exhibit synergistic effects and are able to interact directly with AMPK regulatory binding sites. These data suggest that the appropriate proportion of verbascoside, loganic acid and luteolin-7-diglucuronide in the vegetal mixture could ensure the effectiveness for its use as an anti-obesity supplement.

Acknowledgements

We are grateful to the Cluster of Scientific Computing (http://ccc.umh.es/) of the Miguel Hernández University (UMH) and the Centro de Supercomputación of the University of Granada (ALHAMBRA-CSIRC) for providing computing facilities.

Funding

The Spanish Ministry of Economy and Competitiveness (MINECO, Project RTI2018-096724-B-C21) and the Generalitat Valenciana (PROMETEO/2016/006) supports work in the

laboratory. Scholarships ACIF/2016/230 and APOSTD/2017/023 from Generalitat Valenciana cofinanced with the European Social Fund; and CIBER (CB12/03/30038, Fisiopatologia de la Obesidad y la Nutricion, CIBERobn, Instituto de Salud Carlos III).

Conflict of interest

The authors declare no conflict of interest.

References

1. Mandviwala, T., U. Khalid, and A. Deswal, *Obesity and Cardiovascular Disease: a Risk Factor or a Risk Marker?* Curr Atheroscler Rep, 2016. **18**(5): p. 21.
2. Boles, A., R. Kandimalla, and P.H. Reddy, *Dynamics of diabetes and obesity: Epidemiological perspective.* Biochim Biophys Acta Mol Basis Dis, 2017. **1863**(5): p. 1026-1036.
3. Mobasheri, A. and M. Batt, *An update on the pathophysiology of osteoarthritis.* Ann Phys Rehabil Med, 2016. **59**(5-6): p. 333-339.
4. Ackerman, S.E., et al., *Insights into the Link Between Obesity and Cancer.* Curr Obes Rep, 2017. **6**(2): p. 195-203.
5. Graf, B.L., et al., *Plant-derived therapeutics for the treatment of metabolic syndrome.* Curr Opin Investig Drugs, 2010. **11**(10): p. 1107-15.
6. Boix-Castejon, M., et al., *Hibiscus and lemon verbena polyphenols modulate appetite-related biomarkers in overweight subjects: a randomized controlled trial.* Food Funct, 2018. **9**(6): p. 3173-3184.
7. Aguirre, L., et al., *Resveratrol: anti-obesity mechanisms of action.* Molecules, 2014. **19**(11): p. 18632-55.
8. Jung, C.H., et al., *Quercetin reduces high-fat diet-induced fat accumulation in the liver by regulating lipid metabolism genes.* Phytother Res, 2013. **27**(1): p. 139-43.
9. Peyrol, J., et al., *Involvement of bilitranslocase and beta-glucuronidase in the vascular protection by hydroxytyrosol and its glucuronide metabolites in oxidative stress conditions.* J Nutr Biochem, 2017. **51**: p. 8-15.
10. Quirantes-Pine, R., et al., *Phenylpropanoids and their metabolites are the major compounds responsible for blood-cell protection against oxidative stress after administration of Lippia citriodora in rats.* Phytomedicine, 2013. **20**(12): p. 1112-8.

11. Joven, J., et al., *Plant-derived polyphenols regulate expression of miRNA paralogs miR-103/107 and miR-122 and prevent diet-induced fatty liver disease in hyperlipidemic mice.* Biochim Biophys Acta, 2012. **1820**(7): p. 894-9.
12. Herranz-Lopez, M., et al., *Synergism of plant-derived polyphenols in adipogenesis: perspectives and implications.* Phytomedicine, 2012. **19**(3-4): p. 253-61.
13. Herranz-Lopez, M., et al., *Lemon verbena (Lippia citriodora) polyphenols alleviate obesity-related disturbances in hypertrophic adipocytes through AMPK-dependent mechanisms.* Phytomedicine, 2015. **22**(6): p. 605-14.
14. Funes, L., et al., *Correlation between plasma antioxidant capacity and verbascoside levels in rats after oral administration of lemon verbena extract.* Food Chemistry, 2009. **117**(4): p. 589–598.
15. Funes, L., et al., *Effects of verbascoside, a phenylpropanoid glycoside from lemon verbena, on phospholipid model membranes.* Chem Phys Lipids, 2010. **163**(2): p. 190-199.
16. Herranz-Lopez, M., et al., *Differential effects of a combination of Hibiscus sabdariffa and Lippia citriodora polyphenols in overweight/obese subjects: A randomized controlled trial.* Sci Rep, 2019. **9**(1): p. 2999.
17. Lee, Y.S., et al., *Metabolaid((R)) Combination of Lemon Verbena and Hibiscus Flower Extract Prevents High-Fat Diet-Induced Obesity through AMP-Activated Protein Kinase Activation.* Nutrients, 2018. **10**(9).
18. O'Neill, H.M., G.P. Holloway, and G.R. Steinberg, *AMPK regulation of fatty acid metabolism and mitochondrial biogenesis: implications for obesity.* Mol Cell Endocrinol, 2013. **366**(2): p. 135-51.
19. Hardie, D.G., *Sensing of energy and nutrients by AMP-activated protein kinase.* Am J Clin Nutr, 2011. **93**(4): p. 891s-6.
20. Yan, Y., et al., *Structure and Physiological Regulation of AMPK.* Int J Mol Sci, 2018. **19**(11).
21. Sanz, P., T. Rubio, and M.A. Garcia-Gimeno, *AMPKbeta subunits: more than just a scaffold in the formation of AMPK complex.* Febs j, 2013. **280**(16): p. 3723-33.
22. Hawley, S.A., et al., *Characterization of the AMP-activated protein kinase kinase from rat liver and identification of threonine 172 as the major site at which it phosphorylates AMP-activated protein kinase.* J Biol Chem, 1996. **271**(44): p. 27879-87.
23. Woods, A., et al., *LKB1 is the upstream kinase in the AMP-activated protein kinase cascade.* Curr Biol, 2003. **13**(22): p. 2004-8.
24. Hawley, S.A., et al., *Calmodulin-dependent protein kinase kinase-beta is an alternative upstream kinase for AMP-activated protein kinase.* Cell Metab, 2005. **2**(1): p. 9-19.

25. Chen, S.C., et al., *Metformin suppresses adipogenesis through both AMP-activated protein kinase (AMPK)-dependent and AMPK-independent mechanisms.* Mol Cell Endocrinol, 2017. **440**: p. 57-68.
26. Giri, S., et al., *5-aminoimidazole-4-carboxamide-1-beta-4-ribofuranoside inhibits proinflammatory response in glial cells: a possible role of AMP-activated protein kinase.* J Neurosci, 2004. **24**(2): p. 479-87.
27. Wang, S., et al., *Resveratrol enhances brown adipocyte formation and function by activating AMP-activated protein kinase (AMPK) alpha1 in mice fed high-fat diet.* Mol Nutr Food Res, 2017. **61**(4).
28. Dong, J., et al., *Quercetin reduces obesity-associated ATM infiltration and inflammation in mice: a mechanism including AMPKalpha1/SIRT1.* J Lipid Res, 2014. **55**(3): p. 363-74.
29. Barrajon-Catalan, E., et al., *Molecular promiscuity of plant polyphenols in the management of age-related diseases: far beyond their antioxidant properties.* Adv Exp Med Biol, 2014. **824**: p. 141-59.
30. Jimenez-Sanchez, C., et al., *AMPK modulatory activity of olive-tree leaves phenolic compounds: Bioassay-guided isolation on adipocyte model and in silico approach.* PLoS One, 2017. **12**(3): p. e0173074.
31. Tomas-Menor, L., et al., *The promiscuous and synergic molecular interaction of polyphenols in bactericidal activity: an opportunity to improve the performance of antibiotics?* Phytother Res, 2015. **29**(3): p. 466-73.
32. Cádiz-Gurrea, M.d.l.L., et al., *Bioassay-guided purification of Lippia citriodora polyphenols with AMPK modulatory activity.* Journal of Functional Foods, 2018. **46**: p. 514-520.
33. Cadiz-Gurrea, M.L., Olivares-Vicente, M., Herranz-Lopez, M., Arraez-Roman, D., Fernandez-Arroyo, S., Micol, V., Segura-Carretero, A., *Bioassay-guided purification of Lippia citriodora polyphenols with AMPK modulatory activity.* Journal of Functional Foods, 2018. **46**: p. 514-520.
34. *EUCAST Definitive Document E.Def 1.2, May 2000: Terminology relating to methods for the determination of susceptibility of bacteria to antimicrobial agents.* Clin Microbiol Infect, 2000. **6**(9): p. 503-8.
35. Krieger, E., et al., *Making optimal use of empirical energy functions: force-field parameterization in crystal space.* Proteins, 2004. **57**(4): p. 678-83.
36. Morris, G.M., R. Huey, and A.J. Olson, *Using AutoDock for ligand-receptor docking.* Curr Protoc Bioinformatics, 2008. **Chapter 8**: p. Unit 8.14.
37. Quirantes-Pine, R., et al., *High-performance liquid chromatography with diode array detection coupled to electrospray time-of-flight and ion-trap tandem mass spectrometry*

to identify phenolic compounds from a lemon verbena extract. J Chromatogr A, 2009. **1216**(28): p. 5391-7.

38. Krieger, E. and G. Vriend, *YASARA View - molecular graphics for all devices - from smartphones to workstations.* Bioinformatics, 2014. **30**(20): p. 2981-2.
39. Marston, A., *Role of advances in chromatographic techniques in phytochemistry.* Phytochemistry, 2007. **68**(22): p. 2786-2798.
40. Jiménez-Sánchez, C., et al., *AMPK modulatory activity of olive–tree leaves phenolic compounds: Bioassay-guided isolation on adipocyte model and in silico approach.* PLOS ONE, 2017. **12**(3): p. e0173074.
41. Park, E., et al., *Antiadipogenic Effects of Loganic Acid in 3T3-L1 Preadipocytes and Ovariectomized Mice.* Molecules, 2018. **23**(7).
42. Langendorf, C.G., et al., *Structural basis of allosteric and synergistic activation of AMPK by furan-2-phosphonic derivative C2 binding.* Nat Commun, 2016. **7**: p. 10912.
43. Kim, J., et al., *AMPK activators: mechanisms of action and physiological activities.* Exp Mol Med, 2016. **48**: p. e224.

Figures

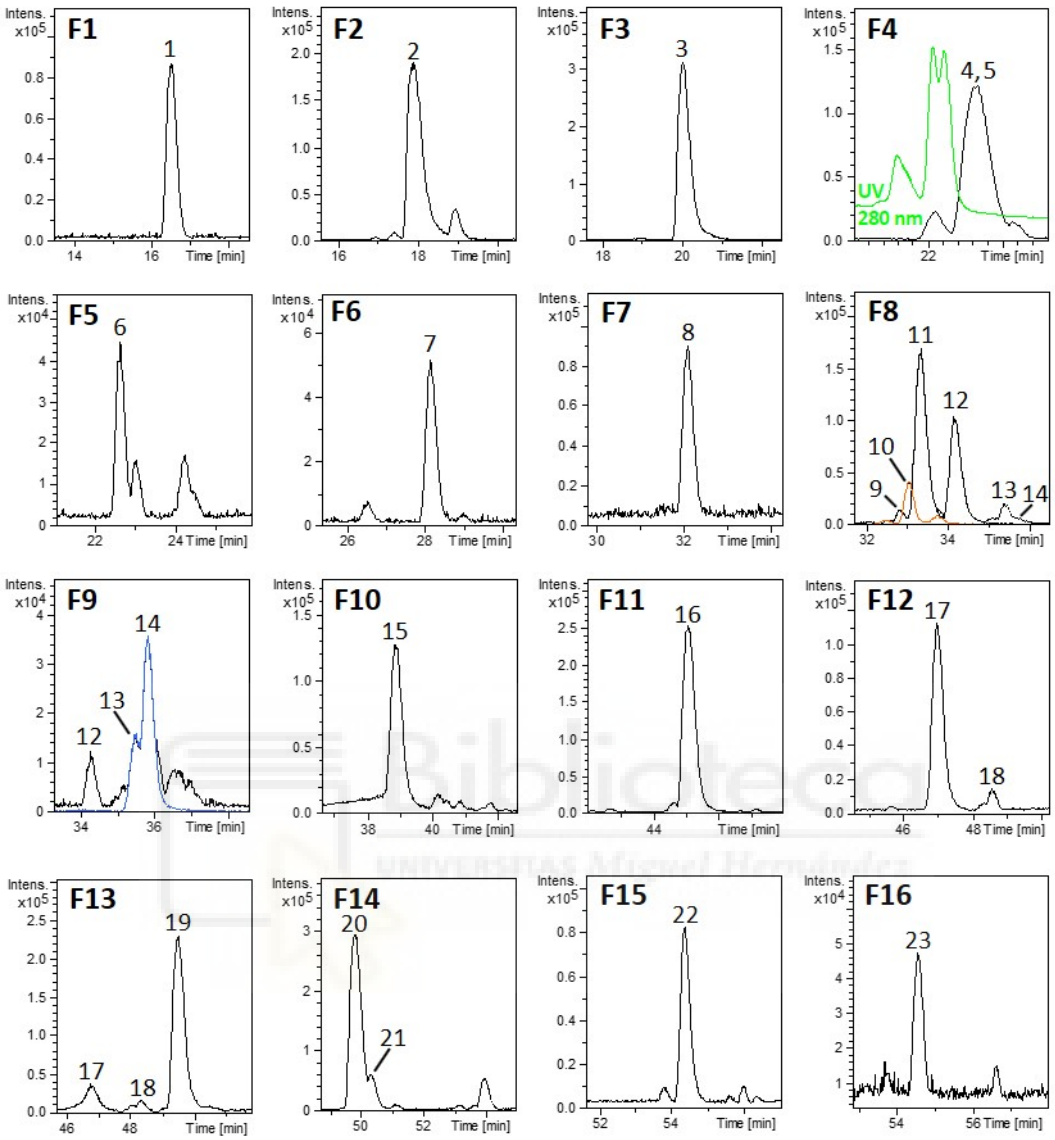

Figure 1. Base peak chromatograms (BPC) of the collected fractions from the LC numbered as F1-F16. Peak numbers were included according to Table 1 and their elution order. UV chromatogram at 280 nm was represented for elucidating the two isomers present in F4, while extracted ion chromatogram (EIC) was remarked in other colors for those cases that were considered necessary.

Table 1. Retention time (RT) and mass spectral data of the compounds characterized in the collected fractions of LC by RP-HPLC-ESI-TOF-MS in negative mode. * indicates the major contribution of a compound in the remarked fraction.

Peak	RT (min)	$[M-H]^-$ measured	$[M-H]^-$ calculated	Error (ppm)	mSigma	Molecular formula	Proposed compound	Fraction	Relative area (%) in fraction
1	16.31	391.1236	391.1246	4.1	6.6	C 16 H 24 O11	Shanziside	F1*	100.0
2	17.79	373.1131	373.114	2.4	2.7	C 16 H 22 O 10	Gardoside	F2*	91.2
3	20.03	461.165	461.1664	3.2	1.5	C 20 H 30 O 12	Verbasoside	F3*	100.0
4	22.5	487.1474	487.1457	-3.5	1.6	C 21 H 28 O 13	Cistanoside F isomer	F4*	38.8
5	22.67	487.148	487.1457	-4.6	2.7	C 21 H 28 O 13	Cistanoside F isomer	F4*	52.1
6	22.81	375.1238	375.1297	15.8	9.8	C 16 H 24 O 10	Loganic acid	F5*	57.1
7	28.27	405.1377	405.1402	6.4	11.6	C 17 H 26 O 11	Shanziside methyl ester	F6*	90.9
8	32.07	389.1082	389.1089	1.9	1.1	C 16 H 22 O 11	Theveside	F7*	100.0
9	32.82	387.1657	387.1661	0.9	4.6	C18 H27 O9	Tuberonic acid glucoside isomer	F8	2.1
10	32.97	445.2075	445.2079	1	5.6	C 21 H 34 O 10	Sacranoside A	F8	7.1
11	33.37	387.1651	387.1661	2.5	6.9	C 18 H 28 O 9	Tuberonic acid glucoside isomer	F8*	51.8
12	34.13	387.2024	387.2024	0.1	3.6	C 19 H 32 O8	UK	F8* / F9	32.4 / 12.1
13	35.38	639.1914	639.1931	2.6	23.7	C 29 H 36 O 16	β-hydroxy-(iso)-verbascoside	F8 / F9*	5.1 / 18.3
14	35.95	639.1909	639.1931	3.3	36	C 29 H 36 O 16	β-hydroxy-(iso)-verbascoside	F8 / F9*	1.4 / 51.6
15	38.83	637.1024	637.1046	3.6	4	C 27 H 26 O 18	Luteolin-7-diglucuronide	F10*	87.9
16	45.05	623.1936	623.1981	7.3	3.3	C 29 H 36 O 15	Verbascoside	F11*	84.4
17	47.04	651.1229	651.1203	-4	2.3	C 28 H 28 O 18	Chrysoeriol-7-diglucuronide	F12* / F13	90.9 / 3.1
18	48.55	621.1879	621.1766	-18.2	21.8	C 36 H 30 O 10	Diooflavone	F12 / F13	6.9 / 3.2
19	49.17	623.2108	623.1981	13.5	8.8	C 29 H 36 O 15	Isoverbascoside	F13*	80.1
20	49.87	623.1992	623.1981	-1.9	0.2	C 29 H 36 O 15	Forsythoside A	F14*	78.2
21	50.44	637.2126	637.2138	1.9	11.3	C 30 H 38 O 15	Leucosceptoside A	F14	9.7
22	54.42	635.1277	635.1254	-3.7	3.4	C 28 H 28 O 17	Acacetin-7-diglucuronide	F15*	90.2
23	54.63	651.2299	651.2294	-0.7	3.8	C 31 H 40 O 15	Martynoside	F16*	89.4

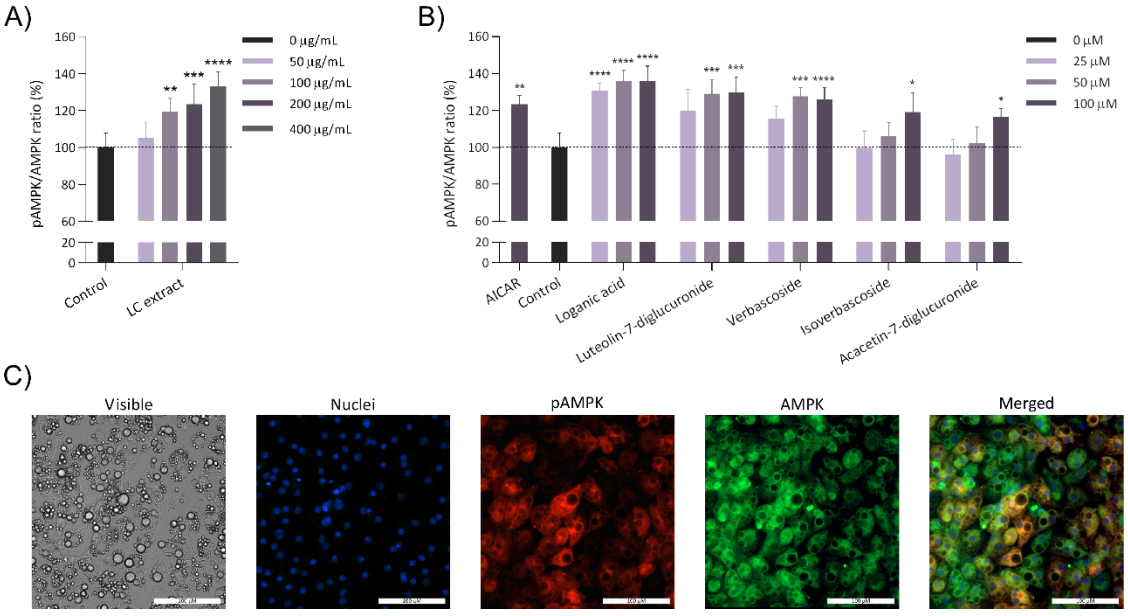

Figure 2. Activity of AMPK in adipocytes 3T3-L1 after 24 h of incubation with LC extract (A) or individual compounds from LC (B). Protein levels of total AMPK and pAMPK were measured by an immunofluorescence assay and the activity of AMPK is represented as the ratio between pAMPK and AMPK levels. Panel **A** shows the effect of the whole extract at 50, 100, 200 and 400 µg/mL, panel **B** shows AMPK activation values of the activator compounds (loganic acid, luteolin-7-diglucuronide, verbascoside, isoverbascoside and acacetin-7-diglucuronide) at 25, 50 and 100 µM. AICAR was incubated at 100 µM for 24 h and represented in panel **B**. All the treatments are normalized to their respective controls in DMSO or water depending on the solubility of the compounds. The data are expressed as the mean ± S.D (n = 5). *, **, *** and **** indicate significant differences with respect to their corresponding controls without extract/compound ($p < 0.5$, $p < 0.01$, $p < 0.001$ and $p < 0.0001$, respectively). Finally, panel **C** illustrates images of adipocytes in phase contrast (visible), blue fluorescence (nuclei), red fluorescence (pAMPK), green fluorescence (AMPK) and merged, after the immunofluorescence assay.

Table 2. Quantitation of compounds in the LC extract by RP-HPLC and analytical parameters from the standard curve used. Compounds were monitored by the DAD detector at 235, 320 and 350 nm wavelengths for loganic acid, verbascoside and luteolin-7-diglucuronide, respectively.

Compound	RT (min)	LOD (µg/mL)	LOQ (µg/mL)	Linear range (µg/mL)	Linear regression equation	r^2	% (w/w) of compound in the LC extract
Loganic acid	14.075	0.15625	0.3125	0.3125-750	y = 19.035x + 60.018	0.9986	0.05 ± 0.01
Luteolin-7-diglucuronide	22.728	0.15625	0.3125	0.3125-750	y = 18.543x - 103.53	0.9996	0.53 ± 0.01
Verbascoside	31.066	0.15625	0.3125	0.3125-1500	y = 11.543x - 40.687	0.9996	0.53 ± 0.01

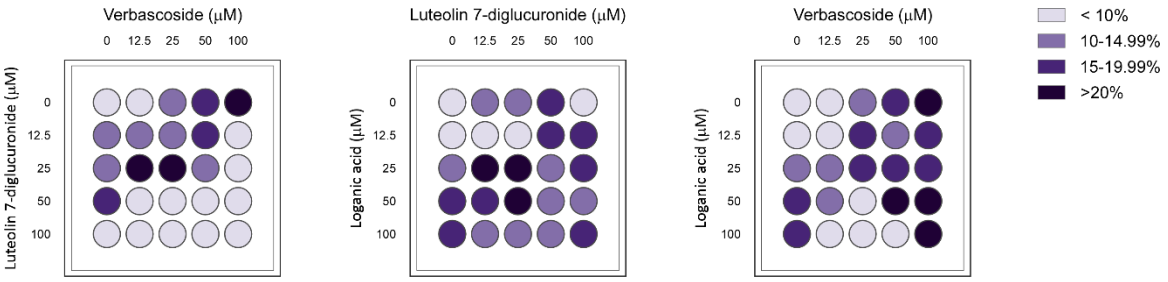

Figure 3. Scheme of the checkerboard method for FICI determination for the pairwise combinations between the best AMPK activators. Four concentrations of the selected compounds from LC (loganic acid, luteolin 7-diglucuronide and verbascoside) were added to adipocytes in 96-well plates in pairwise combinations. One compound was added on the x-axis across the plate at the indicated concentrations and another compound was added on the y-axis. Treated adipocytes were incubated for 24 h and AMPK values were obtained by an immunofluorescence assay. An increase in AMPK activation of 15 % or superior with respect to non-treated cells (0 μM) was considered significant.

Table 3. FICI values and synergy interpretation for the pairwise combinations between the best AMPK activators. FICI values were calculated according to the formula: FICI = (Minimum activating concentration (MAC) of compound X in combination / MAC of compound X alone) + (MAC of compound Y in combination / MAC of compound Y alone).

Combination	FICI	Effect
Verbascoside + Luteolin-7-diglucuronide	0.75	Additivity
Luteolin-7-diglucuronide + Loganic acid	0.5	Synergy
Verbascoside + Loganic acid	0.75	Additivity

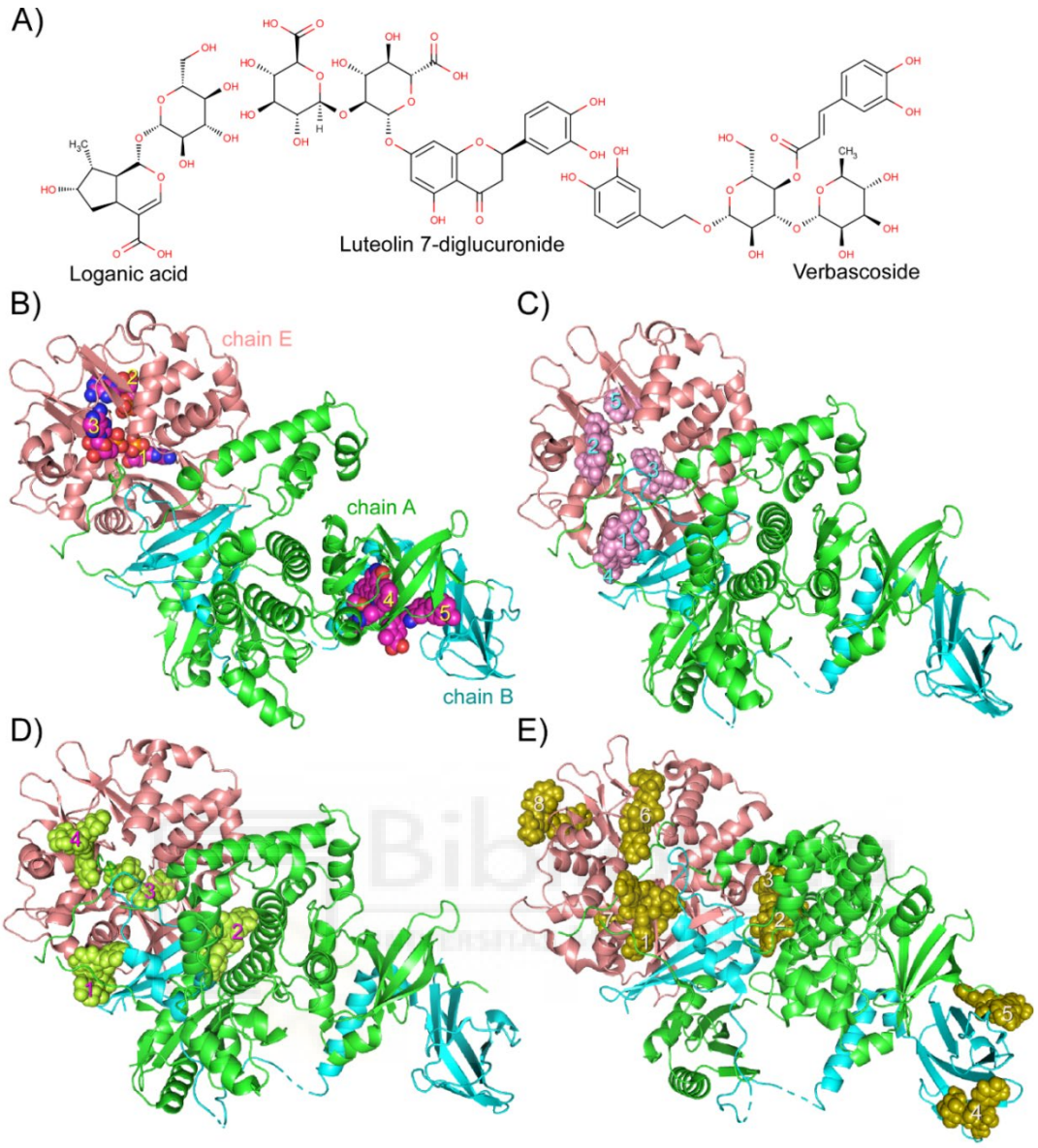

Figure 4. Illustration of the secondary structure for human AMPK with docked loganic acid (C), luteolin-7-diglucuronide (D) and verbascoside (E). For each cluster of the docked compound (loganic acid carbon atoms in pink color, luteolin-7-diglucuronide carbon atoms in lemon color and verbascoside carbon atoms in olive color), the molecule (spheres) with better binding energy is shown (a number indicates each cluster of the different compounds, see supplementary tables). The three AMPK subunits have been shown with different colors (alpha-2 in green as *chain A*, beta-1 in blue as *chain B*, and gamma-1 in salmon as *chain E*). The number of each cluster was indicated. The **5iso** structure has been used (panels **B**, **C**, **D**, **E**) and panel **B** shows the three AMP binding sites (1, 2, 3), the ATP binding site in the catalytic domain (4), and the regulatory site in the interaction zone between the alpha-2 and beta-1 subunits (5). Finally, panel **A** shows the molecular structure of loganic acid, luteolin-7-diglucuronide and verbascoside. The figure has been prepared using the PyMol 2.0 software.

Supplementary

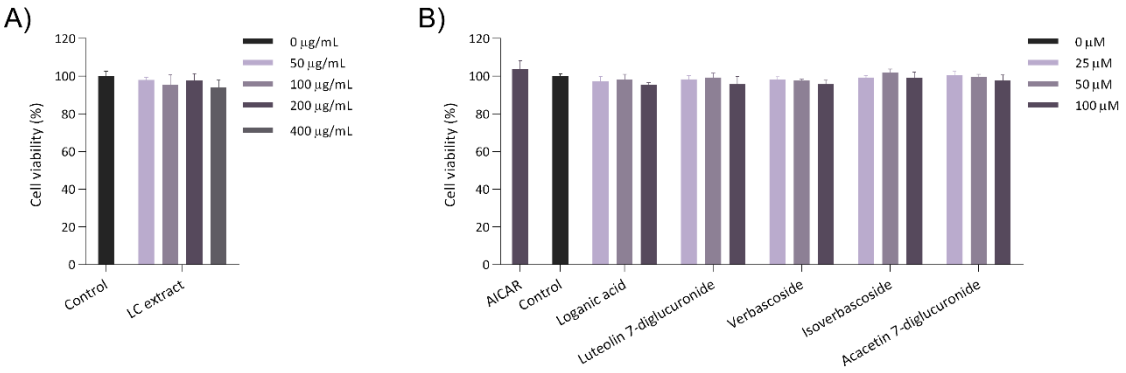

Supplementary Figure 1. Cell viability of adipocytes 3T3-L1 after 24 h of incubation with LC extract (A) or individual compounds (B). Number of cells was counted by staining nuclei with Hoechst. AICAR was incubated at 100 µM for 24 h and represented in panels **B**. All the treatments are normalized to their respective controls in DMSO or water depending on the solubility of the compounds. The data are expressed as the mean ± S.D (n = 5).

Supplementary Table 1. Details of the interaction of loganic acid docked to the human AMPK (see **Fig. 4C**).

Cluster number	ΔG, [kcal/mol]	Dissoc. constant, [µM]	Members	Residues of the AMPK that contact loganic acid
1	-9.735±1.015	0.073095	4.85 %	ARG(A)-369, LYS(A)-399, ALA(A)-400, TRP(A)-402, ILE(B)-214, LEU(B)-215, ASN(B)-216, LYS(B)-217, ASP(B)-218, THR(B)-219, LEU(B)-228, LEU(B)-242, LEU(B)-265, TYR(B)-267, LYS(B)-47, THR(B)-66, ASN(B)-67
2	-9.626±0.899	0.087846	6.06 %	LYS(A)-364, PRO(A)-365, HIS(A)-366, PRO(A)-367, ARG(A)-369, MET(A)-370, PRO(A)-371, ILE(E)-240, PHE(E)-244, ASP(E)-245, ASN(E)-248, LEU(E)-266, HIS(E)-268, ARG(E)-269, TYR(E)-272, PHE(E)-273, GLU(E)-274, GLY(E)-275, VAL(E)-276, LEU(E)-277, VAL(E)-297
3	-9.603±0.892	0.091275	2.12 %	ARG(E)-70, LEU(E)-74, GLY(E)-84, MET(E)-85, LEU(E)-86, THR(E)-87, THR(E)-89, ASP(E)-90, ARG(E)-118, TYR(E)-121, LYS(E)-127, LEU(E)-129, VAL(E)-130, CYS(E)-131, LYS(E)-149, ILE(E)-150, HIS(E)-151, ARG(E)-152, LEU(E)-153, PRO(E)-154, LYS(E)-243
4	-9.340±1.363	0.142345	3.83 %	LEU(A)-373, LYS(A)-398, LYS(A)-399, ALA(A)-400, TRP(A)-402, LEU(B)-215, LEU(B)-242, LYS(B)-245, ASP(B)-246, VAL(B)-248, VAL(B)-250, LEU(B)-265, TYR(B)-267, LYS(E)-59, PHE(E)-62, ALA(E)-63, THR(E)-66, ASN(E)-67

5	-9.121±1.164	0.206011	2.02 %	GLY(E)-199, THR(E)-200, ALA(E)-202, ASN(E)-203, ILE(E)-204, ALA(E)-205, HIS(E)-223, ARG(E)-224, VAL(E)-225, SER(E)-226, ALA(E)-227, LEU(E)-228, PRO(E)-229, ARG(E)-299, ILE(E)-312, VAL(E)-313, SER(E)-314, SER(E)-316, ASP(E)-317

Supplementary Table 2. Details of the interaction of luteolin-7-diglucuronide docked to the human AMPK (see **Fig. 4D**).

Cluster number	ΔG, [kcal/mol]	Dissoc. constant, [μM]	Members	Residues of the AMPK that contact luteolin 7-diglucuronide
1	-11.696±1.722	0.002669	1.11 %	LEU(A)-373, VAL(A)-397, LYS(A)-398, LYS(A)-399, ALA(A)-400, LYS(A)-401, TRP(A)-402, LEU(B)-215, ASN(B)-216, LEU(B)-242, SER(B)-243, LYS(B)-245, ASP(B)-246, VAL(B)-248, VAL(B)-250, TYR(B)-267, LYS(E)-47, LYS(E)-59, PHE(E)-62, ALA(E)-63, THR(E)-66, ASN(E)-67
2	-10.279±1.223	0.029203	1.01 %	ARG(A)-369, MET(A)-370, PRO(A)-371, PRO(A)-372, LEU(A)-373, VAL(A)-397, LYS(A)-398, LYS(A)-399, ALA(A)-400, TRP(A)-402, LEU(B)-215, LYS(B)-217, ASP(B)-218, THR(B)-219, ILE(B)-221, LEU(B)-242, LEU(B)-265, LYS(E)-47, VAL(E)-65, THR(E)-66, ASN(E)-67, GLY(E)-68
3	-11.485±1.304	0.00381	0.91 %	ARG(E)-70, GLY(E)-84, MET(E)-85, LEU(E)-86, THR(E)-87, ILE(E)-88, THR(E)-89, ASP(E)-90, ASN(E)-93, TYR(E)-121, LYS(E)-127, PRO(E)-128, LEU(E)-129, VAL(E)-130, ASN(E)-148, LYS(E)-149, ILE(E)-150, HIS(E)-151, ARG(E)-152, PHE(E)-220, VAL(E)-221, ARG(E)-224, SER(E)-226, LYS(E)-243
4	10.427±1.529	0.022743	2.12 %	LYS(A)-364, PRO(A)-365, HIS(A)-366, PRO(A)-367, GLU(A)-368, ARG(A)-369, MET(A)-370, PRO(A)-371, PHE(E)-244, ASP(E)-245, HIS(E)-268, ARG(E)-269, HIS(E)-271, TYR(E)-272, PHE(E)-273, GLU(E)-274, GLY(E)-275, LEU(E)-277

Supplementary Table 3. Details of the interaction of verbascoside docked to the human AMPK (see **Fig. 4E**).

Cluster number	ΔG, [kcal/mol]	Dissoc. constant, [μM]	Members	Residues of the AMPK that contact verbascoside
1	-10.500±1.226	0.020111	1.05 %	ARG(A)-369, MET(A)-370, PRO(A)-371, PRO(A)-372, LEU(A)-373, LYS(A)-399, ALA(A)-400, TRP(A)-402, LYS(B)-217, ASP(B)-218, THR(B)-219, PRO(B)-225, LEU(B)-228, LEU(B)-242, VAL(B)-250, LEU(B)-265, TYR(B)-267, LYS(E)-47, VAL(E)-65, THR(E)-66, ASN(E)-67, GLY(E)-68
2	-10.190±0.440	0.033937	2.50 %	ASP(A)-128, HIS(A)-131, ARG(A)-132, MET(A)-164, ALA(A)-191, PRO(A)-193, GLU(A)-194, ILE(A)-197, THR(A)-258, ILE(A)-259, LYS(A)-260, GLU(A)-291, HIS(B)-209, GLU(B)-230, PRO(B)-231, ASN(B)-232, HIS(B)-233, LYS(B)-259, TYR(B)-261, THR(E)-44
3	-10.120±1.228	0.038193	3.61 %	GLU(A)-295, GLU(A)-298, LYS(A)-299, PHE(A)-300, GLU(A)-301, ILE(A)-327, ASN(A)-330, ARG(A)-331, MET(A)-334, LYS(B)-258, SER(E)-35, HIS(E)-36, ARG(E)-37, TYR(E)-39, ASP(E)-40, ASN(E)-135
4	-9.700±0.540	0.077597	4.21 %	TRP(B)-84, GLY(B)-86, GLY(B)-87, GLY(B)-88, LYS(B)-89, LYS(B)-126, VAL(B)-129, ASP(B)-130, GLN(B)-132, TRP(B)-133, THR(B)-134, HIS(B)-135, ASP(B)-136, PRO(B)-137, GLY(B)-147, THR(B)-148, VAL(B)-149
5	-9.540±0.362	0.101655	3.85 %	GLY(A)-9, ARG(A)-10, VAL(A)-11, LYS(A)-12, LEU(B)-103, PRO(B)-104, LEU(B)-105, THR(B)-106, ARG(B)-107, VAL(B)-113, ALA(B)-114, ILE(B)-115, LEU(B)-116, ASP(B)-117
6	-11.777±1.159	0.002328	1.07 %	LYS(A)-364, PRO(A)-365, HIS(A)-366, PRO(A)-367, GLU(A)-368, ARG(A)-369, MET(A)-370, PRO(A)-371, ILE(E)-240, PHE(E)-244, ASP(E)-245, HIS(E)-268, ARG(E)-269, TYR(E)-272, PHE(E)-273, GLU(E)-274, GLY(E)-275, VAL(E)-276, LEU(E)-277, LYS(E)-278, ARG(E)-291, ALA(E)-295, VAL(E)-297, ARG(E)-299
7	-10.240±0.232	0.031190	1.06 %	VAL(E)-83, GLY(E)-84, MET(E)-85, THR(E)-89, ASN(E)-93, ARG(E)-118, TYR(E)-121, LEU(E)-122, GLN(E)-123, ASP(E)-124, SER(E)-125, LYS(E)-127, PRO(E)-128, LEU(E)-129, VAL(E)-130, ASN(E)-148, LYS(E)-149, ILE(E)-150, ARG(E)-152, PRO(E)-154, ARG(E)-224, LYS(E)-243
8	-9.880±0.142	0.057267	2.03 %	ILE(E)-204, ALA(E)-205, MET(E)-206, VAL(E)-207, ARG(E)-208, THR(E)-209, THR(E)-210, THR(E)-211, PRO(E)-212, VAL(E)-215, ILE(E)-219, VAL(E)-231, ASP(E)-232, GLU(E)-233

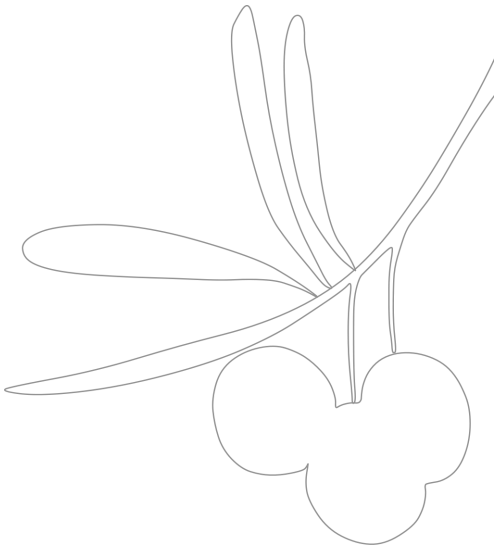

CAPÍTULO 3

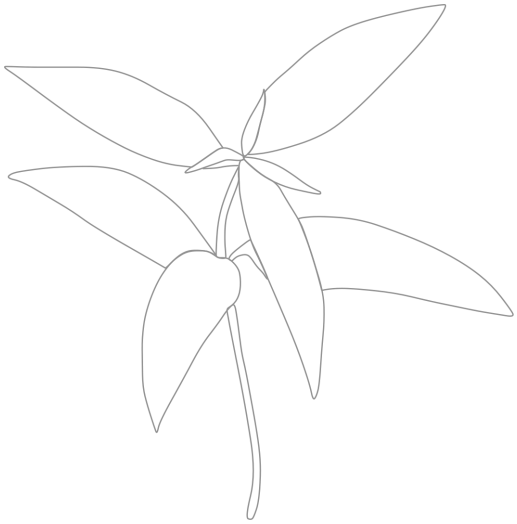

Phytomedicine 25 (2017) 25-28

Correlation between the cellular metabolism of quercetin and its glucuronide metabolite and oxidative stress in hypertrophied 3T3-L1 adipocytes

María Herranz-López[1], Isabel Borrás-Linares[1], Mariló Olivares-Vicente, Julio Gálvez, Antonio Segura-Carretero, Vicente Micol.

[1]These authors contributed equally to this work.

DOI: 10.1016/j.phymed.2016.12.008.

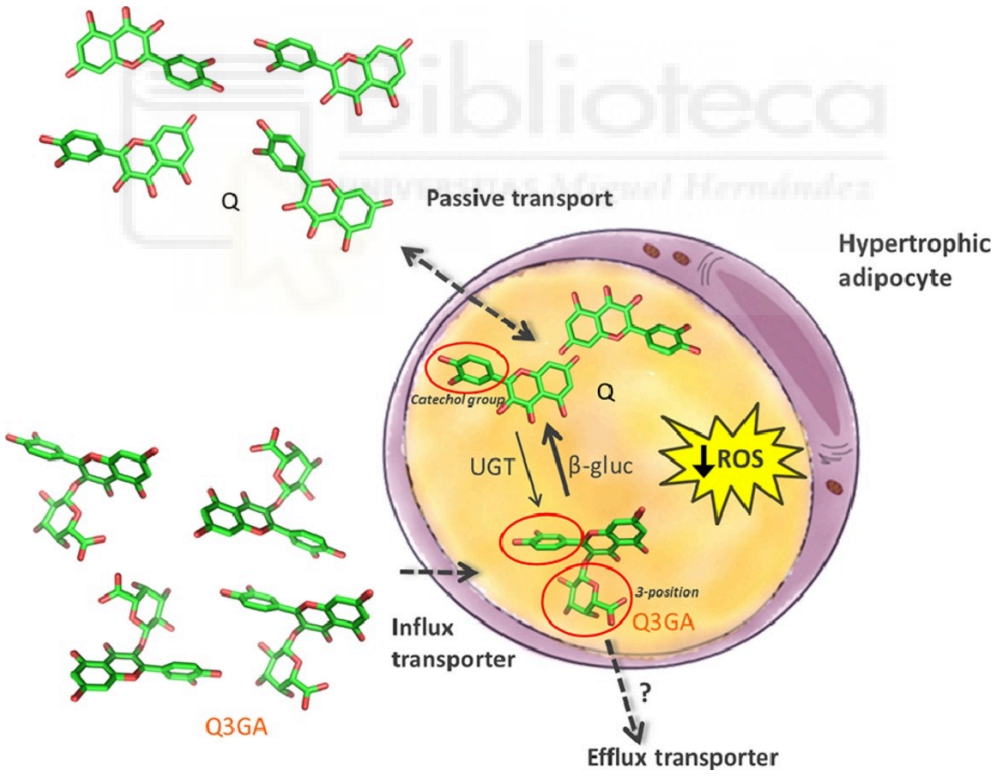

RESUMEN DE LOS RESULTADOS

En este trabajo, se propuso identificar y cuantificar metabolitos intracelulares en adipocitos hipertróficos incubados con quercetina (Q) y quercetina-3-glucurónido (Q3GA), y establecer una correlación entre la presencia de dichos metabolitos de la quercetina y los niveles intracelulares de ERO. Para ello, se trataron adipocitos hipertróficos con Q o Q3GA y se analizaron metabolitos intracelulares y niveles de ERO a las 3, 6, 12 y 18 h de incubación.

Los resultados observados tras la incubación de Q en adipocitos hipertróficos mostraron que la concentración intracelular de este flavonol aumentó rápidamente a las 3 h hasta 1.92 ± 0.03 μg/μg de proteína, decayendo hasta 5.5 veces su concentración a las 6 h. Por el contrario, su metabolito Q3GA apareció progresivamente en el citoplasma, alcanzando su máxima concentración a las 6 h de incubación (0.08 ± 0.0025 μg/μg) y decayendo al final del experimento. Cuando los adipocitos se incubaron en presencia de Q3GA, la máxima concentración intracelular de este metabolito se alcanzó a las 18 h (0.12 ± 0.0015 μg/μg). Sin embargo, también se detectó la presencia de Q alcanzando su máximo valor a las 3 h de incubación (0.03 ± 0.005 μg/mL) y manteniéndose durante el resto del experimento. Estos resultados indicaron una biotransformación intracelular de los dos metabolitos de quercetina en ambas direcciones, siendo más eficiente la conversión de Q a Q3GA que el proceso inverso.

Desde un punto de vista comparativo entre la evolución del estado oxidativo de los adipocitos hipertróficos y la presencia de los metabolitos de quercetina, los niveles de ERO disminuyeron significativamente tras el tratamiento con Q y Q3GA respecto al control (0 h). La mayor reducción de ERO alcanzada tras la incubación con Q fue a las 3 h de incubación (49 % de oxidación en comparación al 100 % del control), coincidiendo con la máxima concentración intracelular de Q. A continuación, el estrés oxidativo aumentó progresivamente a lo largo del experimento hasta alcanzar un 75 % de oxidación, simultáneamente a la disminución de la concentración de Q. Cuando se incubó con Q3GA, la producción de ERO disminuyó de un 82 % de oxidación a las 3 h de incubación hasta un 72 % al final del experimento, estableciéndose una directa correlación entre la acumulación de Q3GA y la disminución de ERO. A pesar de que la Q fue un antioxidante más potente, ambos metabolitos podrían contribuir a la reducción de ERO asociadas a la hipertrofia en adipocitos.

Phytomedicine 25 (2017) 25–28

Contents lists available at ScienceDirect

Phytomedicine

journal homepage: www.elsevier.com/locate/phymed

Correlation between the cellular metabolism of quercetin and its glucuronide metabolite and oxidative stress in hypertrophied 3T3-L1 adipocytes

María Herranz-López[a,1], Isabel Borrás-Linares[b,1], Mariló Olivares-Vicente[a], Julio Gálvez[c], Antonio Segura-Carretero[b], Vicente Micol[a,d,*]

[a] Institute of Molecular and Cell Biology (IMCB), Miguel Hernández University (UMH), Elche 03202, Alicante, Spain
[b] Center for Research and Development of Functional Food (CIDAF), Science Technology Park Health, Armilla, Granada, Spain
[c] CIBER-EHD, Department of Pharmacology, Center for Biomedical Research (CIBM), University of Granada, Avenida del Conocimiento s/n 18016, Armilla, Granada, Spain
[d] CIBER, Fisiopatología de la Obesidad y la Nutrición, CIBERobn, Instituto de Salud Carlos III (CB12/03/30038), Spain

ARTICLE INFO

Article history:
Received 23 August 2016
Revised 14 November 2016
Accepted 15 December 2016

Keywords:
Quercetin
Quercetin-3-O-β-D-glucuronide
Adipocytes
Cellular metabolism
HPLC-DAD-ESI-TOF
ROS

ABSTRACT

Background: Quercetin (Q) is one of the most abundant flavonoids in human dietary sources and has been related to the capacity to ameliorate obesity-related pathologies. Quercetin-3-O-β-D-glucuronide (Q3GA) is supposed to be the main metabolite in blood circulation, but the intracellular final effectors for its activity are still unknown.
Hypothesis/purpose: To identify and quantitate the intracellular metabolites in hypertrophied adipocytes incubated with Q or Q3GA and to correlate them with the intracellular generation of oxygen radical species (ROS).
Methods: Cytoplasmic fractions were obtained and quercetin metabolites were determined by liquid chromatography coupled to a time-of-flight mass detector with electrospray ionization (HPLC-DAD-ESI-TOF). Intracellular ROS generation was measured by a ROS-sensitive fluorescent probe.
Results: Both Q and Q3GA were absorbed by hypertrophied adipocytes and metabolized to some extent to Q3GA and Q, respectively, but Q absorption was more efficient (1.92 ± 0.03 µg/µg protein) and faster than that of Q3GA (0.12 ± 0.0015 µg/µg protein), leading to a higher intracellular concentration of the aglycone. Intracellular decrease of ROS correlated with the presence of the most abundant quercetin metabolite.
Conclusion: Q and Q3GA are efficiently absorbed by hypertrophied adipocytes and metabolized to some extent to Q3GA and Q, respectively. The intracellular decrease of ROS in a hypertrophied adipocyte model treated with Q or Q3GA is correlated with the most abundant intracellular metabolite for the first time. Both compounds might be able to reach other intracellular targets, thus contributing to their bioactivity.

Introduction

Plant-derived polyphenols have demonstrated the potential to improve some disease states by a multitargeted mode of action (Barrajon-Catalan et al., 2014; Joven et al., 2012; Joven et al., 2014). Quercetin (3,3′,4′,5,7-pentahydroxyflavone) (Q) derivatives are the most abundant flavonoids in human dietary sources; ubiquitously present in fruits and vegetables (Ahn et al., 2008), they are converted into aglycone on the cell surface of intestinal epithelial cells and bacteria. Upon absorption, Q is subjected to different types of metabolism, with quercetin-3-O-β-D-glucuronide (Q3GA) as the major metabolite circulating in the bloodstream. The localization of Q3GA in macrophages, atherosclerotic lesions, brain and immune cells and lipid droplets of the liver by using specific antibodies has been reported (Joven et al., 2012; Kawai et al., 2008).

Q3GA is proposed to be deconjugated by β-glucuronidase into hydrophobic Q aglycone in cells, such as macrophages or vascular tissue, which in turn may improve intracellular pathological conditions (Ishisaka et al., 2013; Kawai et al., 2008; Menendez et al., 2011). Nevertheless, no deconjugation has been demonstrated in other cell models.

Abbreviations: Q, quercetin; Q3GA, quercetin-3-O-β-D-glucuronide; ROS, radical oxygen species; UGT, UDP-glucuronosyltransferase; PPAR, peroxisome proliferator-activated receptor; H2DCF-DA, 2′,7′-dichlorodihydrofluorescein diacetate.

* Corresponding author.
E-mail addresses: mherranz@umh.es (M. Herranz-López), vmicol@umh.es (V. Micol).
[1] These authors contributed equally to this work.

http://dx.doi.org/10.1016/j.phymed.2016.12.008
0944-7113/

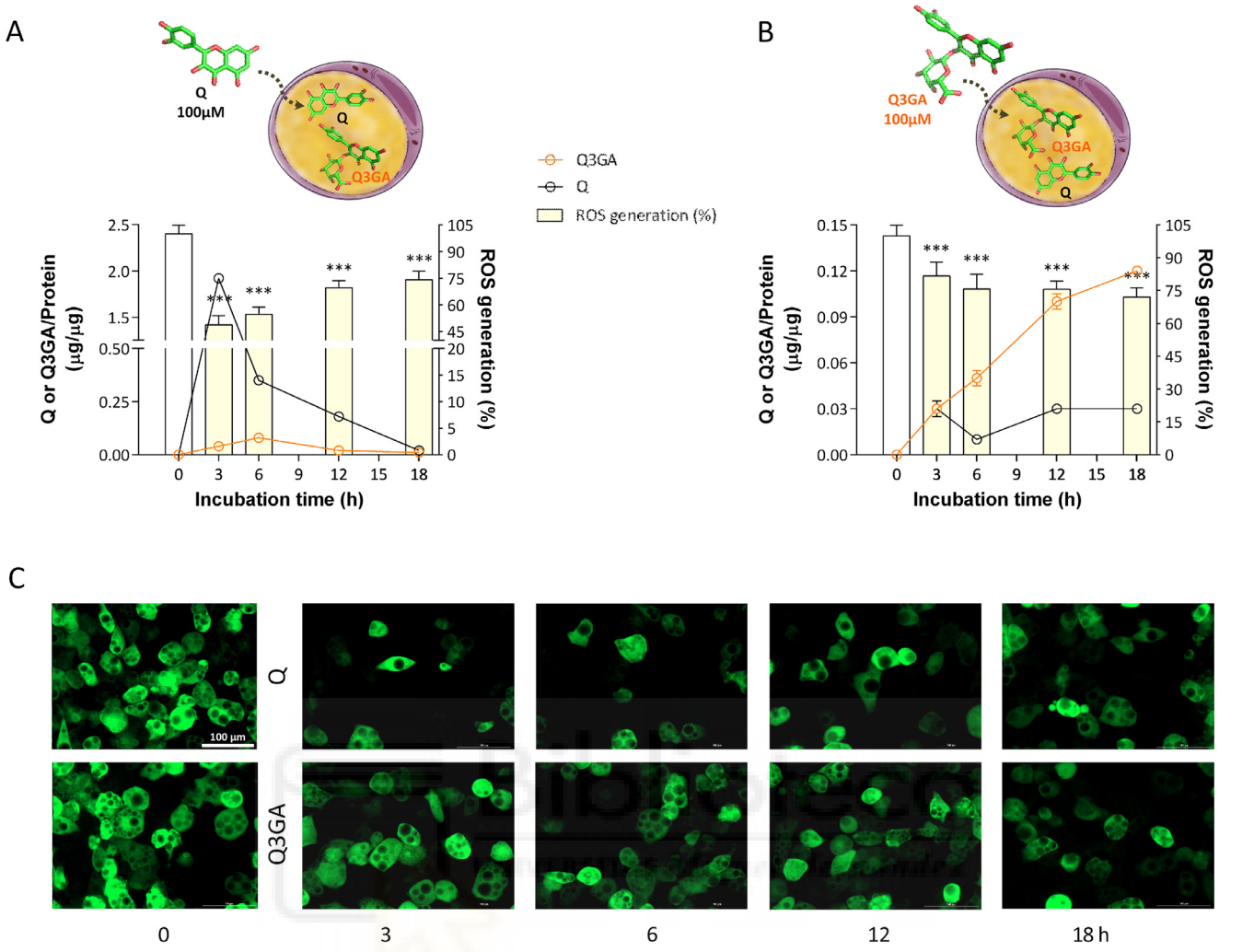

Fig. 1. Cellular metabolism of Q and Q3GA in hypertrophied adipocytes and the concomitant intracellular ROS decrease.
Hypertrophic adipocytes were treated with 100 µM Q (A) or 100 µM Q3GA (B) for 0, 3, 6, 12 and 18 h, and the cellular levels of both the aglycone and glucuronide metabolites were determined by HPLC-ESI-TOF-MS (black and orange circles, respectively). An inverse correlation was observed between intracellular ROS generation, determined by using the ROS-sensitive fluorescent probe H2DCF-DA (yellow bars) and the cytoplasmic levels of Q (A) and Q3GA (B). Representative photomicrographs of intracellular ROS after incubation of adipocytes with Q or Q3GA for 3, 6, 12 and 18 h (C). The intensity of green fluorescence represents the level of intracellular ROS compared to the control (0 h). All data were analyzed by using one-factor ANOVA and Tukey test for multiple comparisons. The results were expressed as the mean ± standard deviation. Differences showing $p < 0.05$ were considered statistically significant (n = 6).

Adipocyte hypertrophy compromises cell function, initiating an oxidative stress-related inflammatory process leading to metabolic disorders associated with obesity (Furukawa et al., 2004). Our findings strongly support that polyphenols from *Hibiscus sabdariffa* L. (Malvaceae) may become an alternative way to alleviate the metabolic disturbances associated with obesity through the modulation of energy management and inflammation pathways (Barrajon-Catalan et al., 2014; Beltran-Debon et al., 2010; Herranz-Lopez et al., 2012). Evidence in animal models leads us to propose that Q and Q3GA, among other flavonols, are the major blood metabolites accounting for these effects (Fig. 1, Supplementary information) (Fernandez-Arroyo et al., 2012; Joven et al., 2012). Nevertheless, the main quercetin metabolites reaching adipocyte intracellular targets are yet to be discovered. In the present work, a comparative study of the cellular metabolism of Q and its glucuronide metabolite was carried out by high performance liquid chromatography coupled to a time-of-flight mass detector with electrospray ionization (HPLC-DAD-ESI-TOF) in hypertrophied adipocytes, and the intracellular metabolites were correlated with the generation of ROS in the cytosol.

Material and methods

Chemicals

LC-MS grade formic acid for mobile phase preparation and the standards Q, Q3GA and naringenin (used as internal standard) were purchased from Fluka, Sigma-Aldrich (Steinheim, Germany). LC-MS grade acetonitrile and analytical reagent grade methanol and ethanol were obtained from Fisher Scientific (Madrid, Spain). Stock solutions containing these analytes were prepared in methanol and stored at −80 °C until use. 3T3-L1 cells and all tissue culture reagents were purchased as reported (Herranz-Lopez et al., 2012). Briefly, 3T3-L1 cells were purchased from the American Type Culture Collection (Manassas, VA, USA). Dexamethasone, 3-isobutyl-1- methylxanthine and insulin were obtained from Sigma–Aldrich (Madrid, Spain). Dulbecco's modified Eagle's medium, calf serum, fetal bovine serum, and an antibiotic mixture (penicillin–streptomycin) were purchased from PAA Laboratories (Linz, Austria). Sodium pyruvate and trypsin–EDTA were obtained from Invitrogen (Carlsbad, CA). Polyvinyldifluoride (PVD) filters, 0.22 µm, were obtained from Millipore (Bedford, MA).

Analysis of Q and Q3GA accumulation in hypertrophied 3T3-L1 adipocytes, sample processing and intracellular ROS measurement

The 3T3-L1 preadipocyte line was propagated and differentiated (Green and Kehinde, 1975). Hypertrophied adipocytes were obtained (Herranz-Lopez et al., 2012) and were treated with 100 µmol/l of Q or Q3GA in serum-free medium. At 0, 3, 6, 12 and 18 h of incubation, cultures were washed with PBS (pH 7.4) twice. Fractionation of cytoplasmic (pooled cell supernatant) and membrane fractions (precipitate) was achieved as reported elsewhere (Borrás-Linares et al., 2015). Briefly, for fractionation of the cells, 1 ml of 0.1% ascorbic acid solution (pH 4) was added to the cells. After three cycles of freezing and thawing, cells were harvested by repetitive pipetting. Pooled mixtures were sonicated three times in an ice-cold bath sonicator (VWR Aquasonic 75D; West Chester, PA) for 10 min each at level 7, then centrifuged at 16,000 x g for 15 min at 4 °C. Pooled supernatant and precipitate fractions are referred to as the cytoplasmic and membrane fractions, respectively. Protein concentration in the cell lysates was analyzed by the Bradford method according to the manufacturer's protocol (Bio-Rad, Hercules, CA). Intracellular ROS generation was measured in hypertrophied adipocytes using 2′,7′-dichlorodihydrofluorescein diacetate (H2DCF-DA, Sigma-Aldrich, Spain) as reported elsewhere (Herranz-Lopez et al., 2015) (see Supplementary information).

For HPLC analysis, the cytoplasmic fractions were spiked with 30 µg/ml of naringenin (methanol solution) used as an internal standard for the analysis. These samples were subjected to protein precipitation using methanol:ethanol (50:50, v/v) at a proportion of 1:5 (sample-solvent), vortex-mixed for 10 s, kept at −20 °C for 2 h and centrifuged at 17,900 x g for 15 min at 4 °C. Finally, the supernatants were collected and evaporated in a vacuum concentrator (Eppendorf Concentrator Plus, Eppendorf AG, Hamburg Germany), dissolved in 100 µl of methanol and stored at −80 °C until their analysis.

HPLC-DAD-ESI-TOF analysis and quantitation

The analyses of the cytoplasmic fractions were carried out using an Agilent 1200 RRLC system (Agilent Technologies, Palo Alto, CA, USA) of the Series Rapid Resolution coupled to a microTOFTM mass analyzer (Bruker Daltonik, Bremen, Germany) via an ESI interface (model G1607A, Agilent Technologies, Palo Alto, CA, USA) operating in negative ionization mode. The chromatographic column, separation conditions, mobile phases, DAD detection and standard calibration data are detailed in Supplementary information (Supplementary Materials and Supplementary Table 1).

Results and discussion

H. sabdariffa polyphenols inhibit triglyceride accumulation, oxidative stress and inflammation in cell models (Herranz-Lopez et al., 2012) and prevent hepatic steatosis in hyperlipidemic mice through the regulation of glucose and lipid homeostasis pathways (Joven et al., 2012). These effects are concomitant with the presence of Q3GA in immune cells and lipid droplets of the liver. Bioavailability studies have demonstrated that Q and Q3GA are the major metabolites found in plasma of rats fed *H. sabdariffa* polyphenols (Fernandez-Arroyo et al., 2012) (Fig. 1, Supplementary information).

To identify the intracellular compounds responsible for these effects, we carried out a comparative study of the uptake of Q and Q3AG by hypertrophied 3T3-L1 adipocytes after 3, 6, 12 and 18 h of incubation (Fig. 1, Supplementary Table 2). When adipocytes were incubated in the presence of Q, their glucuronide metabolite, Q3GA, appeared progressively in the cytoplasm, reaching its maximum concentration after 6 h of incubation (0.08 ± 0.0025 µg/µg protein) and then decaying throughout the assay (Fig. 1A, Supplementary Table 2). In contrast, the Q concentration sharply increased after 3 h of incubation up to a concentration of 1.92 ± 0.03 µg/µg (Fig. 1A). Upon incubation of hypertrophied adipocytes with Q3GA, the intracellular concentration of this compound steadily increased until it reached its maximum concentration at 18 h (0.12 ± 0.0015 µg/µg) (Fig. 1B). However, quercetin aglycone appeared quickly, reaching its maximum value after 3 h of incubation (0.03 ± 0.005 µg/µg) and showing a plateau that was maintained throughout the study.

The uptake of Q was approximately 16-fold higher and was much faster (3 h) compared to the maximum concentration of Q3GA achieved in adipocytes incubated with this metabolite (18 h), highlighting that Q was rapidly absorbed by passive diffusion. In contrast, Q3GA was less efficiently absorbed due to the higher polarity of glucuronic derivatives, which hampers their absorption through the cell membrane, as postulated for other cell lines (Spencer et al., 2003; Youdim et al., 2003). In agreement with our observation, it has been reported that Q-7- and Q-3-glucuronides, but not Q-4-glucuronides, can be absorbed and undergo turnover by intracellular β-glucuronidase activity in human liver hepatocellular cells, most likely by an influx transporter such as the organic anion transport polypeptide (OATP2) (O'Leary et al., 2003).

Interestingly, Q concentrations dropped sharply, approximately 5.5-fold, after 6 h of incubation compared with 3 h, which can be explained on the basis of metabolism/oxidation of Q leading to diverse degradation compounds (*o*-quinones), as reported in a human hepatocellular carcinoma cell line (Boyer et al., 2004). In our case, no degradation compounds were detected in the cytoplasmic fractions by HPLC-DAD-ESI-TOF. Alternatively, low quantities of Q3GA were found, indicating the presence of biotransformation most likely due to UDP-glucuronosyltransferase (UGT) activity.

Our results clearly indicate that biotransformation occurs in both directions in adipocytes, from Q to Q3GA and *vice versa*. Glucuronidation of several flavonoids has been observed in fibroblasts (Proteggente et al., 2003). Isoforms of UGT have been found in several cell lines (Barbier et al., 2003; Beaulieu et al., 1998), and UGT 1A9 has been implicated in the glucuronidation of the synthetic peroxisome proliferator-activated receptor (PPAR) activators (Prueksaritanont et al., 2002; Watanabe et al., 2002) and natural PPARα and PPARγ agonists (Barbier et al., 2003). Furthermore, treatment with PPAR activators, such as plant polyphenols (Encinar et al., 2015; Herranz-López et al., 2015; Wang et al., 2014), results in enhanced glucuronidation activity and UGT expression (Barbier et al., 2003). All these data suggest that glucuronidation reactions can occur *in vivo* in diverse tissues apart from the liver and small intestine and indicate that polyphenols may induce their own glucuronidation. In our hypertrophic adipocyte model, UGT activity seemed to be weaker than that of glucuronidase, since the conversion of Q3GA to Q seemed to be more efficient than the reverse process. According to our results, it has been reported that in cell conditions bearing high levels of inflammation or oxidative stress, as occurs in hypertrophic adipocytes, Q emerges by the action of β-glucuronidase (Terao et al., 2011).

The correlation between the biological effects of polyphenols and the intracellular presence of the responsible metabolites is hard to prove. Therefore, we aimed to study the effects of cytoplasmic metabolites on the evolution of concomitant oxidative stress in a hypertrophied adipocyte model (Han et al., 2007; Herranz-Lopez et al., 2012). Intracellular ROS levels were quantified in the same adipocyte model treated with Q or Q3GA using the fluorescent probe H2DCF-DA (Fig. 1). Adipocytes treated with Q or Q3GA during different times (3–18 h) exhibited a significant reduction of ROS generation compared with the controls (Fig. 1C). The highest reduction of ROS level achieved by Q incubation was obtained after 3 h of incubation (49% of oxidation) (Fig. 1A and C).

After that, oxidative stress gradually increased to reach 74% oxidation after 18 h of incubation with the aglycone. Considering that Q was more abundant than Q3GA and that oxidation behavior correlated with the intracellular accumulation of Q, quercetin aglycone was proposed to be primarily responsible for the ROS decrease in this case. However, when adipocytes were incubated with Q3GA, the intracellular ROS production decreased steadily from 3 h (82% oxidation) up to the minimum achieved at the end of the assay (72% oxidation) (Fig. 1B and C). This result confirms a direct relation between the accumulation of Q3GA and the decrease of ROS. However, we cannot rule out that the total intracellular antioxidant activity is the result of the balanced contribution of all conjugate metabolites (Terao et al., 2011).

Conclusions

In conclusion, both Q and Q3GA were absorbed by hypertrophied adipocytes and metabolized to Q3GA and Q by glucuronosyltransferase and glucuronidase activity, respectively. Absorption was more efficient and faster for Q than Q3GA, leading to a higher intracellular concentration of the aglycone. Both metabolites Q and Q3GA were responsible for an intracellular decrease of ROS in hypertrophied adipocytes. These results support for the first time that both metabolites may account for the strong radical scavenging capacity observed in hypertrophied adipocytes treated with the polyphenolic extract of *H. sabdariffa* (Herranz-Lopez et al., 2012) and might also reach other intracellular targets that contribute to their bioactivity.

Conflict of interest

We confirm that there are no known conflicts of interest associated with this publication.

Acknowledgments

We are grateful for grant AGL2011-29857-C03-03 from MICINN; Grants AGL2015-67995-C3-1-R, AGL2015-67995-C3-2-R, AGL2015-67995-C3-3R, PTQ-13-06429 and PTQ-14-07243 from MINECO; PROMETEO/2012/007 and PROMETEO/2016/006, and ACIF/2016/230 to MOV from Generalitat Valenciana; CIBER (CB12/03/30038, Fisiopatologia de la Obesidad y la Nutricion, CIBERobn, Instituto de Salud Carlos III).

Supplementary materials

Supplementary material associated with this article can be found, in the online version, at doi:10.1016/j.phymed.2016.12.008.

References

Ahn, J., Lee, H., Kim, S., Park, J., Ha, T., 2008. The anti-obesity effect of quercetin is mediated by the AMPK and MAPK signaling pathways. Biochem. Biophys. Res. Commun. 373, 545–549.

Barbier, O., Villeneuve, L., Bocher, V., Fontaine, C., Torra, I.P., Duhem, C., Kosykh, V., Fruchart, J.-C., Guillemette, C., Staels, B., 2003. The UDP-glucuronosyltransferase 1A9 enzyme is a peroxisome proliferator-activated receptor α and γ target gene. J. Biol. Chem. 278, 13975–13983.

Barrajon-Catalan, E., Herranz-Lopez, M., Joven, J., Segura-Carretero, A., Alonso-Villaverde, C., Menendez, J.A., Micol, V., 2014. Molecular promiscuity of plant polyphenols in the management of age-related diseases: far beyond their antioxidant properties. Adv. Exp. Med. Biol. 824, 141–159.

Beaulieu, M., Lévesque, É., Hum, D.W., Bélanger, A., 1998. Isolation and characterization of a human orphan UDP-glucuronosyltransferase, UGT2B11. Biochem. Biophys. Res. Commun. 248, 44–50.

Beltran-Debon, R., Alonso-Villaverde, C., Aragones, G., Rodriguez-Medina, I., Rull, A., Micol, V., Segura-Carretero, A., Fernandez-Gutierrez, A., Camps, J., Joven, J., 2010. The aqueous extract of *Hibiscus sabdariffa* calices modulates the production of monocyte chemoattractant protein-1 in humans. Phytomedicine 17, 186–191.

Borrás-Linares, I., Herranz-López, M., Barrajón-Catalán, E., Arráez-Román, D., González-Álvarez, I., Bermejo, M., Gutiérrez, A.F., Micol, V., Segura-Carretero, A., 2015. Permeability study of polyphenols derived from a phenolic-enriched *Hibiscus sabdariffa* extract by UHPLC-ESI-UHR-Qq-TOF-MS. Int. J. Mol. Sci. 16, 18396–18411.

Boyer, J., Brown, D., Liu, R.H., 2004. Uptake of quercetin and quercetin 3-glucoside from whole onion and apple peel extracts by Caco-2 cell monolayers. J Agric. Food Chem. 52, 7172–7179.

Encinar, J.A., Fernandez-Ballester, G., Galiano-Ibarra, V., Micol, V., 2015. In silico approach for the discovery of new PPARgamma modulators among plant-derived polyphenols. Drug Des. Dev. Ther. 9, 5877–5895.

Fernandez-Arroyo, S., Herranz-Lopez, M., Beltran-Debon, R., Borras-Linares, I., Barrajon-Catalan, E., Joven, J., Fernandez-Gutierrez, A., Segura-Carretero, A., Micol, V., 2012. Bioavailability study of a polyphenol-enriched extract from *Hibiscus sabdariffa* in rats and associated antioxidant status. Mol. Nutr. Food Res. 56, 1590–1595.

Furukawa, S., Fujita, T., Shimabukuro, M., Iwaki, M., Yamada, Y., Nakajima, Y., Nakayama, O., Makishima, M., Matsuda, M., Shimomura, I., 2004. Increased oxidative stress in obesity and its impact on metabolic syndrome. J. Clin. Invest. 114, 1752–1761.

Green, H., Kehinde, O., 1975. An established preadipose cell line and its differentiation in culture. II. Factors affecting the adipose conversion. Cell 5, 19–27.

Han, C.Y., Subramanian, S., Chan, C.K., Omer, M., Chiba, T., Wight, T.N., Chait, A., 2007. Adipocyte-derived serum amyloid A3 and hyaluronan play a role in monocyte recruitment and adhesion. Diabetes 56, 2260–2273.

Herranz-Lopez, M., Barrajon-Catalan, E., Segura-Carretero, A., Menendez, J.A., Joven, J., Micol, V., 2015. *Lemon verbena* (*Lippia citriodora*) polyphenols alleviate obesity-related disturbances in hypertrophic adipocytes through AMPK-dependent mechanisms. Phytomedicine 22, 605–614.

Herranz-Lopez, M., Fernandez-Arroyo, S., Perez-Sanchez, A., Barrajon-Catalan, E., Beltran-Debon, R., Menendez, J.A., Alonso-Villaverde, C., Segura-Carretero, A., Joven, J., Micol, V., 2012. Synergism of plant-derived polyphenols in adipogenesis: perspectives and implications. Phytomedicine 19, 253–261.

Ishisaka, A., Kawabata, K., Miki, S., Shiba, Y., Minekawa, S., Nishikawa, T., Mukai, R., Terao, J., Kawai, Y., 2013. Mitochondrial dysfunction leads to deconjugation of quercetin glucuronides in inflammatory macrophages. PLoS One. 8, e80843.

Joven, J., Espinel, E., Rull, A., Aragones, G., Rodriguez-Gallego, E., Camps, J., Micol, V., Herranz-Lopez, M., Menendez, J.A., Borras, I., Segura-Carretero, A., Alonso-Villaverde, C., Beltran-Debon, R., 2012. Plant-derived polyphenols regulate expression of miRNA paralogs miR-103/107 and miR-122 and prevent diet-induced fatty liver disease in hyperlipidemic mice. Biochem. Biophys. Acta. 1820, 894–899.

Joven, J., Micol, V., Segura-Carretero, A., Alonso-Villaverde, C., Menéndez, J.A., Aragonès, G., Barrajón-Catalán, E., Beltrán-Debón, R., Camps, J., Cufí, S., Fernández-Arroyo, S., Fernández-Gutiérrez, A., Guillén, E., Herranz-López, M., Iswaldi, I., Lozano-Sánchez, J., Martin-Castillo, B., Oliveras-Ferraros, C., Pérez-Sánchez, A., Rodríguez-Gallego, E., Rull, A., Saura, D., Vázquez-Martín, A., 2014. Polyphenols and the modulation of gene expression pathways: can we eat our way out of the danger of chronic disease? Crit. Rev. Food Sci. Nutr. 54, 985–1001.

Kawai, Y., Nishikawa, T., Shiba, Y., Saito, S., Murota, K., Shibata, N., Kobayashi, M., Kanayama, M., Uchida, K., Terao, J., 2008. Macrophage as a target of quercetin glucuronides in human atherosclerotic arteries: implication in the anti-atherosclerotic mechanism of dietary flavonoids. J. Biol. Chem. 283, 9424–9434.

Menendez, C., Duenas, M., Galindo, P., Gonzalez-Manzano, S., Jimenez, R., Moreno, L., Zarzuelo, M.J., Rodriguez-Gomez, I., Duarte, J., Santos-Buelga, C., Perez-Vizcaino, F., 2011. Vascular deconjugation of quercetin glucuronide: the flavonoid paradox revealed? Mol. Nutr. Food Res. 55, 1780–1790.

O'Leary, K.A., Day, A.J., Needs, P.W., Mellon, F.A., O'Brien, N.M., Williamson, G., 2003. Metabolism of quercetin-7- and quercetin-3-glucuronides by an in vitro hepatic model: the role of human beta-glucuronidase, sulfotransferase, catechol-*O*-methyltransferase and multi-resistant protein 2 (MRP2) in flavonoid metabolism. Biochem. Pharmacol. 65, 479–491.

Proteggente, A.R., Basu-Modak, S., Kuhnle, G., Gordon, M.J., Youdim, K., Tyrrell, R., Rice-Evans, C.A., 2003. Hesperetin glucuronide, a photoprotective agent arising from flavonoid metabolism in human skin fibroblasts. Photochem. Photobiol. 78, 256–261.

Prueksaritanont, T., Tang, C., Qiu, Y., Mu, L., Subramanian, R., Lin, J.H., 2002. Effects of fibrates on metabolism of statins in human hepatocytes. Drug Metab. Dispos. 30, 1280–1287.

Spencer, J.P.E., Kuhnle, G.G.C., Williams, R.J., Rice-Evans, C., 2003. Intracellular metabolism and bioactivity of quercetin and its in vivo metabolites. Biochem. J. 372, 173–181.

Terao, J., Murota, K., Kawai, Y, 2011. Conjugated quercetin glucuronides as bioactive metabolites and precursors of aglycone in vivo. Food Funct. 2, 11–17.

Wang, L., Waltenberger, B., Pferschy-Wenzig, E.-M., Blunder, M., Liu, X., Malainer, C., Blazevic, T., Schwaiger, S., Rollinger, J.M., Heiss, E.H., Schuster, D., Kopp, B., Bauer, R., Stuppner, H., Dirsch, V.M., Atanasov, A.G., 2014. Natural product agonists of peroxisome proliferator-activated receptor gamma (PPARγ): a review. Biochem. Pharmacol. 92, 73–89.

Watanabe, Y., Nakajima, M., Yokoi, T., 2002. Troglitazone glucuronidation in human liver and intestine microsomes: high catalytic activity of UGT1A8 and UGT1A10. Drug Metab. Dispos. 30, 1462–1469.

Youdim, K.A., Dobbie, M.S., Kuhnle, G., Proteggente, A.R., Abbott, N.J., Rice-Evans, C., 2003. Interaction between flavonoids and the blood–brain barrier: *in vitro* studies. J. Neurochem. 85, 180–192.

Food and Chemical Toxicology (submitted)

Quercetin-3-O-glucuronide is a major contributor from *Hibiscus sabdariffa* to alleviate glucolipotoxicity-induced metabolic stress

María Herranz-López[1], Mariló Olivares-Vicente[1], Esther Rodríguez Gallego, José Antonio Encinar, Almudena Pérez-Sánchez, Jorge Joven, Enrique Roche, Vicente Micol.

[1]Both authors contributed equally to this study.

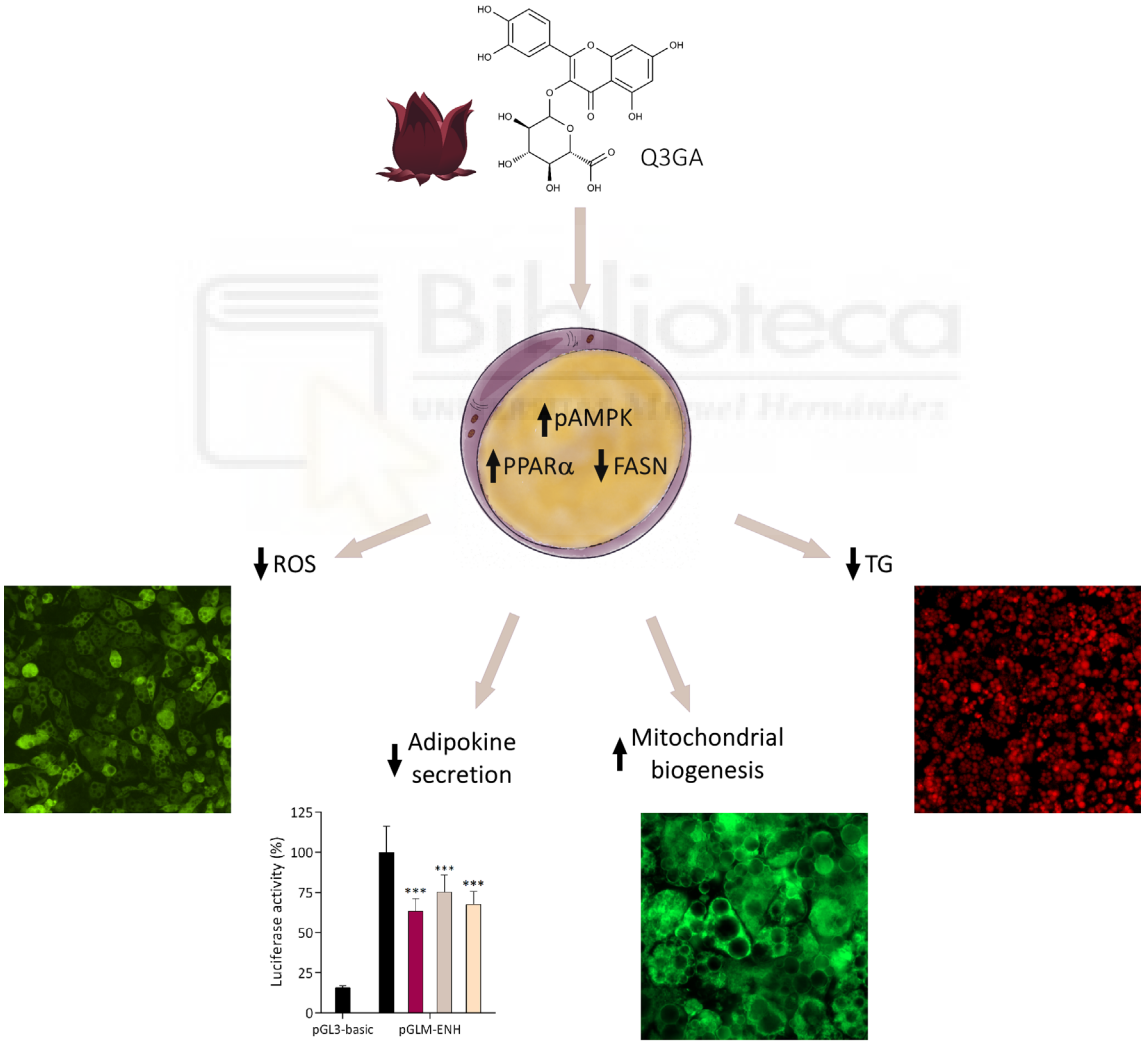

RESUMEN DE LOS RESULTADOS

Con el fin de investigar los posibles metabolitos responsables de los efectos biológicos del extracto polifenólico de HS (PEHS) en la obesidad, se evaluó el efecto del ácido clorogénico, Q y Q3GA (todos ellos metabolitos identificados en plasma de ratas alimentadas con PEHS [98]) en la reversión del estrés metabólico inducido por glucolipotoxicidad en adipocitos 3T3-L1 y células β-pancreáticas INS 832/13.

Los resultados del estudio *in vitro* indicaron un alto estrés oxidativo en adipocitos hipertróficos incubados durante al menos 17 días con altas concentraciones de glucosa (20 mM) comparado con adipocitos maduros tratados con bajos niveles de glucosa (5 mM). Cuando se trataron los adipocitos hipertróficos con PEHS (10 y 30 μg/mL) y los metabolitos (25 y 100 μM) durante 48 h, la Q y la Q3GA mostraron la mayor capacidad de inhibir la oxidación (reduciendo hasta un 37 % y 44 % la producción de ERO, respectivamente). No obstante, el ácido clorogénico, así como el antioxidante de referencia ácido ascórbico, apenas inhibieron la generación de ERO en este modelo celular. Esta capacidad antioxidante de las dos formas de la quercetina se mantuvo en adipocitos y células β-pancreáticas cuando se indujo la glucolipotoxicidad con alta glucosa y palmitato (0.5 mM).

El PEHS y los dos derivados de quercetina redujeron significativamente la secreción de adipoquinas proinflamatorias (leptina, IGF-1, IL-6, VEGF, IL-1α, IL-1β, TNF-α y MCP-1) en adipocitos hipertróficos inducidos por alta glucosa tras 48 h de incubación. Concretamente, la inhibición de MCP-1 puede considerarse de particular interés por la capacidad de esta proteína de atraer macrófagos al tejido adiposo, lo que implicaría una reducción de la respuesta inflamatoria. Cuando se transfectaron adipocitos con el plásmido pGLM-ENH (que contiene la región potenciadora del gen de MCP-1 humano), PEHS, Q y Q3GA inhibieron también la expresión de esta citoquina a nivel transcripcional (valores de actividad luciferasa: 63.4 %, 75.2 % y 67.5 %, respectivamente).

La acumulación de triglicéridos intracelulares en adipocitos hipertróficos disminuyó tras el tratamiento con PEHS, Q y Q3GA hasta un 20 %, 15 % y 27 %, respectivamente, mientras que el ácido clorogénico no mostró ningún efecto sobre la acumulación lipídica. En particular, la Q3GA fue el metabolito que mayor efecto presentó, por lo que se evaluó la capacidad de PEHS y Q3GA de modular tres proteínas implicadas en la homeostasis energética y el metabolismo lipídico: AMPK, FASN y PPARα. En el primer caso, ambos activaron significativamente AMPK, siendo el extracto más activo. No obstante, la Q3GA evidenció una mayor capacidad de reducir la expresión de FASN y aumentar la expresión de PPARα. El análisis de acoplamiento molecular mostró bajas ΔG para Q y Q3GA en posiciones

funcionalmente relevantes para las 3 proteínas: especialmente en la cavidad de unión de los agonistas de PPARα, en la cavidad del dominio catalítico de FASN y en los sitios de unión a AMP de la subunidad γ de AMPK. Estos resultados sugieren que las dos formas de quercetina podrían actuar como moduladores directos de estas tres proteínas metabólicas.

La glucolipotoxicidad induce en los adipocitos defectos en la biogénesis y dinámica mitocondrial. El tratamiento con PEHS y Q3GA aumentó significativamente el contenido de mitocondrias en adipocitos, mientras que la Q no mostró cambios sobre la masa mitocondrial. Las observaciones de microscopía electrónica de transmisión mostraron un desequilibrio en los procesos de fusión y fisión de las mitocondrias, así como la aparición de estructuras relacionadas con autofagosomas en adipocitos hipertróficos inducidos por alta glucosa. Dichas alteraciones parecen ser revertidas por PEHS y Q3GA, ya que no se observaron ni procesos de fusión y fisión mitocondrial, ni vacuolas autofágicas bajo estas condiciones.

Quercetin-3-O-glucuronide is a major contributor from *Hibiscus sabdariffa* to alleviate glucolipotoxicity-induced metabolic stress

María Herranz-López[1#*], Mariló Olivares-Vicente[1#], Esther Rodríguez Gallego[2], Jose Antonio Encinar[1], Almudena Pérez-Sánchez[1], Jorge Joven[3, 4], Enrique Roche[5, 6] and Vicente Micol[1, 6]

[1]Instituto de Investigación, Desarrollo e Innovación en Biotecnología Sanitaria de Elche (IDiBE) e Instituto de Biología Molecular y Celular (IBMC). Miguel Hernández University (UMH), Elche 03202, Alicante, Spain.

[2]Infection and Immunity (INIM). Unitat de Recerca. Hospital Universitari Joan XXIII de Tarragona. 43007, Tarragona.

[3]Universitat Rovira i Virgili, Departament de Cirurgia i Medicina, Unitat de Recerca Biomèdica. 43201 Reus (Tarragona), Spain.

[4]Institut d'Investigació Sanitària Pere Virgili (IISPV), 43204 Reus, Spain.

[5]Institute of Bioengineering and Department of Applied Biology-Nutrition, University Miguel Hernandez, Alicante Institute for Health and Biomedical Research (ISABIAL), Alicante, Spain.

[6]CIBER, Fisiopatología de la Obesidad y la Nutrición, CIBERobn, Instituto de Salud Carlos III (CB12/03/30038). Spain.

*Corresponding author. Address: mherranz@umh.es

[#]Both authors contributed equally to this study.

Abbreviations: HS (*Hibiscus sabdariffa* L.), PEHS (polyphenol-enriched HS extract), Q (quercetin), Q3GA (quercetin-3-O-glucuronide), AMPK (AMP-activated protein kinase), pAMPK (phospho-AMPK), DEX (dexamethasone), ELISA (Enzyme-Linked InmunoSorbent Assay), FASN (fatty acid synthase), H_2DCF-DA (2',7'-dichlorodihydrofluorescein diacetate), IBMX (3-isobutyl-1-methylxanthine), IGF-1 (insulin-like growth factor-1), IL1α (interleukin-1 alpha), IL1β (interleukin-1 beta), IL6 (interleukin 6), MCP-1 (monocyte chemoattractant protein-1), PPARα (peroxisome proliferator-activated receptor alpha), TNF-α (tumor necrosis factor-alpha), VEGF (vascular endothelial growth factor).

Highlights

Plant polyphenols from *H. sabdariffa* (HS) have exhibited the capacity to alleviate obesity-related metabolic complications.

Among quercetin metabolites, Q3GA was found to be the predominant metabolite in rat plasma.

PEHS, Q and Q3GA decreased cytokine secretion and glucolipotoxicity-induced ROS generation in hypertrophic adipocytes.

PEHS, Q and Q3GA reduced lipid accumulation through AMPK-mediated decreased fat storage and increased fatty acid oxidation.

Among quercetin metabolites, Q3GA showed the highest antilipogenic and mitochondrial viability restoration effects.

ABSTRACT

Polyphenols from *Hibiscus sabdariffa* (HS) alleviate obesity-related metabolic complications but the metabolites responsible for such effects are unknown. We aimed to elucidate which of the potential quercetin metabolites derived from polyphenol-enriched HS extract (PEHS) contributed more for the reversion of glucolipotoxicity-induced metabolic stress using 3T3-L1 adipocyte and INS 832/13 pancreatic β-cell models under glucolipotoxic conditions.

PEHS, quercetin (Q) and quercetin-3-O-glucuronide (Q3GA) showed stronger capacity to decrease glucolipotoxicity-induced ROS generation than ascorbic acid or chlorogenic acid. PEHS, Q and Q3GA reduced triglyceride accumulation, decreased cytokine secretion and reduced MCP-1 cytokine expression at transcriptional level. Q3GA and PEHS exhibited stronger capacity than Q to reduce triglyceride accumulation, which occurred through FASN downregulation, AMPK activation and mitochondrial mass and biogenesis restoration via PPARα upregulation. Electron microscopy rationale confirmed that PEHS and Q3GA decreased mitochondrial remodeling and mitophagy. Virtual screening lead us to postulate that Q and Q3GA might act as agonists of these protein targets at specific sites.

These data suggest that Q3GA may be the main responsible for the capacity of HS extract to revert glucolipotoxicity-induced metabolic stress through AMPK-mediated decrease in fat storage and increase in fatty acid oxidation, though other compounds of the extract may contribute to this capacity.

Keywords: glucolipotoxicity; *Hibiscus sabdariffa;* polyphenols; quercetin-3-glucuronide; AMPK; mitochondrial remodeling.

1. Introduction

Adipocytes are far from being an inert fat storage tissue. Recent evidence supports the idea that these cells play an instrumental role in glucose homeostasis by regulating the presence of GLUT-4 receptors on the cell surface. Excess circulating glucose can be incorporated and converted to fatty acids through the activation of the lipogenic pathway. Fatty acids can then be stored in the form of triglycerides in lipid droplets. However, lipid overload generates endoplasmic reticulum stress, mitochondrial dysfunction and increased inflammatory cytokine release from adipocytes, attracting macrophages. This glucolipotoxicity is associated with an oxidative-inflammatory stress condition that, when sustained over time, results in insulin resistance in peripheral cells, mainly hepatocytes and myocytes (Mittra et al., 2008). Additionally, adipocytes become insulin resistant, decreasing glucose uptake and leading to hyperglycemia and the development of type 2 diabetes.

Obesity, considered a triglyceride surplus syndrome, is a risk condition that favors the development of type 2 diabetes and cardiovascular diseases and is considered the main symptom in the diagnosis of metabolic syndrome (Despres and Lemieux, 2006). One-quarter of the world's population suffers from metabolic syndrome, according to International Diabetes Federation (O'Neill and O'Driscoll, 2015). As mentioned before, excess fat accumulation compromises cellular function through severe defects in mitochondrial biogenesis and impaired mitochondrial dynamics, resulting in the overproduction of ROS, which leads to oxidative stress (Addabbo et al., 2009). Since mitochondria are the main site for fat oxidation, mitochondrial dysfunction results in fat accumulation and adipocyte hypertrophy. In this context, the stimulation of the secretion of proinflammatory cytokines, such as interleukin IL-1, IL-6, TNF-α, leptin and monocyte chemoattractant protein-1 (MCP-1), may contribute to the development of insulin resistance (Cancello and Clement, 2006; Han, 2016; Luna-Luna et al., 2015; O'Neill and O'Driscoll, 2015).

Obesity-related dyslipidemia affects other tissues, such as the pancreas, leading to a glucolipotoxic condition that impairs pancreas endocrine function (Miyake et al., 2018). Pancreatic β-cells are located in the endocrine pancreas and secrete insulin. Fat accumulation in this particular cell type inhibits insulin secretion and results in mitochondrial dysfunction, leading to apoptosis. Low insulin production and secretion causes hyperglycemia and dyslipidemia, ultimately culminating in type 2 diabetes (Soria et al., 2003). In fact, both insulin resistance in adipocytes and the dysfunction of pancreatic β-

cells have been reported to be involved in the pathogenesis of metabolic syndrome. Thus, mitochondrial dysfunction might be regarded as a target for therapeutic action in metabolic diseases (Bhatti et al., 2017).

Polyphenols from *Hibiscus sabdariffa* L. (HS) have shown to inhibit adipogenesis in 3T3-L1 preadipocytes (Kim et al., 2007), reduce body weight gain and glycemia in obese/MSG-treated mice (Alarcon-Aguilar et al., 2007) and decrease plasma triglycerides in hyperlipidemic mice (Fernandez-Arroyo et al., 2011). Furthermore, HS extract reduces the plasma concentrations of MCP-1 in humans (Beltran-Debon et al., 2010) and alleviates steatohepatitis in hyperlipidemic mice (Joven et al., 2012) and obese humans (Chang et al., 2014). These findings suggest that the polyphenolic extract of HS may modulate pathways related to energy management and inflammation, improving metabolic disturbances associated with obesity.

Extracts derived from HS calyces show a complex composition and are rich in anthocyanins, such as delphinidin and cyanidin derivatives, and polysaccharides. HS extract also contains organic acids such as hydroxycitric and hibiscus acid, phenolic acids and other flavonoids such as quercetin (Q), luteolin and their derivatives (Herranz-Lopez et al., 2017b). We have previously shown that a polyphenol-enriched HS (PEHS) extract devoid of fiber and polysaccharides exerted a higher capacity than the original aqueous extract to inhibit triglyceride accumulation in hypertrophied and insulin-resistant adipocytes. PEHS also modulated proinflammatory adipokine secretion and reduced reactive oxygen species (ROS) generation in hypertrophied cells (Herranz-Lopez et al., 2012). Nevertheless, attempts to increase this activity by further purification failed, suggesting putative synergistic interactions between several components in the extract.

Experiments aimed at searching for the key compounds responsible for the properties mentioned above are scarce. A bioavailability study of HS extract in a rat model revealed that some flavonol-conjugated forms may be candidate metabolites that contribute to the health effects of PEHS, and quercetin-3-O-glucuronide (Q3GA) was found to be the predominant metabolite in rat plasma. Compared with other alternative plant sources (Nemeth and Piskula, 2007), HS extract has shown greater bioavailability of its flavonol derivatives, displaying a plasma concentration near 5 μM after oral administration in rats (Fernandez-Arroyo et al., 2012). Accordingly, the Q3GA metabolite was identified in the liver of hyperlipidemic mice fed PEHS, concomitantly with steatohepatitis improvements (Joven et al., 2012).

In view of the above, further research is needed to identify the specific metabolites responsible for the health effects of PEHS to develop polyphenolic mixtures from HS with potential applications in obesity. To identify these metabolites, in this work, we studied the effects of PEHS and some of the putative candidate metabolites in obesity-associated metabolic disturbances in 3T3-L1 hypertrophic cells and INS 832/13 pancreatic β-cells under glucolipotoxic conditions. The capacity of these metabolites to activate AMPK and to modulate lipid metabolism and mitochondrial function was also evaluated. Finally, their putative ability to interact with selected target proteins related to energy management was also assessed using virtual screening.

2. Materials and methods

2.1 Chemicals and reagents

Dulbecco's modified Eagle's medium (DMEM), Roswell Park Memorial Institute medium (RPMI 1640), Dulbecco's phosphate-buffered saline (PBS), penicillin-streptomycin and D-glucose were purchased from Gibco (Grand Island, NY, USA). Dexamethasone (DEX), 3-isobutyl-1-methylxanthine (IBMX), insulin, sodium pyruvate, palmitic acid, β-mercaptoethanol, dimethyl sulfoxide (DMSO) and 2′,7′-dichlorodihydrofluorescein diacetate (H_2DCF-DA) were obtained from Sigma-Aldrich (Madrid, Spain). Calf serum (CS) and fetal bovine serum (FBS) were purchased from Thermo Scientific (Cramlington, Northumberland, UK). Fatty acid-poor and endotoxin-free fraction V albumin from bovine serum was obtained from EMD Millipore (Billerica, USA). HS extract was kindly provided by the Biomedical Research Unit (URB) (Reus, Spain) (Herranz-Lopez et al., 2012). Quercetin was obtained from Extrasynthese (France). Quercetin-3-glucuronide, chlorogenic acid and L-ascorbic acid were purchased from Sigma-Aldrich (Europe). Cellulose acetate filters (0.2 μm) were obtained from GE Healthcare Life Sciences (Buckinghamshire, UK). AdipoRed™ Assay Reagent was purchased from Lonza (Walkersville, MD, USA).

2.2 Cell culture, differentiation of the 3T3-L1 cell line and hypertrophied adipocyte model

The 3T3-L1 preadipocytes (American Type Culture Collection, Manassas, VA, USA) were cultured in low glucose (5 mM) DMEM supplemented with 10 % CS, 100 μg/mL streptomycin and 100 U/mL penicillin. INS 832/13 pancreatic β-cells (kindly provided by Dr. Enrique Roche) were cultured in RPMI 1640 supplemented with 11 mM glucose, 10 mM HEPES, 10 % FBS, 2 mM L-glutamine, 1 mM sodium pyruvate and 50 μM β-mercaptoethanol

as previously indicated (Soria et al., 2003). Both cell lines were incubated at 37°C in a humidified (5 % CO_2, 95 % air) atmosphere.

The 3T3-L1 preadipocytes were differentiated using standard protocols (Green and Kehinde, 1975). Briefly, differentiation from preadipocytes to adipocytes was induced by adding 10 % FBS, 1 µM insulin, 1 µM DEX and 0.5 mM IBMX to high glucose (20 mM) DMEM for 48 h. Then, the cells were maintained in high glucose DMEM supplemented with FBS, and insulin and medium were replaced every 2-3 days; mature adipocytes were obtained after 8 days of incubation. Hypertrophied adipocytes were obtained by maintaining mature adipocytes in high glucose DMEM supplemented with FBS and insulin for at least 9 additional days. Once hypertrophied adipocytes were obtained, the cells were treated with PEHS and several pure compounds for 48 h. Before the cell treatments, the extract and all the compounds were dissolved in medium or DMSO-medium and filtered for sterilization.

2.3 Induction of glucolipotoxicity

Glucolipotoxicity was induced in INS 832/13 pancreatic β-cells and mature 3T3-L1 adipocytes by incubation in 20 mM glucose alone or 20 mM glucose plus 0.5 mM palmitate (El-Assaad et al., 2010; Han et al., 2010). Briefly, the cells were incubated in their respective medium with 20 mM glucose (high glucose) alone or with 20 mM glucose in the presence of 0.5 % BSA alone as a control or 0.5 mM palmitate bound to 0.5 % BSA as the glucolipotoxic condition. Glucolipotoxicity was induced in β-cells for 24 h. At the same time, cells were treated with PEHS and quercetin derivatives to determine the effect of these treatments on glucolipotoxicity-induced oxidative stress. On the other hand, 3T3-L1 cells were differentiated and then glucolipotoxicity was induced for 7 days. Finally, PEHS and quercetin derivatives were assayed for 48 h.

2.4 Determination of intracellular reactive oxygen species (ROS) by H_2DCF-DA analysis, evaluation of lipid content by AdipoRed™ and determination of secreted adipokines by ELISA

Intracellular ROS generation was measured in both 3T3-L1 adipocytes and INS 832/13 pancreatic β-cells using 2′,7′-dichlorodihydrofluorescein diacetate (H_2DCF-DA). Briefly, 2x H_2DCF-DA was added when the cells were ready to be analyzed. After 30 minutes at 37°C, the cells were carefully washed with PBS (pH 7.4), and intracellular ROS levels were measured using a fluorescence microplate reader (POLARstar, Omega, BMG LABTECH) at 485 nm excitation and 520 nm emission or a multimode reader (Cytation 3, Biotek, Spain)

at 495 nm excitation and 529 nm emission. The cells were photographed by using a fluorescence microscope (Eclipse TE2000-U, Nikon microscope, Melville, NY) at 10x. The lipid content of hypertrophied adipocytes was assessed using the AdipoRed™ reagent. Briefly, the supernatant was removed from the cells, and the cells were washed carefully with PBS. Then, AdipoRed™ was added, and the cells were incubated for 15 minutes at room temperature. Triglyceride accumulation was measured using the POLARstar microplate reader at 485 nm excitation and 572 nm emission. Fat droplets were photographed using a fluorescence microscope (Eclipse TE2000-U) at 10x. The concentrations of adipokines were determined in the serum-free supernatant of hypertrophied adipocytes by a Mouse Obesity ELISA Strip Analysis kit (Signosis, Inc., Sunnyvale, CA, USA), which determines 8 cytokines (leptin, TNF-α, IGF-1, IL6, VEGF, IL1α, IL1β and MCP-1), following the manufacturer's instructions.

2.5 Quantification of AMPK, pAMPK, PPARα and FASN by Western blot

Hypertrophied adipocytes treated with PEHS and Q3GA for 48 h were washed with PBS and lysed with lysis buffer (20 mM Tris-HCl, 150 mM NaCl, 1 mM EDTA, 1 % CHAPS, 1 mM Pefabloc and 1 % phosphatase inhibitors no. 2, Sigma-Aldrich Inc., Steinheim, Germany). Then, the samples were submitted to ice-cold cycles and centrifuged to remove the cell debris. The protein concentrations were quantified using a NanoDrop spectrophotometer (NanoDrop Technologies, Wilmington, DE). AMPK, phospho-AMPK (pAMPK), FASN, PPARα and actin were analyzed by Western blotting. Electrophoresis was performed with 4-20 % Tris-Gly or 4-12 % Bis-Tris gradient polyacrylamide gels (Invitrogen, Barcelona, Spain). MES buffer (Invitrogen) was used for AMPK, pAMPK, PPARα and actin electrophoresis, and Tris-Gly buffer (Invitrogen) was used for FASN electrophoresis. Proteins were transferred to nitrocellulose membranes using the iBlot transfer system (Invitrogen). The antibodies used were rabbit anti-AMPK (2532, Cell Signaling Tech., Danvers, MA, USA), rabbit anti-pAMPK (Thr172) (2531, Cell Signaling Tech.), rabbit anti-FASN (3180, Cell Signaling Tech.), rabbit anti-PPARα (H-98, St. Cruz Biotech., Heidelberg, Germany) and rabbit anti-actin (H-300, St. Cruz Biotech.). The secondary antibodies were goat anti-rabbit-HRP (Dako, Glostrup, Denmark) and anti-goat-HRP (Dako, Glostrup, Denmark). Chemiluminescent detection was performed using the ECL Advance Western Blotting Detection kit (Amersham, GE Healthcare, Barcelona, Spain), and membranes were analyzed in a ChemiDoc system (Bio-Rad, Spain). Protein levels were quantified by band densitometry normalized to the β-actin signal using Image Lab software (Version 3.0 build 11, Bio-Rad, Madrid, Spain).

2.6 Plasmids and analysis of the human MCP-1 gene enhancer

The pGL3-basic plasmid was obtained from Promega (Madison, WI), and the pGLM-ENH plasmid was obtained from Osaka University (Osaka, Japan). The pGLM-ENH plasmid contains an enhancer region between nucleotides 22742 to 22513 from the human MCP-1 gene (230 bp) and an enhancer region between nucleotides 2107 to 2160 from the same gene (167 bp) coupled to the luciferase gene (Ueda et al., 1997) and linked to the pGL3-basic plasmid. Differentiated adipocytes were harvested by trypsinization (HyQtase, Thermo Scientific). Transfection was performed using 0.05 μg of pGLM-ENH plasmid or pGL3-basic (empty) plasmid as a control. To obtain high transfection efficiency, plasmids were introduced into differentiated adipocytes using the Neon® Transfection System from Invitrogen, following the manufacturer's instructions. Briefly, the adipocytes and corresponding plasmids were submitted to 2 pulses at 1400 V for 20 ms. Moreover, plasmid-free adipocytes were or were not submitted to the microporation process, and both conditions were used as controls. Then, the cells were seeded and incubated 2 days later with PEHS or quercetin derivatives for 48 h. Finally, the cells were washed with PBS and lysed, and luciferase activity was determined using the Luciferase Assay System (Promega). Light production was measured using a luminometer (POLARstar).

2.7 Molecular docking

The structures of Q (PubChem CID: 5280343) and Q3GA (PubChem CID: 5274585) were obtained from the National Center for Biotechnology Information (NCBI) PubChem database (http://www.ncbi.nlm.nih.gov/pccompound). Human PPARα (1.65 Å resolution, PDB code **4P54**), FASN (2.3 Å resolution, PDB code **5C37**) and AMPK (2.63 Å resolution, PDB code **5ISO**) structures were obtained from the Research Collaboratory for Structural Bioinformatics (RCSB) Protein Data Bank (PDB). The specific structure of each protein was visualized using PyMol 2.0 software (The PyMOL Molecular Graphics System, Version 2.0 Schrödinger, LLC, at http://www.pymol.org/) without further optimization. Molecular docking experiments were performed using the YASARA v18.12.27 software (Krieger et al., 2004) that executed the AutoDock 4 algorithm (Morris et al., 2008), in which 999 flexible docking runs were set and clustered (7 Å) around the putative binding sites. The AMBER99 force field was used. The YASARA pH command was set to 7.4. The YASARA software calculated the Gibbs free energy variation (ΔG, kcal/mol), with highly positive energy values indicating strong binding. All the values shown in the table's results included a negative sign. Moreover, the ΔG value for only the best compound docked in each cluster is shown.

Dissociation constants were recalculated from the average binding energy of all the compounds in each cluster. The number of docked molecules (Q or Q3GA) included in each cluster of compounds is indicated as percent "Members". The theoretical dissociation constant of each ligand (Q or Q3GA) at its putative binding site can be determined by calculating the binding energy of the ligand-receptor complex. All the figures were prepared using PyMol 2.0 software.

2.8 Analysis of Mitochondrial Mass and Transmission electron microscopy

The mitochondrial mass of treated hypertrophic adipocytes was measured by using the fluorescent probe MitoTracker™ Green FM (Molecular Probes, Invitrogen, Carlsbad, CA, USA). In brief, the medium was removed, and the fluorescent dye was added at 200 nM in medium and incubated for 45 minutes at 37°C. Then, the staining solution was replaced with PBS, and fluorescence was quantified at 490/520 nm using a cell imaging multimode microplate reader (Cytation 3, Biotek Instruments, Winooski, VT, USA). Representative microphotographs of stained mitochondrial mass were taken with a GFP filter cube at 20x. Hypertrophied adipocytes were collected after trypsin digestion, washed with PBS and fixed with a 2 % glutaraldehyde solution in 0.1 M cacodylate buffer at a pH of 7.4. Samples were then postfixed in 1 % osmium tetroxide (OsO4) for 2 h and dehydrated in graded acetone solutions prior to impregnation in increasing concentrations of resin in acetone over a 24 h period. Semithin sections (500 nm) were stained with 1 % toluidine blue. Ultrathin sections (70 nm) were subsequently cut using a diamond knife, double-stained with uranyl acetate and lead citrate, and examined with a transmission electron microscope (Hitachi, Tokyo, Japan).

2.9 Statistical analyses

The results are expressed as the mean ± standard deviation of the mean from at least three independent experiments. Differences between two or more groups were compared by nonparametric tests and were considered statistically significant at $p < 0.05$. The stimulating or inhibitory effects of extracts and pure compounds versus the control were analyzed by one-way ANOVA and Tukey's test for multiple comparisons. All statistical analyses and graphic representations were performed using GraphPad Prism 5 software (GraphPad, San Diego, CA). $*p<0.05$, $**p<0.01$ and $***p<0.001$ indicate significant differences versus the high glucose control, unless otherwise stated.

3. Results

3.1 Selection of polyphenols and metabolites derived from HS extract

Polyphenols have been proposed to exert their pharmacological effects through their interaction with several metabolic targets (Barrajon-Catalan et al., 2014; Joven et al., 2013). Nevertheless, in most cases, the compounds or metabolites responsible for such effects are still unknown. Several metabolites derived from HS extracts have been found in pharmacokinetic studies performed in a rat model that may account for such effects, i.e., organic acids, phenolic acid derivatives and flavonol-conjugated forms (Herranz-Lopez et al., 2017b). Evidence from our laboratory suggests that flavonol-conjugated forms seem to be the most potent candidates that contribute to the health effects of PEHS (Herranz-Lopez et al., 2017b; Joven et al., 2012). These compounds are more potent antioxidants than phenolic acids such as chlorogenic acid, a reference antioxidant that is also abundant in the extract. Therefore, we selected chlorogenic acid, Q, Q3GA and PEHS to be compared in the development of the present study.

3.2 PEHS and quercetin derivatives show antioxidant effects under glucolipotoxic conditions in different cell types

HS extract has shown the capacity to reduce ROS generation in hypertrophied adipocytes (Herranz-Lopez et al., 2012), but its antioxidant capacity had not yet been compared with the compounds derived from the extract under a glucolipotoxic environment associated with metabolic stress. For this purpose, the antioxidant capacity of the above selected compounds (chlorogenic acid, Q and Q3GA) (Herranz-Lopez et al., 2017b) was determined with 3T3-L1 hypertrophied adipocytes under glucolipotoxic conditions. The differential effects on oxidative stress were assayed by adding extract, pure compounds or metabolites (commercially available) to high glucose-induced hypertrophied adipocytes for 48 h, using ascorbic acid (or vitamin C) as a reference antioxidant (Chambial et al., 2013).

The two forms of quercetin showed a higher capacity to inhibit glucolipotoxicity-associated oxidative stress than the extract and the other compounds analyzed at the different concentrations tested. ROS generation was reduced to 37 % and 44 % of the control with Q and Q3GA, respectively (**Fig. 1A**). Furthermore, among the compounds, Q3GA exerted the most powerful inhibition of ROS generation under these conditions, suggesting that this metabolite could be one of the candidates for the potent antioxidant capacity of PEHS *in*

vivo. Nevertheless, ascorbic acid and chlorogenic acid barely inhibited ROS generation in this cell model. Fluorescence microscopy observations of cells treated with the quercetin derivatives revealed a significant reduction in intracellular ROS generation at the end of the assay (**Fig. 1B**).

Nevertheless, hyperglycemia and hyperlipemia occur together in type 2 diabetes, aggravating the progression of the disease. In this context and as previously shown, exposure to high glucose combined with high palmitate concentrations has shown to increase intracellular ROS generation in 3T3-L1 adipocytes (Han et al., 2010). Therefore, PEHS and quercetin derivatives were also tested on 3T3-L1 adipocytes for 48 h under this highly pathological glucolipotoxic condition. Compared with the control, the extract and the two compounds tested significantly decreased oxidative stress in 3T3-L1 adipocytes. In this particular case, Q was the most potent compound (30 µg/mL PEHS: 42 % mean value reduction; 100 µM Q: 57 % mean value reduction; 100 µM Q3GA: 41 % mean value reduction) (**Fig. 1C**).

Glucolipotoxicity has been shown to increase ROS production in INS 832/13 pancreatic β-cells (El-Assaad et al., 2010), which exhibit β-cell functionality to produce and secrete insulin. When PEHS and quercetin derivatives were incubated with β-cells under glucolipotoxic conditions (incubation with high glucose + palmitate) for 24 h, both the extract and the pure compounds significantly inhibited intracellular ROS production at the highest concentrations tested (30 µg/mL PEHS: 41 % mean value reduction; 100 µM Q: 65 % mean value reduction; 100 µM Q3GA: 64 % mean value reduction) (**Fig. 1D**).

3.3 PEHS and quercetin derivatives modulate adipokine secretion under glucolipotoxic conditions

It is postulated that intracellular ROS generation induces the transactivation of NFκB, which subsequently stimulates inflammation. PEHS has proven to inhibit proinflammatory adipokine secretion, particularly leptin and MCP-1 in an adipocyte model (Herranz-Lopez et al., 2012). Given the marked antioxidant effects of the two forms of quercetin on adipocytes and pancreatic β-cells, we compared the potential effects of these compounds and PEHS on proinflammatory cytokine secretion. To this end, hypertrophied adipocytes were treated for 48 h with PEHS, Q or Q3GA at the highest concentrations tested before cytotoxicity was observed. We focused on a selection of cytokines, i.e., leptin, IGF-1, IL6, VEGF, IL1α, IL1β, TNF-α and MCP-1, which are the highly relevant in the development of

insulin resistance and in inflammation (Makki et al., 2013). The concentrations of these cytokines were determined by ELISA.

The results revealed that compared with the control, PEHS significantly inhibited the secretion of all these proinflammatory cytokines (**Figs. 2A and B**). In addition, the two forms of quercetin showed comparable inhibitory capacities under the same conditions for most of the cytokines evaluated. Similarly, MCP-1 is of particular interest (Fig. 2B) due to its capacity to attract macrophages to hypertrophied adipose tissue and to generate and amplify the inflammatory condition.

3.4 PEHS and quercetin derivatives modulate MCP-1 expression at the transcriptional level

To determine whether the downregulation of MCP-1 by PEHS and quercetin derivatives occurred at the transcriptional level, we transfected the enhancer region of the MCP-1 promoter into adipocytes coupled to the luciferase gene (pGLM-ENH) (Ueda et al., 1997). Transfected cells were incubated under glucolipotoxic conditions with different concentrations of PEHS and quercetin derivatives for 48 h, and MCP-1 gene expression was determined by luciferase activity. Four controls were established for this assay: nontransfected adipocytes; adipocytes transfected without plasmid (data not shown); adipocytes transfected with pGL3-basic (no gene inserted into the plasmid) (Ueda et al., 1997); and adipocytes transfected with pGLM-ENH (**Fig. 2C**).

Adipocytes transfected with pGLM-ENH showed significantly increased luciferase activity compared to control adipocytes under glucolipotoxic conditions. However, PEHS significantly reduced luciferase activity up to 36.6 % compared to the control transfected with pGLM-ENH, indicating that the extract modulated MCP-1 expression at the transcriptional level. Similarly, quercetin derivatives were also able to inhibit the expression of MCP-1 to a similar extent (24.8 % and 32.5 % with Q and Q3GA, respectively) (**Fig. 2C**). Altogether, these findings offer a plausible explanation of the mechanism by which these compounds and the extract exert their action to reduce MCP-1 levels.

3.5 PEHS and quercetin derivatives exhibit antilipogenic effects under glucolipotoxic conditions

To evaluate the effects of pure compounds and metabolites from PEHS on the inhibition of cytoplasmic lipid accumulation, high glucose-induced hypertrophied 3T3-L1 adipocytes

were incubated with the compounds and the extract for 48 h, and the accumulated triglyceride content was determined by AdipoRed™ staining.

Despite the previously observed antioxidant effects of ascorbic and chlorogenic acids, none of these compounds significantly modulated lipid content. Furthermore, no effect was observed for PEHS and Q at the lowest concentrations tested. Nevertheless, both PEHS and the two forms of quercetin (Q and Q3GA) at the highest concentration tested significant differences from the high glucose control (**Fig. 3A**), reducing the accumulated triglyceride content by 20 %, 15 % and 27 %, respectively. Q3GA reduced triglyceride content even at 25 µM, demonstrating a marked antilipogenic capacity after incubation under high glucose concentrations. Microscopic observations of treated cells confirmed that cytoplasmic triglyceride accumulation was significantly decreased with the PEHS and quercetin derivative treatments compared to the control condition (**Fig. 3B**).

3.6 PEHS and the metabolite Q3GA modulate the activity and expression of proteins related to energy and lipid metabolism

The molecular mechanisms by which quercetin derivatives from HS reduce triglyceride accumulation are unknown. To understand the underlying mechanism of these compounds, we selected several key molecular targets related to lipid homeostasis and energy metabolism in adipose tissue. We comparatively analyzed the capacity of PEHS and Q3GA (the most active quercetin derivative in previous assays) to modulate the following three proteins: AMP-activated protein kinase (AMPK), fatty acid synthase (FASN) and peroxisome proliferator-activated receptor alpha (PPARα). AMPK plays an important role in cellular energy metabolism and is activated by phosphorylation (pAMPK). FASN is the last enzyme of the lipogenic pathway. PPARα is the main regulator of lipid metabolism, and its activation induces lipid catabolism through genes related to fatty acid mobilization, transport and oxidation.

PEHS and Q3GA were assayed for 48 h in hypertrophied adipocytes, and both compounds significantly activated AMPK by phosphorylation (activation is expressed as the pAMPK/AMPK ratio), with the polyphenolic extract being more active than the pure compound (**Fig. 3C**). In addition, 30 µg/mL PEHS and Q3GA significantly reduced FASN expression and increased PPARα expression (**Fig. 3C**). Nevertheless, in these particular cases, the metabolite was more active than PEHS at modulating FASN and PPARα,

suggesting that the strong antilipogenic effect observed for Q3GA might be due to its high capacity to inhibit FASN.

3.7 In silico analysis of quercetin derivatives reveals a potential therapeutic drug for obesity treatment

To explore the possibility that quercetin derivatives acted as direct modulators of the previously studied protein targets, we used *in silico* analysis. Molecular docking techniques aim to predict the structure of the ligand-receptor complex using computational methods and require high-resolution structural information on the target structure. The docking software (Autodock in our case) has a scoring function that makes an approximate calculation of the binding free energy between the target (human PPARα, FASN and AMPK) and the ligand (Q and Q3GA) in each binding position. To search for potential binding sites of the aforementioned compounds on each protein of interest, a global molecular docking procedure was performed with AutoDock 4 (Morris et al., 2008) implemented in YASARA software (Krieger and Vriend, 2014), where 999 flexible docking runs were performed and clustered around putative binding sites. Docking results usually cluster around certain hot spot conformations. In our calculations, two complexed compounds belonged to different clusters if the ligand root-mean-square deviation (RMSD) of their atomic positions was larger than 7 Å.

The obtained results are shown in **Fig. 4** and **Supplementary Tables 1 to 6**. A first observation of the obtained results showed that for the three proteins of interest, the clusters with low ΔG for both compounds were located in functionally relevant positions previously described in the literature. For both Q and Q3GA, the best clusters of each compound were located in the broad binding cavity described for physiological agonists of PPARα. However, the best positions for Q3GA showed higher theoretical affinity (low ΔG, approximately -11.2 kcal/mol, see **Fig. 4B** and **Supplementary Table 2**) than those for Q (approximately -9.5 kcal/mol, see **Fig. 4A** and **Supplementary Table 1**). A similar analysis showed that the best clusters for both compounds docked on the deep cavity of the FASN catalytic domain, which under physiological conditions should be occupied by NADPH and a nascent fatty acid. The calculated affinity for Q3GA (ΔG approximately -11 kcal/mol, see **Fig. 4D** and **Supplementary Table 4**) was higher than that for Q (ΔG approximately -9 kcal/mol, see **Fig. 4C** and **Supplementary Table 3**), and in that location these compounds would behave as competitive inhibitors capable of reducing fatty acid biosynthesis. Finally, molecular docking experiments for both Q and Q3GA showed that the clusters with the

highest calculated affinity were located in the AMPKγ regulatory subunit (see **Fig. 4E** and **4F** and **Supplementary Tables 5 and 6**). Specifically, they occupied previously described sites that bind AMP (see chain **E** in **Fig. 4E** and **4F**). Both compounds would behave, therefore, as AMPK agonists. It should be noted that cluster 2 for Q (see **Fig. 4E**) was located in the binding site in the established zone of interaction between the AMPKα catalytic and AMPKβ-regulatory subunits. This site has been described as a binding site for the AMPK activator called A-769662 (Langendorf et al., 2016). It is expected that the binding of Q at the same position also activated the enzyme. In addition, neither of the two compounds significantly bound to the catalytic site of the AMPKα subunit.

3.8 PEHS and the metabolite Q3GA improve mitochondrial biogenesis and restore mitochondrial dynamics

In adipocytes, severe defects in mitochondrial biogenesis and altered mitochondrial dynamics induce triglyceride accumulation and have been linked to defects in the secretion of anti-inflammatory adipokines (Vankoningsloo et al., 2005). Considering the inhibitory effect of PEHS and quercetin derivatives on the secretion of proinflammatory factors and their antilipogenic capacity, we evaluated the potential action of these compounds on mitochondrial remodeling. For this purpose, the differential effects of PEHS, Q and Q3GA on mitochondrial mass were evaluated by using a mitochondrial-selective fluorescent probe. MitoTracker Green accumulates in the mitochondrial matrix, thereby allowing the probe abundance to indicate the amount of active mitochondria. Adipocytes under glucolipotoxic conditions develop mitochondrial stress, showing a significant decrease in mitochondrial content (Gao et al., 2010). In high glucose-induced hypertrophied cells, our results showed that Q did not seem to exert changes in mitochondrial mass and biogenesis relative to the control. Nevertheless, the administration of PEHS and Q3GA increased mitochondrial mass under glucolipotoxic conditions (**Fig. 5A**). Fluorescence photomicrographs showed a significant increase in the mitochondrial content of PEHS- and Q3GA-treated cells compared to that of high glucose-induced hypertrophied adipocytes, revealing a putative mechanism to explain the decrease in intracellular triglycerides and proinflammatory factors induced by these agents (**Fig. 5B**).

Furthermore, to determine whether PEHS and Q3GA had any effect on mitochondrial dynamics, we assessed the ultrastructure of mitochondria in adipocytes after treatment with the most active agents, i.e., PEHS and Q3GA. Transmission electron microscopy observations showed imbalanced mitochondrial biogenesis in high glucose-induced

hypertrophied adipocytes. Fusion and fission, processes that determine mitochondrial turnover, were overrepresented in these cells. This altered mitochondrial biogenesis was also accompanied by the appearance of autophagosome-related structures **(Fig. 5C).** This situation could occur as part of a protective mechanism against glucolipotoxic conditions, in an effort to preserve mitochondrial bioenergetics capacities and eliminate nonviable mitochondria through autophagy. This compromised mitochondrial viability seemed to be recovered by PEHS and Q3GA, since neither fusion-fission processes nor autophagic vacuole structures were observed in adipocytes treated with these agents under glucolipotoxic conditions **(Fig. 5C)**.

4. Discussion

It has been postulated that dietary polyphenols could be used as therapeutic agents for the treatment of obesity (Joven et al., 2014). Different cell lines have been widely used as a model to study metabolic disturbances related to obesity. Despite the limitations of a cell model, the 3T3-L1 adipocytic cell line under glucolipotoxic conditions is a well-established cell model to study the effect of these phytochemicals and their metabolites on a context closed to obesity-associated metabolic disturbances. Moreover pancreatic β-cells under similar conditions represents a valuable resource for spotting potential candidate regulators of insulin resistance and obesity (El-Assaad et al., 2010; Gao et al., 2010; Vankoningsloo et al., 2005). In these models, incubation with high glucose and palmitic acid *in vitro* mimics the physiological condition of excess nutrients, induces cell hypertrophy and simulates a state of inflammation and insulin resistance, similar to that observed under obese conditions (Han et al., 2010; Tanis et al., 2015). In addition, the excessive intracellular lipid storage that occurs in adipocytes as a result of exposure to high extracellular glucose concentrations is another way to mimic glucolipotoxic conditions; this treatment leads to metabolic alterations, mitochondrial dysfunction and increased oxidative stress (Mittra et al., 2008).

Considering that complex mixtures of polyphenols are able to interact with different metabolic targets (Barrajon-Catalan et al., 2014), reliable *in vitro* tools are required to identify the particular compounds in the mixture responsible for the biological activity and to dissect their putative mechanism. Thus, the identification of these candidates will allow us to establish additional plausible approaches and develop synergistic mixtures with improved success rates in clinical trials focused on metabolic disturbances associated with obesity.

Previous evidence has demonstrated that HS might represent a relevant therapeutic tool in the treatment and prevention of obesity and related diseases (Herranz-Lopez et al., 2017b; Hopkins et al., 2013). HS extract contains several compounds such as anthocyanins, organic acids, phenolic acids and flavonoids (Borrás-Linares et al., 2015). Nevertheless, recent data provide evidence that flavonols, especially quercetin derivatives, are the main compounds responsible for the salutary effects of the extract (Fernandez-Arroyo et al., 2012; Joven et al., 2012). Q and its metabolite Q3GA were reported to be the flavonol derivatives with the highest concentrations (Cmax values of 1.57 and 3 μM, respectively) in the plasma of rats after the acute ingestion of PEHS (Fernandez-Arroyo et al., 2012), suggesting that these compounds might be the main candidates for the bioactivity of the whole extract. Indeed, there was a correlation between the long half-life elimination values of quercetin glucuronides and the lipid peroxidation inhibition in plasma after the oral administration of the PEHS. In agreement with our results, other authors have reported that quercetin glucuronides are the most representative quercetin-conjugated forms after the consumption of quercetin-enriched plant sources in both humans and rats (Sesink et al., 2001; Yang et al., 2016). Consistent with these results, Q3GA was detected using an anti-Q3GA antibody in the liver tissue of hyperlipidemic mice fed PEHS (Joven et al., 2012). Because of these findings, we aimed to study the capacity of selected metabolites derived from HS extract to alleviate glucolipotoxicity-induced metabolic stress and to reach target tissues, and we compared these metabolites with the whole extract in hypertrophied 3T3-L1 adipocytes and pancreatic β-cells under glucolipotoxic conditions. We chose the most common quercetin metabolites found in plasma (Q and Q3GA) and a metabolite derived from phenolic acids, i.e., chlorogenic acid (the ester of caffeic acid and (−)-quinic acid).

Our results showed that both Q and Q3GA seemed to be more effective than chlorogenic acid, ascorbic acid and PEHS in reducing ROS generation in adipocytes under glucolipotoxic conditions. These results were in agreement with the strong antioxidant capacity observed for quercetin in a large number of *in vitro* and animal models (Kobori et al., 2011; Li et al., 2016; Makris and Rossiter, 2001; Nabavi et al., 2012; Roche et al., 2009; Sanchez-Reus et al., 2007; Vidyashankar et al., 2013), which indicate that this flavonol and its derivatives may directly act as a free radical scavenger or act through the activation of antioxidant enzymes. The weak capacity of chlorogenic acid to reduce intracellular ROS generation might be related to the difficult metabolism of this compound as an intracellular metabolite in the cell model. In a previous study, it was estimated that the concentration of total flavonols present in adipocytes treated with 30 μg/mL of PEHS was approximately 4 μM of total flavonols (Herranz-Lopez et al., 2012). Therefore, it is reasonable to expect that the whole extract had

a lower capacity to decrease intracellular ROS than Q or Q3GA. The decreased capacity observed for the whole extract compared to the quercetin derivatives could be explained by the aforementioned aspect and by the limited conversion of the glycosylated flavonols in the extract into flavonol-conjugated metabolites that may reach their intracellular targets. The concentrations of flavonol-conjugated metabolites utilized in these cell models may be higher than those found in plasma samples (within the low micromolar range). However, the required dose of HS extract in humans to be continually used in nutritional interventions focused on obesity management should be verified in further clinical studies.

Regarding the molecular mechanism involved, recent evidence suggests that high levels of glucose induce hypertrophy and MCP-1 expression and secretion in adipocytes, which leads to macrophage recruitment and chronic inflammation (Han et al., 2007; Joven et al., 2013). However, not only high levels of glucose but also the combination of high glucose with saturated fatty acids such as palmitate induces inflammation in adipose tissue (Han et al., 2010), a mechanism that seems to be mediated by ROS generation. Therefore, we also analyzed the capacity of PEHS and quercetin derivatives to inhibit oxidative stress in 3T3-L1 adipocytes and INS 832/13 pancreatic β-cells under glucolipotoxic conditions. Our results showed that both the extract and the two quercetin derivatives maintained their antioxidant properties in both cell models. The capacity to reduce oxidative stress in INS 832/13 pancreatic β-cells may mean a positive effect on β-cell viability that could be instrumental in type 2 diabetes management.

Both PEHS and quercetin derivatives were able to reduce the levels of proinflammatory cytokines in an adipocyte model (leptin, TNF-α, IGF-1, IL6, VEGF, IL1α, IL1β and MCP-1). The anti-inflammatory activity of Q has been widely demonstrated in many cells and animal studies (Dong et al., 2014; Indra et al., 2013; Overman et al., 2011; Vidyashankar et al., 2013; Ying et al., 2013). This activity seems to be exerted through the direct modulation of the gene expression of proinflammatory proteins, likely by epigenetic control, or through the modulation of the main transcription factor NFκB (Indra et al., 2013; Overman et al., 2011; Panchal et al., 2012; Ying et al., 2013). MCP-1 was found at high levels in the adipose tissue of obese people (Han et al., 2007; Kim and Park, 2015), and it is postulated that the regulation of the metabolic pathways responsible for the production of this cytokine might prevent chronic inflammatory diseases, such as those associated with obesity. Therefore, MCP-1 or its receptor are postulated to be therapeutic targets to treat the inflammation associated with obesity. The results obtained from the transfection experiments confirmed that both PEHS and quercetin derivatives were able to reduce MCP-1 gene expression.

Again, the anti-inflammatory effect of the whole extract was almost comparable to the quercetin derivatives, indicating that compounds in the extract other than flavonols may be involved in this effect.

The two forms of quercetin and PEHS also significantly reduced triglyceride accumulation in hypertrophied adipocytes, with Q3GA again being the most active compound. In contrast, chlorogenic acid and ascorbic acid did not affect triglyceride content. This result is in agreement with previous results obtained in cell lines and animal models (Ahn et al., 2008; Dong et al., 2014; Imessaoudene et al., 2016; Jung et al., 2013; Kobori et al., 2011; Vidyashankar et al., 2013; Ying et al., 2013), in which quercetin showed antiadipogenic and antilipogenic properties and was able to modify tissue lipid composition and reduce fat deposition and weight gain *in vivo*. These data suggest that Q and its glucuronidated derivative may be applied to the treatment of obesity and its related diseases due to antioxidant properties or lipid metabolism regulation. In particular, in this work, Q3GA was highlighted as having a marked antilipogenic effect even at low doses. Considering the strong capacity of Q3GA to decrease triglyceride accumulation in the hypertrophied adipocyte model, we aimed to elucidate the underlying potential mechanism, focusing on several protein targets closely related to energy metabolism and lipid metabolism regulation. Therefore, we determined the comparative capacity of PEHS and Q3GA to modulate AMPK, FASN and PPARα in 3T3-L1 adipocytes under glucolipotoxic conditions. The results from Western blot analysis suggested that the glucuronidated metabolite has a significant role in decreasing the accumulation of triglycerides via the modulation of these three metabolic targets.

AMPK is a key sensor on energy metabolism (Hwang et al., 2009). AMPK is a serine/threonine kinase that is activated by phosphorylation (pAMPK) when the AMP:ATP ratio increases, activating catabolic pathways and inhibiting anabolic pathways. AMPK is a crucial regulator of the balance between energy supply and energy demand on cells. Thus, pAMPK phosphorylates metabolic enzymes such as acetyl-CoA carboxylase (ACC), a central enzyme in lipid biosynthesis. When phosphorylated by AMPK, ACC is inhibited and reduces the levels of malonyl-CoA, an allosteric inhibitor of carnitine palmitoyl transferase 1 (CPT1) (Saha and Ruderman, 2003). The subsequent activation of CPT1 promotes fatty acid transport to the mitochondrial matrix where β-oxidation occurs. Western blot analysis revealed that PEHS and Q3GA activated AMPK via phosphorylation in a dose-dependent manner. The fact that the extract showed a stronger effect than the quercetin metabolite suggests again that other compounds in the extract may also be implicated. Therefore, AMPK activation could be partly responsible for the decrease in lipid content that could be

684 induced by the reduction in lipogenesis via inhibiting ACC and/or by increasing fatty acid
685 oxidation. Recently, the capacity of Q to activate AMPK has been demonstrated in obese
686 C57BL/6J mice (Dong et al., 2014), which suggests that the activation of this kinase is
687 involved in the suppression of inflammation and insulin resistance in mouse adipose tissue.
688 Therefore, our results provide a reasonable basis to postulate that some plasma compounds
689 and metabolites from PEHS, probably quercetin derivatives, decrease fat deposition and
690 inflammation via AMPK activation when ingested by mice.
691
692 Similarly, Western blot analysis revealed that PEHS and particularly Q3GA were able to
693 reduce FASN expression levels in adipocytes under glucolipotoxic conditions. This protein
694 is a crucial enzyme in the *de novo* synthesis of saturated long-chain fatty acids. The
695 antilipogenic effect of PEHS and Q3GA suggests a complementary action to the inhibition of
696 ACC by AMPK that results in lipolysis, and both effects can explain the observed global
697 decrease in adipocyte triglycerides (Menendez et al., 2009). The inhibition of FASN
698 expression by AMPK activation has been previously reported to be induced either by the
699 AMPK activator AICAR or by the anti-diabetic drug metformin in liver and cancer cells
700 (Xiang et al., 2004; Zhou et al., 2001), most likely due to the strong suppressive effect of
701 AMPK on SREBP1c expression. Whether the effect of PEHS or its metabolite Q3GA on FASN
702 expression and activation is a consequence of the capacity to activate AMPK or whether this
703 compound is able to directly modulate FASN may deserve further research.
704
705 Therefore, we postulate that Q3GA may be one of the main compounds in PEHS responsible
706 for decreasing lipid accumulation in hypertrophied adipocytes via a reduction in FASN
707 expression and the activation of mitochondrial fatty acid oxidation. Furthermore, these data
708 are in agreement with the results obtained in hyperlipidemic mice fed PEHS. In this animal
709 model, the presence of Q3GA in the liver tissue of these mice is correlated with the activation
710 of AMPK and the decreased expression of lipogenic genes such as SREBP1c and FASN (Joven
711 et al., 2012).
712
713 Considering that the concentration of total flavonols in the 10 μg/mL and 30 μg/mL PEHS
714 treatments was approx. 1.3 and 4 μM, respectively, the increased capacity of PEHS to
715 decrease the intracellular ROS in both cell models treated with high concentrations of
716 palmitic acid compared to that of the pure compounds was remarkable. Moreover, PEHS
717 also showed a potent ability to decrease triglyceride content, to activate AMPK and to
718 decrease FASN expression in hypertrophic adipocytes. These results may indicate that

719 compounds other than flavonols likely contribute to the capacity of PEHS to alleviate
720 glucolipotoxicity-induced metabolic stress.
721
722 Our results also demonstrated that Q3GA showed a higher capacity than PEHS to increase
723 PPARα levels. This transcription factor is a main modulator of the expression of genes
724 related to peroxisomal and mitochondrial fatty acid oxidation, mitochondrial biogenesis
725 and antioxidant enzyme synthesis, and its activation results in the fatty acid catabolism,
726 reduced lipid tissue content, and decreased glucolipotoxicity and oxidative stress (Okada-
727 Iwabu et al., 2013). Therefore, we postulate that the reduction in fat accumulation mediated
728 by PEHS and Q3GA was partially due to their antilipogenic effect and also due to an increase
729 in fatty acid oxidation via PPARα activation, preserving mitochondrial function and content.
730 Our results also support that PEHS and Q3GA revert the decrease in mitochondrial mass
731 induced by glucolipotoxicity in hypertrophied adipocytes and restore mitochondrial
732 biogenesis and viability. Proper oxidative mitochondrial function may contribute to the
733 observed decreased lipid content induced by these agents. Considering that mitochondrial
734 dysfunction is partially associated with a reduction in mitochondrial content in obese
735 conditions (Jokinen et al., 2017), Q3GA could prevent mitochondrial degradation. These
736 results are also consistent with the activation of PPARα observed in obese C57BL/6J mice
737 fed Q (Kobori et al., 2011), which significantly reduced liver triglycerides and oxidative
738 stress.
739
740 In correlation with these molecular findings, our *in silico* studies have also demonstrated
741 the potential of quercetin derivatives to interact with several protein targets as part of their
742 putative mechanism. In our study, Q3GA showed a lower ΔG than Q for PPARα and FASN,
743 which indicated that Q3GA is a promising candidate to act as a direct modulator of both
744 proteins, as described for other polyphenols (Encinar et al., 2015; Olivares-Vicente et al.,
745 2018). This fact underwrites the capacity of this compound to modulate lipid metabolism
746 and mitochondrial function beyond simple antioxidant capacity. In addition, molecular
747 docking experiments showed that both quercetin derivatives seemed to be capable of acting
748 as AMPK agonists and interacting with the AMPKγ regulatory subunit. Nevertheless, the
749 strong activation of AMPK induced by PEHS may indicate that other compounds may be
750 involved in the activation of this enzyme.
751
752 We have previously demonstrated that both Q and Q3GA were absorbed by hypertrophied
753 adipocytes and intracellularly metabolized to some extent to Q3GA and Q, respectively
754 (Herranz-Lopez et al., 2017a). Although the absorption of Q was more efficient and faster

than that of Q3GA, both compounds were intracellularly localized and inhibited ROS generation in a similar manner. Our results confirm that Q and Q3GA show similar antioxidant and anti-inflammatory capacities in adipocyte models under glucolipotoxic conditions. However, Q3GA exhibited a higher capacity than Q to reduce triglyceride accumulation, an effect that occurred through FASN downregulation, AMPK activation and mitochondrial mass and viability restoration via PPARα upregulation. All of these data suggest that Q3GA could be the main candidate responsible for the bioactive effects of whole PEHS that revert glucolipotoxicity-induced metabolic stress in adipose tissue. Interestingly, the strong antilipogenic and AMPK-activating capacity observed for the whole extract may deserve further research to elucidate the other compounds that contribute to this capacity in addition to Q3GA.

Acknowledgements

We thank grants AGL2015-67995-C3-1-R and RTI2018-096724-B-C21 from the Spanish Ministry of Economy and Competitiveness (MINECO); PROMETEO/2016/006, APOSTD/2017/023, APOSTD/2018/097 and ACIF/2016/230 from Generalitat Valenciana; CIBER (CB12/03/30038, Fisiopatologia de la Obesidad y la Nutricion, CIBERobn, Instituto de Salud Carlos III). We are grateful to the Cluster of Scientific Computing (http://ccc.umh.es/) of the Miguel Hernandez University (UMH) and the Centro de Supercomputación (ALHAMBRA-CSIRC) of the University of Granada for supporting supercomputing facilities. We also thank SME instrument phase 1 EU funding for grant INNOPREFAT 683933 (H2020-SMEINST-1-2015_18-03-2015) and H2020 SME Phase II project, grant number 783838.

Conflict of interest

The authors declare no conflict of interest.

References

Addabbo, F., Montagnani, M., Goligorsky, M.S. 2009. Mitochondria and reactive oxygen species. Hypertension 53, 885-892.

Ahn, J., Lee, H., Kim, S., Park, J., Ha, T. 2008. The anti-obesity effect of quercetin is mediated by the AMPK and MAPK signaling pathways. Biochem. Biophys. Res. Commun. 373, 545-549.

Alarcon-Aguilar, F.J., Zamilpa, A., Perez-Garcia, M.D., Almanza-Perez, J.C., Romero-Nunez, E., Campos-Sepulveda, E.A., Vazquez-Carrillo, L.I., Roman-Ramos, R. 2007. Effect of *Hibiscus sabdariffa* on obesity in MSG mice. J. Ethnopharmacol. 114, 66-71.

Barrajon-Catalan, E., Herranz-Lopez, M., Joven, J., Segura-Carretero, A., Alonso-Villaverde, C., Menendez, J.A., Micol, V. 2014. Molecular promiscuity of plant polyphenols in the management of age-related diseases: far beyond their antioxidant properties. Adv. Exp. Med. Biol. 824, 141-159.

Beltran-Debon, R., Alonso-Villaverde, C., Aragones, G., Rodriguez-Medina, I., Rull, A., Micol, V., Segura-Carretero, A., Fernandez-Gutierrez, A., Camps, J., Joven, J. 2010. The aqueous extract of *Hibiscus sabdariffa* calices modulates the production of monocyte chemoattractant protein-1 in humans. Phytomedicine 17, 186-191.

Bhatti, J.S., Bhatti, G.K., Reddy, P.H. 2017. Mitochondrial dysfunction and oxidative stress in metabolic disorders — A step towards mitochondria based therapeutic strategies. Biochim. Biophys. Acta Mol. Basis Dis. 1863, 1066-1077.

Borrás-Linares, I., Herranz-López, M., Barrajón-Catalán, E., Arráez-Román, D., González-Álvarez, I., Bermejo, M., Fernández Gutiérrez, A., Micol, V., Segura-Carretero, A. 2015. Permeability Study of Polyphenols Derived from a Phenolic-Enriched Hibiscus sabdariffa Extract by UHPLC-ESI-UHR-Qq-TOF-MS. Int. J. Mol. Sci. 16, 18396-18411.

Cancello, R., Clement, K. 2006. Is obesity an inflammatory illness? Role of low-grade inflammation and macrophage infiltration in human white adipose tissue. Bjog 113, 1141-1147.

Chambial, S., Dwivedi, S., Shukla, K.K., John, P.J., Sharma, P. 2013. Vitamin C in disease prevention and cure: an overview. Indian J. Clin. Biochem. 28, 314-328.

Chang, H.C., Peng, C.H., Yeh, D.M., Kao, E.S., Wang, C.J. 2014. *Hibiscus sabdariffa* extract inhibits obesity and fat accumulation, and improves liver steatosis in humans. Food Funct. 5, 734-739.

Despres, J.P., Lemieux, I. 2006. Abdominal obesity and metabolic syndrome. Nature 444, 881-887.

Dong, J., Zhang, X., Zhang, L., Bian, H.X., Xu, N., Bao, B., Liu, J. 2014. Quercetin reduces obesity-associated ATM infiltration and inflammation in mice: a mechanism including AMPKalpha1/SIRT1. J. Lipid Res. 55, 363-374.

El-Assaad, W., Joly, E., Barbeau, A., Sladek, R., Buteau, J., Maestre, I., Pepin, E., Zhao, S., Iglesias, J., Roche, E., Prentki, M. 2010. Glucolipotoxicity alters lipid partitioning and causes mitochondrial

818 dysfunction, cholesterol, and ceramide deposition and reactive oxygen species production in
819 INS832/13 ss-cells. Endocrinology 151, 3061-3073.

820 Encinar, J.A., Fernandez-Ballester, G., Galiano-Ibarra, V., Micol, V. 2015. In silico approach for the
821 discovery of new PPARgamma modulators among plant-derived polyphenols. Drug Des. Devel. Ther.
822 9, 5877-5895.

823 Fernandez-Arroyo, S., Herranz-Lopez, M., Beltran-Debon, R., Borras-Linares, I., Barrajon-Catalan, E.,
824 Joven, J., Fernandez-Gutierrez, A., Segura-Carretero, A., Micol, V. 2012. Bioavailability study of a
825 polyphenol-enriched extract from Hibiscus sabdariffa in rats and associated antioxidant status. Mol.
826 Nutr. Food Res. 56, 1590-1595.

827 Fernandez-Arroyo, S., Rodriguez-Medina, I., Beltran-Debon, R., Pasini, F., Joven, J., Micol, V., Segura-
828 Carretero, A., Fernandez-Gutierrez, A. 2011. Quantification of the polyphenolic fraction and *in vitro*
829 antioxidant and *in vivo* anti-hyperlipemic activities of *Hibiscus sabdariffa* aqueous extract. Food Res.
830 Int. 44.

831 Gao, C.L., Zhu, C., Zhao, Y.P., Chen, X.H., Ji, C.B., Zhang, C.M., Zhu, J.G., Xia, Z.K., Tong, M.L., Guo, X.R.
832 2010. Mitochondrial dysfunction is induced by high levels of glucose and free fatty acids in 3T3-L1
833 adipocytes. Mol. Cell. Endocrinol. 320, 25-33.

834 Green, H., Kehinde, O. 1975. An established preadipose cell line and its differentiation in culture. II.
835 Factors affecting the adipose conversion. Cell 5, 19-27.

836 Han, C.Y. 2016. Roles of reactive oxygen species on insulin resistance in adipose tissue. Diabetes
837 Metab. J. 40, 272-279.

838 Han, C.Y., Kargi, A.Y., Omer, M., Chan, C.K., Wabitsch, M., O'Brien, K.D., Wight, T.N., Chait, A. 2010.
839 Differential effect of saturated and unsaturated free fatty acids on the generation of monocyte
840 adhesion and chemotactic factors by adipocytes: Dissociation of adipocyte hypertrophy from
841 inflammation. Diabetes 59, 386-396.

842 Han, C.Y., Subramanian, S., Chan, C.K., Omer, M., Chiba, T., Wight, T.N., Chait, A. 2007. Adipocyte-
843 derived serum amyloid A3 and hyaluronan play a role in monocyte recruitment and adhesion.
844 Diabetes 56, 2260-2273.

845 Herranz-Lopez, M., Borras-Linares, I., Olivares-Vicente, M., Galvez, J., Segura-Carretero, A., Micol, V.
846 2017a. Correlation between the cellular metabolism of quercetin and its glucuronide metabolite and
847 oxidative stress in hypertrophied 3T3-L1 adipocytes. Phytomedicine 25, 25-28.

848 Herranz-Lopez, M., Fernandez-Arroyo, S., Perez-Sanchez, A., Barrajon-Catalan, E., Beltran-Debon, R.,
849 Menendez, J.A., Alonso-Villaverde, C., Segura-Carretero, A., Joven, J., Micol, V. 2012. Synergism of
850 plant-derived polyphenols in adipogenesis: perspectives and implications. Phytomedicine 19, 253-
851 261.

852 Herranz-Lopez, M., Olivares-Vicente, M., Encinar, J.A., Barrajon-Catalan, E., Segura-Carretero, A.,
853 Joven, J., Micol, V. 2017b. Multi-Targeted Molecular Effects of Hibiscus sabdariffa Polyphenols: An
854 Opportunity for a Global Approach to Obesity. Nutrients 9.

Hopkins, A.L., Lamm, M.G., Funk, J.L., Ritenbaugh, C. 2013. *Hibiscus sabdariffa* L. in the treatment of hypertension and hyperlipidemia: a comprehensive review of animal and human studies. Fitoterapia 85, 84-94.

Hwang, J.T., Kwon, D.Y., Yoon, S.H. 2009. AMP-activated protein kinase: a potential target for the diseases prevention by natural occurring polyphenols. New Biotechnol. 26, 17-22.

Imessaoudene, A., Merzouk, H., Berroukeche, F., Mokhtari, N., Bensenane, B., Cherrak, S., Merzouk, S.A., Elhabiri, M. 2016. Beneficial effects of quercetin-iron complexes on serum and tissue lipids and redox status in obese rats. J. Nutr. Biochem. 29, 107-115.

Indra, M.R., Karyono, S., Ratnawati, R., Malik, S.G. 2013. Quercetin suppresses inflammation by reducing ERK1/2 phosphorylation and NF kappa B activation in Leptin-induced Human Umbilical Vein Endothelial Cells (HUVECs). BMC Res. Notes 6, 275.

Jokinen, R., Pirnes-Karhu, S., Pietiläinen, K.H., Pirinen, E. 2017. Adipose tissue NAD+-homeostasis, sirtuins and poly(ADP-ribose) polymerases -important players in mitochondrial metabolism and metabolic health. Redox Biol. 12, 246-263.

Joven, J., Espinel, E., Rull, A., Aragones, G., Rodriguez-Gallego, E., Camps, J., Micol, V., Herranz-Lopez, M., Menendez, J.A., Borras, I., Segura-Carretero, A., Alonso-Villaverde, C., Beltran-Debon, R. 2012. Plant-derived polyphenols regulate expression of miRNA paralogs miR-103/107 and miR-122 and prevent diet-induced fatty liver disease in hyperlipidemic mice. Biochim. Biophys. Acta 1820, 894-899.

Joven, J., Micol, V., Segura-Carretero, A., Alonso-Villaverde, C., Menéndez, J.A., Aragonès, G., Barrajón-Catalán, E., Beltrán-Debón, R., Camps, J., Cufí, S., Fernández-Arroyo, S., Fernández-Gutiérrez, A., Guillén, E., Herranz-López, M., Iswaldi, I., Lozano-Sánchez, J., Martin-Castillo, B., Oliveras-Ferraros, C., Pérez-Sánchez, A., Rodríguez-Gallego, E., Rull, A., Saura, D., Vázquez-Martín, A. 2014. Polyphenols and the Modulation of Gene Expression Pathways: Can We Eat Our Way Out of the Danger of Chronic Disease? Crit. Rev. Food Sci. Nutr. 54, 985-1001.

Joven, J., Rull, A., Rodriguez-Gallego, E., Camps, J., Riera-Borrull, M., Hernandez-Aguilera, A., Martin-Paredero, V., Segura-Carretero, A., Micol, V., Alonso-Villaverde, C., Menendez, J.A. 2013. Multifunctional targets of dietary polyphenols in disease: a case for the chemokine network and energy metabolism. Food Chem. Toxicol. 51, 267-279.

Jung, C.H., Cho, I., Ahn, J., Jeon, T.I., Ha, T.Y. 2013. Quercetin reduces high-fat diet-induced fat accumulation in the liver by regulating lipid metabolism genes. Phytother. Res. 27, 139-143.

Kim, J.K., So, H., Youn, M.J., Kim, H.J., Kim, Y., Park, C., Kim, S.J., Ha, Y.A., Chai, K.Y., Kim, S.M., Kim, K.Y., Park, R. 2007. *Hibiscus sabdariffa* L. water extract inhibits the adipocyte differentiation through the PI3-K and MAPK pathway. J. Ethnopharmacol. 114, 260-267.

Kim, T.K., Park, K.S. 2015. Inhibitory effects of harpagoside on TNF-alpha-induced pro-inflammatory adipokine expression through PPAR-gamma activation in 3T3-L1 adipocytes. Cytokine 76, 368-374.

Kobori, M., Masumoto, S., Akimoto, Y., Oike, H. 2011. Chronic dietary intake of quercetin alleviates hepatic fat accumulation associated with consumption of a Western-style diet in C57/BL6J mice. Mol. Nutr. Food Res. 55, 530-540.

Krieger, E., Darden, T., Nabuurs, S.B., Finkelstein, A., Vriend, G. 2004. Making optimal use of empirical energy functions: force-field parameterization in crystal space. Proteins 57, 678-683.

Krieger, E., Vriend, G. 2014. YASARA View - molecular graphics for all devices - from smartphones to workstations. Bioinformatics 30, 2981-2982.

Langendorf, C.G., Ngoei, K.R.W., Scott, J.W., Ling, N.X.Y., Issa, S.M.A., Gorman, M.A., Parker, M.W., Sakamoto, K., Oakhill, J.S., Kemp, B.E. 2016. Structural basis of allosteric and synergistic activation of AMPK by furan-2-phosphonic derivative C2 binding. Nat. Commun. 7, 10912.

Li, C., Zhang, W.J., Frei, B. 2016. Quercetin inhibits LPS-induced adhesion molecule expression and oxidant production in human aortic endothelial cells by p38-mediated Nrf2 activation and antioxidant enzyme induction. Redox. Biol. 9, 104-113.

Luna-Luna, M., Medina-Urrutia, A., Vargas-Alarcon, G., Coss-Rovirosa, F., Vargas-Barron, J., Perez-Mendez, O. 2015. Adipose tissue in metabolic syndrome: onset and progression of atherosclerosis. Arch. Med. Res. 46, 392-407.

Makki, K., Froguel, P., Wolowczuk, I. 2013. Adipose tissue in obesity-related inflammation and insulin resistance: cells, cytokines, and chemokines. ISRN Inflamm. 2013, 139239-139239.

Makris, D.P., Rossiter, J.T. 2001. Comparison of quercetin and a non-orthohydroxy flavonol as antioxidants by competing *in vitro* oxidation reactions. J. Agric. Food Chem. 49, 3370-3377.

Menendez, J.A., Vazquez-Martin, A., Ortega, F.J., Fernandez-Real, J.M. 2009. Fatty acid synthase: association with insulin resistance, type 2 diabetes, and cancer. Clin. Chem. 55, 425-438.

Mittra, S., Bansal, V.S., Bhatnagar, P.K. 2008. From a glucocentric to a lipocentric approach towards metabolic syndrome. Drug Discov. Today 13, 211-218.

Miyake, H., Sakagami, J., Yasuda, H., Sogame, Y., Kato, R., Suwa, K., Dainaka, K., Takata, T., Yokota, I., Itoh, Y. 2018. Association of fatty pancreas with pancreatic endocrine and exocrine function. PLoS One 13, e0209448.

Morris, G.M., Huey, R., Olson, A.J. 2008. Using AutoDock for ligand-receptor docking. Curr. Protoc. Bioinformatics. Chapter 8, Unit 8.14.

Nabavi, S.M., Nabavi, S.F., Eslami, S., Moghaddam, A.H. 2012. *In vivo* protective effects of quercetin against sodium fluoride-induced oxidative stress in the hepatic tissue. Food Chem. 132, 931–935.

Nemeth, K., Piskula, M.K. 2007. Food content, processing, absorption and metabolism of onion flavonoids. Crit. Rev. Food Sci. Nutr. 47, 397-409.

O'Neill, S., O'Driscoll, L. 2015. Metabolic syndrome: a closer look at the growing epidemic and its associated pathologies. Obes. Rev. 16, 1-12.

926 Okada-Iwabu, M., Yamauchi, T., Iwabu, M., Honma, T., Hamagami, K., Matsuda, K., Yamaguchi, M.,
927 Tanabe, H., Kimura-Someya, T., Shirouzu, M., Ogata, H., Tokuyama, K., Ueki, K., Nagano, T., Tanaka, A.,
928 Yokoyama, S., Kadowaki, T. 2013. A small-molecule AdipoR agonist for type 2 diabetes and short life
929 in obesity. Nature 503, 493-499.

930 Olivares-Vicente, M., Barrajon-Catalan, E., Herranz-Lopez, M., Segura-Carretero, A., Joven, J., Encinar,
931 J.A., Micol, V. 2018. Plant-derived polyphenols in human health: biological activity, metabolites and
932 putative molecular targets. Curr. Drug Metab. 19, 351-369.

933 Overman, A., Chuang, C.C., McIntosh, M. 2011. Quercetin attenuates inflammation in human
934 macrophages and adipocytes exposed to macrophage-conditioned media. Int. J. Obes. 35, 1165-1172.

935 Panchal, S.K., Poudyal, H., Brown, L. 2012. Quercetin ameliorates cardiovascular, hepatic, and
936 metabolic changes in diet-induced metabolic syndrome in rats. J. Nutr. 142, 1026-1032.

937 Roche, M., Tarnus, E., Rondeau, P., Bourdon, E. 2009. Effects of nutritional antioxidants on AAPH- or
938 AGEs-induced oxidative stress in human SW872 liposarcoma cells. Cell Biol. Toxicol. 25, 635-644.

939 Saha, A.K., Ruderman, N.B. 2003. Malonyl-CoA and AMP-activated protein kinase: an expanding
940 partnership. Mol. Cell Biochem. 253, 65-70.

941 Sanchez-Reus, M.I., Gomez del Rio, M.A., Iglesias, I., Elorza, M., Slowing, K., Benedi, J. 2007.
942 Standardized *Hypericum perforatum* reduces oxidative stress and increases gene expression of
943 antioxidant enzymes on rotenone-exposed rats. Neuropharmacology 52, 606-616.

944 Sesink, A.L., O'Leary, K.A., Hollman, P.C. 2001. Quercetin glucuronides but not glucosides are present
945 in human plasma after consumption of quercetin-3-glucoside or quercetin-4'-glucoside. J. Nutr. 131,
946 1938-1941.

947 Soria, B., Maestre, I., Reig, J.A., Roche, E., Jordán, J.n., Calvo, S., Ceña, V.n., Prentki, M. 2003.
948 Mitochondrial Dysfunction Is Involved in Apoptosis Induced by Serum Withdrawal and Fatty Acids
949 in the β-Cell Line Ins-1. Endocrinology 144, 335-345.

950 Tanis, R.M., Piroli, G.G., Day, S.D., Frizzell, N. 2015. The effect of glucose concentration and sodium
951 phenylbutyrate treatment on mitochondrial bioenergetics and ER stress in 3T3-L1 adipocytes.
952 Biochim. Biophys. Acta Mol. Cell. Res. 1853, 213-221.

953 Ueda, A., Ishigatsubo, Y., Okubo, T., Yoshimura, T. 1997. Transcriptional regulation of the human
954 monocyte chemoattractant protein-1 gene. Cooperation of two NF-kappaB sites and NF-kappaB/Rel
955 subunit specificity. J. Biol. Chem. 272, 31092-31099.

956 Vankoningsloo, S., Piens, M., Lecocq, C., Gilson, A., De Pauw, A., Renard, P., Demazy, C., Houbion, A.,
957 Raes, M., Arnould, T. 2005. Mitochondrial dysfunction induces triglyceride accumulation in 3T3-L1
958 cells: role of fatty acid beta-oxidation and glucose. J. Lipid. Res. 46, 1133-1149.

959 Vidyashankar, S., Sandeep Varma, R., Patki, P.S. 2013. Quercetin ameliorate insulin resistance and up-
960 regulates cellular antioxidants during oleic acid induced hepatic steatosis in HepG2 cells. Toxicol. In
961 Vitro 27, 945-953.

962 Xiang, X., Saha, A.K., Wen, R., Ruderman, N.B., Luo, Z. 2004. AMP-activated protein kinase activators
963 can inhibit the growth of prostate cancer cells by multiple mechanisms. Biochem. Biophys. Res.
964 Commun. 321, 161-167.

965 Yang, L.-L., Xiao, N., Li, X.-W., Fan, Y., Alolga, R.N., Sun, X.-Y., Wang, S.-L., Li, P., Qi, L.-W. 2016.
966 Pharmacokinetic comparison between quercetin and quercetin 3-O-β-glucuronide in rats by UHPLC-
967 MS/MS. Sci. Rep. 6, 35460.

968 Ying, H.Z., Liu, Y.H., Yu, B., Wang, Z.Y., Zang, J.N., Yu, C.H. 2013. Dietary quercetin ameliorates
969 nonalcoholic steatohepatitis induced by a high-fat diet in gerbils. Food Chem. Toxicol. 52, 53-60.

970 Zhou, G., Myers, R., Li, Y., Chen, Y., Shen, X., Fenyk-Melody, J., Wu, M., Ventre, J., Doebber, T., Fujii, N.,
971 Musi, N., Hirshman, M.F., Goodyear, L.J., Moller, D.E. 2001. Role of AMP-activated protein kinase in
972 mechanism of metformin action. J. Clin. Invest. 108, 1167-1174.

FIGURE LEGENDS

Figure 1: PEHS and quercetin derivatives decrease ROS generation in hypertrophied 3T3-L1 adipocytes and INS 832/13 pancreatic β-cells. A) Measurement of intracellular ROS levels (%) using the H_2DCF-DA fluorescent probe in 3T3-L1 hypertrophied adipocytes following incubation with PEHS and different HS metabolites and antioxidants for 48 h under glucolipotoxic conditions. B) Representative fluorescence images of treated cells are shown. C) Measurement of intracellular ROS levels (%) in hypertrophied adipocytes (C) or pancreatic β-cells (D) under glucolipotoxic conditions after treatment with different concentrations of PEHS, Q or Q3GA for 48 h. Statistical analysis was performed as described in the Materials section.

Figure 2: PEHS and quercetin derivatives modulate adipokine secretion under glucolipotoxic conditions. A and B) Hypertrophied adipocytes were treated for 48 h with PEHS and quercetin derivatives at the most active concentrations tested, and adipokine levels were determined by ELISA. Compared to the control, PEHS and quercetin derivatives significantly inhibited the secretion of all these proinflammatory factors. C) 3T3-L1 adipocytes transfected with the enhancer region of the MCP-1 promoter were treated with PEHS, Q or Q3GA at different concentrations for 48 h, and MCP-1 gene expression was determined by luciferase activity. Statistical analysis was performed as described in the Materials section.

Figure 3: PEHS and quercetin derivatives exhibit antilipogenic effects under glucolipotoxic conditions by modulating the activity and expression of proteins related to energy and lipid metabolism. A and B) High glucose-induced hypertrophied 3T3-L1 adipocytes were incubated with PEHS or pure compounds for 48 h, and the accumulated triglyceride content was determined by AdipoRed™ staining. Compared to the high glucose control, PEHS, Q and Q3GA significantly decreased triglyceride content. The effect was confirmed by microscopic observations of treated cells stained with AdipoRed™. C) Measurement of AMPK activation and expression levels of FASN and PPARα by Western blot analysis in hypertrophied adipocytes treated with PEHS and Q3GA for 48 h. Statistical analysis was performed as described in the Materials section.

Figure 4: Illustration of the secondary structure of human PPARα (A, B), FASN (C, D), and AMPK (E, F) with docked Q (A, C, E) and Q3GA (B, D, F). For each cluster of the docked compound (Q carbon atoms are shown in yellow, and Q3GA carbon atoms are shown in

cyan), the molecules (spheres) with high binding energy are shown. For PPARα (A, B) and FASN (C, D), the secondary structure is shown in rainbow colors from N-terminal (blue) to C-terminal (red). The three AMPK subunits are been shown with different colors (alpha-2 is shown in green as *chain A*, beta-1 is shown in blue as *chain B*, and gamma-1 is shown in salmon as *chain E*). The number of each cluster is indicated. The figure was prepared using PyMol 2.0 software.

Figure 5: PEHS and quercetin derivatives restore mitochondrial mass and integrity. A) High glucose-induced hypertrophied 3T3-L1 adipocytes were incubated with PEHS, Q or Q3GA for 48 h, and mitochondrial mass was determined by the fluorescent probe MitoTracker™ Green FM. B) Representative fluorescence images of treated cells are shown. C) Transmission electron microscopy images representative of the mitochondria in 3T3-L1 hypertrophied adipocytes treated with the polyphenol-enriched HS (PEHS) extract at 30 μg/mL or Q3GA at 100 μM. Circles show fused mitochondria, and arrows show fission events.

FIGURE 1

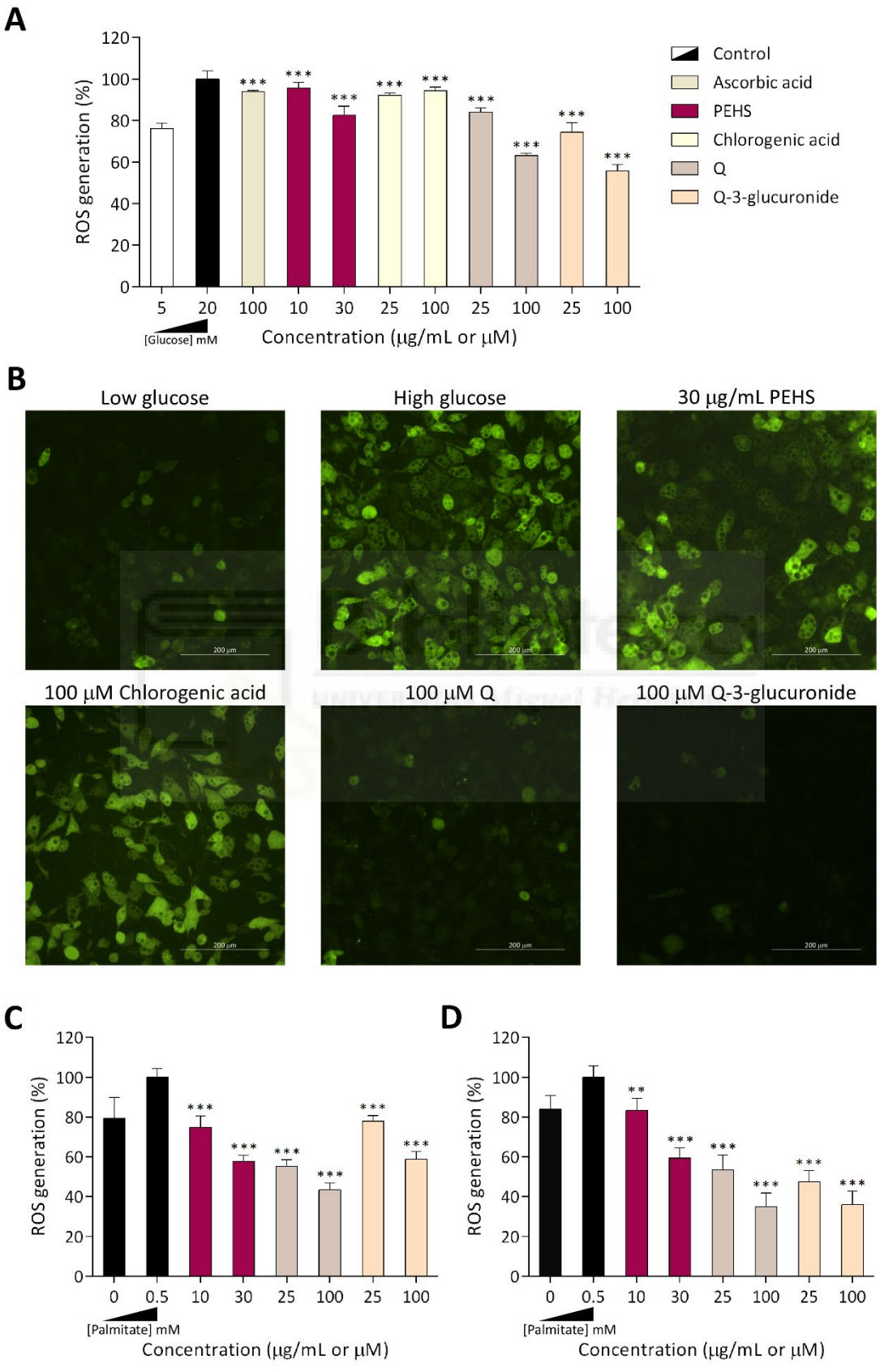
A
ROS generation (%)
Control
Ascorbic acid
PEHS
Chlorogenic acid
Q
Q-3-glucuronide
[Glucose] mM
Concentration (µg/mL or µM)
B
Low glucose
High glucose
30 µg/mL PEHS
100 µM Chlorogenic acid
100 µM Q
100 µM Q-3-glucuronide
C
D
[Palmitate] mM
Concentration (µg/mL or µM)

FIGURE 2

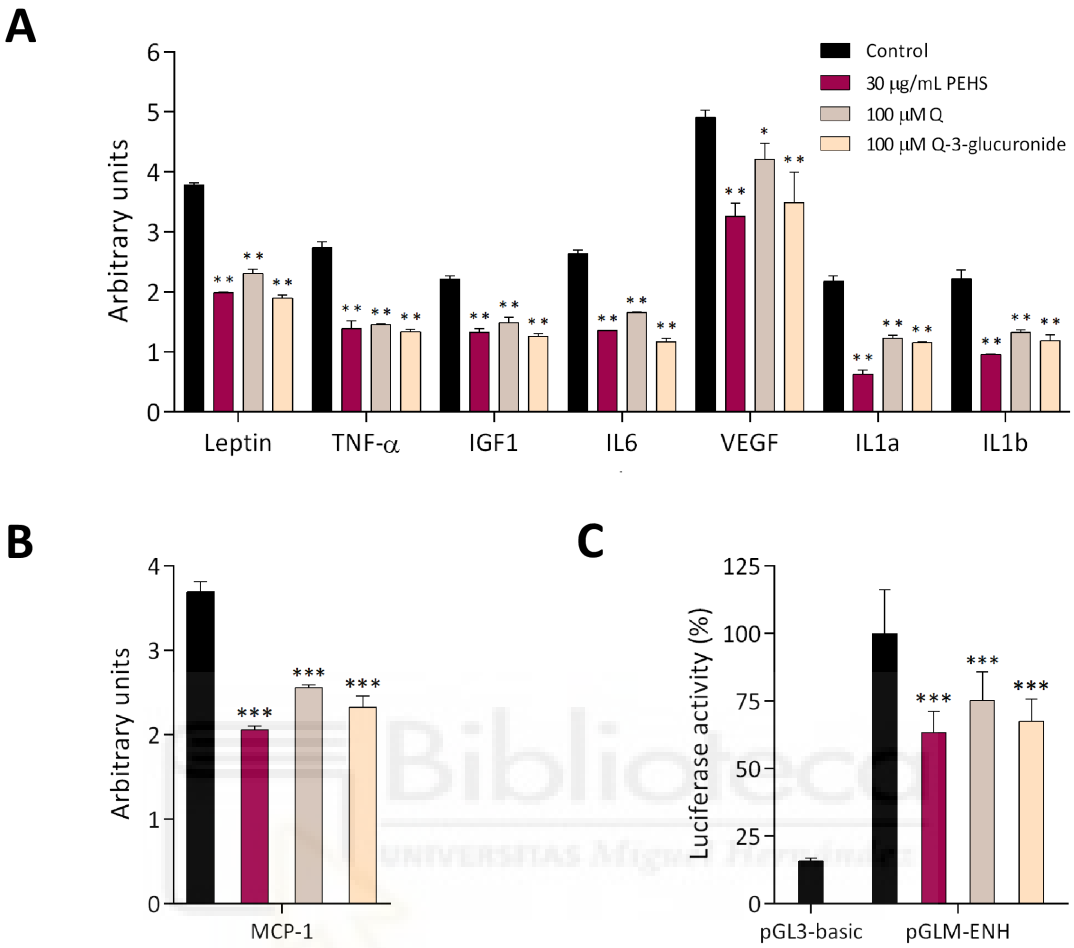
A
Control
30 μg/mL PEHS
100 μM Q
100 μM Q-3-glucuronide
Arbitrary units
Leptin
TNF-α
IGF1
IL6
VEGF
IL1a
IL1b
B
Arbitrary units
MCP-1
C
Luciferase activity (%)
pGL3-basic
pGLM-ENH

FIGURE 3

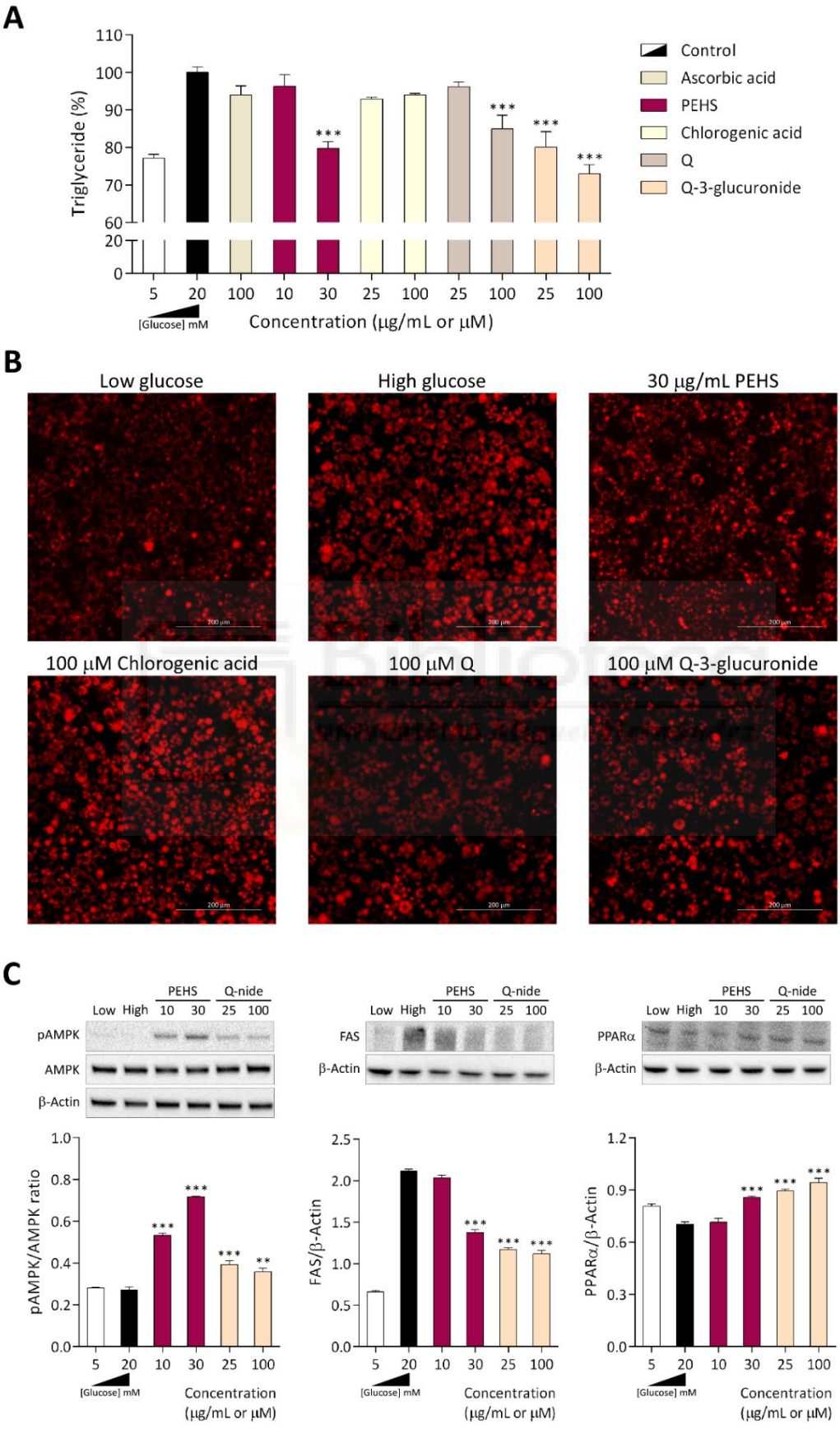
A
Triglyceride (%)
Control
Ascorbic acid
PEHS
Chlorogenic acid
Q
Q-3-glucuronide
[Glucose] mM
Concentration (µg/mL or µM)
B
Low glucose
High glucose
30 µg/mL PEHS
100 µM Chlorogenic acid
100 µM Q
100 µM Q-3-glucuronide
C
PEHS
Q-nide
Low High 10 30 25 100
pAMPK
AMPK
β-Actin
FAS
PPARα
pAMPK/AMPK ratio
FAS/β-Actin
PPARα/β-Actin

FIGURE 4

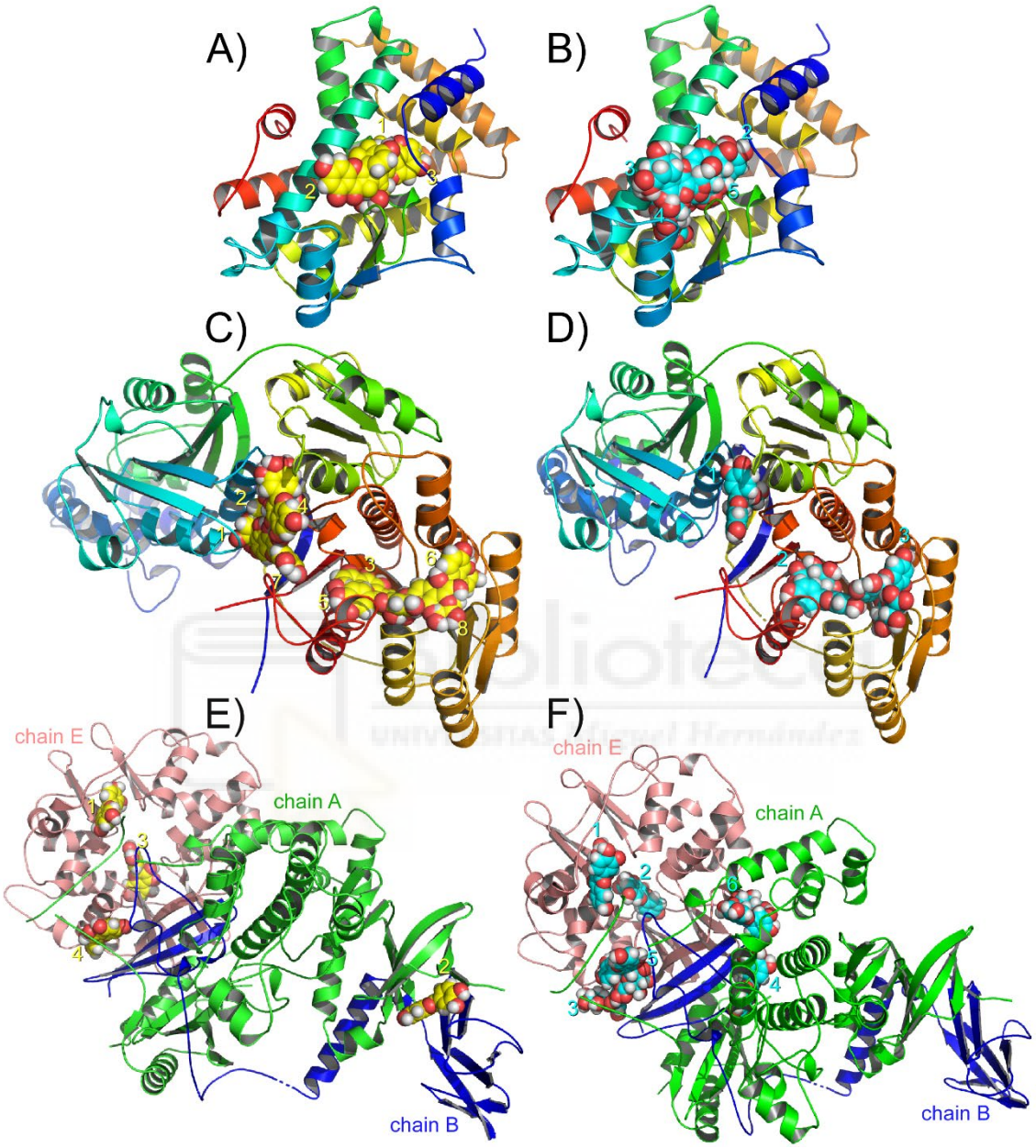

FIGURE 5

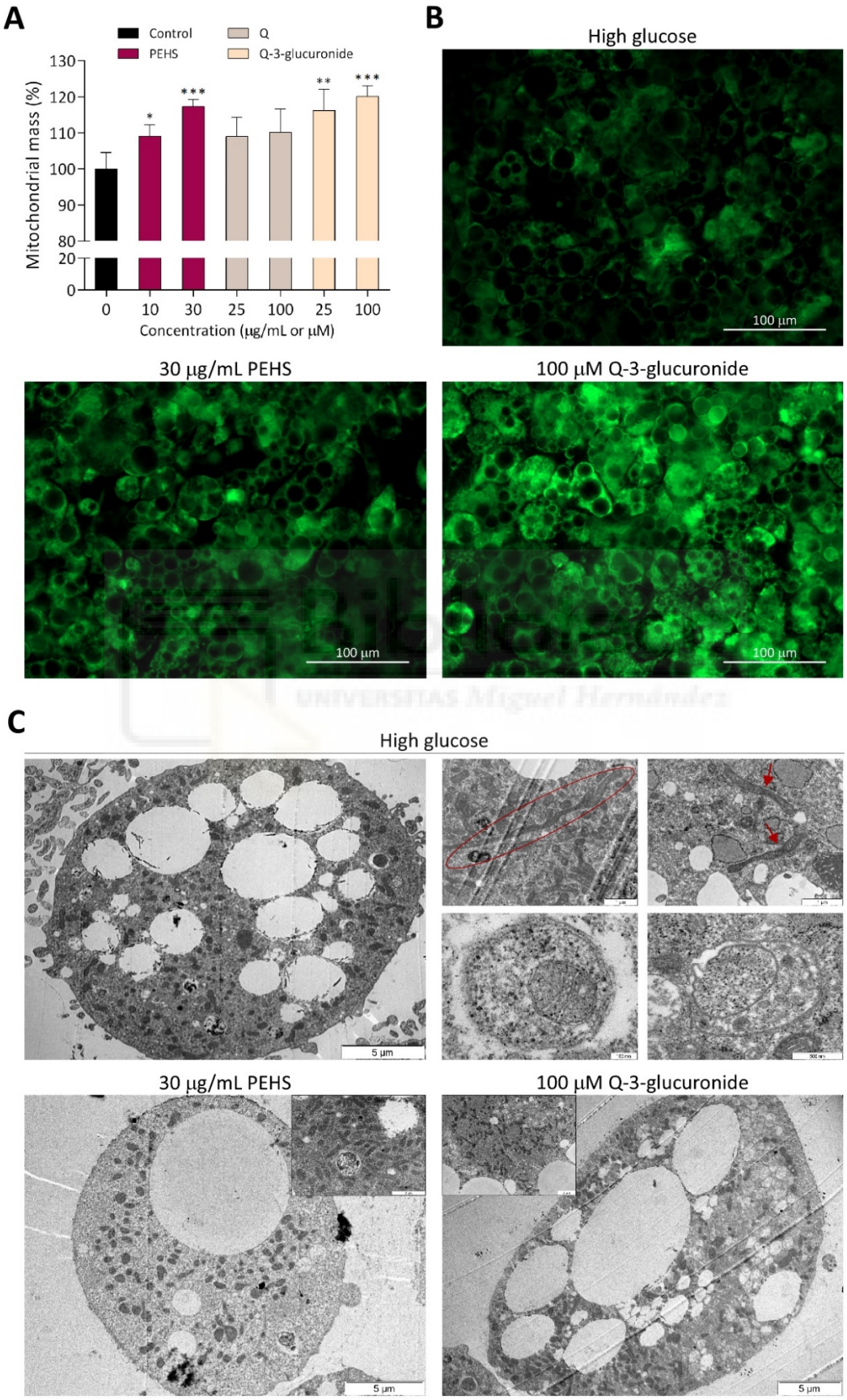
A
Control
PEHS
Q
Q-3-glucuronide
Mitochondrial mass (%)
130
120
110
100
90
80
20
0
*
***
**
***
0
10
30
25
100
25
100
Concentration (µg/mL or µM)
B
High glucose
100 µm
30 µg/mL PEHS
100 µm
100 µM Q-3-glucuronide
100 µm
C
High glucose
5 µm
30 µg/mL PEHS
5 µm
100 µM Q-3-glucuronide
5 µm

Supplementary Table 1: Details of the interaction of quercetin docked to the human PPARα (see **Figure 1A**).

Cluster number	ΔG, [kcal/mol]	Dissoc. constant, [μM]	Members	Residues of the PPARα protein that contact quercetin
1	-10.286±0.603	0.028832	3.50 %	TYR-214, PHE-218, MET-220, ASN-221, LYS-222, THR-279, GLU-282, THR-283, GLU-286, MET-320, SER-323, VAL-324, VAL-332, ALA-333, TYR-334, GLY-335, ASP-372, ILE-375
2	-9.566±0.726	0.097147	4.80 %	PHE-218, ASN-219, MET-220, CYS-275, CYS-278, THR-279, GLU-282, THR-283, GLU-286, LEU-331, VAL-332, ALA-333, TYR-334
3	-9.895±0.186	0.055792	1.10 %	TYR-214, PHE-218, MET-220, ASN-221, LYS-222, THR-279, THR-283, GLU-286, MET-320, LEU-321, SER-323, VAL-324, MET-330, LEU-331, VAL-332, ALA-333, TYR-334, GLY-335, ASP-372, ILE-375

Supplementary Table 2: Details of the interaction of Q3GA docked to the human PPARα (see **Figure 1B**).

Cluster number	ΔG, [kcal/mol]	Dissoc. constant, [μM]	Members	Residues of the PPARα protein that contact quercetin-3-O-glucuronide
1	-11.230±0.323	0.005866	4.80 %	ILE-272, PHE-273, CYS-275, CYS-276, THR-279, SER-280, THR-283, TYR-314, ILE-317, LEU-321, MET-330, VAL-332, ILE-339, LEU-344, ILE-354, MET-355, HIS-440, VAL-444, LEU-460, TYR-464
2	-11.220±0.496	0.005965	5.20 %	VAL-227, ILE-228, LEU-229, SER-230, GLY-231, LYS-232, ALA-233, SER-234, ASN-236, PRO-237, PRO-238, VAL-240, LEU-331, PHE-338
3	-11.030±0.326	0.008221	6.10 %	MET-220, VAL-255, ILE-272, CYS-275, CYS-276, CYS-278, THR-279, GLU-282, VAL-324, MET-330, LEU-331, VAL-332, ALA-333, TYR-334, ILE-339
4	-10.670±0.678	0.015095	3.10 %	PHE-218, ASN-219, MET-220, ASN-221, CYS-276, THR-279, SER-280, THR-283, GLU-286, TYR-314, ILE-317, MET-320, LEU-321, SER-323, VAL-324, MET-330, LEU-331, VAL-332, ALA-333, TYR-334, GLY-335
5	-10.030±0.766	0.044458	4.70 %	MET-220, VAL-255, ILE-272, HIS-274, CYS-275, CYS-276, CYS-278, THR-279, GLU-282, THR-283, GLU-286, MET-330, LEU-331, VAL-332, ALA-333, TYR-334

Supplementary Table 3: Details of the interaction of quercetin docked to the FASN (see **Figure 1C**).

Cluster number	ΔG, [kcal/mol]	Dissoc. constant, [μM]	Members	Residues of the FASN protein that contact quercetin
1	-9.757±0.684	0.070391	7.17 %	GLU-115, PHE-117, LYS-210, ASP-214, VAL-217, GLU-218, LEU-244, LEU-245, PRO-247, HIS-248, LEU-251, ASN-438, MET-483, PHE-494, ARG-495, HIS-496, GLY-651, ARG-652, GLY-653
2	-9.630±0.482	0.087277	5.75 %	PHE-117, LYS-210, ASP-214, VAL-217, GLU-218, MET-220, PRO-221, LEU-223, LEU-245, HIS-248, ASN-438, ARG-441, ARG-442, VAL-482, MET-483, ARG-495, HIS-496, ARG-652
3	-9.496±0.515	0.109386	7.07 %	GLY-517, GLY-520, GLY-521, PHE-522, GLY-523, LEU-597, LYS-621, PHE-645, SER-646, SER-647, VAL-648, TRP-686, GLY-687, ALA-688, ILE-689, GLY-693, ILE-694, LEU-695
4	-9.454±0.604	0.117402	1.51 %	VAL-217, GLU-218, ASN-219, MET-220, LEU-223, HIS-248, PRO-249, LEU-250, ASN-438, ARG-441, ARG-442, VAL-482, ARG-652, GLY-653, ASN-654, ALA-655, SER-707
5	-9.054±0.450	0.230781	2.62 %	GLY-517, GLY-520, GLY-521, PHE-522, GLY-523, LEU-597, VAL-599, PHE-645, ALA-688, ILE-689, VAL-692, GLY-693, ILE-694, LEU-695, VAL-696
6	-9.178±0.371	0.187168	2.42 %	GLY-517, LEU-519, GLY-520, GLY-521, SER-542, ARG-543, SER-544, ASN-571, ILE-572, SER-573, LEU-597, ALA-598, VAL-599, VAL-600, LYS-619, PRO-620
7	-9.118±0.356	0.207018	3.64 %	ILE-113, GLU-115, LYS-210, PRO-247, HIS-248, PRO-249, VAL-648, ARG-652, GLY-687, ALA-688, VAL-706, SER-707, THR-709, PHE-735
8	-9.295±0.232	0.153596	2.22%	GLY-517, LEU-519, GLY-520, THR-541, SER-542, ARG-543, SER-544, GLY-545, GLN-551, SER-570, ASN-571, ILE-572, SER-573, ALA-598, VAL-599, VAL-600, LYS-619, PRO-620

Supplementary Table 4: Details of the interaction of Q3GA docked to the human FASN (see **Figure 1D**).

Cluster number	ΔG, [kcal/mol]	Dissoc. constant, [μM]	Members	Residues of the FASN that contact quercetin-3-O-glucuronide
1	-11.901±0.998	0.001890	1.01 %	PHE-117, LYS-210, ASP-214, VAL-217, GLU-218, ASN-219, MET-220, LEU-223, HIS-248, PRO-249, LEU-250, ASN-438, ARG-441, ARG-442, VAL-482, MET-483, PHE-494, ARG-495, HIS-496, GLY-651, ARG-652, GLY-653, SER-707
2	-11.179±1.347	0.006391	1.21 %	GLY-517, GLY-520, GLY-521, PHE-522, GLY-523, LEU-597, ALA-598, VAL-599, LYS-621, PHE-645, SER-646, SER-647, VAL-648, TYR-660, ASN-664, TRP-686, GLY-687, ALA-688, ILE-689, VAL-692, GLY-693, ILE-694, LEU-695, VAL-696
3	-10.321±1.501	0.027200	1.82 %	ALA-516, GLY-517, GLY-518, LEU-519, GLY-520, THR-541, SER-542, ARG-543, SER-544, GLY-545, ARG-547, GLN-551, ASN-571, ILE-572, SER-573, LEU-597, ALA-598, VAL-599, VAL-600, LYS-619, PRO-620, ILE-694

Supplementary Table 5: Details of the interaction of quercetin docked to the human AMPK protein ternary complex (see **Figure 1E**).

Cluster number	ΔG, [kcal/mol]	Dissoc. constant, [μM]	Members	Residues of the AMPK protein complex that contact quercetin
1	-9.220±0.213	0.174441	4.5 %	PRO-365, HIS-366, PRO-367 (**chain A**) and ILE-240, ASP-245, ARG-269, TYR-272, PHE-273, GLY-275, VAL-276, LEU-277, VAL-297, HIS-298, ARG-299, LEU-300, VAL-301 (**chain E**)
2	-9.202±0.125	0.179822	3.9 %	VAL-11, LEU-18, LYS-29, LYS-31, ILE-46, ASN-48, ASP-88, PHE-90 (**chain A**) and VAL-81, ARG-83, THR-106, ARG-107, SEP-108, ASN-111, VAL-113, ILE-115 (**chain B**)
3	-9.129±0.653	0.203401	6.1 %	ARG-70, MET-85, THR-87, THR-89, ASP-90, ARG-118, TYR-121, LEU-122, LYS-127, ILE-150, HIS-151, ARG-152, SER-226, LYS-243 (**chain E**)
4	-8.508±0.756	0.580167	4.8 %	LYS-398, LYS-399, ALA-400, TRP-402 (**chain A**) and LEU-215, LEU-242, ASP-246, VAL-248, VAL-250, LEU-265, TYR-267 (**chain B**) and LEU-55, LYS-59, PHE-62, ALA-63, THR-66, ASN-67 (**chain E**)

Supplementary Table 6: Details of the interaction of Q3GA docked to the human AMPK protein ternary complex (see **Figure 1E**).

Cluster number	ΔG, [kcal/mol]	Dissoc. constant, [μM]	Members	Residues of the AMPK protein complex that contact quercetin-3-O-glucuronide
1	-10.357±0. 631	0.025598	3.9 %	PRO-365, HIS-366, PRO-367, ARG-369, (**chain A**) and ALA-227, ILE-240, SER-242, PHE-244, ASP-245, HIS-268, ARG-269, TYR-272, PHE-273, GLU-274, GLY-275, VAL-276, LEU-277, ALA-295, VAL-297, HIS-298, ARG-299 (**chain E**)
2	-9.641±0. 372	0.085714	2.6 %	ARG-70, GLY-84, MET-85, THR-87, ILE-88, THR-89, ASP-90, TYR-121, LYS-127, VAL-130, LYS-149, ILE-150, HIS-151, ARG-152, ARG-224, SER-226, LYS-243 (**chain E**)
3	-9.250±0. 238	0.165828	4.6 %	LEU-373, ALA-375, ASP-376, VAL-397, LYS-398, LYS-399, ALA-400, TRP-402 (**chain A**) and LEU-242, LYS-245, ASP-246, VAL-248, TYR-267 (**chain B**) and LYS-59, PHE-62, ALA-63, THR-66, ASN-67, LYS-253 (**chain E**)
4	-9.108±0.205	0.210740	5.1 %	ASP-128, HIS-131, ARG-132, MET-164, ALA-191, PRO-193, GLU-194, ILE-197, PRO-253, LEU-254, ARG-256, ALA-257, THR-258, ILE-259, LYS-260, ARG-263 (**chain A**) and HIS-209, GLU-230, PRO-231, ASN-232, HIS-233, VAL-234, TYR-261 (**chain B**)
5	-9.015±0.157	0.246557	2.4 %	ARG-369, MET-370, PRO-371, PRO-372, LEU-373, VAL-397, LYS-399, ALA-400, TRP-402 (**chain A**) and LEU-215, ASN-216, ASP-218, THR-219, ILE-221 (**chain B**) and LYS-47, VAL-65, THR-66, ASN-67 (**chain E**)
6	-8.502±0.956	0.693828	3.9 %	GLU-279, GLU-291, ARG-331, MET-334, ASN-335, SER-338, TYR-341, LEU-342 (**chain A**) and LYS-259, LYS-260 (**chain B**) and TYR-39, ASP-40, THR-44 (**chain E**)

CAPÍTULO 4

Scientific Reports, 2019, 28;9(1):2999

Differential effects of a combination of *Hibiscus sabdariffa* and *Lippia citriodora* polyphenols in overweight/obese subjects: A randomized controlled trial

María Herranz-López, Mariló Olivares-Vicente, Marina Boix-Castejón, Nuria Caturla, Enrique Roche, Vicente Micol.

María Herranz-López and Mariló Olivares-Vicente contributed equally.

DOI: 10.1038/s41598-019-39159-5

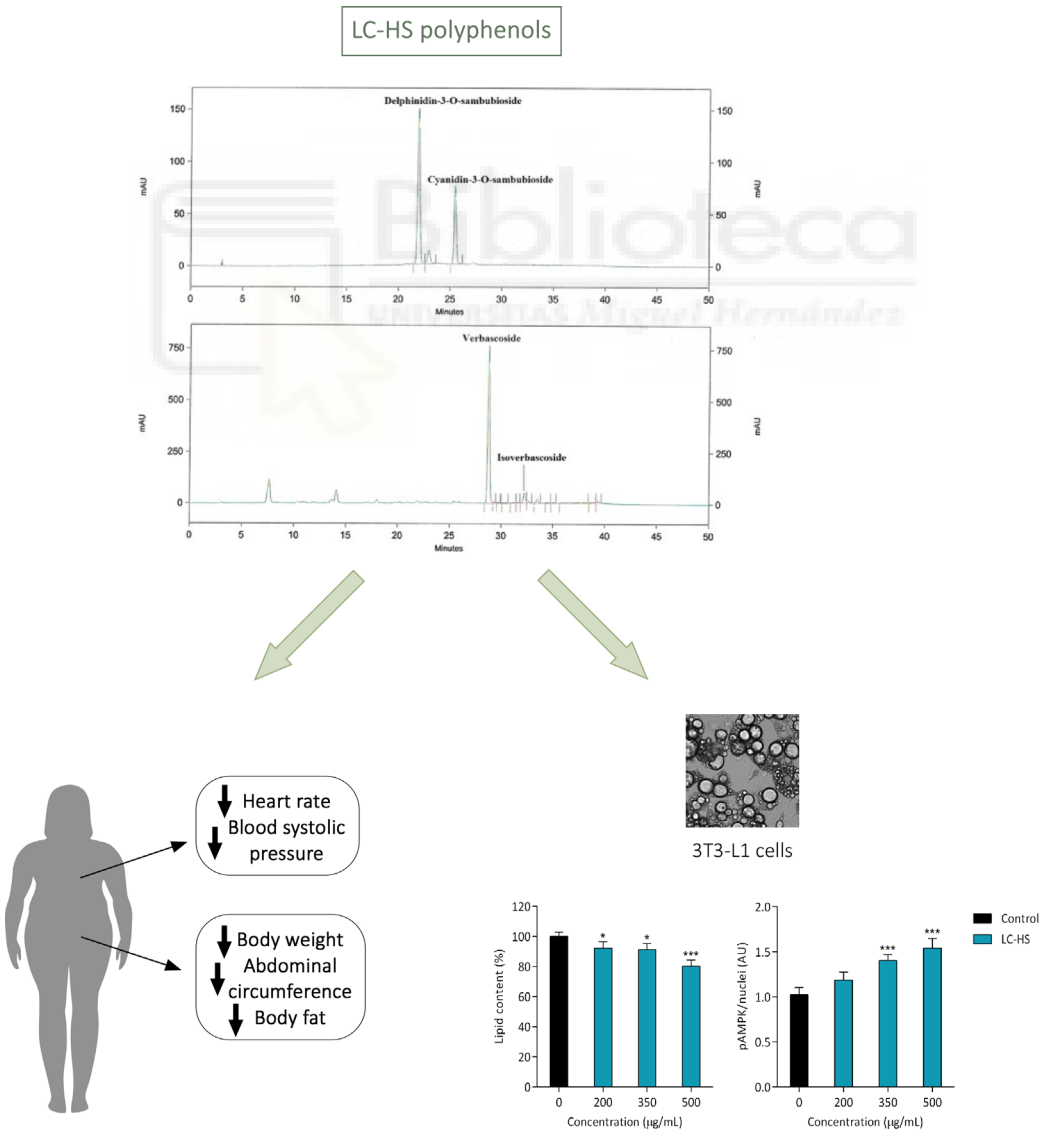

RESUMEN DE LOS RESULTADOS

Considerando los estudios previos del grupo sobre los beneficios de los extractos de LC e HS en la obesidad a través de ensayos en modelos celulares y animales, se evaluó la suplementación de 500 mg de una combinación de ambos extractos acompañada de una dieta isocalórica en mujeres obesas y con sobrepeso en un ensayo doble ciego, aleatorizado y controlado por placebo durante 2 meses. Los resultados mostraron una mejora general de los parámetros antropométricos en el grupo que consumía el suplemento comparado con el control, especialmente en el peso corporal, la circunferencia abdominal (AC) y el porcentaje de grasa corporal (% BF). Asimismo, los cambios fueron más notorios en el grupo de mujeres con sobrepeso.

Al final del estudio, los grupos que recibieron el suplemento exhibieron una mayor disminución del peso corporal respecto a los grupos controles: −1.96 ± 2.49 kg en el grupo control con sobrepeso vs. −3.69 ± 0.34 kg en el grupo LC-HS con sobrepeso ($p < 0.05$) y −2.17 ± 0.95 kg en el grupo control obeso vs. −4.68 ± 0.67 kg en el grupo LC-HS obeso ($p < 0.05$). Ambos parámetros de circunferencia abdominal (AC1 y AC2) también disminuyeron, especialmente en el grupo con sobrepeso que consumía el suplemento: −6.79 ± 0.80 cm en el AC1 del grupo LC-HS comparado con −1.85 ± 0.83 cm de reducción en el grupo control con sobrepeso ($p < 0.001$). A los dos meses, el % BF disminuyó en ambos grupos, obesos y sobrepeso, siendo más significativo en el grupo con sobrepeso que consumía LC-HS (−1.33 ± 0.15 %) comparado con el control (−0.66 ± 0.17 %, $p < 0.05$). El IMC también disminuyó en obesos y sobrepeso, pero el grupo LC-HS con sobrepeso mostró una mayor disminución comparado con su control (−1.46 ± 0.14 vs. −0.78 ± 0.28, respectivamente, $p < 0.05$).

En cuanto a los signos vitales, el ritmo cardíaco disminuyó significativamente en las voluntarias con sobrepeso y obesidad que consumían LC-HS a los 30 y 60 días del estudio, mientras que no cambió en los grupos controles (control: −1.25 ± 2.68 bpm vs. LC-HS: −8.53 ± 1.35 bpm en sobrepeso, $p < 0.05$; control: −1.75 ± 2.09 bpm vs. LC-HS: −8.00 ± 1.14 bpm en obesos, $p < 0.05$). La presión arterial sistólica (SBP) y diastólica (DBP) en los grupos LC-HS con sobrepeso y obesos también se redujo a los 30 y 60 días, especialmente en el caso de la SBP, con valores en torno a 130 al principio del tratamiento que cayeron a 110 al final del tratamiento. Por otro lado, no se observaron diferencias significativas en el grupo control a los 60 días. Entre los grupos control y LC-HS, solo se observaron diferencias significativas en la SBP al final del estudio (20.65 ± 2.88 and 18.42 ± 3.95 mm Hg en los grupos LC-HS con sobrepeso y obesidad, respectivamente; 5.33 ± 2.55 y 13.50 ± 7.11 mm Hg en los grupos control con sobrepeso y obesidad, respectivamente). Asimismo, la reducción de la presión sanguínea fue acompañada de una mejora en el perfil lipídico sanguíneo.

In vitro, la mezcla LC-HS disminuyó significativamente los triglicéridos intracelulares en adipocitos hipertróficos reduciendo hasta un 19.7 % la acumulación lipídica a 500 μg/mL tras 72h de incubación. Asimismo, LC-HS aumentó la activación de AMPK en los adipocitos hasta 1.5 veces comparado con el control.

La mezcla LC-HS fue analizada por HPLC-DAD-ESI-IT-MS. La mayoría de los compuestos identificados pertenecían a las subfamilias de fenilpropanoides y antocianinas. Se identificaron 4 principales compuestos fenólicos: 2 antocianinas (delfinidina-3-O-sambubiósido y cianidina-3-O-sambubiósido) y 2 fenilpropanoides (verbascósido e isoverbascósido). El total de antocianinas constituyó un 3.5 % del peso seco total representando la delfinidina-3-O-sambubiósido el 2.27 % del peso seco total (65 % del total de antocianidinas) y cianidina-3-O-sambubiósido, un 1.23 % (35 %). Respecto a los fenilpropanoides, este grupo representó el 16 % del peso seco total, siendo verbascósido el principal componente y constituyendo el 15 % (93.75 % del total de fenilpropanoides) y el isoverbascósido, el 1 % (6.65 % del total de fenilpropanoides).

SCIENTIFIC REPORTS

OPEN

Differential effects of a combination of *Hibiscus sabdariffa* and *Lippia citriodora* polyphenols in overweight/obese subjects: A randomized controlled trial

Received: 29 June 2018
Accepted: 18 December 2018
Published online: 28 February 2019

María Herranz-López[1], Mariló Olivares-Vicente[1], Marina Boix-Castejón[2], Nuria Caturla[3], Enrique Roche[2,4] & Vicente Micol[1,4]

Plant-polyphenols have shown the capacity to ameliorate obesity-induced metabolic disturbances, both in cell and animal models, where most therapeutic approaches have failed. On the basis of previous research, a dietary supplement containing 500 mg of a combination of polyphenolic extracts from *Lippia citriodora* L. and *Hibiscus sabdariffa* L. (LC-HS), in the context of an equilibrated isocaloric diet, was evaluated in a double blind, placebo-controlled and randomized trial in 56 obese/overweight subjects for two months. Compared to controls, the consumption of the LC-HS polyphenols showed significant improvements in body weight, abdominal circumference of overweight subjects (-6.79 ± 0.80 cm in overweight LC-HS group *vs* -1.85 ± 0.83 cm in controls, $p < 0.001$) and body fat % (-1.33 ± 0.15% in overweight LC-HS group *vs* -0.66 ± 0.17% in controls, $p < 0.05$). Heart rate and systolic blood pressure also presented significant improvements in overweight LC-HS participants. However, changes were more modest in obese subjects. Further, LC-HS extract significantly reduced lipid content and increased AMPK activity in a hypertrophied adipocyte cell model. Therefore, consumption of 500 mg/day of LC-HS extracts enriched in polyphenols for two months in the context of an isocaloric diet by overweight subjects decreased symptoms associated to obesity-related diseases. Modulation of fat metabolism in adipose tissue, probably mediated by AMPK activation, is proposed as a molecular target to be explored in future research.

Obesity has reached global epidemic proportions. Given the absence of effective drugs with no side-effects, improving our understanding of the relationship between diet and health may be a realistic alternative. Obesity is associated with several metabolic abnormalities including insulin resistance, endothelial dysfunction and dyslipidemia, which are involved in the development of type 2 diabetes, hypertension and cardiovascular diseases. Very often, these changes start to be evident during the overweight phase (Body Mass Index <30). While there has been considerable progress in understanding the molecular mechanisms underlying metabolic disorders, their successful treatment remains limited[1,2].

The causal link between excessive fat storage in obesity and metabolic disturbances is mediated by altered metabolic homeostasis in adipose tissue. Excessive accumulation of triglycerides leading to adipocyte hypertrophy compromises cell function, initiating an inflammatory process related to oxidative stress, which can lead to metabolic disorders associated with obesity[3,4]. Among the putative targets to ameliorate metabolic diseases, the

[1]Instituto de Investigación, Desarrollo e Innovación en Biotecnología Sanitaria de Elche (IDiBE) e Instituto de Biología Molecular y Celular (IBMC), Miguel Hernández University (UMH), Elche, 03202, Alicante, Spain. [2]Institute of Bioengineering and Department of Applied Biology-Nutrition, University Miguel Hernandez, Alicante Institute for Health and Biomedical Research (ISABIAL-FISABIO Foundation), Alicante, Spain. [3]Monteloeder S.L., Alicante, Spain. [4]CIBER, Fisiopatología de la Obesidad y la Nutrición, CIBERobn, Instituto de Salud Carlos III (CB12/03/30038), 07122 Palma de Mallorca, Spain. María Herranz-López and Mariló Olivares-Vicente contributed equally. Enrique Roche and Vicente Micol jointly supervised this work. Correspondence and requests for materials should be addressed to V.M. (email: vmicol@umh.es)

energy sensor AMP-activated protein kinase (AMPK) has been proposed as an important therapeutic target for obesity[5–7]. Its activation leads to activation of catabolic pathways such as lipolysis and fatty acid oxidation and to inhibition of anabolic pathways such as lipogenesis and gluconeogenesis[8].

Our previous research has accumulated enough evidence and has identified several herbal extracts with the capacity to alleviate metabolic stress and to modulate different molecular and cellular targets in cell culture and animal models[9–12]. These extracts include *Hibiscus sabdariffa* (HS), *Lippia citriodora* (LC), *Olea europaea* leaf and extra virgin olive oil extracts[13]. Most of these effects were correlated with the activation of the energy sensor AMP-activated protein kinase (AMPK). Using an insulin resistant hypertrophic adipocyte model, we have seen that HS polyphenols decreased metabolic stress in glucotoxicity and/or lipotoxicity events through the modulation of pathways associated with energy management and inflammation[5,6]. Additionally, HS polyphenols exhibited the capacity to inhibit triglyceride accumulation, oxidative stress and the secretion of inflammatory adipokines that regulate the infiltration of non-resident macrophages to adipose tissue[3,9,14]. Moreover, the efficacy of HS polyphenolic extract has also been demonstrated in animal models by preventing hepatic steatosis in hyperlipidemic mice through the regulation of the expression of genes involved in glucose and lipid homeostasis[10], and lowering blood pressure and improving endothelial function[11]. Bioavailability studies performed in rat model and adipocytes suggest that quercetin-3-O-β-D-glucuronide and its aglycone may be responsible for the observed effects[10,12,13,15].

On the other hand, studies on LC, namely lemon verbena, polyphenols showed favorable effects such as decreased lipogenesis, enhanced fatty acid oxidation and activation of the AMPK pathway, probably through PPAR-gamma receptor activation and adiponectin[16]. Similar to the HS polyphenol extract, the continuous administration of LC polyphenolic extract prevented fatty liver disease (FLD) and improved lipid metabolism in hyperlipidemic animal model. Interestingly, the results on lipid and glucose metabolism obtained in the hyperlipidemic mice revealed the possibility that HS and LC reach similar as well as complementary targets[10,16]. These findings prompted us to explore the effects of a combination of HS and LC in obese mice fed a high-fat diet (HFD). A recent report has shown the capacity of this combination to decrease obesity and its complications, improving the metabolism of HFD mice through increased thermogenesis-inducing genes in the white adipose tissue, and correlating with increased phosphorylation of AMPK and fatty-acid oxidation in the liver[17]. Finally, a randomized controlled trial performed in overweight subjects has demonstrated that the combination of HS and LC can modulate appetite-related peptides, as well as reduced blood pressure when compared to placebo, helping probably to a better management of body weight in the context of an equilibrated isocaloric diet[18].

Therefore, the objective of this study was to assess the comparative efficacy of the abovementioned formulation, containing both LC and HS extracts (LC-HS), in two groups of overweight/obese subjects under risk of developing metabolic syndrome to search for differential effects between obese and overweight subjects. The capacity of a dietary supplement containing this combination coupled with isocaloric diet to modulate anthropometric parameters, as well as to improve several metabolic and hematological parameters associated with metabolic syndrome, such as blood pressure and heart rate, was also differentially studied in overweight and/or obese participants. Then, we assayed the potential of this combination to activate the AMPK-enzyme and to reduce triglyceride accumulation in the hypertrophied adipocyte model.

Results

Intervention study results. *Anthropometric parameters.* Subjects in the study were sedentary lifestyle at baseline. Characteristics of the two overweight and the two obese groups were well matched and no significant differences were found at baseline (Table 1A,B). Study design and flow chart are shown in Fig. 1 (see suplementary file for full trial protocol). During the intervention study, participants were instructed to walk every day for 30 minutes as was reflected at weekly meetings. The results showed an overall improvement in the anthropometric parameters determined in the groups taking LC-HS compared to control after two months, particularly in body weight, abdominal circumference and percentage of body fat. Changes were more significant in the overweight group (Table 1A). The LC-HS groups exhibited a higher decrease of body weight compared to the control group, and significant differences were observed mainly between the control and LC-HS overweight groups (-1.96 ± 2.49 kg vs. -3.69 ± 0.34 kg, respectively, $p < 0.05$) and the control and LC-HS obese (-2.17 ± 0.95 kg vs. -4.68 ± 0.67 kg, respectively, $p < 0.05$) groups (Table 2). Both abdominal circumference parameters (ACs) were also reduced over the two months of treatment, particularly in overweight people consuming LC-HS (Table 1). After two months, only the AC1 presented a significantly reduction of -6.79 ± 0.80 cm in the overweight LC-HS group, compared to the -1.85 ± 0.83 cm of reduction in the overweight control group, $p < 0.001$ (Table 2A). Consistently with this data, % body fat (BF) decreased over time in overweight and obese groups (Table 1) but the overweight group consuming the extract lost significantly more body fat ($-1.33 \pm 0.15\%$) compared to the control group ($-0.66 \pm 0.17\%$, $p < 0.05$) after two months (Table 2A). In line with the above, a decrease in BMI was also observed in overweight and obese groups (Table 1), but the overweight LC-HS group exhibited a stronger decrease in BMI compared to the control, showing statistically significant differences (-1.46 ± 0.14 vs. -0.78 ± 0.28, respectively, $p < 0.05$) (Table 2A).

Heart rate and blood pressure. There were no significant differences in baseline heart rate and blood pressures parameters between the LC-HS and control groups of overweight and obese volunteers (Table 1). First, a significant decrease was observed in the heart rate of the volunteers of the overweight and obese groups consuming LC-HS after 30 and 60 days, while the heart rate remained unchanged during the entire study period in the control groups (Table 1). After two months, statistically significant differences were observed for the change in heart rate when the two groups were compared (control: -1.25 ± 2.68 bpm vs. LC-HS: -8.53 ± 1.35 bpm in overweight, $p < 0.05$; Table 2A) (control: -1.75 ± 2.09 bpm vs. LC-HS: -8.00 ± 1.14 bpm in obese, $p < 0.05$; Table 2B). Regarding blood pressure, both systolic and diastolic BP in overweight and obese LC-HS groups also

	LC-HS (N = 16)			Control (N = 10)		
A) OVERWEIGHT	**BASELINE**	**MONTH 1**	**MONTH 2**	**BASELINE**	**MONTH 1**	**MONTH 2**
Anthropometric parameters						
Body weight	67.97 ± 8.42	65.48 ± 8.07****	64.28 ± 8.32****	67.83 ± 6.74	66.25 ± 7.28**	65.87 ± 7.60*
Body mass index (BMI) kg/m^2	26.62 ± 1.85	25.64 ± 1.69****	25.16 ± 1.73****	27.31 ± 1.60	26.67 ± 1.88**	26.53 ± 2.25*
AC1 (cm)	93.91 ± 10.85	87.89 ± 9.00***	86.42 ± 9.71****	83.60 ± 6.32	81.75 ± 5.97**	81.75 ± 5.96*
AC2 (cm)	100.4 ± 10.50	96.58 ± 9.20**	94.61 ± 9.52****	95.69 ± 7.20	92.78 ± 6.79*	90.66 ± 5.92**
Triceps skinfold thickness (mm)	28.13 ± 9.02	25.13 ± 7.94**	23.92 ± 8.64***	27.29 ± 3.05	25.63 ± 2.31*	25.13 ± 2.16**
% Body fat (BF)	44.05 ± 2.89	43.16 ± 2.66****	42.72 ± 2.61****	42.87 ± 1.13	42.39 ± 1.15**	42.21 ± 1.28**
Vital signs						
Heart rate (BPM)	81.40 ± 9.64	75.57 ± 8.23***	72.87 ± 7.30****	74.75 ± 10.06	74.08 ± 13.57	73.50 ± 13.05
Systolic BP mm Hg	129.2 ± 14.84	118.2 ± 15.48****	108.6 ± 9.18****	120.8 ± 15.66	117.8 ± 15.11	115.4 ± 15.40
Diastolic BP mm Hg	79.60 ± 11.89	75.07 ± 10.44	68.53 ± 10.27****	74.75 ± 12.75	75.08 ± 6.68	69.33 ± 10.35
Biochemical parameters						
Glucose mg/dl	90.08 ± 12.35	86.17 ± 11.45	86.75 ± 8.67	92.82 ± 15.83	94.73 ± 11.96	94.73 ± 18.42
Triglycerides mg/dl	80.33 ± 57.87	74.17 ± 40.67	79.17 ± 40.91	77.18 ± 25.63	72.64 ± 20.01	75.73 ± 20.78
Total Cholesterol mg/dl	245.4 ± 25.69	219.8 ± 27.95***	211.8 ± 27.22***	223.7 ± 28.09	197.0 ± 16.61**	196.6 ± 14.53***
HDL mg/dl	61.81 ± 7.70	60.69 ± 7.62	60.69 ± 9.26	59.36 ± 8.00	58.09 ± 7.87	57.91 ± 7.67
LDL mg/dl	165.6 ± 23.70	146.1 ± 20.83***	133.2 ± 18.81****	148 0.8 ± 27.15	124.5 ± 18.19**	123.5 ± 14.04***
	LC-HS (N = 10)			**Control (N = 10)**		
B) OBESE	**BASELINE**	**MONTH 1**	**MONTH 2**	**BASELINE**	**MONTH 1**	**MONTH 2**
Anthropometric parameters						
Body weight	88.23 ± 11.57	86.09 ± 11.14*	83.55 ± 11.57***	86.16 ± 6.85	84.03 ± 6.53**	83.99 ± 6.42*
Body mass index (BMI) kg/m^2	33.92 ± 4.93	33.07 ± 4.48*	32.06 ± 4.50**	34.62 ± 3.50	33.78 ± 3.59**	33.77 ± 3.63*
AC1 (cm)	88.80 ± 10.41	85.35 ± 9.91*	82.63 ± 9.80**	101.9 ± 13.21	100.4 ± 12.35*	98.61 ± 10.84
AC2 (cm)	103.7 ± 9.03	100.6 ± 7.69	97.86 ± 9.08***	112.3 ± 9.74	110.5 ± 10.04	106.6 ± 8.87*
Triceps skinfold thickness (mm)	32.14 ± 9.46	30.43 ± 7.55	28.86 ± 8.15**	34.38 ± 5.04	32.69 ± 4.32	32.0 ± 4.47
% Body fat (BF)	44.92 ± 2.97	44.23 ± 2.98**	43.63 ± 2.84**	47.35 ± 2.42	46.86 ± 2.56**	46.55 ± 2.23**
Vital signs						
Heart rate (BPM)	76.90 ± 10.20	72.85 ± 10.29**	68.90 ± 9.43****	77.25 ± 6.21	76.75 ± 9.35	78.50 ± 9.01
Systolic BP mm Hg	129.5 ± 15.44	118.1 ± 15.93**	111.1 ± 8.19***	135.5 ± 21.25	125.0 ± 20.91	122.0 ± 16.17
Diastolic BP mm Hg	75.60 ± 9.42	67.20 ± 7.64*	64.90 ± 5.71****	83.63 ± 12.55	77.63 ± 10.29	73.75 ± 13.56
Biochemical parameters						
Glucose mg/dl	100.1 ± 19.79	96.71 ± 15.82	95.14 ± 17.74	95.50 ± 8.32	93.13 ± 10.64	89.75 ± 8.57*
Triglycerides mg/dl	115.1 ± 68.99	76.86 ± 23.41	86.0 ± 37.66	97.25 ± 58.40	86.63 ± 36.16	106.6 ± 52.04
Total Cholesterol mg/dl	229.3 ± 27.46	213.7 ± 29.88*	208.7 ± 28.85**	236.5 ± 22.83	217.3 ± 30.34*	222.5 ± 36.90
HDL mg/dl	57.45 ± 7.12	55.73 ± 7.13*	55.09 ± 7.06**	58.50 ± 7.35	55.38 ± 10.77	56.0 ± 10.13
LDL mg/dl	146.5 ± 23.07	130.8 ± 23.58**	121.0 ± 22.80****	160.4 ± 21.23	144.5 ± 25.37*	145.9 ± 32.34

Table 1. Intragroup analysis of anthropometric, vital signs and biochemical measurements after one and two months of intervention. Intra-group statistical analysis at the endpoint compared to the baseline is reported as follows: *$p < 0.05$; **$p < 0.01$; ***$p < 0.001$; ****$p < 0.0001$. Data are expressed as the mean ± se.

showed a significant reduction after 30 and 60 days compared to the basal value (Table 1), and this reduction was greater for the systolic blood pressure, with values of nearly 130 at the beginning of the treatment that dropped below 110 at the end of the treatment (Table 1). However, in the case of the control group, no significant reduction was observed after 60 days. When control and LC-HS groups were compared, we observed significant differences only in the systolic BP at the end of the study (Table 2). Whereas blood pressure dropped 20.65 ± 2.88 and 18.42 ± 3.95 mm Hg in the LC-HS overweight and obese groups respectively, the same parameter decreased only 5.33 ± 2.55 and 13.50 ± 7.11 mm Hg in the overweight and obese control groups respectively (Table 2).

Reduction in blood pressure was accompanied by an improvement in the circulating lipid profile, showing the most significant changes in the overweight group consuming the supplement (Table 1).

Adverse events. Treatment of overweight and obese subjects with LC-HS was well-tolerated. The incidence of a reported diarrhea case in the treated group was caused by a viral infection. No subjects had adverse side effects during the intervention period. Accordingly, safety hematological reference values were normal throughout the intervention study (data not shown).

Appetite assessment. Although appetite assessment was not strictly evaluated, monitoring of the volunteers throughout the study by a simple survey indicated that most individuals of the LC-HS group experienced a satiating effect, confirming previous observations[18].

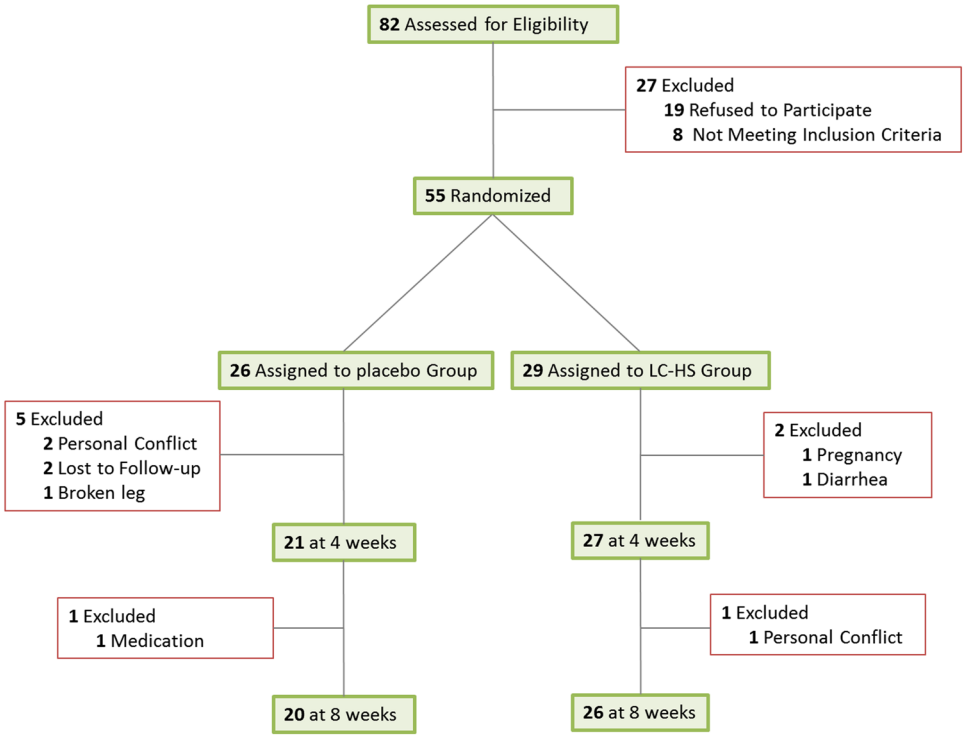

Figure 1. Study design and flow chart of the double blind, placebo controlled and randomized trial using LC-HS combination in 56 overweight volunteers.

Hypertrophied adipocytes model results. Recently, the capacity of LC-HS to activate AMPK in the liver of HFD-induced obesity animal model has been reported[17]. Despite the limitations of a cellular model and recognizing the inherent restrictions using high doses and non-metabolized polyphenols, LC-HS combination was assessed for triglyceride accumulation and AMPK activation in a cell model of adipocyte hypertrophy in the context of insulin resistance. The results of this examination are presented below.

LC-HS polyphenols decrease intracellular triglycerides in hypertrophied adipocytes. The capacity of the combination of polyphenols derived from *H. sabdariffa* and *L. citriodora* to decrease triglyceride accumulation was confirmed in a cellular model of hypertrophy. The results showed a dose response behavior in the decrease of the triglyceride accumulation with an increase in the concentration of the polyphenol combination, reaching a reduction of 19.7% at the maximum concentration assayed; i.e., 500 µg/mL (Fig. 2A).

Activation of AMPK by LC-HS polyphenols in hypertrophied adipocytes. To determine if the selected combination of polyphenols from LC and HS extracts was able to reduce the lipid content concomitantly with the activation of AMPK, the immunofluorescence detection of AMPK in hypertrophied adipocytes was assayed after treatment with the combination. The polyphenolic extract promoted a potent increase in the pAMPK/nuclei ratio in a dose-dependent manner that was significant compared to the control already at 350 µg/mL and reached an increase approximately 1.5-fold at 500 µg/mL of extract with respect to the control (Fig. 2B). Representative immunofluorescence micrographs of the activated pAMPK (red fluorescence) vs. total AMPK (green fluorescence) are shown in Fig. 2C.

Characterization of the dietary supplement by High-Performance Liquid Chromatography (HPLC). The composition of the LC-HS combination was analyzed by HPLC-DAD-ESI-IT-MS. Major compounds identified by their UV spectra and MS/MS data of the peaks belonged to the polyphenolic subfamilies of phenylpropanoids and anthocyanins. Figure 3 shows representative chromatograms of the dietary supplement at 520 nm and 320 nm, upper and lower panel respectively. Four major phenolic compounds were identified, i.e. two anthocyanins, delphinidin-3-O-sambubioside and cyanidin-3-O-sambubioside and two phenylpropanoids, verbascoside, and isoverbascoside. Total anthocyanins represented 3.5% of the total dry weight with delphinidin-3-O-sambubioside constituting 2.27% (65% of total anthocyanidins) and cyanidin-3-O-sambubioside comprising 1.23% (35% of total anthocyanidins). Regarding phenylpropanoids, 16% w/w, verbascoside represented the major compound and constituted 15% (93.75% of total phenylpropanoids) and isoverbascoside represented 1% (6.65% of total phenylpropanoids).

A) OVERWEIGHT	Changes in the first month		Changes in two months	
	LC-HS (N = 16)	Control (N = 10)	LC-HS (N = 10)	Control (N = 10)
Anthropometric parameters				
Body weight	−2.49 ± 0.26	−1.58 ± 0.45	−3.69 ± 0.34*	−1.96 ± 2.49
Body mass index (BMI) kg/m^2	−0.98 ± 0.10	−0.64 ± 0.17	−1.46 ± 0.14*	−0.78 ± 0.28
AC1 (cm)	−5.22 ± 0.94**	−1.85 ± 0.56	−6.79 ± 0.80***	−1.85 ± 0.83
AC2 (cm)	−3.82 ± 1.06	−2.92 ± 0.95	−5.79 ± 1.05	−5.03 ± 1.21
Triceps skinfold thickness (mm)	3.00 ± 0.75	1.67 ± 0.55	−4.21 ± 0.88	−2.16 ± 0.59
% Body fat (BF)	−0.89 ± 0.12*	−0.49 ± 0.13	−1.33 ± 0.15*	−0.66 ± 0.17
Vital signs				
Heart rate (BPM)	−5.83 ± 1.24	−0.67 ± 2.67	−8.53 ± 1.35*	−1.25 ± 2.68
Systolic BP mm Hg	−11.00 ± 1.89	−2.92 ± 4.86	−20.65 ± 2.88***	−5.33 ± 2.55
Diastolic BP mm Hg	−4.53 ± 2.51	0.33 ± 3.54	−11.07 ± ± 1.97	−5.42 ± 2.72
Biochemical parameters				
Glucose mg/dl	−3.91 ± 2.78	1.91 ± 2.10	−3.33 ± 3.00	1.91 ± 2.68
Triglycerides mg/dl	−6.17 ± 17.43	−3.83 ± 5.20	−7.17 ± 10.31	−1.45 ± 6.10
Total Cholesterol mg/dl	−25.67 ± 4.36	−26.73 ± 8.05	−33.67 ± 6.29	−27.09 ± 5.61
HDL mg/dl	−1.12 ± 0.54	−1.27 ± 0.81	−1.13 ± 1.03	−1.45 ± 0.79
LDL mg/dl	−19.47 ± 3.27	−24.36 ± 7.71	−32.40 ± 5.07	−25.30 ± 5.41
	Changes in the first month		**Changes in two months**	
B) OBESE	**LC-HS (N = 10)**	**Control (N = 10)**	**LC-HS (N = 10)**	**Control (N = 10)**
Anthropometric parameters				
Body weight	−2.14 ± 0.68	−2.13 ± 0.64	−4.68 ± 0.67*	−2.17 ± 0.95
Body mass index (BMI) kg/m^2	−0.85 ± 0.30	−0.84 ± 0.23	−1.85 ± 0.34	−0.84 ± 0.34
AC1 (cm)	−3.45 ± 1.15	−1.53 ± 0.45	−6.18 ± 1.16	−3.30 ± 1.49
AC2 (cm)	−3.10 ± 0.86	−1.80 ± 0.74	−5.80 ± 1.16	−5.70 ± 1.79
Triceps skinfold thickness (mm)	−1.71 ± 0.92	−1.68 ± 0.86	−3.29 ± 0.78	−2.38 ± 1.18
% Body fat (BF)	−0.69 ± 0.16	−0.49 ± 0.10	−1.30 ± 0.29	−0.81 ± 0.22
Vital signs				
Heart rate (BPM)	−4.05 ± 1.10	−0.50 ± 3.61	−8.00 ± 1.14*	−1.75 ± 2.09
Systolic BP mm Hg	−11.42 ± 2.46	−10.50 ± 7.46	−18.42 ± 3.95*	−13.50 ± 7.11
Diastolic BP mm Hg	−8.40 ± 2.61	−6.00 ± 4.38	−10.70 ± 1.51	−9.88 ± 6.97
Biochemical parameters				
Glucose mg/dl	−3.40 ± 4.82	−2.38 ± 2.03	−4.96 ± 3.00	−5.75 ± 1.65
Triglycerides mg/dl	−38.29 ± 27.44	−10.63 ± 17.58	−29.10 ± 26.86	9.37 ± 17.73
Total Cholesterol mg/dl	−15.60 ± 4.41	−19.25 ± 7.90	−20.57 ± 4.53	−14.00 ± 10.66
HDL mg/dl	−1.73 ± 0.62	−3.12 ± 1.89	−2.36 ± 0.73	−2.50 ± 1.88
LDL mg/dl	−15.70 ± 3.38	−15.88 ± 6.59	−25.50 ± 3.44	−14.50 ± 8.91

Table 2. Intergroup analysis of changes in anthropometric, vital signs and biochemical measurements after one and two months of dietary supplement use. Intergroup (vs control) statistical analysis is reported as follows: *$p < 0.05$; **$p < 0.01$; ***$p < 0.001$. Data are expressed as the mean ± se.

Discussion

Trial limitations. The limitations of the study may be related with the metabolic variability of the participants since some of them were pre- or post-menopausal women and this may play a role in adiposity and lipid management. However, a similar percentage of women ranged from 45 to 55 years was present in all groups and none of them reported taking hormone replacement therapy. Additional limitations corresponded to the low number of participants and the short time for intervention. Nevertheless, significant differences were observed in anthropometric and cardiovascular parameters when the two groups were compared at the end of the study.

Applicability of trial findings. Female participants in this study were recruited from a Nutrition and Dietetics Centre in a city of the Southeast of Spain. Then, we can state that the results are applicable to women in urban environments with similar life styles and eating habits. Last, since the results may also vary depending on the composition of the dietary supplement, the results of the present study would be only valid for the specific polyphenolic composition of the herbal extracts studied here.

Discussion of results. Obesity is defined as a condition of excessive accumulation of fat in adipose tissue that carries a health risk and predisposes to insulin resistance, hypertension and dyslipidemia. Despite the adverse

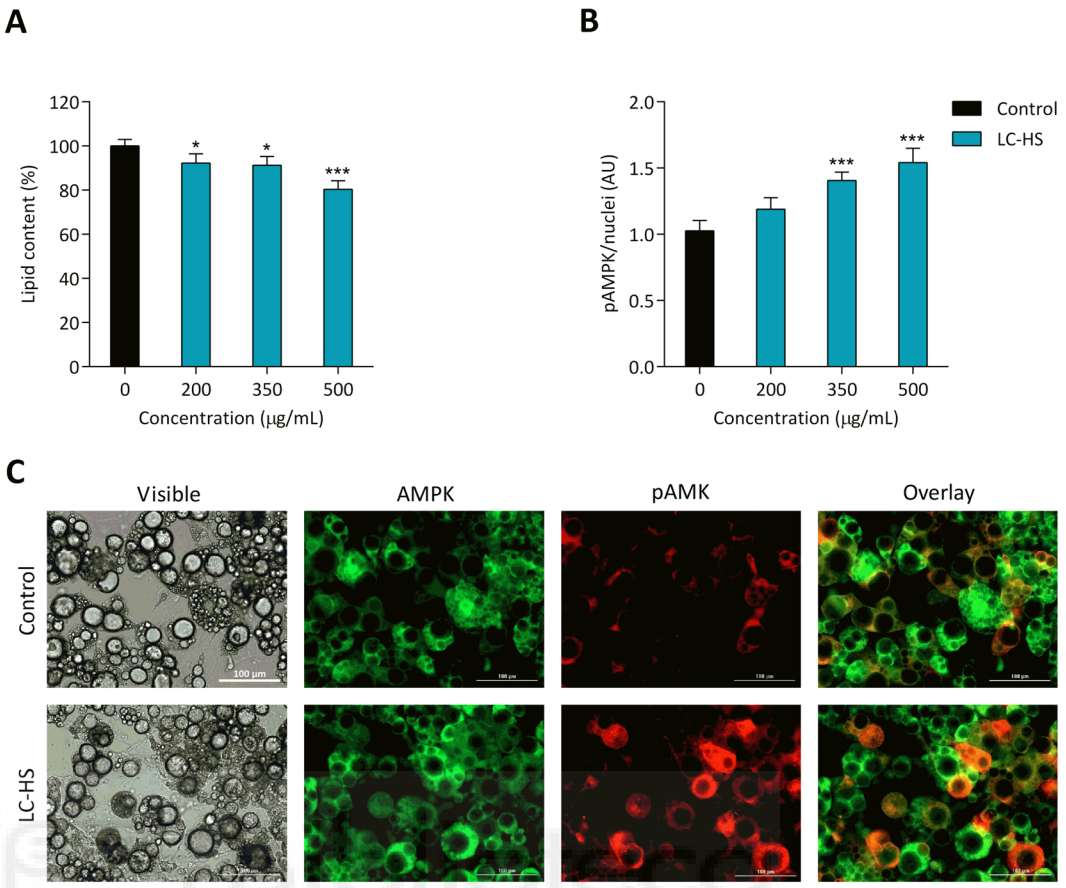

Figure 2. LC-HS combination decreases triglyceride accumulation and activates AMPK in hypertrophied 3T3-L1 adipocytes. Hypertrophied adipocytes were treated with a combination of the polyphenolic extracts, and triglyceride accumulation was monitored by AdipoRed staining as mentioned in the materials section (**A**). Hypertrophied adipocytes were treated with the same concentrations of the polyphenolic combination as in (**A**), and AMPK (non-active) and pAMPK (activated) kinases were quantitated by immunofluorescence microscopy (**B**). Representative photomicrographs of phase contrast, green fluorescence (AMPK), red fluorescence (pAMK) and overlay (**C**). The data are expressed as the mean ± S.D. from three independent experiments performed in octuplicate.

effects of obesity, weight loss can result in a significant reduction in the risk of most of these comorbid diseases[19]. Restricting caloric intake and increasing caloric expenditure via physical activity seem to be the only accepted ways to prevent development of obesity-associated disorders. Nevertheless, in many cases, these changes in lifestyle are not possible, being necessary to implement complementary therapeutical tools, such as bariatric surgery or the intake of dietary supplements containing polyphenolic extracts[20].

In this last context, we recently reported the capacities of LC polyphenolic extract and its major compound verbascoside to ameliorate high glucose-induced metabolic disturbances. These effects were mediated by the PPARγ-dependent transcriptional upregulation of adiponectin, the mRNA expression upregulation of PPAR-α and downregulation of FASN, in correlation to a potent activation of AMPK[16]. Experiments in a hyperlipidemic mice model suggested a significant improvement in fat metabolism (cholesterol and triglycerides), especially in the triglyceride clearance, but the glucose tolerance test was not affected.

In addition, HS polyphenols have been demonstrated to be particularly effective in decreasing inflammation linked to metabolic stress by the inhibition of leptin and MCP-1 secretions[3,9,14]. The polyphenolic HS extract also prevented hepatic steatosis in hyperlipidemic mice through the modulation of the expression of genes involved in glucose and lipid homeostasis. In animals fed a high fat diet, HS polyphenols attenuated the increase in blood glucose levels and the apparent increase in insulin resistance, as well as increased the respiratory quotients, which are closely related to the basal metabolic rate (BMR). A decrease in the expression of lipogenic genes, such as fatty acid synthase (FASN) and the sterol regulatory element-binding protein (Srebp-1c), concomitantly to the activation of hepatic AMPK, was also reported in this animal model[10]. AMPK activation is known to induce peroxisome proliferator-activated receptor γ coactivator 1α (PGC-1α) expression and directly enhances its activity through phosphorylation, which increases mitochondrial biogenesis and function[21]. These results note that the putative mechanism of HS polyphenols may be mediated by modulation of fat utilization, most likely by the inhibition of lipogenesis and activation of lipolysis, probably through enhancing mitochondrial biogenesis. All these

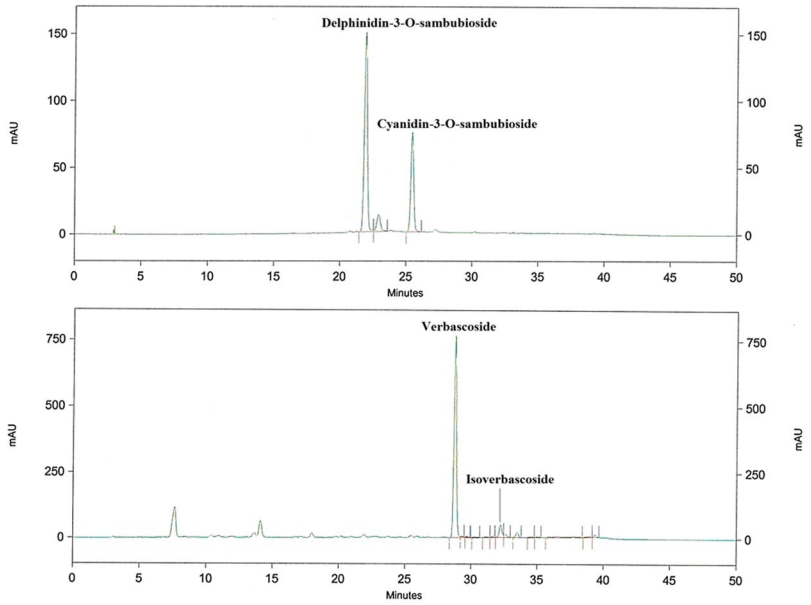

Figure 3. Representative HPLC chromatograms of the LC-HS combination at 320 nm for phenylpropanoids (upper panel) and 520 nm for anthocyanins (lower panel). Four compounds including delphinidin-3-O-sambubioside, cyanidin-3-O-sambubioside, verbascoside and isoverbascoside were determined by HPLC.

events resemble a metabolic situation that reflects high cellular energy demand and improved energy expenditure and probably a higher BMR.

Taking into account the common and complementary molecular targets reached by LC and HS polyphenols, we strongly considered the possibility to combine both extracts to test their role in the management of obesity-related disorders. First, previous *in vitro* and animal trials led us to establish the dose response behavior and the range of effective polyphenol concentrations. In the present work, the optimum proportion of LC and HS extracts was established based on the estimated daily intake of polyphenols derived from our previous human intervention studies using the extracts in a separate manner[11,14,22–24].

In spite of both control and experimental groups were taking an isocaloric diet, the results obtained in this study showed that the consumption of 500 mg per day of LC-HS for two months in overweight women significantly reduced body weight, abdominal circumference and percentage of body fat compared to the control group. A similar tendency was observed in obese volunteers consuming the polyphenolic extract, but results were in general less significant, indicating that the supplement was more effective when obesity changes had not been stablished.

Previous results from our laboratory indicate that control of appetite may be one of the candidate mechanisms by which LC-HS polyphenols may act[18]. The satiating effect was not strictly evaluated in the present report but monitoring of the volunteers revealed that LC-HS exerted a certain satiating effect. Our previous studies showed that HS extract reduced leptin levels in hypertrophic adipocytes[9]. In addition, the LC-HS polyphenolic extract increased anorexigenic (glucagon-like peptide -1) and decreased orexigenic (ghrelin) hormones. Aside from satiety, the same study opens the possibility that the extract could act in other body systems, such as the cardiovascular system and the adipose tissue, that have been addressed in the present report.

Regarding cardiovascular system, the consumption of LC-HS significantly decreased heart rate and systolic blood pressure compared to the control group, particularly in overweight participants. Traditionally, calyxes from *Hibiscus sabdariffa* have been used to treat hypertension, which is a risk factor of cardiovascular diseases. Animal and human studies have shown that consumption of HS extract reduces systolic and diastolic blood pressure[11,25]. Targeted training or endurance exercise promotes skeletal muscle to adapt to higher mitochondrial density and quality, increased oxygen availability and blood flow, as well as enlarged arteries[26], which turns to a lower resting heart rate and blood pressure and increased BMR. In a similar way, we hypothesize that LC-HS polyphenols may mimic the effects of endurance exercise on heart rate and blood pressure. In addition, an elevated resting heart rate is also one of the main predictors of cardiovascular mortality and it is associated with sudden cardiac death[27]. Natural agents able to reduce heart rate might become an important therapy in the prevention of sudden cardiac death. A reduction of heart rate has been observed after omega-3 fatty acids supplementation, and one of the mechanisms proposed is a direct effect on cardiac cell membrane electrical excitability[27]. However, the mechanism through which LC-HS reduces heart rate in overweight women is still unknown and deserves further attention. Finally, the selected participants presented moderate dyslipidemia (Table 1). Healthy obese people often exhibit this clinical phenotype[28]. Circulating LDL-cholesterol levels decrease in both groups, suggesting that the change to an equilibrated isocaloric diet could be the main responsible factor for this observation.

In the context of the adipose tissue, a previous report revealed that the decrease in body fat mass in the LC-HS group correlated with a reduction in circulating leptin levels compared to the control[18]. Our first interpretation

was based on the lipostatic role that leptin plays, otherwise said, the reduction in body fat mass may be accompanied by a decrease in leptin secretion by adipocytes, taking into account that we could not assess the presence of leptin resistance in participants. Since leptin is a hormone secreted by adipocytes, these results strongly suggest a direct action of LC-HS extract on adipocytes. This prompted us to gain more inside by preliminary exploring the possible molecular mechanisms through the use on the *in vitro* adipocyte model. Although cellular systems are limited for studying human diseases, the insulin resistant hypertrophied 3T3-L1 adipocytes induced by a high glucose concentration used in this study and others from our group, resemble the metabolic alterations associated with excessive food storage in adipose tissue of obese subjects[4,29–31] and provides a valid model to explore candidate molecular targets of LC-HS polyphenols[32,33].

Among the putative molecular targets, AMPK is proposed as one of the candidates to consider due to the previous results on the potential molecular complementary effects of HS and LC on lipid and glucose metabolism and the reported activation of AMPK by both polyphenolic extracts *in vitro*[9,16] and in hyperlipidemic mice[10,16,17]. The LC-HS polyphenolic extract resulted in a strong AMPK activation of approximately 1.5-fold compared with that of the control at the highest concentration utilized in hypertrophied 3T3-L1 adipocytes. AMPK activation has been shown to increase mitochondrial biogenesis and density, which in turns should result in an increase in the maximum metabolic rate (MMR), the basal metabolic rate (BMR), and exercise tolerance[34]. In fact, increased voluntary activity has been observed in mice artificially selected for a high BMR[35], whereas mice with impaired AMPK function had decreased voluntary activity[36], which suggests a direct link between the cellular energy state, BMR, and voluntary activity that is likely partly mediated by AMPK. The results obtained in obese rats using a synthetic estrogen have shown an increase in resting energy expenditure, through increased heat production and oxygen consumption and a reduced respiratory quotient in correlation with an induction of liver AMPK phosphorylation with a fatty acid utilization increase[37]. AMPK also enhances the metabolic rate by activating phosphofructokinase-2 (PFK2), a key bifunctional enzyme that regulates the rates of glycolysis and gluconeogenesis[38], by mimicking, in this way, starvation or low glucose conditions. Therefore, we hypothesize that AMPK activation by polyphenols may increase BMR and energy expenditure, leading to improved metabolic and anthropometric parameters, as reported for some alternative weight loss agents capable of increasing the basal metabolism and oxygen consumption[37,39,40]. Conceivably, dietary therapies with bioactive compounds potentially acting on protein kinase AMPK, such as some polyphenols, may have potential benefits in the amelioration of obesity-related diseases.

Interestingly, it is known that activation of AMPK in the hypothalamus enhances food intake and its inhibition by leptin decreases appetite[41]. It may be suggested that our polyphenolic extract might normalize leptin levels in adipose tissue, inhibiting AMPK in the hypothalamus and suppressing feeding behavior. Altogether, the satiating[18] and blood pressure normalization effects (this report) observed suggest that hypothalamus could be a key target organ for the action of the extract together with adipose tissue. Nevertheless, all these hypotheses require further investigation in the future by using animal models. On the basis of the potential activity observed for polyphenols in adipose tissue and liver, efforts to provide data on randomized control trials, as is the case of this study, deserve further consideration in the future.

In conclusion, our results show that the intake of LC-HS polyphenols for two months in overweight women decreased weight, improved anthropometric parameters, decreased systolic BP and heart beat and improved the blood lipid profile. However, changes were more modest in obese volunteers. Probably, more drastic changes in lifestyle or longer treatments should be carried out by obese subjects to achieve more consistent results. Therefore, the consumption of 500 mg/day of LC-HS, in combination with an isocaloric diet, may be considered as a dietary intervention for weight management and the prevention of metabolic syndrome, being AMPK one of the candidate molecular targets to explore in future research.

Materials and Methods

Chemicals and reagents. Dulbecco's modified Eagle's medium (DMEM), Dulbecco's phosphate buffered saline (PBS) and penicillin-streptomycin were purchased from Gibco (Grand Island, NY, USA). Dexamethasone (DEX), 3-isobutyl-1-methylxanthine (IBMX) and insulin were obtained from Sigma-Aldrich (Madrid, Spain). Calf serum (CS) and fetal bovine serum (FBS) were purchased from ThermoFisher Scientific (Cramlington, Northumberland, UK). Cellulose acetate filters (0.2 µm) were obtained from GE Healthcare Life Sciences (Buckinghamshire, UK). *Hibiscus sabdariffa* polyphenolic extract (10% anthocyanins, dry weight), *Lippia citriodora* polyphenolic extract (25% verbascoside, dry weight) and the combination of both extracts selected to be tested in the clinical trial (MetabolAid®) were kindly provided by Monteloeder, SL (Elche, Alicante, Spain).

Characterization of the dietary supplement by HPLC-DAD-ESI-IT-MS. The combination of polyphenolic extracts (LC-HS) was prepared by mixing LC and HS extracts at a weight ratio (w/w) of 65:35. MetabolAid® was provided by Monteloeder S.L. (Alicante, Spain) (Patent application number P201731147). The composition of the combination of extracts was identified and quantified by using an HPLC instrument (Agilent LC 214 1100 series; Agilent Technologies, Inc., Palo Alto, CA, USA) controlled by Chemstation software, as previously reported[9,42]. The HPLC instrument was coupled to an Esquire 3000 + (Bruker Daltonics, GmbH, Bremen, Germany) mass spectrometer equipped with an ESI source and ion trap mass analyzer and controlled by Esquire control and data analysis software. A Merck Lichrospher 100RP-18 (5 µm, 250 × 4 mm) column was used for analytical purposes. The main compounds were identified by HPLC-DAD analysis, comparing the retention time, UV spectra, and MS/MS data of the peaks in the samples with those of authentic standards or data reported in the literature.

Maintenance of the 3T3-L1 cell line and differentiation to hypertrophied adipocytes. The 3T3-L1 preadipocytes (American Type Culture Collection, Manassas, VA, USA) were cultured in low glucose (1 g/L) DMEM supplemented with 10% CS, 100 µg/mL streptomycin and 100 U/mL penicillin and incubated at 37 °C in a humidified (5% CO_2, 95% air) atmosphere. Differentiation from preadipocytes to adipocytes was induced by high glucose (4.5 g/L) DMEM supplemented with 10% FBS, 1 µM insulin, 1 µM DEX and 0.5 mM IBMX for 48 h. Then, cells were maintained in high glucose DMEM with FBS and insulin, and the medium was replaced every 2 days obtaining hypertrophied adipocytes after 20 days of incubation, a well-established insulin resistant adipocyte model bearing metabolic stress[4,16]. Once hypertrophied adipocytes were obtained, cells were treated with LC-HS extract at several concentrations for 72 h. For cell treatment, the extract was dissolved in medium and filtered for sterilization.

Evaluation of lipid content by AdipoRed. Lipid content of hypertrophied adipocytes was assessed using AdipoRed™ Reagent (Lonza, Walkersville, MD, USA). Briefly, supernatant was removed from the cells, and the cells were then washed carefully with PBS. Next, AdipoRed was added and incubated for 15 minutes at room temperature. Triglyceride accumulation was measured using a fluorescence microplate reader (POLARstar, Omega, BMG LABTECH) at 485 nm excitation and 572 nm emission.

Determination of activation of AMPK by immunofluorescence. To study the activation of AMPK in hypertrophied adipocytes, AMPK phosphorylated in Thr172 (pAMPK) was quantified with an immunofluorescence assay. Cells were fixed with a fixation buffer (Cytofix™, BD Biosciences, Europe), permeabilized with 0.3% Triton X-100 (Sigma-Aldrich, Spain) and blocked with 4% goat serum (Sigma-Aldrich). Then, cells were incubated overnight at 4 °C with mouse monoclonal AMPK alpha 1 + AMPK alpha 2 antibodies (Abcam, Cambridge, UK) and rabbit monoclonal phospho-AMPKα (Thr172; Cell Signalling Technology, Danvers, MA, USA). After incubation with primary antibodies, cells were washed with PBS and incubated for 6 h at room temperature together with each corresponding polyclonal secondary antibody, goat anti-rabbit IgG CF™ 594 and anti-mouse-FITC, all from Sigma-Aldrich (St. Louis, MO, USA). Fluorescence from cells was measured using a cell imaging multi-mode microplate reader (Cytation 3, Biotek, Spain) at 593 nm excitation and 614 nm emission for pAMPK levels and 490 nm excitation and 520 nm emission for AMPK levels. Activation of AMPK was expressed as levels of AMPK normalized to total AMPK (pAMPK/AMPK). Microphotographs of pAMPK and AMPK were taken at 20x.

Study design and study population. The study was an 8-week, randomized, double-blind, placebo-controlled trial. The study participants were recruited during 2015 from the city of Elche, Alicante, Spain. Before participation in the study, subjects were informed by the investigators about the purpose and the study procedures. All subjects provided written informed consent (ICF) before entering the study and the Ethical Committee of the Miguel Hernández University of Elche approved the study protocol (reference IB.ER.01.15). The study was conducted in accord with the Helsinki Declaration (1983 version). During the enrollment period, 82 prospective overweight volunteers were recruited at the pharmacy in March 2015.

Exclusion criteria included total cholesterol lower than 200 mg/dL, presence of any obesity-related pathology, use of prescription medication for cholesterol or hypertension, hormone replacement therapy, consumption of antioxidant supplements/drugs, alcohol addiction and women who were pregnant or lactating.

Based on the above criteria, fifty-five healthy women, aged 36–69 years old, with a body mass index (BMI) from 24 to 34 kg/m^2 passed a telephone-based health screening and interview as well as the biochemical and anthropometrical evaluation. After recruitment, the subjects were randomly assigned into the control (N = 26) or experimental group (N = 29) in a 1:1 ratio for BMI using an Excel program by the research team. Participants (identified by a code) and researchers responsible for the follow-up were blinded. During the study (April-July 2015), 9 volunteers dropped out, 6 in the control and 3 in the intervention group, and a total of 46 volunteers completed the study (control, N = 20 and intervention, N = 26) (Fig. 1).

The control group (mean age 51) received two capsules of placebo (400 mg of crystalline microcellulose each), and the treatment group (mean age 52) received two capsules, each one containing 250 mg of LC-HS and 150 mg excipients (crystalline microcellulose). Composition of capsules was established based in previous studies performed in humans[11,14,22,24]. The capsules were made to have the same size, same odor and same color (red capsule), both for LC-HS and placebo. After overnight fasting, volunteers were instructed to take two capsules 20–30 minutes prior to breakfast every day for two months. During the screening visit, demographic and lifestyle information was collected (age, dietary and physical habits, alcohol consumption and smoking habits).

Women were instructed by a qualified dietician to follow an isocaloric and balanced diet of 2,200 kcal. At baseline, all participants completed a validated semiquantitative food frequency questionnaire[43]. The questionnaire included 22 items, among others, grains, pulses, meat, eggs, seafood, dairy products, fruits, vegetables, processed foods, snacks high in fat and sugar and beverages. For each item, participants could select from 3 frequency categories (daily, weekly or monthly) and the number of servings from each food category. Besides, throughout both the pre and post-intervention survey, a 15-min interview, adapted from a validated questionnaire was conducted with each participant to gather information for a 24 h diet recall[43]. Participants in both groups (dietary supplement and placebo) were given personalized advice for dietary changes at achieving a diet as close as possible to isocaloric and balanced diet with normal hydration. During the meeting, women were also asked about daily physical activity. All declared to be absolutely sedentary. Therefore, they were advised walking for at least half an hour per day. Trained dieticians were responsible for all aspects of the intervention. Compliance of the subjects with the ingestion of capsules, diet and exercise was assessed at each visit or by phone every week during the 2 months of study, estimated as a reasonable time to observe anthropometric changes in participants[44]. Measurements were taken before and after 30 and 60 days of the study. Before analysis (Tables 1 and 2), data were

stratified in four groups: overweight and obese control, and overweight and obese volunteers consuming the polyphenolic extract.

Efficacy outcomes. The efficacy outcome measurements were taken at baseline and after 30 and 60 days of the intervention period. Moreover, during each visit, symptoms or side effects were recorded.

The main objective of the study was to assess the effect of taking LC-HS extracts on changes in anthropometric and circulating parameters in volunteers. To this end, the following parameters were assessed. Anthropometric measurements included body weight, height, triceps skinfold thickness and abdominal circumference (AC) measured at two different sites: anteriorly midway between the xiphoid process of the sternum and the umbilicus and laterally between the lower end of the rib cage and iliac crests (AC1) and at umbilicus level (AC2). A scale with a height measuring rod was used for the measurement of body weight and height. Body mass index (BMI) was derived from body weight and height using the equation BMI = body weight (kg)/height^2 (m). Triceps skinfold thickness was measured using a skinfold caliper, and AC1 and AC2 were measured using a tape measure. Percentage of body fat (% BF) was calculated from the weight, height and abdominal circumference (AC1 and AC2) using the Weltman equation for obese women[41]. Fasting blood was collected to determine total glucose and glycosylated hemoglobin (HbA1c) and the lipid profile, which included triglycerides, total cholesterol, high-density lipoprotein (HDL) and low-density lipoprotein (LDL)-cholesterol. Blood was also analyzed for safety parameters, hematology, electrolytes (Na, K), creatinine, urea, uric acid, glutamic-pyruvic transaminase (GPT), glutamic-oxaloacetic transaminase (GOT) and C-reactive protein.

Furthermore, the secondary objective of the study was to assess the effect of taking LC-HS extracts on changes in blood pressure in volunteers. To this end, systolic (SBP) and diastolic blood pressure (DBP) and heart beat were measured at rest at the beginning and at 30 and 60 days after the intervention using an Omron HEM-7320-LA oscillometric blood pressure monitor (Omron Healthcare Co. Ltd, Kyoto, Japan) at the upper arm with a large cuff. Five independent measurements for SBP, DBP and heart rate were taken using a validated protocol[45].

Theoretical estimation of sample size. Theoretical estimation of sample size was essentially as previously described[18]. This allowed to estimate a minimum sample size of around 17 women per group in order to detect significant changes in body composition.

Stopping guidelines. Participants compliance and retention was esentially as described previously[18]. The following reasons were considered for the exclusion of the participants after being included in the trial: personal conflict (n = 2 in control and n = 1 in LC-HS group), protocol violations (n = 2 in control), accident (n = 1 in control), medication intake (n = 1 in control), pathology (n = 1 in LC-HS group) and pregnancy (n = 1 in LC-HS group).

Statistical analysis. Clinical statistical analyses were performed with a Student's t-test using Graphpad Prism software. Outcome variables were assessed for conformance to the normal distribution and Kolmogorov-Smirnov test was utilized for transformation when needed. Data are reported as the mean ± se (standard error of the mean). Reported *p*-values were two-sided and a P-value of 0.05 or less was considered statistically significant for between-group comparisons. Comparisons were established between the control and the LC-HS groups by unpaired Student's t-test. By contrast, intra-group statistical analysis at the endpoint was compared to the baseline and analyzed by paired Student's t-test. Statistically significant differences throughout the study were expressed as $*p < 0.05$; $**p < 0.01$, $***p < 0.001$.

The results of an AdipoRed assay and immunofluorescence assay were represented using Graphpad Prism software and are expressed as the mean ± standard deviation. The parameters studied were compared to controls and analyzed using a one-way ANOVA and Tukey's test for multiple comparisons.

References

1. Lim, J. *et al*. Diet-induced obesity, adipose inflammation, and metabolic dysfunction correlating with PAR2 expression are attenuated by PAR2 antagonism. *FASEB J.* **27**, 4757–67 (2013).
2. Iyer, A. *et al*. Inflammatory lipid mediators in adipocyte function and obesity. *Nat. Rev. Endocrinol.* **6**, 71–82 (2010).
3. Furukawa, S. *et al*. Increased oxidative stress in obesity and its impact on metabolic syndrome. *J. Clin. Invest.* **114**, 1752–61 (2004).
4. Yeop Han *et al*. Differential effect of saturated and unsaturated free fatty acids on the generation of monocyte adhesion and chemotactic factors by adipocytes: dissociation of adipocyte hypertrophy from inflammation. *Diabetes* **59**, 386–96 (2010).
5. Barrajón-Catalán, E. *et al*. Molecular promiscuity of plant polyphenols in the management of age-related diseases: Far beyond their antioxidant properties. *Adv. Exp. Med. Biol.* **824**, 141–159 (2014).
6. J Joven, J. *et al*. Multifunctional targets of dietary polyphenols in disease: a case for the chemokine network and energy metabolism. *Food Chem. Toxicol.* **51**, 267–79 (2013).
7. Carling, D. AMPK signalling in health and disease. *Curr. Opin. Cell Biol.* **45**, 31–37 (2017).
8. Shirwany, N. A. & Zou, M. H. AMPK: a cellular metabolic and redox sensor. A minireview. *Front. Biosci. (Landmark Ed)* **19**, 447–74 (2014).
9. Herranz-Lopez, M. *et al*. Synergism of plant-derived polyphenols in adipogenesis: perspectives and implications. *Phytomedicine* **19**, 253–261 (2012).
10. Joven, J. *et al*. Plant-derived polyphenols regulate expression of miRNA paralogs miR-103/107 and miR-122 and prevent diet-induced fatty liver disease in hyperlipidemic mice. *Biochim. Biophys. Acta* **1820**, 894–9 (2012).
11. Joven, J. *et al*. *Hibiscus sabdariffa* extract lowers blood pressure and improves endothelial function. *Mol. Nutr. Food Res.* **58**, 1374–1378 (2014).
12. Fernandez-Arroyo, S. *et al*. Bioavailability study of a polyphenol-enriched extract from Hibiscus sabdariffa in rats and associated antioxidant status. *Mol. Nutr. Food Res.* **56**, 1590–1595 (2012).
13. Olivares-Vicente, M. *et al*. Plant-derived polyphenols in human health: biological activity, metabolites and putative molecular targets. *Curr. Drug Metab.* **19**, 351–369 (2018).

14. Beltran-Debon, R. *et al*. The aqueous extract of *Hibiscus sabdariffa* calices modulates the production of monocyte chemoattractant protein-1 in humans. *Phytomedicine* **17**, 186–191 (2010).
15. Herranz-Lopez, M. *et al*. Correlation between the cellular metabolism of quercetin and its glucuronide metabolite and oxidative stress in hypertrophied 3T3-L1 adipocytes. *Phytomedicine* **25**, 25–28 (2017).
16. Herranz-Lopez, M. *et al*. Lemon verbena (*Lippia citriodora*) polyphenols alleviate obesity-related disturbances in hypertrophic adipocytes through AMPK-dependent mechanisms. *Phytomedicine* **22**, 605–614 (2015).
17. Lee, Y. S. *et al*. Metabolaid® Combination of Lemon Verbena and Hibiscus Flower Extract Prevents High-Fat Diet-Induced Obesity through AMP-Activated Protein Kinase Activation. *Nutrients* **10**, 1204 (2018).
18. Boix-Castejon, M. *et al*. Hibiscus and lemon verbena polyphenols modulate appetite-related biomarkers in overweight subjects: a randomized controlled trial. *Food Funct.* **9**, 3173–3184 (2018).
19. O'Neill, S. & O'Driscoll, L. Metabolic syndrome: a closer look at the growing epidemic and its associated pathologies. *Obes. Rev.* **16**, 1–12 (2015).
20. Kim, J. *et al*. AMPK activators: mechanisms of action and physiological activities. *Exp. Mol. Med.* **48**, e224 (2016).
21. Fernandez-Marcos, P. J. & Auwerx, J. Regulation of PGC-1alpha, a nodal regulator of mitochondrial biogenesis. *Am. J. Clin. Nutr.* **93**, 884S–890 (2011).
22. Carrera-Quintanar, L. *et al*. Antioxidant effect of lemon verbena extracts in lymphocytes of university students performing aerobic training program. *Scand. J. Med. Sci. Sports* **22**, 454–461 (2012).
23. Carrera-Quintanar, L. *et al*. Effect of polyphenol supplements on redox status of blood cells: a randomized controlled exercise training trial. *Eur. J. Nutr.* **54**, 1081–1093 (2015).
24. Funes, L. *et al*. Effect of lemon verbena supplementation on muscular damage markers, proinflammatory cytokines release and neutrophils' oxidative stress in chronic exercise. *Eur. J. Appl. Physiol.* **111**, 695–705 (2011).
25. Hopkins, A. L. *et al*. *Hibiscus sabdariffa* L. in the treatment of hypertension and hyperlipidemia: a comprehensive review of animal and human studies. *Fitoterapia* **85**, 84–94 (2013).
26. Booth, F. W. *et al*. Endurance Exercise and the Regulation of Skeletal Muscle Metabolism. *Prog. Mol. Biol. Transl. Sci.* **135**, 129–151 (2015).
27. Kang, J. X. Reduction of heart rate by omega-3 fatty acids and the potential underlying mechanisms. *Front. Physiol.* **3**, 416 (2012).
28. Wang, H. & Peng, D.-Q. New insights into the mechanism of low high-density lipoprotein cholesterol in obesity. *Lipids Health Dis.* **10**, 176 (2011).
29. Yu, Y. H. & Zhu, H. Chronological changes in metabolism and functions of cultured adipocytes: a hypothesis for cell aging in mature adipocytes. *Am. J. Physiol. Endocrinol. Metab.* **286**, E402–410 (2004).
30. Jernås, M. *et al*. Separation of human adipocytes by size: hypertrophic fat cells display distinct gene expression. *FASEB J.* **20**, 1540–1542 (2006).
31. Takahashi, K. *et al*. JNK- and IκB-dependent pathways regulate MCP-1 but not adiponectin release from artificially hypertrophied 3T3-L1 adipocytes preloaded with palmitate *in vitro*. *Am. J. Physiol. Endocrinol. Metab.* **294**, E898–E909 (2008).
32. Zebisch, K. *et al*. Protocol for effective differentiation of 3T3-L1 cells to adipocytes. *Anal. Biochem.* **425**, 88–90 (2012).
33. Ji, E. *et al*. Inhibition of adipogenesis in 3T3-L1 cells and suppression of abdominal fat accumulation in high-fat diet-feeding C57BL/6J mice after downregulation of hyaluronic acid. *Int. J. Obes.* **38**(8), 1035–43 (2013).
34. Ross, T. T. *et al*. beta-GPA treatment leads to elevated basal metabolic rate and enhanced hypoxic exercise tolerance in mice. *Physiol. Rep.* **5** (2017).
35. Gebczynski, A. K. & Konarzewski, M. Locomotor activity of mice divergently selected for basal metabolic rate: a test of hypotheses on the evolution of endothermy. *J. Evol. Biol.* **22**, 1212–1220 (2009).
36. Thomson, D. M. *et al*. Skeletal muscle and heart LKB1 deficiency causes decreased voluntary running and reduced muscle mitochondrial marker enzyme expression in mice. *Am. J. Physiol. Endocrinol. Metab.* **292**, E196–202 (2007).
37. Banz, W. J. *et al*. (+)-z-bisdehydrodoisynolic Acid enhances Basal metabolism and Fatty Acid oxidation in female obese zucker rats. *J. Obes.* **2012** (2012).
38. Chaube, B. *et al*. AMPK maintains energy homeostasis and survival in cancer cells via regulating p38/PGC-1alpha-mediated mitochondrial biogenesis. *Cell Death Discov.* **1**, 15063 (2015).
39. Tomas, E. *et al*. GLP-1(32-36)amide Pentapeptide Increases Basal Energy Expenditure and Inhibits Weight Gain in Obese Mice. *Diabetes* **64**, 2409–2419 (2015).
40. Dal-Pan, A., Blanc, S. & Aujard, F. Resveratrol suppresses body mass gain in a seasonal non-human primate model of obesity. *BMC Physiol.* **10**, 11–11 (2010).
41. Weltman, A. *et al*. Accurate assessment of body composition in obese females. *Am. J. Clin. Nutr.* **48**, 1179–1183 (1988).
42. Ahmad-Qasem, M. H. *et al*. Influence of olive leaf processing on the bioaccessibility of bioactive polyphenols. *J. Agric. Food Chem.* **62**, 6190–6198 (2014).
43. Martin-Moreno, J. M. *et al*. Development and validation of a food frequency questionnaire in Spain. *Int. J. Epidemiol.* **22**, 512–519 (1993).
44. Lasa, A. *et al*. Comparative effect of two Mediterranean diets versus a low-fat diet on glycaemic control in individuals with type 2 diabetes. *Eur. J. Clin. Nutr.* **68**, 767–772 (2014).
45. Grover-Paez, F. *et al*. Validation of the Omron HEM-7320-LA, upper arm blood pressure monitor with Intelli Wrap Technology Cuff HEM-FL1 for self-measurement and clinic use according to the European Society of Hypertension International Protocol revision 2010 in the Mexican population. *Blood Press. Monit.* **22**, 375–378 (2017).

Acknowledgements

We thank grants AGL2015-67995-C3-1-R from the Spanish Ministry of Economy and Competitiveness (MINECO); PROMETEO/2016/006, APOSTD/2017/023 and ACIF/2016/230 from Generalitat Valenciana; CIBER (CB12/03/30038, Fisiopatologia de la Obesidad y la Nutricion, CIBERobn, Instituto de Salud Carlos III). We also thank SME instrument phase 1 EU funding for grant INNOPREFAT 683933 (H2020-SMEINST-1-2015_18-03-2015) and H2020 SME Phase II project, grant number 783838.

Author Contributions

All authors have approved the submitted version of the manuscript. V.M., M.H., N.C. and E.R. conceived and designed the experiments and the formulation; M.H., M.O. and M.B. participated in the acquisition, analysis and interpretation of data. V.M., M.H. and E.R. wrote and reviewed the manuscript. V.M. is the guarantor for this article and takes responsibility for the integrity of the work as a whole. N.C. works for Monteloeder S.L.

Additional Information

Supplementary information accompanies this paper at https://doi.org/10.1038/s41598-019-39159-5.

Competing Interests: This study was partially funded by Monteloeder S.L. Monteloeder was involved in the design of the study protocol and provided the test products samples. Employees of the sponsor were not involved in data analysis. The manuscript was prepared by V.M., E.R. and M.H. Monteloeder was permitted to review the manuscript and suggest changes, but the final decision on content was exclusively retained by the corresponding author.

CAPÍTULO 5

Current Drug Metabolism, 2018, 19, 351-369

Plant-derived polyphenols in human health: Biological activity, metabolites and putative molecular targets

Mariló Olivares-Vicente, Enrique Barrajón-Catalán, María Herranz-López, Antonio Segura-Carretero, Jorge Joven, José Antonio Encinar, Vicente Micol.

DOI:10.2174/1389200219666180220095236

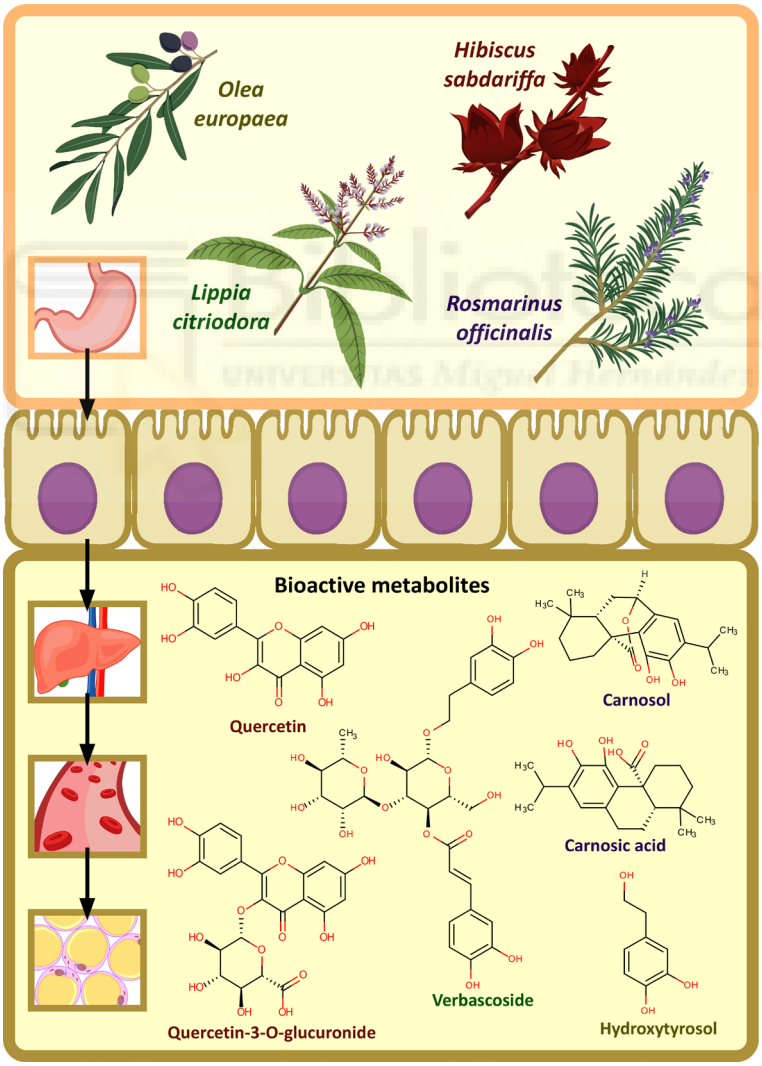

RESUMEN DE LOS RESULTADOS

El capítulo 5 corresponde a un artículo de revisión en el que se ofrece una visión general y actualizada de los estudios *in vitro* e *in vivo* sobre la bioactividad, la absorción intestinal, la biotransformación, la biodisponibilidad y la toxicidad de los compuestos bioactivos presentes en HS, LC, *Rosmarinus officinalis* (romero) y OL. A pesar de que la actividad biológica de estas cuatro plantas y sus compuestos ha sido ampliamente constatada mediante estudios en modelos celulares y animales, el conocimiento sobre los datos farmacológicos en humanos y el perfil farmacocinético y toxicológico de estos extractos es limitado.

El extracto acuoso de HS es rico en ácidos orgánicos, derivados de ácidos fenólicos y flavonoles, fenilpropanoides y antocianinas [77]. No obstante, se ha demostrado que la actividad biológica de HS se ve potenciada por el enriquecimiento del extracto en su contenido polifenólico [55]. Numerosos estudios han confirmado los efectos beneficiosos de HS. La mayoría de estos efectos parecen estar mediados por la potente capacidad antioxidante de sus compuestos bioactivos, actuando como secuestradores de ERO y aumentando la actividad y expresión de enzimas antioxidantes [55, 78]. Asimismo, HS también presenta propiedades antiinflamatorias, reduciendo la secreción de citoquinas proinflamatorias en adipocitos [55]. Cabe destacar el importante papel de HS como agente antihipertensivo en pacientes con síndrome metabólico e hipertensión [110], así como el efecto "anti-obesidad" del extracto polifenólico en adipocitos hipertróficos [55] y en ratones hiperlipidémicos [87]. En este último estudio, se evidenció que el extracto puede mediar sus efectos antilipogénicos a través de cambios en la expresión de miRNAs y genes lipogénicos y la activación de AMPK.

A pesar de que las antocianinas son los polifenoles más abundantes en HS, tienen una baja absorción y biodisponibilidad. Por ello, se postula que la presencia de otros compuestos minoritarios pueda contribuir a la bioactividad del extracto. Entre los compuestos propuestos, se encuentran la quercetina y sus derivados, que demostraron una mayor presencia en el plasma de ratas alimentadas con el extracto polifenólico de HS (especialmente sus formas glucuronidadas) [98]. Concretamente, el metabolito quercetina-3-glucurónido ha sido detectado en el hígado y en las células inmunes que rodean los hepatocitos de ratones hiperlipidémicos alimentados con el extracto polifenólico, los cuales mostraron una mejora de la esteatosis hepática [87]. Por otro lado, un estudio de permeabilidad intestinal en células Caco-2 reveló que unos pocos compuestos presentes en el extracto, como la quercetina y la *N*-feruloil-tiramina, son capaces de atravesar la monocapa celular, probablemente por difusión pasiva [111]. En dicho estudio, el análisis de

permeabilidad con compuestos puros sugirió la existencia de un mecanismo de transporte hacia el lumen intestinal, lo que daría lugar a una disminución de la absorción neta de los compuestos de HS.

El extracto de LC está compuesto mayoritariamente por fenilpropanoides, siendo el verbascósido el más abundante y al que se le atribuyen las propiedades antioxidantes de esta planta [79, 112]. Asimismo, otra clase importante de polifenoles en LC son las flavonas, especialmente presentes en sus formas glucuronidadas, y los iridoides glicósidos [113]. Recientemente, se ha demostrado la capacidad de su principal componente, el verbascósido, y del extracto de LC de reducir el estrés metabólico en adipocitos hipertróficos y mejorar el perfil lipídico en ratones hiperlipidémicos [86]. Se postula que tales efectos puedan estar mediados por mecanismos dependientes de AMPK. No obstante, se ha propuesto que el verbascósido no es el único compuesto responsable de los efectos de LC. Un estudio de biodisponibilidad identificó este polifenol y su isómero isoverbascósido como los principales metabolitos en el plasma de ratas que ingirieron una dosis aguda de extracto de LC [114]. Además, en dicho estudio se identificaron otros metabolitos minoritarios. Entre ellos, compuestos fenólicos derivados probablemente de la hidrólisis del verbascósido, como el hidroxitirosol, el ácido cafeico, el ácido ferúlico o el ácido homoprotocatecuico; o flavonas como acacetina diacetato y los diglucurónidos de luteolina y crisoeriol procedentes probablemente de las biotransformaciones de fase II de las flavonas presentes en LC. Asimismo, otros compuestos como el gardósido, cistanósido F, entre otros, fueron detectados en pequeñas cantidades en sus formas nativas. Estos resultados indicaron que el verbascósido, el isoverbáscósido y otros compuestos de LC son absorbidos y metabolizados, alcanzando el torrente sanguíneo y ejerciendo una respuesta antioxidante en células sanguíneas.

El romero es rico en diterpenoides como el ácido carnósico y sus derivados, triterpenos como el ácido ursólico y el ácido betulínico, ácidos fenólicos como el ácido rosmarínico, y varios flavonoides como apigenina o diosmetina [115]. El extracto de romero ha sido descrito fundamentalmente por su capacidad antioxidante [116] y por ejercer un importante papel anti-proliferativo en diferentes tipos de células tumorales [117], propiedades principalmente atribuidas a los diterpenos como el ácido carnósico y el carnosol y ácidos fenólicos como el ácido rosmarínico. No obstante, se desconocen los procesos farmacocinéticos que pueden sufrir los compuestos del romero *in vivo* y los metabolitos responsables de su bioactividad. Un estudio realizado en ratas alimentadas con un extracto de romero enriquecido en ácido carnósico identificó un total de 26 compuestos en muestras de distintos tejidos, incluyendo el plasma y la barrera intestinal [118]. Entre

ellos, carnosol, ácido carnósico, rosmanol, epirosmanol y su isómero y ácido rosmarínico. La mayoría de los metabolitos fueron detectados en el hígado y el lumen, indicando que la glucuronidación es la principal forma de conjugación. Por otro lado, estudios de permeabilidad en células Caco-2 indican que la mayoría de los compuestos bioactivos del romero son pobremente absorbidos y, fundamentalmente, se absorben por difusión pasiva [119].

El extracto de OL se compone fundamentalmente de secoiridoides como la oleuropeína, flavonoides como derivados de luteolina y apigenina y fenoles simples como hidroxitirosol [97]. Existen numerosas evidencias que demuestran las propiedades beneficiosas del aceite de oliva. Sin embargo, las hojas, que son ricas en polifenoles, han sido menos estudiadas. Ciertos estudios han atribuido importantes propiedades antioxidantes, antitumorales, antimicrobianas, entre otras, al extracto de OL y, especialmente, a su principal componente oleuropeína. Recientemente, se ha demostrado la capacidad del extracto de OL de activar AMPK y reducir la acumulación de triglicéridos en adipocitos hipertróficos, señalando la posible implicación de otros polifenoles del extracto de OL en la obesidad [120]. A pesar de estas evidencias, los datos sobre el metabolismo y biodisponibilidad de los compuestos de OL son escasos. Dada la diferente composición, el comportamiento farmacocinético de los compuestos bioactivos de OL puede diferir de los presentes en el aceite. Estudios en humanos indican que los principales metabolitos que alcanzan el torrente sanguíneo tras la ingesta de OL son derivados del hidroxitirosol (fundamentalmente glucuronidados y sulfatados), algunos derivados de la oleuropeína aglicona y metabolitos del ácido homovanílico [121, 122]. Estos resultados indican que los polifenoles de OL se absorben rápidamente y son altamente biostransformados, especialmente el hidroxitirosol y la oleuropeína, rindiendo metabolitos glucuronidados.

Current Drug Metabolism, 2018, *19*, 351-369

REVIEW ARTICLE

Plant-Derived Polyphenols in Human Health: Biological Activity, Metabolites and Putative Molecular Targets

Mariló Olivares-Vicente[1], Enrique Barrajón-Catalán[1,*], María Herranz-López[1], Antonio Segura-Carretero[2,3], Jorge Joven[4], José Antonio Encinar[1] and Vicente Micol[1,5]

[1]Instituto de Biología Molecular y Celular (IBMC), Universidad Miguel Hernández (UMH), Alicante, Spain; [2]Department of Analytical Chemistry, University of Granada, Granada, Spain; [3]Research and Development of Functional Food Centre (CIDAF), PTS Granada, Granada, Spain; [4]Unitat de Recerca Biomèdica, Hospital Universitari Sant Joan, Institut d'Investigació Sanitària Pere Virgili, Universitat Rovira i Virgili, Reus, Spain; [5]CIBER: CB12/03/30038, Fisiopatología de la Obesidad y la Nutrición, CIBERobn, Instituto de Salud Carlos III (ISCIII), Madrid, Spain

Abstract: ***Background:*** *Hibiscus sabdariffa*, *Lippia citriodora*, *Rosmarinus officinalis* and *Olea europaea*, are rich in bioactive compounds that represent most of the phenolic compounds' families and have exhibited potential benefits in human health. These plants have been used in folk medicine for their potential therapeutic properties in human chronic diseases. Recent evidence leads to postulate that polyphenols may account for such effects. Nevertheless, the compounds or metabolites that are responsible for reaching the molecular targets are unknown.

Objective: data based on studies directly using complex extracts on cellular models, without considering metabolic aspects, have limited applicability. In contrast, studies exploring the absorption process, metabolites in the blood circulation and tissues have become essential to identify the intracellular final effectors that are responsible for extracts bioactivity. Once the cellular metabolites are identified using high-resolution mass spectrometry, docking techniques suppose a unique tool for virtually screening a large number of compounds on selected targets in order to elucidate their potential mechanisms.

Results: we provide an updated overview of the *in vitro* and *in vivo* studies on the toxicity, absorption, permeability, pharmacokinetics and cellular metabolism of bioactive compounds derived from the abovementioned plants to identify the potential compounds that are responsible for the observed health effects.

Conclusion: we propose the use of targeted metabolomics followed by *in silico* studies to virtually screen identified metabolites on selected protein targets, in combination with the use of the candidate metabolites in cellular models, as the methods of choice for elucidating the molecular mechanisms of these compounds.

ARTICLE HISTORY

Received: September 05, 2017
Revised: December 07, 2017
Accepted: January 13, 2018

DOI:
10.2174/1389200219666180220095236

Keywords: Polyphenols, metabolites, molecular docking, *Hibiscus sabdariffa*, *Lippia citriodora*, *Rosmarinus officinalis*, *Olea europaea*.

1. INTRODUCTION

The interest in dietary polyphenols has increased over the past 10 years due to their large abundance in plants and fruits and their multiple beneficial properties for human health. These molecules are synthetized by plants as secondary metabolites and are involved in diverse functions, such as growth, lignification and structure, pigmentation, pollination or defense against pathogens, predators and ultraviolet radiation [1, 2]. These compounds are structurally characterized by the presence of one (phenol) or more (polyphenol) hydroxyl substituents and can be classified into different groups, depending on their carbon skeleton: phenolic acids, flavonoids, stilbenes and lignans. Flavonoids are the most abundant polyphenols in diet and can be divided into flavonols, flavones, isoflavones, flavanones, anthocyanidins and flavanols. The complexity of polyphenols increases since these compounds can be associated with several carbohydrates or organic acids and with other polyphenols, which widely increases their diversity and their ability to reach multiple molecular targets [3-5].

Plant-derived polyphenols have been found to possess antitumor, antimicrobial, antiviral, anti-inflammatory, antiatherogenic, antihypertensive, anti lipogenic and antioxidant activities [6-13]. Over the last decades, polyphenols have been widely designated as strong antioxidant agents, and it has been considered that the supported biological effects are derived from this antioxidant capacity [12]. Recently, a new perspective is emerging, as polyphenols have exhibited a pleiotropic character, so there is an increasing consideration of polyphenols in the prevention and treatment of multifactorial diseases, such as cancer or obesity-related pathologies [14].

Although pharmacological potency strongly influences the *in vivo* activity, polyphenols biological activity (efficacy) depend not only on their potency but also on their bioavailability. Some polyphenols are rapidly absorbed by the gut barrier and reach the circulating plasma in their native form, while others are poorly absorbed and may be highly metabolized or rapidly excreted. Accordingly, the metabolites that reach the circulating blood and target tissues may differ from their native forms and the gastrointestinal tract plays a crucial role in this. These compounds may be first hydrolyzed by gastric fluid in the stomach and later metabolized by the enzymes of intestinal cells or catabolized by the colonic microflora, which may drastically affect the absorption of these molecules through the gut barrier (Fig. **1**). In addition, polyphenols may also undergo important Phase I and Phase II reactions in the liver, promoting their excretion through urine or bile and reducing their bioavailability. The most frequent conjugation reactions are methylation, sulfation and glucuronidation. In the

*Address correspondence to this author at the Instituto de Biología Molecular y Celular (IBMC), Universidad Miguel Hernández (UMH), Alicante, Spain; Tel/Fax: 965222586; E-mail: e.barrajon@umh.esmailto

1875-5453/18 $58.00+.00

circulating plasma, polyphenols or their metabolites may circulate when bound to albumin and may be able to penetrate tissues where they can exert their potential systemic effects. Once in the target tissues, these molecules can also be accumulated into tissue cells or can undergo new biotransformations into other compounds [1, 3, 4] (Fig. **1**).

Therefore, understanding the bioavailability, absorption and metabolism of plant polyphenols from diet is essential in order to clarify their mode of action, and determine the final active metabolites. With this purpose, many researchers have focused their attention on the study of the absorption of polyphenols by measuring plasma concentrations and/or examining urinary and fecal excretions from animal models or humans after consumption of a single dose of the compound or a complex plant extract or beverage [15, 16]. Pharmacokinetic measurements may include several variables: maximum plasma concentration (Cmax), time to reach Cmax (Tmax), area under the plasma concentration-time curve (AUC) and the elimination half-life ($t_{1/2}$) (Fig. **1**). Several factors, such as administration route, gender, age, genetic polymorphisms, hormonal status and food interaction, seriously influence the pharmacokinetics and bioavailability of polyphenols [17]. Nevertheless, studies that consider these influential factors are scarce.

The purpose of this review is to offer a summary, built on our own experience of the bioavailability, absorption, distribution, metabolism and excretion of polyphenols, that are present in four selected edible plants, bearing the most representative polyphenols' families, namely, *Hibiscus sabdariffa*, *Lippia citriodora*, *Rosemary officinalis* and *Olea europaea* (Figs. **2-4**), as well as to propose some of their putative molecular targets. These plants are commonly consumed as beverages, such as teas or juices or food seasonings and some of them have been used in folk medicine. Within the last decade, we have accumulated enough evidence to postulate that compounds derived from these plants may contribute to the prevention and/or the treatment of several metabolic pathologies, such as cancer, obesity, diabetes or cardiovascular diseases. It is postulated that these beneficial effects are mainly due to the presence of phenolic compounds, and studies on their pharmacological activities as pure compounds are extensive and consistent [18]. On the other hand, little is known about the pharmacokinetic behavior of these phenolic compounds after the consumption of plant extracts, and further investigations are required to identify the active metabolites that are responsible for such effects. Furthermore, the toxicological profile and tolerability are also important points that deserve more attention to understand possible side effects and to establish a safe dose to be administered as a dietary supplement in humans.

1.1. *Hibiscus sabdariffa*

1.1.1. Description and Composition

Hibiscus sabdariffa L. (HS) is a tropical plant belonging to the Malvaceae family, a wide family that comprises more than 4000 species. This plant is commonly known as Roselle, Karkade or Jamaica sorrel and is native to India and Malaysia. Currently, it is widely cultivated in the tropics and subtropics of both hemispheres and its flowers are normally consumed throughout the world. HS is an annual, erect and herbaceous sub-shrub that can grow up to 2.4 m in height with a typical red flower (calyx) consisting of five large sepals [19]. Anthocyanins are the natural pigments responsible for the red color of HS calyces, and they make HS a profitable product as a coloring ingredient in drinks. Furthermore, ingredients based on HS calyces have been traditionally used in folk medicine for the treatment of hypertension [20, 21], pyrexia [22] and inflammation [21, 23], kidney [24, 25] and liver [26-28] disorders and even obesity [29, 30]. Likewise, HS extracts have been shown to possess antioxidant [15, 27, 31-33], antitumor [34], anti-atherosclerotic [35, 36] and antimicrobial [37] properties.

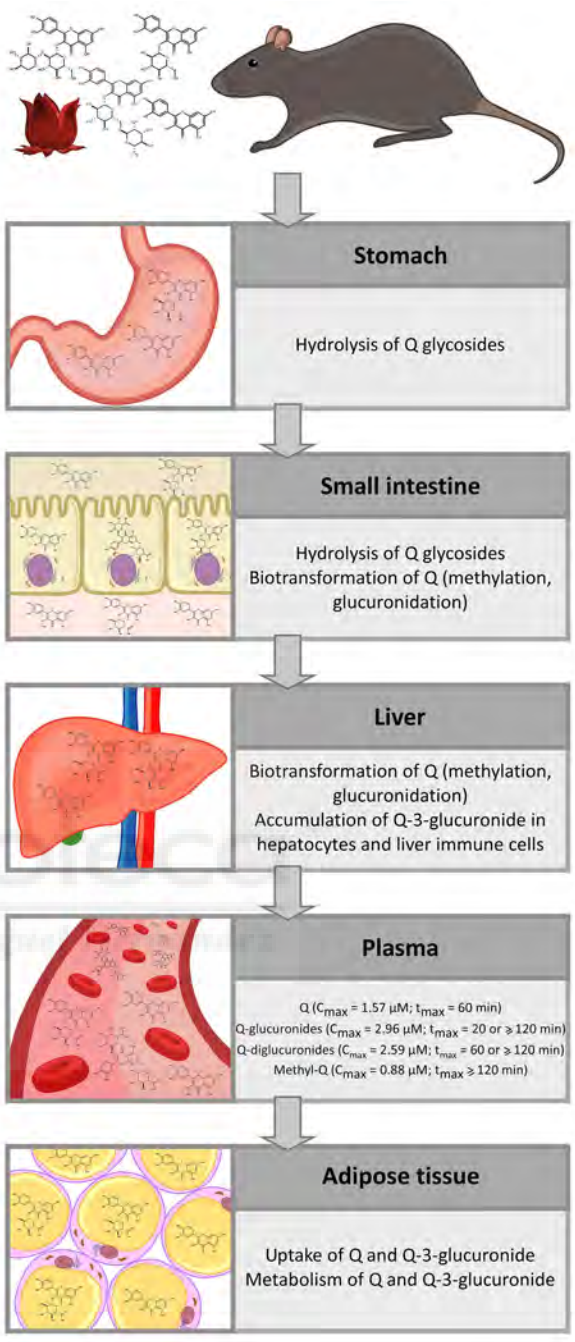

Fig. (1). Schematic flow diagram showing the bioavailability and metabolism of polyphenolic compounds along the different steps involved from the oral ingestion to their arrival to target tissue (adipocytes) in a rat model. Quercetin (Q) and its derivatives from HS extract have been selected to illustrate this process. After oral ingestion, glycosides derivatives are likely hydrolyzed in the stomach. Then, in the small intestine, both in lumen and inside enterocytes, additional hydrolysis reactions occur along with methylation and glucuronidation. Once absorbed, most probably by passive diffusion, first pass effect introduces additional methylation and glucuronidation moieties on liver along with hepatic accumulation of some of the metabolites such as Q-3-glucuronide. After phase I and II metabolism reactions, metabolites reach plasma and exhibit different pharmacokinetic behavior (maximum plasma concentration, C_{max}; time to reach Cmax, t_{max}) depending of their individual characteristics. Finally, metabolites arrive to their target, adipose tissue in this particular case, where not all but only selected compounds (Q and Q-3-glucuronide) are transported into adipocytes and suffer additional intracellular metabolism such as glucuronidation or deglucuronidation. The diagram has been constructed based on the evidence accumulated by our group, and others [15, 28, 46-48].

The qualitative characterization [38] and quantitation [31] of the compounds present in the aqueous extract of HS calyces have been carried out by high-performance liquid chromatography with diode array detection coupled to electrospray time-of-flight mass spectrometry or ion trap tandem mass spectrometry (HPLC-DAD-ESI-TOF-MS or HPLC-DAD-ESI-IT-MS). In these first studies, a total of seventeen compounds were found and quantified in the aqueous extract (Fig. **2A**). Among them, the main constituents were organic acids, phenolic acid derivatives, flavonol derivatives, phenylpropanoids and anthocyanins (Figs. **3** and **4**). Low molecular weight polysaccharides are another abundant group of compounds present in HS [39], but the biological activity of HS extract lies in the polyphenolic content, mainly quercetin and kaempferol derivatives, which are concentrated after ethanol precipitation or affinity chromatography [33]. In this later study, a total of 37 polyphenolic compounds were determined.

1.1.2. Biological Activities

A large amount of *in vitro*, *in vivo* and clinical studies have been published in order to explain the beneficial effects and potential mechanism of HS bioactive compounds. Most of these effects seem to be associated with the potent antioxidant capacity of HS extracts, which may take place through their direct strong scavenging effects on reactive oxygen species (ROS) [31], and also by their capacity to increase the activity/expression of antioxidant enzymes, such as glutathione (GSH), catalase (CAT), superoxide dismutase (SOD) and glutathione peroxidase (GPx) in liver [27]. The relationship between the antioxidant capacity of anthocyanins and their antiatherogenic activity, through the inhibition of *in vitro* low-density lipoprotein (LDL) oxidation and prevention of oxLDL-induced apoptosis, has also been reported [36].

The antioxidant activity of HS has been well correlated with an anti-inflammatory effect since inflammation is normally related to oxidative stress in several chronic diseases as confirmed previously in the liver of Sprague-Dawley rats treated with bacterial lipopolysaccharide (LPS). The inflammatory and oxidative effects induced by LPS were re-established after pretreatment with an extract of HS [40], suggest an important implication of HS extract on the treatment of chronic inflammatory diseases. We have also reported the anti-inflammatory effects of HS polyphenolic extract through the means of reduced pro-inflammatory cytokines in a hypertrophic adipocyte cell model [33] and in humans trials [21, 23].

The vast majority of clinical trials assayed with HS extracts show the antihypertensive effectiveness of this extract in patients with metabolic syndrome and hypertension. According to most studies, the antihypertensive effect of HS extract is related to the inhibition of angiotensin I-converting enzyme (ACE) and a reduction in serum sodium levels [41, 42]. Nevertheless, Joven *et al*. suggested that the inhibition of ACE activity contributes in a lesser degree and that the antioxidant, anti-inflammatory and endothelium-dependent effects are, most likely, the mechanisms involved in the hypotensive effect of HS [21].

Several studies have confirmed the anti-obesity effect of HS, proposing the use of this plant in the treatment of obesity and metabolic syndrome [29, 30, 43, 44]. Previously, a direct effect of compounds from HS extract on an adipose tissue model has been reported. Our research group has evaluated a polyphenol-enriched HS extract in a model of adipogenesis from 3T3-L1 cells and in hypertrophic and insulin resistant adipocytes [33]. The polyphenolic extract of HS extract showed potent activity in inhibiting adipogenesis, triglyceride accumulation, ROS generation and pro-inflammatory cytokine secretion, suggesting that the complex mixture of HS polyphenolic compounds may interact with numerous endogenous molecular targets.

As a sign of the multitargeted action of polyphenols, the capacity of HS polyphenols to modulate gene expression in a hyperlipidemic mouse model has been reported. Mice deficient in LDL receptor (LDLr-/-) were fed a high-fat diet to induce fatty liver disease and were fed HS polyphenols. The results of this study showed that a treatment with HS polyphenols reduced weight gain, ameliorated liver steatosis and modified the composition of liver tissue compared to the control. Furthermore, these changes were associated with a differential expression of liver miRNAs and lipogenic genes and an activation of 5'-adenosine monophosphate-activated protein kinase (AMPK) [28]. All these data support the pleiotropic character of the polyphenols of HS and their potential involvement on multifactorial diseases.

1.1.3. Pharmacokinetics and Toxicology

Despite abundant research on the pharmacology of HS, studies about its pharmacokinetics are scarce, and the main compounds or metabolites responsible for the bioactivity of the plant remain unclear. Furthermore, the final pharmacological effect of HS depends on the composition and dosage of the extract. Therefore, the identification of its bioactive components, its bioavailability in humans and its safety are important issues in order to estimate a suitable formulation and dosage to reach the desired therapeutic effect.

The potential therapeutic superiority of an HS polyphenolic extract enriched in flavonols and its synergic effect has been suggested in adipocyte cell model [33]. Nevertheless, we should be cautious when extrapolating *in vitro* data to an *in vivo* situation. Compounds may be metabolized by the intestinal flora and enzymes in the wall of the intestine, influence the absorption and bioavailability of these compounds and modify their biological activity *in vivo*. Plasma samples from healthy volunteers administered an acute dose of HS aqueous extract (10 g) revealed a significant decrease in monocyte chemoattractant protein-1 (MCP-1) at 1.5 and 3 h after ingestion, suggesting fast absorptions and high circulating concentrations of the bioactive compounds from the extract [23]. A pharmacokinetic study of a single oral dose of HS extract in healthy volunteers revealed very low concentrations of anthocyanins in plasma, which reached the maximum levels at 1.5 h after ingestion, indicating the poor absorption and fast urinary excretion of intact anthocyanins [45]. Several studies have proposed anthocyanidin-3-glucosides as candidates for the beneficial effects of HS. However, the rapid and poor absorption of anthocyanidins and recent evidence in animal models are increasingly pointing to the fact that flavonols, such as quercetin, may also be considered as candidates for such effects [23, 28, 33].

The bioavailability and pharmacokinetics of the HS polyphenol-enriched extract has been evaluated in Wistar rats after an acute oral dose of 1200 mg/kg [15]. A total of seventeen compounds were detected in rat plasma (Fig. **3A**). Several glucoronides of quercetin and kaempferol were found in rat plasma, which most likely were derived from the aglycone forms of these flavonoids after pre- or post-absorption deglycosylation. The organic acids and phenolic acid derivatives not only reached higher concentrations in plasma than flavonols, but also exhibited lower initial elimination half-life values, indicating the lack of accumulation of these compounds in the tissue. Among all the quercetin and kaempferol derivatives found in plasma, the highest concentrations were found for quercetin glucuronide and quercetin aglycone, compounds that showed larger elimination values, revealing a tissue accumulation and probable long-term effects (Fig. **1**). In this study, a correlation between the presence of polyphenols in plasma and antioxidant status was also observed.

Interestingly, the presence of quercetin-3-glucuronide was also detected in the liver and intestinal mucosa of hyperlipidemic LDLr-/- mice fed a polyphenolic-enriched HS extract for 10 weeks [28]. This glucuronide metabolite was also found in immune cells surrounding the surface of lipid droplets in the liver (Fig. **1**). The findings of this study suggested that intestinal mucosa exerts an important enzymatic activity through glucuronyl conjugation of the aglycone form of quercetins derived from HS. Thus, quercetin-3-

glucuronide could be one of the major metabolites from HS to account for the changes in the composition of liver tissue through the modulation of expression of liver miRNAs and lipogenic proteins.

The permeability of the polyphenolic extract from HS has also been evaluated in Caco-2 human cell monolayers, a model of human intestinal absorption [46, 47]. Analysis of the extract by ultra-high-performance liquid chromatography coupled with ultra-high-resolution quadrupole time-of-flight mass spectrometry (UHPLC-ESI-UHR-Qq-TOF-MS) identified most of the compounds that were previously described [31, 33]. In this study, absorption of the major HS metabolite, quercetin-3-glucuronide, and of isolated compounds, which are present at important levels in HS extract, were also studied in Caco-2 cell monolayers (quercetin, quercetin-3-glucoside and N-feruloyltyramine) [15, 28]. Nevertheless, neither phenolic acids nor anthocyanins were selected for their reported poor absorption, which reinforces the hypothesis that these compounds have little or no contribution to HS biological effects. The study revealed a significant absorption in the cell monolayer for all the compounds, especially for quercetin, most likely by passive diffusion and a high basolateral-apical permeability, suggesting a mechanism of transport efflux of these compounds (Fig. **1**).

Intestinal mucosa and liver are not the only tissues where the glucuronidation reactions occur. Recently, Herranz-López *et al*. found glucuronyltransferase and glucuronidase activities in hypertrophied 3T3-L1 adipocytes that were treated with quercetin and its metabolite quercetin-3-glucuronide [48]. In this study, an assessment of the absorption of quercetins was monitored. Both compounds were absorbed by hypertrophied adipocytes, and they were partially metabolized to quercetin-3-glucuronide and quercetin, respectively. Likewise, quercetin absorption was more efficient and faster than its metabolite, most likely indicating a passive diffusion through the plasmatic membrane of adipocytes; this was proposed as the main mechanism responsible for the observed decrease in ROS (Fig. **1**).

In a human intervention study, a systemic antioxidant potential was evaluated in eight healthy volunteers 24 h after the ingestion of 10 g of an aqueous HS extract. A significant increase in plasma and urine antioxidant potential and a reduction in oxidative stress was observed, in agreement with animal studies [49]. Furthermore, the main hibiscus anthocyanins and one glucuronide conjugate were detected in the urine of volunteers. The significant increase in hippuric acid in urinary excretion indicated a high biotransformation of HS polyphenols, which suggested a role of the colonic microbiota in this biotransformation [49].

Reports on the toxicology data of HS are limited. Nevertheless, infusions and aqueous extracts of this plant have been traditionally used in food and folk medicine and are generally considered safe. No acute toxicity was observed within seven days of an oral administration of 15 g/kg of ethanol and aqueous HS extracts in mice [22]. In contrast, liver injury was reported in rats when an aqueous-methanolic extract of HS was administered in at least 15 successive doses of 250 mg/kg/d [50]. Furthermore, total mortality, preceded by a severe loss of weight and diarrhea, was observed in rats after a chronic 90-day oral administration of aqueous and ethanol extracts of HS at 2000 mg/kg [51]. In contrast, neither acute nor chronic toxicity was observed in female rats after a single oral administration of extract at 5000 mg/kg or chronically at doses of 50, 100 and 200 g/kg for 270 days [52]. The discrepancy among different studies is most likely due to the different compositions of the utilized HS extracts. Although no side effects have been reported in human trials to date [29, 41, 42], further studies with well-characterized extracts are required to ensure the safety and tolerability of HS extracts in humans.

1.2. *Lippia citriodora*

1.2.1. Description and Composition

Lippia citriodora (LC) (syn. *Lippia triphylla*, *Aloysia triphylla*), commonly known as lemon verbena, belongs to the genus *Lippia* (Verbenaceae), which includes approximately 200 species of herbs, shrubs and small trees. LC is a deciduous shrub native to South America, however, it is also cultivated in Southern Europe and North Africa, since it was introduced to Europe at the end of the 17th century [53]. The leaves and stems of LC are rich in essential oils; geranial (citral), neral and limonene represent the main components of the total essential oil of the plant and are responsible for its lemony flavor. Furthermore, the individual percentages of these three compounds, especially for geranial and limonene, change depending on the developmental stage, which may be related to flowering [53].

LC extracts are also characterized by the presence of polyphenolic compounds, with phenylpropanoids as the main class of polyphenols of this plant (Fig. **2** and **3B**). Verbascoside (also known as acteoside) is the most abundant among all the phenylpropanoids [54], and it has been proposed as the main compound responsible for the biological activity of LC, especially its potent antioxidant capacity [55-57]. In addition, two verbascoside isomers (isoverbascoside and forsythoside A), two verbascoside derivatives (β-hydroxy-verbascoside and β-hydroxy-isoverbascoside), eukovoside and martynoside are other phenylpropanoids found in LC extracts [54, 55, 58] (Fig. **3B**). Flavones are another class of polyphenols that are present in minor quantities in LC extract. All of them are present in their diglucuronide form, such as luteolin-7-diglucuronide, apigenin-7-diglucuronide, chrysoeriol-7-diglucuronide and acacetin-7-diglucuronide [55, 58]. Other constituents identified by HPLC-DAD-ESI-MS are two iridoid glycosides (gardoside and theveside), verbasoside, cistanoside F and campneoside I and its isomer [58] (Figs. **2** and **3B**). Furthermore, asperuloside, tuberonic acid glucoside (or 5'-hydroxyjasmonic acid 5'-O-glucoside), shanziside and ixoside were also identified when the LC extract was analyzed by capillary electrophoresis-electrospray ionization-mass spectrometry [59].

1.2.2. Biological Activities

The leaves from LC are used as a spice for beverages and food preparations because of their lemony flavor. Additionally, a decoction and infusion of LC have traditionally been taken for the treatment of asthma, colds, fever, stomach ache, indigestion and other gastrointestinal disorders and skin diseases. In addition, it has been used as a diuretic, digestive, analgesic, antispasmodic and anti-inflammatory remedy [60]. In particular, the activity of LC is attributed to verbascoside since this phenylpropanoid represents 0.5 to 3.5% dry weight of the LC leaves, and it has been demonstrated to possess potent antioxidant capacity [55-57] and anti-inflammatory [61], antimicrobial [62] and anti-tumor [63] properties.

Verbascoside exhibited a higher capacity to scavenge free radicals within a hydrophobic environment than other antioxidants, such as hydroxytyrosol and caffeic acid. Furthermore, this phenylpropanoid was much stronger than these compounds and as potent as quercetin in inhibiting lipid peroxidation [55], a fact that may be related to its affinity for phospholipid membranes [64]. Nevertheless, the LC extract tested by Funes *et al*. [55], which contained 25% verbascoside, showed a higher antioxidant capacity than expected, based on the antioxidant capacity of pure verbascoside, suggesting a putative synergistic effect of verbascoside with other minor components, such as the flavones, in agreement with previous suggestions [54].

1.2.3. Pharmacokinetics and Toxicology

In spite of the widespread use of this plant in folk medicine, studies about its pharmacological effects are relatively recent. The capacity of verbascoside and LC extract to alleviate high-glucose

A

Hibiscus sabdariffa

Compound	Family
Hibiscus acid	Organic acids/ Dicarboxylic acids
Delphinidin-3-sambubioside Cyanidin-3-sambubioside	Flavonoids/ Anthocyanins
Chlorogenic acid Methyl digallate Coumaroylquinic acid 5-O-Caffeoylshikimic acid	Phenolic acids
Myricetin-3-arabinogalactose Quercetin-3-sambubioside Quercetin-3-rutinoside Leucoside Quercetin-3-glucoside Kaempferol-3-O-rutinoside Myricetin Quercetin	Flavonoids/ Flavonols
Methyl epigallocatechin	Flavonoids/ Flavanols
N-Feruloyltyramine	Others/ Tyramines

Lippia citriodora

Compound	Family
Shanziside Gardoside Theveside	Iridoid glycosides
Verbascoside Cistanoside F β-Hydroxyverbascoside/ β-Hydroxyisoverbascoside Campenoside I Isoverbascoside Eukovoside Martynoside	Phenylpropanoids
Luteolin-7-diglucuronide Chrysoeriol-7-diglucuronide Acacetin-7-diglucuronide	Flavonoids

Rosmarinus officinalis

Compound	Family
Apigenin Hispidulin Cirsiliol Diosmetin Cirsimaritin Genkwanin	Flavonoids
Rosmanol Epiisorosmanol Epirosmanol Miltipolone Carnosol Rosmadial Rosmaridiphenol Carnosic acid 12-Methoxy carnosic acid Hinokione	Diterpenes
Anemosapogenin Augustic acid Benthamic acid Micromeric acid Betulinic acid Ursolic acid	Triterpenes
9-Shogaol	Phenylpropanoid derivatives

Olea europaea

Compound	Family
(Epi)loganic acid isomers Oleoside/ Secologanoside isomers Hydroxytyrosol-glucoside isomers Hydroxytyrosol Tyrosol glucoside Elenolic acid glucoside/methyloleoside isomers Oleuropein aglycone Demethyloleuropein Oleuropein glucoside/neonuezhenide isomers Hydroxyoleuropein isomers Hydro-oleuropein Oleuropein/oleuroside isomers Methoxyoleuropein Dimethyl hydroxy octenoyloxi secologanoside isomers Ligstroside isomers Oleuropein methyl ether Piperchabaoside/(epi)frameroside/ ligustalisode dimethylacetal	Secoiridoids
Verbascoside	Phenylpropanoids
p-Coumaric acid glucoside Calceolarioside isomers Caffeoylglucoside	Hydroxycinnamic acids
Glucosyl rhamnosylquercetin (rutin) isomers Luteolin rutinoside/luteolin neohesperidoside/apigenin diglucoside Luteolin glucoside isomers Apigenin rutinoside/apigenin neohesperidoside Diosmetin rhamnoside glucoside (diosmin) isomers Apigenin glucoside Diosmetin glucoside Luteolin Quercetin Resinoside Apigenin	Flavonoids
Phenethyl primeveroside Ethyl-glucopyranosyloxy-oxopropyl-cyclohexaneacetic acid	Others
Olivil Olivil glucoside	Others/ Lignans
Esculin	Others/ Hydrocoumarins
Trihydroxystearic acid Trihydroxy-octadecenoic acid Dihydroxyhexadecanoic acid	Others/ Fatty acid derivatives
Sucrose	Others/ Disaccharides
Quinic acid	Others/ Carboxylic acids

Fig. (2) contd….

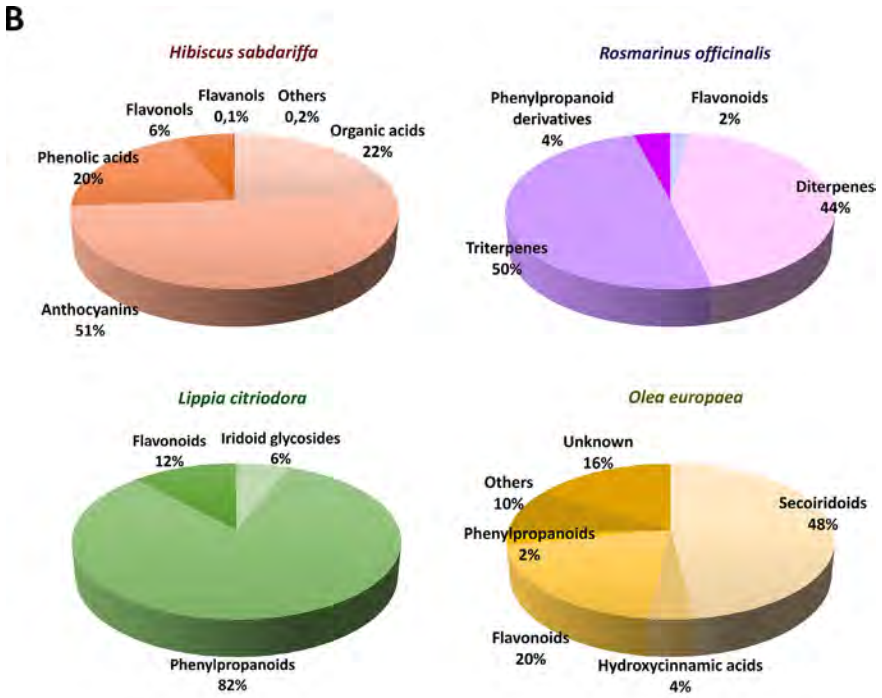

Fig. (2). Major bioactive compounds identified in *H. sabdariffa, L. citriodora, R. officinalis* and *O. europaea* extracts by liquid chromatography coupled to high resolution mass spectrometry (A). Compounds are grouped in families according to their chemical structure. (B) Percentage (w/w) of the different families of identified compounds on each extract. Identified compounds not included in families are shown as "others". Non-identified but quantified compounds are shown as "unknown". The complete characterization of the extracts has been previously reported [33, 65, 100, 181].

induced metabolic stress in hypertrophic adipocytes through AMPK-dependent mechanisms and to improve fat metabolism in hyperlipidemic mice has been recently reported [65]. Nevertheless, the data on the bioavailability and pharmacokinetics of phenolic compounds derived from LC extract are scarce, and little is known about the metabolites that could contribute to the biological activity of this plant. The studies carried out to date have focused on the bioavailability and pharmacokinetics of the main candidate for exerting the beneficial effects of LC, verbascoside. Nonetheless, as postulated from previous findings, other metabolites derived from LC compounds could also contribute to its bioactivity [16], which deserves further studies.

The pharmacokinetics of verbascoside derived from an LC extract studied in an animal model was reported [55]. In this study, Wistar rats were orally treated with a high acute dose of LC extract that contained a 25% of verbascoside, and blood samples were taken at different times after ingestion. Verbascoside was the only metabolite found in plasma samples, and its maximum concentration was reached at 20 min (2.3 μM), which correlated with the maximum antioxidant activity in the plasma of the rats. These results indicated a fast absorption of verbascoside in the gut barrier but a very low bioavailability, which may compromise to assign the observed effects to verbascoside. The low oral bioavailability of pure verbascoside was also corroborated in rats and the binding of this compound to plasma proteins was also shown, which could suggest a restricted distribution of this compound [66]. Nevertheless, there is evidence of the bioactivity of phenylpropanoids at very low concentrations in cell models (at the micromolar range), so low micromolar concentrations of verbascoside over a long-term in plasma could be responsible for some of the effects of LC.

The effect of the consumption of an oral acute dose of LC extract (1440 mg/kg) on the antioxidant response of blood cells was further studied in rats using high-resolution mass spectrometry in order to determine other potential metabolites in plasma [16]. In this study, verbascoside and isoverbasoside were identified as the most abundant metabolites (within the low micromolar range), suggesting that both compounds could be absorbed in their native forms. Five other metabolites, most probably derived from these two by deglycosylation (hydrolysis), methylation or glucuronidation [67], were also found in plasma, namely, hydroxytyrosol, caffeic acid, ferulic acid, ferulic acid glucuronide, and homoprotocatechuic acid, together with eight other phenolic compounds (some structural formulas shown in Fig. **3B**). Three flavone derivatives were also detected in plasma, namely, acacetin diacetate, luteolin diglucuronide and chrysoeriol diglucuronide. Acacetin diacetate could come from the conjugation of two acetate groups after the deglucuronidation of acacetin-7-diglucuronide, while luteolin and chrysoeriol diglucuronides could arise from the absorption of intact compounds present in the extract or from the absorption of free flavones in the gut and their successive glucuronidation (Fig. **3B**). Also, small amounts of gardoside, cistanoside F, theveside, eukovoside and martynoside were detected in plasma, suggesting that these compounds could be absorbed in their native forms. Therefore, the findings of this study indicated that the antioxidant response in blood cells may be due to the combined action of verbascoside, isoverbascoside and their metabolites, which could derive from the deglycosylation of phenylpropanoid glycosides in the gastrointestinal tract and the subsequent glucuronidation, sulfation or methylation of the aglycone forms.

The presence of verbascoside and isoverbascoside in the urine of healthy rats after the consumption of LC polyphenols has also been confirmed, which corroborates the absorption at the intestinal level of both compounds in their intact forms [68]. This study also revealed the possible deglycosylation or deglucuronidation of glycoside or diglucuronide derivatives present in the LC extract, respectively, and their subsequent glucuronidation or sulfation in the gut barrier. They concluded that the urinary and fecal excretion of LC in rats is low and that the influence of the gut microflora in the degradation of the polyphenolic compounds of LC deserves further attention.

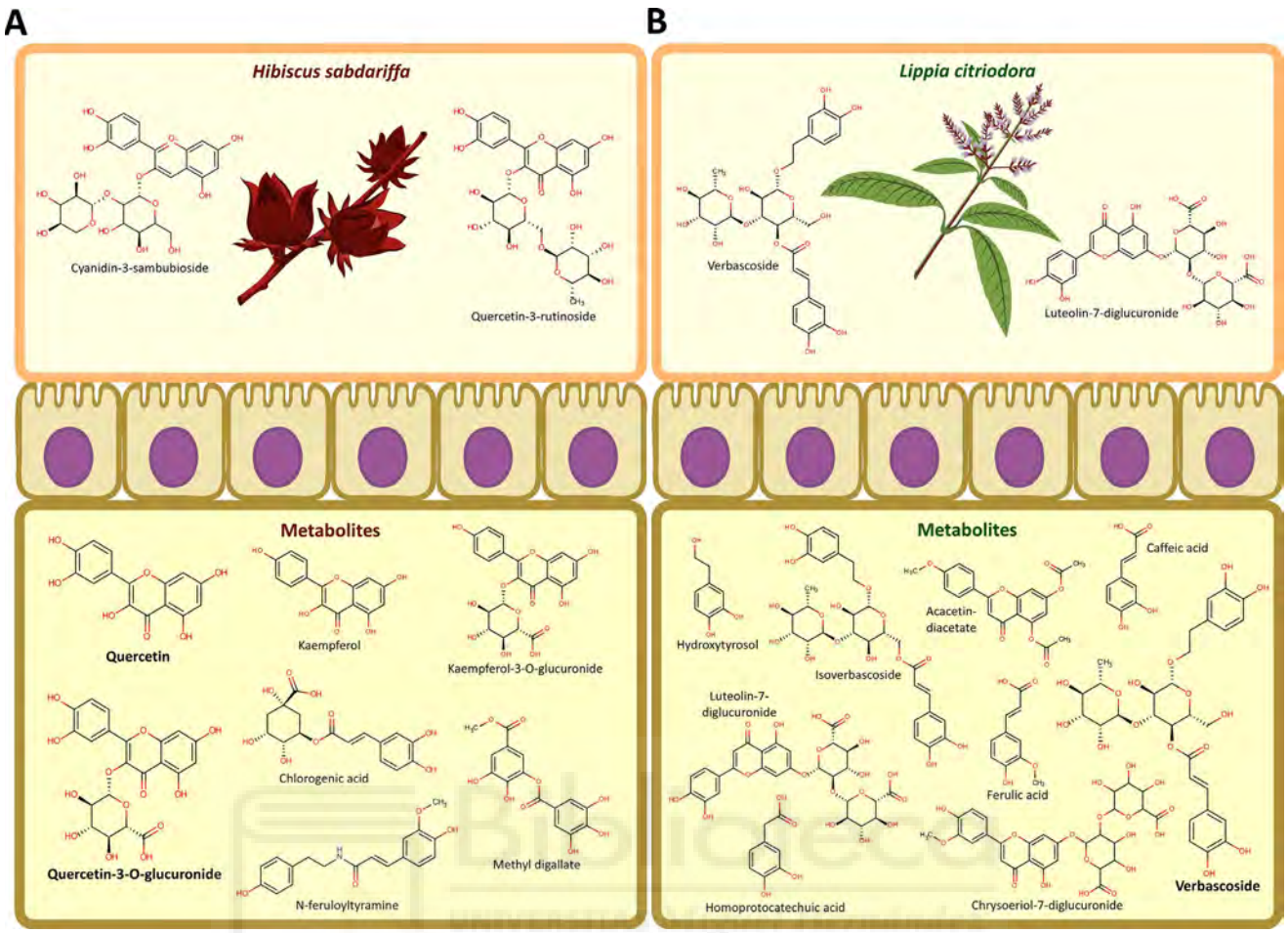

Fig. (3). Main polyphenolic compounds and metabolites from *H. sabdariffa* (**A**) and *L. citriodora* (**B**). Upper part shows a pictogram of each plant and the main polyphenolic compounds found in their respective extracts. The intestinal barrier is represented by the illustration of the enterocyte monolayer in the middle of the figure. Lower part shows the major metabolites derived from each plant found in plasma or tissues; the most significant ones are highlighted using bold letters.

No metabolites derived from LC consumption have been identified to date in plasma samples from human trials. Nevertheless, the effects of LC consumption on the oxidative damage and muscular injury related to intense physical activity has been studied in depth. Several single-blind, randomized and placebo-controlled trials have assessed the effects of LC extract consumption after exercise on several circulating parameters, antioxidant enzyme activities and expression and oxidative stress markers. The results evidenced the activation of glutathione reductase in erythrocytes and lymphocytes, lower levels of oxidative stress markers, such as malondialdehyde (MDA) and protein carbonyls in plasma, a modulation of the circulating lipid profile with an increase in high-density lipoprotein (HDL)-cholesterol, a modest decrease in acute inflammation and an increase in circulating urea after extract intake [69-73]. Furthermore, the protective effect of LC in muscle tissue was found through a 20% decrease in circulating myoglobin, while no interference was detected with an increase in glutathione-disulfide reductase gene expression due to cell adaptation to oxidative stress [71]. Although these effects are supposed to be due to the major compound of LC, verbascoside, further research on the potentially responsible metabolites is required to verify this hypothesis.

There is a lack of data about the toxicology and tolerability in the prolonged consumption of LC. In this sense, the acute oral toxicity was assessed in mice after an oral administration of 2000 mg/kg of LC extract; the extract did not show toxicity and could be classified as GHS Category 5 (Globally Harmonized System) or unclassified [55]. Moreover, several human intervention studies focused on sports nutrition have used dietary supplements based on LC extracts containing 10-20% verbascoside with a daily dosage varying from 500-1800 mg and a duration of the intervention from 3 to 9 weeks [69-71, 74, 75]. As a conclusion, no adverse effects were reported in any of these studies. Nevertheless, further studies on the toxicology of LC consumption are needed to establish safe doses of LC in humans.

To conclude, the absorption and permeability of LC polyphenols are also poorly characterized. The Caco-2 human colon cell line represents a useful model of human intestine in order to study the absorption and metabolism of polyphenols from LC. Information on the metabolites of LC reaching the blood circulation needs to be improved in order to try to explain their potential molecular targets and consequently explain the therapeutic effect of LC. Furthermore, little is known about the tissue distribution of these compounds, in which they could also be further metabolized. Therefore, further research to understand the complete absorption, metabolism and distribution mechanisms of LC polyphenols requires more attention.

1.3. *Rosmarinus officinalis*

1.3.1. Description and Composition

Rosmarinus officinalis L., commonly known as rosemary, is a shrub that belongs to the family Lamiaceae, which contains approximately 3500 species. It is a perennial, evergreen, aromatic plant that grows about one meter in height with whitish-blue flow-

ers and needle-like leaves. This herb blossoms twice a year (spring and autumn) and easily grows in all kinds of areas, especially in dry and sandy soils. Rosemary grows wild throughout the Mediterranean area and is currently cultivated worldwide due to its multiple uses as a culinary spice in food [76].

There is a wealth of information on the identification and quantification of the main components of rosemary-leaf extracts. The most representative classes of polyphenolic compounds present in this matrix are abietane-type diterpenoids, phenolic acids and flavonoids (flavones, flavanones and flavanols) (Fig. **2**). The main phenolic diterpenoid of rosemary is carnosic acid, and several derivatives of this compound can be found as well, namely, carnosol**,** rosmadial, rosmanol, 12-methoxycarnosic acid and its isomers epirosmanol and epiisorosmanol (Fig. **4A**). Triterpene acids are also abundant in rosemary-leaf extracts, such as ursolic and betulinic acids (Fig. **4A**). The most abundant phenolic acid is rosmarinic acid, followed by caffeic and ferulic acids, and several flavonoids, such as genkwanin, hispidulin, cirsimaritin, homoplantaginin, scutellarein, gallocatechin, apigenin, diosmetin, nepetrin, hesperidin, 6-hydroxyluteolin-7-glucoside and luteolin-3'-glucuronide, and phenylpropanoid derivatives, such as (9)-shogaol, are also detected in this plant [77-83] (structural formulas shown in Fig. **4A**).

The composition and quantity of compounds present in the different rosemary-leaf extracts depend on numerous factors, such as the soil type, climate, plant age and, more importantly, the extraction procedure. Basically, rosemary extracts can be classified into three main groups based on its chemical composition: essential oils, hydrophilic and hydrophobic extracts. The essential oil has been valued for its antibacterial, antioxidant and antiproliferative properties [81]. The major compounds found in the essential oil are 1,8-cineol, camphor, α-pinene, limonene, camphene and linalool. On the other hand, rosmarinic acid and other minor compounds, such as hydroxycinnamic acids and glycosylated flavonoids, are the major representative compounds in water-soluble extracts, while abietane diterpenes, such as carnosic acid, carnosol or rosmadial, and other hydrophobic compounds, such as methylated flavones genkwanin and cirsimaritin, and the flavone hesperetin are abundant in the non-water soluble extract. It is well known that the antioxidant activity of rosemary extracts is mainly due to phenolic abietane diterpenes and the phenolic rosmarinic acid. Nevertheless, this behavior depends on the hydrophobicity of the environment, where the hydrosoluble extract exhibits a high antioxidant activity in the absence of a membrane-based system, while the hydrophobic extract shows a higher antioxidant capacity in the presence of a membrane system [79].

1.3.2. Biological Activities

Rosemary, especially the leaf extract, is one of the most popular herbs, traditionally consumed as a culinary spice to adjust food flavor, and is widely used in the food and cosmetic industries as a natural antioxidant agent due to its inherently high antioxidant activity. Moreover, this plant has been used for centuries in folk medicine, and a wide variety of pharmacological activities have been attributed, such as hepatoprotective [84], antibacterial [85], anti-atherogenic [86], antidiabetic [87], antinociceptive [88-89], anti-inflammatory [89-91], anti-tumor [92, 93] and antioxidant [94, 95] activities. In addition, rosemary extracts and their isolated components have been shown to exert an antiproliferative effect on breast, liver, prostate, lung and colon cancer cells [96-100].

Most of the biological activities described for rosemary are associated with its phenolic content. In this sense, its strong antioxidant capacity is mainly due to phenolic diterpenes, such as carnosol, carnosic acid [101], rosmadial, rosmanol and epirosmanol, as well as the phenolic acid rosmarinic acid [79, 95, 102]. Although other phenolic compounds also contribute to the antioxidant activity of this aromatic plant, such as flavonoids like genkwanin and cirsimaritin. The mechanisms proposed for the antioxidant capacity of polyphenols are mainly related to the capacity of polyphenols to scavenge reactive oxygen species, such as peroxide ($^{\bullet-}O_2$), hydroxyl ($^{\bullet}OH$) or lipoperoxyl ($ROO^{\bullet}$) radicals. As mentioned above, the abietane diterpenes from rosemary have been shown to have a preference for a membrane environment, suggesting that the antioxidant effect against peroxidative damage that is induced by free radicals could be mediated by a membrane-related mechanism [79].

In addition to their potent antioxidant capacity, phenolic compounds from rosemary have been proposed to exert an important antiproliferative effect against several types of cancer cells. Researchers have focused their attention on the multiple mechanisms involved in this protective effect as well as the main responsible compounds [100]. For instance, it has been reported that two of the major compounds present in rosemary extract (carnosic acid and carnosol) inhibit the proliferation of colon cancer HT-29 cells by increasing oxidative stress, which results in the transcriptional activation of detoxifying genes by cells [99]. In the same cell model, rosmarinic acid exerted a preventive effect against the activation of the pro-inflammatory gene cyclooxygenase-2 (COX-2) [93], an inducible enzyme involved in metastatic mechanisms.

On the other hand, the literature on the therapeutic implications of rosemary in metabolic syndrome is also extensive since this aromatic plant possesses antidiabetic [87], anti-atherogenic [86] and hypocholesterolemic [103] activities, among others. These effects are basically related to the modulation of enzymes, transcriptional factors and the expression of key genes involved in several key metabolic pathways [104]. Definitively, rosemary represents another example of how medicinal herbs are composed of a complex mixture of phenolic compounds that exerts an important role in multifactorial diseases by interacting with a large number of metabolic targets.

1.3.3. Pharmacokinetics and Toxicology

In spite of a large number of studies focused on the potential therapeutic activities of rosemary extracts and the potential molecular mechanisms involved, little is known about the presence of these molecules and their metabolites *in vivo*. Therefore, research on the absorption, distribution, metabolism and elimination of rosemary components is needed to fully understand their activity *in vivo* and to establish a more effective and safe dosage in humans.

The pharmacokinetics of carnosic acid has been determined in the plasma, liver, intestinal content, urine and feces of rats receiving a single dose of the compound, intravenously or orally [105]. The results of the study revealed that carnosic acid has a slow absorption, but its elimination in the blood needs to be further clarified. The bioavailability was approximately 40% at 360 min after oral administration, likely due to the limited stability of carnosic acid in the stomach and the low uptake in the gut barrier. Moreover, only traces of carnosic acid were detected in the liver and intestinal contents, and there were no signs of enterohepatic recirculation. The analysis of the feces showed that part of carnosic acid is not metabolized; it is cleared by the liver into the intestine and mainly eliminated through the fecal route.

In an attempt to clear up the metabolism of some of the main diterpenes from rosemary, the bioavailability of the main compounds of a carnosic acid-enriched rosemary extract (0.5% w/w) has been studied in Zucker rats after oral administration of the extract for 15 days [106]. A total of 26 compounds were detected as early as 25 min after administration in the gut content, plasma and tissue samples, including carnosol, carnosic acid, rosmanol, epirosmanol, epiisorosmanol and rosmarinic acid. Most of the compounds and metabolites were identified in the liver and the gut lumen, with carnosic acid 12-methyl ether as the main derivative found in the liver, followed by 5,6,7,10-tetrahydro-7-hydroxyrosmariquinone, carnosic acid glucuronide, carnosic acid and epiisorosmanol (structural formulas in Fig. **4A**). On the other

hand, the main metabolites detected in the lumen of the small intestine were carnosic acid glucuronide, rosmanol glucuronide and carnosol glucuronide, suggesting that glucuronidation is the main form of conjugation, both within the intestinal epithelium and in the liver. The most abundant metabolites identified in plasma within the range of 150-300 μM were 5,6,7,10-tetrahydro-7-hydroxyrosmariquinone, which was probably derived from cell oxidative stress, and carnosic acid 12-methyl ether, due to the action of catechol-O-methyltransferases present in the intestine and the liver (Fig. **4A**). Further attention should be paid to these two latter compounds and their molecular targets since they may be relevant to explaining the biological activity of rosemary extract.

Recently, the permeability of 24 bioactive compounds derived from a rosemary extract enriched in diterpenes and triterpenes has been studied in the Caco-2 cell monolayer model, indicating that carnosic acid and epiisorosmanol showed the highest permeability values [107]. The flavonoids hispidulin, diosmetin, genkwanin and cirsimaritin exhibited significant permeation values, with cirsimaritin and genkwanin being the flavonoids with the highest permeations. Among the diterpenoids, carnosic acid, followed by epiisorosmanol and its isomers epirosmanol and rosmanol showed the highest permeability values, while triterpenoids were the class of compounds with the lowest permeability values (Fig. **4A**). The results of this study suggested that most bioactive compounds from rosemary extract are scarcely absorbed, and the major mechanism of absorption for most compounds is passive diffusion transport. Furthermore, the use of liposomes to vehiculize rosemary compounds does not improve their permeability.

Despite these studies, the lack of information about the absorption and pharmacokinetics of rosemary extract compounds is evidenced. Further research should be oriented to study the transportation mechanism at the gut barrier using cell models of human intestine. Moreover, special efforts should be made to identify the plasma metabolites derived from rosemary in human samples. Also, the study of tissue distribution and biotransformation of the plasma compounds or metabolites in animal models requires further attention. Putting all this information together may allow us to identify the specific molecular targets of rosemary metabolites.

The potential toxicity of the consumption of rosemary extracts is another issue that should be clarified. In this regard, only one study of acute oral toxicity (2000 mg/kg dose) in rats with two rosemary extracts, mainly enriched in diterpenes and containing a lower number of flavonoids, has been reported to date [108]. This study showed that the extracts were well-tolerated and had no adverse effects or mortality. Lastly, few human studies have been carried out to investigate the efficacy of rosemary extract on a prolonged basis. In a study performed in 90 subjects who daily consumed a mixture of a rosemary and citrus extracts for 3 months, no adverse effects were reported, and the polyphenol extract showed decreases in the UVB- and UVA-induced skin alterations and improvements in skin wrinkledness and elasticity [109]. Therefore, the toxicity and tolerability of rosemary require further research to set the maximum recommended dose for high effectiveness of the extract.

1.4. *Olea europaea*

1.4.1. Description and Composition

Olive tree (*Olea europaea*) is one of the most popular members of the family Oleaceae, which comprises approximately 30 genera of deciduous trees and shrubs [110]. The olive tree represents one of the oldest and most widespread tree species grown in the coastal areas of the eastern Mediterranean basin, southeastern Europe, western Asia and northern Africa. It is a short, thick tree that can reach up to 15 m in height with many branches. Its leaves are lanceolate and narrow and the olive fruit is small, ovoid and green and turns blackish-violet when ripe [111].

The olive fruit is widely consumed as either a ripe fruit or an unripe green fruit. Furthermore, olive oil constitutes the main food ingredient of the common "Mediterranean diet" and is the major source of dietary fat in the countries where olives are distributed [112, 113]. Likewise, several beneficial effects, such as a reduced risk of coronary artery disease [114, 115], neurodegenerative disease [116, 117] and certain types of cancer [118-120], have been widely attributed to the consumption of olive oil that is rich in phenolic compounds. Nevertheless, olive leaves were commonly discarded as byproducts of fruit harvesting [121] but have recently attracted more attention as nutraceuticals with health purposes due to their high content of phenolic compounds [122].

The chemical compositions of different parts of the olive tree have been extensively studied [122-129]. Fruits, seeds, leaves and oil of the olive tree are rich in phenols, flavonoids and secoiridoids. In particular, secoiridoids are the main phenolic compounds detected in olive leaf (OL) extracts, with oleuropein reported as the most representative compound. Other secoiridoids, such as oleuroside, hydroxyoleuropein, oleuropein diglucoside, oleoside, secologanoside, elenolic acid glucoside, 7-epiloganin or ligstroside, are also found in olive leaves. In addition, flavonoids represent another important group of phenolic compounds in the olive tree. Among them, luteolin, luteolin-7-O-glucoside, luteolin-7,4-O-diglucoside, luteolin-7-O-rutinoside, luteolin-4-O-glucoside, apigenin, apigenin-7-O-glucoside, apigenin-7-O-rutinoside, rutin and quercetin have been detected in OL extracts. Simple phenols were also identified in olive leaves, with hydroxytyrosol being one of the main components of OL extracts. In addition, cinnamic acid derivatives or phenylpropanoids (such as verbascoside and *p*-coumaric acid), other simple phenolic compounds (such as vanillin and *p*-hydroxybenzoic acid) and triterpene acids (such as oleanolic acid and ursolic acid) have also been identified in OL extracts [122, 127] (Fig. **2**).

1.4.2. Biological Activities

O. europaea has a large number of uses in folk medicine for the treatment of cardiovascular diseases, respiratory and urinary tract infections, diarrhea, stomach and intestinal diseases, asthma or rheumatism [111]; a wide range of beneficial health properties are attributed to their components as antidiabetic [130, 131], antihypertensive [132, 133], anti-inflammatory [134], antioxidant [131, 135, 136], antitumor [118, 137] and antimicrobial agents [136, 138]. Although previous literature on the phenolic compounds of the olive plant has focused on olive oil consumption, phenolic compounds in the olive tree are mostly concentrated in the olive leaves [121]. Furthermore, the leaves of *O. europaea* can be consumed as an herbal tea, and they have also been used as a traditional remedy in countries where it is cultivated. Several studies have shown antioxidant [128, 136], hypoglycemic [139], antihypertensive [140], antimicrobial [136, 141], tumoricidal [127], antiviral [142] and antiatherosclerotic [143] effects. Therefore, olive leaves may be considered a cheap and easily available natural source of phenolic compounds.

Certain researchers have studied the biological activities of isolated components from the olive plant. Oleuropein, which is the major phenolic compound present in OL extracts, represents a pharmacologically active molecule since several beneficial effects of this compound have been extensively reported, among them anti-inflammatory [144], anti-atherogenic [145], anticancer [146], antimicrobial [147] and antiviral [142] properties. In addition, this secoiridoid glycoside has skin photoprotective [148] and anti-aging [149] properties and is a potent antioxidant and radical scavenger [150]. In addition to its antioxidant activity, it is postulated that some of these effects could be related to the capacity of oleuropein to interact with biological membranes, consequently promoting changes in the membrane's physical properties and the function of membrane-related proteins [151].

1.4.3. Pharmacokinetics and Toxicology

In spite of the beneficial effects reported for the main components of *O. europaea*, such as oleuropein, the *in vivo* bioactivity depends on the absorption and metabolism of these compounds. *In vitro* gastric digestion of the breakdown of complex olive oil polyphenols [152] revealed that the relative amounts of hydroxytyrosol and tyrosol in the small intestine increased after gastric biotransformation of the complex secoiridoids derivatives of olive oil polyphenols. Likewise, these simple phenols crossed the human Caco-2 cell monolayer and the rat segments of the jejunum and ileum, while oleuropein was not absorbed. However, this secoiridoid glycoside was rapidly degraded by the colonic microflora, yielding hydroxytyrosol, which may then be absorbed. The findings of this study also indicated that hydroxytyrosol and tyrosol could be metabolized to O-methylated, glucuronidated and glutathionylated conjugates.

Hydroxytyrosol is the main derivative from oleuropein. While the secoiridoid glycoside is found in high amounts in unprocessed olive leaves and fruit, the higher concentrations of hydroxytyrosol may appear in the fruit and olive oil due to the chemical and enzymatic reactions that occur during the maturation of the fruit [153]. In addition, hydroxytyrosol has also been shown to be a strong antioxidant *in vitro* and in animal studies [154, 155]. The bioavailability of this simple phenol has been explored in humans (Fig. **4B**). Miro-Casas *et al*. quantified hydroxytyrosol and its main metabolite, 3-O-methylhydroxytyrosol, in plasma and urine after a dose of 25 mL of virgin olive oil in healthy humans and showed that approximately 98% of hydroxytyrosol was present in conjugated forms, mainly glucuronoconjugates [156]. It was suggested that the ingested hydroxytyrosol may be extensively first-pass metabolized in the intestine and liver and that the biological activity of this compound is most likely derived from its metabolites. The bioavailability of olive polyphenols in healthy volunteers after the consumption of twenty olives rich in hydroxytyrosol has also been examined [157]. From the fifteen phenolic compounds detected in olives, seven compounds significantly increased in plasma and urine after administration, namely, tyrosol, *p*-hydroxyphenylacetic acid, *p*-hydroxybenzoic acid, hydroxytyrosol, and three metabolites derived from hydroxytyrosol (homovanillic alcohol, homovanillic acid and 3,4-di-hydroxyphenylacetic acid) (structural formulas shown in Fig. **4B**). Moreover, other phenolic compounds were detected in plasma, mainly in their conjugated form as glucuronides. The results indicated that olive polyphenols are bioavailable, rapidly absorbed and metabolized, especially for the catechol-O-methyltransferase action of hydroxytyrosol in the liver and kidneys. In addition, a correlation between the increase on phenolic compounds after the ingestion of olives and an enhancement of antioxidant status in plasma was found.

The bioavailability of pure oleuropein in rats or in the same animal model supplemented with extra virgin olive oil (EVOO) has also been studied by HPLC-ESI-MS/MS of plasma samples after being consumed for 80 days [158]. The potential phenolic metabolites of oleuropein described in the literature are: hydroxytyrosol, 2-(3,4-dihydroxyphenyl)acetic acid, 4-(2-hydroxyethyl)-2-methoxyphenol or homovanillyl alcohol, 2-(4-hydroxy-3-methoxyphenyl) acetic acid or homovanillic acid, and elenolic acid [158] (Fig. **4B**). In the latter study, the metabolite homovanillic alcohol was found in plasma basal levels, whereas intact hydroxytyrosol was not detected, corroborating the biotransformation of this compound. The metabolites homovanillic acid and 3,4-di-hydroxyphenylacetic acid were detected but were not found in all the plasma samples of rats. This intraindividual variability on metabolite content was also reported in the plasma of volunteers after the ingestion of olives [157], which may suggest a genetic polymorphism of the enzymes involved in the metabolism of olive polyphenols or differential epigenetic regulation.

The above mentioned studies evidenced that EVOO phenolic compounds are absorbed by the small intestine upon oral administration and their levels are dose-dependently increased in plasma and urine [159]. Maximum concentrations of these compounds in urine have been detected within the first 4 h, with their free forms not exceeding 15%. The formation of hydroxytyrosol, tyrosol and their metabolites (especially as glucuronide conjugates) is also a key step in the biotransformation of olive polyphenols (Fig. **4B**). Oleuropein undergoes extensive non-enzymatic hydrolysis by the gastric environment [152] or decomposition by colon microflora [160], forming hydroxytyrosol, which enters the small intestine and is absorbed by passive diffusion or by the colon [158]. However, studies on the absorption of oleuropein are controversial since other studies have proposed that this secoiridoid glycoside can also be absorbed and subjected to phase II metabolism in humans [161].

The form of administration (oily or aqueous) or the administration route (intravenous or oral) significantly affects the bioavailability of EVOO phenolic compounds [162]. Nevertheless, most of the studies have been carried out with olive oil and fruit, while literature considering the absorption and metabolism of these compounds after consuming OL extract is scarce. Furthermore, given the unclear fate of oleuropein, it seems relevant to investigate the behavior of oleuropein from OL extract ingestion (rather than olive oil) since olive leaves are more concentrated in phenolic compounds, especially in oleuropein, and their bioavailability may differ from that of OL from EVOO.

Accordingly, the first study to assess the absorption and metabolism of oleuropein and hydroxytyrosol in human plasma after an ingestion of OL extract evidenced that the main olive phenolic metabolites found in plasma and urine were conjugated metabolites of hydroxytyrosol (mainly glucuronidated and sulfated), while homovanillic acid was detected in traces [121] (Fig. **4B**). Furthermore, the metabolites of hydroxytyrosol were rapidly detected in plasma after ingestion and the primary compounds were present in urine. Heterogeneous bioavailability and metabolism of oleuropein were also observed among volunteers in this study, suggesting a high dependence on several factors, such as the delivery method and gender. Nevertheless, whether the bioactivity of phenolic compounds from olive comes from hydroxytyrosol or its glucuronide metabolites, remains unclear. One study in rats showed that hydroxytyrosol metabolites, such as 3-O-glucuronide conjugate, were more potent than their precursor on radical scavenging activity [163], while another study carried out in humans reported that none of the glucuronides of hydroxytyrosol that were detected in plasma after an ingestion of olive oil contributed to antioxidant activity at real biological doses [164].

The bioavailability of phenolic compounds has also been studied in a human intervention study focused on the effect of the consumption of 250 mg of OL extract (>40% OL) on the menopausal status of women and its potential benefit in the prevention of osteoporosis [165]. Fifteen olive phenolic compounds were rapidly found in plasma and urine and were mainly phase II-derived metabolites; three were metabolites derived from hydroxytyrosol, four were oleuropein aglycon derivatives and two were homovanillic acid metabolites. Hydroxytyrosol glucuronide was the most abundant and tyrosol glucuronide, hydroxytyrosol-acetate glucuronide and luteolin glucuronide and its respective aglycone were found at trace levels. New metabolites derived from oleuropein were identified in urine, such as homovanillic alcohol sulfate, elenolic acid, and elenolic acid glucuronide. These findings confirmed the fast absorption of phenolic compounds from OL extract and the extensive biotransformation of hydroxytyrosol and oleuropein into metabolites, mainly as glucuronidated conjugates, as previously reported [121] (Fig. **4B**).

The toxicology of OL extract has been performed in Wistar rats fed several doses of the extract for 6 weeks [166]. The treated groups showed a significant increase in serum levels of alkaline

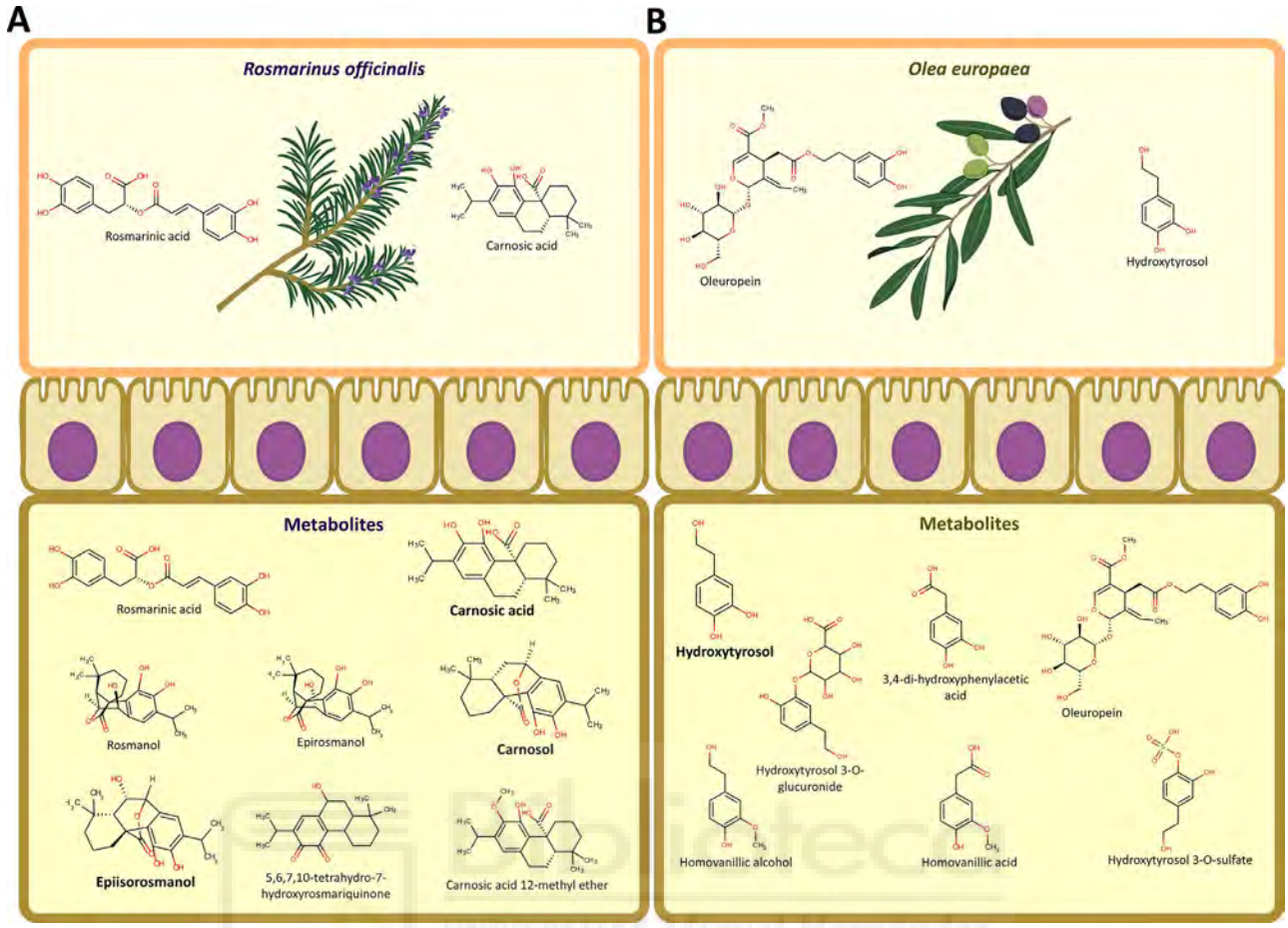

Fig. (4). Main polyphenolic compounds and metabolites from *R. officinalis* (**A**) and *O. europaea* (**B**). Upper part shows a pictogram of each plant and the main compounds found in their respective extracts. The intestinal barrier is represented by the illustration of the enterocyte monolayer in the middle of the figure. Lower part shows the major metabolites derived from each plant found in plasma or tissues; the most significant ones are highlighted using bold letters.

phosphatase and bilirubin and a significant decrease in serum triglyceride, glucose and cholesterol. Furthermore, the group with the higher dose showed decreases in red blood cells and hemoglobin and histological alterations in the liver and kidneys. The findings of this study proposed a careful use of OL extract, especially at higher doses for longer periods of times. Recently, a study on the efficacy and safety of a combination of two extracts (*Opuntia ficus-indica* and OL extracts) on gastroesophageal reflux showed that the consumption of 6 g/day of this formulation for two weeks did not exert any adverse effects and was well-tolerated [167]. In addition, the toxicological safety of OL extract was assessed in a preclinical study in which no evidence of mutagenicity or genotoxicity in the bacterial reverse mutation test, *in vitro* mammalian chromosomal aberration test or *in vivo* mouse micronucleus test was observed [168]. Moreover, the NOAEL derived from the 90-day study in rats was 1000 mg/kg per day.

To conclude, more studies are needed in order to investigate the accumulation of olive-leaf metabolites in tissues and their physiological significance *in vivo*. Furthermore, the pharmacokinetics of oleuropein from olive leaves requires further investigation to elucidate its absorption in the gut barrier, metabolism and various means of excretion, as well as its degradation into other phenolic compounds by the colonic microflora. The toxicological profile of the consumption of OL extract should be further studied in order to clarify a safe and well-tolerated dose for administration in humans, although the frequent consumption of olives and olive oil by humans, which contain many of the same components, has not shown any adverse events to date.

2. MOLECULAR DOCKING AS A TOOL FOR THE DISCOVERY OF POTENTIALLY BIOACTIVE METABOLITES

Biochemical pathways of energy metabolism have, as main objectives, the degradation of molecules to obtain energy (catabolism), the synthesis of simple molecules that polymerize, giving rise to macromolecules (anabolism) and the elimination of molecules that are toxic waste. These biochemical processes involve a large number of enzyme-catalyzed reactions that allow the transformation of numerous metabolites. The Kyoto Encyclopedia of Genes and Genomes contains annotations of 10,476 biochemical reactions and 17,931 metabolites and other small molecules [169]. With these numbers, it is easy to imagine the multiple possibilities of bioactive compounds to modulate the activity of enzymes involved in metabolic processes, either by acting directly on their catalytic or regulatory sites or by modifying their levels of expression. Human diseases, such as diabetes, obesity, neurodegeneration or cancer, lead to metabolic alterations through the modulation of certain key regulatory metabolic pathways of the cell [14, 28, 65, 118-120, 170]. In this context, the development of bioactive compounds that can counteract metabolic alterations has great therapeutic interest. Natural products have traditionally been a source of compounds for the development of drugs and having solved many of the technical problems associated with screening of these products in tests of high performance against specific molecular targets, there is a revived interest in them by pharmaceutical companies [171]. Natural products, such as polyphenols possess a high degree of stereochemistry and are usually substrates of various transport systems that can release them intracellularly, where they must interact with their

molecular target (metabolite-likeness property) [172]. In practice, it is economically impossible to test libraries of millions of compounds looking for bioactive molecules, and many compounds are not commercially available in the quantities suitable for *in vitro* experiments. For this reason, it is necessary to implement a guided search by computational methods to reduce the vast chemical space to a number of compounds that is experimentally approachable.

Metabolite identification is one of the key challenges in current mass spectrometry-based untargeted metabolomics studies. Identifying metabolites derived from plant polyphenols is a necessary task to establish candidate compounds that may interact with their cell targets and then can be correlated with the salutary effects of plant compounds in human health. Nevertheless, this may become a difficult task due to its high complexity in terms of protein targets and candidate compounds. These mass spectrometry-based metabolomics studies are generating an increasing number of metabolites whose data are incorporated into the main metabolomic databases: Human Metabolome DataBase (HMDB), Madison Metabolomics Consortium Database (MMCD), Metlin, and LIPID MAPS.

A simulated physiological approach for elucidating the molecular mechanisms of polyphenols uses computational techniques to search for protein-ligand interactions (Fig. **5**). Molecular docking techniques are widely used for the study of protein-ligand interactions. They enable the virtual screening of millions of compounds against known molecular targets with a reasonable economic cost. Docking experiments usually start with the crystallographic structure of a protein of medical interest and can predict bound conformations and the binding free energy of small molecules to the catalytic or allosteric binding sites [173]. Alternatively, when there are no high-resolution structures of a protein of interest, it is very useful to model its structure by homology to the resolved structures of other proteins with a minimum of 30% sequence identity [174]. After choosing the target protein and its possible binding sites for possible modulation of its activity by ligands, the next step is to have a chemical library with abundant structural variety in electronic format (Fig. **5**). The chemical structures of highly diverse structure compounds are available in different searchable databases, and these compounds can be used to perform virtual screening [175]. In some of these databases, we can also find valuable information on the chemical suppliers of these products, bearing in mind that, in later stages, we will need to have these compounds available for *in vitro* or *in vivo* testing to demonstrate their ability to modulate the activity of our protein of interest.

The computing time required to conduct molecular docking experiments is directly related to not only the size of the library of compounds to be tested but also to the precision of the virtual screening methods and the structural complexity of the compounds to be tested. Fast docking methods at atomic resolution that consider the receptor to be rigid (*i.e.*, protein) with flexible ligands require a few minutes (5-20 min) per ligand [176]. In contrast, molecular dynamics-based approaches require hundreds or thousands of hours per ligand [177]. We can also reduce the computation time if we perform a previous selection of the ligands. We must not forget that the final success of a modulator candidate is directly related to factors such as absorption, biodistribution, the rate at which it is metabolized, excretion, and toxicity (*i.e.*, ADMET profile) upon its administration [178]. Therefore, only compounds with an optimum ADMET profile will be evaluated *in silico* (Fig. **5**). We can consider different ADMET criteria for this selection: calculated logP value must not be greater than 5.0, calculated logS (logarithm base 10 of the solubility measured in mol/L) must be greater than -4.0, fragment-based druglikeness ≥ 0, drugscore ≥ 0.5, molecular weight ≤ 500, five or fewer hydrogen bond donor sites, and ten or fewer

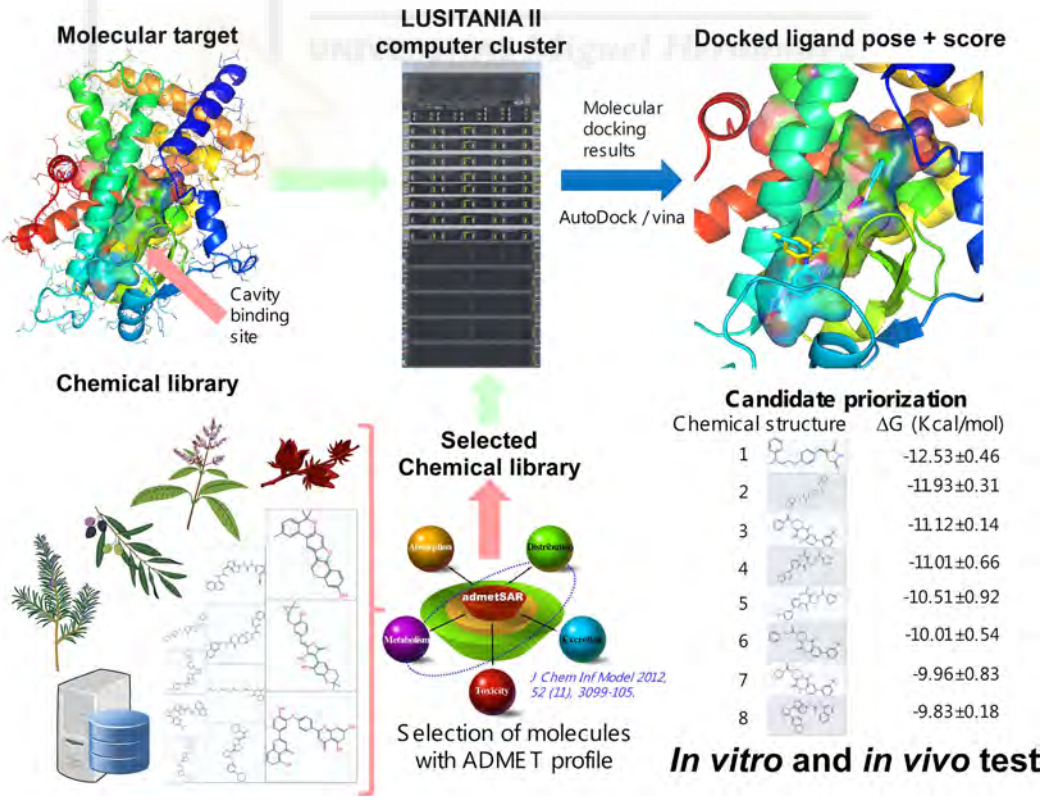

Fig. (5). Schematic representation of a virtual screening process of a phenolic compounds chemical library against the PPAR-gamma receptor structure using molecular docking techniques. On the one hand, a chemical library containing chemical structures to be screened must be built and asked to follow some ADMET criteria. On the other hand, molecular target high resolution structures must be obtained. Once both steps have been fulfilled, using computer clusters with a high computation capability, target structures are challenged with the chemical library to find the best docking results according ΔG binding values. Finally, all tested compounds are prioritized as a function of minor ΔG and proposed as candidates for subsequent *in vitro* and *in vivo* tests.

hydrogen bond acceptor sites [179, 180]. To facilitate the reader's understanding, we share the following data: a library of one million compounds, previously selected with ADMET criteria, can be tested *in silico* with molecular docking experiments, using AutoDock/vina [176] software, in one week. We are running similar calculations under a computing cluster with a Linux operating system that uses 20 computing nodes with 10 processors per node (LUSITANIA II cluster at the Research, Technological Innovation and Supercomputing Center of Extremadura-CenitS and COMPUTAEX). Obviously, the volume of data generated makes it necessary for the user to develop his own scripts to analyze this information. We use Python scripts to select the compounds with the lowest calculated free energy (ΔG, Kcal/mol) as possible modulators of different protein targets [179, 180].

We have applied these *in silico* screening techniques to select compounds from two sources, a library of olive polyphenols derived from OL extract and a library of plant-derived phenolic compounds and metabolites, as possible modulators of two proteins of pharmacological interest: the transcription factor receptor PPAR-gamma [179] and the AMP-activated protein kinase (AMPK) [181] (Fig. **5**). The cellular energy state is detected by various dynamic mechanisms that regulate the balance between catabolism and anabolism. AMPK is a cellular fuel sensitive kinase activated in deficient bioenergetic states that are caused by a lack of nutrients or hypoxia [182]. AMPK-phosphorylation of different proteins promotes inactivation of the energy-consuming pathways and activates the catabolism of fatty acids and other fuels. Therefore, this mechanism increases the available energy for the cell and decreases its content of reserves. In an attempt to identify the molecular targets of olive polyphenols derived from OL extract, our research group has recently reported the AMPK modulatory activity of olive phenolic compounds of an OL extract. In this paper, we demonstrated that OL extract (enriched in polyphenolic compounds) decreased the intracellular lipid accumulation through AMPK-dependent mechanisms in hypertrophic adipocytes [181]. A bioassay-guided approach was utilized to isolate the fractions from the extract that exhibited AMPK modulatory activity on the adipocyte cell model and to further identify the potential compounds responsible for such activity. Molecular docking experiments revealed that several polyphenols may be AMPK-gamma subunit modulators: secoiridoids, cinnamic acids, phenylethanoids and phenylpropanoids, flavonoids and lignans. Ongoing research is focused on corroborating the direct effect of these compounds and their metabolites on AMPK.

Thiazolidinediones (TZDs) are full agonists of the human PPARγ receptor, a nuclear soluble protein that, after binding to the agonist heterodimerize with the retinoic X receptor, recruits different transcriptional cofactors that bind to the promoter region of the fuel-related target genes and initiate their transcription. These synthetic drugs have been used in clinical practice to treat type 2 diabetes, and they effectively lower blood glucose levels and improve insulin sensitivity. However, their administration has been associated with severe side effects, and this makes this protein a target of interest in the search for new, safe modulators using *in silico* screening techniques. In our first paper [179], we performed molecular docking experiments with a big library of plant-derived phenolic compounds and metabolites to select 83 candidates with free energy variations ranging from -10.0±0.6 to -11.0±0.6 kcal/mol. Some of these compounds were tested *in vitro*, and the best candidates displayed encouraging bioactivities (manuscript in preparation).

CONCLUSION

Hibiscus sabdariffa, *Lippia citriodora*, *Rosmarinus officinalis* and *Olea europaea* are four medicinal plants with food uses that also represent a valuable source of the most representative plant bioactive polyphenols. There is abundant data about the biological and pharmacological effects of extracts derived from these plants as well as their isolated compounds, most of them by using *in vitro* or animal models, but human data are scarce. Several studies have reported the complex metabolism that its phenolic components undergo after ingestion in animal models and, in some cases, in humans. Available data provide information on the metabolites that reach the circulating plasma, but advanced research using targeted metabolomics should be utilized to elucidate the final intracellular metabolites that interact with the molecular targets and their associated biomarkers [183, 184].

In this review, we have compiled our own data as well as that of others on the wide biological effects and the metabolites of extracts derived from the abovementioned plants in cell and animal models, as well as in human trials. Most studies support that plant polyphenols exhibit rapid gut absorption, are highly metabolized through intestinal and hepatic cells or by colonic microflora and undergo mainly deglycosylations, glucuronidations, sulfations and methylations. The low bioavailability of the main phenolic compounds of these extracts has been reported, leading to plasma metabolite concentrations within the low micromolar range. Despite these low concentrations, the salutary effects of the consumption of these plants have been well documented in animal models and in humans. Biotransformation of these metabolites by target tissues deserves special attention in the future to find the final effectors of these metabolic effects and their protein targets. Molecular docking techniques provide a powerful method for virtually screening a large number of metabolites on selected protein targets in order to elucidate their potential mechanisms. The pleiotropic character of the polyphenols and its metabolites and the observed effect at multiple targets have led to propose that epigenetic regulation might be involved.

In summary, to fully elucidate the molecular mechanisms of plant polyphenols, targeted metabolomics in plasma and tissue samples, virtual screening on protein and membrane targets and cellular models using metabolites must be combined. This would also enable us to design more effective polyphenolic extracts or new drug candidates for pharmaceutical uses. Finally, most of the studies demonstrate that these plants are generally well-tolerated by humans. Nevertheless, further toxicological studies should be conducted on a chronic or subchronic basis to determine their effects when consumed in a concentrated form for medicinal purposes.

LIST OF ABBREVIATIONS

ACE	=	Angiotensin I-converting enzyme
AMPK	=	5'-adenosine monophosphate-activated protein kinase
DAD	=	Diode Array Detection
ESI	=	Electrospray
EVOO	=	Extra Virgin Olive Oil
GSH	=	Glutathione
HPLC	=	high-performance Liquid Chromatography
HS	=	*Hibiscus sabdariffa*
LC	=	*Lippia citriodora*
LDL	=	low-density Lipoprotein
LDLr	=	LDL Receptor
LPS	=	Lipopolysaccharide
MS	=	Mass Spectrometry
OL	=	Olive Leaf
ROS	=	Reactive Oxygen Species
TOF	=	Time-of-Flight

CONSENT FOR PUBLICATION

Not applicable.

CONFLICT OF INTEREST

The authors declare no conflict of interest, financial or otherwise.

ACKNOWLEDGEMENTS

Some of the investigations expressed in this review have been partially or fully supported by competitive public grants from the following institutions: AGL2011-29857-C03-03 and IDI-20120751 grants (Spanish Ministry of Science and Innovation), projects *AGL2015-67995-C3-1-R, AGL2015-67995-C3-2-R, AGL2015-67995-C3-3-R, Torres Quevedo grants PTQ-13-06429 and PTQ-14-07243 from the Spanish Ministry of Economy and Competitiveness (MINECO);* PROMETEO/2012/007, *PROMETEO/2016/006,* ACOMP/2013/093, ACIF/2010/162 and *ACIF/2016/230 grants from Generalitat Valenciana and CIBER (CB12/03/30038, Fisiopatologia de la Obesidad y la Nutricion, CIBERobn, Instituto de Salud Carlos III).*

REFERENCES

[1] Duthie, G. G.; Gardner, P. T.; Kyle, J. A. Plant polyphenols: are they the new magic bullet? *Proc. Nutr. Soc.*, **2003**, *62* (3), 599-603.

[2] Whiting, D. A. Natural phenolic compounds 1900-2000: a bird's eye view of a century's chemistry. *Nat. Prod. Rep.*, **2001**, *18* (6), 583-606.

[3] Manach, C.; Scalbert, A.; Morand, C.; Remesy, C.; Jimenez, L. Polyphenols: food sources and bioavailability. *Am. J. Clin. Nutr.*, **2004**, *79* (5), 727-747.

[4] Manach, C.; Williamson, G.; Morand, C.; Scalbert, A.; Remesy, C. Bioavailability and bioefficacy of polyphenols in humans. I. Review of 97 bioavailability studies. *Am. J. Clin. Nutr.*, **2005**, *81* (1 Suppl), 230s-242s.

[5] Scalbert, A.; Williamson, G. Dietary intake and bioavailability of polyphenols. *J. Nutr.*, **2000**, *130* (8S Suppl), 2073s-2085s.

[6] Mukhtar, H.; Ahmad, N. Tea polyphenols: prevention of cancer and optimizing health. *Am. J. Clin. Nutr.,* **2000**, *71* (6 Suppl), 1698S-1702S, discussion 1703S-1704S.

[7] Barrajon-Catalan, E.; Fernandez-Arroyo, S.; Saura, D.; Guillen, E.; Fernandez-Gutierrez, A.; Segura-Carretero, A.; Micol, V. *Cistaceae* aqueous extracts containing ellagitannins show antioxidant and antimicrobial capacity, and cytotoxic activity against human cancer cells. *Food Chem. Toxicol.*, **2010**, *48* (8-9), 2273-2282.

[8] Loke, W. M.; Proudfoot, J. M.; Hodgson, J. M.; McKinley, A. J.; Hime, N.; Magat, M.; Stocker, R.; Croft, K. D. Specific dietary polyphenols attenuate atherosclerosis in apolipoprotein E-knockout mice by alleviating inflammation and endothelial dysfunction. *Arterioscler. Thromb. Vasc. Biol.*, **2010**, *30* (4), 749-757.

[9] Daglia, M. Polyphenols as antimicrobial agents. *Curr. Opin. Biotech.*, **2012**, *23* (2), 174-181.

[10] Negishi, H.; Xu, J. W.; Ikeda, K.; Njelekela, M.; Nara, Y.; Yamori, Y. Black and green tea polyphenols attenuate blood pressure increases in stroke-prone spontaneously hypertensive rats. *J. Nutr.*, **2004**, *134* (1), 38-42.

[11] Vendrame, S.; Klimis-Zacas, D. Anti-inflammatory effect of anthocyanins via modulation of nuclear factor-kappaB and mitogen-activated protein kinase signaling cascades. *Nutr. Rev.*, **2015**, *73* (6), 348-358.

[12] Li, A. N.; Li, S.; Zhang, Y. J.; Xu, X. R.; Chen, Y. M.; Li, H. B. Resources and biological activities of natural polyphenols. *Nutrients*, **2014**, *6* (12), 6020-6047.

[13] Beltran-Debon, R.; Rull, A.; Rodriguez-Sanabria, F.; Iswaldi, I.; Herranz-Lopez, M.; Aragones, G.; Camps, J.; Alonso-Villaverde, C.; Menendez, J. A.; Micol, V.; Segura-Carretero, A.; Joven, J. Continuous administration of polyphenols from aqueous rooibos (*Aspalathus linearis*) extract ameliorates dietary-induced metabolic disturbances in hyperlipidemic mice. *Phytomedicine*, **2011**, *18* (5), 414-424.

[14] Barrajon-Catalan, E.; Herranz-Lopez, M.; Joven, J.; Segura-Carretero, A.; Alonso-Villaverde, C.; Menendez, J. A.; Micol, V. Molecular promiscuity of plant polyphenols in the management of age-related diseases: far beyond their antioxidant properties. *Adv. Exp. Med. Biol.*, **2014**, *824*, 141-159.

[15] Fernandez-Arroyo, S.; Herranz-Lopez, M.; Beltran-Debon, R.; Borras-Linares, I.; Barrajon-Catalan, E.; Joven, J.; Fernandez-Gutierrez, A.; Segura-Carretero, A.; Micol, V. Bioavailability study of a polyphenol-enriched extract from *Hibiscus sabdariffa* in rats and associated antioxidant status. *Mol. Nutr. Food. Res.*, **2012**, *56* (10), 1590-1595.

[16] Quirantes-Pine, R.; Herranz-Lopez, M.; Funes, L.; Borras-Linares, I.; Micol, V.; Segura-Carretero, A.; Fernandez-Gutierrez, A. Phenylpropanoids and their metabolites are the major compounds responsible for blood-cell protection against oxidative stress after administration of *Lippia citriodora* in rats. *Phytomedicine*, **2013**, *20* (12), 1112-1118.

[17] Cassidy, A.; Brown, J. E.; Hawdon, A.; Faughnan, M. S.; King, L. J.; Millward, J.; Zimmer-Nechemias, L.; Wolfe, B.; Setchell, K. D. Factors affecting the bioavailability of soy isoflavones in humans after ingestion of physiologically relevant levels from different soy foods. *J. Nutr.*, **2006**, *136* (1), 45-51.

[18] Joven, J.; Micol, V.; Segura-Carretero, A.; Alonso-Villaverde, C.; Menéndez, J. A.; Aragonès, G.; Barrajón-Catalán, E.; Beltrán-Debón, R.; Camps, J.; Cufí, S.; Fernández-Arroyo, S.; Fernández-Gutiérrez, A.; Guillén, E.; Herranz-López, M.; Iswaldi, I.; Lozano-Sánchez, J.; Martin-Castillo, B.; Oliveras-Ferraros, C.; Pérez-Sánchez, A.; Rodríguez-Gallego, E.; Rull, A.; Saura, D.; Vázquez-Martín, A. Polyphenols and the modulation of gene expression pathways: can we eat our way out of the danger of chronic disease? *Crit. Rev. Food Sci. Nutr.*, **2014**, *54* (8), 985-1001.

[19] Morton, J. F. Roselle In: *Fruits of Warm Climates*; Creative Resource Systems: Miami, **1987**; pp. 281-286.

[20] Serban, C.; Sahebkar, A.; Ursoniu, S.; Andrica, F.; Banach, M. Effect of sour tea (*Hibiscus sabdariffa* L.) on arterial hypertension: a systematic review and meta-analysis of randomized controlled trials. *J. Hypertens.*, **2015**, *33* (6), 1119-1127.

[21] Joven, J.; March, I.; Espinel, E.; Fernandez-Arroyo, S.; Rodriguez-Gallego, E.; Aragones, G.; Beltran-Debon, R.; Alonso-Villaverde, C.; Rios, L.; Martin-Paredero, V.; Menendez, J. A.; Micol, V.; Segura-Carretero, A.; Camps, J. *Hibiscus sabdariffa* extract lowers blood pressure and improves endothelial function. *Mol. Nutr. Food. Res.*, **2014**, *58* (6), 1374-1378.

[22] Reanmongkol, W.; Itharat, A. Antipyretic activity of the extracts of *Hibiscus sabdariffa* calyces L. in experimental animals. *Songklanakarin J. Sci. Technol.*, **2007**, *29* (1), 29-38.

[23] Beltran-Debon, R.; Alonso-Villaverde, C.; Aragones, G.; Rodriguez-Medina, I.; Rull, A.; Micol, V.; Segura-Carretero, A.; Fernandez-Gutierrez, A.; Camps, J.; Joven, J. The aqueous extract of *Hibiscus sabdariffa* calices modulates the production of monocyte chemoattractant protein-1 in humans. *Phytomedicine*, **2010**, *17* (3-4), 186-191.

[24] Chou, S. T.; Lo, H. Y.; Li, C. C.; Cheng, L. C.; Chou, P. C.; Lee, Y. C.; Ho, T. Y.; Hsiang, C. Y. Exploring the effect and mechanism of *Hibiscus sabdariffa* on urinary tract infection and experimental renal inflammation. *J. Ethnopharmacol.*, **2016**, *194*, 617-625.

[25] Seujange, Y.; Leelahavanichkul, A.; Yisarakun, W.; Khawsuk, W.; Meepool, A.; Phamonleatmongkol, P.; Saechau, W.; Onlamul, W.; Tantiwarattanatikul, P.; Oonsook, W.; Eiam-Ong, S. *Hibiscus sabdariffa* Linnaeus aqueous extracts attenuate the progression of renal injury in 5/6 nephrectomy rats. *Ren. Fail.*, **2013**, *35* (1), 118-125.

[26] Villalpando-Arteaga, E. V.; Mendieta-Condado, E.; Esquivel-Solis, H.; Canales-Aguirre, A. A.; Galvez-Gastelum, F. J.; Mateos-Diaz, J. C.; Rodriguez-Gonzalez, J. A.; Marquez-Aguirre, A. L. *Hibiscus sabdariffa* L. aqueous extract attenuates hepatic steatosis through down-regulation of PPAR-gamma and SREBP-1c in diet-induced obese mice. *Food Funct.*, **2013,** *4* (4), 618-626.

[27] Adeyemi, D. O.; Ukwenya, V. O.; Obuotor, E. M.; Adewole, S. O. Anti-hepatotoxic activities of *Hibiscus sabdariffa* L. in animal model of streptozotocin diabetes-induced liver damage. *BMC Complement. Altern. Med.*, **2014**, *14*, 277.

[28] Joven, J.; Espinel, E.; Rull, A.; Aragones, G.; Rodriguez-Gallego, E.; Camps, J.; Micol, V.; Herranz-Lopez, M.; Menendez, J. A.; Borras, I.; Segura-Carretero, A.; Alonso-Villaverde, C.; Beltran-Debon, R. Plant-derived polyphenols regulate expression of miRNA paralogs miR-103/107 and miR-122 and prevent diet-induced fatty liver disease in hyperlipidemic mice. *Biochim. Biophys. Acta*, **2012**, *1820* (7), 894-899.

[29] Chang, H. C.; Peng, C. H.; Yeh, D. M.; Kao, E. S.; Wang, C. J. *Hibiscus sabdariffa* extract inhibits obesity and fat accumulation, and improves liver steatosis in humans. *Food. Funct.*, **2014**, *5* (4), 734-739.

[30] Alarcon-Aguilar, F. J.; Zamilpa, A.; Perez-Garcia, M. D.; Almanza-Perez, J. C.; Romero-Nunez, E.; Campos-Sepulveda, E. A.; Vazquez-Carrillo, L. I.; Roman-Ramos, R. Effect of *Hibiscus sab-*

dariffa on obesity in MSG mice. *J. Ethnopharmacol.*, **2007**, *114* (1), 66-71.

[31] Fernandez-Arroyo, S.; Rodriguez-Medina, I.; Beltran-Debon, R.; Pasini, F.; Joven, J.; Micol, V.; Segura-Carretero, A.; Fernandez-Gutierrez, A. Quantification of the polyphenolic fraction and *in vitro* antioxidant and *in vivo* anti-hyperlipemic activities of *Hibiscus sabdariffa* aqueous extract. *Food Res. Int.*, **2011**, *44* (5), 1490-1495.

[32] Zhen, J.; Villani, T. S.; Guo, Y.; Qi, Y.; Chin, K.; Pan, M. H.; Ho, C. T.; Simon, J. E.; Wu, Q., Phytochemistry, antioxidant capacity, total phenolic content and anti-inflammatory activity of *Hibiscus sabdariffa* leaves. *Food Chem.*, **2016**, *190*, 673-680.

[33] Herranz-Lopez, M.; Fernandez-Arroyo, S.; Perez-Sanchez, A.; Barrajon-Catalan, E.; Beltran-Debon, R.; Menendez, J. A.; Alonso-Villaverde, C.; Segura-Carretero, A.; Joven, J.; Micol, V. Synergism of plant-derived polyphenols in adipogenesis: perspectives and implications. *Phytomedicine*, **2012**, *19* (3-4), 253-261.

[34] Malacrida, A.; Maggioni, D.; Cassetti, A.; Nicolini, G.; Cavaletti, G.; Miloso, M. Antitumoral effect of *Hibiscus sabdariffa* on human squamous cell carcinoma and multiple myeloma cells. *Nutr. Cancer*, **2016**, *68* (7), 1161-1170.

[35] Chen, C. C.; Hsu, J. D.; Wang, S. F.; Chiang, H. C.; Yang, M. Y.; Kao, E. S.; Ho, Y. C.; Wang, C. J. *Hibiscus sabdariffa* extract inhibits the development of atherosclerosis in cholesterol-fed rabbits. *J. Agric. Food. Chem.*, **2003**, *51* (18), 5472-5477.

[36] Chang, Y. C.; Huang, K. X.; Huang, A. C.; Ho, Y. C.; Wang, C. J. Hibiscus anthocyanins-rich extract inhibited LDL oxidation and oxLDL-mediated macrophages apoptosis. *Food Chem. Toxicol.,* **2006**, *44* (7), 1015-1023.

[37] Hassan, S. T.; Berchova, K.; Sudomova, M. Antimicrobial, antiparasitic and anticancer properties of *Hibiscus sabdariffa* (L.) and its phytochemicals: *in vitro* and *in vivo* studies. *Ceska Slov. Farm.*, **2016**, *65* (1), 10-14.

[38] Rodriguez-Medina, I. C.; Beltran-Debon, R.; Molina, V. M.; Alonso-Villaverde, C.; Joven, J.; Menendez, J. A.; Segura-Carretero, A.; Fernandez-Gutierrez, A. Direct characterization of aqueous extract of *Hibiscus sabdariffa* using HPLC with diode array detection coupled to ESI and ion trap MS. *J. Sep. Sci.*, **2009**, *32* (20), 3441-3448.

[39] Muller, B. M.; Franz, G. Chemical structure and biological activity of polysaccharides from *Hibiscus sabdariffa*. *Planta Med.*, **1992**, *58* (1), 60-67.

[40] Kao, E. S.; Hsu, J. D.; Wang, C. J.; Yang, S. H.; Cheng, S. Y.; Lee, H. J. Polyphenols extracted from *Hibiscus sabdariffa* L. inhibited lipopolysaccharide-induced inflammation by improving antioxidative conditions and regulating cyclooxygenase-2 expression. *Biosci. Biotechnol. Biochem.,* **2009,** *73* (2), 385-390.

[41] Herrera-Arellano, A.; Miranda-Sanchez, J.; Avila-Castro, P.; Herrera-Alvarez, S.; Jimenez-Ferrer, J. E.; Zamilpa, A.; Roman-Ramos, R.; Ponce-Monter, H.; Tortoriello, J. Clinical effects produced by a standardized herbal medicinal product of *Hibiscus sabdariffa* on patients with hypertension. A randomized, double-blind, lisinopril-controlled clinical trial. *Planta Med.*, **2007**, *73* (1), 6-12.

[42] Nwachukwu, D. C.; Aneke, E.; Nwachukwu, N. Z.; Obika, L. F.; Nwagha, U. I.; Eze, A. A. Effect of *Hibiscus sabdariffa* on blood pressure and electrolyte profile of mild to moderate hypertensive Nigerians: A comparative study with hydrochlorothiazide. *Niger J. Clin. Pract.*, **2015**, *18* (6), 762-770.

[43] Ajiboye, T. O.; Raji, H. O.; Adeleye, A. O.; Adigun, N. S.; Giwa, O. B.; Ojewuyi, O. B.; Oladiji, A. T. *Hibiscus sabdariffa* calyx palliates insulin resistance, hyperglycemia, dyslipidemia and oxidative rout in fructose-induced metabolic syndrome rats. *J. Sci. Food Agric.*, **2016**, *96* (5), 1522-1531.

[44] Gurrola-Diaz, C. M.; Garcia-Lopez, P. M.; Sanchez-Enriquez, S.; Troyo-Sanroman, R.; Andrade-Gonzalez, I.; Gomez-Leyva, J. F. Effects of *Hibiscus sabdariffa* extract powder and preventive treatment (diet) on the lipid profiles of patients with metabolic syndrome (MeSy). *Phytomedicine*, **2010**, *17* (7), 500-505.

[45] Frank, T.; Janssen, M.; Netzel, M.; Strass, G.; Kler, A.; Kriesl, E.; Bitsch, I., Pharmacokinetics of anthocyanidin-3-glycosides following consumption of *Hibiscus sabdariffa* L. extract. *J. Clin. Pharmacol.*, **2005**, *45* (2), 203-210.

[46] Borras-Linares, I.; Herranz-Lopez, M.; Barrajon-Catalan, E.; Arraez-Roman, D.; Gonzalez-Alvarez, I.; Bermejo, M.; Fernandez Gutierrez, A.; Micol, V.; Segura-Carretero, A. Permeability study of polyphenols derived from a phenolic-enriched *Hibiscus sabdariffa* extract by UHPLC-ESI-UHR-Qq-TOF-MS. *Int. J. Mol. Sci.*, **2015**, *16* (8), 18396-18411.

[47] del Mar Contreras, M.; Borrás-Linares, I.; Herranz-López, M.; Micol, V.; Segura-Carretero, A. Further exploring the absorption and enterocyte metabolism of quercetin forms in the Caco-2 model using nano-LC-TOF-MS. *Electrophoresis*, **2016**, *37* (7-8), 998-1006.

[48] Herranz-López, M.; Borrás-Linares, I.; Olivares-Vicente, M.; Gálvez, J.; Segura-Carretero, A.; Micol, V. Correlation between the cellular metabolism of quercetin and its glucuronide metabolite and oxidative stress in hypertrophied 3T3-L1 adipocytes. *Phytomedicine*, **2017**, *25*, 25-28.

[49] Frank, T.; Netzel, G.; Kammerer, D. R.; Carle, R.; Kler, A.; Kriesl, E.; Bitsch, I.; Bitsch, R.; Netzel, M. Consumption of *Hibiscus sabdariffa* L. aqueous extract and its impact on systemic antioxidant potential in healthy subjects. *J. Sci. Food Agric.*, **2012**, *92* (10), 2207-2218.

[50] Akindahunsi, A. A.; Olaleye, M. T. Toxicological investigation of aqueous-methanolic extract of the calyces of *Hibiscus sabdariffa* L. *J. Ethnopharmacol.*, **2003**, *89* (1), 161-164.

[51] Fakeye, T. O.; Pal, A.; Bawankule, D. U.; Yadav, N. P.; Khanuja, S. P. Toxic effects of oral administration of extracts of dried calyx of *Hibiscus sabdariffa* Linn. (Malvaceae). *Phytother. Res.*, **2009**, *23* (3), 412-416.

[52] Sireeratawong, S.; Itharat, A.; Khonsung, P.; Lertprasertsuke, N.; Jaijoy, K. Toxicity studies of the water extract from the calyces of *Hibiscus sabdariffa* L. in rats. *Afr. J. Tradit. Complement. Altern. Med.*, **2013**, *10* (4), 122-127.

[53] Argyropoulou, C.; Daferera, D.; Tarantilis, P. A.; Fasseas, C.; Polissiou, M. Chemical composition of the essential oil from leaves of *Lippia citriodora* H.B.K. (Verbenaceae) at two developmental stages. *Biochem. Syst. Ecol.*, **2007**, *35* (12), 831–837.

[54] Bilia, A. R.; Giomi, M.; Innocenti, M.; Gallori, S.; Vincieri, F. F. HPLC-DAD-ESI-MS analysis of the constituents of aqueous preparations of verbena and lemon verbena and evaluation of the antioxidant activity. *J. Pharm. Biomed. Anal.*, **2008**, *46* (3), 463-470.

[55] Funes, L.; Fernández-Arroyo, S.; Laporta, O.; Pons, A.; Roche, E.; Segura-Carretero, A.; Fernández-Gutiérrez, A.; Micol, V. Correlation between plasma antioxidant capacity and verbascoside levels in rats after oral administration of lemon verbena extract. *Food Chem.*, **2009**, *117* (4), 589-598.

[56] Liu, M. J.; Li, J. X.; Guo, H. Z.; Lee, K. M.; Qin, L.; Chan, K. M. The effects of verbascoside on plasma lipid peroxidation level and erythrocyte membrane fluidity during immobilization in rabbits: a time course study. *Life Sci.*, **2003**, *73* (7), 883-892.

[57] Wong, I. Y.; He, Z. D.; Huang, Y.; Chen, Z. Y. Antioxidative activities of phenylethanoid glycosides from *Ligustrum purpurascens*. *J. Agric. Food. Chem.*, **2001**, *49* (6), 3113-3119.

[58] Quirantes-Pine, R.; Funes, L.; Micol, V.; Segura-Carretero, A.; Fernandez-Gutierrez, A. High-performance liquid chromatography with diode array detection coupled to electrospray time-of-flight and ion-trap tandem mass spectrometry to identify phenolic compounds from a lemon verbena extract. *J. Chromatogr. A*, **2009**, *1216* (28), 5391-5397.

[59] Quirantes-Pine, R.; Arraez-Roman, D.; Segura-Carretero, A.; Fernandez-Gutierrez, A. Characterization of phenolic and other polar compounds in a lemon verbena extract by capillary electrophoresis-electrospray ionization-mass spectrometry. *J. Sep. Sci.*, **2010**, *33* (17-18), 2818-2827.

[60] Pascual, M. E.; Slowing, K.; Carretero, E.; Sanchez Mata, D.; Villar, A. Lippia: traditional uses, chemistry and pharmacology: a review. *J Ethnopharmacol.*, **2001**, *76* (3), 201-214.

[61] Diaz, A. M.; Abad, M. J.; Fernandez, L.; Silvan, A. M.; De Santos, J.; Bermejo, P., Phenylpropanoid glycosides from *Scrophularia scorodonia*: *in vitro* anti-inflammatory activity. *Life Sci.*, **2004**, *74* (20), 2515-2526.

[62] Avila, J. G.; de Liverant, J. G.; Martinez, A.; Martinez, G.; Munoz, J. L.; Arciniegas, A.; Romo de Vivar, A. Mode of action of *Buddleja cordata* verbascoside against *Staphylococcus aureus*. *J Ethnopharmacol.*, **1999**, *66* (1), 75-78.

[63] Ohno, T.; Inoue, M.; Ogihara, Y.; Saracoglu, I., Antimetastatic activity of acteoside, a phenylethanoid glycoside. *Biol. Pharm. Bull.*, **2002,** *25* (5), 666-668.

[64] Funes, L.; Laporta, O.; Cerdán-Calero, M.; Micol, V. Effects of verbascoside, a phenylpropanoid glycoside from lemon verbena, on

phospholipid model membranes. *Chem. Phys. Lipids,* **2010**, *163* (2), 190-199.

[65] Herranz-López, M.; Barrajón-Catalán, E.; Segura-Carretero, A.; Menéndez, J. A.; Joven, J.; Micol, V. Lemon verbena (*Lippia citriodora)* polyphenols alleviate obesity-related disturbances in hypertrophic adipocytes through AMPK-dependent mechanisms. *Phytomedicine*, **2015**, *22* (6), 605-614.

[66] Wu, Y. T.; Lin, L. C.; Sung, J. S.; Tsai, T. H. Determination of acteoside in *Cistanche deserticola* and *Boschniakia rossica* and its pharmacokinetics in freely-moving rats using LC-MS/MS. *J. Chromatogr. B Analyt. Technol. Biomed. Life Sci.*, **2006**, *844* (1), 89-95.

[67] Quirantes-Pine, R.; Verardo, V.; Arraez-Roman, D.; Fernandez-Arroyo, S.; Micol, V.; Caboni, M. F.; Segura-Carretero, A.; Fernandez-Gutierrez, A. Evaluation of different extraction approaches for the determination of phenolic compounds and their metabolites in plasma by nanoLC-ESI-TOF-MS. *Anal. Bioanal. Chem.*, **2012**, *404* (10), 3081-3090.

[68] Felgines, C.; Fraisse, D.; Besson, C.; Vasson, M. P.; Texier, O. Bioavailability of lemon verbena (*Aloysia triphylla*) polyphenols in rats: impact of colonic inflammation. *Br. J. Nutr.*, **2014**, *111* (10), 1773-1781.

[69] Funes, L.; Carrera-Quintanar, L.; Cerdan-Calero, M.; Ferrer, M. D.; Drobnic, F.; Pons, A.; Roche, E.; Micol, V. Effect of lemon verbena supplementation on muscular damage markers, proinflammatory cytokines release and neutrophils' oxidative stress in chronic exercise. *Eur. J. Appl. Physiol.*, **2011**, *111* (4), 695-705.

[70] Carrera-Quintanar, L.; Funes, L.; Viudes, E.; Tur, J.; Micol, V.; Roche, E.; Pons, A., Antioxidant effect of lemon verbena extracts in lymphocytes of university students performing aerobic training program. *Scand. J. Med. Sci. Sports*, **2012**, *22* (4), 454-461.

[71] Carrera-Quintanar, L.; Funes, L.; Vicente-Salar, N.; Blasco-Lafarga, C.; Pons, A.; Micol, V.; Roche, E. Effect of polyphenol supplements on redox status of blood cells: a randomized controlled exercise training trial. *Eur. J. Nutr.*, **2015**, *54* (7), 1081-1093.

[72] Mestre-Alfaro, A.; Ferrer, M. D.; Sureda, A.; Tauler, P.; Martinez, E.; Bibiloni, M. M.; Micol, V.; Tur, J. A.; Pons, A. Phytoestrogens enhance antioxidant enzymes after swimming exercise and modulate sex hormone plasma levels in female swimmers. *Eur. J. Appl. Physiol.*, **2011**, *111* (9), 2281-2294.

[73] Martinez-Rodriguez, A.; Moya, M.; Vicente-Salar, N.; Brouzet, T.; Carrera-Quintanar, L.; Cervello, E.; Micol, V.; Roche, E. Biochemical and psychological changes in university students performing aerobic exercise and consuming lemon verbena extracts. *Curr. Top. Nutraceut. R.*, **2015,** *13* (2), 95-102.

[74] Caturla, N.; Funes, L.; Perez-Fons, L.; Micol, V. A randomized, double-blinded, placebo-controlled study of the effect of a combination of lemon verbena extract and fish oil omega-3 fatty acid on joint management. *J. Altern. Complement. Med.*, **2011**, *17* (11), 1051-1063.

[75] Mauriz, E.; Vallejo, D.; Tunon, M. J.; Rodriguez-Lopez, J. M.; Rodriguez-Perez, R.; Sanz-Gomez, J.; Garcia-Fernandez Mdel, C. Effects of dietary supplementation with lemon verbena extracts on serum inflammatory markers of multiple sclerosis patients. *Nutr. Hosp.*, **2014**, *31* (2), 764-771.

[76] Miroddi, M.; Calapai, G.; Isola, S.; Minciullo, P. L.; Gangemi, S. *Rosmarinus officinalis* L. as cause of contact dermatitis. *Allergol. Immunopathol. (Madr)*, **2014**, *42* (6), 616-619.

[77] Troncoso, N.; Sierra, H.; Carvajal, L.; Delpiano, P.; Gunther, G. Fast high performance liquid chromatography and ultraviolet-visible quantification of principal phenolic antioxidants in fresh rosemary. *J. Chromatogr. A*, **2005**, *1100* (1), 20-25.

[78] Peng, Y.; Yuan, J.; Liu, F.; Ye, J. Determination of active components in rosemary by capillary electrophoresis with electrochemical detection. *J. Pharm. Biomed. Anal.*, **2005**, *39* (3-4), 431-437.

[79] Perez-Fons, L.; Garzon, M. T.; Micol, V. Relationship between the antioxidant capacity and effect of rosemary (*Rosmarinus officinalis* L.) polyphenols on membrane phospholipid order. *J. Agric. Food Chem.*, **2010**, *58* (1), 161-171.

[80] Bai, N.; He, K.; Roller, M.; Lai, C. S.; Shao, X.; Pan, M. H.; Ho, C. T. Flavonoids and phenolic compounds from *Rosmarinus officinalis*. *J. Agric. Food Chem.*, **2010**, *58* (9), 5363-5367.

[81] Hussain, A. I.; Anwar, F.; Chatha, S. A.; Jabbar, A.; Mahboob, S.; Nigam, P. S. *Rosmarinus officinalis* essential oil: antiproliferative, antioxidant and antibacterial activities. *Braz. J. Microbiol.*, **2010**, *41* (4), 1070-1078.

[82] Borras-Linares, I.; Stojanovic, Z.; Quirantes-Pine, R.; Arraez-Roman, D.; Svarc-Gajic, J.; Fernandez-Gutierrez, A.; Segura-Carretero, A. *Rosmarinus officinalis* leaves as a natural source of bioactive compounds. *Int. J. Mol. Sci.*, **2014**, *15* (11), 20585-20606.

[83] Mena, P.; Cirlini, M.; Tassotti, M.; Herrlinger, K. A.; Dall'Asta, C.; Del Rio, D. Phytochemical profiling of flavonoids, phenolic acids, terpenoids, and volatile fraction of a rosemary (*Rosmarinus officinalis* L.) extract. *Molecules*, **2016**, *21* (11).

[84] Al-Attar, A. M.; Shawush, N. A. Influence of olive and rosemary leaves extracts on chemically induced liver cirrhosis in male rats. *Saudi J. Biol. Sci.*, **2015**, *22* (2), 157-163.

[85] Klancnik, A.; Guzej, B.; Kolar, M. H.; Abramovic, H.; Mozina, S. S. *In vitro* antimicrobial and antioxidant activity of commercial rosemary extract formulations. *J. Food Prot.*, **2009**, *72* (8), 1744-1752.

[86] Chae, I. G.; Yu, M. H.; Im, N. K.; Jung, Y. T.; Lee, J.; Chun, K. S.; Lee, I. S. Effect of *Rosemarinus officinalis* L. on MMP-9, MCP-1 levels, and cell migration in RAW 264.7 and smooth muscle cells. *J. Med. Food*, **2012**, *15* (10), 879-886.

[87] Ramadan, K. S.; Khalil, O. A.; Danial, E. N.; Alnahdi, H. S.; Ayaz, N. O., Hypoglycemic and hepatoprotective activity of *Rosmarinus officinalis* extract in diabetic rats. *J. Physiol. Biochem.,* **2013**, *69* (4), 779-783.

[88] Martinez, A. L.; Gonzalez-Trujano, M. E.; Chavez, M.; Pellicer, F. Antinociceptive effectiveness of triterpenes from rosemary in visceral nociception. *J. Ethnopharmacol.*, **2012**, *142* (1), 28-34.

[89] Takaki, I.; Bersani-Amado, L. E.; Vendruscolo, A.; Sartoretto, S. M.; Diniz, S. P.; Bersani-Amado, C. A.; Cuman, R. K. Anti-inflammatory and antinociceptive effects of *Rosmarinus officinalis* L. essential oil in experimental animal models. *J. Med. Food*, **2008**, *11* (4), 741-746.

[90] Rocha, J.; Eduardo-Figueira, M.; Barateiro, A.; Fernandes, A.; Brites, D.; Bronze, R.; Duarte, C. M.; Serra, A. T.; Pinto, R.; Freitas, M.; Fernandes, E.; Silva-Lima, B.; Mota-Filipe, H.; Sepodes, B. Anti-inflammatory effect of rosmarinic acid and an extract of *Rosmarinus officinalis* in rat models of local and systemic inflammation. *Basic Clin. Pharmacol. Toxicol.*, **2015**, *116* (5), 398-413.

[91] Medicherla, K.; Ketkar, A.; Sahu, B. D.; Sudhakar, G.; Sistla, R. *Rosmarinus officinalis* L. extract ameliorates intestinal inflammation through MAPKs/NF-kappaB signaling in a murine model of acute experimental colitis. *Food Funct.,* **2016**, *7* (7), 3233-3243.

[92] Gonzalez-Vallinas, M.; Molina, S.; Vicente, G.; Zarza, V.; Martin-Hernandez, R.; Garcia-Risco, M. R.; Fornari, T.; Reglero, G.; Ramirez de Molina, A. Expression of microRNA-15b and the glycosyltransferase GCNT3 correlates with antitumor efficacy of Rosemary diterpenes in colon and pancreatic cancer. *PLoS One*, **2014**, *9* (6), e98556.

[93] Scheckel, K. A.; Degner, S. C.; Romagnolo, D. F. Rosmarinic acid antagonizes activator protein-1-dependent activation of cyclooxygenase-2 expression in human cancer and nonmalignant cell lines. *J. Nutr.*, **2008**, *138* (11), 2098-2105.

[94] Moreno, S.; Scheyer, T.; Romano, C. S.; Vojnov, A. A. Antioxidant and antimicrobial activities of rosemary extracts linked to their polyphenol composition. *Free Radic. Res.*, **2006**, *40* (2), 223-231.

[95] Zeng, H. H.; Tu, P. F.; Zhou, K.; Wang, H.; Wang, B. H.; Lu, J. F. Antioxidant properties of phenolic diterpenes from *Rosmarinus officinalis*. *Acta Pharmacol. Sin.*, **2001**, *22* (12), 1094-1108.

[96] Yesil-Celiktas, O.; Sevimli, C.; Bedir, E.; Vardar-Sukan, F. Inhibitory effects of rosemary extracts, carnosic acid and rosmarinic acid on the growth of various human cancer cell lines. *Plant Foods Hum. Nutr.*, **2010**, *65* (2), 158-163.

[97] Barni, M. V.; Carlini, M. J.; Cafferata, E. G.; Puricelli, L.; Moreno, S. Carnosic acid inhibits the proliferation and migration capacity of human colorectal cancer cells. *Oncol. Rep.*, **2012**, *27* (4), 1041-1048.

[98] Gonzalez-Vallinas, M.; Molina, S.; Vicente, G.; Sanchez-Martinez, R.; Vargas, T.; Garcia-Risco, M. R.; Fornari, T.; Reglero, G.; Ramirez de Molina, A. Modulation of estrogen and epidermal growth factor receptors by rosemary extract in breast cancer cells. *Electrophoresis*, **2014**, *35* (11), 1719-1727.

[99] Valdes, A.; Garcia-Canas, V.; Simo, C.; Ibanez, C.; Micol, V.; Ferragut, J. A.; Cifuentes, A. Comprehensive foodomics study on the mechanisms operating at various molecular levels in cancer

cells in response to individual rosemary polyphenols. *Anal. Chem.*, **2014**, *86* (19), 9807-9815.

[100] Borras-Linares, I.; Perez-Sanchez, A.; Lozano-Sanchez, J.; Barrajon-Catalan, E.; Arraez-Roman, D.; Cifuentes, A.; Micol, V.; Carretero, A. S. A bioguided identification of the active compounds that contribute to the antiproliferative/cytotoxic effects of rosemary extract on colon cancer cells. *Food Chem. Toxicol.*, **2015**, *80*, 215-222.

[101] Richheimer, S. L.; Bernart, M. W.; King; A., G.; Kent, M. C.; Beiley, D. T. Antioxidant activity of lipid-soluble phenolic diterpenes from rosemary. *J. Am. Oil Chem. Soc.,* **1996**, *73* (4), 507-514.

[102] Zhang, Y.; Chen, X.; Yang, L.; Zu, Y.; Lu, Q., Effects of rosmarinic acid on liver and kidney antioxidant enzymes, lipid peroxidation and tissue ultrastructure in aging mice. *Food Funct.,* **2015**, *6* (3), 927-931.

[103] Afonso, M. S.; de, O. S. A. M.; Carvalho, E. B.; Rivelli, D. P.; Barros, S. B.; Rogero, M. M.; Lottenberg, A. M.; Torres, R. P.; Mancini-Filho, J. Phenolic compounds from Rosemary (*Rosmarinus officinalis* L.) attenuate oxidative stress and reduce blood cholesterol concentrations in diet-induced hypercholesterolemic rats. *Nutr. Metab. (Lond)*, **2013**, *10* (1), 19.

[104] Hassani, F. V.; Shirani, K.; Hosseinzadeh, H. Rosemary (*Rosmarinus officinalis*) as a potential therapeutic plant in metabolic syndrome: a review. *Naunyn Schmiedebergs Arch. Pharmacol.*, **2016**, *389* (9), 931-949.

[105] Doolaege, E. H.; Raes, K.; De Vos, F.; Verhe, R.; De Smet, S. Absorption, distribution and elimination of carnosic acid, a natural antioxidant from *Rosmarinus officinalis*, in rats. *Plant. Foods Hum. Nutr.*, **2011**, *66* (2), 196-202.

[106] Romo Vaquero, M.; Garcia Villalba, R.; Larrosa, M.; Yanez-Gascon, M. J.; Fromentin, E.; Flanagan, J.; Roller, M.; Tomas-Barberan, F. A.; Espin, J. C.; Garcia-Conesa, M. T. Bioavailability of the major bioactive diterpenoids in a rosemary extract: metabolic profile in the intestine, liver, plasma, and brain of Zucker rats. *Mol. Nut. Food Res.*, **2013,** *57* (10), 1834-1846.

[107] Perez-Sanchez, A.; Borras-Linares, I.; Barrajon-Catalan, E.; Arraez-Roman, D.; Gonzalez-Alvarez, I.; Ibanez, E.; Segura-Carretero, A.; Bermejo, M.; Micol, V. Evaluation of the intestinal permeability of rosemary (*Rosmarinus officinalis* L.) extract polyphenols and terpenoids in Caco-2 cell monolayers. *PLoS ONE*, **2017**, *12* (2), e0172063.

[108] Anadon, A.; Martinez-Larranaga, M. R.; Martinez, M. A.; Ares, I.; Garcia-Risco, M. R.; Senorans, F. J.; Reglero, G. Acute oral safety study of rosemary extracts in rats. *J. Food Prot.*, **2008**, *71* (4), 790-795.

[109] Nobile, V.; Michelotti, A.; Cestone, E.; Caturla, N.; Castillo, J.; Benavente-Garcia, O.; Perez-Sanchez, A.; Micol, V. Skin photoprotective and antiageing effects of a combination of rosemary (*Rosmarinus officinalis*) and grapefruit (*Citrus paradisi*) polyphenols. *Food Nutr. Res.*, **2016**, *60*, 31871.

[110] Grohmann, F. Oleaceae In: *Flora of West Pakistan*. Libraries Australia: Pakistan, **1974**; Vol. *59*, p. 9.

[111] Hashmi, M. A.; Khan, A.; Hanif, M.; Farooq, U.; Perveen, S. Traditional uses, phytochemistry, and pharmacology of *Olea europaea* (olive). *Evid. Based Complement. Alternat. Med.*, **2015**, *2015*, 541591.

[112] Waterman, E.; Lockwood, B. Active components and clinical applications of olive oil. *Altern. Med. Rev.*, **2007**, *12* (4), 331-342.

[113] Wahrburg, U.; Kratz, M.; Cullen, P. Mediterranean diet, olive oil and health. *Eur. J. Lipid Sci. Tech.*, **2002**, *104* (9‐10), 698-705.

[114] Estruch, R.; Martinez-Gonzalez, M. A.; Corella, D.; Salas-Salvado, J.; Ruiz-Gutierrez, V.; Covas, M. I.; Fiol, M.; Gomez-Gracia, E.; Lopez-Sabater, M. C.; Vinyoles, E.; Aros, F.; Conde, M.; Lahoz, C.; Lapetra, J.; Saez, G.; Ros, E. Effects of a Mediterranean-style diet on cardiovascular risk factors: a randomized trial. *Ann. Intern. Med.*, **2006**, *145* (1), 1-11.

[115] Fito, M.; Guxens, M.; Corella, D.; Saez, G.; Estruch, R.; de la Torre, R.; Frances, F.; Cabezas, C.; Lopez-Sabater Mdel, C.; Marrugat, J.; Garcia-Arellano, A.; Aros, F.; Ruiz-Gutierrez, V.; Ros, E.; Salas-Salvado, J.; Fiol, M.; Sola, R.; Covas, M. I. Effect of a traditional Mediterranean diet on lipoprotein oxidation: a randomized controlled trial. *Arch. Intern. Med.*, **2007**, *167* (11), 1195-1203.

[116] Scarmeas, N.; Luchsinger, J. A.; Mayeux, R.; Stern, Y., Mediterranean diet and Alzheimer disease mortality. *Neurology*, **2007**, *69* (11), 1084-1093.

[117] Trichopoulou, A.; Costacou, T.; Bamia, C.; Trichopoulos, D. Adherence to a Mediterranean diet and survival in a Greek population. *N. Engl. J. Med.*, **2003**, *348* (26), 2599-2608.

[118] Menendez, J. A.; Vazquez-Martin, A.; Oliveras-Ferraros, C.; Garcia-Villalba, R.; Carrasco-Pancorbo, A.; Fernandez-Gutierrez, A.; Segura-Carretero, A. Analyzing effects of extra-virgin olive oil polyphenols on breast cancer-associated fatty acid synthase protein expression using reverse-phase protein microarrays. *Int. J. Mol. Med.*, **2008**, *22* (4), 433-439.

[119] Menendez, J. A.; Vazquez-Martin, A.; Colomer, R.; Brunet, J.; Carrasco-Pancorbo, A.; Garcia-Villalba, R.; Fernandez-Gutierrez, A.; Segura-Carretero, A. Olive oil's bitter principle reverses acquired autoresistance to trastuzumab (Herceptin) in HER2-overexpressing breast cancer cells. *BMC Cancer*, **2007**, *7*, 80.

[120] Menendez, J. A.; Joven, J.; Aragones, G.; Barrajon-Catalan, E.; Beltran-Debon, R.; Borras-Linares, I.; Camps, J.; Corominas-Faja, B.; Cufi, S.; Fernandez-Arroyo, S.; Garcia-Heredia, A.; Hernandez-Aguilera, A.; Herranz-Lopez, M.; Jimenez-Sanchez, C.; Lopez-Bonet, E.; Lozano-Sanchez, J.; Luciano-Mateo, F.; Martin-Castillo, B.; Martin-Paredero, V.; Perez-Sanchez, A.; Oliveras-Ferraros, C.; Riera-Borrull, M.; Rodriguez-Gallego, E.; Quirantes-Pine, R.; Rull, A.; Tomas-Menor, L.; Vazquez-Martin, A.; Alonso-Villaverde, C.; Micol, V.; Segura-Carretero, A. Xenohormetic and anti-aging activity of secoiridoid polyphenols present in extra virgin olive oil: A new family of gerosuppressant agents. *Cell Cycle*, **2013**, *12* (4), 555-578.

[121] de Bock, M.; Thorstensen, E. B.; Derraik, J. G.; Henderson, H. V.; Hofman, P. L.; Cutfield, W. S. Human absorption and metabolism of oleuropein and hydroxytyrosol ingested as olive (*Olea europaea* L.) leaf extract. *Mol. Nutr. Food Res.*, **2013**, *57* (11), 2079-2085.

[122] Quirantes-Pine, R.; Lozano-Sanchez, J.; Herrero, M.; Ibanez, E.; Segura-Carretero, A.; Fernandez-Gutierrez, A. HPLC-ESI-QTOF-MS as a powerful analytical tool for characterising phenolic compounds in olive-leaf extracts. *Phytochem. Anal.*, **2013**, *24* (3), 213-223.

[123] Savournin, C.; Baghdikian, B.; Elias, R.; Dargouth-Kesraoui, F.; Boukef, K.; Balansard, G. Rapid high-performance liquid chromatography analysis for the quantitative determination of oleuropein in *Olea europaea* leaves. *J. Agric. Food Chem.*, **2001**, *49* (2), 618-621.

[124] Tovar, M. J.; Motilva, M. J.; Romero, M. P. Changes in the phenolic composition of virgin olive oil from young trees (*Olea europaea* L. cv. Arbequina) grown under linear irrigation strategies. *J. Agric. Food Chem.*, **2001**, *49* (11), 5502-5508.

[125] Campeol, E.; Flamini, G.; Cioni, P. L.; Morelli, I.; Cremonini, R.; Ceccarini, L., Volatile fractions from three cultivars of *Olea europaea* L. collected in two different seasons. *J. Agric. Food Chem.*, **2003**, *51* (7), 1994-1999.

[126] Perez-Bonilla, M.; Salido, S.; van Beek, T. A.; Linares-Palomino, P. J.; Altarejos, J.; Nogueras, M.; Sanchez, A. Isolation and identification of radical scavengers in olive tree (*Olea europaea*) wood. *J. Chromatogr. A*, **2006**, *1112* (1-2), 311-318.

[127] Fu, S.; Arraez-Roman, D.; Segura-Carretero, A.; Menendez, J. A.; Menendez-Gutierrez, M. P.; Micol, V.; Fernandez-Gutierrez, A. Qualitative screening of phenolic compounds in olive leaf extracts by hyphenated liquid chromatography and preliminary evaluation of cytotoxic activity against human breast cancer cells. *Anal. Bioanal. Chem.*, **2010**, *397* (2), 643-654.

[128] Briante, R.; Patumi, M.; Terenziani, S.; Bismuto, E.; Febbraio, F.; Nucci, R. *Olea europaea* L. leaf extract and derivatives: antioxidant properties. *J. Agric. Food Chem.*, **2002**, *50* (17), 4934-4940.

[129] Ammar, S.; Contreras, M. D.; Gargouri, B.; Segura-Carretero, A.; Bouaziz, M. RP-HPLC-DAD-ESI-QTOF-MS based metabolic profiling of the potential *Olea europaea* by-product "wood" and its comparison with leaf counterpart. *Phytochem. Anal.*, **2017**, *28* (3), 217-229.

[130] Eidi, A.; Eidi, M.; Darzi, R. Antidiabetic effect of *Olea europaea* L. in normal and diabetic rats. *Phytother. Res.*, **2009**, *23* (3), 347-350.

[131] Al-Azzawie, H. F.; Alhamdani, M. S., Hypoglycemic and antioxidant effect of oleuropein in alloxan-diabetic rabbits. *Life Sci.*, **2006**, *78* (12), 1371-1377.

[132] Khayyal, M. T.; el-Ghazaly, M. A.; Abdallah, D. M.; Nassar, N. N.; Okpanyi, S. N.; Kreuter, M. H. Blood pressure lowering effect of an olive leaf extract (*Olea europaea*) in L-NAME induced hypertension in rats. *Arzneimittelforschung*, **2002**, *52* (11), 797-802.

[133] Perrinjaquet-Moccetti, T.; Busjahn, A.; Schmidlin, C.; Schmidt, A.; Bradl, B.; Aydogan, C., Food supplementation with an olive (*Olea europaea* L.) leaf extract reduces blood pressure in borderline hypertensive monozygotic twins. *Phytother. Res.*, **2008**, *22* (9), 1239-1242.

[134] Eidi, A.; Moghadam-kia, S.; Moghadam, J. Z.; Eidi, M.; Rezazadeh, S. Antinociceptive and anti-inflammatory effects of olive oil (*Olea europeae* L.) in mice. *Pharm. Biol.*, **2012**, *50* (3), 332-337.

[135] Bouaziz, M.; Chamkha, M.; Sayadi, S. Comparative study on phenolic content and antioxidant activity during maturation of the olive cultivar Chemlali from Tunisia. *J. Agric. Food Chem.*, **2004**, *52* (17), 5476-5481.

[136] Lee, O. H.; Lee, B. Y. Antioxidant and antimicrobial activities of individual and combined phenolics in *Olea europaea* leaf extract. *Bioresour. Technol.*, **2010**, *101* (10), 3751-3754.

[137] Marchetti, C.; Clericuzio, M.; Borghesi, B.; Cornara, L.; Ribulla, S.; Gosetti, F.; Marengo, E.; Burlando, B. Oleuropein-enriched olive leaf extract affects calcium dynamics and impairs viability of malignant mesothelioma cells. *Evid. Based Complement. Alternat. Med.*, **2015**, *2015*, 908493.

[138] Pereira, A. P.; Ferreira, I. C.; Marcelino, F.; Valentao, P.; Andrade, P. B.; Seabra, R.; Estevinho, L.; Bento, A.; Pereira, J. A. Phenolic compounds and antimicrobial activity of olive (*Olea europaea* L. Cv. Cobrancosa) leaves. *Molecules*, **2007**, *12* (5), 1153-1162.

[139] Wainstein, J.; Ganz, T.; Boaz, M.; Bar Dayan, Y.; Dolev, E.; Kerem, Z.; Madar, Z., Olive leaf extract as a hypoglycemic agent in both human diabetic subjects and in rats. *J. Med. Food*, **2012**, *15* (7), 605-610.

[140] Susalit, E.; Agus, N.; Effendi, I.; Tjandrawinata, R. R.; Nofiarny, D.; Perrinjaquet-Moccetti, T.; Verbruggen, M. Olive (*Olea europaea*) leaf extract effective in patients with stage-1 hypertension: comparison with Captopril. *Phytomedicine*, **2011**, *18* (4), 251-258.

[141] Sudjana, A. N.; D'Orazio, C.; Ryan, V.; Rasool, N.; Ng, J.; Islam, N.; Riley, T. V.; Hammer, K. A. Antimicrobial activity of commercial *Olea europaea* (olive) leaf extract. *Int. J. Antimicrob. Agents*, **2009**, *33* (5), 461-463.

[142] Micol, V.; Caturla, N.; Perez-Fons, L.; Mas, V.; Perez, L.; Estepa, A. The olive leaf extract exhibits antiviral activity against viral haemorrhagic septicaemia rhabdovirus (VHSV). *Antiviral Res.*, **2005**, *66* (2-3), 129-136.

[143] Singh, I.; Mok, M.; Christensen, A. M.; Turner, A. H.; Hawley, J. A. The effects of polyphenols in olive leaves on platelet function. *Nutr. Metab. Cardiovasc. Dis.*, **2008**, *18* (2), 127-132.

[144] de la Puerta, R.; Ruiz Gutierrez, V.; Hoult, J. R. Inhibition of leukocyte 5-lipoxygenase by phenolics from virgin olive oil. *Biochem. Pharmacol.*, **1999**, *57* (4), 445-449.

[145] Carluccio, M. A.; Siculella, L.; Ancora, M. A.; Massaro, M.; Scoditti, E.; Storelli, C.; Visioli, F.; Distante, A.; De Caterina, R. Olive oil and red wine antioxidant polyphenols inhibit endothelial activation: antiatherogenic properties of Mediterranean diet phytochemicals. *Arterioscler. Thromb. Vasc. Biol.*, **2003**, *23* (4), 622-629.

[146] Acquaviva, R.; Di Giacomo, C.; Sorrenti, V.; Galvano, F.; Santangelo, R.; Cardile, V.; Gangia, S.; D'Orazio, N.; Abraham, N. G.; Vanella, L. Antiproliferative effect of oleuropein in prostate cell lines. *Int. J. Oncol.*, **2012**, *41* (1), 31-38.

[147] Bisignano, G.; Tomaino, A.; Lo Cascio, R.; Crisafi, G.; Uccella, N.; Saija, A. On the *in-vitro* antimicrobial activity of oleuropein and hydroxytyrosol. *J. Pharm. Pharmacol.*, **1999**, *51* (8), 971-974.

[148] Perugini, P.; Vettor, M.; Rona, C.; Troisi, L.; Villanova, L.; Genta, I.; Conti, B.; Pavanetto, F. Efficacy of oleuropein against UVB irradiation: preliminary evaluation. *Int. J. Cosmet. Sci.*, **2008**, *30* (2), 113-120.

[149] Katsiki, M.; Chondrogianni, N.; Chinou, I.; Rivett, A. J.; Gonos, E. S. The olive constituent oleuropein exhibits proteasome stimulatory properties in vitro and confers life span extension of human embryonic fibroblasts. *Rejuvenation Res.*, **2007**, *10* (2), 157-172.

[150] Kruk, I.; Aboul-Enein, H. Y.; Michalska, T.; Lichszteld, K.; Kladna, A. Scavenging of reactive oxygen species by the plant phenols genistein and oleuropein. *Luminescence*, **2005**, *20* (2), 81-89.

[151] Caturla, N.; Perez-Fons, L.; Estepa, A.; Micol, V. Differential effects of oleuropein, a biophenol from Olea europaea, on anionic and zwiterionic phospholipid model membranes. *Chem. Phys. Lipids*, **2005**, *137* (1-2), 2-17.

[152] Corona, G.; Tzounis, X.; Assunta Dessi, M.; Deiana, M.; Debnam, E. S.; Visioli, F.; Spencer, J. P. The fate of olive oil polyphenols in the gastrointestinal tract: implications of gastric and colonic microflora-dependent biotransformation. *Free Radic. Res.*, **2006**, *40* (6), 647-658.

[153] Brenes, M.; Garcia, A.; Garcia, P.; Garrido, A. Acid hydrolysis of secoiridoid aglycons during storage of virgin olive oil. *J. Agric. Food Chem.*, **2001**, *49* (11), 5609-5614.

[154] Visioli, F.; Bellomo, G.; Galli, C. Free radical-scavenging properties of olive oil polyphenols. *Biochem. Biophys. Res. Commun.*, **1998**, *247* (1), 60-64.

[155] Visioli, F.; Galli, C.; Plasmati, E.; Viappiani, S.; Hernandez, A.; Colombo, C.; Sala, A. Olive phenol hydroxytyrosol prevents passive smoking-induced oxidative stress. *Circulation*, **2000**, *102* (18), 2169-2171.

[156] Miro-Casas, E.; Covas, M. I.; Farre, M.; Fito, M.; Ortuno, J.; Weinbrenner, T.; Roset, P.; de la Torre, R. Hydroxytyrosol disposition in humans. *Clin. Chem.*, **2003**, *49* (6 Pt 1), 945-952.

[157] Kountouri, A. M.; Mylona, A.; Kaliora, A. C.; Andrikopoulos, N. K. Bioavailability of the phenolic compounds of the fruits (drupes) of *Olea europaea* (olives): impact on plasma antioxidant status in humans. *Phytomedicine*, **2007**, *14* (10), 659-667.

[158] Bazoti, F. N.; Gikas, E.; Tsarbopoulos, A. Simultaneous quantification of oleuropein and its metabolites in rat plasma by liquid chromatography electrospray ionization tandem mass spectrometry. *Biomed. Chromatogr.*, **2010**, *24* (5), 506-515.

[159] Vissers, M. N.; Zock, P. L.; Katan, M. B. Bioavailability and antioxidant effects of olive oil phenols in humans: a review. *Eur. J. Clin. Nutr.*, **2004**, *58* (6), 955-965.

[160] Rechner, A. R.; Kuhnle, G.; Hu, H.; Roedig-Penman, A.; van den Braak, M. H.; Moore, K. P.; Rice-Evans, C. A. The metabolism of dietary polyphenols and the relevance to circulating levels of conjugated metabolites. *Free Radic. Res.*, **2002**, *36* (11), 1229-1241.

[161] Garcia-Villalba, R.; Carrasco-Pancorbo, A.; Nevedomskaya, E.; Mayboroda, O. A.; Deelder, A. M.; Segura-Carretero, A.; Fernandez-Gutierrez, A. Exploratory analysis of human urine by LC-ESI-TOF MS after high intake of olive oil: understanding the metabolism of polyphenols. *Anal. Bioanal. Chem.*, **2010**, *398* (1), 463-475.

[162] Tuck, K. L.; Freeman, M. P.; Hayball, P. J.; Stretch, G. L.; Stupans, I. The *in vivo* fate of hydroxytyrosol and tyrosol, antioxidant phenolic constituents of olive oil, after intravenous and oral dosing of labeled compounds to rats. *J. Nutr.*, **2001**, *131* (7), 1993-1996.

[163] Tuck, K. L.; Hayball, P. J.; Stupans, I. Structural characterization of the metabolites of hydroxytyrosol, the principal phenolic component in olive oil, in rats. *J. Agric. Food Chem.*, **2002**, *50* (8), 2404-2409.

[164] Khymenets, O.; Fito, M.; Tourino, S.; Munoz-Aguayo, D.; Pujadas, M.; Torres, J. L.; Joglar, J.; Farre, M.; Covas, M. I.; de la Torre, R. Antioxidant activities of hydroxytyrosol main metabolites do not contribute to beneficial health effects after olive oil ingestion. *Drug Metab. Dispos.*, **2010**, *38* (9), 1417-1421.

[165] Garcia-Villalba, R.; Larrosa, M.; Possemiers, S.; Tomas-Barberan, F. A.; Espin, J. C., Bioavailability of phenolics from an oleuropein-rich olive (*Olea europaea*) leaf extract and its acute effect on plasma antioxidant status: comparison between pre- and postmenopausal women. *Eur. J. Nutr.*, **2014**, *53* (4), 1015-1027.

[166] Omer, S. A.; Elobeid, M. A.; Elamin, M. H.; Hassan, Z. K.; Virk, P.; Daghestani, M. H.; Al-Olayan, E. M.; Al-Eisa, N. A.; and Almarhoon, Z. M. Toxicity of olive leaves (*Olea europaea* L.) in Wistar albino rats. *Asian J. Anim. Vet. Adv.*, **2012**, *7* (11), 1175-1182.

[167] Alecci, U.; Bonina, F.; Bonina, A.; Rizza, L.; Inferrera, S.; Mannucci, C.; Calapai, G. Efficacy and safety of a natural remedy for the treatment of gastroesophageal reflux: a double-blinded randomized-controlled study. *Evid. Based Complement. Alternat. Med.*, **2016**, *2016*, 2581461.

[168] Clewell, A. E.; Beres, E.; Vertesi, A.; Glavits, R.; Hirka, G.; Endres, J. R.; Murbach, T. S.; Szakonyine, I. P. A comprehensive toxicological safety assessment of an extract of *Olea europaea* L. leaves (Bonolive). *Intl. Jl. Toxicoll.*, **2016**, *35* (2), 208-221.

[169] Kanehisa, M.; Goto, S.; Sato, Y.; Kawashima, M.; Furumichi, M.; Tanabe, M. Data, information, knowledge and principle: back to metabolism in KEGG. *Nucleic Acids Res.*, **2014**, *42* (Database issue), D199-205.

[170] McKnight, S. L. On getting there from here. *Science*, **2010**, *330* (6009), 1338-1339.

[171] Harvey, A. L.; Edrada-Ebel, R.; Quinn, R. J. The re-emergence of natural products for drug discovery in the genomics era. *Nature reviews. Drug Discov.*, **2015**, *14* (2), 111-129.

[172] Gupta, S.; Aires-de-Sousa, J. Comparing the chemical spaces of metabolites and available chemicals: models of metabolite-likeness. *Mol. Divers.*, **2007**, *11* (1), 23-36.

[173] Forli, S.; Huey, R.; Pique, M. E.; Sanner, M. F.; Goodsell, D. S.; Olson, A. J. Computational protein-ligand docking and virtual drug screening with the AutoDock suite. *Nat. Protoc.*, **2016**, *11* (5), 905-919.

[174] Biasini, M.; Bienert, S.; Waterhouse, A.; Arnold, K.; Studer, G.; Schmidt, T.; Kiefer, F.; Gallo Cassarino, T.; Bertoni, M.; Bordoli, L.; Schwede, T. SWISS-MODEL: modelling protein tertiary and quaternary structure using evolutionary information. *Nucleic Acids Res.*, **2014**, *42* (Web Server issue), W252-8.

[175] Banerjee, P.; Erehman, J.; Gohlke, B. O.; Wilhelm, T.; Preissner, R.; Dunkel, M. Super Natural II--a database of natural products. *Nucleic Acids Res.*, **2015**, *43* (Database issue), D935-939.

[176] Trott, O.; Olson, A. J., AutoDock Vina: improving the speed and accuracy of docking with a new scoring function, efficient optimization, and multithreading. *J. Comput Chem.*, **2010**, *31* (2), 455-461.

[177] Perez-Sanchez, H.; Wenzel, W. Optimization methods for virtual screening on novel computational architectures. *Curr. Comput. Aided Drug Des.*, **2011**, *7* (1), 44-52.

[178] Cheng, F.; Li, W.; Zhou, Y.; Shen, J.; Wu, Z.; Liu, G.; Lee, P. W.; Tang, Y. admetSAR: a comprehensive source and free tool for assessment of chemical ADMET properties. *J. Chem. Inf. Model.*, **2012**, *52* (11), 3099-3105.

[179] Encinar, J. A.; Fernandez-Ballester, G.; Galiano-Ibarra, V.; Micol, V. *In silico* approach for the discovery of new PPARgamma modulators among plant-derived polyphenols. *Drug Des. Dev. Ther.*, **2015**, *9*, 5877-5895.

[180] Galiano, V.; Garcia-Valtanen, P.; Micol, V.; Encinar, J. A. Looking for inhibitors of the dengue virus NS5 RNA-dependent RNA-polymerase using a molecular docking approach. *Drug Des. Dev. Ther.*, **2016**, *10*, 3163-3181.

[181] Jimenez-Sanchez, C.; Olivares-Vicente, M.; Rodriguez-Perez, C.; Herranz-Lopez, M.; Lozano-Sanchez, J.; Segura Carretero, A.; Fernandez-Gutierrez, A.; Micol, V. AMPK modulatory activity of olive–tree leaves phenolic compounds: Bioassay-guided isolation on adipocyte model and *in silico* approach. *PLoS ONE*, **2017**, *12* (3), e0173074.

[182] Hardie, D. G. AMP-activated protein kinase: an energy sensor that regulates all aspects of cell function. *Genes Dev.*, **2011**, *25* (18), 1895-1908.

[183] Riera-Borrull, M.; Rodriguez-Gallego, E.; Hernandez-Aguilera, A.; Luciano, F.; Ras, R.; Cuyas, E.; Camps, J.; Segura-Carretero, A.; Menendez, J. A.; Joven, J.; Fernandez-Arroyo, S. Exploring the process of energy generation in pathophysiology by targeted metabolomics: performance of a simple and quantitative method. *J. Am. Soc. Mass Spectr.*, **2016**, *27* (1), 168-177.

[184] Massucci, F. A.; Wheeler, J.; Beltran-Debon, R.; Joven, J.; Sales-Pardo, M.; Guimera, R. Inferring propagation paths for sparsely observed perturbations on complex networks. *Science advances*, **2016**, *2* (10), e1501638.

DISCUSIÓN/ DISCUSSION

DISCUSIÓN

Considerando la falta de terapias farmacológicas efectivas enfocadas en la pérdida de peso y la mejora de las alteraciones relacionadas con la obesidad, se postula que el uso de polifenoles a través de la intervención nutricional podría ser una estrategia alternativa para tratar o prevenir los trastornos metabólicos asociados con la ganancia de peso [110]. Diferentes modelos celulares de obesidad han sido empleados para estudiar el proceso de adipogénesis y la expansión del tejido adiposo y entender los mecanismos moleculares implicados [51]. Por ejemplo, el uso de cultivos primarios permite el estudio del tejido adiposo de diferentes localizaciones y de animales de diferentes estadios de desarrollo. Asimismo, los estudios con preadipocitos primarios humanos reflejan con mayor fidelidad la situación patológica de la obesidad. Sin embargo, los cultivos primarios presentan una baja reproducibilidad y una capacidad de renovación limitada. Estas desventajas llevan a considerar el uso alternativo de líneas celulares establecidas, como la línea de preadipocitos 3T3-L1 derivada de embrión de ratón suizo 3T3 [123].

Tras la diferenciación de fibroblastos 3T3-L1 a adipocitos maduros, estas células se vuelven hipertróficas cuando se incuban de forma prolongada con concentraciones altas de glucosa. Los altos niveles de glucosa extracelular promueven un excesivo almacenamiento de lípidos en el citoplasma de los adipocitos. En consecuencia, se produce estrés oxidativo, disfunción mitocondrial y otras alteraciones metabólicas que llevan a un estado de inflamación y resistencia a la insulina, como ocurre en el tejido adiposo obeso [103, 124]. Por tanto, este modelo celular es válido para estudiar el efecto y los mecanismos de los polifenoles y sus metabolitos en el tejido adiposo dentro de un contexto de estrés metabólico.

Como se observa en este trabajo, los extractos procedentes de plantas como *Hibiscus sabdariffa* (HS), *Lippia citriodora* (LC) y *Olea europaea* muestran efectos beneficiosos frente a los trastornos metabólicos asociados con la obesidad. Sin embargo, los extractos de plantas son mezclas complejas de moléculas con una amplia variedad estructural que pueden interactuar con múltiples dianas metabólicas [125], lo que dificulta la identificación de los compuestos implicados en dichos efectos. Para este propósito, el fraccionamiento guiado por bioensayo mediante HPLC semi-preparativa es un enfoque adecuado para delimitar la actividad biológica de un extracto complejo a unos pocos compuestos. Esta metodología se llevó a cabo para atribuir la capacidad moduladora de AMPK a las diferentes fracciones obtenidas de la hoja de olivo (OL) (Capítulo 1) [120] y LC [126] en adipocitos 3T3-L1 hipertróficos. Asimismo, la optimización del método de aislamiento confiere la posibilidad de obtener fracciones altamente puras que contienen compuestos individuales

difíciles de adquirir comercialmente, como se alcanzó en el Capítulo 2. En este capítulo, la evaluación de fracciones de LC conteniendo compuestos principalmente puros, o junto con uno o dos compuestos minoritarios, indicó que el verbascósido y, en menor medida, el ácido logánico y la luteolina-7-diglucurónido podrían ser los principales contribuidores del extracto de LC de activar AMPK en adipocitos.

No obstante, los datos de compuestos procedentes de plantas en modelos celulares deben ser interpretados con cautela cuando se extrapolan a situaciones *in vivo*. Tras una ingesta oral, estos compuestos pueden ser altamente metabolizados, por lo que los metabolitos que alcanzan la circulación sanguínea pueden diferir considerablemente de sus formas nativas. Muchos compuestos fenólicos están glicosilados en las plantas, como los flavonoides de HS [55] u OL (Capítulo 1) [120] o los iridoides de LC [126], y algunos de estos compuestos pueden ejercer un efecto biológico en células cuando se añaden al medio extracelular. En el Capítulo 1, se demostró que algunos polifenoles glicosilados como la oleuropeína o los glucósidos de luteolina y diosmetina presentes en OL pueden contribuir a la capacidad activadora de AMPK del extracto en adipocitos 3T3-L1 [120]. De acuerdo con estos hallazgos, otros autores han mostrado que la apigenina y la luteolina glucósidos inhiben la adipogénesis en estas células disminuyendo la expresión de C/EBPα y PPARγ [127].

Sin embargo, los polifenoles glicosilados no se absorben en la barrera intestinal, sino que requieren la previa deglicosilación enzimática por los enterocitos o la microflora intestinal a sus formas agliconas. Un estudio de biodisponibilidad en ratas mostró que las quercetinas glicosiladas de un extracto de HS enriquecido en polifenoles son hidrolizadas a quercetina y después conjugadas mediante reacciones de Fase II [98]. En este estudio, los principales metabolitos de flavonoles identificados en el plasma tras la ingestión oral del extracto fueron quercetina y sus derivados glucuronidados (detectados en un rango micromolar bajo), los cuales exhibieron valores de vida media de eliminación largos mostrando una alta presencia en el torrente sanguíneo. De acuerdo con estos resultados, otros autores han señalado que los glucurónidos de quercetina son las principales formas conjugadas en el plasma tras el consumo de fuentes de quercetina en ratas y humanos [128, 129]. Estos hallazgos respaldan la suposición de que estos son los metabolitos que alcanzan los tejidos diana. En concreto, se ha reportado la presencia de quercetina-3-glucurónido en células inmunes y en vacuolas lipídicas de hígado de rata [87] y en macrófagos de lesiones ateroscleróticas en aortas humanas [99].

Asimismo, los metabolitos pueden ser absorbidos y sufrir nuevas biotransformaciones dentro de los tejidos diana, afectando a su eliminación y a su efecto biológico. Este aspecto se abordó en el primer estudio del Capítulo 3, en el que se monitorizó el metabolismo celular

de la quercetina y la quercetina-3-glucurónido en adipocitos 3T3-L1 hipertróficos [130]. Como se deriva de este estudio, la quercetina es rápidamente absorbida por los adipocitos y alcanza concentraciones citoplasmáticas más altas que su glucurónido. Estos datos sugieren que las formas agliconas atraviesan la membrana plasmática por difusión pasiva, mientras que los derivados glucuronidados requieren algún transportador para su absorción debido a su mayor polaridad comparada con la aglicona. Previamente, otros autores también propusieron dicho mecanismo para la quercetina-3-glucurónido y la quercetina-7-glucurónido en otras líneas celulares, como los hepatocitos de hígado humano [131].

Asimismo, también se detectaron pequeñas cantidades de quercetina-3-glucurónido en el citoplasma de los adipocitos que se incubaron con quercetina, y viceversa. Estos resultados sugieren que la biotransformación ocurre en ambas direcciones debido a la presencia de actividad uridinadifosfato glucuroniltransferasa (UGT) y β-glucuronidasa en adipocitos, como han reportado otros autores [132, 133]. No obstante, la conversión de quercetina a quercetina-3-glucurónido fue más notoria que el proceso contrario. Curiosamente, Barbier *et al.* manifestaron que los activadores de PPARα y PPARγ, como podrían ser ciertos polifenoles [134], pueden aumentar la expresión de la enzima UGT 1A9 resultando en una mayor actividad de glucuronidación [132]. Esto indicaría que los polifenoles podrían inducir su propia glucuronidación. Finalmente, los dos derivados de quercetina exhibieron una fuerte capacidad antioxidante en el modelo de adipocitos hipertróficos, lo que sugiere que estos metabolitos pueden alcanzar dianas intracelulares y disminuir las ERO, a pesar de su baja biodisponibilidad en el citoplasma de los adipocitos (Capítulo 3) [130].

En vista de lo anteriormente mencionado, conocer el comportamiento farmacocinético de los polifenoles es crucial para centrar el estudio en el efecto de sus metabolitos en los experimentos celulares y elucidar los mecanismos implicados en la bioactividad de las plantas [135]. Este enfoque se llevó a cabo en el segundo estudio del Capítulo 3. En este trabajo, se seleccionaron los principales metabolitos plasmáticos encontrados tras la ingestión oral de HS en ratas [98] para evaluar su capacidad de mejorar el estrés metabólico inducido por glucolipotoxicidad en adipocitos (entre ellos, ácido clorogénico, quercetina y quercetina-3-glucurónido). Nuestros resultados mostraron que los derivados de quercetina ejercen una mayor capacidad de reducir la producción de ERO en adipocitos bajo condiciones glucolipotóxicas. Este efecto antioxidante puede deberse al papel de estas moléculas como secuestradoras de radicales libres [136]. Asimismo, otros autores indican que algunos metabolitos de quercetina pueden inducir la expresión de enzimas antioxidantes a través de la activación de Nrf2 [137] o inhibir la xantina oxidasa [138], una

enzima principal en la producción de ERO en algunas condiciones patológicas como las enfermedades cardiovasculares.

Nuestros resultados también demostraron que los metabolitos de quercetina disminuyen la inflamación inducida por glucolipotoxicidad, disminuyendo la secreción de adipoquinas como leptina, TNF-α, IGF-1, IL-6, VEGF, IL-1α, IL-1β and MCP-1. La expresión reducida de MCP-1 en adipocitos transfectados con el promotor de este gen sugirió que los derivados de quercetina pueden modular la secreción de adipoquinas a nivel transcripcional, como confirmaron previamente otros autores [139]. Este último estudio demostró que la quercetina atenúa la expresión de genes inflamatorios en macrófagos humanos, probablemente a través de la inhibición de factores transcripcionales proinflamatorios como NFκB, c-Jun y JNK, previniendo la inflamación inducida por macrófagos y la resistencia a la insulina en adipocitos primarios humanos.

Los metabolitos de quercetina también redujeron la acumulación intracelular de triglicéridos, siendo la quercetina-3-glucurónido el más activo. Estas evidencias llevaron a postular que dicho metabolito puede promover la oxidación de ácidos grasos e inhibir la lipogénesis aumentando la expresión de PPARα y reduciendo la de FASN, respectivamente, como parte de su mecanismo de acción. De acuerdo con esto, se ha asociado la presencia de quercetina-3-glucurónido en la superficie de las gotas lipídicas del hígado de ratones hiperlipidémicos alimentados con HS con cambios en la composición de los lípidos y la mejora de la esteatosis hepática [87]. En este último estudio, los polifenoles modularon la expresión de miRNAs implicados en vías metabólicas, como miR-103/107 y miR-122. Estos descubrimientos sugieren que los derivados de quercetina podrían reducir el almacenamiento de grasa modulando la expresión de genes metabólicos a través de cambios epigenéticos.

La quercetina-3-glucurónido también activó AMPK, el principal regulador del metabolismo celular. Esta proteína se activa por fosforilación en la Thr172 y modula un arsenal de sustratos con el fin de mantener la homeostasis energética. En este sentido, uno de los mecanismos que podría explicar la supresión de la expresión de FASN es mediante la inhibición mediada por AMPK de su factor transcripcional, la proteína de unión al elemento regulador del esterol 1 c (SREBP-1c) [140]. Así, la activación de AMPK mediada por polifenoles culmina en la modulación de múltiples vías que ayudan a prevenir y tratar la obesidad. Por ejemplo, el resveratrol ha demostrado inducir el pardeamiento del tejido adiposo aumentando la expresión de genes específicos del adipocito marrón a través de la activación de AMPK, entre ellos, la del coactivador de PPAR 1 alfa (PGC1α), un regulador clave de la biogénesis mitocondrial [141]. En correlación con esto, nuestros resultados

mostraron que los derivados de quercetina aumentan el contenido mitocondrial en adipocitos hipertróficos, lo que podría mejorar la función oxidativa de la mitocondria resultando en una disminución del contenido lipídico. No obstante, se requiere profundizar si el restablecimiento de la biogénesis mitocondrial por quercetinas se debe a la expresión de PGC1α mediada por AMPK.

Por otro lado, los mecanismos moleculares por los que los polifenoles pueden activar AMPK requieren una mayor aclaración. Por ejemplo, algunos polifenoles inducen la activación de AMPK mediante la activación de LKB1, como el resveratrol [142], o a través de la fosforilación de CaMKKβ, como la epigalocatequina-3-galato del té verde [143]. Se ha propuesto que el fármaco antidiabético metformina activa AMPK disminuyendo los niveles celulares de ATP a través de la inhibición del complejo respiratorio mitocondrial I [67], y se piensa que los polifenoles podrían llevar a cabo este mecanismo también [144]. Además, existe la posibilidad de que estas moléculas puedan actuar como activadores directos de AMPK, como se propuso para los metabolitos de quercetina en el experimento de acoplamiento molecular en el Capítulo 3.

El acoplamiento molecular computacional es un enfoque útil para predecir las potenciales interacciones entre los polifenoles y los sitios de unión de una proteína diana. Esta estrategia se desarrolló también en los Capítulos 1 [120] y 2 para predecir las interacciones putativas de los polifenoles de OL y LC, respectivamente, frente a los sitios de unión de las diferentes subunidades de AMPK. Concretamente, los resultados del Capítulo 2 mostraron que el ácido logánico (un iridoide), la luteolina-7-diglucurónido (un flavonoide) y el verbascósido (un fenilpropanoide) presentes en LC activan AMPK. De acuerdo con estos datos, la fracción más activa de OL en el estudio de fraccionamiento guiado por bioensayo se componía principalmente de verbascósido (Capítulo 1) [120]. Además, la luteolina-7-diglucurónido y el verbascósido han sido detectados como metabolitos plasmáticos en ratas alimentadas con LC [114], sugiriendo que podrían alcanzar el tejido adiposo en sus formas nativas a pesar de su alto peso molecular.

Los experimentos de acoplamiento molecular indicaron que los polifenoles bioactivos de LC (verbascósido, ácido logánico y luteolina-7-diglucurónido) podrían actuar como agonistas de AMPK a través de la interacción con diferentes sitios de unión. Entre ellos, estos compuestos exhibieron bajas ΔG para cualquiera de los tres sitios de unión a AMP de la subunidad γ. Estos datos sugieren que los polifenoles pueden inducir la activación de AMPK mimetizando el mecanismo alostérico del nucleótido AMP, como se describió para el agonista AICAR [145]. También se observó que los polifenoles de LC establecían interacciones en posiciones diferentes a los sitios de unión a nucleótidos de adenina en la

subunidad γ. No se descarta que estas interacciones atípicas puedan modular la actividad de AMPK, como se ha observado con el activador ácido 5-(5-hidroxil-isoxasol-3-il)-furan-2-fosfónico [70]. Se han descrito otras posiciones reguladoras a través de las cuales los polifenoles podrían promover la conformación activa de la quinasa. Por ejemplo, la interfaz establecida entre el KD de la subunidad α y el CBM de la subunidad β (llamado sitio ADaM) es un sitio de unión de activadores como A-769662, compuesto 911 y salicilato [66, 70]. Además, la amarogentina es un glucósido secoiridoide presente en *Gentiana lutea* que ejerce propiedades anti-ateroscleróticas y ha sido descrita como un activador directo de AMPK. Novedosamente, este polifenol parece unirse a la región AID de la subunidad α, lo que indicaría que la ocupación de esta región puede impedir su interacción con el KD y favorecer la conformación activa [146].

Con todo lo mencionado, existe un gran número de estudios celulares y animales que demuestran los efectos farmacológicos de los polifenoles de plantas en patologías metabólicas. Sin embargo, el impacto beneficioso sobre la salud en humanos no está extensamente estudiado y las dosis efectivas para los ensayos clínicos no están todavía claras. Como se observó en este y otros trabajos previos, los polifenoles de los extractos de HS y LC ejercen mecanismos comunes y complementarios en los trastornos relacionados con la obesidad [86, 87]. En consecuencia, el objetivo del Capítulo 4 fue evaluar el efecto de una combinación de ambos extractos en mujeres obesas y con sobrepeso [147]. Nuestros resultados mostraron que el consumo de 500 mg al día de LC-HS (65:35, p/p) acompañado con una dieta isocalórica y ejercicio diario durante dos meses redujo significativamente el peso corporal, la circunferencia abdominal y el porcentaje de grasa corporal en mujeres con sobrepeso y, de manera menos significativa, en mujeres obesas comparado con el grupo placebo.

Como muchos fármacos "anti-obesidad", los polifenoles podrían actuar a nivel del tracto gastrointestinal alterando la digestión y absorción de macronutrientes. De acuerdo con datos de acoplamiento molecular previos, se propone que los polifenoles de HS pueden tener la capacidad de inhibir enzimas digestivas interactuando con ciertas glucosidasas y con el complejo triacilglicerol lipasa/colipasa [148]. Asimismo, otro mecanismo por el que los polifenoles de LC-HS pueden promover la pérdida de peso es a través del control hipotalámico del apetito. En un trabajo previo del grupo, se demostró que la mezcla polifenólica LC-HS aumenta hormonas anorexigénicas, como GLP-1, y disminuye hormonas orexigénicas, como la grelina, en sujetos con sobrepeso [149].

No obstante, la combinación polifenólica podría ejercer mecanismos de acción a otros niveles corporales. Como se observó en el Capítulo 4, el consumo del suplemento LC-HS

disminuyó el pulso cardíaco y la presión arterial sistólica, especialmente en mujeres con sobrepeso. El efecto antihipertensivo de los extractos de HS ha sido ampliamente reportado en la bibliografía [110, 150]. Al igual que ocurre con el entrenamiento de resistencia, que induce adaptaciones en el músculo esquelético incrementando la densidad mitocondrial, el flujo sanguíneo y la dilatación de las arterias [151], o con los ácidos grasos omega-3, que han mostrado reducir el pulso cardíaco a través de la excitabilidad eléctrica de la membrana de miocitos cardíacos [152], se postula que los polifenoles de LC-HS podrían ejercer mecanismos similares para explicar la bajada del pulso cardíaco y la presión arterial. Aun así, estas especulaciones necesitan ser demostradas.

Los datos obtenidos en el modelo *in vitro* de adipocitos llevan a considerar que los polifenoles de LC-HS ejercen una acción directa sobre el tejido adiposo. En el Capítulo 4, se demostró una fuerte capacidad de la combinación LC-HS de inducir la activación de AMPK en adipocitos 3T3-L1 hipertróficos, acompañada de una reducción en la acumulación de lípidos intracelulares. Aunque no se consideró el metabolismo *in vivo* de los polifenoles de LC-HS en este modelo celular, este mecanismo se sostiene por la fuerte actividad AMPK de sus principales metabolitos (verbascósido y quercetina-3-glucurónido) demostrada en este trabajo (Capítulos 2 y 3). Asimismo, la activación de AMPK parece resultar en un aumento de la tasa metabólica basal y de la actividad voluntaria [153], como se ha descrito en el caso de algunos agentes reductores de grasa [154, 155]. De forma similar, se propone que los polifenoles pudieran aumentar el gasto energético en reposo a través de la activación de AMPK, resultando en una mejora de los parámetros metabólicos y antropométricos.

En resumen, las evidencias obtenidas en este estudio soportan la hipótesis de que los metabolitos de LC y HS, como el verbascósido y la quercetina-3-glucurónido, parecen ser los responsables de mejorar las alteraciones metabólicas asociadas a la obesidad, reduciendo el estrés metabólico y la inflamación y restableciendo la homeostasis lipídica, un efecto probablemente mediado por la activación de AMPK. Además, estos efectos han sido corroborados mediante ensayos de intervención en humanos. No obstante, la perspectiva futura es profundizar en la identificación de los metabolitos plasmáticos y confirmar la posible activación de AMPK en humanos, así como elucidar el mecanismo detallado por el que ocurre la reducción de lípidos observada y su posible control epigenético.

DISCUSSION

Considering the lack of effective pharmacological therapies focused on weight loss and amelioration of obesity-related alterations, it is postulated that plant-derived polyphenols could be an alternative strategy to treat or prevent metabolic disturbances associated with weight gain through nutritional intervention [110]. Different cell models of obesity have been used to study the process of adipogenesis and adipose tissue expansion and to understand the molecular mechanisms involved [51]. For instance, the use of primary cultures allows the study of the adipose tissue from different fat locations and from animals of different ages. Furthermore, studies with human primary preadipocytes are far more reliable as they reflect better the situation of human obesity. Nevertheless, primary cultures exhibit a low reproducibility and a limited renewal capacity. These disadvantages lead to consider the use of established cell lines, such as the preadipose 3T3-L1 cell line derived from Swiss 3T3 mouse embryos [123].

After the differentiation of 3T3-L1 fibroblasts to mature adipocytes, these cells can become hypertrophic when incubated with high glucose concentrations for a long period. The high extracellular glucose promotes excessive cytoplasmic lipid storage in adipocytes accompanied by oxidative stress, mitochondrial dysfunction and other metabolic alterations. As a consequence, these disturbances lead to a state of inflammation and insulin resistance, as occurs in obese adipose tissue [103, 124]. Therefore, this cell model is valid to study the effect and mechanisms of polyphenols and their metabolites in adipose tissue in a context of metabolic stress.

As derived from this work, extracts from plants such as *Hibiscus sabdariffa* (HS), *Lippia citriodora* (LC) and *Olea europaea* show beneficial effects against obesity-associated metabolic disturbances. Nevertheless, plant extracts are complex mixtures of molecules with a wide variety of structures that can interact with multiple metabolic targets [125], what hinders the identification of compounds involved in such effects. For this purpose, bioassay-guided fractionation by semi-preparative HPLC is a suitable approach to delimit the biological activity of a complex extract to a few compounds. This methodology was carried out to attribute the AMPK modulatory activity to the different fractions obtained from olive leaf (OL) (Chapter 1) [120] and LC [126] on hypertrophic 3T3-L1 adipocytes. Likewise, the optimization of isolation method confers the possibility of obtaining highly pure fractions containing single compounds that are difficult to acquire commercially, as achieved in Chapter 2. In this chapter, the evaluation of LC fractions containing mostly pure compounds, or together with one or two minor compounds, indicated that verbascoside

and, to a lesser extent, loganic acid and luteolin-7-diglucuronide may be the major contributors for the AMPK activity of LC extract in adipocytes.

However, data of plant-derived compounds in cell models should be taken with caution when extrapolated to *in vivo* situations. After an oral intake, these compounds can be highly metabolized, so metabolites that reach circulating blood may differ substantially from their native forms. Many phenolic compounds are glycosylated in plants, such as flavonoids from HS [55] or OL (Chapter 1) [120] or iridoids from LC [126], and some of these compounds can exert a biological effect in cells when added to the extracellular medium. In Chapter 1, it was shown that some glycosylated polyphenols such as oleuropein, luteolin or diosmetin glucosides from OL may contribute to the AMPK activating capacity of the extract in 3T3-L1 adipocytes [120]. In agreement with these findings, other authors have reported that apigenin and luteolin glucosides inhibit adipogenesis of these cells by decreasing C/EBPα and PPARγ expression [127].

Nevertheless, glycosylated polyphenols are not absorbed through the gut barrier but require prior enzymatic deglycosylation by enterocytes or colon microflora to their aglycone forms. A bioavailability study in rats showed that glycosylated quercetins of a polyphenol-enriched extract from HS are hydrolyzed into quercetin and then conjugated through Phase II reactions [98]. In this study, the main flavonol metabolites identified in plasma after the oral ingestion of the extract were quercetin and their glucuronide derivatives (detected in the low micromolar range), which showed long half-time elimination values displaying a great presence in the bloodstream. In agreement with these results, other authors have stated that quercetin glucuronides are the major conjugated forms in plasma after the consumption of quercetin sources in rats and humans [128, 129]. These findings support the assumption that these are the metabolites that reach target tissues. In particular, it has been reported the presence of quercetin-3-glucuronide in immune cells and lipid droplets of rat liver [87] and in macrophages of atherosclerotic lesions of human aortas [99].

In addition, metabolites can be absorbed and undergo new biotransformations in target tissues, affecting their elimination and their biological effect. This aspect was addressed in the first study of Chapter 3, in which the cellular metabolism of quercetin and quercetin-3-glucuronide was monitored in hypertrophic 3T3-L1 adipocytes [130]. As derived from this study, quercetin is rapidly absorbed by adipocytes and reaches higher concentrations than its glucuronide. These data suggest that aglycone forms cross the plasmatic membrane by passive diffusion, while glucuronide derivatives would require some transporter for its absorption due to their higher polarity compared to the aglycone. Previously, this

mechanism has also been proposed for quercetin-3-glucuronide and quercetin-7-glucuronide in other cell lines, such as human liver hepatocytes [131].

A second observation from our study was the detection of low quantities of quercetin-3-glucuronide in the cytoplasm of adipocytes when quercetin was incubated, and *vice versa*. These results suggested that biotransformation occurs in both directions due to the presence of UDP-glucuronosyltransferase (UGT) and β-glucuronidase activity in adipocytes, as reported by other authors [132, 133]. However, the conversion of quercetin to quercetin-3-glucuronide was more notorious than the reverse process. Interestingly, Barbier *et al.* manifested that PPARα and PPARγ activators, such as certain polyphenols [134], can increase UGT 1A9 enzyme expression resulting in enhanced glucuronidation activity [132]. This would indicate that polyphenols could induce their own glucuronidation. Finally, both quercetin derivatives exhibited a strong antioxidant capacity in the model of hypertrophic adipocytes, suggesting that these metabolites may reach intracellular targets and decrease ROS despite their low bioavailability detected in the cytoplasm of adipocytes (Chapter 3) [130].

Given the above mention, the knowledge of the pharmacokinetic behavior of polyphenols is crucial to focus the study on the effect of their metabolites in cell experiments and elucidate the mechanisms involved in the bioactivity of plants [135]. This approach was carried out in the second study of Chapter 3. In this work, we selected the major plasma metabolites found after the oral ingestion of HS in rats [98] to evaluate their capacity on amelioration of glucolipotoxicity-induced metabolic stress in adipocytes, i.e., chlorogenic acid, quercetin and quercetin-3-glucuronide. Our results showed that quercetin derivatives exert a stronger capacity to reduce ROS production in adipocytes under glucolipotoxic conditions. This antioxidant effect may be due to the role of these molecules as free radical scavengers [136]. In addition, other authors indicate that some quercetin metabolites can induce antioxidant enzyme expression through nuclear factor erythroid 2-related factor 2 (Nrf2) activation [137] or inhibit xanthine oxidase [138], a major enzyme involved in ROS production in some pathological conditions such as cardiovascular diseases.

Our results also demonstrated that quercetin metabolites decrease glucolipotoxicity-induced inflammation by decreasing adipokine secretion such as leptin, TNF-α, IGF-1, IL-6, VEGF, IL-1α, IL-1β and MCP-1. The reduced MCP-1 expression in adipocytes transfected with the promoter of this gene suggested that quercetin derivatives may modulate adipokine secretion at the transcriptional level, as confirmed previously by other authors [139]. This latter study showed that quercetin attenuates inflammatory gene expression in human macrophages likely through inhibition of proinflammatory transcription factors

such as NFκB, c-Jun and JNK, preventing macrophage-induced inflammation and insulin resistance in primary human adipocytes.

Triglyceride intracellular accumulation was also reduced by quercetin metabolites, being quercetin glucuronide the most active one. Our evidences lead us to postulate that this metabolite may promote fatty acid oxidation and inhibit lipogenesis by increasing PPARα expression and reducing FASN expression, respectively, as part of its mechanism of action. In agreement with this, the presence of quercetin-3-glucuronide at the surface of hepatic lipid droplets in hyperlipidemic mice fed HS was associated to changes in lipid composition of liver tissue and the amelioration of liver steatosis [87]. In this study, polyphenols modulated expression of miRNA involved in metabolic pathways, such as miR-103/107 and miR-122. These findings suggest that quercetin derivatives could reduce fat storage by modulating metabolic gene expression through epigenetic changes.

AMPK, the master regulator of cellular metabolism, was also activated by quercetin-3-glucuronide. This protein is activated by phosphorylation of Thr172 and modulate an arsenal of substrates in order to maintain energy homeostasis. In this sense, one of the mechanisms to explain the suppression of FASN expression might be through inhibition of its transcriptional factor sterol regulatory element binding protein 1c (SREBP-1c) via AMPK [140]. Interestingly, activation of AMPK by polyphenols culminates in the modulations of multiple pathways that help to prevent and treat obesity. For instance, resveratrol has shown to induce browning of white adipose tissue by increasing expression of specific genes of brown adipocytes through AMPK activation, among them, the master regulator of mitochondrial biogenesis peroxisome proliferator-activated receptor γ co-activator 1 α (PGC1α) [141]. In correlation with this, our results showed that quercetin derivatives increase mitochondrial content in hypertrophic adipocytes that could lead to a proper oxidative mitochondrial function resulting in a decrease on lipid content. Nevertheless, whether restoration of mitochondrial biogenesis by quercetins is due through AMPK-mediated PGC1α expression deserves further research.

On the other hand, the molecular mechanisms by which polyphenols can activate AMPK need to be further clarified. For instance, some polyphenols induce AMPK activation by increasing LKB1 activity, such as resveratrol [142], or through CaMKKβ phosphorylation, such as epigallocatechin-3-gallate of green tea [143]. It has been proposed that the antidiabetic drug metformin activates AMPK by decreasing ATP cell levels through inhibition of mitochondrial respiratory complex I [67], and it is thought that this mechanism could be exerted by polyphenols as well [144]. In addition, there is a chance that these

molecules might act as direct activators of AMPK, as suggested for quercetin metabolites in a molecular docking experiment in Chapter 3.

Computational molecular docking is a useful approach to predict potential interactions between polyphenols and the binding sites of a protein target. This strategy was also developed in Chapters 1 [120] and 2 to predict putative interactions of polyphenols from OL and LC, respectively, against binding sites of the different AMPK subunits. Particularly in Chapter 2, our results showed that loganic acid (an iridoid), luteolin-7-diglucuronide (a flavonoid) and verbascoside (a phenylpropanoid) from LC activate AMPK. In agreement with these data, the most active fraction of OL in the bioassay-guided fractionation study was mainly composed of verbascoside (Chapter 1) [120]. Furthermore, luteolin-7-diglucuronide and verbascoside have been detected as plasma metabolites in rats fed LC [114], suggesting that they could reach the adipose tissue in their native forms despite their high molecular weight.

As derived from our computational docking experiments, the bioactive polyphenols of LC (verbascoside, loganic acid and luteolin-7-diglucuronide) could act as AMPK agonists through interaction at different binding sites. Among them, these compounds exhibited low ΔG for any of the three AMP binding sites of the γ subunit. These data suggest that polyphenols may induce AMPK activation by mimicking allosteric mechanism of the nucleotide AMP, as reported for the agonist AICAR [145]. It was also observed that LC polyphenols established interactions in different positions to adenine nucleotide binding sites in the γ subunit. It is not excluded that these atypical interactions could modulate the activity of AMPK, as reported for the activator 5-(5-hydroxyl-isoxasol-3-yl)-furan-2-phosphonic acid [70]. Other regulatory positions through which polyphenols could promote the active conformation of the kinase have been described. For instance, the interface established between KD of alpha subunit and CBM of β subunit (called ADaM site) is a binding site for activators such as A-769662, compound 911 and salicylate [66, 70]. As well, amarogentin is a secoiridoid glycoside present in *Gentiana lutea* that exerts anti-atherosclerotic properties and has been described as a direct activator of AMPK. Interestingly, this polyphenol seems to bind to the AID region of alpha subunit, meaning that occupation of this region may disrupt its interaction with KD and favors the active conformation [146].

With all the above, there is a large number of cell and animal studies that demonstrate the pharmacological effects of plant-derived polyphenols in metabolic pathologies. However, the beneficial impact on human health is not widely studied and effective doses for clinical trial are still unclear. As derived from this and also previous work, polyphenols from HS and

LC extracts exert common and complementary mechanisms in obesity-related disorders [86, 87]. Accordingly, the aim of Chapter 4 was to evaluate the effect of a combination of both extracts in overweight and obese women [147]. Our results showed that the consumption of 500 mg per day of LC-HS (65:35, w/w) accompanied by an isocaloric diet and daily exercise for two months significantly reduced body weight, abdominal circumference and percentage of body fat in overweight women and less significant in obese women, compared to the placebo group.

Like many anti-obesity drugs, polyphenols could act at the gastrointestinal level by altering macronutrient digestion and absorption. According to previous molecular docking data, we propose that HS polyphenols may have the capacity to inhibit digestive enzymes by interacting with some glucosidase enzymes and the triacylglycerol lipase/colipase complex [148]. In addition, another mechanism by which LC-HS polyphenols can promote weight loss might be through hypothalamic control of appetite. We previously reported that LC-HS polyphenolic mixture have shown to increase anorexigenic hormones such as glucagon-like peptide-1 and decrease orexigenic hormones such as ghrelin in overweight subjects [149].

Nevertheless, the polyphenolic combination could exert mechanisms of action at other body levels. As observed in Chapter 4, the consumption of LC-HS supplement decreased heart rate and systolic blood pressure, especially in overweight women. The antihypertensive effect of HS extracts has been widely reported in the literature [110, 150]. As with endurance training, that induces skeletal muscle adaptations in terms of high mitochondrial density and increased blood flow accompanied by enlarged arteries [151], or with omega-3 fatty acids, that have shown to reduce heart rate through membrane electrical excitability of cardiac myocytes [152], we hypothesize that LC-HS polyphenols could exert similar mechanisms to explain the decrease on heart rate and blood pressure. Even so, these speculations need to be demonstrated.

According to our previous data in the *in vitro* adipocyte model, we strongly consider a direct action of LC-HS polyphenols on adipose tissue. In Chapter 4, we demonstrated a strong capacity of LC-HS combination to induce AMPK activation in hypertrophic 3T3-L1 adipocytes, accompanied by a reduction on intracellular lipid accumulation. Although we did not consider the *in vivo* metabolism of LC-HS polyphenols in this cell model, this mechanism is sustained by the strong AMPK activity of their main metabolites (verbascoside and quercetin-3-glucuronide) demonstrated in this work (Chapters 2 and 3). Likewise, activation of AMPK seems to result in an increase of basal metabolic rate and voluntary activity [153], as reported for some alternative weight loss agents [154, 155]. Similarly, we hypothesize that LC-HS polyphenols could increase resting energy

expenditure through AMPK activation, resulting in improved metabolic and anthropometric parameters.

In summary, the evidence obtained in this study support the hypothesis that metabolites from LC and HS, such as verbascoside and quercetin-3-glucuronide, seem to be the responsible for improving the metabolic alterations associated to obesity, by reducing oxidative stress and inflammation and restoring lipid homeostasis, an effect probably mediated by AMPK activation. Furthermore, these effects have been corroborated in human intervention trials. However, the future perspective is to deepen the identification of plasma metabolites, confirm the possible activation of AMPK in humans and elucidate the detailed mechanism of the observed lipid reduction and its possible epigenetic control.

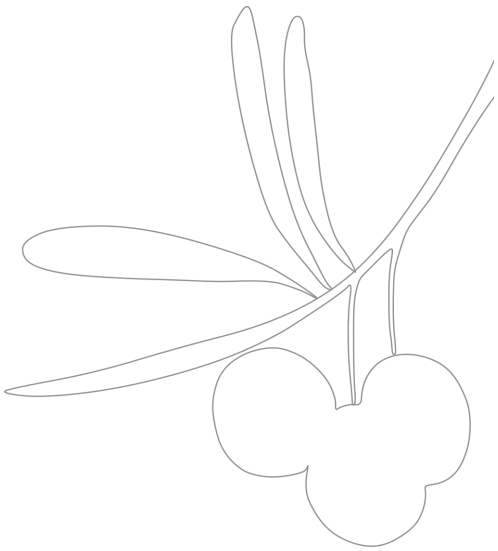

CONCLUSIONES/ CONCLUSIONS

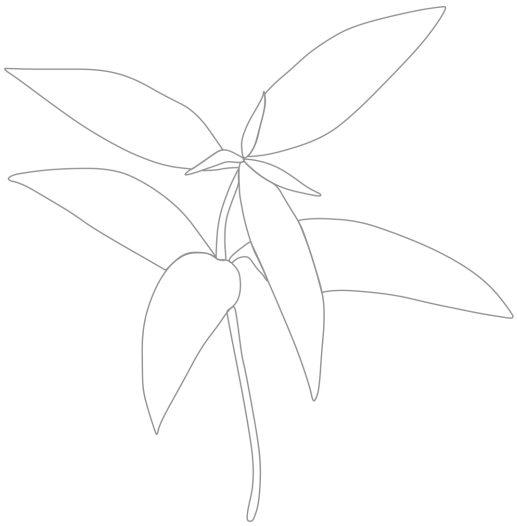

CONCLUSIONES

1. El extracto de OL reduce significativamente la acumulación de triglicéridos a través de mecanismos dependientes de AMPK en adipocitos hipertróficos. De acuerdo con el fraccionamiento guiado por bioensayo del extracto, se postula que polifenoles pertenecientes a las subclases de los secoiridoides, ácidos cinámicos, feniletanoides, fenilpropanoides, flavonoides y lignanos pueden ser los principales responsables de dichos efectos. Además, los datos de los experimentos de acoplamiento molecular sugieren que algunos de estos compuestos podrían actuar como agonistas directos de AMPK, interactuando con cualquiera de los tres sitios de unión de la subunidad γ.

2. El extracto de LC induce significativamente la activación de AMPK en adipocitos. La evaluación de los compuestos identificados y aislados del extracto mostraron que el ácido logánico, la luteolina-7-diglucurónido y el verbascósido son capaces de activar la quinasa, siendo el verbascósido el principal candidato para la actividad del extracto por su mayor abundancia. No obstante, el estudio de sinergia mostró un comportamiento sinérgico entre el ácido logánico y la luteolina-7-diglucurónido y efectos aditivos en combinación por parejas con el verbascósido, lo que sugiere que estos compuestos minoritarios en proporciones óptimas podrían aumentar la actividad de LC. Además, el experimento de acoplamiento molecular sugiere que cualquiera de los tres compuestos podría actuar como agonista directo de AMPK.

3. Quercetina y quercetina-3-glucurónido (metabolitos representativos de HS) son absorbidos por adipocitos hipertróficos y metabolizados a quercetina-3-glucurónido y quercetina por glucuronosiltransferasas y glucosidasas, respectivamente. La quercetina se absorbe más rápido, probablemente mediante un mecanismo de difusión pasiva, alcanzando una concentración celular más alta que la de su metabolito glucuronidado, el cual presenta una polaridad más alta. Además, la correlación entre la acumulación de metabolitos de quercetina en el citoplasma y la reducción de la generación de ERO intracelulares indica que ambos metabolitos son responsables de la fuerte capacidad antioxidante observada en adipocitos hipertróficos.

4. La quercetina y quercetina-3-glucurónido revierten el estrés metabólico inducido por glucolipotoxicidad en adipocitos hipertróficos. Concretamente, ambos metabolitos reducen significativamente la generación de ERO y la secreción de adipoquinas proinflamatorias. En particular, la quercetina-3-glucurónido es más potente

reduciendo la acumulación de lípidos intracelulares, probablemente mediante la oxidación de ácidos grasos y la inhibición de la lipogénesis a través del aumento de PPARα, la disminución de FASN, la activación de AMPK y el restablecimiento de la función mitocondrial.

5. La ingesta de 500 mg de una combinación polifenólica preparada a partir de extractos de LC y HS acompañada por una dieta isocalórica durante dos semanas mejora los parámetros antropométricos como el peso corporal, la circunferencia abdominal y el porcentaje de grasa corporal, disminuye la presión arterial sistólica y el pulso cardíaco y mejora el perfil lipídico en mujeres con sobrepeso. No obstante, los cambios son más modestos en voluntarias obesas. Estos cambios podrían llevarse a cabo por la acción de los polifenoles de LC-HS sobre el sistema cardiovascular y la activación de AMPK en el tejido adiposo.

6. Los datos farmacocinéticos disponibles sobre los polifenoles de plantas medicinales como HS, LC, OL y *Rosmarinus officinalis* revelan que la mayoría de estos polifenoles presentan una rápida absorción en el intestino, son altamente metabolizados por los enterocitos, hepatocitos y flora intestinal siendo principalmente deglicosilados, glucuronidados, sulfatados y metilados, y exhiben una baja biodisponibilidad alcanzando concentraciones en un rango micromolar bajo. Además, muchos de los estudios indican que estas plantas son generalmente bien toleradas. Sin embargo, se requieren más estudios de biodisponibilidad y toxicología para establecer las dosis seguras y efectivas para el consumo a largo plazo.

7. A pesar de las altas concentraciones empleadas en los experimentos celulares y la baja biodisponibilidad de los polifenoles, los resultados obtenidos en este trabajo demuestran que el consumo de polifenoles tiene efectos saludables frente a las alteraciones metabólicas asociadas a la obesidad. Sin embargo, es necesario realizar estudios enfocados en la metabolómica dirigida en muestras de plasma y de tejidos, así como experimentos *in silico* con dianas proteicas y modelos celulares usando metabolitos con el fin de identificar los metabolitos efectores y elucidar los mecanismos moleculares implicados en los efectos beneficiosos de los polifenoles.

CONCLUSIONS

1. OL extract significantly reduces triglyceride accumulation through AMPK-dependent mechanisms in hypertrophic adipocytes. According to the bioassay-guided fractionation of the extract, it is postulated that polyphenols belonging to the secoirioids, cinnamic acids, phenylethanoids and phenylpropanoids, flavonoids and lignans subclasses may be the main responsible for such effects. Furthermore, docking experiment data suggest that some of these compounds could act as direct agonists of AMPK, interacting with any of the three binding sites of the γ subunit.

2. LC extract significantly induces AMPK activation in adipocytes. The evaluation of compounds identified and isolated from the extract showed that loganic acid, lutelin-7-diglucuronide and verbascoside are able to activate the kinase, being verbascoside the main candidate for the AMPK activating capacity of the extract due to its high abundance. Nevertheless, a synergy study indicated a synergistic behavior between loganic acid and luteolin-7-diglucuronide and additive effects in pairwise combinations with verbascoside, suggesting that these minor compounds in an appropriate proportion could enhance the activity of LC. In addition, the molecular docking experiment suggest that any of the three activator compounds could act as direct agonists of AMPK.

3. Quercetin and quercetin-3-glucuronide (representative metabolites from HS) are absorbed by hypertrophic adipocytes and metabolized to quercetin-3-glucuronide and quercetin by glucuronosyltransferase and glucosidase activity, respectively. Quercetin is absorbed faster, probably through a passive diffusion mechanism, reaching a higher intracellular concentration than its glucuronide metabolite, which presents a higher polarity. In addition, the correlation between the accumulation of quercetin metabolites in the cytoplasm of adipocytes and the reduction of intracellular ROS generation indicates that both metabolites are responsible for the strong antioxidant capacity observed in hypertrophic adipocytes.

4. Quercetin and quercetin-3-glucuronide reverse glucolipotoxicity-induced metabolic stress in hypertrophic adipocytes. Specifically, both metabolites significantly reduce ROS generation and proinflammatory adipokine secretion. In particular, quercetin-3-glucuronide is more potent reducing intracellular lipid accumulation, probably by

oxidation of fatty acids and inhibition of lipogenesis through PPARα upregulation, FASN downregulation, AMPK activation and mitochondrial function restoration.

5. The intake of 500 mg of a polyphenolic combination based on LC and HS extracts accompanied by an isocaloric diet for two months improves anthropometric parameters such as body weight, abdominal circumference and percentage of body fat, decreases systolic blood pressure and heart rate and improves blood lipid profile in overweight women. However, changes are more modest in obese volunteers. These changes could be achieved by the action of LC-HS polyphenols on cardiovascular system and AMPK activation in adipose tissue.

6. Available pharmacokinetic data about polyphenols from medicinal plants such as HS, LC, OL and *Rosmarinus officinalis* reveal that most of these polyphenols present a fast absorption in intestine, are highly metabolized by enterocytes, hepatocytes and colonic microflora being mainly deglycosylated, glucuronidated, sulfated and methylated and exhibit a low bioavailability reaching plasma concentrations in the low micromolar range. In addition, most of the studies indicate that these plants are generally well-tolerated. Nevertheless, further bioavailability and toxicological studies are required to establish safe and effective doses for long-term consumption.

7. Despite the high concentrations used on cell experiments and the low bioavailability of polyphenols, the results obtained in this work demonstrate that polyphenol consumption has salutary effects against metabolic disturbances associated to obesity. However, further research focused on targeted metabolomics in plasma and tissue samples and *in silico* experiments with protein targets and cell models using metabolites are required to identify effector metabolites and elucidate the molecular mechanisms involved in the beneficial effects of polyphenols.

PROYECCIÓN FUTURA

PROYECCIÓN FUTURA

En vista de los resultados obtenidos en este proyecto, se destaca la importancia de integrar los estudios que investigan los efectos biológicos de las moléculas bioactivas con el conocimiento sobre los procesos que sufren dichas moléculas una vez ingeridas. La forma en la que estas moléculas llegan a la circulación sanguínea determina la manera en la que alcanzan el lugar de acción, repercutiendo en la efectividad de su actividad farmacológica.

Por ello, el objetivo futuro que se plantea es llevar a cabo una estrategia analítica de metabolómica dirigida para estudiar el perfil metabólico de los polifenoles tras el consumo humano. De esta manera, el uso de modelos celulares y técnicas *in silico* tiene mayor relevancia cuando se emplean metabolitos y no los polifenoles en sus formas nativas. Estos descubrimientos nos permitirían centrar el enriquecimiento de los extractos de plantas en aquellos compuestos que dan lugar a los metabolitos activos para su implicación clínica en patologías asociadas a la obesidad.

REFERENCIAS

REFERENCIAS

1. WHO, *Physical status: the use and interpretation of anthropometry: report of a World Health Organization (WHO) expert committee. Geneve, Switzerland*. 1995, World Health Organization.
2. Nuttall, F.Q., *Body Mass Index: Obesity, BMI, and Health: A Critical Review*, in *Nutr Today*. 2015. p. 117-28.
3. WHO, *Obesity: preventing and managing the global epidemic. Report of a WHO Consultation (WHO Technical Report Series 894)*, in *WHO*. 2000, World Health Organization.
4. NCD-RisC, *Worldwide trends in body-mass index, underweight, overweight, and obesity from 1975 to 2016: a pooled analysis of 2416 population-based measurement studies in 128.9 million children, adolescents, and adults.* Lancet, 2017. **390**(10113): p. 2627-2642.
5. *NCD Risk Factor Collaboration*. Available from: http://ncdrisc.org/index.html.
6. Choe, S.S., et al., *Adipose Tissue Remodeling: Its Role in Energy Metabolism and Metabolic Disorders.* Front Endocrinol (Lausanne), 2016. **7**: p. 30.
7. Mead, J.R., S.A. Irvine, and D.P. Ramji, *Lipoprotein lipase: structure, function, regulation, and role in disease.* J Mol Med (Berl), 2002. **80**(12): p. 753-69.
8. Morak, M., et al., *Adipose triglyceride lipase (ATGL) and hormone-sensitive lipase (HSL) deficiencies affect expression of lipolytic activities in mouse adipose tissues.* Mol Cell Proteomics, 2012. **11**(12): p. 1777-89.
9. Vazquez-Vela, M.E., N. Torres, and A.R. Tovar, *White adipose tissue as endocrine organ and its role in obesity.* Arch Med Res, 2008. **39**(8): p. 715-28.
10. Vegiopoulos, A., M. Rohm, and S. Herzig, *Adipose tissue: between the extremes.* Embo j, 2017. **36**(14): p. 1999-2017.
11. Marlatt, K.L. and E. Ravussin, *Brown Adipose Tissue: an Update on Recent Findings.* Curr Obes Rep, 2017. **6**(4): p. 389-396.
12. Fedorenko, A., P.V. Lishko, and Y. Kirichok, *Mechanism of fatty-acid-dependent UCP1 uncoupling in brown fat mitochondria.* Cell, 2012. **151**(2): p. 400-13.
13. Lee, M.J., Y. Wu, and S.K. Fried, *Adipose tissue heterogeneity: implication of depot differences in adipose tissue for obesity complications.* Mol Aspects Med, 2013. **34**(1): p. 1-11.
14. Virtanen, K.A., et al., *Functional brown adipose tissue in healthy adults.* N Engl J Med, 2009. **360**(15): p. 1518-25.
15. Cypess, A.M., et al., *Identification and importance of brown adipose tissue in adult humans.* N Engl J Med, 2009. **360**(15): p. 1509-17.
16. Aune, U.L., L. Ruiz, and S. Kajimura, *Isolation and differentiation of stromal vascular cells to beige/brite cells.* J Vis Exp, 2013(73).
17. Sidossis, L. and S. Kajimura, *Brown and beige fat in humans: thermogenic adipocytes that control energy and glucose homeostasis.* J Clin Invest, 2015. **125**(2): p. 478-86.
18. Wang, S., et al., *Resveratrol enhances brown adipocyte formation and function by activating AMP-activated protein kinase (AMPK) alpha1 in mice fed high-fat diet.* Mol Nutr Food Res, 2017. **61**(4).
19. Cohen, P., et al., *Ablation of PRDM16 and beige adipose causes metabolic dysfunction and a subcutaneous to visceral fat switch.* Cell, 2014. **156**(1-2): p. 304-16.
20. Zhang, X., et al., *Dietary luteolin activates browning and thermogenesis in mice through an AMPK/PGC1alpha pathway-mediated mechanism.* Int J Obes (Lond), 2016. **40**(12): p. 1841-1849.
21. Brestoff, J.R. and D. Artis, *Immune regulation of metabolic homeostasis in health and disease.* Cell, 2015. **161**(1): p. 146-160.
22. Coelho, M., T. Oliveira, and R. Fernandes, *Biochemistry of adipose tissue: an endocrine organ.* Arch Med Sci, 2013. **9**(2): p. 191-200.

23. Dandona, P., A. Aljada, and A. Bandyopadhyay, *Inflammation: the link between insulin resistance, obesity and diabetes.* Trends Immunol, 2004. **25**(1): p. 4-7.
24. Trayhurn, P. and I.S. Wood, *Signalling role of adipose tissue: adipokines and inflammation in obesity.* Biochem Soc Trans, 2005. **33**(Pt 5): p. 1078-81.
25. Kloting, N. and M. Bluher, *Adipocyte dysfunction, inflammation and metabolic syndrome.* Rev Endocr Metab Disord, 2014. **15**(4): p. 277-87.
26. Ghaben, A.L. and P.E. Scherer, *Adipogenesis and metabolic health.* Nat Rev Mol Cell Biol, 2019. **20**(4): p. 242-258.
27. Hoffstedt, J., et al., *Regional impact of adipose tissue morphology on the metabolic profile in morbid obesity.* Diabetologia, 2010. **53**(12): p. 2496-503.
28. Murphy, M.P., *How mitochondria produce reactive oxygen species.* Biochem J, 2009. **417**(1): p. 1-13.
29. Maslov, L.N., et al., *Is oxidative stress of adipocytes a cause or a consequence of the metabolic syndrome?* J Clin Transl Endocrinol, 2019. **15**: p. 1-5.
30. Tormos, K.V., et al., *Mitochondrial complex III ROS regulate adipocyte differentiation.* Cell Metab, 2011. **14**(4): p. 537-44.
31. Ma, M., et al., *Bidirectional modulation of insulin action by reactive oxygen species in 3T3L1 adipocytes.* Mol Med Rep, 2018. **18**(1): p. 807-814.
32. Castro, J.P., T. Grune, and B. Speckmann, *The two faces of reactive oxygen species (ROS) in adipocyte function and dysfunction.* Biol Chem, 2016. **397**(8): p. 709-24.
33. Gao, C.L., et al., *Mitochondrial dysfunction is induced by high levels of glucose and free fatty acids in 3T3-L1 adipocytes.* Mol Cell Endocrinol, 2010. **320**(1-2): p. 25-33.
34. Kim, M.J., et al., *Rg3 Improves Mitochondrial Function and the Expression of Key Genes Involved in Mitochondrial Biogenesis in C2C12 Myotubes.* Diabetes Metab J, 2016. **40**(5): p. 406-413.
35. Woo, C.Y., et al., *Mitochondrial Dysfunction in Adipocytes as a Primary Cause of Adipose Tissue Inflammation.* Diabetes Metab J, 2019.
36. Ohashi, K., et al., *Adiponectin Promotes Macrophage Polarization toward an Anti-inflammatory Phenotype**, in *J Biol Chem*. 2010. p. 6153-60.
37. Kern, P.A., et al., *Adiponectin expression from human adipose tissue: relation to obesity, insulin resistance, and tumor necrosis factor-alpha expression.* Diabetes, 2003. **52**(7): p. 1779-85.
38. Goyal, R., et al., *Evaluation of TNF-alpha and IL-6 Levels in Obese and Non-obese Diabetics: Pre- and Postinsulin Effects.* N Am J Med Sci, 2012. **4**(4): p. 180-4.
39. Anusree, S.S., et al., *Insulin resistance in 3T3-L1 adipocytes by TNF-alpha is improved by punicic acid through upregulation of insulin signalling pathway and endocrine function, and downregulation of proinflammatory cytokines.* Biochimie, 2018. **146**: p. 79-86.
40. Rotter, V., I. Nagaev, and U. Smith, *Interleukin-6 (IL-6) induces insulin resistance in 3T3-L1 adipocytes and is, like IL-8 and tumor necrosis factor-alpha, overexpressed in human fat cells from insulin-resistant subjects.* J Biol Chem, 2003. **278**(46): p. 45777-84.
41. Trim, W., J.E. Turner, and D. Thompson, *Parallels in Immunometabolic Adipose Tissue Dysfunction with Ageing and Obesity.* Front Immunol, 2018. **9**: p. 169.
42. O'Neill, S. and L. O'Driscoll, *Metabolic syndrome: a closer look at the growing epidemic and its associated pathologies.* Obes Rev, 2015. **16**(1): p. 1-12.
43. Schuster, D.P., *Obesity and the development of type 2 diabetes: the effects of fatty tissue inflammation.* Diabetes Metab Syndr Obes, 2010. **3**: p. 253-62.
44. Gauthier, M.S. and N.B. Ruderman, *Adipose tissue inflammation and insulin resistance: all obese humans are not created equal.* Biochem J, 2010. **430**(2): p. e1-4.
45. Kersten, S., *Peroxisome proliferator activated receptors and obesity.* Eur J Pharmacol, 2002. **440**(2-3): p. 223-34.
46. Han, L., et al., *PPARs: regulators of metabolism and as therapeutic targets in cardiovascular disease. Part II: PPAR-beta/delta and PPAR-gamma.* Future Cardiol, 2017. **13**(3): p. 279-296.

47. Moseti, D., A. Regassa, and W.K. Kim, *Molecular Regulation of Adipogenesis and Potential Anti-Adipogenic Bioactive Molecules.* Int J Mol Sci, 2016. **17**(1).
48. Guo, L., X. Li, and Q.Q. Tang, *Transcriptional regulation of adipocyte differentiation: a central role for CCAAT/enhancer-binding protein (C/EBP) beta.* J Biol Chem, 2015. **290**(2): p. 755-61.
49. Rosen, E.D., et al., *C/EBPalpha induces adipogenesis through PPARgamma: a unified pathway.* Genes Dev, 2002. **16**(1): p. 22-6.
50. de Villiers, D., et al., *The Role of Reactive Oxygen Species in Adipogenic Differentiation.* Adv Exp Med Biol, 2018. **1083**: p. 125-144.
51. Ruiz-Ojeda, F.J., et al., *Cell Models and Their Application for Studying Adipogenic Differentiation in Relation to Obesity: A Review.* Int J Mol Sci, 2016. **17**(7).
52. Gabrielli, M., et al., *Exchange protein activated by cyclic AMP is involved in the regulation of adipogenic genes during 3T3-L1 fibroblasts differentiation.* Dev Growth Differ, 2014. **56**(2): p. 143-51.
53. Park, Y.K. and K. Ge, *Glucocorticoid Receptor Accelerates, but Is Dispensable for, Adipogenesis.* Mol Cell Biol, 2017. **37**(2).
54. Merck. *Adipogenesis Assay | ECM950*. Available from: https://www.merckmillipore.com/ES/es/product/Adipogenesis-Assay,MM_NF-ECM950#anchor_DS.
55. Herranz-Lopez, M., et al., *Synergism of plant-derived polyphenols in adipogenesis: perspectives and implications.* Phytomedicine, 2012. **19**(3-4): p. 253-61.
56. Ross, F.A., C. MacKintosh, and D.G. Hardie, *AMP-activated protein kinase: a cellular energy sensor that comes in 12 flavours.* Febs j, 2016. **283**(16): p. 2987-3001.
57. Yan, Y., et al., *Structure and Physiological Regulation of AMPK.* Int J Mol Sci, 2018. **19**(11).
58. Sanz, P., T. Rubio, and M.A. Garcia-Gimeno, *AMPKbeta subunits: more than just a scaffold in the formation of AMPK complex.* Febs j, 2013. **280**(16): p. 3723-33.
59. Garcia, D. and R.J. Shaw, *AMPK: Mechanisms of Cellular Energy Sensing and Restoration of Metabolic Balance.* Mol Cell, 2017. **66**(6): p. 789-800.
60. Hardie, D.G., *AMP-activated protein kinase: maintaining energy homeostasis at the cellular and whole-body levels.* Annu Rev Nutr, 2014. **34**: p. 31-55.
61. Fujiwara, Y., et al., *Differential AMP-activated Protein Kinase (AMPK) Recognition Mechanism of Ca2+/Calmodulin-dependent Protein Kinase Kinase Isoforms.* J Biol Chem, 2016. **291**(26): p. 13802-8.
62. Zhang, Y.L., et al., *AMP as a low-energy charge signal autonomously initiates assembly of AXIN-AMPK-LKB1 complex for AMPK activation.* Cell Metab, 2013. **18**(4): p. 546-55.
63. Hawley, S.A., et al., *Phosphorylation by Akt within the ST loop of AMPK-alpha1 down-regulates its activation in tumour cells.* Biochem J, 2014. **459**(2): p. 275-87.
64. Li, X., et al., *Structural basis of AMPK regulation by adenine nucleotides and glycogen.* Cell Res, 2015. **25**(1): p. 50-66.
65. Galic, S., et al., *AMPK signaling to acetyl-CoA carboxylase is required for fasting- and cold-induced appetite but not thermogenesis.* Elife, 2018. **7**.
66. Kim, J., et al., *AMPK activators: mechanisms of action and physiological activities.* Exp Mol Med, 2016. **48**: p. e224.
67. Owen, M.R., E. Doran, and A.P. Halestrap, *Evidence that metformin exerts its anti-diabetic effects through inhibition of complex 1 of the mitochondrial respiratory chain.* Biochem J, 2000. **348 Pt 3**: p. 607-14.
68. Rizos, C.V., A. Kei, and M.S. Elisaf, *The current role of thiazolidinediones in diabetes management.* Arch Toxicol, 2016. **90**(8): p. 1861-81.
69. Brass, E.P. and C.L. Hoppel, *Mitochondria as targets of drug toxicity: Lessons from the R118 phase I experience.* Clin Pharmacol Ther, 2015. **98**(5): p. 464-6.
70. Langendorf, C.G., et al., *Structural basis of allosteric and synergistic activation of AMPK by furan-2-phosphonic derivative C2 binding.* Nat Commun, 2016. **7**: p. 10912.

71. Ruban, A., et al., *Current treatments for obesity.* Clin Med (Lond), 2019. **19**(3): p. 205-212.
72. Narayanaswami, V. and L.P. Dwoskin, *Obesity: Current and potential pharmacotherapeutics and targets.* Pharmacol Ther, 2017. **170**: p. 116-147.
73. Duthie, G.G., P.T. Gardner, and J.A. Kyle, *Plant polyphenols: are they the new magic bullet?* Proc Nutr Soc, 2003. **62**(3): p. 599-603.
74. Li, A.N., et al., *Resources and biological activities of natural polyphenols.* Nutrients, 2014. **6**(12): p. 6020-47.
75. Mopuri, R. and M.S. Islam, *Medicinal plants and phytochemicals with anti-obesogenic potentials: A review.* Biomed Pharmacother, 2017. **89**: p. 1442-1452.
76. Furukawa, S., et al., *Increased oxidative stress in obesity and its impact on metabolic syndrome.* J Clin Invest, 2004. **114**(12): p. 1752-61.
77. Fernandez-Arroyo, S., et al., *Quantification of the polyphenolic fraction and in vitro antioxidant and in vivo anti-hyperlipemic activities of Hibiscus sabdariffa aqueous extract.* Food Research International, 2011. **44**(5).
78. Adeyemi, D.O., et al., *Anti-hepatotoxic activities of Hibiscus sabdariffa L. in animal model of streptozotocin diabetes-induced liver damage.* BMC Complement Altern Med, 2014. **14**: p. 277.
79. Funes, L., et al., *Correlation between plasma antioxidant capacity and verbascoside levels in rats after oral administration of lemon verbena extract.* Food Chemistry, 2009. **117**(4): p. 589–598.
80. Funes, L., et al., *Effects of verbascoside, a phenylpropanoid glycoside from lemon verbena, on phospholipid model membranes.* Chem Phys Lipids, 2010. **163**(2): p. 190-9.
81. Lee, O.H. and B.Y. Lee, *Antioxidant and antimicrobial activities of individual and combined phenolics in Olea europaea leaf extract.* Bioresour Technol, 2010. **101**(10): p. 3751-4.
82. Martínez-Huélamo, M., et al., *Modulation of Nrf2 by Olive Oil and Wine Polyphenols and Neuroprotection*, in *Antioxidants (Basel)*. 2017.
83. Beltran-Debon, R., et al., *The aqueous extract of Hibiscus sabdariffa calices modulates the production of monocyte chemoattractant protein-1 in humans.* Phytomedicine, 2010. **17**(3-4): p. 186-91.
84. Ezzat, S.M., et al., *Metabolic profile and hepatoprotective activity of the anthocyanin-rich extract of Hibiscus sabdariffa calyces.* Pharm Biol, 2016. **54**(12): p. 3172-3181.
85. Kao, E.S., et al., *Polyphenols extracted from Hibiscus sabdariffa L. inhibited lipopolysaccharide-induced inflammation by improving antioxidative conditions and regulating cyclooxygenase-2 expression.* Biosci Biotechnol Biochem, 2009. **73**(2): p. 385-90.
86. Herranz-Lopez, M., et al., *Lemon verbena (Lippia citriodora) polyphenols alleviate obesity-related disturbances in hypertrophic adipocytes through AMPK-dependent mechanisms.* Phytomedicine, 2015. **22**(6): p. 605-14.
87. Joven, J., et al., *Plant-derived polyphenols regulate expression of miRNA paralogs miR-103/107 and miR-122 and prevent diet-induced fatty liver disease in hyperlipidemic mice.* Biochim Biophys Acta, 2012. **1820**(7): p. 894-9.
88. Fernandes, G.F.S., et al., *Epigenetic Regulatory Mechanisms Induced by Resveratrol.* Nutrients, 2017. **9**(11).
89. Cuyas, E., et al., *Extra Virgin Olive Oil Contains a Phenolic Inhibitor of the Histone Demethylase LSD1/KDM1A.* Nutrients, 2019. **11**(7).
90. *The Surprising Health Benefits of Hibiscus*. Available from: https://webdesigninstitute.wixsite.com/herbaltea/single-post/2014/01/15/The-Surprising-Health-Benefits-of-Hibiscus.
91. *Lippia triphylla*. Available from: https://www.somsegarra.cat/flora/noticia/878/marialluisa-(lippia-triphylla).

92. *Olear europaea*. Available from: http://vineveracosmetics.com/2014/05/20/ingredient-spotlight-olea-europaea/.
93. Scalbert, A. and G. Williamson, *Dietary intake and bioavailability of polyphenols.* J Nutr, 2000. **130**(8S Suppl): p. 2073s-85s.
94. Kawabata, K., Y. Yoshioka, and J. Terao, *Role of Intestinal Microbiota in the Bioavailability and Physiological Functions of Dietary Polyphenols*, in *Molecules*. 2019.
95. Olivares-Vicente, M., et al., *Plant-Derived Polyphenols in Human Health: Biological Activity, Metabolites and Putative Molecular Targets.* Curr Drug Metab, 2018. **19**(4): p. 351-369.
96. van Duynhoven, J., et al., *Metabolic fate of polyphenols in the human superorganism.* Proc Natl Acad Sci U S A, 2011. **108 Suppl 1**: p. 4531-8.
97. Quirantes-Pine, R., et al., *HPLC-ESI-QTOF-MS as a powerful analytical tool for characterising phenolic compounds in olive-leaf extracts.* Phytochem Anal, 2013. **24**(3): p. 213-23.
98. Fernandez-Arroyo, S., et al., *Bioavailability study of a polyphenol-enriched extract from Hibiscus sabdariffa in rats and associated antioxidant status.* Mol Nutr Food Res, 2012. **56**(10): p. 1590-5.
99. Kawai, Y., et al., *Macrophage as a target of quercetin glucuronides in human atherosclerotic arteries: implication in the anti-atherosclerotic mechanism of dietary flavonoids.* J Biol Chem, 2008. **283**(14): p. 9424-34.
100. Lee, Y.S., et al., *Metabolaid((R)) Combination of Lemon Verbena and Hibiscus Flower Extract Prevents High-Fat Diet-Induced Obesity through AMP-Activated Protein Kinase Activation.* Nutrients, 2018. **10**(9).
101. Maestre, I., et al., *Mitochondrial dysfunction is involved in apoptosis induced by serum withdrawal and fatty acids in the beta-cell line INS-1.* Endocrinology, 2003. **144**(1): p. 335-45.
102. Mittra, S., V.S. Bansal, and P.K. Bhatnagar, *From a glucocentric to a lipocentric approach towards metabolic syndrome.* Drug Discov Today, 2008. **13**(5-6): p. 211-8.
103. Yeop Han, C., et al., *Differential effect of saturated and unsaturated free fatty acids on the generation of monocyte adhesion and chemotactic factors by adipocytes: dissociation of adipocyte hypertrophy from inflammation.* Diabetes, 2010. **59**(2): p. 386-96.
104. Tanis, R.M., et al., *The effect of glucose concentration and sodium phenylbutyrate treatment on mitochondrial bioenergetics and ER stress in 3T3-L1 adipocytes.* Biochim Biophys Acta, 2015. **1853**(1): p. 213-21.
105. El-Assaad, W., et al., *Glucolipotoxicity alters lipid partitioning and causes mitochondrial dysfunction, cholesterol, and ceramide deposition and reactive oxygen species production in INS832/13 ss-cells.* Endocrinology, 2010. **151**(7): p. 3061-73.
106. Tomas-Menor, L., et al., *The promiscuous and synergic molecular interaction of polyphenols in bactericidal activity: an opportunity to improve the performance of antibiotics?* Phytother Res, 2015. **29**(3): p. 466-73.
107. *EUCAST Definitive Document E.Def 1.2, May 2000: Terminology relating to methods for the determination of susceptibility of bacteria to antimicrobial agents.* Clin Microbiol Infect, 2000. **6**(9): p. 503-8.
108. Krieger, E. and G. Vriend, *YASARA View - molecular graphics for all devices - from smartphones to workstations.* Bioinformatics, 2014. **30**(20): p. 2981-2.
109. Weltman, A., et al., *Accurate assessment of body composition in obese females.* Am J Clin Nutr, 1988. **48**(5): p. 1179-83.
110. Joven, J., et al., *Hibiscus sabdariffa extract lowers blood pressure and improves endothelial function.* Mol Nutr Food Res, 2014. **58**(6): p. 1374-8.
111. Borras-Linares, I., et al., *Permeability Study of Polyphenols Derived from a Phenolic-Enriched Hibiscus sabdariffa Extract by UHPLC-ESI-UHR-Qq-TOF-MS.* Int J Mol Sci, 2015. **16**(8): p. 18396-411.

112. Bilia, A.R., et al., *HPLC-DAD-ESI-MS analysis of the constituents of aqueous preparations of verbena and lemon verbena and evaluation of the antioxidant activity.* J Pharm Biomed Anal, 2008. **46**(3): p. 463-70.
113. Quirantes-Pine, R., et al., *High-performance liquid chromatography with diode array detection coupled to electrospray time-of-flight and ion-trap tandem mass spectrometry to identify phenolic compounds from a lemon verbena extract.* J Chromatogr A, 2009. **1216**(28): p. 5391-7.
114. Quirantes-Pine, R., et al., *Phenylpropanoids and their metabolites are the major compounds responsible for blood-cell protection against oxidative stress after administration of Lippia citriodora in rats.* Phytomedicine, 2013. **20**(12): p. 1112-8.
115. Borras-Linares, I., et al., *Rosmarinus officinalis leaves as a natural source of bioactive compounds.* Int J Mol Sci, 2014. **15**(11): p. 20585-606.
116. Perez-Fons, L., M.T. Garzon, and V. Micol, *Relationship between the antioxidant capacity and effect of rosemary (Rosmarinus officinalis L.) polyphenols on membrane phospholipid order.* J Agric Food Chem, 2010. **58**(1): p. 161-71.
117. Borras-Linares, I., et al., *A bioguided identification of the active compounds that contribute to the antiproliferative/cytotoxic effects of rosemary extract on colon cancer cells.* Food Chem Toxicol, 2015. **80**: p. 215-22.
118. Romo Vaquero, M., et al., *Bioavailability of the major bioactive diterpenoids in a rosemary extract: metabolic profile in the intestine, liver, plasma, and brain of Zucker rats.* Mol Nutr Food Res, 2013. **57**(10): p. 1834-46.
119. Perez-Sanchez, A., et al., *Evaluation of the intestinal permeability of rosemary (Rosmarinus officinalis L.) extract polyphenols and terpenoids in Caco-2 cell monolayers.* PLoS One, 2017. **12**(2): p. e0172063.
120. Jimenez-Sanchez, C., et al., *AMPK modulatory activity of olive-tree leaves phenolic compounds: Bioassay-guided isolation on adipocyte model and in silico approach.* PLoS One, 2017. **12**(3): p. e0173074.
121. de Bock, M., et al., *Human absorption and metabolism of oleuropein and hydroxytyrosol ingested as olive (Olea europaea L.) leaf extract.* Mol Nutr Food Res, 2013. **57**(11): p. 2079-85.
122. Khymenets, O., et al., *Antioxidant activities of hydroxytyrosol main metabolites do not contribute to beneficial health effects after olive oil ingestion.* Drug Metab Dispos, 2010. **38**(9): p. 1417-21.
123. Green, H. and M. Meuth, *An established pre-adipose cell line and its differentiation in culture.* Cell, 1974. **3**(2): p. 127-33.
124. Han, C.Y., et al., *Adipocyte-derived serum amyloid A3 and hyaluronan play a role in monocyte recruitment and adhesion.* Diabetes, 2007. **56**(9): p. 2260-73.
125. Barrajon-Catalan, E., et al., *Molecular promiscuity of plant polyphenols in the management of age-related diseases: far beyond their antioxidant properties.* Adv Exp Med Biol, 2014. **824**: p. 141-59.
126. Cádiz-Gurrea, M.d.l.L., et al., *Bioassay-guided purification of Lippia citriodora polyphenols with AMPK modulatory activity.* Journal of Functional Foods, 2018. **46**: p. 514-520.
127. Kim, J., et al., *Vitexin, orientin and other flavonoids from Spirodela polyrhiza inhibit adipogenesis in 3T3-L1 cells.* Phytother Res, 2010. **24**(10): p. 1543-8.
128. Sesink, A.L., K.A. O'Leary, and P.C. Hollman, *Quercetin glucuronides but not glucosides are present in human plasma after consumption of quercetin-3-glucoside or quercetin-4'-glucoside.* J Nutr, 2001. **131**(7): p. 1938-41.
129. Yang, L.L., et al., *Pharmacokinetic comparison between quercetin and quercetin 3-O-beta-glucuronide in rats by UHPLC-MS/MS.* Sci Rep, 2016. **6**: p. 35460.
130. Herranz-López, M., et al., *Correlation between the cellular metabolism of quercetin and its glucuronide metabolite and oxidative stress in hypertrophied 3T3-L1 adipocytes.* 2017. **25**: p. 25–28.

131. O'Leary, K.A., et al., *Metabolism of quercetin-7- and quercetin-3-glucuronides by an in vitro hepatic model: the role of human beta-glucuronidase, sulfotransferase, catechol-O-methyltransferase and multi-resistant protein 2 (MRP2) in flavonoid metabolism.* Biochem Pharmacol, 2003. **65**(3): p. 479-91.
132. Barbier, O., et al., *The UDP-glucuronosyltransferase 1A9 enzyme is a peroxisome proliferator-activated receptor alpha and gamma target gene.* J Biol Chem, 2003. **278**(16): p. 13975-83.
133. Terao, J., K. Murota, and Y. Kawai, *Conjugated quercetin glucuronides as bioactive metabolites and precursors of aglycone in vivo.* Food Funct, 2011. **2**(1): p. 11-7.
134. Encinar, J.A., et al., *In silico approach for the discovery of new PPARgamma modulators among plant-derived polyphenols.* Drug Des Devel Ther, 2015. **9**: p. 5877-95.
135. Qian, Y., et al., *Metabolites of flavonoid compounds preserve indices of endothelial cell nitric oxide bioavailability under glucotoxic conditions.* Nutr Diabetes, 2017. **7**(9): p. e286.
136. Di Meo, F., et al., *Free radical scavenging by natural polyphenols: atom versus electron transfer.* J Phys Chem A, 2013. **117**(10): p. 2082-92.
137. Li, C., W.J. Zhang, and B. Frei, *Quercetin inhibits LPS-induced adhesion molecule expression and oxidant production in human aortic endothelial cells by p38-mediated Nrf2 activation and antioxidant enzyme induction.* Redox Biol, 2016. **9**: p. 104-113.
138. Mohos, V., et al., *Inhibitory Effects of Quercetin and Its Human and Microbial Metabolites on Xanthine Oxidase Enzyme.* Int J Mol Sci, 2019. **20**(11).
139. Overman, A., C.C. Chuang, and M. McIntosh, *Quercetin attenuates inflammation in human macrophages and adipocytes exposed to macrophage-conditioned media.* Int J Obes (Lond), 2011. **35**(9): p. 1165-72.
140. Li, Y., et al., *AMPK phosphorylates and inhibits SREBP activity to attenuate hepatic steatosis and atherosclerosis in diet-induced insulin-resistant mice.* Cell Metab, 2011. **13**(4): p. 376-388.
141. Wang, S., et al., *Resveratrol induces brown-like adipocyte formation in white fat through activation of AMP-activated protein kinase (AMPK) alpha1.* Int J Obes (Lond), 2015. **39**(6): p. 967-76.
142. Lan, F., et al., *Resveratrol-Induced AMP-Activated Protein Kinase Activation Is Cell-Type Dependent: Lessons from Basic Research for Clinical Application.* Nutrients, 2017. **9**(7).
143. Collins, Q.F., et al., *Epigallocatechin-3-gallate (EGCG), a green tea polyphenol, suppresses hepatic gluconeogenesis through 5'-AMP-activated protein kinase.* J Biol Chem, 2007. **282**(41): p. 30143-9.
144. Turner, N., et al., *Berberine and its more biologically available derivative, dihydroberberine, inhibit mitochondrial respiratory complex I: a mechanism for the action of berberine to activate AMP-activated protein kinase and improve insulin action.* Diabetes, 2008. **57**(5): p. 1414-8.
145. Giri, S., et al., *5-aminoimidazole-4-carboxamide-1-beta-4-ribofuranoside inhibits proinflammatory response in glial cells: a possible role of AMP-activated protein kinase.* J Neurosci, 2004. **24**(2): p. 479-87.
146. Potunuru, U.R., et al., *Amarogentin, a secoiridoid glycoside, activates AMP- activated protein kinase (AMPK) to exert beneficial vasculo-metabolic effects.* Biochim Biophys Acta Gen Subj, 2019. **1863**(8): p. 1270-1282.
147. Herranz-Lopez, M., et al., *Differential effects of a combination of Hibiscus sabdariffa and Lippia citriodora polyphenols in overweight/obese subjects: A randomized controlled trial.* Sci Rep, 2019. **9**(1): p. 2999.
148. Herranz-Lopez, M., et al., *Multi-Targeted Molecular Effects of Hibiscus sabdariffa Polyphenols: An Opportunity for a Global Approach to Obesity.* Nutrients, 2017. **9**(8).
149. Boix-Castejon, M., et al., *Hibiscus and lemon verbena polyphenols modulate appetite-related biomarkers in overweight subjects: a randomized controlled trial.* Food Funct, 2018. **9**(6): p. 3173-3184.

150. Hopkins, A.L., et al., *Hibiscus sabdariffa L. in the treatment of hypertension and hyperlipidemia: a comprehensive review of animal and human studies.* Fitoterapia, 2013. **85**: p. 84-94.
151. Booth, F.W., et al., *Endurance Exercise and the Regulation of Skeletal Muscle Metabolism.* Prog Mol Biol Transl Sci, 2015. **135**: p. 129-51.
152. Kang, J.X., *Reduction of heart rate by omega-3 fatty acids and the potential underlying mechanisms.* Front Physiol, 2012. **3**: p. 416.
153. Ross, T.T., et al., *beta-GPA treatment leads to elevated basal metabolic rate and enhanced hypoxic exercise tolerance in mice.* Physiol Rep, 2017. **5**(5).
154. Banz, W.J., et al., *(+)-z-bisdehydrodoisynolic Acid enhances Basal metabolism and Fatty Acid oxidation in female obese zucker rats.* J Obes, 2012. **2012**: p. 154145.
155. Tomas, E., et al., *GLP-1(32-36)amide Pentapeptide Increases Basal Energy Expenditure and Inhibits Weight Gain in Obese Mice.* Diabetes, 2015. **64**(7): p. 2409-19.

ANEXOS

Información suplementaria (Capítulo 1)

AMPK modulatory activity of olive–tree leaves phenolic compounds: bioassay-guided isolation on adipocyte model and in silico approach

Cecilia Jiménez–Sánchez[1,2], Mariló Olivares–Vicente[3], Celia Rodríguez–Pérez[1,2], María Herranz–López[3], Jesús Lozano–Sánchez[1,2], Antonio Segura–Carretero[1,2], Alberto Fernández–Gutiérrez[1,2], José Antonio Encinar[3¶], Vicente Micol[3,4*¶]

[1] Department of Analytical Chemistry, University of Granada. Granada, Spain.

[2] Research and Development of Functional Food Centre (CIDAF), PTS, Granada, Spain.

[3] Instituto de Biología Molecular y Celular (IBMC), Miguel Hernández University (UMH), Elche, Alicante, Spain.

[4] CIBER: CB12/03/30038, Fisiopatología de la Obesidad y la Nutrición, CIBERobn, Instituto de Salud Carlos III (ISCIII), Palma de Mallorca, Spain.

* Corresponding author
Email: vmicol@umh.es (VM)

¶ These authors share co-senior authorship

S1 Fig. Proposed molecular structure of the identified compounds showed on Table 1 for selected fractions with biological activity over AMPK kinase.

Peaks 5, 8 and 15

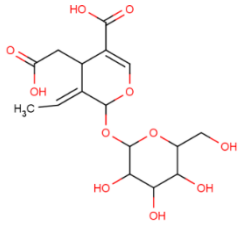

4-(carboxymethyl)-3-ethenyl-2-{(3.4.5-trihydroxy-6-(hydroxymethyl)oxan-2-yl)oxy}-3.4-dihydro-2H-pyran-5-carboxylic acid
PubChem CID: 101042548, Oleoside.

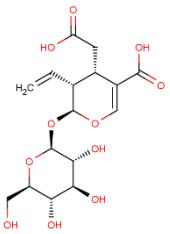

(3E)-4-(carboxymethyl)-3-ethylidene-2-{(3.4.5-trihydroxy-6-(hydroxymethyl)oxan-2-yl)oxy}-3.4-dihydro-2H-pyran-5-carboxylic acid
PubChem CID: 14136854, Secologanoside.

Peaks 6 and 7

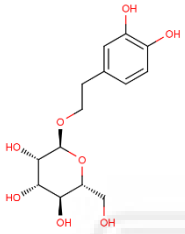

2-(2-(3.4-dihydroxyphenyl)ethoxy)-6-(hydroxymethyl)oxane-3.4.5-triol
PubChem CID: 13845930, Hydroxytyrosol 1-O-glucoside.

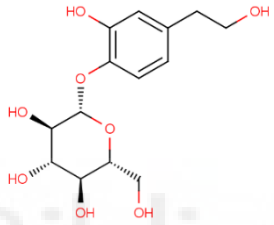

2-(2-hydroxy-4-(2-hydroxyethyl)phenoxy)-6-(hydroxymethyl)oxane-3.4.5-triol
PubChem CID: 6453057, Hydroxytyrosol 4-beta-D-glucoside.

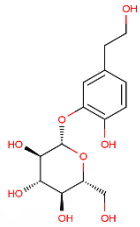

2-(2-hydroxy-5-(2-hydroxyethyl)phenoxy)-6-(hydroxymethyl)oxane-3.4.5-triol
PubChem CID: 5315870, Cimidahurinine.

Peak 9

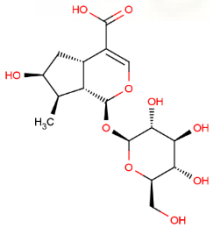

6-hydroxy-7-methyl-1-{(3.4.5-trihydroxy-6-(hydroxymethyl)oxan-2-yl)oxy}-1H.4aH.5H.6H.7H.7aH-cyclopenta(c)pyran-4-carboxylic acid
PubChem CID: 158144, 8-Epiloganic acid.

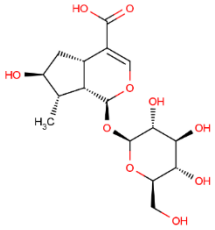

6-hydroxy-7-methyl-1-{(3.4.5-trihydroxy-6-(hydroxymethyl)oxan-2-yl)oxy}-1H.4aH.5H.6H.7H.7aH-cyclopenta(c)pyran-4-carboxylic acid
PubChem CID: 89640, Loganic Acid.

Peaks 16 and 22

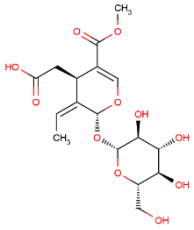

methyl 3-formyl-2-methyl-4-{2-oxo-2-{(3.4.5-trihydroxy-6-(hydroxymethyl)oxan-2-yl)oxy}ethyl)-3.4-dihydro-2H-pyran-5-carboxylate
PubChem CID: 24121278, oleoside 11-methyl ester.

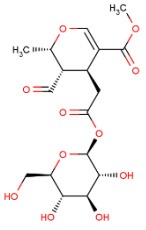

2-((3Z)-3-ethylidene-5-(methoxycarbonyl)-2-{(3.4.5-trihydroxy-6-(hydroxymethyl)oxan-2-yl)oxy}-3.4-dihydro-2H-pyran-4-yl]acetic acid

Peak 17

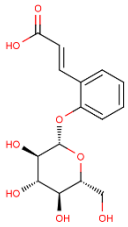

(2E)-3-(2-{(3.4.5-trihydroxy-6-(hydroxymethyl)oxan-2-yl)oxy}phenyl)prop-2-enoic acid
PubChem CID: 6275271.

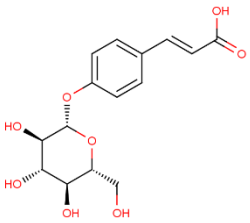

(2E)-3-(4-{(3.4.5-trihydroxy-6-(hydroxymethyl)oxan-2-yl)oxy}phenyl)prop-2-enoic acid
PubChem CID: 9840292.

Peak 24

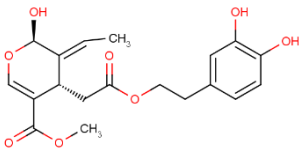

methyl (3E)-4-{2-(2-(3.4-dihydroxyphenyl)ethoxy)-2-oxoethyl}-3-ethylidene-2-hydroxy-3.4-dihydro-2H-pyran-5-carboxylate
PubChem CID: 56842347, Oleuropein Aglycone.

Peak 25 and 33

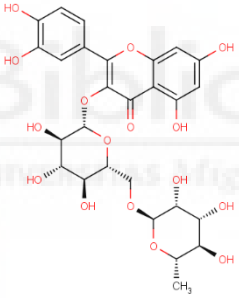

2-(3.4-dihydroxyphenyl)-5.7-dihydroxy-3-((3.4.5-trihydroxy-6-{((3.4.5-trihydroxy-6-methyloxan-2-yl)oxy)methyl}oxan-2-yl)oxy)-4H-chromen-4-one
PubChem CID: 5280805, Rutin.

Peak 27

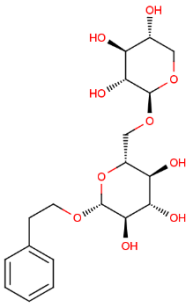

2-(2-phenylethoxy)-6-{((3.4.5-trihydroxyoxan-2-yl)oxy)methyl}oxane-3.4.5-triol
PubChem CID: 131129, 2-Phenylethyl beta-primeveroside.

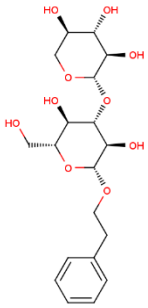

2-{(3.5-dihydroxy-2-(hydroxymethyl)-6-(2-phenylethoxy)oxan-4-yl)oxy}oxane-3.4.5-triol
PubChem CID: 100930979.

Peak 28

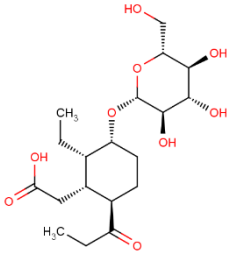

2-{2-ethyl-6-propanoyl-3-{{3.4.5-trihydroxy-6-(hydroxymethyl)oxan-2-yl)oxy}cyclohexyl)acetic acid

Peak 30

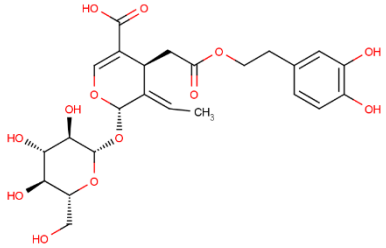

(3E)-4-{2-(2-(3.4-dihydroxyphenyl)ethoxy]-2-oxoethyl}-3-ethylidene-2-{(3.4.5-trihydroxy-6-(hydroxymethyl)oxan-2-yl)oxy}-3.4-dihydro-2H-pyran-5-carboxylic acid

PubChem CID: 6450302, Demethyloleuropein.

Peaks 32 and 39

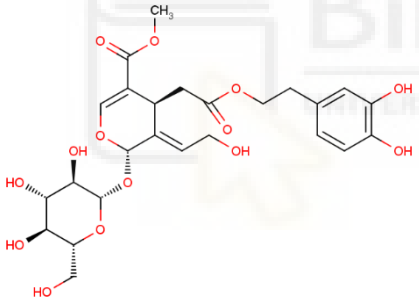

methyl (3E)-4-{2-(2-(3.4-dihydroxyphenyl)ethoxy)-2-oxoethyl}-3-(2-hydroxyethylidene)-2-{(3.4.5-trihydroxy-6-(hydroxymethyl)oxan-2-yl)oxy}-3.4-dihydro-2H-pyran-5-carboxylate
PubChem CID: 6440747, 10-Hydroxyoleuropein.

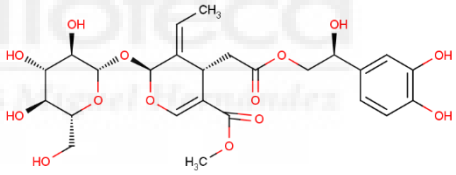

methyl (3E)-4-{2-(2-(3.4-dihydroxyphenyl)-2-hydroxyethoxy)-2-oxoethyl}-3-ethylidene-2-{(3.4.5-trihydroxy-6-(hydroxymethyl)oxan-2-yl)oxy}-3.4-dihydro-2H-pyran-5-carboxylate
PubChem CID: 102461563, (7''S)-Hydroxyoleuropein.

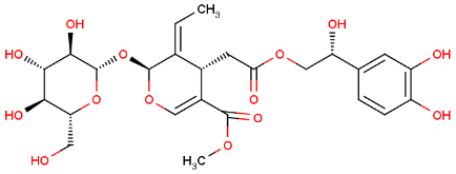

methyl (3E)-4-{2-(2-(3.4-dihydroxyphenyl)-2-hydroxyethoxy)-2-oxoethyl}-3-ethylidene-2-{(3.4.5-trihydroxy-6-(hydroxymethyl)oxan-2-yl)oxy}-3.4-dihydro-2H-pyran-5-carboxylate
PubChem CID: 102461562, (2''R)-2''-Hydroxyoleuropein.

Peak 34

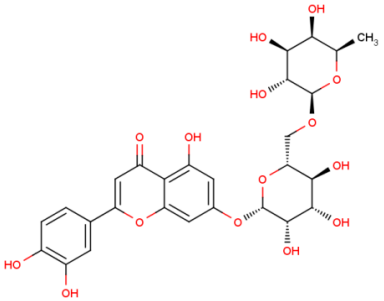

2-(3.4-dihydroxyphenyl)-5-hydroxy-7-((3.4.5-trihydroxy-6-{((3.4.5-trihydroxy-6-methyloxan-2-yl)oxy)methyl}oxan-2-yl)oxy)-4H-chromen-4-one
PubChem CID: 44258082, Luteolin 7-rutinoside.

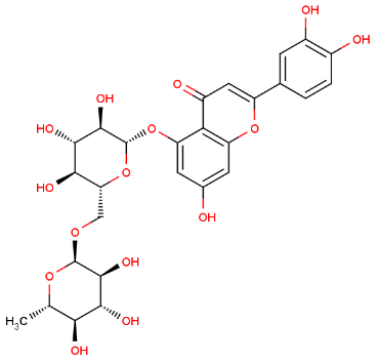

2-(3.4-dihydroxyphenyl)-7-hydroxy-5-((3.4.5-trihydroxy-6-{((3.4.5-trihydroxy-6-methyloxan-2-yl)oxy)methyl}oxan-2-yl)oxy)-4H-chromen-4-one
PubChem CID: 44258131, Luteolin 5-O-rutinoside.

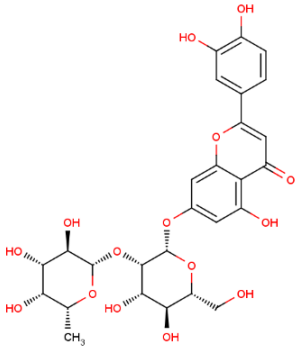

7-{(4.5-dihydroxy-6-(hydroxymethyl)-3-{(3.4.5-trihydroxy-6-methyloxan-2-yl)oxy}oxan-2-yl)oxy}-2-(3.4-dihydroxyphenyl)-5-hydroxy-4H-chromen-4-one
PubChem CID: 44258083, Luteolin 7-neohesperidoside.

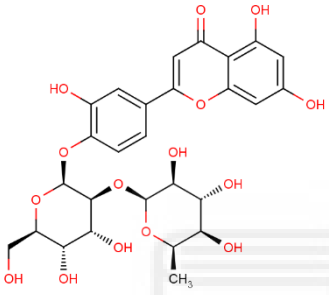

2-(4-{(4.5-dihydroxy-6-(hydroxymethyl)-3-((3.4.5-trihydroxy-6-methyloxan-2-yl)oxy)oxan-2-yl)oxy}-3-hydroxyphenyl)-5.7-dihydroxy-4H-chromen-4-one
PubChem CID: 44258098, Luteolin 4'-neohesperidoside.

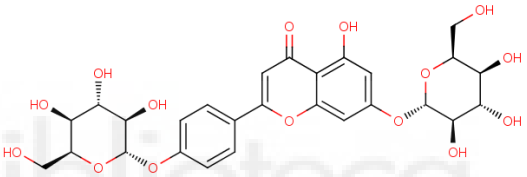

5-hydroxy-7-{(3.4.5-trihydroxy-6-(hydroxymethyl)oxan-2-yl)oxy}-2-(4-{(3.4.5-trihydroxy-6-(hydroxymethyl)oxan-2-yl)oxy}phenyl)-4H-chromen-4-one
PubChem CID: 44257819.

Peak 35

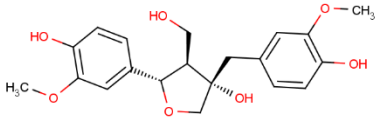

5-(4-hydroxy-3-methoxyphenyl)-3-((4-hydroxy-3-methoxyphenyl)methyl)-4-(hydroxymethyl)oxolan-3-ol
PubChem CID: 5273570, Olivil.

Peak 36

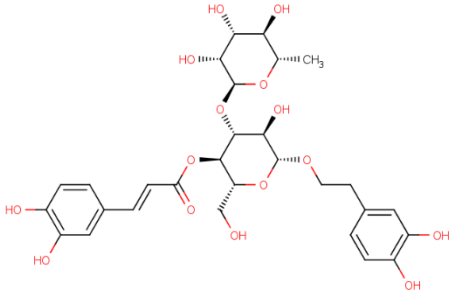

6-(2-(3.4-dihydroxyphenyl)ethoxy)-5-hydroxy-2-(hydroxymethyl)-4-((3.4.5-trihydroxy-6-methyloxan-2-yl)oxy)oxan-3-yl (2E)-3-(3.4-dihydroxyphenyl)prop-2-enoate
PubChem CID: 5281800, Acteoside.

Peaks 37, 48 and 55

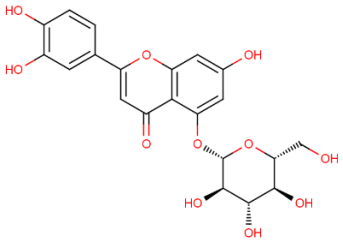

2-(3.4-dihydroxyphenyl)-7-hydroxy-5-{(3.4.5-trihydroxy-6-(hydroxymethyl)oxan-2-yl)oxy}-4H-chromen-4-one
PubChem CID: 5317471, Luteolin-5-O-b-D-glucopyranoside.

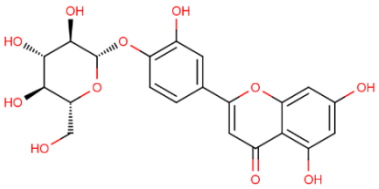

5.7-dihydroxy-2-(3-hydroxy-4-{(3.4.5-trihydroxy-6-(hydroxymethyl)oxan-2-yl)oxy}phenyl)-4H-chromen-4-one
PubChem CID: 5319116, Luteolin 4'-O-glucoside.

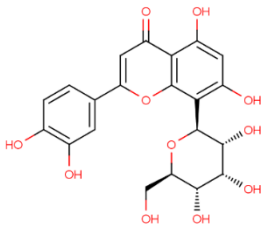

2-(3.4-dihydroxyphenyl)-5.7-dihydroxy-8-(3.4.5-trihydroxy-6-(hydroxymethyl)oxan-2-yl)-4H-chromen-4-one
PubChem CID: 44257907, Luteolin 8-C-beta-D-glucopyranoside.

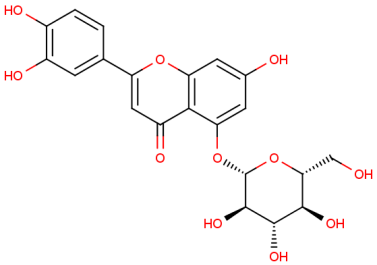

2-(3.4-dihydroxyphenyl)-7-hydroxy-5-{(3.4.5-trihydroxy-6-(hydroxymethyl)oxan-2-yl)oxy}-4H-chromen-4-one
PubChem CID: 5317471, Luteolin-5-O-b-D-glucopyranoside.

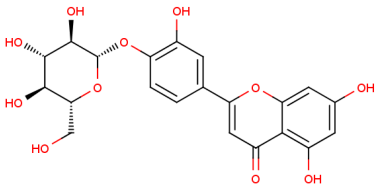

5.7-dihydroxy-2-(3-hydroxy-4-{(3.4.5-trihydroxy-6-(hydroxymethyl)oxan-2-yl)oxy}phenyl)-4H-chromen-4-one
PubChem CID: 5319116, Luteolin 4'-O-glucoside.

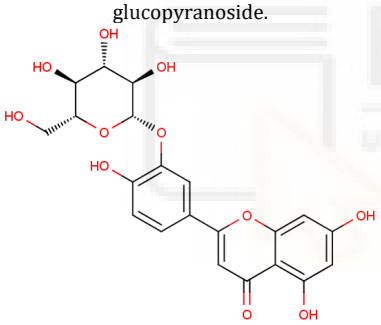

5.7-dihydroxy-2-(4-hydroxy-3-{(3.4.5-trihydroxy-6-(hydroxymethyl)oxan-2-yl)oxy}phenyl)-4H-chromen-4-one
PubChem CID: 12309350, Luteolin 3'-glucoside.

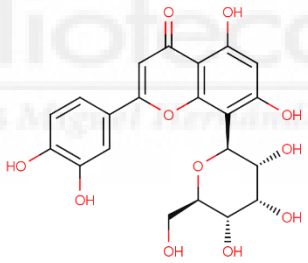

2-(3.4-dihydroxyphenyl)-5.7-dihydroxy-8-(3.4.5-trihydroxy-6-(hydroxymethyl)oxan-2-yl)-4H-chromen-4-one
PubChem CID: 44257907, Luteolin 8-C-beta-D-glucopyranoside.

Peaks 40, 42, 43 and 44

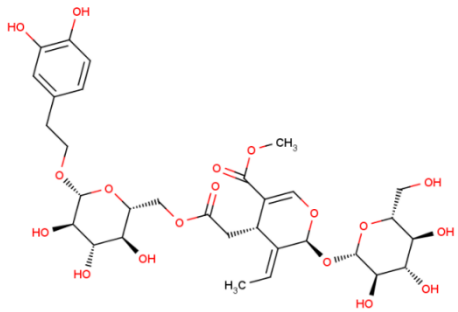

methyl (3E)-4-(2-({6-(2-(3.4-dihydroxyphenyl)ethoxy)-3.4.5-trihydroxyoxan-2-yl}methoxy)-2-oxoethyl)-3-ethylidene-2-{(3.4.5-trihydroxy-6-(hydroxymethyl)oxan-2-yl)oxy}-3.4-dihydro-2H-pyran-5-carboxylate
PubChem CID: 101720830, Neonuezhenide.

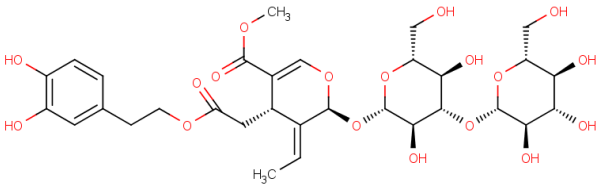

methyl (3E)-2-{(3.5-dihydroxy-6-(hydroxymethyl)-4-{(3.4.5-trihydroxy-6-(hydroxymethyl)oxan-2-yl)oxy}oxan-2-yl)oxy}-4-{2-(2-(3.4-dihydroxyphenyl)ethoxy)-2-oxoethyl}-3-ethylidene-3.4-dihydro-2H-pyran-5-carboxylate
PubChem CID: 102031346, Oleuropein 3'-glucoside.

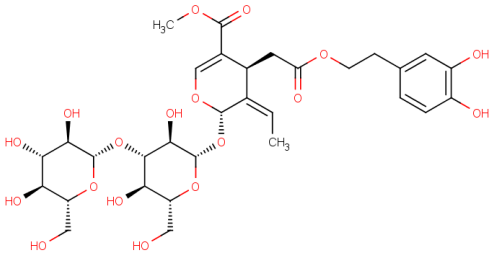

methyl (3Z)-2-{(3.5-dihydroxy-6-(hydroxymethyl)-4-{(3.4.5-trihydroxy-6-(hydroxymethyl)oxan-2-yl)oxy}oxan-2-yl)oxy}-4-{2-(2-(3.4-dihydroxyphenyl)ethoxy)-2-oxoethyl}-3-ethylidene-3.4-dihydro-2H-pyran-5-carboxylate
PubChem CID: 101447987.

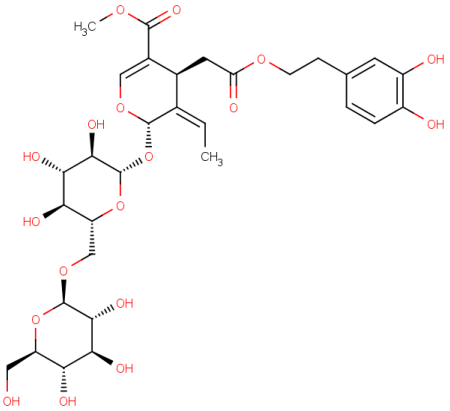

methyl (3Z)-4-{2-(2-(3.4-dihydroxyphenyl)ethoxy)-2-oxoethyl}-3-ethylidene-2-{(3.4.5-trihydroxy-6-({(3.4.5-trihydroxy-6-(hydroxymethyl)oxan-2-yl)oxy}methyl)oxan-2-yl)oxy}-3.4-dihydro-2H-pyran-5-carboxylate
PubChem CID: 102078602, 6'-O-beta-D-Glucopyranosyloleuropein.

Peaks 45 and 46

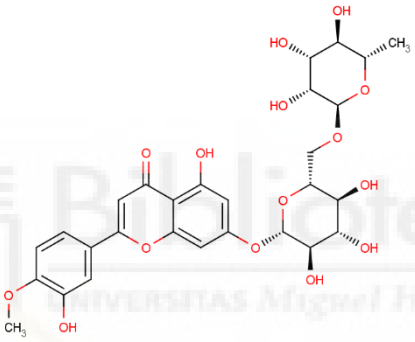

5-hydroxy-2-(3-hydroxy-4-methoxyphenyl)-7-((3.4.5-trihydroxy-6-{{(3.4.5-trihydroxy-6-methyloxan-2-yl)oxy)methyl}oxan-2-yl)oxy)-4H-chromen-4-one
PubChem CID: 5281613, Diosmin.

Peak 47

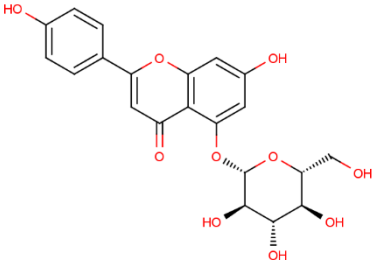

7-hydroxy-2-(4-hydroxyphenyl)-5-{(3.4.5-trihydroxy-6-(hydroxymethyl)oxan-2-yl)oxy}-4H-chromen-4-one
PubChem CID: 14730806.

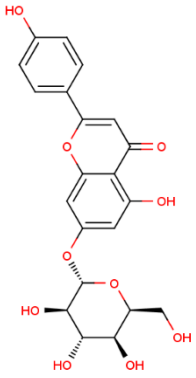

5-hydroxy-2-(4-hydroxyphenyl)-7-{(3.4.5-trihydroxy-6-(hydroxymethyl)oxan-2-yl)oxy}-4H-chromen-4-one
PubChem CID: 44257792.

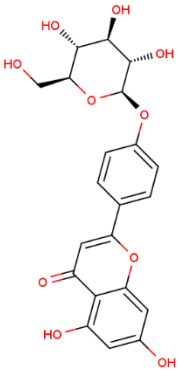

5.7-dihydroxy-2-(4-{(3.4.5-trihydroxy-6-(hydroxymethyl)oxan-2-yl)oxy}phenyl)-4H-chromen-4-one
PubChem CID: 101135001.

Peak 49

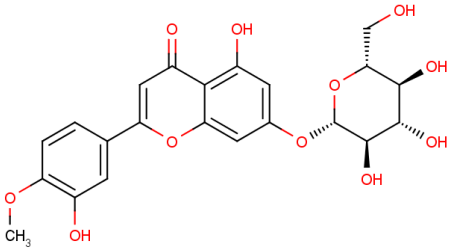

5-hydroxy-2-(3-hydroxy-4-methoxyphenyl)-7-{(3.4.5-trihydroxy-6-(hydroxymethyl)oxan-2-yl)oxy}-4H-chromen-4-one
PubChem CID: 11016019, Diosmetol 7-glucoside.

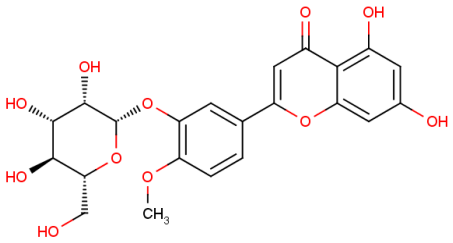

5.7-dihydroxy-2-(4-methoxy-3-{(3.4.5-trihydroxy-6-(hydroxymethyl)oxan-2-yl)oxy}phenyl)-4H-chromen-4-one
PubChem CID: 44258229, Diosmetin 3'-glucoside.

Peak 50

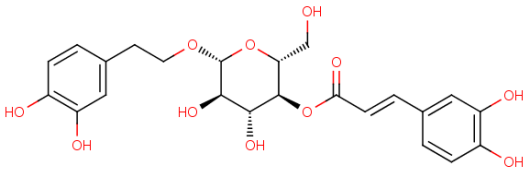

6-(2-(3.4-dihydroxyphenyl)ethoxy)-4.5-dihydroxy-2-(hydroxymethyl)oxan-3-yl (2E)-3-(3.4-dihydroxyphenyl)prop-2-enoate
PubChem CID: 5273566, Calceolarioside A.

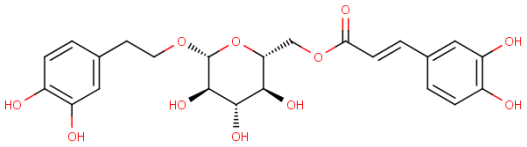

{6-(2-(3.4-dihydroxyphenyl)ethoxy)-3.4.5-trihydroxyoxan-2-yl}methyl (2E)-3-(3.4-dihydroxyphenyl)prop-2-enoate
PubChem CID: 5273567, Calceolarioside B.

Peaks 59 and 68

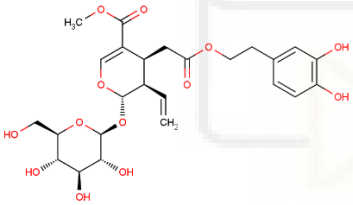

methyl 4-{2-(2-(3.4-dihydroxyphenyl)ethoxy)-2-oxoethyl}-3-ethenyl-2-{(3.4.5-trihydroxy-6-(hydroxymethyl)oxan-2-yl)oxy}-3.4-dihydro-2H-pyran-5-carboxylate
PubChem CID: 102016333, Oleuroside.

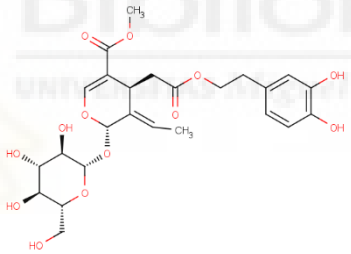

methyl (3E)-4-{2-(2-(3.4-dihydroxyphenyl)ethoxy)-2-oxoethyl}-3-ethylidene-2-{(3.4.5-trihydroxy-6-(hydroxymethyl)oxan-2-yl)oxy}-3.4-dihydro-2H-pyran-5-carboxylate
PubChem CID: 5281544, Oleuropein.

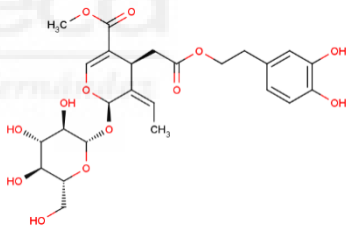

methyl (3Z)-4-{2-(2-(3.4-dihydroxyphenyl)ethoxy)-2-oxoethyl}-3-ethylidene-2-{(3.4.5-trihydroxy-6-(hydroxymethyl)oxan-2-yl)oxy}-3.4-dihydro-2H-pyran-5-carboxylate
PubChem CID: 53297357, Oleuropein.

Peak 62

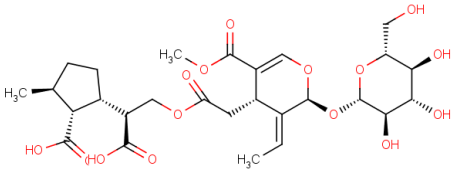

2-(1-carboxy-2-({2-((3E)-3-ethylidene-5-(methoxycarbonyl)-2-{(3.4.5-trihydroxy-6-(hydroxymethyl)oxan-2-yl)oxy}-3.4-dihydro-2H-pyran-4-yl)acetyl}oxy)ethyl)-5-methylcyclopentane-1-carboxylic acid
PubChem CID: 102461565, Frameroside.

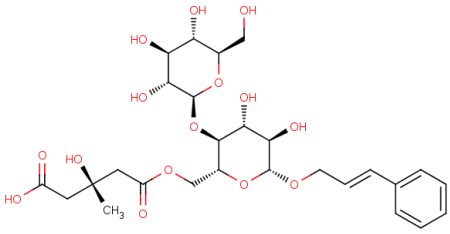

5-((4.5-dihydroxy-6-{((2E)-3-phenylprop-2-en-1-yl)oxy}-3-{(3.4.5-trihydroxy-6-(hydroxymethyl)oxan-2-yl)oxy}oxan-2-yl)methoxy)-3-hydroxy-3-methyl-5-oxopentanoic acid
PubChem CID: 44521607, Piperchabaoside B.

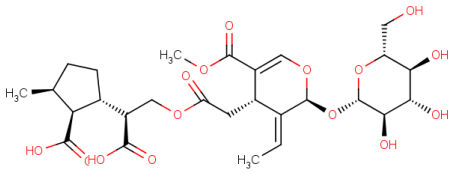

2-(1-carboxy-2-({2-[(3E)-3-ethylidene-5-(methoxycarbonyl)-2-{[3.4.5-trihydroxy-6-(hydroxymethyl)oxan-2-yl]oxy}-3.4-dihydro-2H-pyran-4-yl]acetyl}oxy)ethyl)-5-methylcyclopentane-1-carboxylic acid
PubChem CID: 11968448, 2''-epi-Frameroside.

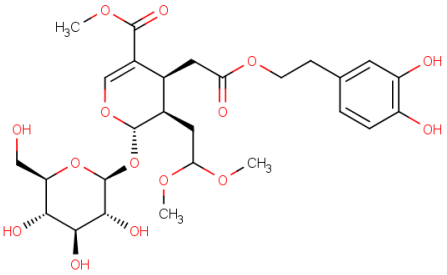

methyl 4-{2-(2-(3.4-dihydroxyphenyl)ethoxy)-2-oxoethyl}-3-(2.2-dimethoxyethyl)-2-{[3.4.5-trihydroxy-6-(hydroxymethyl)oxan-2-yl]oxy}-3.4-dihydro-2H-pyran-5-carboxylate
PubChem CID: 44521607, Piperchabaoside B.

Peaks 63 and 66

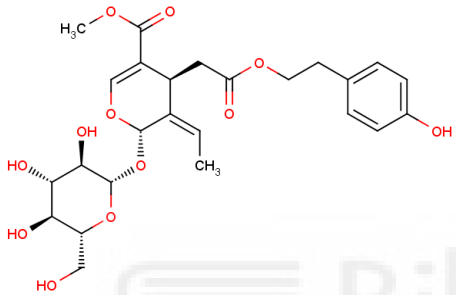

methyl (3Z)-3-ethylidene-4-{2-(2-(4-hydroxyphenyl)ethoxy)-2-oxoethyl}-2-{[3.4.5-trihydroxy-6-(hydroxymethyl)oxan-2-yl]oxy}-3.4-dihydro-2H-pyran-5-carboxylate
PubChem CID: 10392063, (8Z)-Ligstroside.

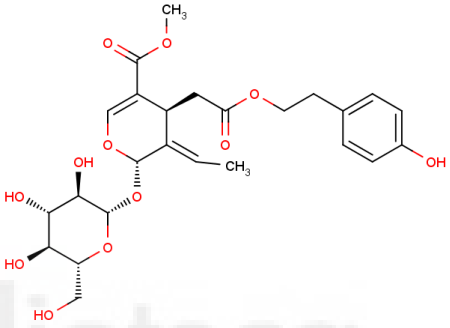

methyl (3E)-3-ethylidene-4-{2-(2-(4-hydroxyphenyl)ethoxy)-2-oxoethyl}-2-{[3.4.5-trihydroxy-6-(hydroxymethyl)oxan-2-yl]oxy}-3.4-dihydro-2H-pyran-5-carboxylate
PubChem CID: 14136859, Ligstroside.

Peak 65

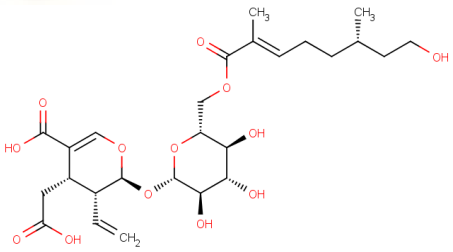

4-(carboxymethyl)-3-ethenyl-2-{[3.4.5-trihydroxy-6-({[(2E)-8-hydroxy-2.6-dimethyloct-2-enoyl]oxy}methyl)oxan-2-yl]oxy}-3.4-dihydro-2H-pyran-5-carboxylic acid
PubChem CID: 101406919.

Peak 67

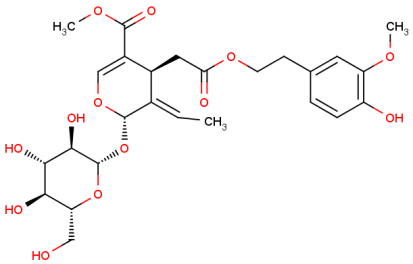

methyl (3E)-3-ethylidene-4-{2-(2-(4-hydroxy-3-methoxyphenyl)ethoxy)-2-oxoethyl}-2-{[3.4.5-trihydroxy-6-(hydroxymethyl)oxan-2-yl]oxy}-3.4-dihydro-2H-pyran-5-carboxylate
PubChem CID: 102047330.

Peak 69

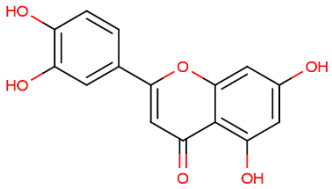

2-(3.4-dihydroxyphenyl)-5.7-dihydroxy-4H-chromen-4-one
PubChem CID: 5280445, Luteolin.

Peak 70

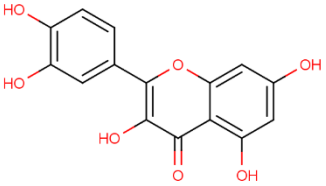

2-(3.4-dihydroxyphenyl)-3.5.7-trihydroxy-4H-chromen-4-one
PubChem CID: 5280343, Quercetin.

Peak 71

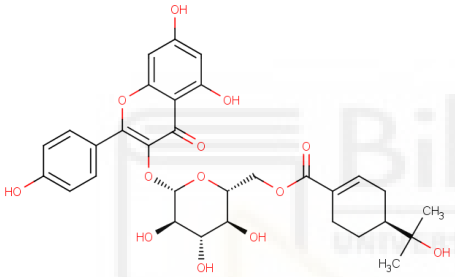

(6-{(5.7-dihydroxy-2-(4-hydroxyphenyl)-4-oxo-4H-chromen-3-yl)oxy}-3.4.5-trihydroxyoxan-2-yl)methyl 4-(2-hydroxypropan-2-yl)cyclohex-1-ene-1-carboxylate
PubChem CID: 15172373, Resinoside A.

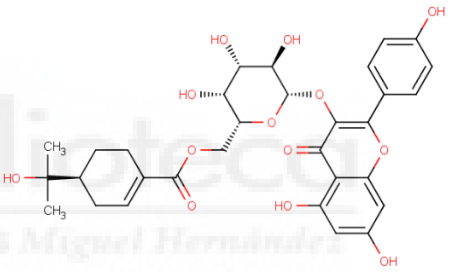

(6-{(5.7-dihydroxy-2-(4-hydroxyphenyl)-4-oxo-4H-chromen-3-yl)oxy}-3.4.5-trihydroxyoxan-2-yl)methyl 4-(2-hydroxypropan-2-yl)cyclohex-1-ene-1-carboxylate
PubChem CID: 101618995, Resinoside B.

Peak 74

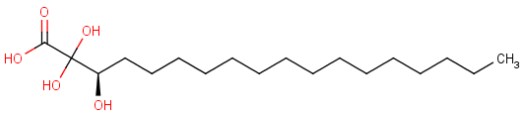

2.2.3-trihydroxyoctadecanoic acid
PubChem CID: 147011, 2,2,3-trihydroxyoctadecanoic acid.

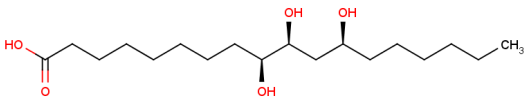

9.10.12-trihydroxyoctadecanoic acid
PubChem CID: 4252742, 9,10,12-trihydroxyoctadecanoic Acid.

Peak 75

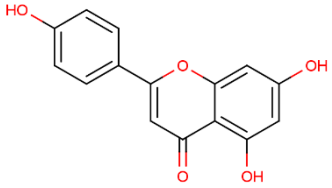

5.7-dihydroxy-2-(4-hydroxyphenyl)-4H-chromen-4-one
PubChem CID: 5280443.

Peak 76

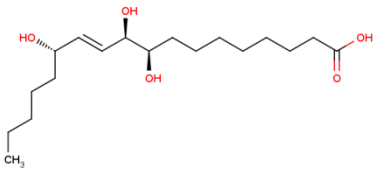

(11E)-9.10.13-trihydroxyoctadec-11-enoic acid
PubChem CID: 5282965.

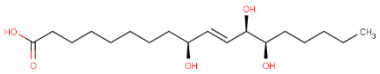

(10E)-9.12.13-trihydroxyoctadec-10-enoic acid
PubChem CID: 5282966.

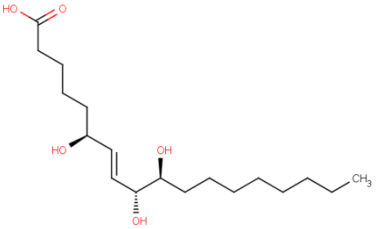

(7E)-6.9.10-trihydroxyoctadec-7-enoic acid
PubChem CID: 53248432.

Peak 78

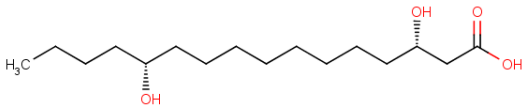

3.12-dihydroxyhexadecanoic acid
PubChem CID: 125639.

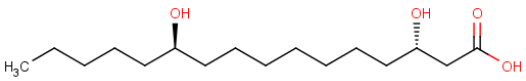

3.11-dihydroxyhexadecanoic acid
PubChem CID: 170969.

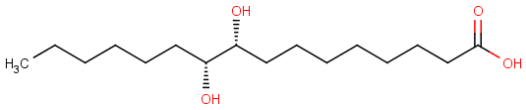

9.10-dihydroxyhexadecanoic acid
PubChem CID: 193113.

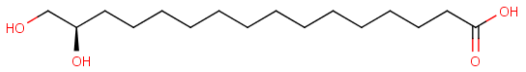

15.16-dihydroxyhexadecanoic acid
PubChem CID: 5282925.

S2 Fig. Base peak chromatogram (BPC) made by HPLC-ESI-TOF. This BPC was obtained in negative ion mode of the olive leaf extract, with the optimized semi-preparative conditions, and the collected fractions highlighted in blue.

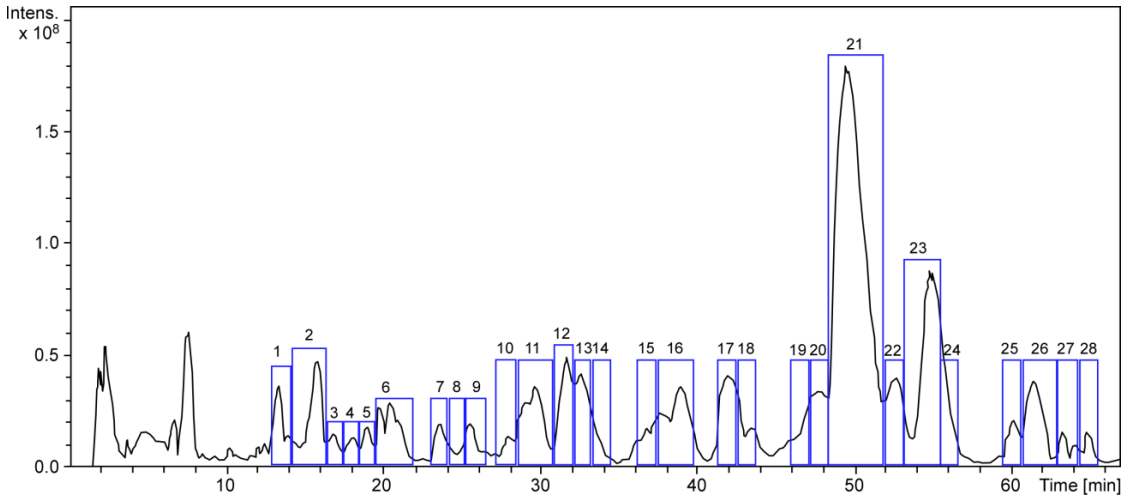

S3 Fig. AMPK binding sites. Panels A, C and E show the secondary structure of alpha, beta and gamma subunits of AMPK kinase (4CFE.pdb), respectively. Panels B, D and F represent the electrostatic potential surface with a co-crystalized ligand indicating the position of each binding sites.

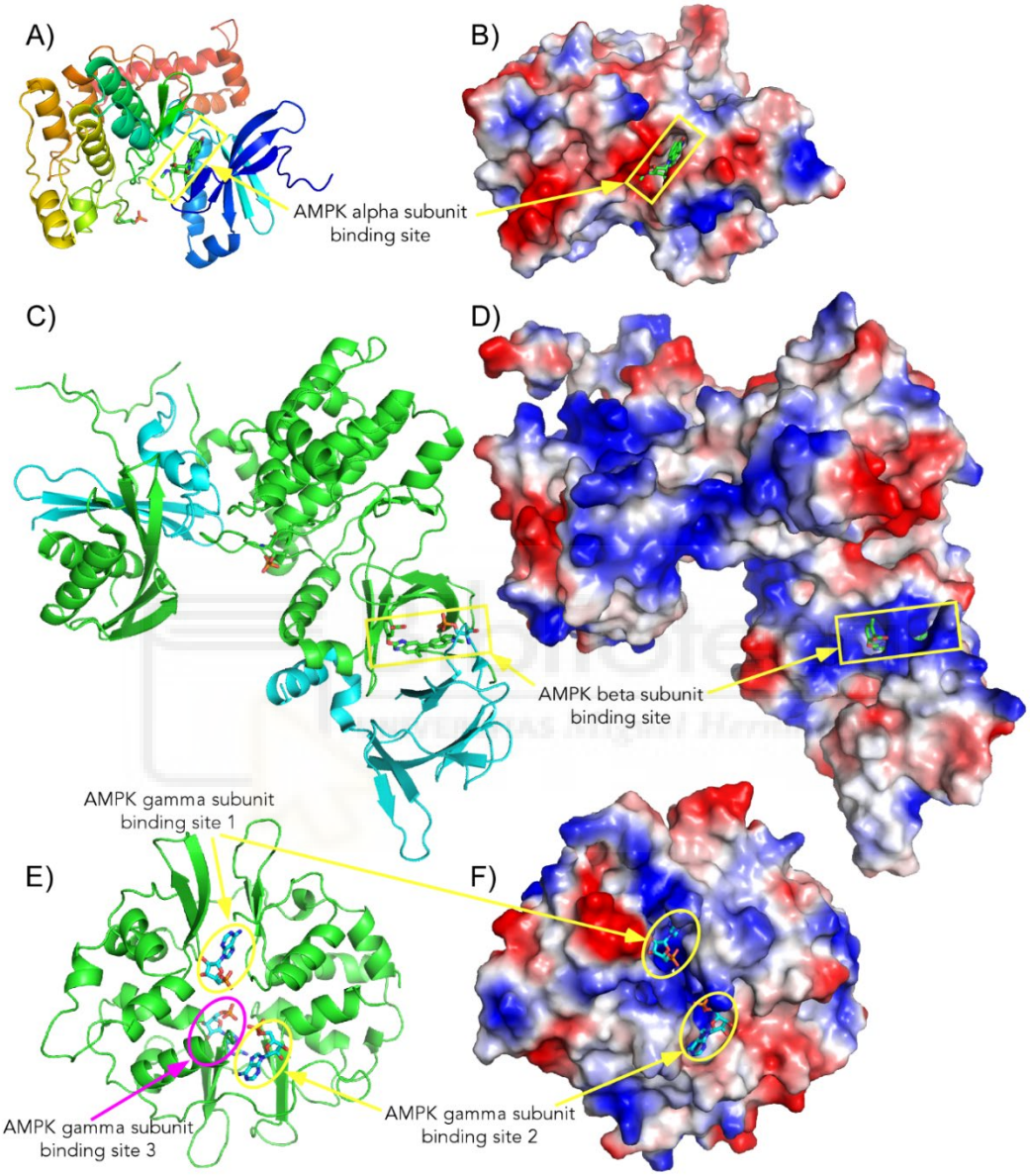

Información suplementaria (Capítulo 3)

Correlation between the cellular metabolism of quercetin and its glucuronide metabolite and oxidative stress in hypertrophied 3T3-L1 adipocytes

María Herranz-López[a,1], Isabel Borrás-Linares[b,1], Mariló Olivares-Vicente[a], Julio Gálvez[c], Antonio Segura-Carretero[b,‡] and Vicente Micol[a,d,‡,*]

[a]Institute of Molecular and Cell Biology (IMCB). Miguel Hernández University (UMH). Elche-03202, Alicante. Spain.

[b]Center for Research and Development of Functional Food (CIDAF), Science Technology Park Health, Armilla, Granada, Spain.

[c]CIBER-EHD, Department of Pharmacology, ibs.GRANADA, Center for Biomedical Research (CIBM), University of Granada, Avenida del Conocimiento s/n 18016-Armilla, Granada, Spain.

[d]CIBER, Fisiopatología de la Obesidad y la Nutrición, CIBERobn, Instituto de Salud Carlos III (CB12/03/30038).

Materials and methods

HPLC-DAD-ESI-TOF analysis and quantitation

The analyses of the cytoplasmic fractions were carried out using an Agilent 1200 RRLC system (Agilent Technologies, Palo Alto, CA, USA) of the Series Rapid Resolution equipped with a vacuum degasser, an autosampler, a binary pump, and a UV-Vis detector. The chromatographic separation was performed on a Zorbax Eclipse Plus C18 analytical column (4.6 x 150 mm, 1.8 µm particle size) at a flow rate of 0.3 ml/min. The temperature of the column was maintained at 25 °C and the injection volume was 10. Prefilters were used as precolumn RRLC in-line filters, 4.6 mm, 0.2 µm (Agilent Technologies, Palo Alto, CA, USA). The mobile phases used were water:acetonitrile (90:10, v/v) plus 0.5 % of formic acid as mobile phase A and acetonitrile as mobile phase B. The separation was conducted using the following multi-step gradient: 0 min, 5 % B; 20 min, 20 % B; 25 min, 40 % B; 30 min 5 % B and, finally, a conditioning cycle of 5 min with the initial conditions for the next analysis. The UV-Vis detection was performed in a wavelength range 190-950 nm.

For MS detection a microTOF™ mass analyzer (Bruker Daltonik, Bremen, Germany) was used coupled to the HPLC system via an ESI interface (model G1607A, Agilent Technologies, Palo Alto, CA, USA) operating in negative ionization mode showing the molecular ions [M-H]-. External mass spectrometer calibration was performed with a sodium formate cluster solution containing 5 mM sodium hydroxide and 0.2 % formic acid in water/2-propanol (1:1, v/v). The calibration solution was injected at the beginning of the run and all the spectra were calibrated prior to identification. This external calibration eliminates the necessity of a dual sprayer setup for internal mass calibration due to the compensation of temperature drift in the micro-TOF analyzer, providing accurate mass values (better than 5 ppm). For quantitative purposes, standard calibration curves of Q and Q3GA were prepared by using naringenin at a concentration of 30 µg/ml as internal standard (Table 1, Supplementary).

Source and transfer parameters were optimized for good sensitivity and a reasonable resolution of the mass range for the compounds of interest in order to improve ionization performance. The optimum values of source parameters were: capillary voltage, -4500 V; drying gas temperature, 200 °C; drying gas flow, 9 L/min; nebulizing gas pressure, 2 bar; and end plate offset, -500 V. The values of transfer parameters were: capillary exit, -120 V; skimmer 1, -40 V; hexapole 1, - 23 V; RF hexapole, 100 Vpp; skimmer 2, -22.5 V; transfer time, 50 µs; and pre-pulse storage time, 3 µs.

The accurate mass data of the molecular ions were processed through the software Data Analysis 4.0 (Bruker Daltonik, Bremen, Germany), which provided a list of possible elemental formulas by using the Generate Molecular Formula Editor™. This software provides standard functionalities such as minimum/maximum electron configuration, elemental range, and ring-plus double-bond equivalent, as well as a sophisticated comparison of the theoretical with the measured isotopic pattern (Sigma-Value) for increased confidence in the suggested molecular formula.

Determination of intracellular reactive oxygen species (ROS) by H_2DCF-DA analysis

Intracellular ROS generation was measured in hypertrophied adipocytes using 2′,7′-dichlorodihydrofluorescein diacetate (H2DCF-DA, Sigma-Aldrich, Spain). Briefly, 2x H_2DCF-DA was added into the cells after incubation of Q or Q3GA for 3, 6, 12 and 18 h. After 1 h at 37 °C, cells were carefully washed with PBS (pH 7.4) and intracellular ROS levels were measured using a cell imaging multi-mode microplate reader (Cytation 3, Biotek, Spain) at 495 nm excitation and 529 nm emission. Fluorescence in the cells was photographed using the GFP imaging filter cube of the Cytation 3 at 4x. The results were expressed as mean ± standard deviation. Differences showing a $p < 0.05$ were considered statistically significant. All the parameters studied were compared to positive controls and analyzed using one-way ANOVA and Tukey test for multiple comparisons.

Table 1

Analytical parameters for the standards used for quantitation purposes. The limits of detection (LODs) and limits of quantification (LOQs) for individual compounds in standards solutions were also calculated as the signal to noise ratio: S/N = 3 and S/N = 10, respectively. Repeatability of the proposed method was measured as the relative standard deviation (RSD, %) in terms of concentration. A mixed solution containing the analytes was utilized to determine intraday repeatability (n=3), and interday repeatability (n = 9).

Analyte	LOD (µg/ml)	LOQ (µg/ml)	Interday Repeatability	Intraday Repeatability	Calibration range (µg/ml)	Calibration equations	r^2
Quercetin	0.004	0.012	0.06	0.10	0.1- 45	y = 3.5734 x + 0.0035	0.997
Quercetin-3-O-β-D-glucuronide	0.004	0.013	0.34	0.86	0.05-40	y = 4.2045 x + 0.0041	0.996

Table 2

Quantification of quercetin intracellular metabolites upon incubation of hypertrophied 3T3-L1 adipocytes with Q or Q3GA. Hypertrophied adipocytes were treated with 100 µM Q or 100 µM Q3GA for 0, 3, 6, 12 and 18 h and the cytoplasmic fractions were isolated. Quercetin metabolites were identified and quantitated by HPLC-DAD-ESI-TOF as described in Methods section. Concentration of metabolites was expressed as µg compound/µg total protein. ND: Non detected compound.

Incubated compound	Q		Q3GA	
Incubation time (h)	Intracellular compound (µg/µg protein)		Intracellular compound (µg/µg protein)	
	Q	Q3GA	Q3GA	Q
Control (0)	ND	ND	ND	ND
3	1.92 ± 0.03	0.04 ± 0.005	0.03 ± 0.002	0.03 ± 0.005
6	0.35 ± 0.01	0.08 ± 0.0025	0.05 ± 0.005	0.01 ± 0.002
12	0.18 ± 0.01	0.02 ± 0.005	0.10 ± 0.005	0.03 ± 0.001
18	0.02 ± 0.005	0.01 ± 0.0005	0.12 ± 0.0015	0.03 ± 0.003

Fig. 1. Molar percentage of phenolic compounds and their metabolites in rat plasma after oral administration of *H. sabdariffa*.

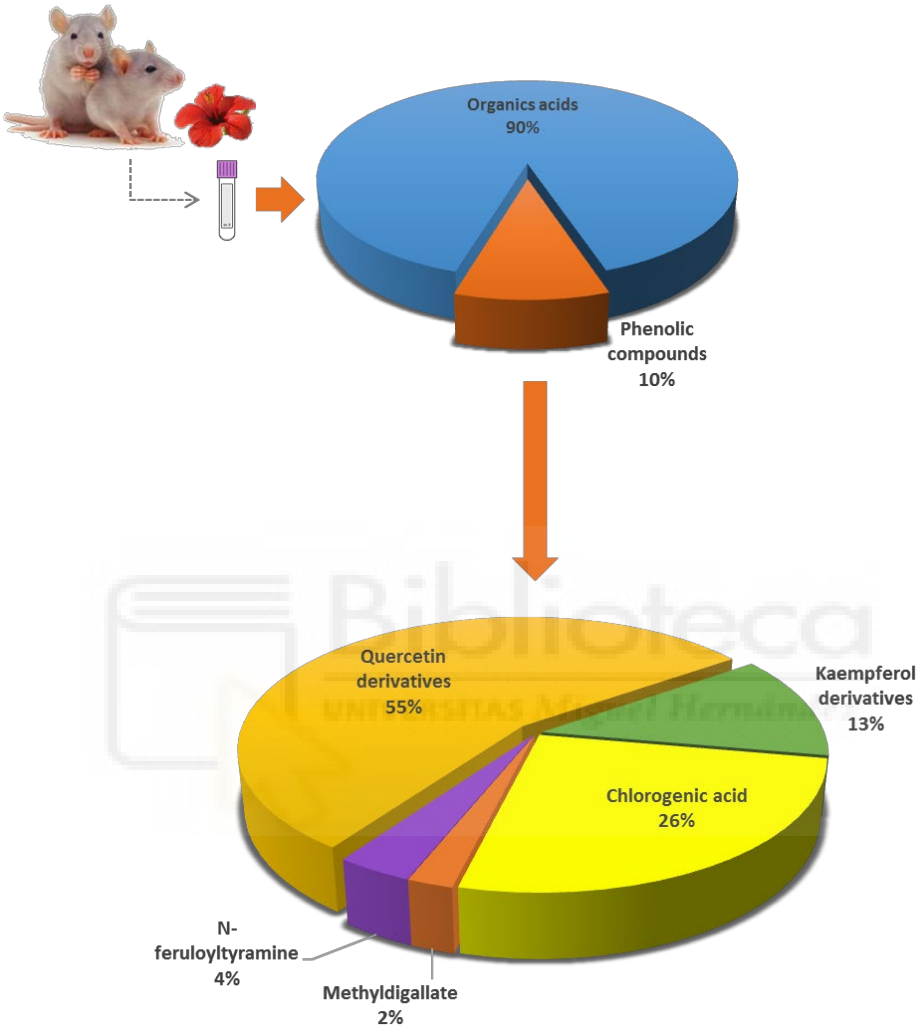

Información suplementaria (Capítulo 4)

CLINICAL TRIAL PROTOCOL

Differential effects of a combination of *Hibiscus sabdariffa* and *Lippia citriodora* polyphenols in overweight/obese subjects: A randomized controlled trial

María Herranz-López [1]†, Mariló Olivares-Vicente [1]†, Marina Boix-Castejón [2], Nuria Caturla [3], Enrique Roche [2, 4, ‡], and Vicente Micol [1, 4, ‡, *]

Affiliation:

[1] Instituto de Investigación, Desarrollo e Innovación en Biotecnología Sanitaria de Elche (IDiBE) e Instituto de Biología Molecular y Celular (IBMC). Miguel Hernández University (UMH), Elche 03202, Alicante, Spain.

[2] Institute of Bioengineering and Department of Applied Biology-Nutrition, University Miguel Hernandez, Alicante Institute for Health and Biomedical Research (ISABIAL-FISABIO Foundation), Alicante, Spain

[3] Monteloeder S.L., Alicante, Spain

[4] CIBER, Fisiopatología de la Obesidad y la Nutrición, CIBERobn, Instituto de Salud Carlos III (CB12/03/30038). Spain

† These authors contributed equally to this work.

‡ These authors shared author co-seniorship.

***Corresponding author:**

Vicente Micol, Tel: 34966658430, Fax: 34966658758 email: vmicol@umh.es

Co-authors email: mherranz@umh.es (Maria Herranz-López), maria.olivaresv@umh.es (Mariló Olivares-Vicente), marinaboix@hotmail.com (Marina Boix-Castejón), nuriacaturla@monteloeder.com (Nuria Caturla), eroche@umh.es (Enrique Roche).

Project summary

Our previous research in hypertrophied adipocytes and obese animal models has identified *Hibiscus sabdariffa* (HS) and *Lippia citriodora* (LC) with the capacity to activate the AMPK enzyme, decrease metabolic stress in glucotoxicity and/or lipotoxicity events, inhibit triglyceride accumulation, oxidative stress, secretion of inflammatory adipokines, decreased lipogenesis, enhanced fatty acid oxidation, prevention of hepatic steatosis, lowering blood pressure and improving endothelial function. Therefore, a randomized controlled trial was conducted to evaluate if a dietary supplement, containing 500 mg of both LC and HS extracts (LC+HS), is capable to normalize anthropometric and circulating parameters in overweight/obese subjects under risk of developing metabolic syndrome. In this trial, 26 women were supplemented with capsules containing 500 mg of *LC+HS* for a 2-month period. A placebo group was formed by 20 women consuming capsules containing 400 mg of crystalline microcellulose. The consumption of the dietary supplement for two months showed significant decreases of body weight, abdominal circumference, body fat %, heart rate and systolic blood pressure compared to the placebo. Changes were more prominent in overweight volunteers consuming the polyphenolic extract. The outcomes support that LC+HS can decrease obesity/overweight-related diseases, probably through the complementary effects between LC and HS polyphenols.

General information

1. **Protocol title**: Evaluation of a dietary supplement for weight control in overweight/obese volunteers (approved by the Ethics Committee of University Miguel Hernandez, Spain).
2. **Protocol code**: NCT03568877 (22/06/2018)
3. **Ethical approval**: University Miguel Hernandez code: IB.ER.01.15 (approval date: March 12th, 2015). The official approval letter is attached herewith for reference (Appendix section).
4. **Sponsors:**
    i. *Spanish Ministry of Economy and Competitiveness (MINECO). Code: AGL2015-67995-C3-1-R*.
    ii. Generalitat Valenciana. Codes: *PROMETEO/2016/006, APOSTD/2017/023 and ACIF/2016/230.*
    iii. Instituto de Salud Carlos III, *Fisiopatologia de la Obesidad y la Nutricion, CIBERobn*. Code: *(CB12/03/30038.*
    iv. *SME instrument phase 1* European Union funding. Code: *INNOPREFAT 683933 (*H2020-SMEINST-1-2015_18-03-2015).

5. Investigators details, address and roles:

i. Dr Maria Herranz-Lopez
Associated Professor
Institute of Molecular and Cell Biology (IBMC),
University Miguel Hernandez (UMH), Avda de la Universidad sn, 03202-Elche, Alicante, Spain.
Tel: +34966658430
Role: Investigator

ii. Marilo Olivares-Vicente
Pre-doctoral fellow
Institute of Molecular and cell Biology (IBMC),
University Miguel Hernandez (UMH), Avda de la Universidad sn, 03202-Elche, Alicante, Spain.
Tel: +34966658430
Role: Investigator

iii. Marina Boix-Castejon
Pre-doctoral fellow
Institute of Bioengineering (IB),
University Miguel Hernandez (UMH), Avda de la Universidad sn, 03202-Elche, Alicante, Spain.
Tel: +34965222029
Role: Investigator

iv. Dr Nuria Caturla
Company Research Officer
Monteloeder SL,
Elche Industrial Park, Miguel Servet 16, 03203-Elche, Alicante, Spain.
Tel: +34965685275
Role: Company Consultant

v. Dr Enrique Roche
Head of Research,
Institute of Bioengineering (IB)
University Miguel Hernandez (UMH), Avda de la Universidad sn, 03202-Elche, Alicante, Spain.
Tel: +34965222029
Role: Investigator

vi. Dr Vicente Micol

Head of Research
Institute of Molecular and Cell Biology (IBMC)
University Miguel Hernandez (UMH), Avda de la Universidad sn, 03202-Elche, Alicante, Spain.
Tel: +34966658430
Role: Main Investigator

6. Clinical laboratories:

i. Pharmacy Office (Maria A Iborra-Campos)
Material for determination of anthropometric parameters and blood pressure
101, Carrer Dr Caro
03201-Elche
Alicante, Spain.
Tel: +34965442985

ii. Clinical Analysis Laboratory (Jose M Adsuar-Pomares)
Chemicals and devices for blood analysis
7, Carrer Ample
03202-Elche
Alicante, Spain.
Tel: +34965457945

7. Rationale and background information

Obesity has reached global epidemic proportions. In addition, obesity is associated with several metabolic disorders including insulin resistance, endothelial dysfunction and dyslipidemia, which are involved in the development of type 2 diabetes, hypertension and cardiovascular diseases. While there has been considerable progress in understanding the molecular mechanisms underlying metabolic disorders, their successful treatment remains limited [1]. Recently, the energy sensor AMP-activated protein kinase (AMPK) has been proposed as an important therapeutic target for obesity therapy that can be modulated by diet and exercise [2]. Our proposal is to investigate the modulation of AMPK by dietary supplements.

Our previous research has accumulated enough evidence and has identified several herbal extracts with the capacity to activate the AMPK enzyme, i.e., *Hibiscus sabdariffa* (*HS*), *Lippia citriodora* (*LC*) and *Olea europaea* leaf and extra virgin olive oil extracts [3-6]. Using an insulin resistant hypertrophic adipocyte model, we have seen that *HS* polyphenols have the capability to decrease metabolic stress in glucotoxicity and/or lipotoxicity events through the modulation of pathways associated with energy management and inflammation [7].

Additionally, HS polyphenols have exhibited the capacity to inhibit triglyceride accumulation, oxidative stress and the secretion of inflammatory adipokines that regulate the infiltration of circulating macrophages to adipose tissue [6]. Moreover, the efficacy of *HS* polyphenolic extract has also been demonstrated in animal models, preventing hepatic steatosis in hyperlipidemic mice through the regulation of the expression of genes involved in glucose and lipid homeostasis, lowering blood pressure and improving endothelial function [8, 9]. In fact, a bioavailability study conducted in rats showed that the major *HS* metabolites found in the plasma of rats were quercetin aglycone and its glucuronide [10].

On the other hand, studies on *LC*, namely lemon verbena, polyphenols showed favorable effects such as decreased lipogenesis, enhanced fatty acid oxidation and activation of the AMPK pathway, probably through PPAR-gamma receptor activation and adiponectin, which are involved in the observed beneficial effects [4]. Similar to the *HS* polyphenol extract, the effects observed for *LC* extract have also been corroborated in animal hyperlipidemic models in which the continuous consumption of the *LC* extract prevented fatty liver disease and improved lipid metabolism. Interestingly, the results on lipid and glucose metabolism obtained in the hyperlipidemic mice revealed the possibility that *HS* and *LC* reach complementary targets [4, 8], which prone us to design a dietary supplement in which both extracts were present.

References:

[1] Iyer, A.; Fairlie, D.P.; Prins, J.B.; Hammock, B.D.; Brown, L. Inflammatory lipid mediators in adipocyte function and obesity. *Nat. Rev. Endocrinol.* **6**, 71-82 (2010).

[2] Carling, D. AMPK signalling in health and disease. *Curr. Opin. Cell Biol.* **45**, 31-37 (2017).

[3] Beltran-Debon, R. *et al*. The aqueous extract of *Hibiscus sabdariffa* calices modulates the production of monocyte chemoattractant protein-1 in humans. *Phytomedicine.* **17**, 186-191 (2010).

[4] Herranz-Lopez, M. *et al*. Lemon verbena (*Lippia citriodora*) polyphenols alleviate obesity-related disturbances in hypertrophic adipocytes through ampk-dependent mechanisms. *Phytomedicine.* **22**, 605-614 (2015).

[5] Jimenez-Sanchez, C. *et al*. AMPK modulatory activity of olive–tree leaves phenolic compounds: Bioassay-guided isolation on adipocyte model and in silico approach. *PLoS ONE.* **12**, e0173074 (2017).

[6] Menendez, J.A. *et al.* Xenohormetic and anti-aging activity of secoiridoid polyphenols present in extra virgin olive oil: A new family of gerosuppressant agents. *Cell Cycle.* **12**, 555-578 (2013).

[7] Joven, J. *et al.* Multifunctional targets of dietary polyphenols in disease: A case for the chemokine network and energy metabolism. *Food Chem. Toxicol.* **51**, 267-279 (2013).

[8] Joven, J. *et al.* Plant-derived polyphenols regulate expression of miRNA paralogs miR-103/107 and miR-122 and prevent diet-induced fatty liver disease in hyperlipidemic mice. *Biochim. Biophys. Acta.* **1820**, 894-899 (2012).

[9] Joven, J. *et al. Hibiscus sabdariffa* extract lowers blood pressure and improves endothelial function. *Mol. Nutr. Food. Res.* **58**, 1374-1378 (2014).

[10] Fernandez-Arroyo, S. *et al*. Bioavailability study of a polyphenol-enriched extract from *Hibiscus sabdariffa* in rats and associated antioxidant status. *Mol. Nutr. Food. Res.* **56**, 1590-1595 (2012).

8. Study objectives

i. To assess the effect of taking LC-HS extracts on changes in anthropometric parameters in overweight/obese volunteers.

ii. To assess the effect of taking LC-HS extracts on changes in circulating parameters in overweight/obese volunteers.

iii. To assess the effect of taking LC-HS extracts on changes in blood pressure in overweight/obese volunteers.

9. Study protocol

9.1 Study design

The study was an 8-week, randomized, double-blind, placebo-controlled trial, designed to evaluate the potential of *HS+LC* extracts in modulation of anthropometric and circulating parameters as well blood pressure in overweight and obese Spanish women.

82 women, habitual clients of a Pharmacy Office in Elche (Spain), passed a health evaluation protocol. Anthropometric parameters, including weight, height and waste/hip ratio were determined on-site at the Pharmacy Office. Blood pressure determinations were taken with a monitor in the same Pharmacy Office, according to current regulations provided by the European Society of Hypertension. Finally, circulating glucose, cholesterol and triglyceride levels were measured with a Rapid Control Gauge Reflotron® Plus (Roche). To proceed to selection, contacted volunteers passed a telephone health screening interview based in the inclusion and exclusion criteria. Demographic and lifestyle information was collected as well during the telephone interview, including age, dietary and physical habits. Once recruited (N= 55), women were randomly assigned into the control (N = 26) or experimental group (N = 29) in a 1:1 ratio according to BMI (24-34 kg/m^2) using an Excel program by the research team. The control group (mean age 51) received capsules of

placebo (400 mg of crystalline microcellulose each), and the experimental group (mean age 52) received capsules, each one containing 250 mg of *HS*+*LC* plus 150 mg excipients (crystalline microcellulose). The capsules provided to both groups were made to have the same size, same odour and same colour (red capsule).

During the 60-days intervention, volunteers were instructed to take two capsules 20–30 min after overnight fasting and prior to breakfast every day. In addition, women were instructed by a qualified dietician to follow an isocaloric and balanced diet (55 % carbohydrates, 33 % lipids and 12 % proteins) of 2,200 kcal. At baseline, all participants completed a validated semiquantitative food frequency questionnaire. The questionnaire included 22 items to determine habitual consumption of grains, pulses, meat, eggs, seafood, dairy products, fruits, vegetables, processed foods, snacks high in fat and sugar and beverages. For each item, participants could select from 3 frequency categories (daily, weekly or monthly) and the number of servings from each food category. Besides, throughout both the pre and post-intervention survey, a 15-min interview, adapted from a validated questionnaire was conducted with each participant to gather information for a 24 h diet recall. Participants in both groups (dietary supplement and placebo) were given personalized advice for dietary changes at achieving a diet as close as possible to isocaloric and balanced diet with normal hydration. During the meeting, women were also asked about daily physical activity and were advised to walk for at least 30 minutes per day. Trained dieticians were responsible for all aspects of the intervention. Compliance of the subjects with the ingestion of capsules, diet and exercise was assessed at each clinic visit or by phone every week during the 2 months of study.

Measurements were taken at the beginning (day 0) and at day 30^{th} and 60^{th} of the intervention. Data were analysed and compared to the start of the study and between groups at the same time period of the intervention. These comprised anthropometric determinations, circulating parameters and blood pressure values. Anthropometric measurements included body weight, height, triceps skinfold thickness and abdominal circumference (AC) measured at two different sites: anteriorly midway between the xiphoid process of the sternum and the umbilicus and laterally between the lower end of the rib cage and iliac crests (AC1) and at umbilicus level (AC2). Body weight and height were measured using a scale with a height measuring rod. Body mass index (BMI) was derived from body weight and height using the equation BMI = body weight (kg) / height^2 (m). Triceps skinfold thickness was measured using a skinfold caliper, and AC1 and AC2 were measured using a tape measure. Percentage of body fat (% BF) was calculated from the

weight, height and abdominal circumference (AC1 and AC2) using the Weltman equation for obese women.

Regarding circulating parameters, fasting blood was collected to determine total glucose and glycosylated hemoglobin (HbA1c) and the lipid profile, which included triglycerides, total cholesterol, high-density lipoprotein (HDL) and low-density lipoprotein (LDL)-cholesterol. Blood was also analysed for safety parameters, hematology, electrolytes (Na, K), creatinine, urea, uric acid, glutamic-pyruvic transaminase (GPT), glutamic-oxaloacetic transaminase (GOT) and C-reactive protein.

Finally, systolic (SBP) and diastolic blood pressure (DBP) and heart beats were measured at rest, using an Omron HEM-7320-LA oscillometric blood pressure monitor (Omron Healthcare Co. Ltd, Kyoto, Japan) at the upper arm with a large cuff. Five independent measurements for SBP, DBP and heart rate were taken using a validated protocol. The study flow diagram is shown in Figure 1.

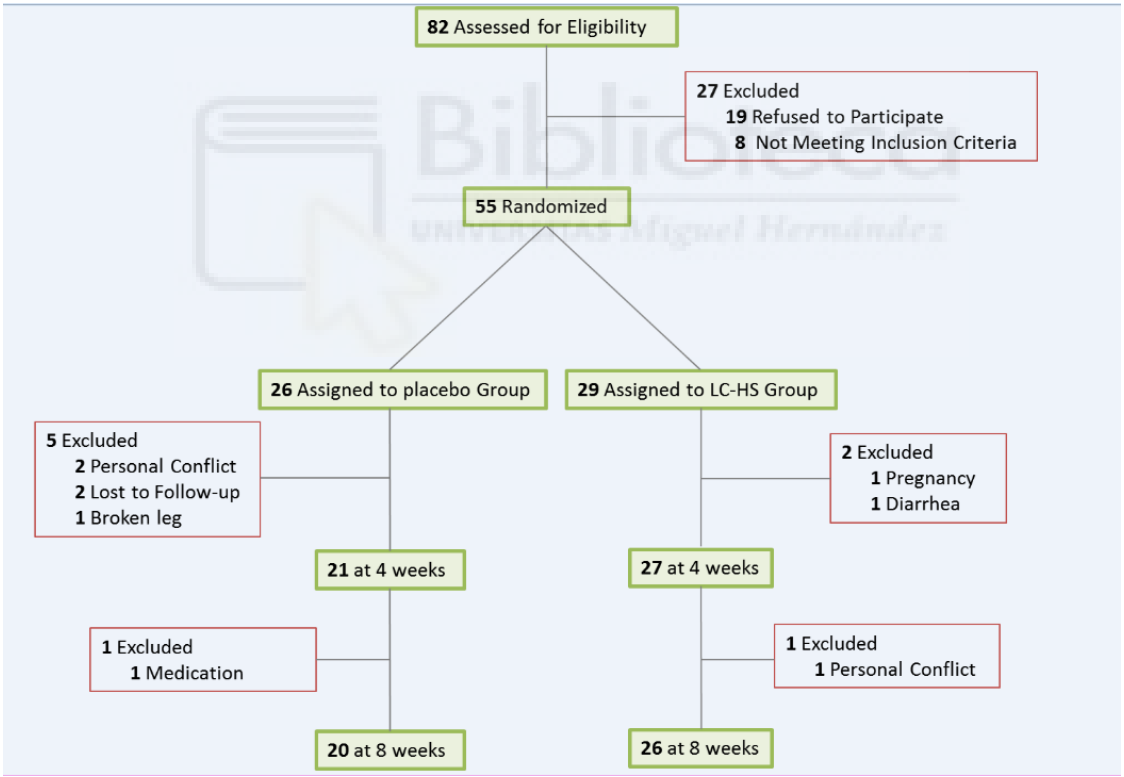

Figure 1: Study flow chart.

9.1.2 Recruitment of volunteers

55 volunteers were recruited from 82 initially contacted women at the Pharmacy Office in Elche (Spain). Volunteers were selected according to several inclusion and exclusion criteria, as follows:

9.1.2.1 Inclusion criteria

i. Written informed consent obtained from volunteers after detailed information provided by investigators about the purpose and procedures of the study.
ii. Volunteers age between 36 and 69 years.
iii. Diastolic blood pressure > 75 mmHg, Systolic blood pressure > 120 mmHg
iv. Women.
v. Having a good record of compliance.

9.1.2.2 Exclusion criteria

a. Total cholesterol < 200 mg/dL.
b. Evident presence of an obesity related pathology.
c. Use of medication to treat hypercholesterolemia and/or hypertension.
d. Hormone replacement therapy.
e. Consumption of antioxidant supplements, including vitamins and herbal extracts.
f. Consumption of alcohol and/or drugs.
g. Smoking habits.
h. Women in pregnancy or in lactation periods.

9.1.2.3 Rights of volunteers to drop out of the study

Volunteers were free to drop out from the study at any time for any reason without giving explanations. Volunteers may also be dropped out from the study for the following reasons: pathology diagnosis, prescription of medication, accident, protocol violations and at any time at discretion of the investigator. The drop out document must be provided to participants at the same time that the written consent at the beginning of the study.

9.2 Methodology

9.2.1 Blood sampling

Fasting blood sample were drawn from the volunteers by experienced and well-trained health professionals. 5 mL of blood were transferred into an EDTA (ethylenediamine tetra acetic acid) tube and processed for analysis according to laboratory standard protocols.

9.2.2 Measured blood parameters:

- Circulating cells and related parameters*:

- Red blood cell counts.
- Hematocrit, mean corpuscular volume, mean corpuscular hemoglobin, mean corpuscular hemoglobin concentration and red blood cell distribution width.

- Leucocyte counts: Neutrophils, lymphocytes, monocytes, eosinophils and basophils.

- Platelet counts.

- Glycemia profiles:** Glucose and glycosylated hemoglobin (HbA1C).

- Lipid profile:** Triglycerides, total cholesterol, LDL-cholesterol and HDL-cholesterol.

- Metabolites for kidney function*: Creatinine, urea and uric acid.

- Liver and muscle markers*: Glutamic-pyruvic transaminase (GPT) and glutamic-oxaloacetic transaminase (GOT).

- Electrolytes*: Na^+ and K^+.

- Stress markers*: C-reactive protein (CRP).

(*) Safety parameters to control the health status of participants.

(**) Parameters analyzed in the study.

9.2.3 Statistical method

For analysis, data were stratified in four groups: overweight and obese placebo, and overweight and obese volunteers consuming the polyphenolic extract. Clinical statistical analyses were performed with a Student's t-test using Graphpad Prism software. Outcome variables were assessed for conformance to the normal distribution and transformed if necessary, by a KS-test. Data are reported as the mean ± SEM. Reported *p*-values were two-sided and a *p*-value of 0.05 or less was considered statistically significant for between-group comparisons. Comparisons were established between the placebo and the LC-HS groups by unpaired Student's t-test. By contrast, intra-group statistical analysis at the endpoint was compared to the baseline and analyzed by paired Student's t-test. Statistically significant differences throughout the study were expressed as $*p < 0.05$; $** p < 0.01$, $*** p < 0.001$.